NUCLEAR DATA IN SCIENCE AND TECHNOLOGY

VOL. I

PROCEEDINGS OF A SYMPOSIUM, PARIS, 12-16 MARCH 1973

INTERNATIONAL ATOMIC ENERGY AGENCY, VIENNA, 1973

NUCLEAR DATA
IN SCIENCE AND TECHNOLOGY

VOL. I

The following States are Members of the International Atomic Energy Agency:

AFGHANISTAN
ALBANIA
ALGERIA
ARGENTINA
AUSTRALIA
AUSTRIA
BANGLADESH
BELGIUM
BOLIVIA
BRAZIL
BULGARIA
BURMA
BYELORUSSIAN SOVIET SOCIALIST REPUBLIC
CAMEROON
CANADA
CHILE
CHINA
COLOMBIA
COSTA RICA
CUBA
CYPRUS
CZECHOSLOVAK SOCIALIST REPUBLIC
DENMARK
DOMINICAN REPUBLIC
ECUADOR
EGYPT, ARAB REPUBLIC OF
EL SALVADOR
ETHIOPIA
FINLAND
FRANCE
GABON
GERMANY, FEDERAL REPUBLIC OF
GHANA
GREECE
GUATEMALA
HAITI
HOLY SEE
HUNGARY
ICELAND
INDIA
INDONESIA
IRAN
IRAQ
IRELAND
ISRAEL
ITALY
IVORY COAST
JAMAICA
JAPAN
JORDAN
KENYA
KHMER REPUBLIC
KOREA, REPUBLIC OF
KUWAIT
LEBANON
LIBERIA
LIBYAN ARAB REPUBLIC
LIECHTENSTEIN
LUXEMBOURG
MADAGASCAR
MALAYSIA
MALI
MEXICO
MONACO
MOROCCO
NETHERLANDS
NEW ZEALAND
NIGER
NIGERIA
NORWAY
PAKISTAN
PANAMA
PARAGUAY
PERU
PHILIPPINES
POLAND
PORTUGAL
ROMANIA
SAUDI ARABIA
SENEGAL
SIERRA LEONE
SINGAPORE
SOUTH AFRICA
SPAIN
SRI LANKA
SUDAN
SWEDEN
SWITZERLAND
SYRIAN ARAB REPUBLIC
THAILAND
TUNISIA
TURKEY
UGANDA
UKRAINIAN SOVIET SOCIALIST REPUBLIC
UNION OF SOVIET SOCIALIST REPUBLICS
UNITED KINGDOM OF GREAT BRITAIN AND NORTHERN IRELAND
UNITED STATES OF AMERICA
URUGUAY
VENEZUELA
VIET-NAM
YUGOSLAVIA
ZAIRE, REPUBLIC OF
ZAMBIA

The Agency's Statute was approved on 23 October 1956 by the Conference on the Statute of the IAEA held at United Nations Headquarters, New York; it entered into force on 29 July 1957. The Headquarters of the Agency are situated in Vienna. Its principal objective is "to accelerate and enlarge the contribution of atomic energy to peace, health and prosperity throughout the world".

Printed by the IAEA in Austria
September 1973

PROCEEDINGS SERIES

NUCLEAR DATA IN SCIENCE AND TECHNOLOGY

PROCEEDINGS OF THE SYMPOSIUM ON
APPLICATIONS OF NUCLEAR DATA
IN SCIENCE AND TECHNOLOGY
HELD BY THE
INTERNATIONAL ATOMIC ENERGY AGENCY
IN PARIS, 12 - 16 MARCH 1973

In two volumes

VOL. I

INTERNATIONAL ATOMIC ENERGY AGENCY
VIENNA, 1973

NUCLEAR DATA IN SCIENCE AND TECHNOLOGY
IAEA, VIENNA, 1973
STI/PUB/343

FOREWORD

The IAEA Symposium on "Applications of Nuclear Data in Science and Technology" was convened by the International Atomic Energy Agency on 12 - 16 March 1973 in Paris at the invitation of the French Government. The meeting was held on the recommendation of the International Nuclear Data Committee (INDC) and the International Working Group on Nuclear Structure and Reaction Data (IWGNSRD). The main purpose of the Symposium was to illuminate the needs for nuclear data in the technological and scientific community. Over 200 delegates attended, representing 30 countries and five international organizations. A total of 74 papers was presented, including the Keynote Address and the Symposium Summary.

For many years the mechanisms for satisfying the nuclear data needs related to neutron-induced reactions have been fairly well organized by those concerned with neutron-reactor technology, which is a major field of application for this kind of data. However, for several years it has become increasingly evident that there is a strong need for better, up-to-date compilations of nuclear data for a large number of other applications. The IAEA was therefore requested to convene a symposium in order to review the status of and needs for new nuclear data evaluation activities. During the preparation, it became evident that the symposium should emphasize data needs in the various applications rather than existing data compilation activities.

The program committee attempted to achieve a balance between reactor and non-reactor applications as well as a balance between the needs for various applications and the needs for compilation work. As a result, four of the sixteen regular sessions were devoted to applications related to nuclear energy, seven to other applications and five to topics related to data compilations. In contrast to the International Conferences on Nuclear Data for Reactors (Paris, 17 - 21 October 1966, and Helsinki, 15 - 19 June 1970), this Symposium was not meant to be a forum for the presentation of experimental data.

The Symposium demonstrated that the compilation of structure and decay data would benefit from considerably increased support. These data are basic to most other data-application-oriented compilations. The long delay in bringing compilations of this type up to date causes unacceptable hold-ups in the process of bringing such data from producers to users. Under the heading 'Symposium Summary', Dr. W.B. Lewis, at the end of the meeting, discussed the most important conclusions to be drawn from the symposium with regard to data needs and the status of compilations. A further summary of the meeting, by L. Hjärne, appears in Atomic Energy Review, 1973, Vol.11, No.2, 395.

The Proceedings are divided into two volumes, the first of which contains, besides the Keynote Address, thirty-two papers in the fields of Future Technology Requirements, Reactor Technology, Safeguards, Life Sciences, Radioisotopes in Chemistry, Fission-Product Nuclear Data and

Accelerator and Space Shielding. The second volume – with forty contributions, in addition to the Symposium Summary – covers the fields of Fusion Research, Evaluated Neutron Data Files, Activation Analysis (General and Neutrons), Compilation and Evaluation – Data Centres, Large-Volume Compilations, Various Applications, Activation Analysis: Charged Particles and Photons, and Application-Oriented Computations and Evaluations.

The Agency wishes to thank the French authorities for their hospitality and active support of the Symposium, and the authors and participants for their valuable contributions. Special thanks are due to the Chairmen of the individual sessions for their successful efforts in guiding the discussions.

EDITORIAL NOTE

The papers and discussions incorporated in the proceedings published by the International Atomic Energy Agency are edited by the Agency's editorial staff to the extent considered necessary for the reader's assistance. The views expressed and the general style adopted remain, however, the responsibility of the named authors or participants.

For the sake of speed of publication the present Proceedings have been printed by composition typing and photo-offset lithography. Within the limitations imposed by this method, every effort has been made to maintain a high editorial standard; in particular, the units and symbols employed are to the fullest practicable extent those standardized or recommended by the competent international scientific bodies.

The affiliations of authors are those given at the time of nomination.

The use in these Proceedings of particular designations of countries or territories does not imply any judgement by the Agency as to the legal status of such countries or territories, of their authorities and institutions or of the delimitation of their boundaries.

The mention of specific companies or of their products or brand-names does not imply any endorsement or recommendation on the part of the International Atomic Energy Agency.

CONTENTS OF VOL. I

KEYNOTE ADDRESS
OPENING OF THE SYMPOSIUM

CRITERIA OF CHOICE FOR COMPILATIONS OF NUCLEAR DATA*

D.J. HOREN, A.M. WEINBERG
Oak Ridge National Laboratory, Oak Ridge, Tenn.,
United States of America

About twelve years ago, when the scientific community began to realize that priorities in science were inevitable, one of us (AMW) proposed what are now called "criteria for scientific choice" [1]. These amounted to a set of principles – admittedly much easier to formulate in the abstract than to apply in specific cases – that could help one decide the relative merit of, and therefore priority to be assigned to, different scientific activities.

The criteria of choice were divided into two categories: internal and external. Internal criteria arose out of the logic and structure of a field: they were concerned with such questions as, "Is the field ripe for exploitation – i.e. are there pressing scientific issues in which knowledgeable practitioners see ways of making progress? Or does the field itself attract very able people?" These internal criteria address themselves to the solvability of scientific problems. (Peter Medawar describes science – in a clever paraphrase of Disraeli – as the Art of the Soluble [2].) Internal criteria measure a scientific activity by the extent to which it yields results that are worthwhile as judged by the standards of the field in which the results are obtained.

External criteria measure a scientific activity from the standpoint of the universe outside the activity. They address themselves to the usefulness (as contrasted to the solvability) of scientific research: its usefulness to other sciences, to engineering and technology, to society at large. In a general sort of way, it was argued that where large sums of public money were required to support a scientific activity, external criteria must loom prominently in judging relative priorities.

About the time of the publications on criteria for scientific choice, one of us (AMW) chaired a panel of the President's Science Advisory Committee (PSAC) concerned with scientific information. That report, entitled "Science, Government, and Information" [3], is probably familiar to many in this audience. Its main emphasis was on the specialized information centre. The report viewed such secondary handlers of scientific information as a key to restoring order to what seemed like a chaotic expansion of scientific knowledge. In retrospect, it seems that the panel was graced with good luck in stressing the role of the specialized information centre. Such centres have proliferated even beyond what we enthusiasts anticipated when writing the report. In nuclear structure and reactions alone, there are now at least 28 such centres throughout the world according to the studies of the International Working Group on Nuclear Structure and Reaction Data (IWGNSRD) [4].

It therefore seemed appropriate, in talking to an audience that includes both compilers of nuclear data and users of nuclear data, to try to synthesize

---

* Presented by A.M. Weinberg.

these two separate threads from earlier works: Scientific Information, in this instance, Nuclear Information, and Criteria for Scientific Choice. For just as science itself, and certainly nuclear science, must adjust to limited resources, so scientific compilation, and in particular compilation of nuclear data, is similarly constrained. Thus the problem of priorities – what to do first, where to allocate resources in science – also faces the community of compilers. They too must decide what to compile and what to leave for later. Can we establish a-priori criteria of choice for scientific compilation? Can such criteria be regarded as more than a philosophic exercise?

THE NECESSITY FOR CHOICE

The compilers of scientific data have in recent years lagged behind the producers of scientific data, and have had to establish priorities. In nuclear science, technical developments have greatly magnified this discrepancy between the mass of data and the compiler's capacity to handle it.

The use of high-resolution solid-state detectors, as well as other improved techniques, has multiplied the number of recorded bound states per nucleus five- to ten-fold during the past decade; and the widespread utilization of automatic processing has created a heavy glut of undigested nuclear data. There are now some 3000-4000 nuclear-structure scientists who publish about 3500 papers annually. The data contained in each paper varies anywhere from a single number – e.g. the reporting of a half-life measurement, or spin, etc. – to thousands of numbers. For example, Mühlbauer has observed more than 2000 gamma-ray transitions below 1.4 MeV following neutron capture in ^{152}Eu [5]! Ignoring the quantities – level energies and properties – that can be deduced from this particular data, but, considering only the energies, intensities, and uncertainties on each quantity, one has to deal with 4×2000 or 8000 numbers!

The history of the Nuclear Data Project from 1959-1972 illustrates how this increase in data has complicated the life of the compiler of mass-chain data. Prior to 1963 the number of compilations per man-year was 3.5-5, with each compilation having 100 times the quantity of data reported in an average research paper; today this number has fallen to about 1.8 compilations per man-year. Since 1959 the number of research papers per man-year (at least in the United States) has remained relatively constant at about one. The average quantity of reported data, however, has increased by a factor of ten, and the ratio of data per compilation versus that per average research paper has remained about constant at 100/1. Thus the compiler has increased his ability to handle data by a factor of four to five – i.e. $(1.8/5) \times 10$ – but this has not been sufficient to cope with the ten-fold increased production of data.[1] Thus one can make a serious argument for relatively more, rather than less, money going into secondary treatment of data.

[1] We have tried to estimate the cost of gathering and compiling nuclear data. The average research paper reports approximately 30 measured numbers (including uncertainties), which is equivalent to about $1500 per number; in the United States an average research paper costs approximately $45 000. Data producers are generating some 110 000 numbers annually. An average Data Project compilation contains approximately 3000 numbers at a cost of approximately $10 per number, or one per cent of the production cost.
In this connection the authors would like to point to the importance of establishing a uniform and international system of key words and indexing as a means of amplifying the compilers' increasingly difficult job of keeping up with the data.

INTERNAL CRITERIA: NUCLEAR COMPILATION AS PART OF NUCLEAR SCIENCE

Scientific compilation is, of course, part of science. One could therefore argue that criteria of choice that are appropriate for science ought to be applicable to scientific compilation. Moreover, the motivations for scientific compilation in a way parallel the motivations for science itself. We say we do science, on the one hand, to find order in nature where none had hitherto been perceived (the Newtonian view) or, on the other hand, to enable man, through application of science, to control nature for man's benefit (Baconian view). In a parallel sense, the scientific compiler is motivated, on the one hand, by his desire to find scientific regularities and new insights where none have been found before, or to help scientists in his own field find such regularities; and, on the other hand, his desire to make the results of his compilations useful to scientists in other fields, and to those who apply science to the useful arts. We would call the first motivation for scientific compilation internal, the second external.

Within the field of nuclear science one can find both internally and externally motivated compilation groups. The approach as to what they compile, as well as their methods, is usually reflected to some degree by their histories. Most of the internally motivated groups were established by active researchers, mainly as an aid to cope with the data or to detect systematic trends.

Most of the compilers in this audience are familiar with instances in which compilations have proved of some significance in the creation of new nuclear science. To mention a few examples, we would cite the nuclear shell model which stemmed mainly from a combination of compiled data and the injection of a new idea, strong spin-orbit coupling.[2] The highly successful description of nuclear properties in the rare-earth and actinide regions in terms of a non-spherical model has been refined through an intermingling of experiments, compilations, and theoretical ideas. Compilations played an important role also in the evolving description of the vibrations of near-spherical nuclei, or the development of the optical-model description for nuclear reactions. Other examples in which compilations have played a significant part in the discovery of new nuclear science can of course, be given.

The compiler, in pursuing his aims that are part of nuclear science – i.e. finding regularities, discrepancies, and lacunae – must be guided by some internal criteria. He must decide what data are most likely to yield such nuggets, are most worth spending his time on. It would be our impression that the compiler's sensitivity to what is important, and therefore his ordering of priorities, is established in much the same way as are the sensitivities toward priorities of nuclear science itself. Moreover, since the compilers, at least in those centres serving basic nuclear science,

---

[2] Although a number of workers, some before 1930, had suggested the possibility of nuclear shell structure based on theoretical and sketchy experimental grounds [see, e.g. ELSASSER, W., J. Phys. Radium 5 (1934) 625], it remained until early 1949 for Maria MAYER [Phys. Rev. 75 (1949) 1969] and independently the team of HAXEL, O., JENSEN, J.H.D., SUESS, H.E. [Phys. Rev. 75 (1949) 1766] to present a totally convincing case for the existence of magic numbers, as well as a rationale for them in terms of strong spin-orbit coupling (suggested to Mayer by Fermi).

TABLE I. AREAS OF APPLICATION OF NUCLEAR DATA AND TECHNIQUES

Applied area	Usage	Main data requirements	Level of knowledge of nuclear physics required by user
Electrical power	Fission reactors Design Radioactive waste disposal Regulation Environmental Fuel element control (i.e. safeguards)	Neutron data, fission data, decay data, nuclear structure	High
	Radioisotope batteries	Decay data	Low
	Controlled thermal fusion	Charged-particle reactions, neutron reactions	High
Biology and medicine	Diagnostic studies	Decay data (some reaction data)	Medium to low
	Therapy	Decay data, neutron and charged-particle reactions (protons, π-mesons, heavy ions)	Medium to high
	Research		
Agriculture	Food preservation Genetic studies Plant studies	Decay data	Low
Geology Archeology Forensic	Activation analysis	Decay data, neutron capture, X-ray fluorescence by means of charged particles or γ's	Low to medium
Industrial	Leak detection Gauges (thickness, density) Controls Fire detection devices Filters Materials treatment Solid-state devices Materials analysis Radiography	Various types noted above depending upon application	Low to medium
Physical sciences	Nuclear physics Astrophysics Solid state Chemistry		Low to high depending on specific area

are themselves an integral part of the nuclear science community, there is little problem of what to compile next: at least, it is not more difficult than the problem of what to measure next. This is determined by the state of knowledge of the science and is largely a personal judgment.

A second, and perhaps more important, question of priority is the depth and complexity of a compilation. For some purposes, only a broad, but not deep, compilation is necessary (the initial stages of the optical model, for example). However, where one is interested in a microscopic test of a theoretical model, an in-depth compilation is required. Again, however, since these are so integral a part of nuclear science, it is hard for us to prescribe criteria that are different from the intrinsic criteria of choice appropriate for nuclear science itself. After all, nuclear science, like all science, is the Art of the Soluble: one goes where one's instincts, sharpened by the scientific ambience in which one operates, lead. The main point is that as long as nuclear compilation is supported at a level sufficient for the compiler to be au courant with the data, and the compiler maintains his contacts with the nuclear community, significant new nuclear science will come from nuclear compilations.

EXTERNAL CRITERIA: NUCLEAR COMPILATION AS AN AID TO APPLICATION

In Table I we summarize some of the areas in which nuclear data or techniques are being applied. As one sees, these range from power generation to nuclear medicine, from agriculture to forensic science, and, of course, include the basic physical sciences – nuclear physics, astrophysics, solid state, chemistry, etc. Most striking is the wide variation in sophistication both in the use of the data and in the user's knowledge of nuclear science. In view of this, one easily surmises that the need for critical evaluation of the data will be somewhat dependent upon the specific application for which it is intended.

Papers to be presented at this symposium suggest that these points will be aptly demonstrated in the respective sessions. Hence we confine ourselves to two specific examples of the use of nuclear data: as it applies to emergency core-cooling systems (ECCS) and its present and possible future role in biological applications.

(1) ECCS: Perhaps an apt example of heavily applied use for compiled non-neutron nuclear data is the estimate of the afterheat in a light-water reactor. This is one of the factors needed to asses the performance of the ECCS, and some 22 000 pages of testimony pertaining to this topic have been amassed during the past year. Among the important technical questions involved is whether or not the fuel elements heat up too much during the first few seconds after blow-down. To obtain this information from in-situ measurements would be extremely difficult. Therefore, to estimate the heat build-up, two calculational approaches have been considered – one based upon experimental measurements of the gamma and beta power associated with the thermal fission of ^{235}U, the other on a detailed knowledge of the yields and decays of the fission products. The latter information has been compiled since the beginning of the Manhattan Project, particularly, through the active work of Katharine Way, who is generally recognized as one of the founders of modern nuclear data compilation.

Partly because of the work of T.R. England [6], questions were recently raised concerning the validity of accepted procedures for handling the fission product after-heat. This has led to a re-examination of the problem, and once again exemplifies a fundamental contribution that can be made to applied programs by the nuclear scientist in his role as compiler/evaluator.

Given a choice, the reactor engineer or scientist would certainly prefer to have available all the evaluated nuclear data required to calculate the heat release after blow-down. An engineer is unlikely to have had sufficient training and experience to evaluate the experimental data, whereas a nuclear scientist would probably find it difficult were he too long removed from the experimental details. Furthermore, to perform the calculation by going back to the fission product yields and decays would be almost impossible if he were forced to start at the beginning and compile and evaluate all the data himself.

A look at data on direct measurement of the gamma and beta powers illustrates the engineer's difficulty. In Fig. 1 we show the results of four independent measurements of the beta power. It takes little imagination to visualize the bewilderment which the nuclear engineer will experience when confronted with such data. Should he, or can he, examine the detailed measurements to try to determine the sources of the apparent discrepancies? Should he treat the data as four equal and independent sets? Should he accept the uncertainties quoted by the authors? Here is a place where the experience of the compilation community could well be brought to bear on an important technical matter.

(2) Biological applications: The use of nuclear data and techniques for biological purposes continues to grow. At present 20 to 30 radioisotopes are in routine clinical use, mainly as diagnostic tools. Approximately 120 others are being used in research studies. Recently, there has been a resurgence in the use of neutrons in cancer therapy. With the new high-energy proton accelerators coming on-line, as well as heavy-ion accelerators,

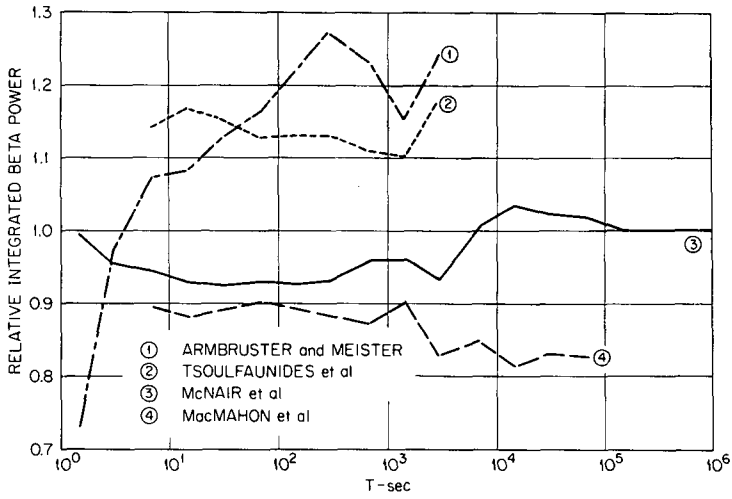

FIG. 1. Comparison of differential beta experiments. The integrated beta power from four differential measurements is plotted relative to a weighted average (this figure was kindly provided by A.M. Perry of ORNL).

new techniques in medical radiology that exploit the interactions of such projectiles (and also π-mesons) with tissue will most likely be developed. This will entail detailed knowledge of many nuclear interactions as well as phenomena associated with atomic physics, such as charged-particle stopping powers.

In this area alone one can find examples for which the quality of the data is relatively unimportant and others for which it is critical. The typical role of the compiler, as a supplier of evaluated data, probably will not suffice in all cases. The medical user, in the application of π-mesons, will need assistance that goes far beyond that historically provided by a compiler; undoubtedly, he will often have to communicate directly with the compiler/evaluator.

In general, though, the needs of the applied scientist are for evaluated nuclear data and, in particular, data that have been evaluated with his needs in mind. To be sure, there now are many nuclear compilation centres, such as the Brookhaven National Neutron Cross Section Center, which compile and evaluate data for special classes of users. Of the centres listed by IWGNSRD, about two-thirds are externally motivated and are part of the applied community; one-third are internally motivated – i.e. consider themselves part of nuclear science rather than of nuclear applications.

Obviously, insofar as barriers exist between the internally and externally motivated data compilers, these barriers ought to be removed. This has happened in the case of evaluated neutron cross-section data – through the operation of the Neutron Cross-Section Advisory Committees, both national and international. And the creation of the U.S. Nuclear Data Committee to cover broader nuclear data (including that for nuclear science itself) is an experiment well worth serious attention.

THE PROBLEM IN PERSPECTIVE

By the year 2000 we anticipate that in the United States alone there will be 500 operating reactors. The rest of the world will not be far behind. It will be a world in which the existence of radioactive nuclei will not be a scientific curiosity but an ever present factor in our daily lives. All kinds of people will have to know about radioactive nuclei: chemical engineers, geologists, geochemists, atmospheric scientists, oceanographers, paleographers, ecologists, anthropologists, veterinarians, agricultural scientists, soil scientists, economists, and political scientists. Each group will want information in a format that is easy to use, easy to transmit, and easy to remember. It will be the task of the compilers to be responsive to the needs of many sectors of our society and to provide nuclear data in specific formats for each sector.

We see therefore a strong and growing need for externally motivated nuclear compilations. It is unlikely that potential users will come uninvited to the compilers and ask for particularly useful kinds of compilations. The compiler must seek out potential users continuously and energetically. Several mechanisms might make this task a little less than impossible.

(1) There are conferences such as this one where users and compilers meet to exchange views on major problems and to work out together useful courses of action.

(2) It is possible to embed nuclear data centres in large multidisciplinary organizations. This is currently the case in the nuclear laboratories of many countries, and leads to reasonably good communication channels between compilers and obvious potential users who are connected with the nuclear energy enterprise.

(3) Committees which we mentioned earlier, such as the US Nuclear Data Committee, may be very useful in helping to establish priorities for compilation of nuclear data. Certainly the various Neutron Cross-Section Advisory Committees have been helpful both in the measurement and evaluation of data for reactor design. However, the more general fields of nuclear science and application do not have the same unifying theme or, for that matter, the centralized managerial structure as does reactor design and engineering. This will make it harder for committees to sense accurately the needs of this larger community. Moreover, committees are cumbersome: will they impose further delays on the transfer of information from experimenter to user – which after all is what we are trying to expedite?

(4) Finally, the most important ingredient is the intelligence, the energy, and vision of the individual compiler or of compiler organizations. One important issue here is how one can make the centres that have a tradition of internal motivation, a commitment to basic nuclear science, more useful to the community of applied science. One obvious, and quite simple, answer is to urge that these compilers of nuclear data become more familiar with the needs of users. After all, when a compiler establishes a priority according to the internal logic of nuclear science, it is necessary to familiarize himself with that logic – to decide what is needed to strengthen the edifice of nuclear science. Is one being unrealistic to urge that nuclear compilers themselves accept some responsibility for the needs of the applied community that their data may serve so that, though their primary commitment remains to their science, and their primary criteria of choice remain internal, they use some cues from the applied world in setting their priorities? As a practical matter, this means that at least a few compilers in each of the basic compilation groups would acquire knowledge of and sensitivity to the applied sciences.

Establishing priorities in nuclear compilation is hardly any easier than is establishing priorities in nuclear science itselt. And indeed, rather than proposing specific priorities, we have alluded to mechanisms for establishing priorities – in particular, the steering or guiding committee, and the informed individual compiler, especially the one who works in a broad, interdisciplinary setting. The two mechanisms, of course, do not exclude each other. We would only hope that this present-day tendency to centralize decisions in science by setting up central committees does not work to lessen the individual compiler's own responsibility to become acquainted with, and sensitive to, the needs of the basic and applied communities his compilations serve.

REFERENCES

[1] "Criteria for Scientific Choice", Minerva I, pp. 159-171 (Winter 1963); "Criteria for Scientific Choice II: The Two Cultures", Minerva III, pp. 3-14 (Autumn 1964).

[2] MEDAWAR, P.B., The Art of the Soluble, Methuen and Company Ltd., London (1967).

[3] A report of the President's Science Advisory Committee, U.S. Government Printing Office, Washington (January 10, 1963).

[4] International Working Group on Nuclear Structure and Reaction Data, Minutes of First Meeting, INDC(SEC)-29/G (and minutes of subsequent meetings), IAEA Nuclear Data Section, Vienna (October 1972).
[5] MÜHLBAUER, K., Z. Phys. 230 (1970) 18.
[6] ENGLAND, T.R., "An Investigation of Fission Product Behavior and Decay Heating in Nuclear Reactors", Ph.D. Thesis, University of Wisconsin (August 1969).

Section I

FUTURE TECHNOLOGY REQUIREMENTS

Chairman

G.A. KOLSTAD (USA)

FISSIONING URANIUM PLASMAS

K. THOM
AEC/NASA Space Nuclear Systems Office,
Washington, D.C.
and
R.T. SCHNEIDER
University of Florida, Gainesville, Fla.,
United States of America

Abstract

FISSIONING URANIUM PLASMAS.

Several concepts for cavity reactors have been proposed in which the nuclear fuel is in the plasma state. Motives for conducting research related to such high-temperature reactors are the possible application of these reactors for high-specific-impulse propulsion in space, magnetohydrodynamic electrical power generation at high efficiency, direct nuclear pumping of lasers, and as a source for process heat.

The confinement of the fissioning uranium plasma within the cavity is sought by means of fluid mechanics. The extraction of power is accomplished by radiative transfer. These requirements impose specific problems upon criticality calculations.

A significant difference exists between the neutron temperature (thermal) and the uranium plasma temperature. For this reason, more accurate neutron scattering and capture cross-section data in the several-eV-region are needed. Temporal fluctuation of the fuel density and variation of the spatial fuel distribution during operation and start-up require new codes. Reactivity perturbations due to possible uranium influx variations have to be carefully analysed for power excursions and subsequent disturbances of the balanced system of flow confinement and radiative power transmission.

In connection with some of the concepts under consideration, research on nuclear radiation damage of optical transparent material is needed.

The US National Aeronautics and Space Administration has conducted an intensive research program on various aspects of fissioning plasmas, analytically and in simulation, particularly regarding the feasibility of two major concepts of cavity reactors. Such work is described. The needs for further research, especially in view of required nuclear data, is discussed.

A significant step forward will be the realization of a proposed hybrid research facility consisting of a solid-fuel driver section enclosing the fissioning plasma. This facility would allow basic research on fissioning plasmas. The requirements for codes for design of such a two-component fuel-reactor system are discussed.

INTRODUCTION

A fissioning plasma is a reacting fissionable fuel that by its own fission power is sufficiently energized to exist in a gaseous partially ionized state. Fissioning plasmas have so far only been produced in nuclear explosions. Steady-state fissioning plasmas are expected to be useful because of the high temperature at which they exist. However, theoretical investigations have shown that the realization of a plasma-core reactor represents a major development effort. With the exception of space propulsion at a high specific impulse and at a high level of thrust, no technological needs for the high-temperature capabilities of fissioning plasmas in the past were pressing enough to warrant the cost of such a development. However, for the purpose of space propulsion, the U.S. National Aeronautics and Space Administration has conducted research on fissioning plasmas [1, 2]. More recently, problems such as power shortages and thermal pollution have developed that make plasma-core reactors desirable for more applications than space propulsion. Advanced propulsion remains, however, a principal motivation for plasma-core reactor research.

A frequently used term in rocket propulsion is "specific impulse". It is the ratio of thrust and mass flow rate and is proportional to the propellant exhaust velocity. At low specific impulse, such as in chemical propulsion, the propellant and fuel weights are much larger than the weight of structures. In this case the payload fraction depends exponentially on the ratio of the final speed of the rocket and the exhaust velocity; during low specific impulse propulsion, lunar-return missions and particularly planetary missions, diminishing payload fractions result.

High exhaust velocities can be achieved in ion propulsion or by electromagnetic plasma acceleration. However, the jet power is the product of thrust and exhaust velocity and thus increases with the cube of the latter. At high specific impulse, power requirements can become so large that the dead weight of the power plant offsets gains in payload fraction, such that the ratio of the power plant weight and jet power becomes the dominant characteristic of propulsion. This ratio is called the specific mass. It is determined by dividing the kilograms of power plant mass by the kilowatts of jet power and is obviously an expression for power density. A fissioning plasma, burning nuclear fuel at very high temperatures and densities, is a very high power density energy source. In prospective plasma core rockets, shielding, neutron moderation and reflection impose a large dead weight. After analysis it turns out, however, that such minimum weight is not incompatible with more ambitious space missions, because the inherently low specific mass of fissioning plasma rockets will lead to significant gains in payload fraction and in reductions of trip times. Such advantages are compared with the capabilities of other propulsion methods for a manned round trip to Mars (fig. 1). For plasma core propulsion, the initial mass in earth orbit is an order of magnitude smaller than for chemical propulsion. It has been estimated that the resulting reduction of cost for such a mission could compensate for the cost of the development of plasma core reactors in one or two such flights, but that may remain questionable because advances in other propulsion modes may alter such present comparisons. In this treatise of fissioning plasmas a broader view of technological usefulness than space propulsion is taken as to lead to various detailed scientific and engineering problems, of which, nuclear data are a significant part.

FISSIONING PLASMA REACTOR CONCEPTS

Major concepts of plasma core reactors are the coaxial flow system, the nuclear light bulb engine, the nuclear pumped laser system, and the nuclear piston engine. These concepts, particularly the first two, have motivated a program of specific research aimed at demonstrating their feasibility. The magnitude of this research effort, extending over the past 15 years, is about 200 professional manyears [3]. Accordingly, the present schemes of plasma core reactors should be regarded as mature in the sense of careful probing in theory and experiment, short mainly of fission tests at larger power.

The coaxial flow scheme, originally conceived for advanced space propulsion, is based on fluid mechanics confinement of the fissioning plasma (fig. 2), and is analyzed in [4, 5, 6]. Enriched ^{235}U is introduced into the cavity in the form of a fast moving wire. The fissioning plasma is held in a central position by a rapid flow of hydrogen injected through porous cavity walls or through an array of slots. This propellant flow separates the hot plasma from the walls and also intercepts the powerful thermal radiation from the plasma. Thereby it is heated up for expansion through a nozzle. Some uranium plasma is entrained in the propellant flow and subsequently lost. The cavity is surrounded by a beryllium oxide moderator-reflector, and all is contained in a pressure vessel.

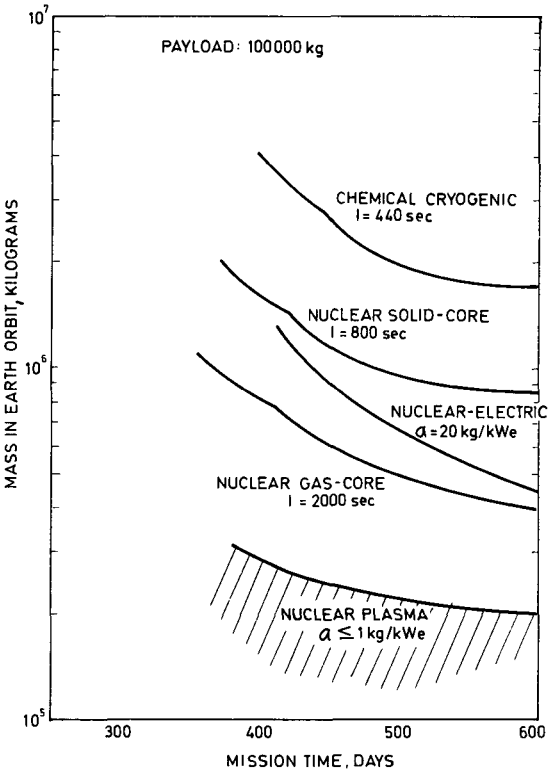

FIG. 1. Principal modes of propulsion.

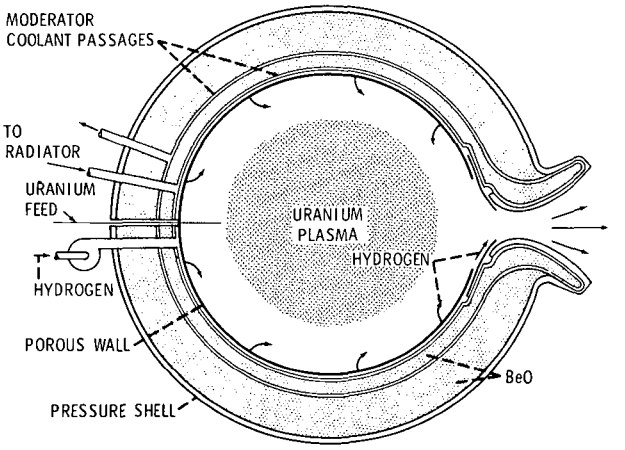

FIG. 2. Open-cycle gas-core concept.

Three requirements determine the characteristics of the system: fuel mass and density to achieve criticality, sufficiently high temperatures to achieve a high specific impulse, and a low rate of fuel loss through the exhaust nozzle, for economic operation. These requirements result in rather rigid boundaries for power and weight. A "best" configuration can, however, not be determined because of trade-offs among the variables. Typically, a coaxial flow plasma reactor for space propulsion operates at 6000 MW power, producing thrust at 4000 sec specific impulse. The cavity diameter is about 4 meters, the pressure ranges from 400 to 600 atm., and the total weight of the system is of the order of 500000 kg figuring present radiator technology. The fissioning plasma temperature is up to 50000°K in the center of the fuel region, decreasing to less than 25000°K at the edge of the fuel. The critical mass is about 40 to 80 kg ^{235}U depending on poison.

The nuclear light bulb engine concept consists of seven modules, such as shown in Fig. 3, contained in a pressure vessel together with a BeO and graphite moderator reflector [7]. In contrast to the coaxial flow system, the nuclear light bulb scheme provides for full containment of the fuel within a transparent internally cooled wall configuration, thereby circumventing the problem of fuel losses through the exhaust. The fissioning plasma is kept away from the transparent walls by a tangentially injected swirl flow of buffer gas, which is recirculated. Some uranium plasma that is entrained in the buffer gas flow is separated out during the recirculation process and is fed back to the fuel region. Thermal radiation from the fissioning plasma penetrates the buffer gas flow and the transparent walls and is intercepted by a flow of seeded hydrogen propellant. Typical data for the nuclear light bulb engine are power: 4600 MW; specific impulse: 1870 sec; weight: 35000 kg; edge-of-the-fuel temperature: 5000°K; and pressure: 500 atm.

Both of these fissioning plasma reactor concepts represent machines of enormous power and stresses. It is not apparent that these schemes can be scaled down significantly because of criticality requirements combined with the need of high temperature operation. However, at significantly decreased temperature, the pressure decreases accordingly as does the power. In such a case, the plasma core reactor operates in a nonequilibrium mode, in which

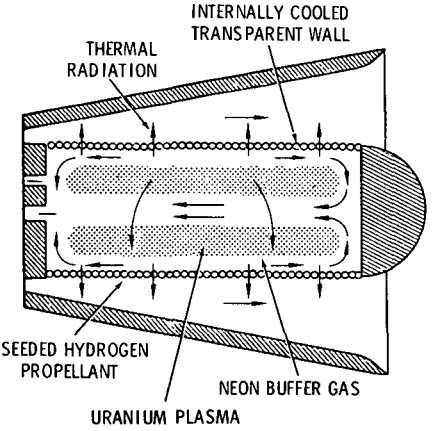

FIG.3. Nuclear light-bulb gas-core concept.

the plasma is optically thin. Extraction of power would most efficiently be effected by laser radiation [8]. In such a self-critical nuclear powered laser system, nuclear energy is directly converted into coherent light by elastic and inelastic collisions of fission fragments with the uranium atoms (and possibly other gas admixtures), Fig. 4. Population inversion is expected to result from the vastly different energies of the fission fragments over most of the lengths of their stopping distances as compared to the energy level of the plasma. In order to maintain the fissionable fuel in a partially ionized gaseous state, one may have to resort to UF_6.

Another fissioning plasma reactor concept is the nuclear piston engine [9]. This engine resembles an Otto-motor as indicated in Fig. 5. During the intake stroke a mixture of enriched UF_6 and helium is drawn into a cylinder that is surrounded by a moderator-reflector. During the compression stroke the density of the gas is increased until criticality is reached. The chain reaction is initiated by an external neutron source. Because of the buildup of power, temperature and pressure are increased in the cylinder and can be extracted as shaft horsepower in the following power stroke. An exhaust stroke ejects the now again subcritical UF_6 and He mixture into a cooling and reprocessing loop.

In Fig. 5 an auxiliary precompression piston is shown which follows the working piston at high compression to provide time for buildup of power and to assure that maximum power is released as the piston passes dead center. Preliminary calculations [10] show that a one cylinder engine requires a minimum volume of 0.23 m^3 and a compression ratio of 1:10. Crankshaft speed of 100 to 500 rev/min and a critical mass of about 3 kg ^{235}U seem to be feasible. Power outputs of several megawatts per cylinder at an efficiency up to 60% seem to be realizable. The main problem to be solved seems to be the handling of the chemically aggressive UF_6. A comprehensive knowledge of thermodynamic properties of UF_6 and UF_6-He mixtures at high temperatures is required. This includes dissociation temperatures and interaction of fission fragments with UF_6.

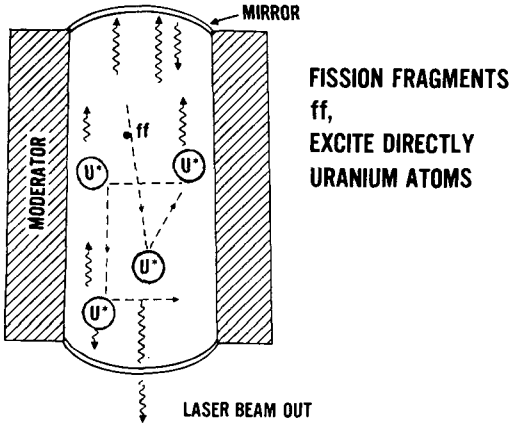

FIG.4. Nuclear pumped laser.

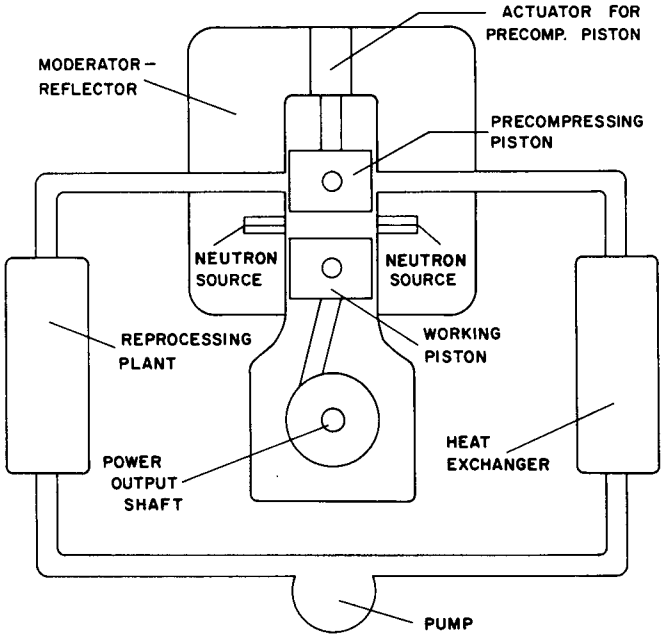

FIG.5. Nuclear piston engine.

POTENTIAL APPLICATIONS

The aforementioned plasma core reactor concepts involve the fissioning plasma as a source of radiation. In contrast to the conditions in a solid nuclear fuel, fission fragments and photons in a plasma have relatively large mean free paths such that the fission energy is not thermalized locally, i.e., in a close proximity of the locus of the fission event. Fission fragments traversing the plasma undergo up to 10^5 collisions with the plasma uranium atoms. As a result of deexcitation and recombination processes and in combination with bremsstrahlung, a broad spectrum of optical radiation is generated, which, depending on density and temperature, can escape from the plasma. A model of possible radiation is depicted in Fig. 6. In the process of energy loss resulting from collisions, the fission fragment energy decays from an original level of 100 MeV to that of the average plasma temperature. A scheme of possible radiation levels is illustrated in the form of a tower with radiative power outlets at various energies. The fissioning plasma is seen as a source of photons at ranges of energy and intensity by orders of magnitude greater than those of any other terrestrial steady state energy source. Possible technological applications of fissioning plasmas more general than are apparent in the previous discussion of plasma core reactor concepts are envisioned by figuring direct uses of such photon fluxes. The complex of desirable relevant investigations may, in a provocative manner, be called "photonics" research.

Radiation in the range of 0.1 to 10 eV is expected to be useful in photochemistry, because molecular bond energies range up to 4 eV in organic matter and up to more than 10 eV for very stable inorganic solids. Intense

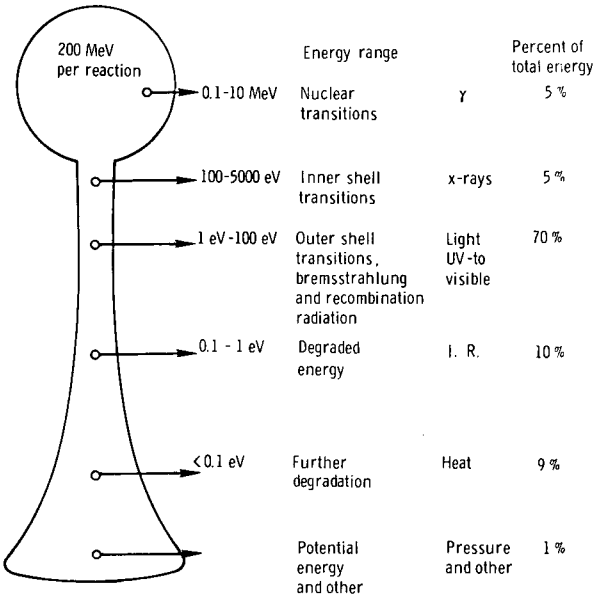

FIG.6. Plasma-core reactor-energy outlets.

4 to 10 eV photon fluxes lead to more rapid chemical reactions through excitation, and may have significance in industrial processing. Powerful radiation in the u.v. spectrum should be useful for photolytic dissociation of water for large scale production of hydrogen, which in present discussions of a forthcoming energy crisis is considered to become a major fuel in the future. Photosynthesis may be approached by using the radiation in the visible spectrum.

The processing of photons themselves may be defined as photophysics, including laser techniques, nonlinear optics, and electro-optics. Current development in these fields bears clear analogies with previous development of electronics. Many technological innovations should be expected from progress in photonics. The optical pumping of lasers by the radiation from a fissioning plasma at high intensities (multiphoton absorption and emission) and at high energy levels and the direct pumping of lasers by fission fragments for the achievement of very high laser power at frequencies up to the x-ray spectrum appear possible.

The aspects and possibilities of photonics are too numerous to recount in this article.

Intensive studies have been conducted concerning the use of thermal radiation of fissioning plasmas for rocket propulsion in space and for magnetohydrodynamic (MHD) power generation. Propulsion capabilities of plasma core nuclear rockets in respect to payload fractions and trip times are calculated [4] for lunar ferry missions, for space-tug applications in cis-lunar space, for manned trips to the nearby planets, and for missions to the major planets. For missions requiring small payloads, such as current automated space probes, the plasma core reactor is too heavy.

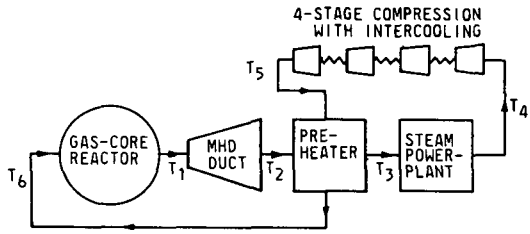

FIG.7. Block design of plasma-core MHD power plant.

Because of its high specific impulse, however, the plasma core rocket is superior to other propulsion systems for manned missions to the nearby planets. For missions deep into space, beyond perhaps Jupiter or Saturn, the projected thermonuclear fusion rocket becomes superior because of its higher specific impulse. In lunar ferry and space tug service, the plasma core propulsion unit would be employed in a reusable fashion, to result in greatly improved economy of cargo transport between earth orbit and the lunar surface. It is presently not contemplated to use plasma core rockets for launch from the earth surface into orbit.

The needs for crew shielding from radiation of fission products present in the reactor cavity and in the exhaust have been investigated [11]. Shielding requirements, depending on fission fragment retention times, have been derived. Only qualitative consideration has been given so far to the effect of fission products deposition in near earth space. This problem warrants more investigation because in the state of ionization such fission products will be trapped by the geomagnetic field and can be deflected back to the atmosphere.

MHD power generation using a plasma core reactor is investigated in [12]. Both the plasma core reactor exhaust and the MHD channel flow are at very high temperatures to yield a large overall efficiency. In addition, at such high temperatures the working gas stream is sufficiently ionized in equilibrium to circumvent nonequilibrium ionization problems that have impeded the development of MHD power generation from solid fuel nuclear reactor energy sources. A schematic of a projected plasma core reactor MHD terrestrial power plant is shown in Fig. 7. Computations show an efficiency of 70%, a reduction of thermal pollution per unit power by factor of 3 to 5 compared with that of contemporary power plants, and a high fuel economy. In addition, such a system appears to be essentially safe because no excess reactivity is in the plasma cavity. The fissile fuel is in continuous recirculation and allows for continuous removal of fission products.

RESEARCH

Confinement

The objective of plasma core reactor fluid mechanics confinement is to isolate the hot gaseous fuel from the cavity walls and, simultaneously, to intercept the thermal radiation from the fissioning plasma in a propellant flow for heating and subsequent expansion. In present plasma core reactor concepts, the nuclear fuel and propellant are injected into the cavity at different locations and are exhausted together from the reactor through a nozzle. For criticality it is necessary that the fuel volume be not less

than 20% of the cavity volume, and for economy it is required that the ratio of the fuel mass flow rate to the propellant mass flow rate, m_F/m_p, be as small as possible. For rocket application, an acceptable level of m_F/m_p depends on the cost to lift the weight into earth orbit. At present this is figured at m_F/m_p = 1:100 to 1:200. For other applications involving closed loop configurations, m_F/m_p does not appear to be a critical parameter.

A series of experimental studies has been conducted [13] to demonstrate the feasibility of fluid mechanics confinement. Air/freon and air/air combinations were used to simulate propellant and fuel flows and were injected into a cavity at greatly different velocities. In earlier experiments, the gas injection was spatially sharply discontinuous at the cavity inlet region, resulting in turbulent boundary layer mixing. Supported by theoretical analysis a method was devised for producing a wide shear layer between the flows with a gradual transition from high to low velocity streaming. As a result, in cold flow simulation, a fuel-to cavity-volume ratio greater than 0.2 was achieved, at m_F/m_p = 70. Hot flow simulation is conducted in relatively small volumes by radiofrequency induction heating, with the indication that the temperature gradient across the boundary layer tends to suppress the formation of eddies and, consequently, results in a better confinement. Increasing size, temperature and density, in order to approach plasma core reactor conditions, requires low frequencies and large power. A 10 to 100 kHz tunable 4 megawatt hot flow research apparatus is under construction.

Radiative Heat Transfer

Most of the power generated by the fissioning plasma inside the cavity of a plasma core reactor is transmitted to the propellant, or working fluid, by optical radiation. Relevant research is consequently concerned with the spectral distribution of radiated power and with the absorption of such radiative power in the propellant. Simultaneously, one has to consider the deposition of energy in structures from all the energy fluxes from the fissioning plasma. In the nuclear light bulb engine concept, the fissioning plasma is confined by a swirl flow buffer gas within transparent fused silica tubing. Because of this additional structural element, radiative heat transfer has been studied with particular care for the nuclear light bulb system.

The total power of the conceptual full scale nuclear light bulb engine is computed to be 4600 MW. Eighty-nine per cent is in the fission fragments and is rapidly converted into optical radiation; the remainder is in neutrons, prompt gamma rays, delayed gamma rays, and beta particles, most of which are deposited in structures and must be carried away by coolants.

The spectral distribution of the radiant heat fluxes from the fissioning plasma was calculated [14] using a one-dimensional neutron transport theory computer code. There is a steep temperature gradient across the boundary region between the fuel volume and the confining swirl flow. The optical radiation will therefore be that of a blackbody one optical depth into the steep temperature gradient, such that the emitted spectrum is that of a blackbody at much higher temperatures than those at the edge of the fuel. Measurements of the absorption coefficient of uranium plasma under similar conditions [15] confirm theoretical predictions. As a result, the radiated power has a large fraction of u.v. radiation at wavelengths less than 0.18 μm, which is the cutoff of the silica tubing. A remedy to this problem is to seed the neon swirl flow with silicon particles, which absorb

the short wavelength radiation. The associated power is, however, not all carried away with the buffer gas flow but can largely be reemitted in longer wavelength radiation.

In experiment, isothermal two-component vortex flow simulation tests were conducted to demonstrate confinement by buffer gas flow within silica tubes. High intensity radiant flux simulation was carried out using a 1.2 MW rf induction heater to heat a vortex stabilized argon plasma up to 11000°K at 19 atm. The radiant flux was at 7.6 kw/cm^2, but that of a full scale engine would be 28 KW/cm^2. Further development of this simulation technique promises to approach plasma core conditions. In addition, the experimental results are quite encouraging for small scale in-core experiments.

At ranges of pressure and thickness of interest, hydrogen and most of the other light gases are optically transparent at temperatures less than about 15000°K. Therefore, propellant seeding with micrometre sized particles has to be applied for absorption of the radiation from the fissioning plasma. Such a process appears to be more a matter of technique than physics, and approaches have been developed that, in experiment, have demonstrated, for example, the heating of a tungsten seeded argon flow up to 4500°K. Propellant exhaust temperatures of plasma core reactors for propulsion must be higher than that, however, so that seed particles will vaporize. The opacity of propellants with vaporized seed materials is under current investigation.

Ballistic Piston Compressor

A ballistic compressor is used to simulate conditions in the nuclear piston engine and to measure the thermodynamic properties of UF_6 under extreme conditions. The behavior of enriched compressed UF_6 under bombardment with fission fragments, neutrons and other nuclear radiation will be explored.

Fig. 8 is a schematic diagram of the ballistic compressor. The apparatus is able to produce a temperature up to 10000°K at a pressure up to 5000 atm. The basic properties of temperature, volume, and pressure are measured and the equation of state for UF_6 is determined. The van der Waals' coefficients, the ratio of specific heats for pure UF_6 and UF_6-He mixtures, and the viscosity for UF_6 have been determined [16]. The results of these measurements show that by choosing optimum mixing ratios of UF_6 and He, values of specific heat ratios as high as 1.47 can be obtained.

For research on the interaction of the compressed $^{235}UF_6$ with fission fragments, the high-pressure part of the ballistic compressors will be inserted in a reactor and exposed to a neutron flux.

Nuclear Pumped Lasers

Research on nuclear pumped lasers has been underway for several years. Two types of experimental configurations have been used. Tubes coated with uranium oxide and filled with laser gas mixtures were exposed to a neutron flux in a reactor. Fission fragments emanating from the coating caused nuclear laser pumping. Another configuration was an uncoated tube filled with laser gas mixtures plus a certain partial pressure of ^3He. When exposed to a neutron flux the ^3He (n,p)T reaction resulted in laser excitation. The results obtained can be grouped in nuclear augmentation and pure nuclear pumping. In the case of nuclear augmentation, the performance of an electrical discharge laser is improved by nuclear effects, in the pure nuclear pumping no electrical energy is used to maintain the laser action.

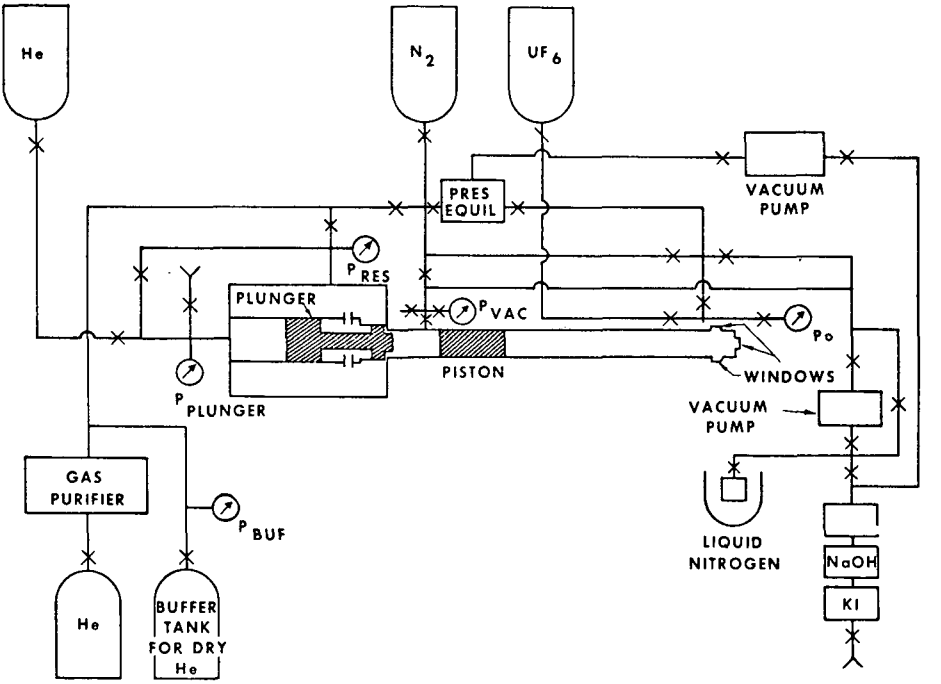

FIG. 8. Ballistic piston device.

Results in both categories are reviewed in [8]. Additional results on pure nuclear pumping are reported in [17], where an argon ion laser cavity without electrodes was employed.

In-core testing of lasers is very meticulous because of the high radiation environment to which the optical components are exposed and the inaccessibility of the laser experiment in the reactor.

Results of this research indicate the possibility of nuclear pumping of lasers. In a broader view they substantiate the concept of a fissioning plasma existing in possible nonequilibrium states.

Criticality

Research on the criticality of low-power (500 W) gaseous core cavity reactors was conducted at the National Reactor Testing Station in Idaho, USA, using enriched gaseous $^{235}UF_6$ [18]. A relatively clean spherical geometry was used and thus could be analyzed by one-dimensional reactor physics codes. The deviations from perfect spherical geometry were experimentally evaluated as being worth less than 0.75 %Δk. The fuel core region was 1.27 m in diameter in a cavity of 1.83 m in diameter and was reflected by 0.91 m of D_2O. Correlation with theory was attempted using S_4 transport theory with 19 energy groups, seven of which were thermal. The absolute multiplication factor was calculated at 1.04, 3 %Δk higher than the corrected experimental value. The worth of the addition of hydrogen for propellant flow simulation was underpredicted by approximately 50%.

Three critical experiments were conducted in an attempt to determine empirically the feasibility of the plasma-core reactor concept. One was without hydrogen propellant and with a 0.005-m Al cavity wall. In the second, 1.1×10^{21} hydrogen atoms/cm^3 of simulated propellant (foamed polystyrene and polyethylene sheets) were added, the critical masses were 8.43 and 12.9 kg, respectively, and the fuel worth was 2.96 %Δk/kg, and 2.02 %Δk/kg, respectively. In the third experiment a 0.008-m stainless steel liner was added on the cavity wall to evaluate the effect of 0.019 mean free path thermal absorber material. The critical mass increased to 29.2 kg, and the fuel worth decreased to 0.44 %Δk/kg.

General conclusions from these and other criticality experiments, also involving cylindrical configurations, accompanied by theoretical analysis, are that a plasma-core reactor must be designed with an absolute minimum of nonessential reactivity penalties, that the effect of a hydrogen propellant flow between the fuel region and the reflector requires serious consideration, and that the ratio of fuel radius to cavity radius be not less than 0.5 in order to obtain criticality at a pressure of less than 1000 atm and at the projected plasma core reactor temperatures.

Instabilities

The nonlinear evolution of unstable sound waves in a fissioning uranium plasma has been calculated [19] using a multiple time-scale asymptotic expansion scheme. A spectrum of standing sound waves in a bounded region of the fissioning plasma was considered, with a constant background thermal neutron flux density. In the wave compressions, the fissioning power density, P_{fiss}, increases because of the increased uranium density, and in the rarefractions P_{fiss} decreases. This leads to a transfer of fission power to the wave. Competing with this effect is thermal electromagnetic radiation, which tends to transport the extra thermal energy out of the wave compressions. Such radiation diffusion disperses the energy accumulation in waves more rapidly for shorter wavelengths. This results in a critical wavelength below which waves are stable and above which they are unstable. The calculations show that nonlinear mode coupling causes an energy flow from the long-wavelength unstable modes to the short-wavelength modes, such that the system stabilizes at defined amplitudes. For plasma-core conditions as assumed in this analysis, this occurs at relative pressure fluctuations of the order of $\delta P/P = 10^{-5}$. In addition, neutronic feedback in the regimes of rarefraction contributes to stabilization. In a first-order approximation, the stability of fissioning plasmas seems to be indicated. However, the analysis needs to be expanded to include gross flow fluctuations and the effects of inhomogenous neutron flux and fuel distributions.

Gaseous Core Reactor Dynamics Studies

An analysis of the dynamics of the coaxial flow plasma-core reactor is presented in [20]. The theoretical model is described by a set of 22 first-order differential equations in 22 unknowns, involving neutron, heat, and mass balances of the system. The fuel region is assumed to remain spherical in shape during all deviations from steady state. Six reactivity feedback mechanisms are taken into account: fuel temperature, propellant temperature, fuel mass, propellant density, fuel cloud radius, and moderator temperature. According to this analysis, at 0.1% positive reactivity insertion the power of the reactor raises first, but rapid increases in propellant density and fuel temperature generate sufficient negative feedback to decrease the excess reactivity, which in turn reduces the power. About 200 msec after the initial perturbation, the propellant density feedback becomes positive and

causes a slow increase in power which continues later in time because of positive feedback from the expansion of the fuel ball. Neither the fuel mass nor the moderator temperature feedback are significant.

The progression of power excursion is less than 10% within 1 sec indicating possibilities of easy control. The system response to larger reactivity insertions is qualitatively the same, but at a step insertion of $1 reactivity, fluctuations become more rapid and larger in amplitude to cause more serious control problems. Whereas the system is relatively insensitive to the rate of fuel inflow, it exhibits strong responses to variations of propellant flow. For example, losses of propellant flow result in an expansion of the fuel region, which is a positive feedback, and in a decrease of the negative reactivity of the propellant layer. Although the corresponding rates of power increase are larger than those of the previously discussed reactivity insertion, the time scale is likewise in seconds.

Similar analysis using a digital computer simulation program has been conducted for the nuclear light bulb concept [21] and shows that such a system can be controlled by the fuel flow rate, regulated by valves that are activated in response to the amount of neutron flux increases and to the rate of such neutron flux increases.

Fissioning Plasma Research Facility

A significant advance in understanding fissioning plasmas is expected to result from investigations conducted in a special research facility. Such a Fissioning Plasma Research Facility is presently projected as a system involving a solid fuel driver reactor particularly designed to produce an unperturbed thermal neutron flux at 10^{15} n/cm^2 sec in a relatively large inside test volume and in interchangeable test section to investigate the various configurations of fissioning plasmas derived from the concepts and schemes presented earlier. A primary objective, however, would be to create a steady state fissioning plasma for basic research, under conditions best suited for comprehensive diagnostics.

A possible fissioning plasma research facility is shown in Fig. 9. The reactor and test section are contained in a pressure vessel for operation at 200 to 300 atm. The top section plus the upper part of the Be reflector and the test section can easily be removed for interchanging experiments. At the bottom, not shown in the figure, are an effluent handling and a cleanup system. Almost all reactivity is contained in the solid fuel. Feedback from the fissioning plasma appears to be negligible and small enough to be overridden by conventional control methods. There appear several tradeoffs resulting from the best choices of fuel elements, coolants, and moderator-reflector materials as to the required power level of the reactor and the affiliated coolant flow capacities. A desirable feature would be the possibility of boosting the neutron flux in pulsed operation up to 10^{16} n/cm^2 sec and higher.

In the depicted scheme, the coaxial flow concept of fissioning plasma confinement is shown in which seeded hydrogen enters a spherical cavity tangentially through an array of slots, while enriched uranium fuel is fed through a central cadmium-shielded pipe system. In the cavity, the uranium undergoes fission, thereby creating a fissioning uranium plasma fireball. The edge of the fuel temperature has to be not less than that of uranium evaporation. A typical temperature profile for an in-core coaxial flow configuration operating at a pressure of 200 atm is shown in Fig. 10. In the central region, the fissioning plasma has a temperature of about 20000°K.

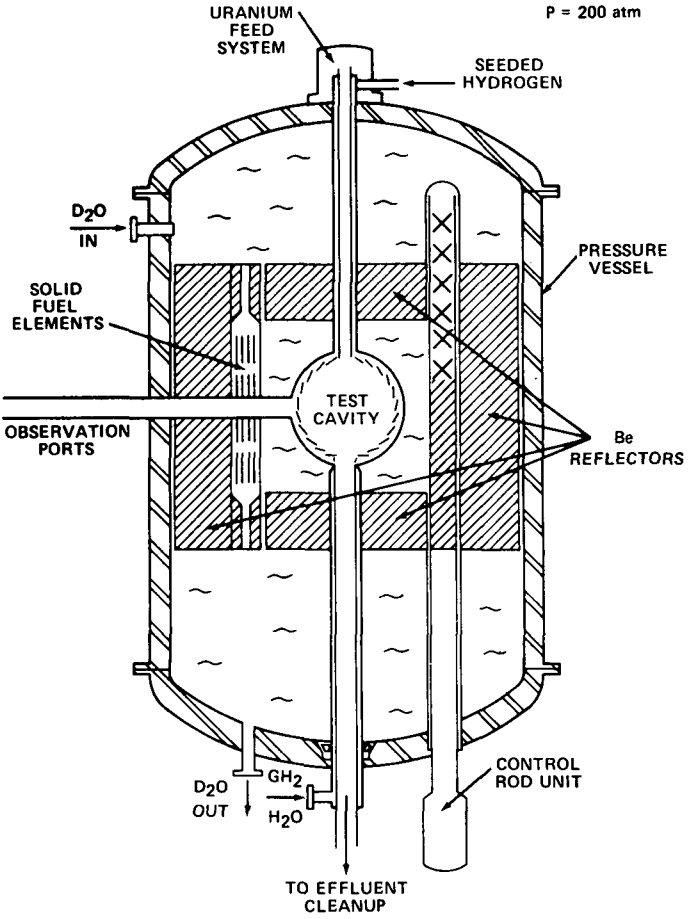

FIG. 9. Possible fissioning plasma research facility.

At the edge of the fuel, the temperature drops to about 5000°K, a temperature at which the uranium is expected not to condense (exact data for the uranium vapor pressure at the edge of the fuel are not yet at hand; however, recent measurements [22] allow for confident estimates and extrapolations). For a pressure of 300 atm and an unperturbed neutron flux of 10^{15} n/cm^2 sec, the fission power is 14 kW/g, and the edge of the fuel temperature is 7400°K. At the wall, the flow has absorbed all radiation such that the cavity wall remains essentially at room temperature. In this case the cavity would appear black for optical observation from the wall region, for diagnostics purposes, an undesirable effect.

Calculations of the total power balance for such a system, with a plasma diameter of about 0.38 m, show that the fission power in the plasma is a few megawatts, while the driver reactor has to operate at 50 to 200 megawatts, depending on reactor design. Appreciable alterations of the power balance should result from variations of the radiant heat flux. When,

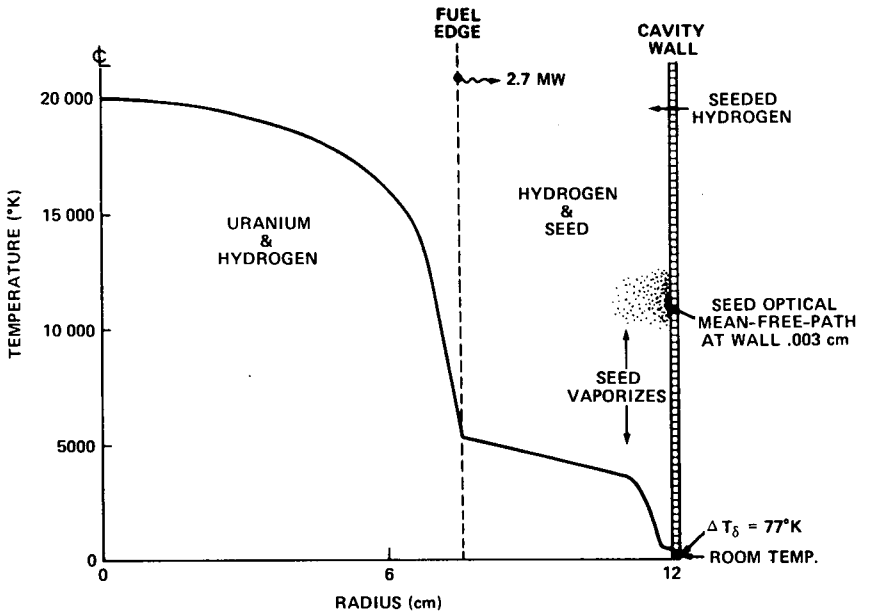

FIG.10. Temperature profile in test cavity.

for example, in the cavity an argon flow is used instead of hydrogen flow, the possibility of increased seed loading results in such greatly enhanced reflection of radiation back to the plasma that plasma conditions are maintained even if fission power drops to 0.5 MW or the temperature may be increased if the power level is maintained. Simultaneously, the pressure may vary to about 50%. An unseeded flow may be used in conjunction with reflecting cavity walls, as to control the power loss from the plasma. It appears thus that a fissioning uranium plasma research facility can be built with some flexibility in respect to power, temperature, and pressure.

Experimental investigations of the overall power balance, and some details of radiation transport and stability, can be carried out by measuring cavity outlet flow temperature, cavity wall temperature, cavity neutron flux, cavity pressure, and the variations thereof depending on perturbations of propellant and fuel flow rates and neutron flux density. It should be possible to deduce various reactivity feedback coefficients from such measurements to supplement analysis of self-critical systems. Diagnostics of the fissioning plasma, for example, the determination of the spectral power distribution of thermal radiation, the spatial temperature distribution in the fissioning plasma, and the possible nonequilibrium states of excitation and ionization does not appear to be impossible, but development of special techniques may be required.

Beyond the purpose of obtaining basic information a fissioning plasma research facility should be used to test functional components of plasma-core reactor applications, such as propulsion in space, MHD power generation, and the nuclear pumping of lasers.

Small Light Bulb Engine

The critical fuel density and the size of a cavity reactor depend on the flow of thermalized neutrons back into the cavity. In the plasma reactor concepts previously discussed, the high-temperature propellant flow in between the fissioning plasma and the moderator-reflector region represents a significant neutron flux barrier. A concept [23] has been forwarded to largely circumvent this problem by dividing the surface area surrounding the fissioning plasma such that only a part of it is propellant flow and the other is an optically reflecting material that is highly transparent for neutrons. Part of the thermal radiation from the fuel region is directly absorbed in an array of segmented propellant flow ducts embedded in the reflecting cavity walls. Another part of the radiation is focused indirectly by reflection from such walls to such ducts. In addition, use is made of the large transparency of cold beryllium for thermal neutrons having energies below 0.006 eV.

A figure of merit for the performance of reflector-moderator materials in cavity reactors is the ratio of the square root of the age of fission neutrons and the thermal neutron mean free path. For example, if this ratio is 7.25, that is, for a graphite moderator at 300°K, the critical density for ^{235}U in a spherical cavity of 1 m radius must be greater than 10^{19} atoms/cm^3. In contrast, a beryllium moderator at 100°K yields 0.47 for this ratio with a resulting critical density of 2 to 4 x 10^{17} atoms/cm^3.

The combined effects of a super-cooled beryllium neutron moderator and drastically reduced propellant flow areas should result in appreciably reduced critical mass for the plasma-core reactor and a low operational power. The cold beryllium has to be surrounded by a D_2O reflector to prevent neutron leakage from the system. Analysis was conducted for a spherical geometry using one-dimensional multigroup neutron transport theory calculations. Seventeen neutron energy groups were employed, including five thermal groups of which two were below 0.006 eV. Scattering cross sections were taken from literature or were computed by standard methods. The neutron transport calculations were performed on a computer with the ANISN code. The system involved an argon buffer gas flow for the confinement of the fissioning plasma within the cavity and away from the walls. Results show that moderator temperature is a strong negative reactivity feedback. For example, using ^{233}U, the critical mass is slightly higher than 1 kg at a beryllium temperature of 40°K. It increases to about 2.8 kg at room temperature. The use of ^{235}U instead of ^{233}U results in an increase of the critical mass of about 20%. The presence of hot hydrogen in the discrete propellant channels does not appear to have a large effect on critical mass for the system studied.

Operating power depends largely on the reflectivity of the reflecting surfaces of the cavity, which in the calculations is assumed to be of the order of 0.9. Radiation damage may, however, degrade this quality. With the previously mentioned temperature requirements for the fissioning plasma, the power is calculated to be in the range of 40 to 400 MW. The pressure may vary from 250 to 500 atm, and the weight of the system, including a pressure shell, is in the range of 16000 to 22000 kg. Applications are seen for space propulsion at specific impulse values as large as 1550 sec and for MHD power conversion.

NUCLEAR DATA REQUIREMENTS

The special characteristics of plasma-core reactor schemes pose a number of problems for computing criticality conditions not hitherto encountered in

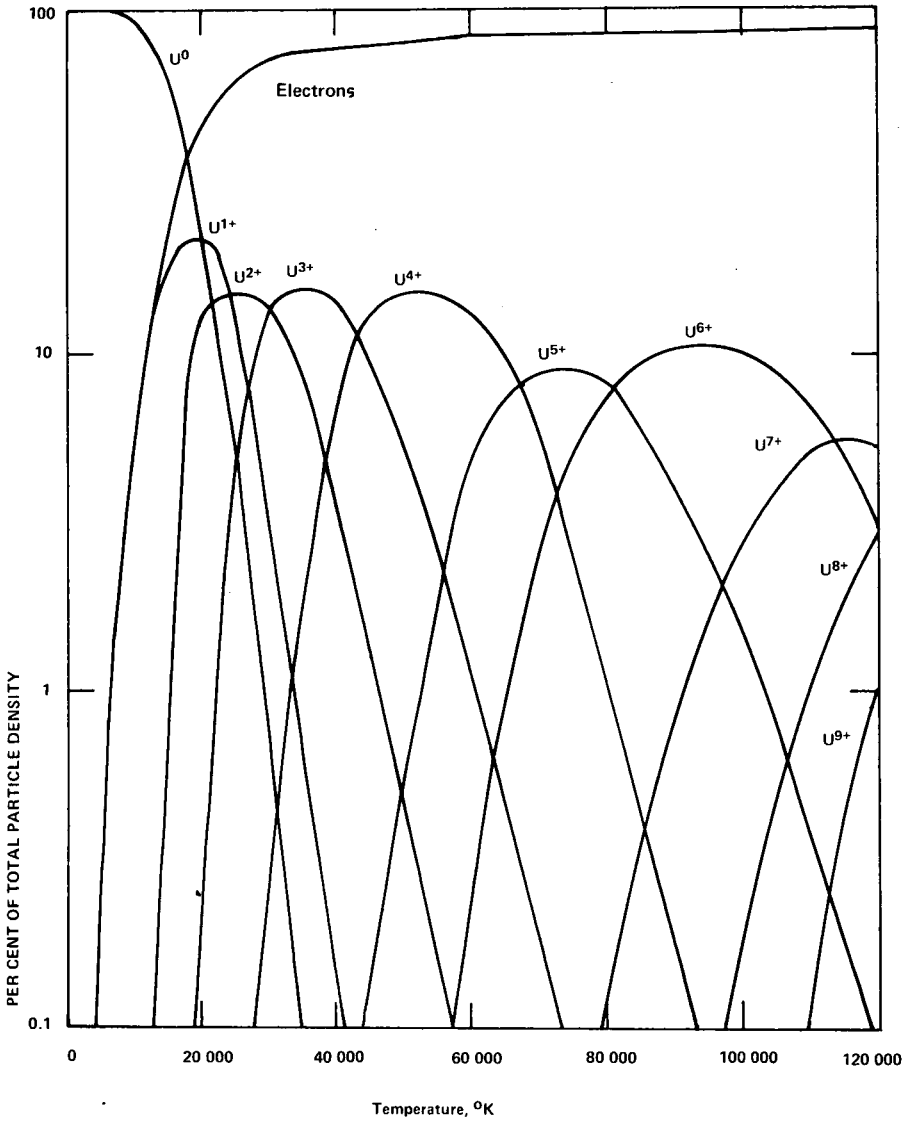

FIG.11. Uranium-plasma composition at pressure of 500 atmospheres [32].

reactor physics calculations. More precise knowledge of certain nuclear data that play a more important role in plasma-core reactor schemes is required. A predominant new aspect is the intimate relationship between plasma physics and reactor physics. For typical plasma-core reactor conditions at 40000°K and 500 atm, more than 70% of the particles that account for this pressure are electrons. About 15% are U IV, as can be seen from Fig. 11. Composition calculations have thus to be included in criticality calculation and their

accuracy is as important as that of the nuclear calculations. Theoretical approximations have been performed [24] and the results incorporated in current plasma-core reactor analysis.

Data required for improved composition calculations are electronic partition functions and the ionization energies for the uranium atom and its ions. The partition functions are not yet known to a desirable degree of precision. Ionization energies are theoretically predicted but not yet verified by experiment.

For precisely predicting the radiant heat transfer, depending on the plasma composition, transition probabilities and atomic energy levels of the uranium atom and its ions have to be known as well as the optical absorption and emission coefficients of the uranium plasma. A weak reactivity feedback exists depending on these quantities, which in turn can alter the power and subsequently the plasma temperature that governs its composition.

Some measurements of emission and absorption coefficients exist [15]. Also transition probabilities for U I and U II are known [25]. However, the transition probabilities for U III and U IV are not known. U III and U IV will be major species in the reactor core.

At a fuel temperature of the order of 40000°K (or about 4 eV), the neutrons see high target velocities; the result is reduced average fission cross sections. This fuel temperature effect does not appear to be critical (owing to the large mass of the uranium nucleus); however, it is not negligible. An increase of the critical mass by less than 5% is typical. Possible bulk motion of the fuel would result in similar effects.

More important is the upscattering of thermal neutrons by the hot hydrogen propellant [26, 27] which in plasma-core reactor schemes is placed between the fuel and the moderator. The reflected and moderated neutrons have to pass through this high-temperature hydrogen region before they can reenter the fuel region. Upscatter of neutron energy results in a substantial penalty for the critical mass requirement. This effect can become so severe that for a given temperature a maximum operating pressure and hydrogen layer thickness exist beyond which criticality cannot be achieved. Because of the strong negative reactivity feedback of the propellant flow, a sudden interruption of this flow can result in a severe reactor power excursion.

In the coaxial flow concept hydrogen migrates into the fuel region by diffusion and eventually will establish and maintain a certain hydrogen partial pressure in the fuel region. The temperature of the hydrogen in the fuel region will be equal to the fuel temperature. Fig. 12 shows the consequences for the 500-atm case assuming a mixing ratio of 1:1. At 40000°K, about 68% of the particles would be electrons, 15% would be protons, 10% would be U IV, 4% U III, and 4% U V. Because of the high temperature of the hydrogen ($\sim$4 eV) a substantial hardening of the neutron spectrum would occur, with a larger penalty for critical mass requirement than due to the hardening caused by the hydrogen in the working fluid. Competing with this effect is the moderation of fission neutrons by this hydrogen component.

In order to compute all these effects properly, a better knowledge of the still unresolved resonances would be helpful. Also computation models for scattering kernels for hydrogen up to 40000°K are required. Doppler coefficients for similar temperatures are also required. New codes for criticality calculations involving the effects of fuel mixing ought to be developed.

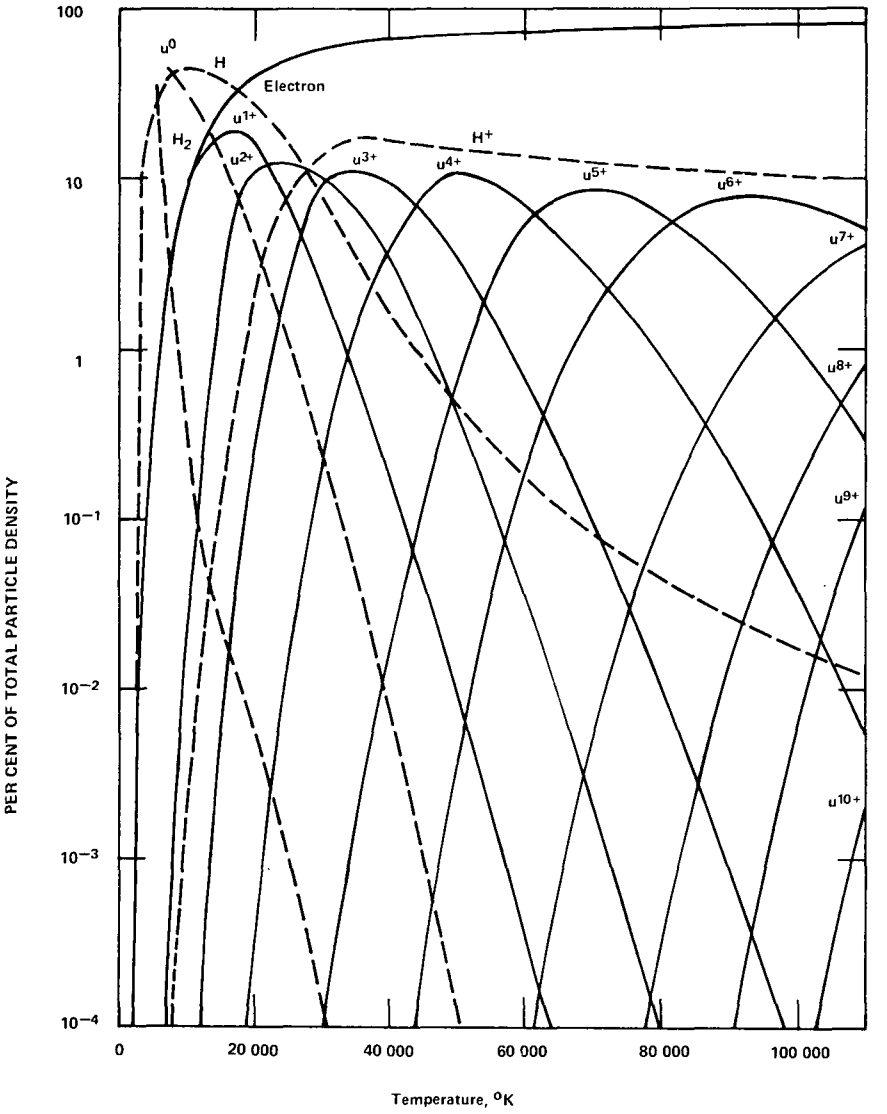

FIG.12. Composition of hydrogen-uranium plasma at pressure of 500 atmospheres. Mixing ratio = 1:1 [32].

In contrast to conditions in solid-core reactors, the fuel in plasma core reactors has such a short residence time in the core that a portion of the delayed neutrons do not contribute to criticality. According to [28] there are more delayed neutrons in the low-energy region than previously assumed. These are competing effects whose relative contributions to criticality computations require more attention. Special analysis of the delayed neutron spectrum appears to be in order.

The radial diffusion coefficient for the plasma core, including modifications due to deviations from true spherical shape of the fuel region, needs to be developed for a good description of the flux distribution. Such deviations of the fuel geometry are caused by the proximity of the nozzle and by dynamic effects in the uranium plasma like eddies and pressure oscillations.

Another major difference between plasma-core reactors and solid fuel reactors is that the interaction mean free path of neutrons is equal to or larger than the core diameter. This has an effect on the moderator design requirements for reactor control. The reactor has to be undermoderated to achieve a negative temperature coefficient.

Gamma ray heating of the moderator and reflector is important in space propulsion and should be calculable to a better precision [29]. Heat loads in the range of 300 to 400 MW will have to be radiated to space. Calculated gamma ray heating may be low by 35% to 60%. Relying on calculations, the gamma ray heat shield of a 6000 MW reactor has heat loads of 100 W/g, which are present day technology maximum, but in actual operation the load might be 150 W/g, which would be intolerable.

The nuclear data required to rectify this situation are neutron capture cross sections and gamma ray spectra emitted by low cross section elements like deuterium, oxygen, and beryllium. Available data are of substantial uncertainty; e.g., the thermal neutron absorption cross sections recommended in BNL-235 for D, Be and O list uncertainties of 20% for D, 10% for Be,and 14% for O.

Radiation damage plays a most important role in the nuclear light bulb concept, in which the radiant (light) energy is transferred from the fissioning plasma to the propellant through fused-silica walls. Experimental studies [30] indicate that around 2150A the absorption coefficient of fused silica can increase substantially by nuclear radiation. Absorption coefficients induced by radiation as high as 14.5 cm^{-1} for the 2100A band were reported. Other research [31] yields more optimistic results (5 cm^{-1}). The consequences of a large absorption coefficient are heating of the transparent wall material of the nuclear light bulb engine and ultimate destruction of this solid interface between fuel region and working fluid. Moderate heating of the fused silica can, however, have a beneficial effect. At about 600°C to 800°C, thermal annealing of color centers takes place. In [30] an equilibrated condition is reported to exist in which the rate of radiation-induced absorption is balanced by annealing such that a steady state good transparency at 0.1 cm^{-1} is maintained.

Reliable information on neutron- and gamma-induced increases of the absorption coefficient of quartz and other transparent materials of potential use as barrier material (e.g., aluminum oxide, beryllium oxide, and titanium oxide) is essential.

For calculations pertaining to problems germane to the plasma-core reactor, numerous codes established for conventional reactors have been used successfully (e.g., DTK, DDK, TDSN, GAM II, GATHER II, QADHD, ANISN, EXTERMINATOR-II, PHROG, and DOT II-W). However, there is a need for development of new codes capable of handling specific problems of the plasma-core reactor, that cannot be handled or can only be handled tortuously by existing codes.

Codes that need to be developed include those for handling extreme temperature and density gradients of the working fluid, the temperature and density gradients of hot uranium and hot hydrogen in the fuel region, and

neutronic feedback resulting from rarefraction waves in the fuel region. Also necessary is a code dealing with the radial motion of the fuel within the cavity. These properties eventually should be described with three-dimensional codes.

For the projected fissioning plasma research facility codes to deal with the coupling of both fuel components, the plasma-core and the solid drives region are required.

CONCLUSION

In the foregoing it has been shown that a need for improvement of nuclear data exists. There is also a need for reactor codes dealing with the specific problems of plasma-core reactors. The most striking feature of this new technology however is the intimate interrelationship between reactor physics and plasma physics, which calls for more precise knowledge of plasma data that have a strong effect on the nuclear behavior of the system. These plasma data have to be considered in this connection as nuclear data as well.

The following nuclear data and computational codes appear at present significant for plasma-core reactor analysis and design:

(1) Neutron fission cross sections at low energies (including resonances)

(2) Kernels for neutron scattering in hot hydrogen (up to 40000°K)

(3) Spectra of delayed neutrons

(4) Neutron capture cross sections and gamma ray spectra of low cross-section elements

(5) Radiation damage of optically transparent material

(6) Codes for criticality calculations involving angular and radial distributions, two and three dimensions, coupled fuel systems, and mixed fuel (U + H)

ACKNOWLEDGMENTS

The authors had the privilege of discussions with most of the authors cited in this article. Particularly valuable advice was obtained from F. C. Schwenk, SNSO, AEC/NASA, R. G. Ragsdale, NASA Lewis Research Center, and M. J. Ohanian, The University of Florida.

REFERENCES

[1] THOM, K., SCHNEIDER, R.T., Symposium on Research on Uranium Plasmas and Their Technological Applications, NASA-SP 236 (1971) (U.S. Government Printing Office).

[2] RAGSDALE, R.G., Second Symposium on Uranium Plasmas: Research and Applications, AIAA, New York (1971).

[3] THOM, K., Review of fission engine concepts, J. Spacecr. Rockets, 9, 9 (1972).

[4] RAGSDALE, R., WILLIS, E.A., Gas-Core Rocket Reactors - A new Look, NASA TM X-67823 (1971).

[5] CLEMENT, J.D., WILLIAMS, J.R., Gas core reactor technology, Reactor Technol. 13 3 (1970).

[6] SCHWENK, F.C., FRANKLIN, C.E., "Comparison of closed and open cycle systems", Symposium on Research on Uranium Plasmas and Their Technological Applications, NASA SP-236 (1971) (U.S. Government Printing Office).

[7] LATHAM, T.S., Summary of the Performance Characteristics of the Nuclear Light Bulb Engine, AIAA 71-642 (1971).

[8] THOM, K., SCHNEIDER, R.T., Nuclear pumped gas lasers, AIAA J. 10 4 (1972).

[9] SCHNEIDER, R.T., OHANIAN, M.J., Patent disclosure to NASA, 1970.

[10] KYLSTRA, C.D., COOPER, J.L., MILLER, B.E., "UF_6 plasma engine", Second Symposium on Uranium Plasmas: Research and Applications, AIAA, New York (1971).

[11] MASSER, C.C., Radiation hazard from backflow of fission fragments from the plume of a gas core nuclear rocket, Symposium on Research on Uranium Plasmas and Their Technological Applications, NASA SP-236 (1971) (U.S. Government Printing Office).

[12] WILLIAMS, R.J., KIRBY, K.D., Exploratory investigation of an electric power plant utilizing a gaseous core reactor with MHD conversion (American Nuclear Society Topical Meeting, Atlantic City, New Jersey, 1972).

[13] BENNETT, J.C., JOHNSON, B.V., Experimental Study of One- and Two-Component Low-Turbulence Confined Coaxial Flows, NASA CR-1851 (1971). (U.S. National Technical Information Service).

[14] RODGERS, R.J., LATHAM, T.S., KRASCELLA, N.L., "Radiant heat transfer calculations for the uranium free containment region of the nuclear light bulb engine", Second Symposium on Uranium Plasmas: Research and Applications, AIAA, New York (1971).

[15] SCHNEIDER, R.T., CAMPBELL, H.D., MACK, J.M., Part I, University of Florida Annual Report, NASA Grant NGL 10-005-089 (1972).

[16] SCHNEIDER, R.T., STERRIT, D.L., LALOS, G.A., Part II, University of Florida Annual Report, NASA Grant NGL 10-005-089 (1972).

[17] WALTERS, R.A., SCHNEIDER, R.T., Part III, University of Florida Annual Report, NASA Grant NGL 10-005-089 (1972).

[18] LOFTHOUSE, J.H., KUNZE, J.F., Spherical Gas Core Reactor Critical Experiment, NASA CR-72781 (1971). (U.S. National Technical Information Service).

[19] TIDMAN, D.A., "Instabilities in uranium plasmas", Second Symposium on Uranium Plasmas: Research and Applications, AIAA, New York (1971).

[20] TURNER, K.H., A Dynamic Model of Coaxial Flow Gaseous Core Nuclear Rocket System, Ph. D. thesis, Georgia Institute of Technology (1971).

[21] LATHAM, T.S., BAUER, H.E., RODGERS, R.J., "Investigation of nuclear light bulb startup and engine dynamics", Symposium on Research on Uranium Plasmas and Their Technological Applications, NASA SP-236 (1971) (U.S. Government Printing Office).

[22] RANDOL, A.G., III, SCHNEIDER, R.T., KYLSTRA, C.D., "Boiling point of uranium", Symposium on Research on Uranium Plasmas and Their Technological Applications, NASA SP-236 (1971) (U.S. Government Printing Office).

[23] LATHAM, T.S., RODGERS, R.J., "Small nuclear light bulb engines with cold beryllium reflectors", AIAA/SAE Joint Propulsion Specialist Conference (New Orleans, Louisiana, 1972) 8.

[24] PARKS, D.E., LANE, G., STEWARD, J.C., PEYTON, S., Optical Constants of Uranium Plasma, NASA CR-72348 (1968). (U.S. National Technical Information Service).

[25] CORLISS, C.H., BOZMAN, W.R., NBS Monograph 53 (1962). (U.S. Government Printing Office).

[26] WHITMARSH, J.C., Neutronic Analysis of Open-Cycle High-Impulse Gas-Core Reactor Concept, NASA TMX-2534 (1972).

[27] KUNZE, J.F., LOFTHOUSE, J.H., SHAFFER, C.J., Hydrogen effect on a demonstration test for open-cycle gas core reactors, American Nuclear Society Trans. 15 (1972).

[28] SLOAN, W.R., WOODRUFF, G.L., Delayed-neutron energy spectra, American Nuclear Society Trans. 15 (1972) 942.

[29] LOFTHOUSE, J.H., KUNZE, J.F., YOUNG, R.C., YOUNG, T.E., Gamma heating in gas core rocket reflector, American Nuclear Soceity Trans. 15 1 (1972) 7.

[30] SMITH, A.B., Optical Absorption in Fused Silica at Elevated Temperatures During 1.5 MeV Electron Irradiation, NASA TN D-6840 (1972) (U.S. National Technical Information Service).

[31] PALMA, G.E., Measurement of the UV and VUV Transmission of Optical Materials During High-Energy Electron Irradiation, United Aircraft Research Laboratories Report L-990929-3 (1972).

[32] ATWATER, H.F., Fissioning Uranium Plasma for Rocket Propulsion, Ph. D. dissertation, University of Florida, Gainesville, Florida (1968).

DISCUSSION

F. RUSTICHELLI: What is the situation as regards the energy loss of fission fragments at high temperature? Do you need stopping power data relating to this condition and have you done any experiments on the subject?

K. THOM: At high temperature the uranium target gas is partially ionized. Large Coulomb collision cross-sections should result in a different stopping power than in a neutral target gas. Important data are those on the number of inelastic collisions of the fission fragments with the gas atoms and ions versus the number of eleastic collisions, and the fractional

energy losses involved in such collisions. In addition, one would like to know the partition among states of ionization and excitation during the slowing down of the fission fragments. Ionization produces free electrons whose presence in the fissioning plasma can add appreciably to the total pressure of the system. The result could be an unacceptable increase in pressure and size of a plasma core reactor, i.e. from the point of view of achieving criticality. The effect of excitation from fission fragment interactions is related to electromagnetic radiation at discrete energy levels from the plasma. Since the fission fragment energy is very much larger than the average energy of the plasma, the excitation from fission fragments collisions may result in a population inversion of excited states and could thus be exploited for the direct conversion of fission fragments energies into coherent light, that is into work! I think this is the most important characteristic of fissioning plasmas.

We have conducted some experiments in which light was, in fact, produced by the fission fragment interactions with gas targets. In one case, in which the target gas was argon, even lasing was achieved.

Much more detailed data are needed, however. For example, in a high-Z target gas, such as a uranium plasma, fission fragment collision may lead to bound-bound electron transitions at energy levels ranging from a few eV up to many keV. Knowledge of the distribution of such transitions would have far-reaching consequences.

NUCLEAR DATA REQUIREMENTS FOR FUSION-FISSION (HYBRID) REACTORS

W.C. WOLKENHAUER, B.R. LEONARD, Jr.
Pacific Northwest Laboratories,
Richland, Wash.,
United States of America

Abstract

NUCLEAR DATA REQUIREMENTS FOR FUSION-FISSION (HYBRID) REACTORS.

The hybrid (fusion-fission) reactor is a class of power-producing reactors which has fusion and fission reactors as its extreme members. There are two distinctly different hybrid systems: Hybrid systems which optimize on the breeding of fissile fuel for fission reactors or tritium for D-T fusion reactors, and hybrid systems which optimize on power production and utilization of energy resources. Studies have been made on the hybrid since 1953 with the most recent work being carried out by the authors at Battelle-Northwest.

The justification for pursuing the study of hybrid systems is the possibility of achieving a power plant which couples the short doubling times associated with the fusion reactor to the high power densities associated with the fission reactor while at the same time being able to extract power from the available uranium reserves from an essentially safe (subcritical) fission lattice.

The design and optimization of hybrid plants places new restraints on the required nuclear data needed for the analysis. All of the usual reactions considered in fission reactor design must be covered by the data but now the requirement is for good data from thermal to 14 MeV. In addition, n,2n and n,3n reactions which are not normally significant in fission reactor design become important. Finally, of course, plasma physics data and reaction cross-sections of structural materials for 14 MeV neutrons are required.

Most hybrid concepts are based upon the nuclear reactions of ^{238}U with 14-MeV neutrons. There are several neutron-producing reactions which take place. They include n,2n, n,3n, and fission reactions. While data on these reactions are currently available in the Evaluated Nuclear Data File (ENDF/B-III) of the USAEC, credible optimization of hybrid concepts to determine the potential advantages cannot be made without significant reevaluation of the ^{238}U data file. Hybrid systems can also be designed based on the thorium fuel cycle. In this regard, the same type of data is required here but the available data are inferior to those of ^{238}U.

The fusion-fission or hybrid reactor is generally defined as a Controlled Thermonuclear Reactor (CTR) with a fissionable blanket surrounding it. The concept is based upon the neutron multiplication properties of heavy isotopes in a 14 MeV (deuterium-tritium plasma) neutron flux and the large energy release of neutron-induced fission relative to neutron capture events or neutron absorption in lithium.[1]

While a number of different concepts have been proposed, there appear to be only two distinct classes of hybrid systems. One of these is a system which is optimized for the breeding of fissile fuel for fission reactors. The other concept is the hybrid which is optimized for power production directly.[2]

Because the hybrid concept is not well understood, we will first review the historical development of the concept. We will then develop some of the principle characteristics of the system. After this, a specific hybrid design will be given. A review of the analytical techniques applied to this specific design will then allow for development of the nuclear data required for hybrid reactor design.

1. History of Development

The first suggestion for a hybrid device was apparently made in the early 1950's.[3] A United States patent application describing a hybrid was filed in 1957.[4] A British patent application was filed by Lawson, et al., in 1958 on a similar idea.[5] The first applicable measurements in the open literature appear to have been made by Weale et al., in 1961.[6] The most systematic study of a hybrid concept which is optimized for the breeding of fissile fuel for fission reactors was carried out by Lidsky [7]. Some of the most recent work on a hybrid concept optimized for power production has been carried out by Lee[8] and by the authors [1]. There does not however, seem to have been a consistent development program on the hybrid concept even though it was first introduced some twenty years ago. Interest in the hybrid may grow, however, when the emphasis in fusion reactor development changes from technical feasibility to engineering and economic feasibility.

2. The Characteristics of a Hybrid Reactor

A hybrid reactor can be defined as a CTR with a blanket which contains fissile or fertile material. Such a machine, independent of the market it is optimized for, has certain characteristics which identify its potential advantages or disadvantages as a source of power.

First of all, consider the characteristics of the plasma of the fusion device employed in the hybrid machine. It is often mentioned that a possible advantage of the hybrid is that, as a result of its energy multiplication possibilities, it can be used with a sub-Lawson plasma which would allow for early exploitation of the fusion reaction. The plasma characteristics of a hybrid can be more accurately defined by pointing out that a hybrid must operate with a sub-Lawson plasma [9]. This conclusion results from engineering considerations. A certain level of energy or neutron multiplication must take place in the blanket in order to breed fuel for the device. For a given blanket design, there is a limit on blanket power density and a limit on fissile fuel depletion rate which can be determined for that design. For known materials, these blanket limits result in plasma limits which are, in all cases surveyed, substantially sub-Lawson in nature. Therefore, the first characteristic of a hybrid machine is that it must operate with a sub-Lawson plasma. This result implies that exotic refractory metals for structure and fuel cladding are not required for hybrid reactors.

Another characteristic of hybrid machines is the nature of the energy multiplication. For a hybrid design with a fissile blanket, the rate of multiplication, or the number of fissions per fusion event, (N) can be estimated by the equation [10]:

$$N = \frac{1}{\nu} \frac{k_{eff}}{1 - k_{eff}}$$

where k_{eff} is the neutron balance of the fissile blanket as usually defined by standard reactor physics terminology and ν is the average number of neutrons per fission. From this equation, one can see that very large energy multiplication is possible with values of $k_{eff} < 1$. Therefore, hybrid fertile/fissile blankets will be subcritical. For a deuterium-tritium plasma, the energy multiplication (Q) of a given design can be estimated by the equation:

$$Q = \frac{200 + 17}{17} \times \frac{1}{\nu} \times \frac{k_{eff}}{1 - k_{eff}}$$

assuming an average fission energy release of 200 MeV, an average fusion energy release of 17 MeV, and also assuming that all of the fusion energy is available to the energy balance. Therefore, a second characteristic of the hybrid machine can be developed. Not only does the hybrid operate with a sub-Lawson plasma, but also it employs a subcritical blanket assembly. The design goal, of course, is to develop a machine with the above characteristics which has a favorable output to input energy balance. For a wide range of interesting designs, this appears to be possible.

A third general characteristic of hybrid machines relates to the breeding function of the blanket. If the blanket, in its role as a fissile breeder, utilizes depleted or natural uranium as a fertile material, the bred fissile material is found to be almost all Pu-239 [1]. This is due to two phenomena. The hybrid reactor, if it utilizes the deuterium-tritium reaction, gives off 14 MeV neutrons as a primary source. The value of $\alpha(\alpha = \sigma_c/\sigma_f)$ approaches zero for Pu-239 above 2 MeV or so [11]. Therefore, the buildup of higher plutonium isotopes in a hybrid reactor can be greatly retarded depending upon the specific concept.

The blanket of a hybrid reactor must perform several functions. It must produce neutron and energy multiplication by means of n, 2n, n,3n, and fission reactions. It must breed sufficient tritium in order to maintain the fusion reaction. It must breed sufficient fissile material in order to maintain the fission reaction. Finally, it may be used to extract energy by means of neutron moderation and cooling. The two breeding functions and the energy multiplication functions compete with each other for neutrons. One of the difficulties the authors observed in their work was how to suppress breeding in order to obtain the desired energy multiplication. In the case of a graphite moderated blanket, the authors found that it was difficult to achieve all of the requirements with a natural uranium fueled blanket. However, it was found that a slightly enriched blanket provided breakeven breeding for both reactions and a overall system output to input energy ratio in excess of 25. In this case, the results indicate that an additional slight enrichment would provide remarkably short breeding doubling times which are a feature of fusion machines. Thus, two more design characteristics emerge. They are that hybrid blankets would probably operate with a slight fissile enrichment and that the hybrid could have the breeding doubling times characteristic of fusion reactors [9].

Finally, one can list some of the environmental characteristics of hybrid reactors. The hybrid reactor will contain large quantities of tritium and fission products. A properly designed hybrid will, contrary to fission reactors, contain only small amounts of nonfissile actinides. The tritium inventory will be small compared to that of a fusion reactor. Thus, the ash from a hybrid reactor will be similar to that found in a fully enriched fission reactor. If one assumes that the relatively cheap uranium currently available will be exploited for power, if one recognizes the unique problems associated with tritium containment, and if one recognizes that the higher actinides represent a major waste disposal problem associated with fission reactors, then it appears that the hybrid reactor might have attractive environmental features [2].

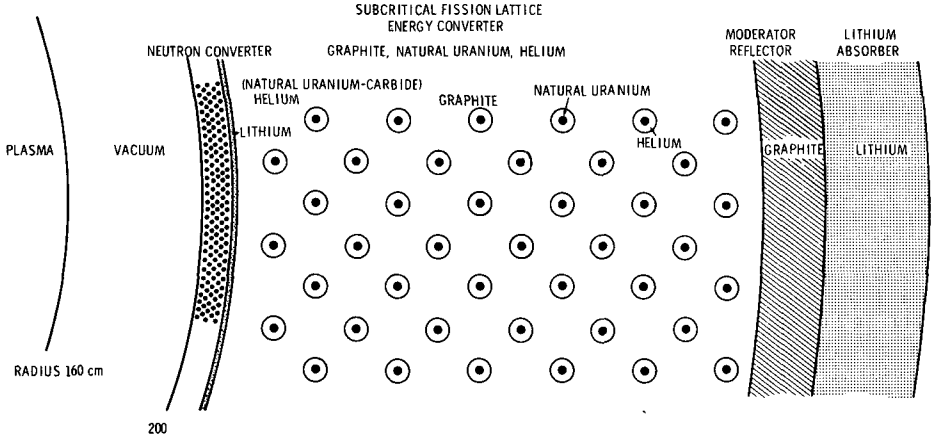

FIG. 1. Hybrid blanket.

In summary then, a hybrid reactor is a sub-Lawson plasma coupled to a subcritical fissile/fertile assembly which can produce a positive energy balance. Some of the potential advantages of the device are:

- Has high energy densities associated with fission reactors.
- Has short doubling times associated with fusion reactors.
- Breeds relatively pure fissile material.
- Allows for exploitation of uranium reserves in subcritical assemblies.
- Eliminates major radioactive hazards associated with pure fusion and pure fission devices.
- Development can progress to fruition based on known technology.

The authors have been studying a specific hybrid design based upon the neutron convertor concept [1,2,9,10]. One variation of this approach is shown in Figure 1.

The fissile blanket is divided into a number of regions. These include the neutron convertor, the energy convertor, a reflector, and an outer absorber for tritium production. The design shown here is helium cooled and, at least for the energy convertor, is generally consistent with gas cooled fission lattice design.

The neutron convertor concept is of general interest here as it serves several purposes [1]. It provides direct utilization of the U-238 fission energy by 14 MeV neutron induced fission and multiplication of the 14 MeV neutron source through fission, n,2n, and n,3n reactions. The absorption in the convertor of these secondary neutrons and neutrons leaking back from the fission lattice result in further fast neutron fissions and neutron capture in U-238 to produce Pu-239. The lithium

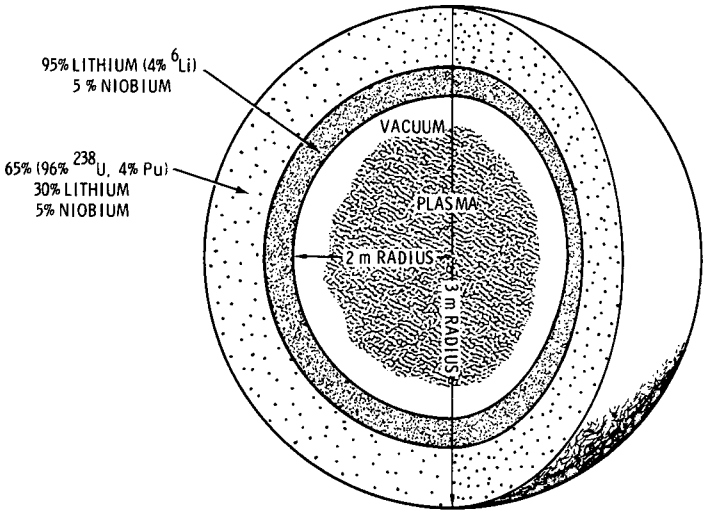

FIG.2. Spherical hybrid.

serves to breed tritium, inhibit Pu-239 fission and in addition, it decouples neutronically one side of the fission lattice from the other side of the cylinder.

The design shown here is, in general, typical of the studies being carried out on this concept. The hybrid is usually studied somewhat independently of a specific plasma device. However, it is usually based on a deuterium-tritium plasma due to the high potential neutron multiplication of the energetic (14 MeV) neutrons. In addition, a specific blanket design will, as mentioned previously, dictate the desired plasma conditions.

In contrast to this system, Figure 2 shows a spherical design developed by Lee [8]. In principle, this system operates much in the manner of that shown in Figure 1. This type of hybrid probably places more stringent requirements on nuclear data than the coupled convertor-thermal system. In order to analyze this system, one must have continuous data describing the slowing down of neutrons from 14 MeV to thermal energies throughout the system and for all isotopes of the system.

3. The Analysis of a Hybrid

In order to develop the minimum nuclear data requirements needed to analyze some of these previously described systems, a method of performing an analysis of hybrids will be described. A flow chart of the approach is shown in Figure 3. Other analytical techniques which have been used include Monte Carlo analysis and other computer codes which solve the neutron transport equation directly.

The analysis of a hybrid begins with a microscopic data library for the required isotopes with data being available for the required reactions over an energy range from 14 MeV to thermal. The minimum data requirements

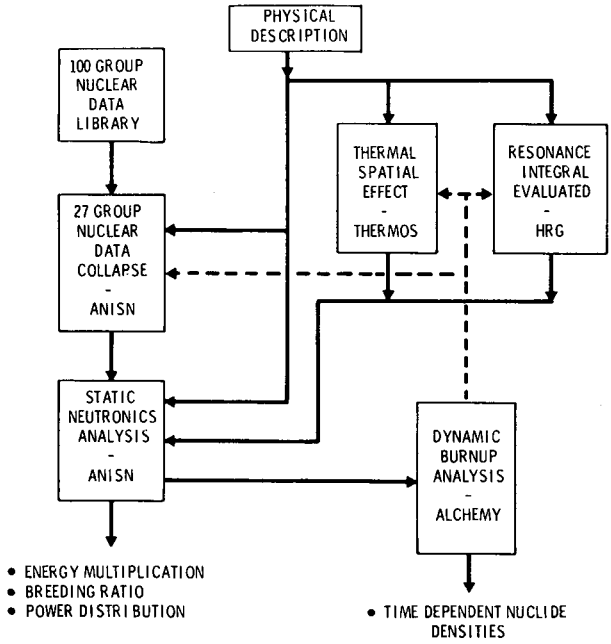

FIG. 3. An analysis model for hybrid reactors.

are summarized in Figures 7 and 8. In Figure 2, to save computer space, the data are collapsed by means of the neutron transport code ANISN[12] to a 27 energy group set. The THERMOS[13] and HRG[14] codes are used to calculate thermal spatial and resonance absorption spatial effects. These effects are particularly strong with respect to U-238 and Pu-240. The ANISN code is used to calculate the static neutron flux distribution. The ALCHEMY[15] code is used to calculate the burnup rate of the various isotopes. Dashed lines are used to indicate the need for periodic spectral updating of the data as the analysis proceeds to higher neutron exposure. The computer codes used here are generally available and have been used in the analysis of similar devices [16].

4. The Important Neutron Reactions

The major neutronic reactions involved in the analysis of hybrid blankets are the neutron producing reactions and the fuel breeding reactions. These reactions are reviewed below along with some of the other relevant reactions. The results are then summarized to develop the minimum nuclear data needs for hybrid analysis.

4.1 The Neutron Producing Reactions

The neutron producing reactions for U-238 are shown in Figure 4 as a function of energy. They are the n,2n, n,3n and fission reactions and are shown here as a function of energy. The curves were obtained from version 3 of ENDF/B[17] which is the Evaluated Nuclear Data File of the

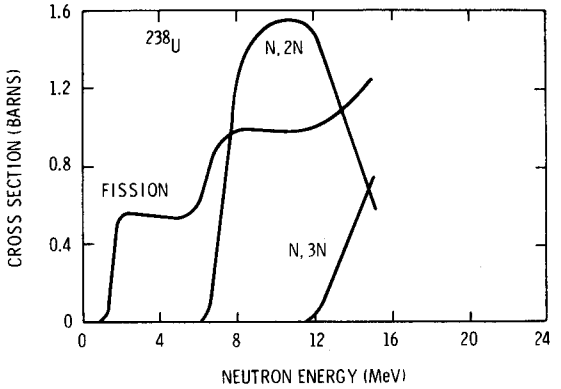

FIG.4. Neutron-producing reactions of ^{238}U.

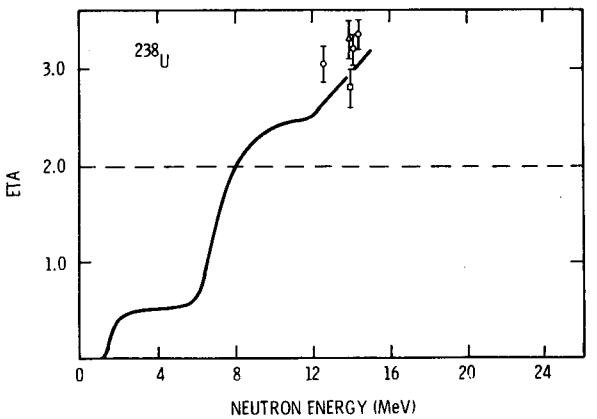

FIG.5. Neutrons produced per neutron absorbed for ^{238}U.

USAEC. If these data are weighted by the specific reaction neutron production, a continuous curve of the number of neutrons produced per neutron absorbed can be developed. This composite curve is shown in Figure 5 [9]. If this curve is compared to experimental points, as shown on Figure 5, one can see that the file may not be a best estimate at 14 MeV. While Figure 5 demonstrates the high neutron multiplication which can be obtained from 14 MeV neutrons impinging upon a fissile/fertile assembly, it also indicates some inadequacy in the available data for neutron producing reactions. This inadequacy may, however, be due to inadequacies in the library data file description as opposed to inadequacies in the data themselves. In any case, the nuclear data needs for hybrid reactor analysis not only include specific requirements for nuclear data for energies far above the fission spectrum, but also, there are requirements for data on nuclear reactors often not given emphasis in fission reactors. (i.e., n,2n, n,3n).

4.2 The Fuel Breeding Reactions

There are several neutron absorbing fuel breeding reactions associated with the hybrid reactor. Assuming a fusion device based upon the deuterium-tritium reaction, tritium must be bred at a breakeven rate by neutron absorption in lithium. The specific reactions are [18]:

$$^{6}Li_{3} + {}^{1}n_{o} \rightarrow {}^{3}H_{1} + {}^{4}He_{2}$$

$$^{7}Li_{3} + {}^{1}n_{o} \rightarrow {}^{3}H_{1} + {}^{4}He_{2} + {}^{1}n_{o}$$

The ^{6}Li reaction is a thermal neutron reaction and is exothermic. The $^{7}Li_{3}$ reaction is an epithermal neutron reaction and is endothermic. In a typical hybrid blanket, about one-third of the tritium is bred by the $^{7}Li_{3}$ reaction and the rest by the thermal reaction.

Plutonium may be bred in a hybrid blanket to supply fissile fuel either for energy production in the machine itself or in a separate reactor. The pertinent reactions are:

$$^{238}U + {}^{1}n_{o} \rightarrow {}^{239}U \xrightarrow{\beta^-} {}^{239}Np \xrightarrow{\beta^-} {}^{239}Pu$$

If the fissile fuel is bred by means of neutron absorption in thorium such that ^{233}U is bred as the fissile fuel, the reactions are [19]:

$$^{232}Th + {}^{1}n_{o} \rightarrow {}^{233}Th \xrightarrow{\beta^-} {}^{233}Pa \xrightarrow{\beta^-} {}^{233}U$$

The neutron absorption cross sections for the isotopes involved in these reactions must be known over the energy range from 14 MeV to thermal.

4.3 Other Relevant Neutron Reactions

In a hybrid blanket, energy is extracted by moderation of the energetic neutrons. Typical moderating materials include graphite and beryllium. Structural materials which may be used for the vacuum wall and the blanket structure would be alloys of stainless steel in contrast to the exotic metals such as niobium, and vanadium which have been proposed for "pure" fusion reactors. Therefore, inelastic and elastic scattering data are required for these materials, along with neutron absorption data, for the whole energy range from 14 MeV to thermal energies. Supplementary information on the neutron damage characteristics of these materials as a function of energy may also be required.

5. Minimum Data Requirements

The data requirements for hybrid analysis are dictated, in part, by the complexity of the transmutation chain for fertile materials in a

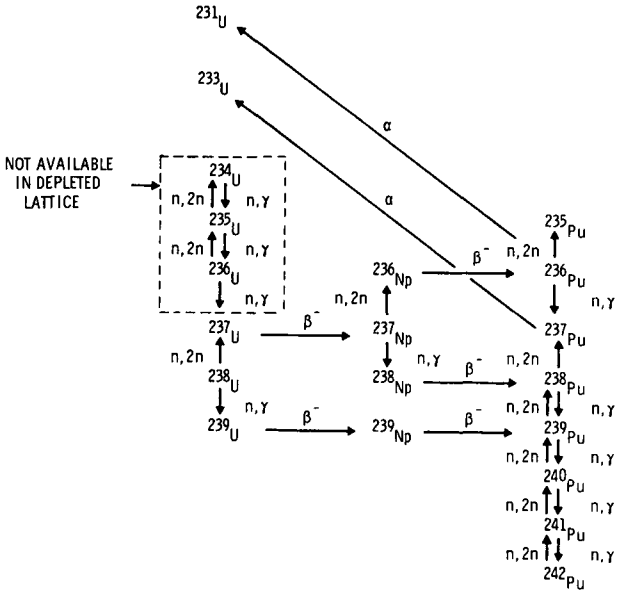

FIG.6. The uranium transmutation chain in a hybrid blanket.

14 MeV neutron flux. Figure 6 displays the uranium transmutation chain in a high energy flux. One can see that such reactions as n,2n, which have a threshold in the range of 8 MeV, become important in the hybrid system.

The nuclear data needs for the analysis of a hybrid lattice such as shown in Figure 1 and which uses the uranium burnup chain shown in Figure 6 can be developed for the analysis model shown in Figure 3. Such a compilation of requirements is shown in Figure 7.

The data needs are so extensive in part, because the uranium burnup and transmutation equations have been shown to be quite complex. In addition, one needs to analyze fusion fuel breeding, neutron moderation, neutron production, and possible damage effects. The sum of these requirements leads to the extensive compilation listed in this figure.

Figure 7 itemizes the data requirements for the analytical model. However, there are additional specific data requirements over certain energy ranges which are of special concern. These requirements are shown in Figure 8.

While plasma reaction data is not of great importance directly in hybrid design, there will eventually develop a need for accurately controlling the degree to which the plasma lacks being a breakeven plasma. For fusion reactors, the emphasis has been placed upon knowing the charged-particle reaction cross section in the range of 10-100 keV. Because hybrid reactors require a degraded plasma, accurate data must be obtained in the range of a few keV. Because the cross section is very small and changing rapidly in this energy region, accurate data in this range might be difficult to obtain [20].

REACTION / ISOTOPE	n, γ	n, α	n, P	n, 2n	n, 3n	n, n'α	FISSION	ν	ELASTIC SCATTER	INELASTIC SCATTER
$^{4}He_{2}$	X			X					X	X
$^{6}Li_{3}$		X		X					X	X
$^{7}Li_{3}$				X		X			X	X
^{12}C	X	X							X	X
^{16}O									X	X
Fe	X		X	X						
^{234}U	X									
^{235}U	X	X		X			X	X		
^{236}U	X			X						
^{238}U	X			X	X		X	X		
^{237}Np	X			X						
^{236}Pu	X			X						
^{237}Pu		X								
^{238}Pu	X			X						
^{239}Pu	X			X			X	X		
^{240}Pu	X			X						
^{241}Pu	X			X			X	X		
^{242}Pu				X						

FIG. 7. Minimum data requirements for hybrid design.

ISOTOPE	REACTION	ENERGY RANGE	COMMENT
^{239}Pu	FISSION	10-15MeV	INTERACTION OF 14MeV AND DEGRADED NEUTRONS WITH ^{232}U, ^{238}U, AND ^{239}Pu LEAD TO NEED FOR IMPROVED DATA
^{238}U AND ^{232}Th	ν	8-15MeV	
	n, 2n	THERMAL-15MeV	
	n, 3n	THERMAL-15MeV	
	INELASTIC SCATTER	8-14MeV	
	RESONANCE CAPTURE	THERMAL- 1MeV	IMPORTANT FARTHER OUT IN THE BLANKET
Fe	CAPTURE	THERMAL- 2MeV	STAINLESS STEEL IS LIKELY HYBRID STRUCTURAL MATERIAL.
	n, 2n	THERMAL-14MeV	
	n, 3n	THERMAL-14MeV	
	ELASTIC SCATTER	THERMAL-14MeV	
	INELASTIC SCATTER	THERMAL-14MeV	
FISSION NEUTRON SPECTRA		4-15MeV	THIS IS NEEDED TO CALCULATE SPECTRA NEAR THE VACUUM WALL.

FIG. 8. Specific data which need improved measurement.

6. Summary

At present, the nuclear data used in hybrid design are found, for the most part, in ENDF/B[17] and other similar data libraries. They are, however, all lacking in some of the required reactions either because it has not been evaluated or because it has not been measured. Immediate requirements are for improved measurements of the minimum indicated reactions as shown in Figure 8 for the indicated energy range. Beyond the basic measurements, the data must be evaluated by data evaluation experts, and just as importantly, it must be placed upon the available nuclear data files.

7. References

[1] LEONARD, B. R., Jr., and WOLKENHAUER, W. C., Fusion-fission hybrids: A subcritical thermal fission lattice for a DT fusion reactor, presented at a conference on Technology of Controlled Thermonuclear Fusion Experiments and the Engineering Aspects of Fusion Reactors, University of Texas, Austin, Texas, (November 1972).

[2] LEONARD, B. R., Jr., and WOLKENHAUER, W. C., Fusion-Fission (Hybrid) Systems, USAEC Report, BNWL-B-162, Pacific Northwest Laboratories, (Feb. 1972).

[3] POWELL, F., Proposal for a Driven Thermonuclear Reactor, USAEC Report, LWS-24920 (revised), (October 1953).

[4] BARRETT, L. G., A Fusion-Fission Reactor, KAPL, Report M-LOB-14, (June 1957).

[5] LAWSON, J. D., THONEMANN, P. C., POOLE, M. J., and TAIT, J. H., Patent Specification 830, 255, United Kingdom Patent, complete specification filed January 15, 1958.

[6] WEALE, J. W., GOODFELLOW, N., MCTAGGERT, M. H., and MOLLENDER, M. L., Measurements of the reaction rate distribution produced by a source of 14 MeV neutrons at the centre of a uranium metal pile, J. Nucl. Energy, A/B, 14, (1961) 91.

[7] LIDSKY, L. M, Fission-fusion symbiosis: General considerations and a specific example, Nuclear Fusion Reactors Conf. (September 1969) UKAEA, Culham Laboratory, Abingdon, Berks.

[8] LEE, J. D., Subcritical fast fission blanket, Thermonuclear Reactor Memorandum 20, LRL (Nov. 1970).

[9] LEONARD, B. R., Jr., Fusion-fission hybrid systems; a presentation prepared for the staff of the USAEC, Div. of Controlled Thermonuclear Research, BNWL-B-216 (July 1972).

[10] WOLKENHAUER, W. C., Editor, The Pacific Northwest Laboratory Annual Controlled Thermonuclear Reactor Technology Report - 1971, BNWL-1604, (July 1971).

[11] Neutron Cross Sections, BNL-325, Second Edition, Supp. 2, (Feb. 1965)

[12] ENGLE, W. W., Jr, A User's Manual for ANISN, a One-Dimensional Discrete Ordinates Transport Code with Anisotropic Scattering, K-1693, (March 1967)

[13] SKEEN, D. R. and PAGE, L. J., THERMOS/BATTELLE: The Battelle Version of the THERMOS Code, BNWL-516, (September 1967).

[14] CARTER, J. L., HRG-3: A Code for Calculating the Slowing Down Spectrum in the P-1 or B-1 Approximation, BNWL-1432 (June 1970).

[15] DUANE, B. H., Time-Variant Isotopic Transmutation, GE-HL Program ALCHEMY, HW-80020, (December 1963)

[16] ABDOR, M , and MAYNARD, C. W., Computational Techniques for Neutronics and Photonics Calculations for Fusion Reactor Blankets and Magnet Shields, FDM3, Nucl. Engng. Report, University of Wisconsin, Madison, Wisconsin, (June 1972)

[17] HONECK, H. C., ENDF/B, Specifications for an Evaluated Nuclear Data File for Reactor Applications, BNWL-50066, USAEC (1966).

[18] STEINER, D., The nuclear performance of fusion reactor blankets, Nucl Applications & Tech. Vol 9, (July 1970).

[19] GLASSTONE, S., and SESONSKE, A., Nuclear Reactor Engineering, D. Van Nostrand Company, Inc., (1967).

[20] GLASSTONE, S., and LOVBERG, R. H., Controlled Thermonuclear Reactions, D. Van Nostrand Company, Inc., Princeton, N. J., (1960).

DISCUSSION

A.M. WEINBERG: How far sub-Lawson is the plasma?

W.C. WOLKENHAUER: For the device considered by the authors, the design called for an $n\tau$ of 3.5×10^{13} and an ion temperature of 10 keV. Thus the device operates one decade below the Lawson condition and, in addition, represents a level of technology which will be achieved shortly.

J.J. SCHMIDT: Do you see any need for nuclear data which are not available from present-day compilations and evaluations such as ENDF/B but knowledge of which is critical and decisive for the success of your present design studies or those for the near future, considering that the hybrid reactor concept (e.g. the fusion reactor) will probably not be realized and find practical application before, say, the year 2000?

W.C. WOLKENHAUER: First of all, the available data, as shown in Fig. 5 of our paper, are not adequate for hybrid design. In a typical ENDF/B file, one finds a maximal point at 14 MeV and quite a few points below 2 MeV. The important range from 14 MeV to 2 MeV is often approximated by a theoretical model.

Current predictions state that a competitive fusion reactor may be available by the year 2000. However, the technology for building the hybrid, if not yet in hand, should be available shortly. If fission power proves to be cheaper than fusion power, the hybrid will allow for exploitation of fissile reserves at comparable power densities in subcritical arrays while retaining the short doubling times of fusion reactors.

NUCLEAR DATA REQUIREMENTS IN THE DESIGN OF THE BIFOLD NUCLEAR POWER SOURCE

W.F. STUBBINS, R.A. WOLFE
University of Cincinnati, Cincinnati, Ohio
and
Mound Laboratory, Monsanto Research Corporation,
Miamisburg, Ohio,
United States of America

Abstract

NUCLEAR DATA REQUIREMENTS IN THE DESIGN OF THE BIFOLD NUCLEAR POWER SOURCE.

The BIFOLD Nuclear Power Source joins SNAP isotopic heat source and SNAP reactor technology to provide reliable uninterruptable base power which is augmented during periods of high-demand power by operation in a critical reactor mode. Plutonium-238 is an alpha-emitting heat source material which has been shown to be able to form a small critical system. The design of the reactor aspects with production-grade ^{238}Pu (80% ^{238}Pu, 16% ^{239}Pu, and 4% other plutonium isotopes) requires estimates of three unmeasured basic nuclear properties: one, the fast-neutron spectrum from the fission of ^{238}Pu; two, the average number of neutrons per fission as a function of neutron energy groups; and three, the delayed-neutron fraction in ^{238}Pu fission. Estimates based upon fission systematics give unconfirmed values of parameters which directly affect the critical size and control parameters. BIFOLD is a small, compact power source using heat pipes with thermoelectric or other energy-converting components operating in an isothermal state at its base power of 11 kWt to 200 kWt or more to meet demand power needs. The split core of BIFOLD permits all operational tests to be completed economically with zero-power reactor operation which avoids induced radioactivity in components and the build-up of fission-fragment inventory. Variations in and ranges of final design parameters owing to uncertainties in nuclear data, plans for the resolution of uncertainties and the economic impact of inadequate nuclear data sources are presented.

Introduction

The possibility of the joint use of isotopic heat source material as a reactor fuel was recognized because of measurements made to access the criticality hazards of processing, storing and using Plutonium-238, (1, 2). Thus, a new and versatile power source concept arose directly in the process of seeking new and reliable nuclear data.

The concept is called BIFOLD since it produces power by two distinctly different means, radioactive decay and nuclear fission, in the same device. BIFOLD is believed to be unique in the annals of energy souces because of this feature. It is described elsewhere, (3, 4, 5).

In recent years legions of diverse applications have been proposed and are being considered for both isotopic and reactor Systems for Nuclear Auxiliary Power (SNAP) in space, under the seas and on land. Nearly all the applications are characterized by short periods of high power demands and extended periods of quiescent operation with a tenth or less of the demand level. BIFOLD provides an uninterruptable base power from radioactive decay capable of meeting needs of normal operation

and functions. The base power is augmented during high demand power periods by operation in a critical reactor mode as a fission energy source.

In fashioning a practical power source from the concept of dual use of isotopic heat source material, ^{238}Plutonium, only proven technology is used in as innovative manner as possible. BIFOLD is a compact power source with a number of important advantages and can match a wide range of mission requirements. The design of the prototypic BIFOLD power source involves thermal and nuclear considerations which interact strongly to determine the parameters. For example, the heat removal rate establishes the size of the heat removal penetrations which in turn govern the core density. The latter sets the critical size and the power density. The thermal conductivity requirements of the fuel governs the possible fuel form and configurations, and the size and number of heat removal penetrations. The iterative process finds the optimum design for the power range to match the mission. A strongly governing parameter is the temperature required or desired for the conversion system to provide electrical energy from the thermal energy.

Gas-controlled heat pipes (6) provide heat removal from the core for both the quiescent base power from radioactive decay and the augumented power from reactor operation. Heat pipes give several important advantages in the form and performance of BIFOLD. Heat pipes are most effective in heat removal and require the smallest heat removal penetrations which yield the greatest density, and thus, the smallest core. They have two other advantages, one is the absence of the need for power to pump a heat transfer fluid. The pumping power in many SNAP devices is the major consumer of the energy released. The second advantage is the possibility of operating BIFOLD in an isothermal mode from the base power to its maximum demand power level.

In accord with our conservative position of using proven technology we chose thermoelectric elements with modest temperatures as the electrical conversion devices. Analyses show that electrical conversion systems such as Rankine and Brayton cycles are fully adaptable to BIFOLD and thermonics are not excluded. In the prototype of BIFOLD a design constraint is that the fuel PuO2 should remain well below its melting temperature if one or more heat removal elements fail. This constraint was chosen to avoid considerations which might be used to challenge the feasibility of BIFOLD. The prototype of BIFOLD is illustrated by a wooden model in Figure 1 and its characteristics are tabulated in Table I.

Nuclear Design of BIFOLD

The nuclear fuel of BIFOLD is production grade Plutonium-238 which is 80% ^{238}Pu, 16% ^{239}Pu and 4% other plutonium isotopes. The composition is given in Table II. It is important to note that the prototypic design is applicable to a fast reactor with less or no isotopic heat source material, ^{238}Pu, and fueled with ^{239}Pu or other isotopes fissioning in a fast neutron flux. In the reducing the ^{238}Pu the base power is diminished or surren-

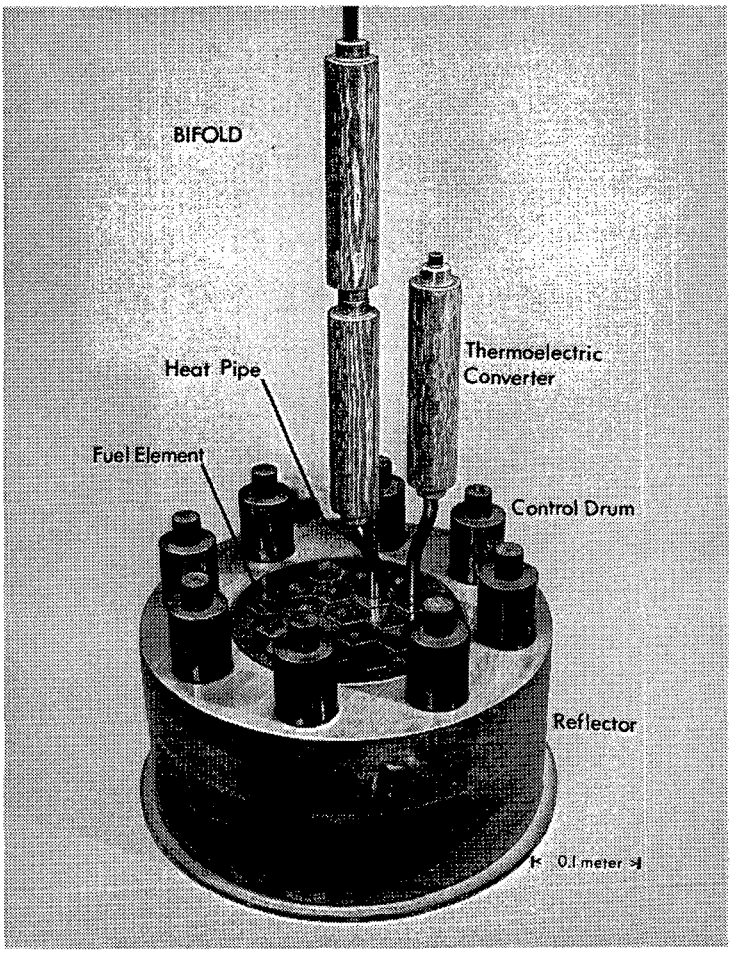

FIG. 1. BIFOLD device.

dered but the fast reactor features are unchanged. The uninterruptable base power can be set at any value less than the maximum for production grade ^{238}Pu by diluting the isotopic mixture or, preferably, by using production grade ^{238}Pu in some of the fuel elements and none in others.

The nuclear design involves two aspects. One is the change in the fuel owing to the alpha decay of ^{238}Pu and the build-up of $^{234}Uranium$. This requires the continual removal of heat and results in the continual change in the composition of the fuel. The half life of ^{238}Pu is 87.8 $\pm$ 0.02 years (7) and produces 0.56 watts per gram of heat by alpha decay. It has been widely

TABLE I. CHARACTERISTICS OF THE BIFOLD SOURCE

General Performance Parameters		
- Power Range	Isotopic Mode	10 Kwt 0.6 Kwe
	Fast Reactor Mode	Up to 150 - 200 Kwt 9 to 12 Kwe
- Application Environment	Space, Terrestrial, Under Sea	
- Lifetime	5 to 25 years	
- Conversion System	Thermoelectric	
- Energy Transfer System	Heat pipes	
- Nuclear Fuel	Plutonium (80% ^{238}Pu)	
BIFOLD Prototype (Reference) Design Parameters		
- Fuel Form	PMC Plutonia-Molybdenum Cermet (PMC)	
- Critical Mass	27.5 Kg (PuO_2) 33.4 Kg (PMC)	
- Nuclear Fuel Element	19 each Hexagonal 3.8 cm Horizontal Width 16 cm in length	
- Thermal Conductivity	0.094 watts/cm^{o}C	
- Melting Temperature of Fuel	2400^{o}C	
- Melting Temperature of Tantalum Cladding	3000^{o}C	
- Maximum Temperature in Fuel Element at		
9.5 Kwt	680^{o}C	
100 Kwt	1100^{o}C	
150 Kwt	1300^{o}C	
200 Kwt	1530^{o}C	

TABLE I. (cont.)

- Heat Pipe:	
Diameter	1.27 Cm
Fluid	Potassium or sodium (K or Na)
Operating Temperature	640°C
- Reflector:	
Material	^{238}U or W
Thickness	9.1 Cm
Control	Rotating Drum
- Size:	
Diameter including Reflector	38 Cm
Height including Reflector	36 Cm
- Approximate Weight	400 Kg
Thermoelectric Element:	
Material	Lead Telluride (PbTe)
Type	Tubular Design
Temperature	
Hot Junction	640°C
Cold Junction	300°C

used as a heat source material because of its relatively high specific heat and its quite low radiation of gammas. A gram of ^{238}Pu produces a gamma dose rate of 0.64 Rads per hour at 1 meter in air. The spontaneous fission half life of ^{238}Pu is $(4.77 \pm 0.14) \times 10^{10}$ years (8) and with almost three neutrons per fission yields 3×10^3 neutrons per second per gram. Additional neutrons come from the alpha-neutron reaction with Oxygen-18 when plutonium is in the form of an oxide, (9). Prior to operation in the reactor mode BIFOLD has both gamma and neutron radiation intensities less than 10^{-6} as a reactor producing the same base power. Between intermittent reactor operation at demand power BIFOLD has significantly lower radiation than a reactor providing the base power.

The change in the fuel composition by the alpha decay of ^{238}Pu does not reduce the excess reactivity as the half life of ^{238}Pu. This is so because the daughter, ^{234}U has a reasonable fast fission cross section, (10). The change in total fissile atoms is shown in Figure 2. The effects of fuel burn-up at a constant power level of 100 kwt is included.

TABLE II. TYPICAL PuO_2 FUEL COMPOSITION USED IN HEAT SOURCES

1. Typical Composition, PuO_2

   a. Oxygen 11.8 wt. %

   b. Plutonium 88.2 wt. %

Isotope	Concentration (Wt. %)
^{236}Pu	0.00012
^{238}Pu	80.2
^{239}Pu	15.9
^{240}Pu	3.022
^{241}Pu	0.643
^{242}Pu	0.132

c. Actinide Impurities	Concentration (Wt. %)
^{241}Am	0.0033
^{237}Np	0.130
^{234}U	0.140 increases at the rate of decay of ^{238}Pu

The total of other isotopic impurities including ^{231}Pa, ^{232}Th, ^{233}U, ^{235}U, ^{236}U, and ^{227}Ac does not exceed 1 wt.% of the fuel.

The second nuclear aspect is that of fast reactor design. The confirmation that ^{238}Pu could form a fast critical system was obtained by replacing an equal amount of ^{239}Pu by 10 grams of ^{238}Pu in a spherical metal ^{239}Pu critical reactor, (1). The criticality worth of ^{238}Pu is nearly the same as ^{239}Pu in the neutron spectrum characteristic of the metal ^{239}Pu reactor. With a thick heavy metal reflector the critical mass of a sphere of metal ^{238}Pu is estimated to be as little as 7.8 kilograms, (11, 12, 13), and it may be even less.

The fission cross section for ^{238}Pu was obtained the Persimmon nuclear test (14) and in earlier measurements (15) from a few eV to 3 MeV. The thermal fission cross section is 18 barns and the thermal capture cross section is 489 barns (16).

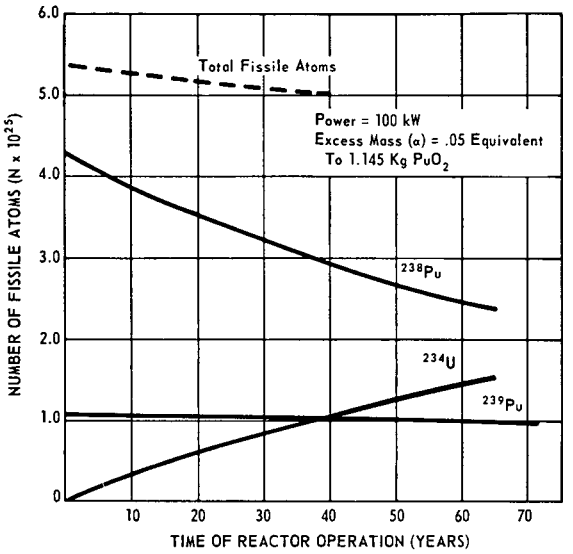

FIG.2. Change in fuel composition within BIFOLD core during reactor mode operation.

The large thermal capture-to-fission ratio makes ^{238}Pu safe from a criticality standpoint in a fully moderated neutron flux. Several neutron multiplication experiments with heat source elements support this conclusion (17, 18). The capture and scattering cross sections for ^{238}Pu have not been systematically reported. The best data are the results of calculations based on the optical model (19).

The absence of data for ^{238}Pu makes it necessary to make some simple, but very questionable, assumptions. One assumes that the unknown cross sections are in magnitude and behavior similar to those of related near nuclei. With the exception of fission cross sections the behavior of elastic, inelastic and capture cross sections is probably reasonably predictable for neutrons above a few hundred kilovolts and are generally small.

The absence of reliable nuclear data for the principle isotope in BIFOLD and equal uncertainties for other isotopes demand a pragmatic design technique. Thus, for the prototype of BIFOLD we use a three group reactor calculation and the homogenization of the core. The 3-energy groups averaged in a "hard" neutron spectrum and the cross sections of the principle isotopes taken from a LASL tabulation for ^{238}Pu (20) and ANL-5800 (21) for the other constituents of the core are shown in Table III. The neutron spectrum arising in the fast fission of production grade ^{238}Pu, is not known. We assume that the spectrum of neutrons from fission of ^{239}Pu is identical to that for production grade ^{238}Pu. As illustrated below different neutron spectra seriously affect the critical mass.

TABLE III. 3-GROUP CROSS-SECTIONAL SET FOR A FAST-NEUTRON SPECTRUM AND USED FOR THE CRITICALITY CALCULATIONS OF BIFOLD SOURCE

ISOTOPE	ENERGY GROUP* (i)	ν	σ_f	$\nu\sigma_f$	σ_c	σ_{tr}	$\sigma_{i\to i+1}$	$\sigma_{i\to i+2}$	$\sigma_{i\to i}$
^{238}Pu	1	3.58	2.47	8.84	0.062	4.38	0.145	0.097	1.61
	2	3.01	2.09	6.29	0.210	6.18	0.280	0.122	3.45
	3	2.93	0.98	2.87	0.272	10.30	0.051	0	9.00
^{239}Pu	1	3.10	1.95	6.05	0.10	4.6	0.45	0.45	----
	2	2.98	1.75	5.21	0.12	6.0	0.50	----	----
	3	2.91	1.80	5.24	0.35	10.0	----	----	----
^{16}O	1	----	----	----	0.020	1.25	0.303	----	0.927
	2	----	----	----	----	3.52	0.578	----	2.925
	3	----	----	----	----	3.59	0.344	----	3.284
Fe	1	----	----	----	0.005	2.00	0.600	0.100	----
	2	----	----	----	0.006	2.13	0.220	----	----
	3	----	----	----	0.006	3.24	----	----	----

*The Energy Spectrum per group was that established for the LASL cross-sectional set in ANL-5800.

i	ENERGY RANGE (Mev)	NEUTRON SPECTUM (x)
1	∞-1.35	0.575
2	1.35-0.4	0.326
3	0.4 -0	0.099

Nevertheless, we judge that there is not great uncertainty in the neutron spectrum so it is not a major source of uncertainty in our criticality calculations but our experience cautions us against discounting it.

As a check of our three-group fast reactor calculations the critical masses for both a bare core and a reflected core were determined with adequate cross sections data and were within five per cent of the experimentally measured critical masses of Jezebel (21) and Popsy (21), two small fast reactors. Configurations applicable to BIFOLD with different arrangements of heat removal penetrations and reflectors were analyzed to evaluate the critical masses. A summary is presented in Table IV.

The critical mass is the governing feature in selecting possible configurations for a practical power source since the fuel costs are so great for the man-made materials. The selection of production grade ^{238}Pu as an oxide in molybdenum as a cermet does not give the smallest critical mass but it allows the demand power maximum to be about twenty times the base power level. The factor of twenty is believed to be significant in that it gives higher power than any proposed isotopic heat source and matches a large number of postulated power needs for space and undersea applications. The use of the cermet PMC, Plutonia-Molybdenum Cermet, is dictated by the thermal conductivity necessary to meet the criterium that the fuel melting temperature would not be reached if one or more of the heat removal elements fail. A smaller core can be achieved with plutonium oxide but the maximum power is limited to 60 kilowatts thermal. A core to provide a maximum of a half of a megawatt as the demand power is about 40 per cent larger than the prototype of BIFOLD specified in Table I.

The selection of the temperature at which the heat energy of BIFOLD is used, in our case the hot side of the thermoelectric converter at 650°K, establishes the temperature at which the thermal energy is accepted by the gas-controlled heat pipes. Heat pipes have the advantage that the heat energy is transferred with a very small thermal gradient, so the temperature in the core is nearly the same as the hot side of the thermoelectric elements. The operation at higher power can be had with the same temperature limits by increasing the diameter of the heat pipes to provide for more heat removal. The core parameters are adjusted to account for the greater penetrations and an increase in the size and critical mass occurs.

The iterative reactor physics calculation results in a critical configuration which is specified by a term called the "buckling". The buckling simultaneously characterizes the composition of the core in terms of nuclear parameters and its geometrical size. The conservation of neutrons is enhanced by the use of a heavy metal jacket completely surrounding the core. This jacket, called the reflector, returns a portion of the neutrons leaking away from a core back to it by neutrons scattering. We have used a reflector thickness to maximize the return of neutrons and minimized the core size and the fuel inventory. The reflector thickness specified in Table I is that

TABLE IV. CRITICALITY REQUIREMENTS OF DIFFERENT FORMS OF THE BIFOLD NUCLEAR POWER SOURCE

Core Configuration	Fuel Form	Critical Buckling	Bare Critical Mass of PuO_2	Critical Mass With Infinite Reflector	Core Dimensions	
					Radius	Height
Solid Sphere	^{239}Pu Metal	0.160 cm^{-2}	15.4 kg	5.45 kg	4.38 cm	
Solid Sphere	$^{238}PuO_2$	0.0918	20.3	9.15	5.94	
Right Cylinder	$^{238}PuO_2$	0.0918	23.2	15.3 (Radial Reflector Only)	5.4	13.4 cm
Cylinderical Iron Block With 1-inch Diameter Fuel Pins	$^{238}PuO_2$	0.0134	190.0			
Cylinderical Iron Block With ½-inch Diameter Fuel Pins	$^{238}PuO_2$	0.0266	93.0			
Hexagonal Fuel Elements With Reflector	$^{238}PuO_2$	0.0660	31.8	17.5	7.13	12.96
Hexagonal Fuel Elements With Reflector	PuO_2 (80% ^{238}Pu) (20% ^{239}Pu)	0.0650	32.4	19.4	7.28	13.26
Hexagonal Fuel Elements With Reflector	PuO_2 as PMC (82.5% PuO_2) (17.5% Mo) (80% ^{238}Pu) (20% ^{239}Pu)	0.0590	45.0	27.5	8.84	15.92

of an infinite reflector, i.e., one for which an additional thickness would not significantly improve the fraction of neutrons returned to the core.

Transformation from base power to more power by the addition of fission power is accomplished by changing the reflector properties by the rotation or insertion of the control elements shown in Figure 1. The system is subcritical with the highest loss rate of neutrons and becomes critical when enough neutrons are conserved to sustain the neutron chain reaction. The control elements act like shutters for neutrons and are one of the ways of effectively controlling a fast reactor which is not readily poisoned, as are thermal reactors, with materials, such as cadmium, which absorb slow neutrons. Removal of fuel or the separation of the core parts are other means of controlling criticality.

Variations in BIFOLD Owing to Uncertain Nuclear Data

The lack of data and uncertainties in data were encountered in the design of the prototypic BIFOLD and required estimates of some quantities and the judgement of the best data to be used in others. In the cases where data uncertainties exist we found it important to evaluate the resulting uncertainties in the parameters of BIFOLD.

Important uncertain parameters are the cross sections for fission, capture and elastic and inelastic scattering; the number of neutrons per fission as a function on neutron energy; and the fraction of delayed neutrons per fission. The fission neutron energy spectrum for the principle isotope in BIFOLD, ^{238}Pu, was assumed to be identical to that for ^{239}Pu and in the absence of any data the same relation was taken for the delayed neutron fraction.

We now outline the uncertainties which we recognize as arising from the present state on nuclear data. As an introduction we wish to point to the initial measurements which gave rise to the BIFOLD concept, (1,2). In planning for the processing of kilogram quantities of ^{238}Pu an assessment of criticality control was made. The lore that even-even heavy nuclei would not have thermal fission cross sections was well established and it was early assumed that ^{238}Pu would be very much like ^{238}U. However, calculations based on ^{238}Uranium cross sections were used to guide planning even for non-thermal systems in absence of data. But there was other information about the expected properties of ^{238}Pu and attention was brought to it. The less direct data were the systematics of fission and particularly the dependence of the neutron induced fission cross section at 3 MeV which as a function of the parameter $Z^{4/3}/A$ increases nearly linearly (10). Thus the ^{238}Pu fast fission cross sections is larger at 3.0 MeV than ^{239}Pu and much larger than that of ^{238}U. Z is the atomic number and A is the mass number of the heavy isotope. Subsequent fission cross section measurements (1,14,15) verified the greater cross section of ^{238}Pu. It is still necessary to use less direct data to proceed with nuclear designs of all but ^{235}U and ^{239}Pu systems.

A. Effect of $\bar{\nu}(E_n)$

The single nuclear parameter that most influences the estimates of the critical mass is the number of neutrons released per fission. This quantity, called $\bar{\nu}$ (nu-bar), depends upon the energy of the neutron causing fission and has been of importance to us in analyses for criticality control of processing, handling, storing and using ^{238}Pu. In the absence of reliable data we estimated $\bar{\nu}(E_n)$ for thermal neutrons and as a function of the neutron energy. We believe that $\bar{\nu}(E)$ is larger than the values in common use and we were encouraged by a measurement of $\bar{\nu}$ (thermal) (22) which matched our prediction.

The quantity, $\bar{\nu}$, for ^{238}Pu has been reported in two separate measurements for neutrons from spontaneous fission (23, 24). Its dependence on neutron energy has not been reported but two estimates have been made and the average of them is in common use. They are

$$\bar{\nu} = 2.88 + 0.097\ E_n \qquad \text{Reference (19)}$$

$$\bar{\nu} = 2.75 + 0.118\ E_n \qquad \text{Reference (25)}$$

and their average is $\bar{\nu} = 2.81 + 0.107\ E_n$. E_n is the neutron energy in MeV.

In seeking the best values of $\bar{\nu}(E_n)$ we considered reports of fission systematics related to nuclear temperature and excitation of fission fragments including a number which relate the neutron release with the fission fragment mass distribution (26,27,28). Our calculations for ^{238}Pu from the analysis of Bondarenko, et al. (26) indicated a higher value for thermal fission and a steeper slope than seen in measurements of other isotopes. We suggest

$$\bar{\nu} = 2.895 + 0.129\ E_n$$

as a better estimate for ^{238}Pu fast neutron fission (29).

Our calculated $\bar{\nu}$ (thermal) = 2.895 is within two per cent of the reported measurement (22). On the basis of this agreement we have used our $\bar{\nu}(E_n)$ in our reactor analysis of BIFOLD, and, indeed, we expect experimental confirmation when the measurements are made. Figure 3 shows our calculation of ^{238}Pu and the reported $\bar{\nu}(E_n)$ for ^{233}U, ^{235}U and ^{239}Pu.

The importance of $\bar{\nu}(E_n)$ in determining the critical size is illustrated by Table V. Table V shows the critical mass for bare spheres of production grade ^{238}Pu as an oxide calculated using $\bar{\nu}(E_n)$ of three different dependences, A) our calculation, b) the $\bar{\nu}(E_n)$ in general use for ^{238}Pu, and C) $\bar{\nu}(E_n)$ for ^{239}Pu. (22). The relation between buckling, B^2, and the dimensions for a bare cylindrical reactor is

$$B^2 = \left(\frac{\pi}{H}\right)^2 + \left(\frac{2.405}{R}\right)^2$$

H is the cylinder height and R its radius.

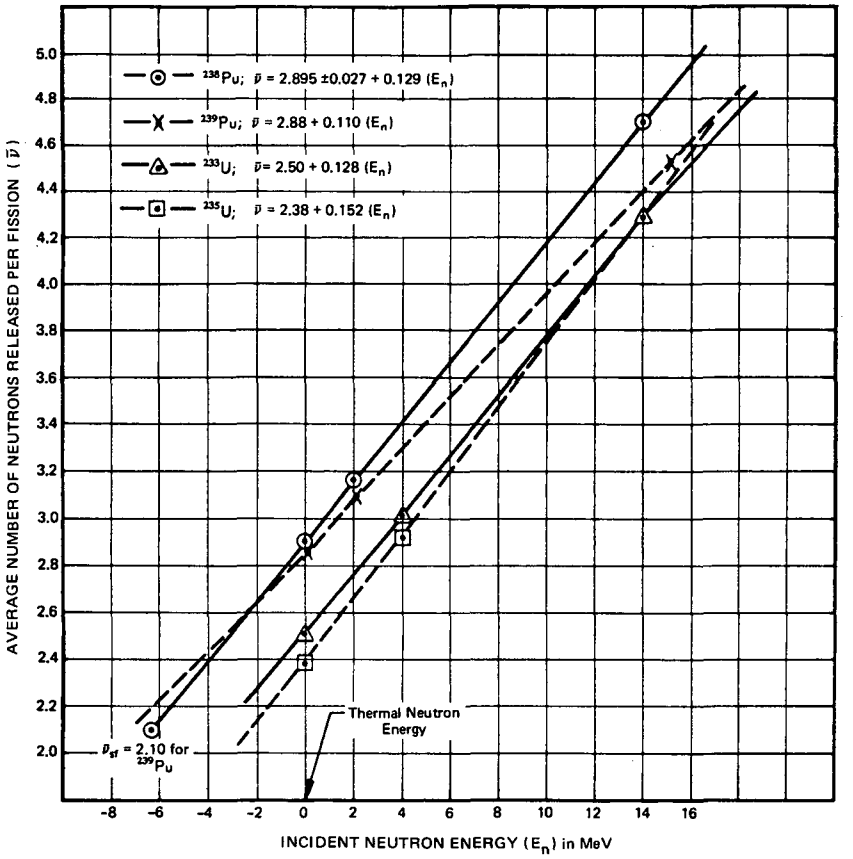

FIG.3. Average neutron number, $\bar{\nu}(E_n)$, as a function of energy of the neutron-inducing fission for ^{238}Pu. (The points shown on the ^{238}Pu curve are based on calculations and not experimental.)

A small decrease in buckling increases the dimensions which add a shell of material in a manner to most effectively increase the critical mass.

B. Effect of Neutron Spectrum

The energy spectrum of prompt neutrons released in the fission of ^{238}Pu has not been reported. Usually the spectrum of ^{239}Pu is used and probably is not far from the spectrum to be found for ^{238}Pu but in the absence of data the knowledge of the effect of spectrum is important. Initially calculations were made of the effect of different spectra in studies for the criticality control of ^{238}Pu by Monte Carlo calculations (13).

TABLE V. EFFECT OF $\nu(E_n)$ ON CRITICAL MASS

A.	$\bar{\nu}(E_n) = 2.895 + 0.129\ E_n$	Our Estimate for ^{238}Pu
B.	$\bar{\nu}(E_n) = 2.810 + 0.107\ E_n$	In General Use for ^{238}Pu
C.	$\bar{\nu}(E_n) = 2.880 + 0.110\ E_n$	Ref. (21) for ^{239}Pu

Neutron Group	Energy Range (MeV)	Spectrum Fraction	Case A	Case B	Case C
				$\nu(E_n)$	
1	∞ - 1.35	0.575	3.58	3.03	3.10
2	1.35 - 0.4	0.326	3.01	2.91	2.98
3	0.4 - 0	0.099	2.93	2.83	2.91
			(Buckling) = B^2		
			0.0488 cm^{-2}	0.0424	0.441
			Bare Critical Mass		
			45.0 Kg	61.0	56.3

In order to evaluate the effect of uncertainties in ^{238}Pu neutron spectra in the parameters of BIFOLD we used three different spectra in the calculation of the critical mass. The spectra are shown in Table VI and are seen to be the ^{239}Pu spectrum in use (21) and two modifications of it which shift the spectrum to lower energies. This shift is seen in Table VI to increase the critical mass and is expected for a predominately ^{238}Pu core since the fission cross section becomes smaller as the neutron energy decreases and the capture cross section increases. We do not believe that the spectra we used in our earlier Monte Carlo calculations and also for this study corresponds to ^{238}Pu but were chosen to provide an evaluation of the effect.

In a recently completed measurement of the neutron energy spectrum in ^{239}Pu photofission near threshold (30) we found that the neutron energy spectrum corresponds to that of thermal neutron fission of ^{239}Pu. We expect to make similar measurements of ^{238}Pu and through them we will gain some insight into its spectrum which can be applied to the specification of BIFOLD.

TABLE VI. EFFECT OF NEUTRON ENERGY SPECTRA ON THE CRITICAL MASS OF BIFOLD

Neutron Energy Group	Energy Range	Fraction of Neutrons in Group (a)		
		χ_A (b)	χ_B	χ_C
1	∞ - 1.35 MeV	0.575	0.538	0.402
2	1.35 - 0.4	0.326	0.333	0.430
3	0.4 - 0	0.099	0.129	0.168
	Buckling	0.0488	0.0471	0.0462
	Critical Mass of PuO_2 (c)	45.0 kg	50.0	51.8
	Per Cent Change		11.1	15.1

(a) The neutron fractions χ_B and χ_C do not correspond to ^{238}Pu which has not been reported. They were only chosen to evaluate spectral effects.

(b) This column corresponds to ^{239}Pu neutron spectrum in use (21).

(c) The critical mass is for a non-reflected minimum right circular cylindrical BIFOLD core.

C. Delayed Neutron Fraction

Another unknown quantity which is fundamental for nuclear design is the fraction of neutrons released in fission which are delayed. The control of a critical reactor depends on the time interval for all the neutrons of one generation to be replaced. The small number of neutrons are delayed because they are released coincident with the beta decay of a neutron rich fission fragment. The neutrons follow the radioactive half life of the fragment. The delayed neutrons make the effective generation time several seconds rather than a few microseconds or less. The control of a fast reactor is governed by the generation time in a crucial way.

The delayed neutron fraction is called beta by reactor physicists. For fast and thermal neutron fission of ^{239}Pu the delayed neutron fraction is $\beta = 0.0026 \pm 0.0002$ (21) and the

average time of retardation is 14.4 seconds (31). We use the data for ^{239}Pu in the absence of data for ^{238}Pu and ^{234}U and recognize it as a possibly serious assumption.

Fabrication and Testing

The BIFOLD source is a compact fast reactor as well as an isotopic heat source. For small compact power sources with the energy conversion devices coupled to the core by heat pipes the entire operational testing and system component verification for reactor operation can be done with auxilliary heating elements rather than reactor operation. For base power all tests are completed with isotopic heat. Analysis of the advantage of compact nuclear space power systems by Breitwieser (32) is applicable to BIFOLD.

By splitting the core into halves the reactor aspects of BIFOLD can be completely investigated with a split-table critical facility. Thus, the induced radioactivity and fission fragment buildup from reactor operation is eliminated since all reactor tests can be at zero power. A second advantage of a split core is the redundancy in BIFOLD as a isotopic heat source for use. Splitting also provides for separation for storage, shipment and handling prior to assembly for mission purposes requiring demand power levels. The criticality control of fabrication and handling are minimized by parts which are so much smaller than the critical configuration. A third advantage is the possibility of using the disassembly of BIFOLD into its halves as an emergency reactor shut-down (scram) precedure.

The advantages of BIFOLD with a split core and external electrical conversion devices which permits all nuclear and non-nuclear testing to be done without the complications of reactor power operation are most clearly realized when the cost of a power system development program is considered. The modular fabrication of fuel elements and heat pipes contributes to the economy. The importance of reliable nuclear data is clearly shown by the cost of design latitudes required to accomodate the ranges of parameters of BIFOLD that arise in data uncertainties at this time.

It is clear from Table V and Table VI that a significant misjudgement in critical size can result from the absence of reliable nuclear data. Were such to occur the redesign of the nuclear power system would yield different fuel element size and loading and general dimensional changes of the entire unit. The economic advantage that we believe BIFOLD has over other energy sources for applications with time varying power demands would be greatly diminished if refabrication would be required.

Plans for the Resolution of Nuclear Data Uncertainties

A. $\bar{\nu}(E_n)$

The measurement of $\bar{\nu}(E)$ is planned by using time-of-flight neutrons to establish E_n and detecting the associated fission event and one or more fission neutrons in coincidence with the fission. A statistical analysis of the single, double

and triple neutron coincidences can yield the average number of neutrons released per fission by the energetic neutron. A neutron fission measurement at the single high energy, for instance E_n = 2.4 MeV with neutrons from the $^2H(^2H,n)^3He$ reaction or E_n = 14.0 MeV from $^3H(^2H,n)^4He$, will provide a point to be associated with the thermal neutron measurement (22) to remove considerable uncertainty in $\bar{\nu}(E_n)$ for the isotopes of interest.

B. Neutron Energy Spectrum

The measurement of the energy spectrum of neutrons released in fission can most readily be done by continuing the photofission measurements completed for ^{239}Pu (30) to ^{238}Pu and ^{234}U, and, indeed, this is planned. The assumption that the spectrum found corresponds to that for neutron induced fission of the isotope will introduce an uncertainty and the dependence of the spectrum on the energy of the fast neutrons inducing fission will not be resolved in photofission studies.

C. Delayed Neutrons

The fraction of neutrons which are delayed and the effective half life can only be measured when a critical assembly of ^{238}Pu is formed. This will be an early quantity sought from the first reactor tests of BIFOLD. However, a study of the fission fragments of the principle isotope can allow an important estimate of beta by identifying the precursors of the delayed neutrons. The radio chemical study of ^{238}Pu fission fragments will be useful.

D. Cross Sections

The measurements of capture, elastic and inelastic scattering cross sections are far more difficult than the measurement of the fission cross section which has such a distinctive signature. Careful experiments will have to seek reliable data.

Conclusions and Summary

BIFOLD is a compact fast reactor which matches time-dependent energy needs with the reliability of an isotopic heat source for base power needs. Considerable uncertainties in the cross sections and other nuclear data exist and strongly influence estimates of BIFOLD's size and cost. BIFOLD has been studied by combining nuclear data of the principal isotopes with the systematics of the physics of fission to yield, as far as possible, consistent data for design.

A continuing program of nuclear data acquisition for ^{238}Pu and ^{234}U is required. The data acquisition must embrace microscopic measurements to give cross sections and macroscopic measurements with critical assemblies to yield delayed neutron fractions and similar reactor physics quantities. The pursuit of the BIFOLD concept must include data acquisition and, indeed, BIFOLD itself can contribute considerable data.

The economics of special purpose power systems for space and elsewhere are favored in BIFOLD because of its energy producing flexibility and the prospects of low development costs compared to other power systems.

The very activity of providing new and improving the reliability and range of present nuclear data will yield new concepts in nuclear and other technologies. The origin of the BIFOLD concept through nuclear data acquisition efforts is evidence for this expectation.

References

(1) W. F. Stubbins, D. M. Barton and F. D. Lonadier, Nucl. Sci. Enging, 25 (1966)377.

(2) W. F. Stubbins, A BIFOLD Nuclear Power Source, USAEC Report. MLM 1357, June 15, 1967, Declassified March 1970.

(3) R. A. Wolfe and W. F. Stubbins, A BIFOLD Nuclear Power Source, USAEC Report MLM 1982, November 17, 1972.

(4) W. F. Stubbins and R. A. Wolfe, BIFOLD Nuclear Power Source, To be published.

(5) W. F. Stubbins and R. A. Wolfe, The BIFOLD Nuclear Power Source, Invited Paper, Am. Nucl. Soc. 19th Annual Meeting, June 10-15, 1973, Chicago, Illinois.

(6) G. Y. Eastman, The Heat pipe - A Progress Report, Fourth Intersociety Energy Conversion Engineering Conference, Washington, D. C. September, 1969.

(7) W. W. Smith, D. R. Rogers and G. L. Silver, Plutonium-238 Isotopic Fuel Form Data Sheets, USAEC Report MLM 1691 (1971)

(8) J. D. Hastings and W. W. Strohm, Jour. Inorganic and Nucl. Chem., 34 (1972) 25.

(9) W. M. Rutherford, G. N. Huffman and D. L. Coffey, Nucl. Applications, 3 (1967)366.

(10) R. L. Henkel, Fission by Fast Neutrons, Fast Neutron Physics Part II, (J. B. Marion and J. L. Fowler, Eds.) Interscience Publishers, New York (1963)

(11) W. F. Stubbins, An Interim Report and Evaluation of the Critical Mass of Plutonium-238 Fast Neutron Assemblies, July 21, 1964, Unpublished.

(12) L. L. Carter, Physics Research Quaterly Report, July-Sept. 1964, USAEC Report HW-84369 (1964).

(13) R. A. Wolfe, The Nuclear Criticality Safety Aspects of Plutonium-238, Nucl. Appl. and Tech. Aug (1970) 9.

(14) M. G. Silbert, Fission Cross Section of Plutonium-238 from Persimmon, USAEC Report LASL-4108-MS (1969).

(15) W. F. Stubbins, C. D. Bowman, G. F. Auchampaugh and M. S. Coops, Phys. Rev. 154 (1967) 1111.

(16) E. K. Hyde, The Nuclear Properties of Heavy Elements, III, Prentice-Hall, New Jersey (1964).

(17) R. A. Wolfe and W. F. Stubbins, Subcritical Neutron Multiplication Experiments with Four SNAP-19B (IRHS) Heat Sources Containing Plutonium-238, USAEC Report MLM 1523 (1969).

(18) R. A. Wolfe and D. A. Edling, Subcritical Neutron Multiplication Experiments with SNAP-19C-2 and SNAP 19B Heat Sources Containing Plutonium-238, USAEC Report MLM-1416 (1967).

(19) A. Prince, Neutron Cross Sections for Cm^{244} and Pu^{238}, USAEC Report GEMP-411 (1966).

(20) 16 Group ^{238}Pu Cross Sections Compiled at LASL, Unpublished, Private Communication (1969).

(21) Reactor Physics Constants, USAEC Report ANL-5800 (1963).

(22) A. H. Jaffey and J. L. Lerner, Nucl. Phys., A145 (1970)1.

(23) D. A. Hicks, J. Ise and R. V. Pyle, Phys. Rev. 101(1956) 1016.

(24) W. W. T. Crane, G. H. Higgins and H. R. Bowman, Phys. Rev. 101(1956)1804.

(25) C. L. Dunford, Evaluated Neutron Cross Section for ^{238}Pu and ^{244}Cm, USAEC Report AI65190 (1965).

(26) I. I. Bondarenko, D. B. Kuzminov, L. S. Kutsageva, L. I. Prokhorova and G. N. Smirenkin, United Nations Conf. on Peaceful Uses of Atomic Energy, Geneva, (1958)p. 353.

(27) R. B. Leachman, Phys. Rev. 101 (1955) 1005.

(28) J. Terrell, Phys. Rev. 108 (1957) 783.

(29) R. A. Wolfe and W. F. Stubbins, An Estimate of $\bar{\nu}(E_n)$ for ^{238}Pu. (To be published).

(30) W. F. Stubbins, The Neutron Energy Spectrum in ^{239}Pu Photofission Near Threshold. Bulletin Am. Phys. Society, Washington D. C. Meeting, April 23-26, 1973, and to be published.

(31) A. M. Weinberg and E. P. Wigner, The Physical Theory of Neutron Chain Reactors, Univ. of Chicago Press, Chicago, Ill. (1958).

(32) R. Breitwieser, An Out-of-Core Thermonic-Convertor System for Nuclear Space Power, Third International Conference on Thermonic Electrical Power Generation, Julich, Germany, June 5-9, 1972, also NASA Tech. Memo. TMX-68049.(1972).

A STUDY OF LONG-TERM HEAT GENERATION IN NUCLEAR BY-PRODUCTS FROM LWR AND LMFBR SYSTEMS

J.A. ANGELO, Jr., R.G. POST,
F.E. HASKIN, C. LEWIS
University of Arizona, Tucson, Arizona, United States of America

Abstract

A STUDY OF LONG-TERM HEAT GENERATION IN NUCLEAR BY-PRODUCTS FROM LWR AND LMFBR SYSTEMS.

Thermal outputs of high-level radioactive by-products from both a 1000-MW(e) reference LWR and a 1000-MW(e) reference LMFBR were calculated for cooling times ranging from one year to one thousand years. Both graphical and tabular representations of the data are useful in a wide variety of long-range by-product management studies.

A relatively fast and simple computer code, RADEC, was developed at the University to perform the bulk of the computations. Excellent agreement was obtained with the more extensive ORIGEN code developed at Oak Ridge National Laboratory.

In-core effects of fission product transmutation and actinide element build-up were included in the computations and were found to be significant. The former effect can account for as much as 25 per cent of the by-product afterheat during the first decade of cooling primarily due to the production of ^{134}Cs in neutron absorption by the fairly abundant fission product ^{133}Cs. Heat generation rates for LWR and LMFBR by-products are comparable during the first century of cooling but diverge rapidly thereafter with the actinide elements predominating after 120 years for the LMFBR and after 225 years for the LWR. Detailed, time-dependent analyses of the more thermally significant fission products and actinide elements were calculated and plotted.

One of the most significant problems facing the world's expanding nuclear power industry is the safe and economic management of the high-level radioisotopes generated by nuclear power reactors and separated in the reprocessing of spent reactor fuels. These by-products contain radioisotopes which decay so slowly that they must be controlled for hundreds to thousands of years. One method that is currently being considered in the United States is permanent removal from the biosphere by storage in deep geologic formations. Geologic storage [1, 2] includes excavation of a deep cavity, filling with radioactive material, sealing and allowing melting of the material and the surroundings for a short distance. The extent of melting and the time required to reach the maximum radius requires detailed heat transfer analyses. Most other schemes for management of radioactive by-products also require heat transfer calculations. These thermal analyses [3] require the development of detailed, time-dependent heat generation data for the radioisotopes formed in burning advanced reactor fuels. In addition to heat transfer studies concerned with permanent storage concepts, the contribution of a particular fission product or actinide nuclide to the total thermal power output of these high-level radioactive materials is frequently required in performing by-product management optimization studies. These studies, for example, may be concerned with reprocessing procedures, by-product thermal applications, or selective isotope recovery concepts.

Since the development of the first nuclear reactor, engineering design has required evaluation and prediction of the heat generated by the radioactive by-products of fission as functions of time [4]. Since then, many calculations have been made to evaluate thermal power output as a function of cooling time. Almost all of these past efforts, including several subject to wide use [5-7], made one or both of two major approximations. The first is to neglect neutron capture by the fission product nuclides during irradiation. The second approximation omits the contribution of the transplutonium actinides. The errors introduced were not readily apparent because the majority of earlier decay heat studies were concerned with the first year or so of cooling, following discharge of the spent fuel from the reactor. It is only recently, with high burn-ups and long-term radioactive by-product management, that isotopes from nuclear transmutation during irradiation and the actinide nuclides have become important to heat generation.

A recent study [8] has shown that by neglecting the process of nuclear transmutation for caesium [$^{133}Cs(n,\gamma)^{134}Cs$] the fission product heat generation rate from a typical advanced design LWR could be underestimated by as much as 25% during the first decade of decay. The ^{133}Cs isotope is a fairly abundant fission product in the thermal fission of ^{235}U (approximately six atoms per one hundred atoms fissioned) and has a fairly large thermal capture cross-section (approximately forty barns). The transmuted population of ^{134}Cs in discharged thermal reactor fuel is much higher than anticipated even by the more recent of these studies [7].

The contribution of the actinide nuclides to the overall heat generation rate of radioactive by-products has also been neglected in the majority of previous decay heat studies. Recently, calculations show [8] that the actinide nuclides contained in spent fuel from typical LWR or LMFBR systems are significant heat generators after about the first decade or two of cooling. These actinide nuclides dominate the LMFBR spent fuel thermal power output after approximately one century of cooling and the LWR after about two centuries of cooling.

To permit comparison with previous studies [1, 9], this study chose the nuclear by-products from two representative reactors: a 1000-MW(e) reference LWR and a 1000-MW(e) reference LMFBR. Design and performance

TABLE I. LWR DESIGN AND PERFORMANCE CHARACTERISTICS [10]

Fuel form:	Oxide pellets
Power:	3083 MW (thermal)
Thermal efficiency:	35.4%
Core:	
Average specific power	34.8 MW/t
Burn-up	33000 MWd/t
Charge (U)	88.6 t
Enrichment (^{235}U)	3.3%
Refuelling interval	~365 full power days
Refuelling fraction	1/3

TABLE II. LMFBR DESIGN AND PERFORMANCE CHARACTERISTICS [10]

Fuel form:	Oxide pellets
Power:	2500 MW (thermal)
Thermal efficiency:	40%
Core:	
Average specific power	175 MW/t
Burn-up	80000 MW/t
Charge (U + Pu)	12.6 t
Enrichment (^{239}Pu)	15.6%
Refuelling interval	153 full power days
Refuelling fraction	1/3
Axial blanket:	
Average specific power	5.5 MW/t
Burn-up	2500 MWd/t
Charge (U)	7.32 t
Enrichment (^{235}U)	0.3%
Refuelling interval	153 full power days
Refuelling fraction	1/3
Radial blanket:	
Average specific power	10 MW/t
Burn-up	8100 MWd/t
Charge (U)	26.7 t
Enrichment (^{235}U)	1.96%
Refuelling interval	153 full power days
Refuelling fraction	~ 3/16

TABLE III. THERMALLY SIGNIFICANT FISSION PRODUCT NUCLIDES IN TYPICAL ADVANCED LWR AND LMFBR SPENT FUEL (1 TO 1000 YEARS COOLING)

^{85}Kr	^{125}Sb	^{147}Pm
^{90}Sr/^{90}Y*	^{125m}Te	^{151}Sm
^{95}Zr	^{126}Sb	^{152}Eu
^{95}Nb	^{134}Cs	^{154}Eu
^{99}Tc	^{137}Cs/^{137m}Ba*	^{155}Eu
^{106}Ru/^{106}Rh*	^{144}Ce/^{144}Pr*	

* Short-lived daughter

TABLE IV. THERMALLY SIGNIFICANT ACTINIDE NUCLIDES IN TYPICAL ADVANCED LWR AND LMFBR SPENT FUEL (1 TO 1000 years cooling)

^{244}Cm	^{242}Pu	^{237}Np
^{243}Cm	^{241}Pu	^{238}U
^{242}Cm	^{240}Pu	^{236}U
$^{243}Am/^{239}Np$*	^{239}Pu	^{235}U
$^{242m}Am/^{242}Am$*	^{238}Pu	^{234}U
^{241}Am	^{236}Pu	^{232}U

* Short-lived daughter

characteristics for these reactors are displayed in Tables I and II respectively. Extensive time-dependent heat generation rate data have been computed, using the ORIGEN and RADEC computer codes for nuclear by-products from these two reference reactors. The ORIGEN isotope generation and depletion code was developed at Oak Ridge National Laboratory. Their calculations of the isotopic changes that took place in the LWR and LMFBR nuclear fuels for an exposure of 33 000 MWd/t were used [10]. The RADEC computer code was developed at the University of Arizona to calculate extensive heat generation rate data as a function of cooling time for all fission product and actinide nuclides with significant heat generation (see Tables III and IV). The cooling ranges from one to one thousand years. Using data calculated by ORIGEN at ORNL and reported by them [9] as its initial conditions, RADEC computed the time-varying populations of all appropriate by-product nuclides, determined the heat generation rate associated with each particular isotope, computed a total thermal power output, and finally computed the fractional decay heat contribution for each thermally significant by-product nuclide.

Since the actual actinide nuclide population in reprocessing by-products is extremely sensitive to reprocessing efficiencies and techniques, the actinide nuclide heat generation was treated separately from the fission product heat generation. In these computations it was assumed that 0.5% of the uranium and 0.5% of the plutonium present in the discharged reactor fuel appeared in the spent-fuel reprocessing by-products. The contribution of each thermally significant nuclide as the fraction of the total fission product thermal power output or the total actinide thermal power output as a function of decay time can be used in optimization studies involving reprocessing procedures, by-product thermal applications, or permanent storage concepts.

TABLE V. TOTAL HEAT GENERATION RATE FOR NUCLEAR BY-PRODUCTS FROM A 1000-MW(e) REFERENCE LWR

Cooling Time	Heat Generation Rate		Fractional Contribution	
(Years)	(W/t)	(W/MWd)	Fission Product	Actinide
1	1.026E+4	3.110E-1	96.92	3.08
2	5.531E+3	1.676E-1	97.49	2.51
3	3.491E+3	1.058E-1	97.16	2.84
4	2.466E+3	7.472E-1	96.42	3.58
5	1.914E+3	5.800E-2	95.62	4.38
6	1.596E+3	4.835E-2	94.94	5.06
7	1.398E+3	4.235E-2	94.42	5.58
8	1.266E+3	3.835E-2	94.04	5.96
9	1.172E+3	3.551E-2	93.78	6.22
10	1.101E+3	3.337E-2	93.59	6.41
11	1.046E+3	3.169E-2	93.47	6.52
12	1.001E+3	3.032E-2	93.40	6.60
13	9.620E+2	2.915E-2	93.35	6.65
14	9.284E+2	2.813E-2	93.33	6.67
15	8.985E+2	2.723E-2	93.33	6.67
16	8.711E+2	2.640E-2	93.33	6.67
17	8.460E+2	2.564E-2	93.35	6.65
18	8.224E+2	2.492E-2	93.37	6.63
19	8.001E+2	2.425E-2	93.40	6.60
20	7.789E+2	2.360E-2	93.43	6.57

TABLE VI. TOTAL HEAT GENERATION RATE FOR NUCLEAR BY-PRODUCTS FROM A 1000-MW(e) REFERENCE LWR

Cooling Time	Heat Generation Rate		Fractional Contribution	
(Years)	(W/t)	(W/MWd)	Fission Product	Actinide
5	1.914E+3	5.8000E-2	95.62	4.38
10	1.101E+3	3.337E-2	93.59	6.41
15	8.985E+2	2.723E-2	93.33	6.67
20	7.789E+2	2.360E-2	93.43	6.57
25	6.845E+2	2.074E-2	93.59	6.41
30	6.037E+2	1.829E-2	93.73	6.27
35	5.332E+2	1.616E-2	93.84	6.16
40	4.714E+2	1.429E-2	93.92	6.08
45	4.172E+2	1.264E-2	93.96	6.04
50	3.694E+2	1.120E-2	93.97	6.03
55	3.274E+2	9.921E-3	93.93	6.07
60	2.904E+2	8.799E-3	93.85	6.15
65	2.577E+2	7.809E-3	93.72	6.28
70	2.289E+2	6.937E-3	93.55	6.45
75	2.035E+2	6.166E-3	93.33	6.67
80	1.810E+2	5.486E-3	93.05	6.95
85	1.612E+2	4.884E-3	92.72	7.28
90	1.436E+2	4.352E-3	92.33	7.67
95	1.281E+2	3.881E-3	91.87	8.13
100	1.143E+2	3.465E-3	91.35	8.65

TABLE VII. TOTAL HEAT GENERATION RATE FOR NUCLEAR BY-PRODUCTS FROM A 1000-MW(e) REFERENCE LWR

Cooling Time	Heat Generation Rate		Fractional Contribution	
(Years)	(W/t)	(W/MWd)	Fission Product	Actinide
100	1.143E+2	3.465E-3	91.35	8.65
110	9.140E+1	2.770E-3	90.09	9.91
120	7.339E+1	2.224E-3	88.50	11.50
130	5.922E+1	1.794E-3	86.56	13.44
140	4.806E+1	1.456E-3	84.23	15.77
150	3.926E+1	1.190E-3	81.48	18.52
160	3.231E+1	9.790E-4	78.29	21.71
170	2.681E+1	8.124E-4	74.67	25.33
180	2.245E+1	6.803E-4	70.61	29.39
190	1.899E+1	5.755E-4	66.17	33.83
200	1.624E+1	4.921E-4	61.41	38.59
210	1.404E+1	4.256E-4	56.41	43.59
220	1.229E+1	3.724E-4	51.29	48.71
230	1.088E+1	3.297E-4	46.16	53.84
240	9.746E+0	2.953E-4	41.13	58.87
250	8.828E+0	2.675E-4	36.31	63.69
260	8.082E+0	2.449E-4	31.79	68.21
270	7.473E+0	2.265E-4	27.63	72.37
280	6.972E+0	2.113E-4	23.87	76.13
290	6.556E+0	1.987E-4	20.53	79.47

TABLE VIII. TOTAL HEAT GENERATION RATE FOR NUCLEAR BY PRODUCTS FROM A 1000-MW(e) REFERENCE LWR

Cooling Time	Heat Generation Rate		Fractional Contribution	
(Years)	(W/t)	(W/MWd)	Fission Product	Actinide
50	3.694E+2	1.120E-2	93.97	6.03
100	1.143E+2	3.465E-3	91.35	8.65
150	3.926E+1	1.190E-3	81.48	18.52
200	1.624E+1	4.921E-4	61.41	38.59
250	8.828E+0	2.675E-4	36.31	63.69
300	6.210E+0	1.882E-4	17.59	82.41
350	5.110E+0	1.549E-4	8.09	91.91
400	4.522E+0	1.370E-4	4.05	95.95
450	4.125E+0	1.250E-4	2.37	97.63
500	3.815E+0	1.156E-4	1.61	98.39
550	3.553E+0	1.077E-4	1.22	98.78
600	3.324E+0	1.007E-4	1.01	98.99
650	3.121E+0	9.457E-5	0.87	99.13
700	2.938E+0	8.902E-5	0.80	99.20
750	2.772E+0	8.398E-5	0.75	99.25
800	2.620E+0	7.940E-5	0.73	99.27
850	2.482E+0	7.521E-5	0.72	99.28
900	2.355E+0	7.136E-5	0.73	99.27
950	2.238E+0	6.782E-5	0.74	99.26
1000	2.131E+0	6.457E-5	0.76	99.24

TABLE IX. TOTAL HEAT GENERATION RATE FOR NUCLEAR BY-PRODUCTS FROM A 1000-MW(e) REFERENCE LMFBR

Cooling Time	Heat Generation Rate		Fractional Contribution	
(Years)	(W/t)	(W/MWd)	Fission Product	Actinide
1	1.432E+4	4.343E-1	95.19	4.81
2	6.728E+3	2.040E-1	96.55	3.45
3	3.709E+3	1.125E-1	96.38	3.62
4	2.298E+3	6.968E-2	95.10	4.90
5	1.613E+3	4.890E-2	93.38	6.62
6	1.266E+3	3.840E-2	91.76	8.24
7	1.082E+3	3.280E-2	90.50	9.50
8	9.761E+2	2.960E-2	89.62	10.38
9	9.104E+2	2.761E-2	89.01	10.99
10	8.653E+2	2.624E-2	88.58	11.42
11	8.314E+2	2.521E-2	88.27	11.73
12	8.039E+2	2.438E-2	88.01	11.99
13	7.803E+2	2.366E-2	87.79	12.21
14	7.591E+2	2.302E-2	87.60	12.40
15	7.396E+2	2.243E-2	87.42	12.58
16	7.214E+2	2.188E-2	87.24	12.76
17	7.041E+2	2.135E-2	87.07	12.93
18	6.877E+2	2.085E-2	86.91	13.09
19	6.719E+2	2.037E-2	86.74	13.26
20	6.567E+2	1.991E-2	86.57	13.48

TABLE X. TOTAL HEAT GENERATION RATE FOR NUCLEAR BY-PRODUCTS FROM A 1000-MW(e) REFERENCE LMFBR

Cooling Time	Heat Generation Rate		Fractional Contribution	
(Years)	(W/t)	(W/MWd)	Fission Product	Actinide
5	1.613E+3	4.890E-2	93.38	6.62
10	8.653E+2	2.624E-2	88.58	11.42
15	7.396E+2	2.243E-2	87.42	12.58
20	6.567E+2	1.991E-2	86.57	13.43
25	5.875E+2	1.781E-2	85.70	14.30
30	5.272E+2	1.599E-2	84.75	15.25
35	4.741E+2	1.438E-2	83.70	16.30
40	4.272E+2	1.300E-2	82.54	17.46
45	3.857E+2	1.170E-2	81.27	18.73
50	3.489E+2	1.058E-2	79.89	20.11
55	3.162E+2	9.589E-3	78.39	21.61
60	2.872E+2	8.710E-3	76.78	23.22
65	2.615E+2	7.929E-3	75.06	24.94
70	2.386E+2	7.235E-3	73.22	26.78
75	2.182E+2	6.617E-3	71.27	28.73
80	2.001E+2	6.067E-3	69.22	30.78
85	1.839E+2	5.578E-3	67.07	32.93
90	1.695E+2	5.141E-3	64.83	35.17
95	1.567E+2	4.752E-3	62.51	37.49
100	1.452E+2	4.404E-3	60.13	39.87

TABLE XI. TOTAL HEAT GENERATION RATE FOR NUCLEAR BY-PRODUCTS FROM A 1000-MW(e) REFERENCE LMFBR

Cooling Time	Heat Generation Rate		Fractional Contribution	
(Years)	(W/t)	(W/MWd)	Fission Product	Actinide
100	1.452E+2	4.404E-3	60.13	39.87
110	1.258E+2	3.814E-3	55.17	44.83
120	1.103E+2	3.344E-3	50.13	49.87
130	9.780E+1	2.966E-3	45.08	54.92
140	8.774E+1	2.661E-3	40.15	59.85
150	7.958E+1	2.413E-3	35.43	64.57
160	7.292E+1	2.211E-3	31.01	68.99
170	6.746E+1	2.046E-3	26.95	73.05
180	6.295E+1	1.909E-3	23.28	76.72
190	5.920E+1	1.795E-3	20.02	79.98
200	5.604E+1	1.699E-3	17.15	82.85
210	5.337E+1	1.618E-3	14.66	85.34
220	5.108E+1	1.549E-3	12.52	87.48
230	4.910E+1	1.489E-3	10.70	89.30
240	4.738E+1	1.437E-3	9.15	90.85
250	4.585E+1	1.390E-3	7.84	92.16
260	4.449E+1	1.349E-3	6.73	93.27
270	4.326E+1	1.312E-3	5.81	94.19
280	4.214E+1	1.278E-3	5.03	94.97
290	4.112E+1	1.247E-3	4.38	95.62

TABLE XII. TOTAL HEAT GENERATION RATE FOR NUCLEAR BY-PRODUCTS FROM A 1000-MW(e) REFERENCE LMFBR

Cooling Time	Heat Generation Rate		Fractional Contribution	
(Years)	(W/t)	(W/MWd)	Fission Product	Actinide
50	3.489E+2	1.058E-2	79.89	20.11
100	1.452E+2	4.404E-3	60.13	39.87
150	7.958E+1	2.413E-3	35.43	64.57
200	5.604E+1	1.699E-3	17.15	82.85
250	4.585E+1	1.390E-3	7.84	92.16
300	4.017E+1	1.218E-3	3.83	96.17
350	3.620E+1	1.098E-3	2.12	97.88
400	3.304E+1	1.002E-3	1.34	98.66
450	3.034E+1	9.199E-4	0.92	99.08
500	2.796E+1	8.480E-4	0.68	99.32
550	2.585E+1	7.838E-4	0.52	99.48
600	2.394E+1	7.260E-4	0.41	99.59
650	2.221E+1	6.736E-4	0.34	99.66
700	2.065E+1	6.261E-4	0.29	99.71
750	1.922E+1	5.828E-4	0.26	99.74
800	1.791E+1	5.432E-4	0.24	99.76
850	1.672E+1	5.069E-4	0.23	99.77
900	1.562E+1	4.737E-4	0.22	99.78
950	1.461E+1	4.432E-4	0.22	99.78
1000	1.369E+1	4.151E-4	0.23	99.77

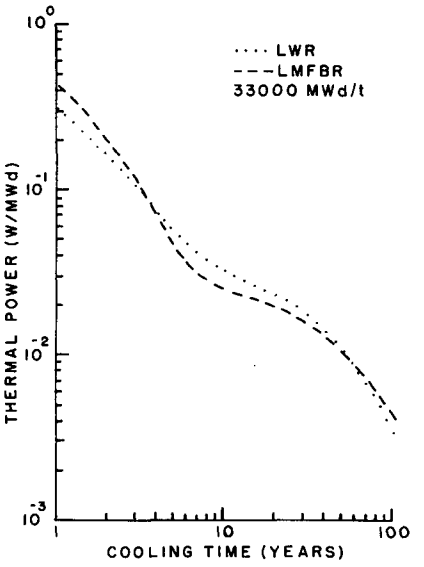

FIG.1. Total thermal power output for nuclear by-products from typical LWR and LMFBR spent fuel (1 to 100 years cooling).

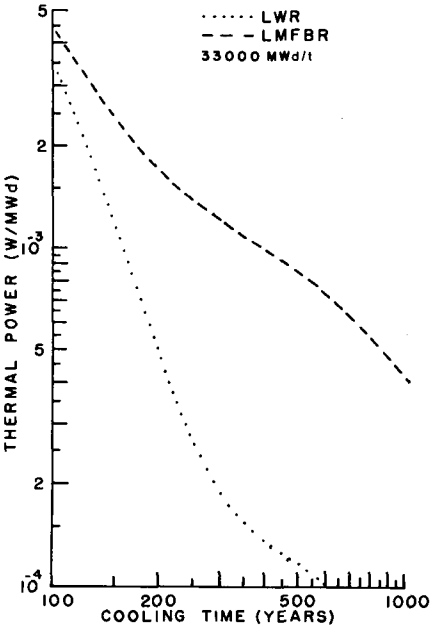

FIG.2. Total thermal power output for nuclear by-products from typical LWR and LMFBR spent fuel (100 to 1000 years cooling).

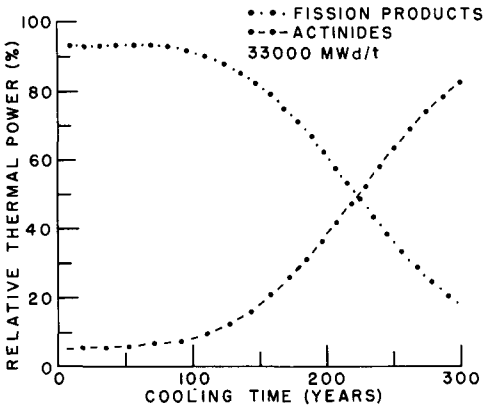

FIG.3. Relative contribution of fission product and actinide nuclides to the total thermal power output from typical LWR spent fuel.

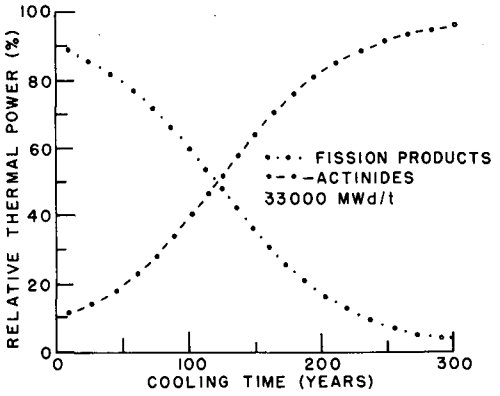

FIG.4. Relative contribution of fission product and actinide nuclides to the total thermal power output from typical LMFBR spent fuel.

Tables V through VIII contain the total heat generation rate data (fission product and actinide) for the reference LWR. Similarly, Tables IX through XII contain the LMFBR nuclear by-product thermal power output for various cooling times. Consistent with previous studies [1, 9, 10] these heat generation rate data are based on one metric tonne (t) of uranium charged to the LWR system and one metric tonne of uranium plus plutonium originally charged to the "homogenized" LMFBR core and blankets. However, in an effort to make these results more versatile and

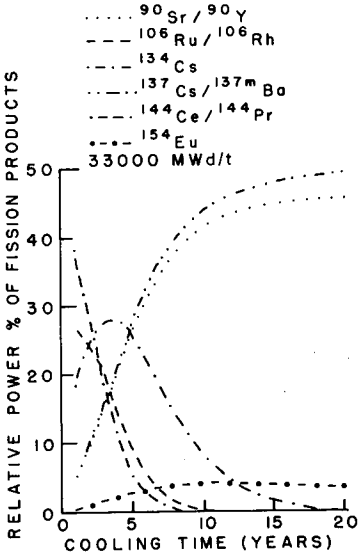

FIG.5. Relative heat contributions of selected fission products in typical LWR spent fuel for 1 to 20 years cooling.

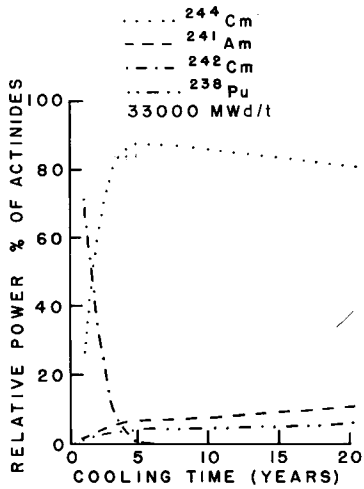

FIG.6. Relative heat contributions of selected actinide nuclides in typical LWR spent fuel for 1 to 20 years cooling.

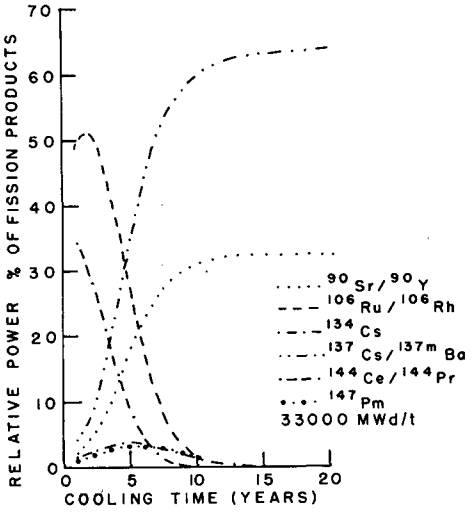

FIG.7. Relative heat contributions of selected fission products in typical LMFBR spent fuel for 1 to 20 years cooling.

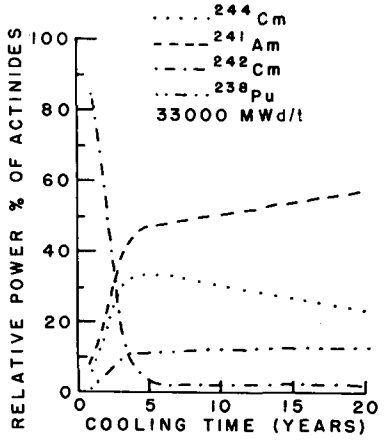

FIG.8. Relative heat contributions of selected actinide nuclides in typical LMFBR spent fuel for 1 to 20 years cooling.

potentially applicable to other burn-up scenarios, a normalizing unit, the watt-per-megawatt day (W/MWd) was also chosen as an ordinate in presenting the decay heat data. (See Figs 1 and 2). It is of interest to note that although the heat generation rates for the LWR and LMFBR by-products appear to be comparable during the first century of cooling, they diverge rapidly after about 100 years, with the actinide nuclides playing a dominant role in determining the LMFBR by-product thermal power output.

The relative contribution of the fission product nuclides versus the actinide nuclides to the total heat generation rate is displayed in Figs 3 and 4 for LWR and LMFBR by-products, respectively.

Extensive heat generation rate data and the associated fractional decay heat contributions for selected fission product and actinide nuclides of unusual thermal significance are presented in Figs 5 through 8.

In summary, discrepancies between the afterheat data presented in this study and those appearing in previous studies arise from two approximations used by the previous studies: the neglect of nuclear transmutation of fission product nuclides during irradiation and the heat contribution of the actinide nuclides. Decay heat computations presented here do not neglect these contributions and provide more complete long-term thermal power output data, which can be utilized in a variety of nuclear by-product management studies, particularly those involving deep geologic disposal of high-level radioisotopes.

REFERENCES

[1] COHEN, J.J., LEWIS, A.E., BRAUN, R.L., Use of a Deep Nuclear Chimney for the In-situ Incorporation of Nuclear-reprocessing Waste in Molten Silicate Rock, UCRL-51044, Lawrence Livermore Lab., Livermore, Calif. (May, 1971).

[2] SHEFF, J.R., Battelle Northwest Labs., Richland, Wash., Private communication (Nov., 1972).

[3] ANGELO, J.A., Jr., Heat Transfer from Radioactive Wastes in Deep Rock, Doctoral Dissertation (in preparation), The University of Arizona (1973).

[4] WAY, K., WIGNER, E.P., The rate of decay of fission products, Phys. Rev. 73 11 (June, 1948).

[5] PERKINS, J.F., KING, R.W., Energy release from the decay of fission products, Nucl. Sci. Eng. 3 (1958) 726.

[6] STEHN, J.R., CLANCY, E.P., "Fission-product Radioactivity and heat generation", 2nd Int. Conf. peaceful Uses atom. Energy (Proc. Conf. Geneva, 1958), UN, New York (P/1071 USA).

[7] VARTERESSIAN, K.A., BURRIS, L., Fission-product Spectra from Fast and Thermal Fission of ^{235}U and ^{239}Pu, Arg. Natl. Lab., Argonne, Ill., ANL-7678 (1970).

[8] ANGELO, J., Jr., POST, R.G., HASKIN, F.E., LEWIS, C., Nuclear by-product long-term heat generation rates, Trans. Amer. Nucl. Soc. 15 2 (1972) 663.

[9] ORNL-4451, Siting Fuel Reprocessing Plants and Waste Management Facilities, ORNL, Oak Ridge, Tenn. (1970 and 1971).

[10] BELL, M.J., Radiation Properties of Spent Plutonium Fuels, ORNL-TM-3641, ORNL, Oak Ridge, Tenn. (1972).

DISCUSSION

W.B. LEWIS: You have separated the fission-product and actinide heat contributions and the compared them. They may, however, be chemically separated. Only the heat from strontium and caesium is highly important for the first hundred years. Is not cooling of the actinides of relatively minor concern?

J.A. ANGELO: On the contrary, the heat generated by the actinides may actually be a major concern even during the first hundred years of decay. The scenario for by-product reprocessing employed in this paper assumed that only 0.5% of the uranium and 0.5% of the plutonium present in the discharged fuel ultimately appeared in the reprocessing by-products.

However, different by-product management schemes – perhaps, say, intact burial of the discharged fuel – will result in different, possibly higher, levels of heavy metals appearing in the wastes. This, of course, could result in much higher "heavy-metal" or actinide heat generation rates.

D. J. HOREN: Is it obvious why the earlier workers ignored the ^{133}Cs problem?

J. A. ANGELO: It was not readily obvious to me during my reviews of the literature. Perhaps it had been assumed that nuclear transmutation of the fission product nuclides could be neglected in the case of short irradiation times or low exposure levels without introducing serious errors. Perhaps they were limited in their calculations by the lack of high-speed computational facilities, which would have enabled the numerical solution of the large number of coupled differential equations describing the fission product inventories.

J. Y. BARRE: Would your conclusions for fast-neutron reactors be changed if:
(1) a burn-up of 100 000 MWd/t was used, which is a much more realistic value than the 33 000 MWd/t which you used?
(2) the isotopic composition of the initial plutonium was different from the one selected, which was not mentioned?

J. A. ANGELO: The answer to both parts of your question is yes. The total heat generation rate for the LMFBR by-products would be changed by using a different burn-up value or a different isotopic composition of plutonium appearing in the reprocessing by-products.

In these computations an average equivalent exposure of 33 000 MWd/t was used. However, this represented a post-irradiation, homogeneous blending (to create an average equivalent burn-up of 33 000 MWd/t) of discharged fuel from the core and radial and axial blanket regions. The discharged core material itself experienced a burn-up of 80 000 MWd/t as indicated in Table II of our paper. Furthermore, it was assumed that only 0.5% of the plutonium and 0.5% of the uranium present in the discharged fuel ultimately appeared in the spent-fuel-reprocessing by-products.

SECTIONS EFFICACES DE CREATION DE DOMMAGES

M. LOTT*, J.P. GENTHON**, F. GERVAISE**,
P. MAS†, J.C. MOUGNIOT††, NGUYEN VAN DOAN**
Commissariat à l'énergie atomique,
France

Abstract-Résumé

CROSS-SECTIONS FOR THE CREATION OF DAMAGE.

Differential cross-sections reporesenting the rate of creation of damage are established; with these it is possible to calculate the simplest quantities associated with irradiation - i.e. the energy imparted to the material in the form of elastic collisions and the number of displacements per atom. The data necessary for calculating these damage functions are: (a) the neutron cross-sections (elastic and inelastic) with their angular distributions; with these it is possible to calculate the spectrum of the (primary) recoil atoms associated with a neutron collision; (b) the energy given up and the number of atoms displaced by the primary atom, which are calculated by means of Lindhardt's universal curve, the results of which are compared with those of a collision-by-collision calculation of the displacement cone. The ARTUS and SOURCE codes are used in calculating with these data the energy imparted to the lattice and the number of displacements per atom. ARTUS X is linked with the UKNDF file. Results are given for all usual cases of common metals and steel. The cross-sections necessary for calculating rates of creation of gas (H and He) in irradiated metals are reviewed.

SECTIONS EFFICACES DE CREATION DE DOMMAGES.

Des sections efficaces différentielles de taux de création de dommages sont établies qui permettent de calculer les grandeurs les plus simples associées à l'irradiation, c'est-à-dire: l'énergie cédée au matériau sous forme de chocs élastiques et le nombre de déplacements par atome. Les données nécessaires au calcul de ces fonctions de dommage sont: a) les sections efficaces neutroniques, élastique, inélastique avec leur distribution angulaire qui permettent de calculer le spectre des atomes de recul (primaire) associés à un choc neutronique; b) l'énergie cédée et le nombre d'atomes déplacés par cet atome primaire qui sont calculés au moyen de la courbe universelle de Lindhardt dont les résultats sont comparés à ceux d'un calcul choc par choc de la gerbe de déplacement. Les codes de calcul ARTUS et SOURCE traitent ces données pour calculer l'énergie cédée au réseau et le nombre de déplacements par atome. ARTUS X est couplé sur la bibliothèque UKNDF. Les résultats sont donnés dans quelques cas usuels des métaux courants et de l'acier. Les sections efficaces nécessaires au calcul des taux de création de gaz (H et He) dans les métaux irradiés sont passées en revue.

INTRODUCTION

Pour caractériser l'irradiation neutronique des matériaux de structure des réacteurs, on s'est longtemps contenté de grandeurs intégrales telles que le flux supérieur à 1 MeV ou l'activation d'un détecteur à seuil.

Compte tenu de l'ensemble des progrès réalisés dans les techniques d'examen des matériaux irradiés, dans la connaissance des sections efficaces et des spectres neutroniques, dans l'étude des mécanismes de transfert d'énergie aux

* Centre d'études nucléaires de Fontenay-aux-Roses.
** Centre d'études nucléaires de Saclay.
† Centre d'études nucléaires de Grenoble.
†† Centre d'études nucléaires de Cadarache.

matériaux, il est devenu possible de rapporter les dommages à des grandeurs liées au matériau lui-même, par exemple : l'énergie cédée au réseau ou le nombre de déplacements par atome.

L'intérêt de l'utilisation de telles unités apparaît encore plus nettement quand il s'agit de comparer les irradiations neutroniques et les irradiations ioniques. Malheureusement, ces grandeurs ne sont pas directement mesurables, elles ne peuvent qu'être calculées et pour le faire, il faut mettre en oeuvre un nombre important de données dont la normalisation est nécessaire pour que la mesure de la même grandeur soit indépendante de l'expérimentateur. Pour ce qui concerne les sections efficaces, compte tenu de la généralisation de l'emploi d'un nombre très restreint d'évaluations : ENDF/B [1] et UKNDF [2] , la normalisation devient possible et il semble qu'il en soit de même pour le calcul du nombre de déplacements par atome primaire dans un métal pour lequel l'abaque de LINDHARD [3] , est maintenant généralement employé.

Après avoir rappelé les formules et les conventions utilisées, nous donnons les sections efficaces de création de dommages d'éléments entrant dans la composition des matériaux de structure les plus courants et celles de l'acier inoxydable.

FORMALISME GENERAL

Lors de l'interaction d'un neutron et d'un atome, celui-ci peut acquérir suffisamment d'énergie pour être déplacé de son site et déplacer à son tour de leur site, tout au long de son parcours, un grand nombre d'autres atomes qui deviennent des interstitiels et laissent sur place des sites lacunaires. C'est au nombre de sites lacunaires ou de paires lacunes interstitiels par unité de volume ainsi créés lors d'une irradiation qu'il est convenu, de façon générale, de rapporter les dommages bien que dans certains cas particuliers, d'autres modèles peuvent être préférables suivant les propriétés des matériaux étudiés.

La connaissance des sections efficaces différentielles neutroniques et de l'ensemble des grandeurs relatives aux réactions permet de calculer le spectre des premiers atomes choqués, les travaux de LINDHARD permettent de calculer l'énergie cédée au réseau et ceux de KINCHIN et PEASE [4] , SIGMUND [5] , TORRENS et ROBINSON [6] , de relier cette énergie cédée au réseau au nombre d'atomes déplacés.

I. ENERGIE DES PREMIERS ATOMES CHOQUES

L'énergie $T(\mu)$ du premier atome choqué dans le système du laboratoire, émis dans une direction faisant un angle $\theta_{c.m.}$ ($\mu = \cos\theta_{c.m.}$) avec la direction du neutron incident dans le système du centre de masse dépend du type d'interaction. Elle est donnée par les expressions suivantes où E est l'énergie du neutron incident (laboratoire) et A la masse atomique du noyau cible.

I.1. Choc élastique

$$T_N(\mu) = E \frac{2A}{(1+A)^2}(1+\mu)$$

I.2. Choc inélastique - niveaux séparés (n,n'γ)

$$T_{N_1'}(\mu) = E \frac{2A}{(1+A)^2}\left\{1 - \frac{A+1}{2A}\frac{Q}{E} + \mu\left(1 - \frac{A+1}{A}\frac{Q}{E}\right)^{1/2}\right\}$$

Dans cette expression $Q>0$ correspond à l'énergie emportée par le γ dont la quantité de mouvement est négligée, ce qui entraîne une erreur de quelques pour mille sur l'énergie du primaire.

I.3. Choc inélastique (n,n'γ) niveaux non résolus

Pour les neutrons d'énergie élevée, les niveaux d'énergie ne sont pas résolus et les bibliothèques de données nucléaires donnent généralement le spectre d'énergie des neutrons émergents dans le système du centre de masse et leur distribution angulaire, souvent isotrope. L'énergie du primaire dépend alors de μ et de l'énergie $E'_{C.M.}$ du neutron émis dans la direction opposée (C.M.) par l'expression :

$$T_{N_2'}(\mu, E'_{CM}) = A\left\{\frac{E}{(A+1)^2} + \frac{E'_{CM}}{A^2} + 2\mu\frac{\sqrt{EE'_{CM}}}{A(A+1)}\right\}$$

I.4. Choc (n,2n)

En supposant l'émission neutronique isotrope dans le système du centre de masse et les directions d'émission des deux neutrons non liées entre elles, l'énergie de recul moyenne de l'atome de recul est donnée par l'expression :

$$T_{2N}(\mu) = (A-1)\left\{\frac{E}{(A+1)^2} + \frac{EA-Q(A+1)}{A(A+1)(A-1)} + 2\mu\left(\frac{E(EA-Q(A+1))}{(A+1)^3 A (A-1)}\right)^{1/2}\right\}$$

où $Q>0$ caractérise l'énergie de la réaction.

I.5. Capture (nγ)

La réaction nγ ne prend de l'importance qu'aux faibles énergies où la quantité de mouvement du neutron incident peut être négligée. Dans ces conditions, en faisant l'hypothèse simplificatrice de non-corrélation angulaire des

γ émis, l'énergie de l'atome de recul est donnée par l'expression de M.S. WECHSLER [7]

$$T_\gamma = \frac{\sum_i N_i E_i^2}{2(A+1)C^2}$$

N_i étant le nombre de rayons γ d'énergie E_i émis par capture et $(A+1)C^2$ l'énergie à l'état fondamental du noyau formé.

Les valeurs de T_γ sont extraites du travail de R.R. COLTMAN [15] .

II. ENERGIE CEDEE AU RESEAU ET NOMBRE D'ATOMES DEPLACES PAR UN PRIMAIRE

Quand l'atome primaire est de même nature que le matériau cible et que celui-ci est constitué d'une seule espèce d'atomes, l'énergie cédée au réseau E_D au cours du ralentissement d'un primaire d'énergie initiale T est donnée par l'abaque de LINDHARD mis sous forme analytique par ROBINSON[8],[9]

$$E_D = \frac{T}{1 + K g(\varepsilon)}$$

où K est donné par l'expression : $K = 0,1337\ Z^{2/3}\ A^{-1/2}$ et $g(\varepsilon)$, fonction de l'énergie réduite du primaire $\varepsilon = 1.15.10^{-2}\ Z^{-7/3} T$ (eV) est donnée par l'expression $g(\varepsilon) = \varepsilon + 0,4024\ \varepsilon^{3/4} + 3,4\ \varepsilon^{1/6}$

Z et A sont respectivement le numéro atomique et la masse atomique communs à l'atome cible et au primaire.

Conformément au modèle de KINCHIN et PEASE, trois cas sont considérés dans le calcul du nombre de paires lacunes interstitiels créés lors du ralentissement du primaire

- $T < E_d$	$N_D = 0$	E_d, pris arbitrairement égal à 40 eV dans les calculs, est le seuil de déplacement.
- $E_d < T < E'_d$	$N_D = 1$	
- $E'_d < T$	$N_D = \beta E_D$	La constante β a été prise égale à 10 keV^{-1}, l'énergie E_D étant exprimée en keV.

Cette formule correspond à la recommandation de l'A.I.E.A. faite au colloque de SEATTLE [13] et à celle faite par le Groupe de Dosimétrie de l'EURATOM. Elle a été justifiée par les calculs de simulation de cascades de TORRENS et ROBINSON [6] et reprise dans le travail de synthèse de NORGETT, ROBINSON et TORRENS [10] .

L'énergie E'_d, limite entre les deux dernières régions est prise telle qu'il n'y ait pas de discontinuité dans N_D. Elle est solution de l'équation :

$$\beta\, E_D(E'_d) = 1$$

/Remarque/ Pour le graphite, l'A.I.E.A. [13] maintient pour l'instant la recommandation d'utiliser le modèle de THOMPSON et WRIGHT[17] pour le calcul des taux de déplacement.

III. SECTIONS EFFICACES DE TRANSFERT D'ENERGIE ET DE TAUX DE DEPLACEMENT

Par l'abaque de LINDHARD et les conventions exposées, on a donc fait correspondre à un primaire d'énergie T (μ), une énergie cédée au réseau E_D (μ) et un nombre de paires de FRENKEL N_D (μ). Lors du bombardement d'un gramme de matériau pur contenant N atomes par un flux unité ($cm^{-2}s^{-1}$) de neutrons d'énergie E, la puissance cédée au réseau D (E) et le nombre de paires de FRENKEL créées par seconde DPG (E) sont donnés par l'expression suivante :

$$Y(E) = N \left\{ \sigma_N \int_{-1}^{+1} \chi_N(\mu)\, p_N(\mu)\, d\mu + \sigma_{N'_1} \int_{-1}^{+1} \chi_{N'_1}(\mu)\, p_{N'_1}(\mu)\, d\mu \right.$$
$$\left. + \sigma_{N'_2} \int_{-1}^{+1} d\mu \int_{E'} \chi_{N'_2}(\mu, E')\, p_{N'_2}(\mu, E')\, dE' + \frac{1}{2}\sigma_{2N} \int_{-1}^{+1} \chi_{2N}(\mu)\, d\mu + \sigma_{N,\gamma}\, \chi_\gamma \right\}$$

N est le nombre d'atomes par gramme

σ les sections efficaces totales des différents types d'interaction (élastique, inélastique...)

$p(\mu)$ les distributions angulaires d'un neutron émergent dans la direction $-\mu$ dans le système du centre de masse

$$\int_{-1}^{+1} p(\mu)\, d\mu = 1 \qquad \int_{-1}^{+1} \int_{E'} p(\mu, E')\, d\mu\, dE' = 1$$

$\chi = E_D(\mu)$ correspond à $Y(E) = D(E)$ — puissance cédée au réseau eV $cm^2/g.s$

$\chi = N_D(\mu)$ correspond à $Y(E) = DPG(E)$ nombre de déplacement par gramme et par seconde.

Cas d'un mélange de matériaux

Pour obtenir les grandeurs correspondant à un mélange de corps de numéros atomiques voisins, on ajoute linéairement les grandeurs relatives à chacun des constituants

$$X = \sum_i \rho_i X_i$$

où ρ_i représente le nombre de gramme du constituant i par gramme de mélange.

IV. EXEMPLES D'APPLICATIONS

Les codes ARTUS X [11] et SOURCE [12] bâtis sensiblement sur les mêmes principes ont été réalisés pour calculer les quantités précédentes. SOURCE est en cours de couplage avec la bibliothèque ENDF et ARTUS X est couplé sur la bibliothèque UKNDF.

Les figures n° 1 à 9 sont les résultats de calculs ARTUS X pour Al, Si, Cr, Fe, Ni, Cu, Zr, Mo, W. Les courbes en tirets correspondent à la réaction élastique, les courbes en pointillés aux autres réactions.

Dans les tableaux I à IX correspondants, les résultats sont donnés en 99 groupes du code de transport ANISN [14], la pondération dans les groupes de basse énergie étant faite selon un spectre en 1/E et dans les groupes de haute énergie selon un spectre de fission.

La première colonne du tableau est la borne inférieure du groupe, la seconde colonne l'énergie totale cédée par les neutrons T ($T = \int T(\mu) d\psi$, la troisième l'énergie cédée au réseau D(E) ($eV.cm^2.g^{-1}$) et la quatrième le nombre de déplacements atomiques DPG (E) ($cm^2.g^{-1}$). De plus, nous donnons dans le tableau X les mêmes grandeurs pour le groupe thermique correspondant à 0,0253eV.

Un travail semblable a été réalisé par D.G. DORAN [16] à partir de la bibliothèque ENDF/B pour le tantale et l'acier inoxydable. La comparaison entre les deux estimations pour l'acier inoxydable est présentée figure 10. Le coefficient de proportionnalité β utilisé par DORAN étant de 15,15 keV^{-1} pour comparer les résultats nous avons reporté le rapport DPG (présent travail)/ DPG (DORAN) x 1,515. Il apparaît que les estimations sont en moyenne concordantes au-dessus de 10^{-2}MeV.

Pour les énergies inférieures, les différences observées tiennent à la différence entre les seuils de déplacement, 33 eV pour DORAN et 40 eV pour le présent travail et à la différence des énergies de recul T_γ correspondant à une capture.

L'écart entre les taux de déplacements obtenus en intégrant ces deux évaluations sur un spectre de neutrons de fission est, compte tenu du facteur de correction 1,515, égal à 3,5%.

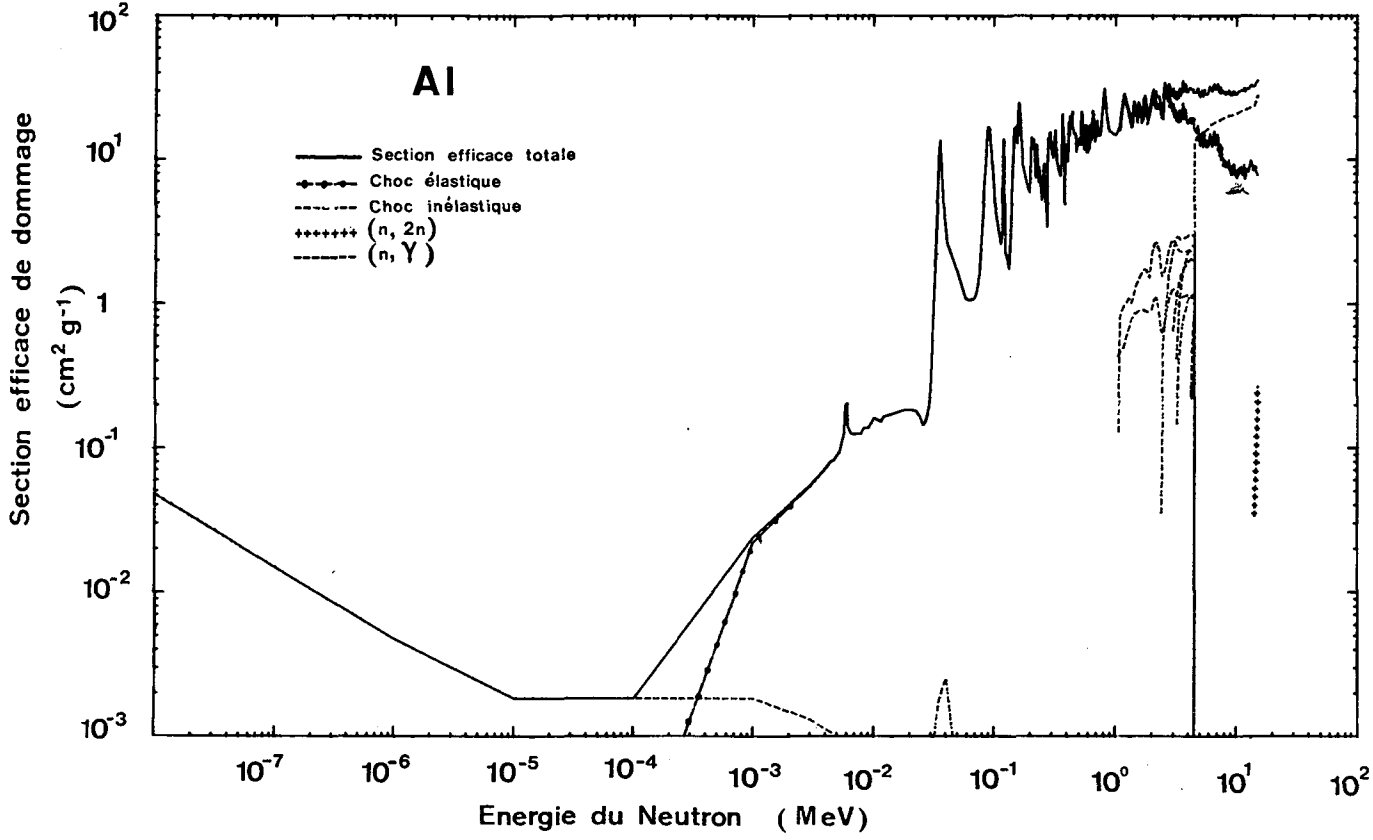

FIG. 1. Résultats de calculs ARTUS X pour l'aluminium.

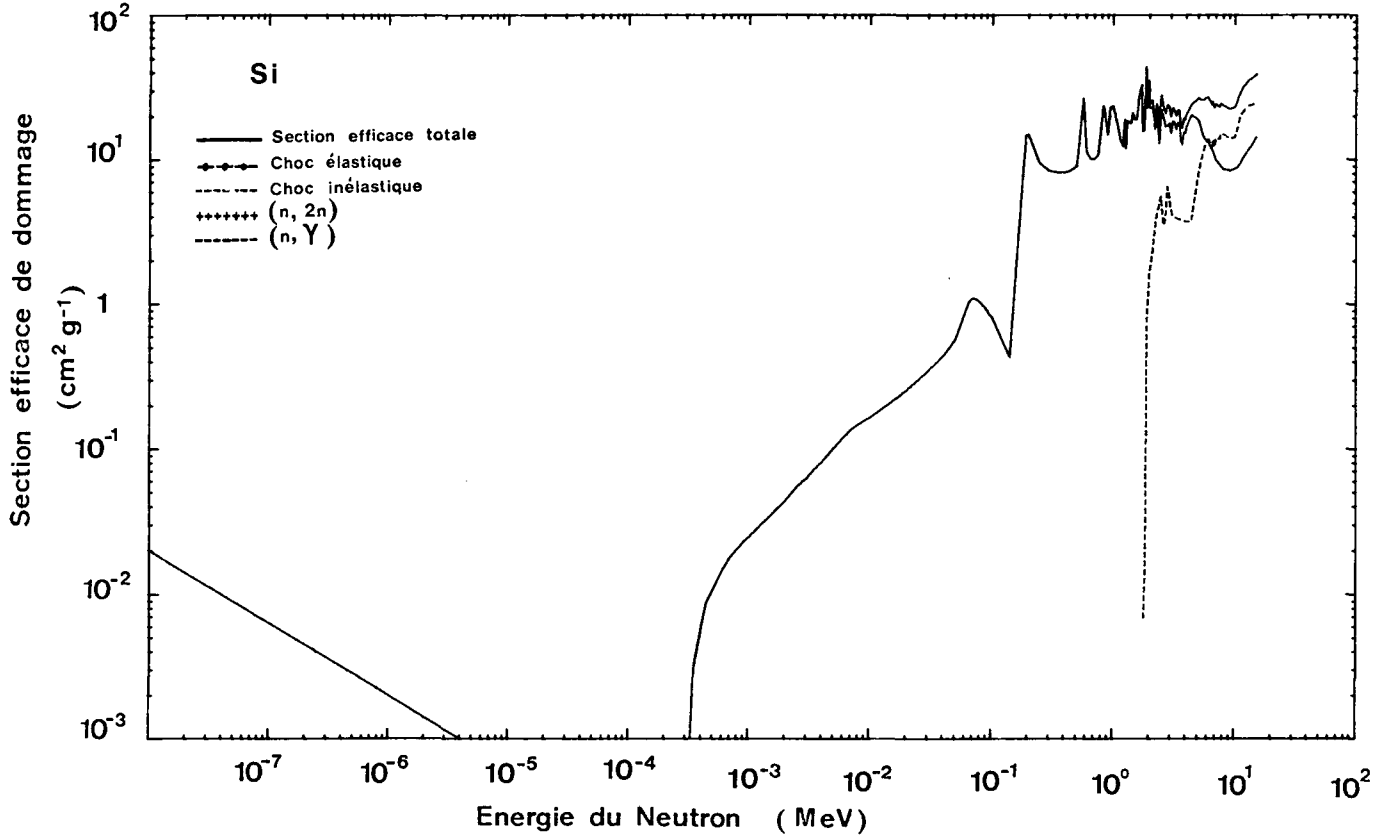

FIG.2. Résultats de calculs ARTUS X pour le silicium.

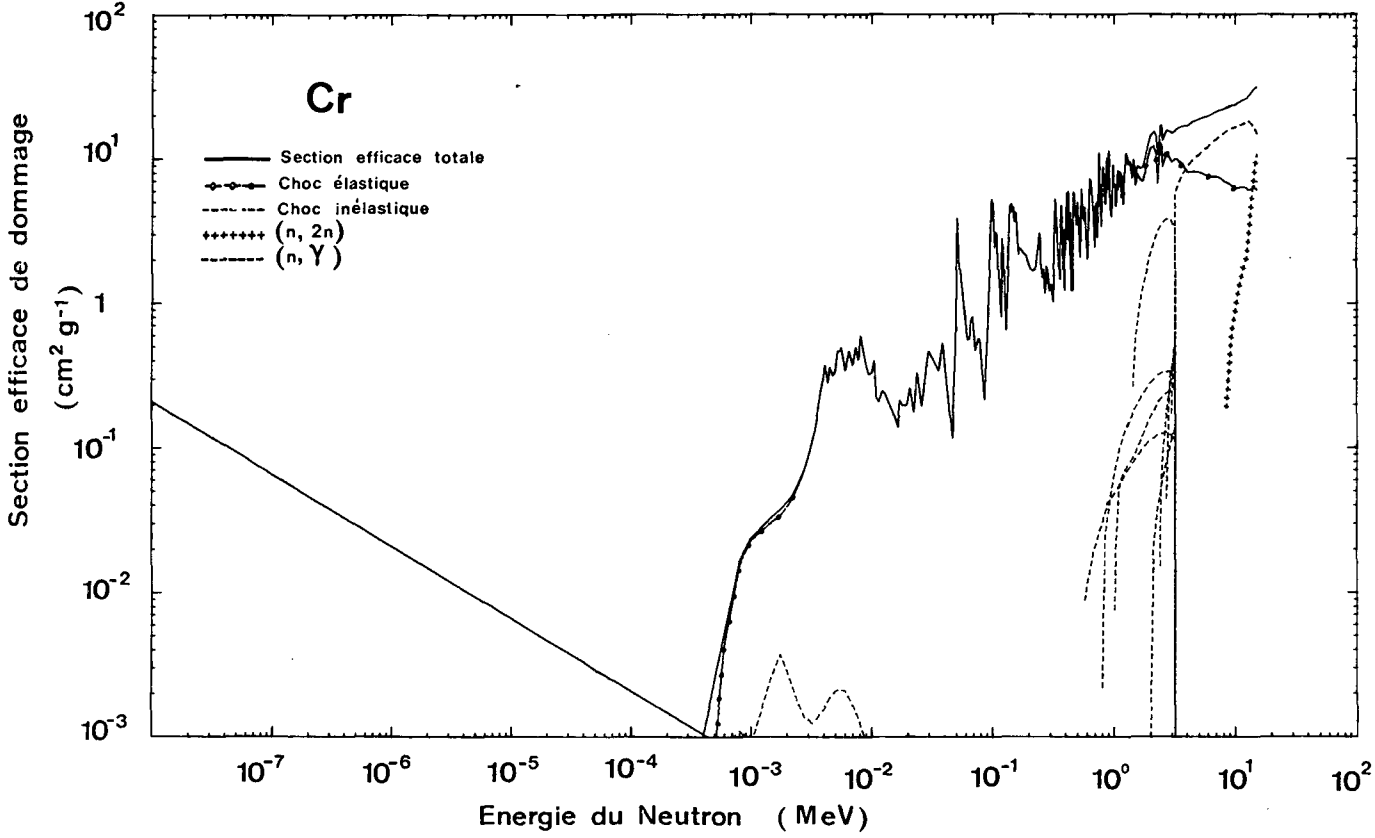

FIG. 3. Résultats de calculs ARTUS X pour le chrome.

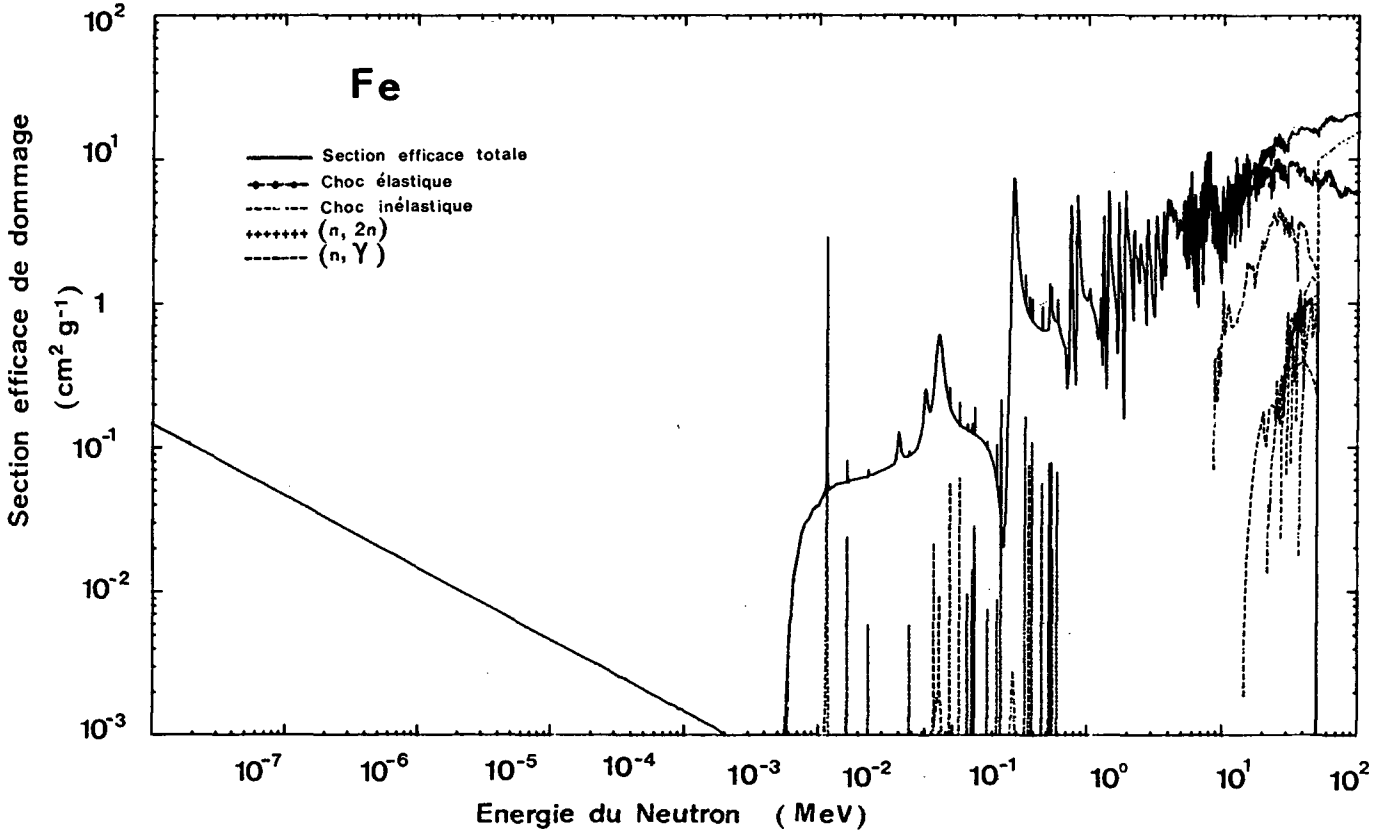

FIG. 4. Résultats de calculs ARTUS X pour le fer.

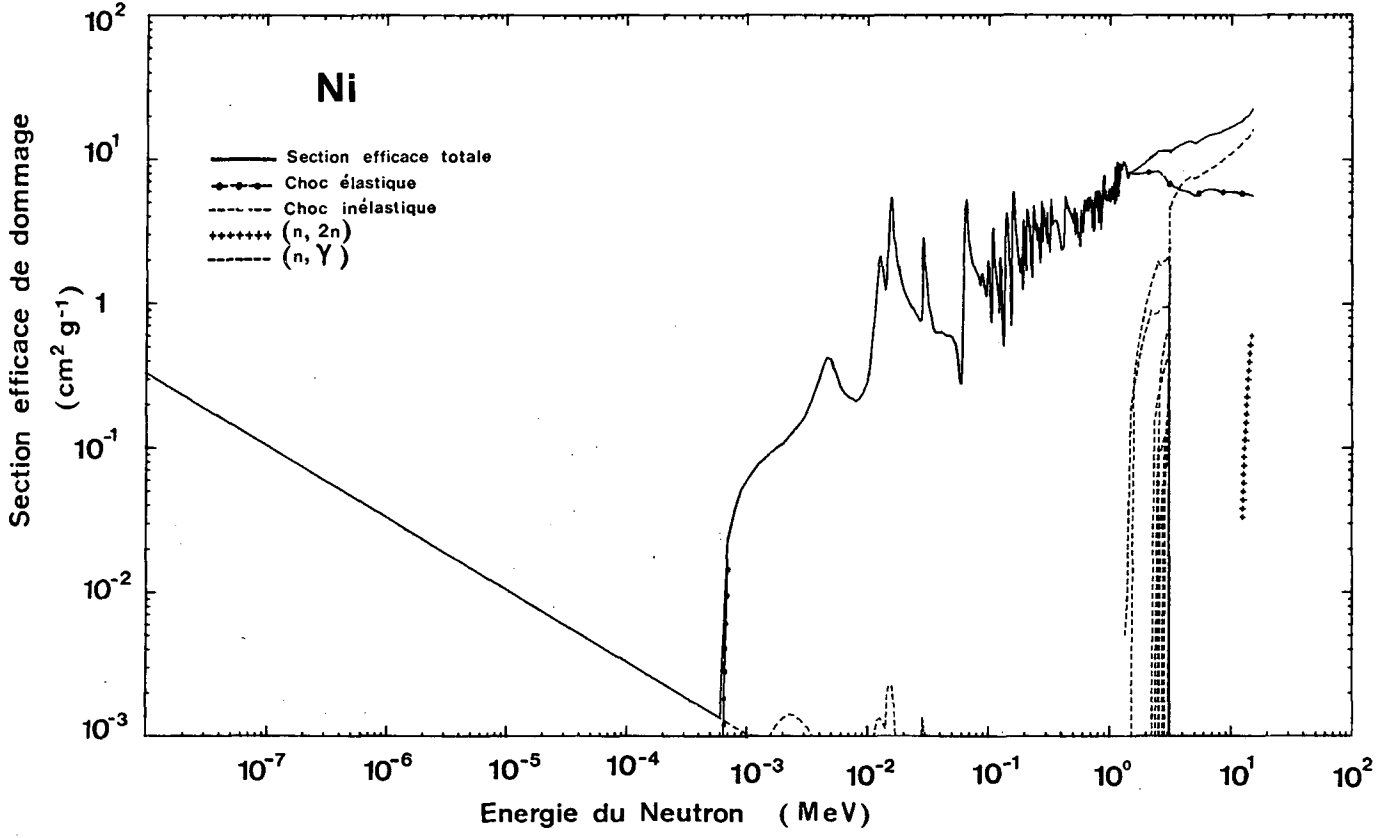

FIG. 5. Résultats de calculs ARTUS X pour le nickel.

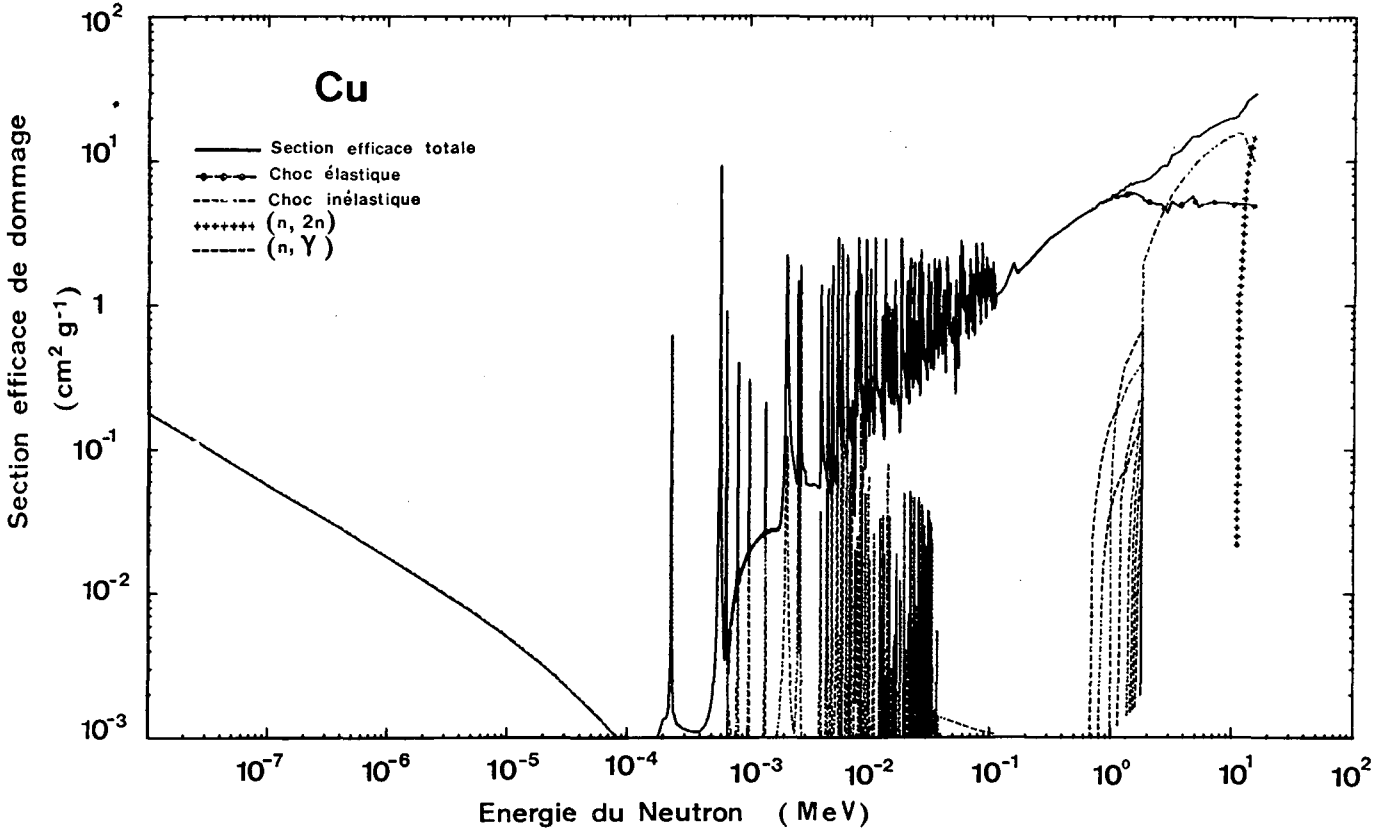

FIG. 6. Résultats de calculs ARTUS X pour le cuivre.

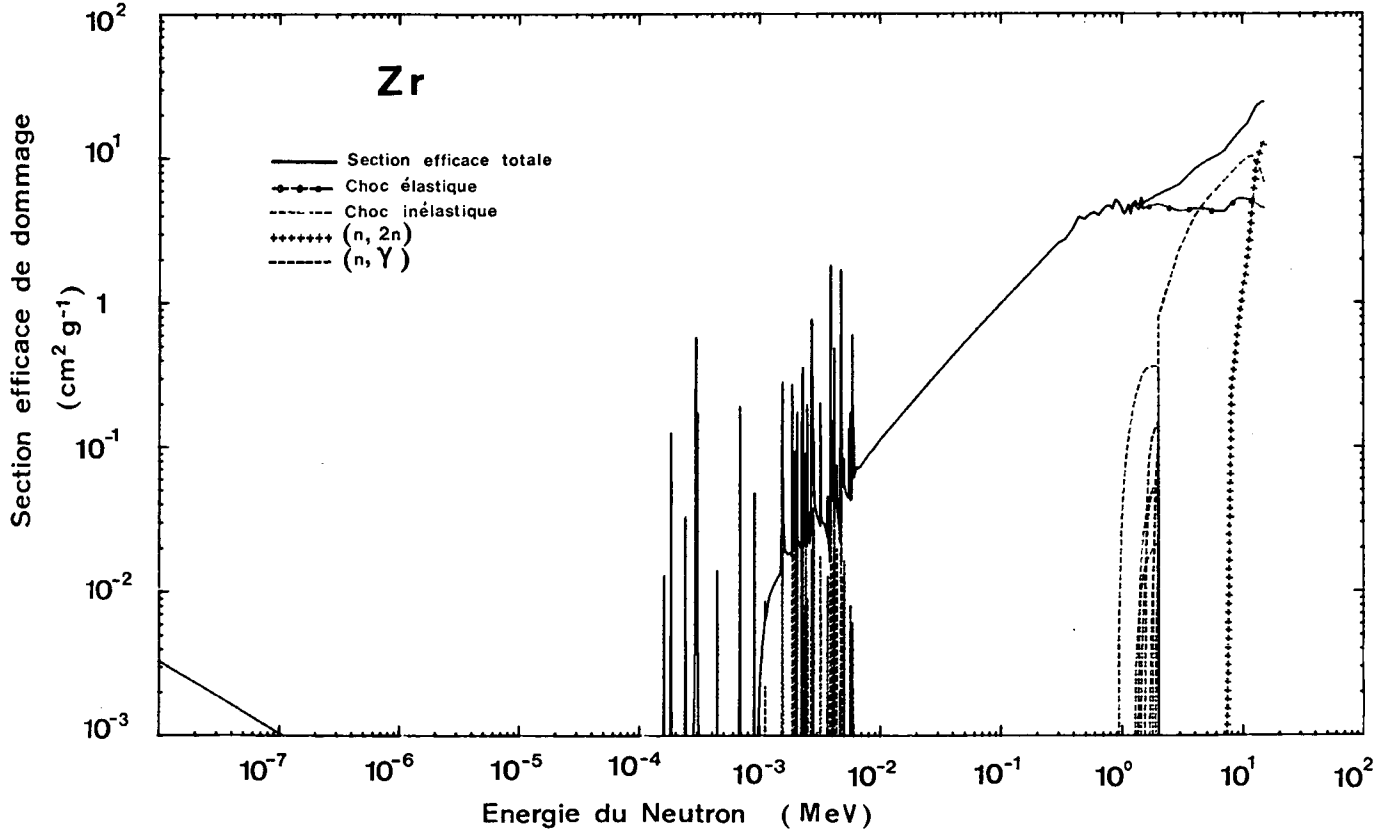

FIG. 7. Résultats de calculs ARTUS X pour le zirconium.

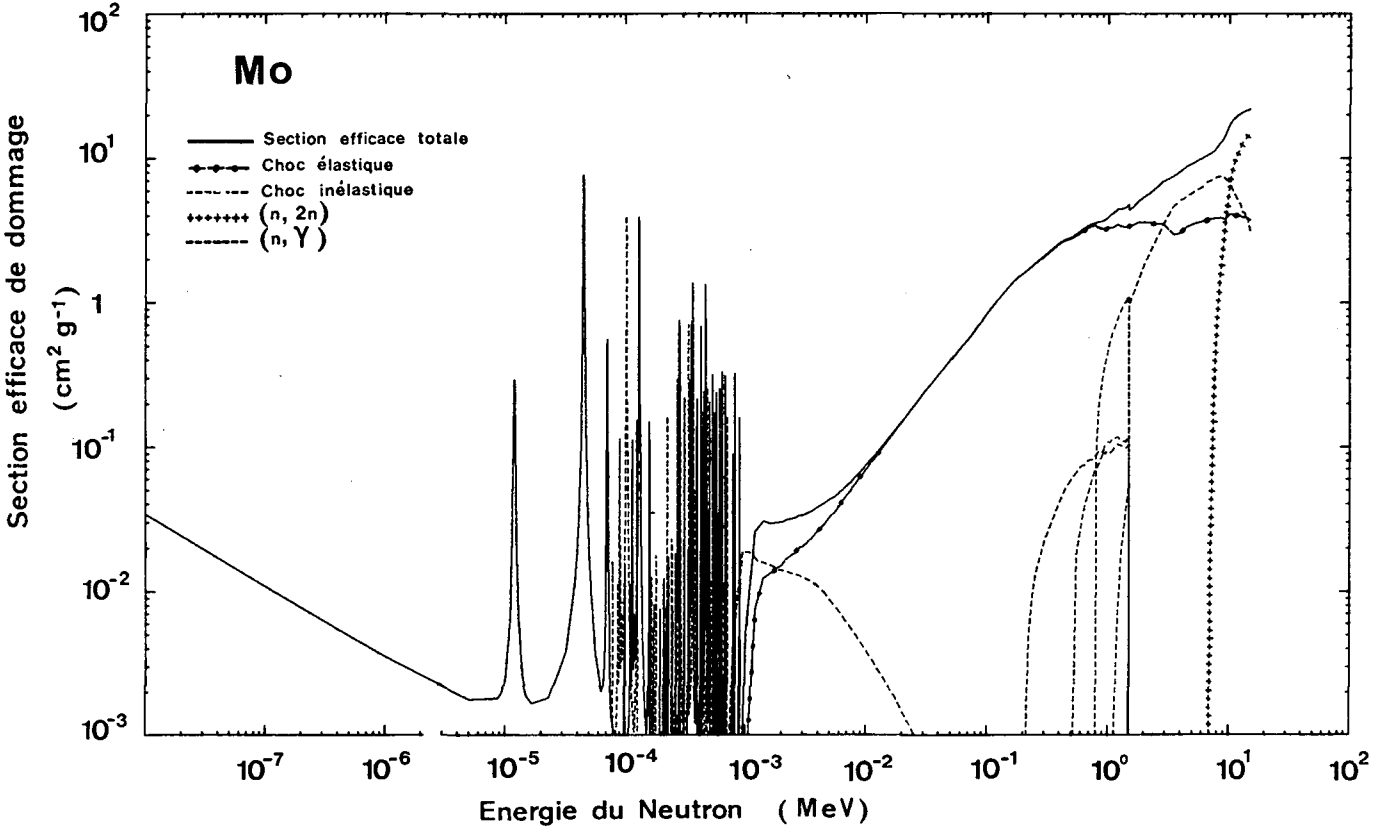

FIG. 8. Résultats de calculs ARTUS X pour le molybdène.

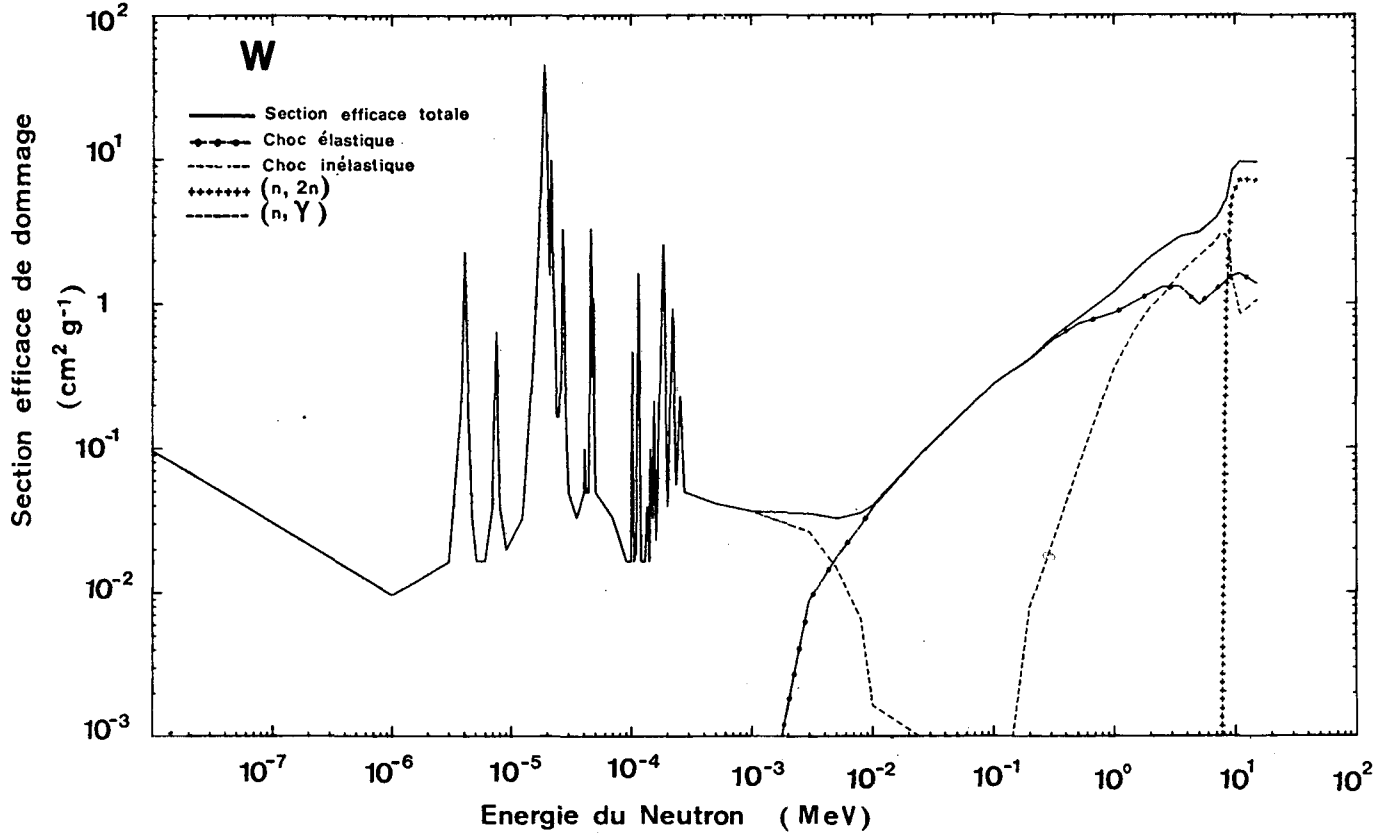

FIG.9. Résultats de calculs ARTUS X pour le tungstène.

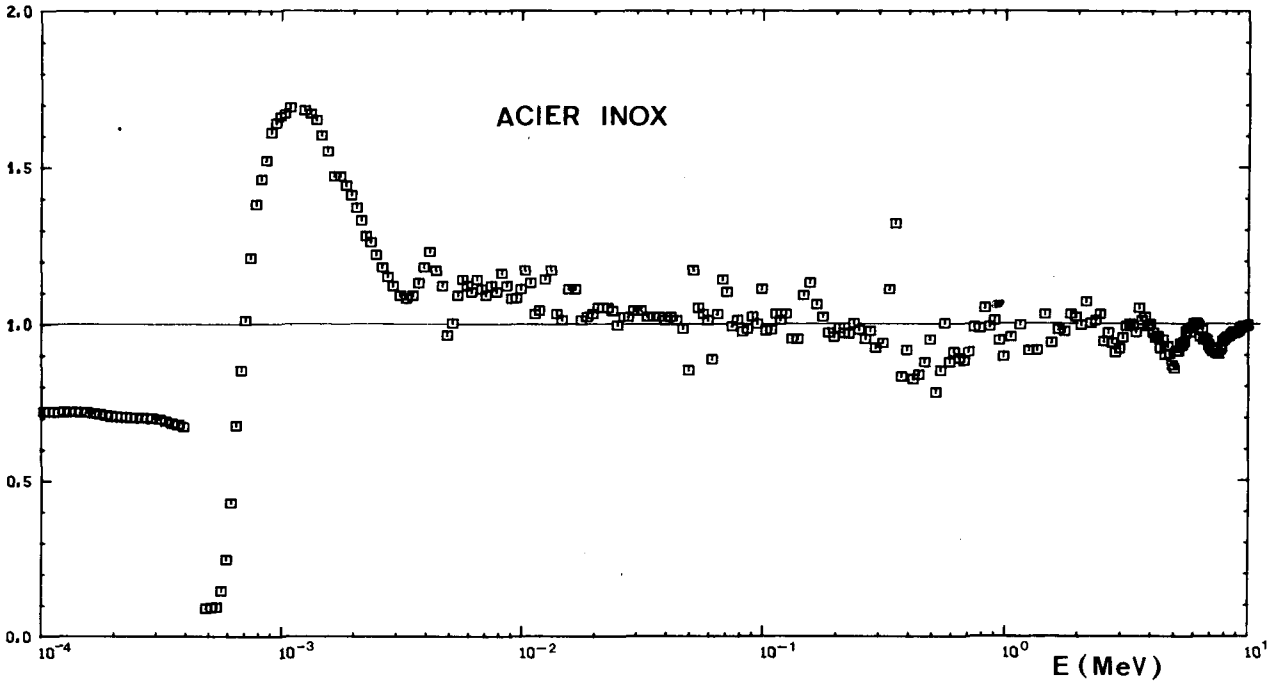

FIG. 10. Comparaison des valeurs des auteurs avec celles de Doran.

CONCLUSION

Nous avons posé comme un principe que les dommages dus à l'irradiation neutronique doivent être rapportés à des grandeurs liées au matériau irradié. Le nombre de paires lacunes interstitiels créés pendant l'irradiation n'est certainement pas la seule grandeur intéressante : le spectre d'énergie des primaires, déterminant la taille des gerbes de déplacement, intervient certainement particulièrement à basse température où la vitesse de migration des défauts élémentaires est trop faible pour que la gerbe soit dispersée et que l'irradiation du matériau puisse être considérée comme uniforme. Néanmoins, le nombre de déplacements atomique est actuellement un bon point de départ au moyen duquel il serait très souhaitable de faire un travail de synthèse de l'ensemble des résultats expérimentaux disponibles sur les différents aspects des dommages : variation dimensionnelle, fragilisation, fluage. L'harmonisation du langage qui semble se faire actuellement est un élément indispensable pour réaliser une telle synthèse et nous avons mis en évidence le fait très positif que les deux évaluations de sections efficaces UKNDF et ENDF/B conduisent, à un facteur de normalisation près, à des résultats très voisins pour les spectres de neutrons rapides.

D'une nature toute différente, mais également liés à l'irradiation neutronique, les taux de production d'impuretés dus aux réactions nucléaires sont également très importants à considérer, particulièrement quand les impuretés sont gazeuses (n,p), (n α), car alors elles favorisent le gonflement qui est un problème technologique grave pour les réacteurs à neutrons rapides. Dans ce domaine, il serait très souhaitable que l'A.I.E.A. fasse également une recommandation.

TABLEAU I

SECTIONS EFFICACES DE TRANSFERT D'ENERGIE ET TAUX DE DEPLACEMENT DANS L'ALUMINIUM (N=2.23E22 AT/G)

B.INF(MEV)	T EV.CM2/G	D EV.CM2/G	DPG CM2/G	
0.4140E-06	0.1423E 01	0.1126E 01	0.1125E-01	1./E
0.5316E-06	0.1222E 01	0.9677E 00	0.9665E-02	1./E
0.6826E-06	0.9649E 00	0.7638E 00	0.7623E-02	1./E
0.8764E-06	0.6765E 00	0.5356E 00	0.5336E-02	1./E
0.1125E-05	0.6163E 00	0.4881E 00	0.4855E-02	1./E
0.1445E-05	0.6015E 00	0.4765E 00	0.4732E-02	1./E
0.1855E-05	0.5826E 00	0.4616E 00	0.4575E-02	1./E
0.2382E-05	0.5583E 00	0.4425E 00	0.4372E-02	1./E
0.3058E-05	0.5270E 00	0.4180E 00	0.4112E-02	1./E
0.3928E-05	0.4869E 00	0.3864E 00	0.3778E-02	1./E
0.5043E-05	0.4354E 00	0.3460E 00	0.3349E-02	1./E
0.6476E-05	0.3693E 00	0.2940E 00	0.2798E-02	1./E
0.8315E-05	0.2881E 00	0.2303E 00	0.2121E-02	1./E
0.1068E-04	0.2664E 00	0.2137E 00	0.1904E-02	1./E
0.1371E-04	0.2738E 00	0.2203E 00	0.1904E-02	1./E
0.1760E-04	0.2832E 00	0.2287E 00	0.1904E-02	1./E
0.2260E-04	0.2953E 00	0.2394E 00	0.1904E-02	1./E
0.2902E-04	0.3108E 00	0.2532E 00	0.1904E-02	1./E
0.3727E-04	0.3308E 00	0.2710E 00	0.1904E-02	1./E
0.4785E-04	0.3564E 00	0.2938E 00	0.1904E-02	1./E
0.6144E-04	0.3893E 00	0.3231E 00	0.1904E-02	1./E
0.7889E-04	0.4315E 00	0.3606E 00	0.1905E-02	1./E
0.1013E-03	0.4857E 00	0.4074E 00	0.2274E-02	1./E
0.1301E-03	0.5554E 00	0.4661E 00	0.3076E-02	1./E
0.1670E-03	0.6448E 00	0.5416E 00	0.4106E-02	1./E
0.2144E-03	0.7596E 00	0.6384E 00	0.5428E-02	1./E
0.2754E-03	0.9070E 00	0.7627E 00	0.7126E-02	1./E
0.3536E-03	0.1096E 01	0.9224E 00	0.9305E-02	1./E
0.4540E-03	0.1339E 01	0.1127E 01	0.1210E-01	1./E
0.5829E-03	0.1651E 01	0.1391E 01	0.1570E-01	1./E
0.7485E-03	0.2052E 01	0.1729E 01	0.2031E-01	1./E
0.9611E-03	0.2564E 01	0.2154E 01	0.2541E-01	1./E
0.1234E-02	0.3217E 01	0.2683E 01	0.3035E-01	1./E
0.1585E-02	0.4056E 01	0.3362E 01	0.3665E-01	1./E
0.2035E-02	0.5132E 01	0.4233E 01	0.4474E-01	1./E
0.2613E-02	0.6525E 01	0.5358E 01	0.5526E-01	1./E
0.3355E-02	0.8420E 01	0.6862E 01	0.6997E-01	1./E
0.4307E-02	0.1107E 02	0.8945E 01	0.9021E-01	1./E
0.5531E-02	0.1772E 02	0.1421E 02	0.1431E 00	1./E
0.7102E-02	0.1655E 02	0.1316E 02	0.1320E 00	1./E
0.9119E-02	0.1969E 02	0.1551E 02	0.1552E 00	1./E
0.1171E-01	0.2184E 02	0.1702E 02	0.1707E 00	1./E
0.1503E-01	0.2372E 02	0.1830E 02	0.1832E 00	1./E
0.1930E-01	0.2337E 02	0.1782E 02	0.1784E 00	1./E
0.2479E-01	0.4452E 02	0.3339E 02	0.3339E 00	1./E
0.3183E-01	0.8816E 03	0.6545E 03	0.6545E 01	1./E
0.4087E-01	0.2752E 03	0.2016E 03	0.2016E 01	1./E
0.5247E-01	0.1591E 03	0.1147E 03	0.1147E 01	1./E
0.6738E-01	0.6642E 03	0.4669E 03	0.4669E 01	1./E

TABLEAU I (SUITE)

SECTIONS EFFICACES DE TRANSFERT D'ENERGIE ET TAUX DE DEPLACEMENT DANS L'ALUMINIUM (N=2.23E22 AT/G)

B.INF(MEV)	T EV.CM2/G	D EV.CM2/G	DPG CM2/G	
0.8652E-01	0.1362E 04	0.9504E 03	0.9504E 01	1./E
0.1111E 00	0.8574E 03	0.5875E 03	0.5875E 01	1./E
0.1228E 00	0.3419E 03	0.2326E 03	0.2326E 01	1./E
0.1357E 00	0.1454E 04	0.9788E 03	0.9788E 01	1./E
0.1500E 00	0.2679E 04	0.1790E 04	0.1790E 02	1./E
0.1657E 00	0.1507E 04	0.9987E 03	0.9987E 01	1./E
0.1832E 00	0.1054E 04	0.6913E 03	0.6913E 01	1./E
0.2024E 00	0.1775E 04	0.1153E 04	0.1153E 02	1./E
0.2237E 00	0.1337E 04	0.8592E 03	0.8592E 01	1./E
0.2472E 00	0.9362E 03	0.5941E 03	0.5941E 01	1./E
0.2732E 00	0.1986E 04	0.1242E 04	0.1242E 02	FIS.
0.3020E 00	0.1869E 04	0.1152E 04	0.1152E 02	FIS.
0.3337E 00	0.1722E 04	0.1045E 04	0.1045E 02	FIS.
0.3688E 00	0.1753E 04	0.1050E 04	0.1050E 02	FIS.
0.4076E 00	0.2918E 04	0.1724E 04	0.1724E 02	FIS.
0.4505E 00	0.2324E 04	0.1356E 04	0.1356E 02	FIS.
0.4979E 00	0.2768E 04	0.1594E 04	0.1594E 02	FIS.
0.5502E 00	0.2513E 04	0.1425E 04	0.1425E 02	FIS.
0.6081E 00	0.3065E 04	0.1705E 04	0.1705E 02	FIS.
0.6721E 00	0.2820E 04	0.1540E 04	0.1540E 02	FIS.
0.7427E 00	0.4334E 04	0.2323E 04	0.2323E 02	FIS.
0.8208E 00	0.3642E 04	0.1938E 04	0.1938E 02	FIS.
0.9072E 00	0.2903E 04	0.1509E 04	0.1509E 02	FIS.
0.1003E 01	0.3178E 04	0.1604E 04	0.1604E 02	FIS.
0.1108E 01	0.5135E 04	0.2553E 04	0.2553E 02	FIS.
0.1225E 01	0.4514E 04	0.2197E 04	0.2197E 02	FIS.
0.1353E 01	0.4667E 04	0.2206E 04	0.2206E 02	FIS.
0.1496E 01	0.4886E 04	0.2255E 04	0.2255E 02	FIS.
0.1653E 01	0.5426E 04	0.2433E 04	0.2433E 02	FIS.
0.1827E 01	0.5580E 04	0.2427E 04	0.2427E 02	FIS.
0.2019E 01	0.6745E 04	0.2854E 04	0.2854E 02	FIS.
0.2231E 01	0.5869E 04	0.2419E 04	0.2419E 02	FIS.
0.2466E 01	0.7873E 04	0.3096E 04	0.3096E 02	FIS.
0.2725E 01	0.8053E 04	0.3010E 04	0.3010E 02	FIS.
0.3012E 01	0.7645E 04	0.2808E 04	0.2808E 02	FIS.
0.3329E 01	0.8649E 04	0.3095E 04	0.3095E 02	FIS.
0.3679E 01	0.8904E 04	0.3072E 04	0.3072E 02	FIS.
0.4066E 01	0.9278E 04	0.3061E 04	0.3061E 02	FIS.
0.4493E 01	0.9282E 04	0.2975E 04	0.2975E 02	FIS.
0.4966E 01	0.9276E 04	0.2895E 04	0.2895E 02	FIS.
0.5488E 01	0.9949E 04	0.2926E 04	0.2926E 02	FIS.
0.6065E 01	0.1078E 05	0.3034E 04	0.3034E 02	FIS.
0.6703E 01	0.1126E 05	0.2984E 04	0.2984E 02	FIS.
0.7408E 01	0.1102E 05	0.2780E 04	0.2780E 02	FIS.
0.8187E 01	0.1156E 05	0.2777E 04	0.2777E 02	FIS.
0.9048E 01	0.1187E 05	0.2769E 04	0.2769E 02	FIS.
0.1000E 02	0.1293E 05	0.2862E 04	0.2862E 02	FIS.
0.1105E 02	0.1394E 05	0.2925E 04	0.2925E 02	FIS.
0.1221E 02	0.1549E 05	0.3076E 04	0.3076E 02	FIS.
0.1350E 02	0.1719E 05	0.3221E 04	0.3221E 02	FIS.
0.1492E 02				

TABLEAU II

SECTIONS EFFICACES DE TRANSFERT D'ENERGIE ET TAUX DE DEPLACEMENT DANS LE SILICIUM (N=2.14E22 AT/G)

B.INF(MEV)	T EV.CM2/G	D EV.CM2/G	DPG CM2/G	
0.4140E-06	0.3830E 00	0.3085E 00	0.3075E-02	1./E
0.5316E-06	0.3369E 00	0.2714E 00	0.2701E-02	1./E
0.6826E-06	0.2979E 00	0.2400E 00	0.2384E-02	1./E
0.8764E-06	0.2641E 00	0.2128E 00	0.2107E-02	1./E
0.1125E-05	0.2405E 00	0.1940E 00	0.1912E-02	1./E
0.1445E-05	0.2137E 00	0.1724E 00	0.1689E-02	1./E
0.1855E-05	0.1857E 00	0.1500E 00	0.1455E-02	1./E
0.2382E-05	0.1702E 00	0.1377E 00	0.1318E-02	1./E
0.3058E-05	0.1517E 00	0.1230E 00	0.1154E-02	1./E
0.3928E-05	0.1346E 00	0.1094E 00	0.9976E-03	1./E
0.5043E-05	0.1227E 00	0.1001E 00	0.8770E-03	1./E
0.6476E-05	0.1138E 00	0.9334E-01	0.7738E-03	1./E
0.8315E-05	0.1077E 00	0.8896E-01	0.6845E-03	1./E
0.1068E-04	0.1062E 00	0.8840E-01	0.6205E-03	1./E
0.1371E-04	0.1063E 00	0.8922E-01	0.5538E-03	1./E
0.1760E-04	0.1072E 00	0.9105E-01	0.4758E-03	1./E
0.2260E-04	0.1150E 00	0.9867E-01	0.4285E-03	1./E
0.2902E-04	0.1263E 00	0.1094E 00	0.3777E-03	1./E
0.3727E-04	0.1421E 00	0.1243E 00	0.3232E-03	1./E
0.4785E-04	0.1664E 00	0.1464E 00	0.2851E-03	1./E
0.6144E-04	0.1993E 00	0.1761E 00	0.2503E-03	1./E
0.7889E-04	0.2433E 00	0.2154E 00	0.2200E-03	1./E
0.1013E-03	0.3017E 00	0.2669E 00	0.1956E-03	1./E
0.1301E-03	0.3776E 00	0.3336E 00	0.1721E-03	1./E
0.1670E-03	0.4762E 00	0.4197E 00	0.1510E-03	1./E
0.2144E-03	0.6042E 00	0.5307E 00	0.1333E-03	1./E
0.2754E-03	0.7719E 00	0.6752E 00	0.1182E-02	1./E
0.3536E-03	0.9855E 00	0.8579E 00	0.6073E-02	1./E
0.4540E-03	0.1260E 01	0.1091E 01	0.1139E-01	1./E
0.5829E-03	0.1610E 01	0.1386E 01	0.1677E-01	1./E
0.7485E-03	0.2069E 01	0.1772E 01	0.2187E-01	1./E
0.9611E-03	0.2661E 01	0.2264E 01	0.2674E-01	1./E
0.1234E-02	0.3425E 01	0.2897E 01	0.3286E-01	1./E
0.1585E-02	0.4401E 01	0.3698E 01	0.4048E-01	1./E
0.2035E-02	0.5652E 01	0.4717E 01	0.5105E-01	1./E
0.2613E-02	0.7282E 01	0.6034E 01	0.6317E-01	1./E
0.3355E-02	0.9383E 01	0.7714E 01	0.7920E-01	1./E
0.4307E-02	0.1207E 02	0.9839E 01	0.1002E 00	1./E
0.5531E-02	0.1536E 02	0.1242E 02	0.1256E 00	1./E
0.7102E-02	0.1860E 02	0.1491E 02	0.1504E 00	1./E
0.9119E-02	0.2140E 02	0.1700E 02	0.1706E 00	1./E
0.1171E-01	0.2505E 02	0.1971E 02	0.1981E 00	1./E
0.1503E-01	0.2979E 02	0.2321E 02	0.2331E 00	1./E
0.1930E-01	0.3586E 02	0.2764E 02	0.2770E 00	1./E
0.2479E-01	0.4388E 02	0.3345E 02	0.3348E 00	1./E
0.3183E-01	0.5464E 02	0.4114E 02	0.4114E 00	1./E
0.4087E-01	0.7150E 02	0.5398E 02	0.5308E 00	1./E
0.5247E-01	0.1180E 03	0.8627E 02	0.8627E 00	1./E
0.6738E-01	0.1463E 03	0.1055E 03	0.1055E 01	1./E

TABLEAU II(SUITE)

SECTIONS EFFICACES DE TRANSFERT D'ENERGIE ET TAUX DE DEPLACEMENT DANS LE SILICIUM (N=2.14E22 AT/G)

B.INF(MEV)	T EV.CM2/G	D EV.CM2/G	DPG CM2/G	
0.8652E-01	0.1172E 03	0.8320E 02	0.8320E 00	1./E
0.1111E 00	0.9287E 02	0.6528E 02	0.6528E 00	1./E
0.1228E 00	0.7691E 02	0.5362E 02	0.5362E 00	1./E
0.1357E 00	0.2073E 03	0.1403E 03	0.1403E 01	1./E
0.1500E 00	0.8148E 03	0.5480E 03	0.5481E 01	1./E
0.1657E 00	0.1519E 04	0.1021E 04	0.1021E 02	1./E
0.1832E 00	0.2151E 04	0.1442E 04	0.1442E 02	1./E
0.2024E 00	0.2035E 04	0.1355E 04	0.1355E 02	1./E
0.2237E 00	0.1675E 04	0.1105E 04	0.1105E 02	1./E
0.2472E 00	0.1413E 04	0.9203E 03	0.9203E 01	1./E
0.2732E 00	0.1335E 04	0.8601E 03	0.8601E 01	FIS.
0.3020E 00	0.1300E 04	0.8272E 03	0.8272E 01	FIS.
0.3337E 00	0.1300E 04	0.8166E 03	0.8166E 01	FIS.
0.3688E 00	0.1320E 04	0.8173E 03	0.8173E 01	FIS.
0.4076E 00	0.1364E 04	0.8320E 03	0.8320E 01	FIS.
0.4505E 00	0.1454E 04	0.8736E 03	0.8736E 01	FIS.
0.4979E 00	0.2582E 04	0.1520E 04	0.1520E 02	FIS.
0.5502E 00	0.3339E 04	0.1946E 04	0.1946E 02	FIS.
0.6081E 00	0.1813E 04	0.1039E 04	0.1039E 02	FIS.
0.6721E 00	0.1822E 04	0.1026E 04	0.1026E 02	FIS.
0.7427E 00	0.2892E 04	0.1593E 04	0.1593E 02	FIS.
0.8208E 00	0.3583E 04	0.1945E 04	0.1945E 02	FIS.
0.9072E 00	0.4073E 04	0.2163E 04	0.2163E 02	FIS.
0.1003E 01	0.3715E 04	0.1935E 04	0.1935E 02	FIS.
0.1108E 01	0.2712E 04	0.1380E 04	0.1380E 02	FIS.
0.1225E 01	0.3405E 04	0.1692E 04	0.1692E 02	FIS.
0.1353E 01	0.3942E 04	0.1910E 04	0.1910E 02	FIS.
0.1496E 01	0.4725E 04	0.2228E 04	0.2228E 02	FIS.
0.1653E 01	0.5086E 04	0.2340E 04	0.2340E 02	FIS.
0.1827E 01	0.6847E 04	0.3072E 04	0.3072E 02	FIS.
0.2019E 01	0.5176E 04	0.2291E 04	0.2291E 02	FIS.
0.2231E 01	0.4948E 04	0.2141E 04	0.2141E 02	FIS.
0.2466E 01	0.5611E 04	0.2339E 04	0.2339E 02	FIS.
0.2725E 01	0.5522E 04	0.2226E 04	0.2226E 02	FIS.
0.3012E 01	0.5535E 04	0.2138E 04	0.2138E 02	FIS.
0.3329E 01	0.5290E 04	0.1963E 04	0.1963E 02	FIS.
0.3679E 01	0.5410E 04	0.1918E 04	0.1918E 02	FIS.
0.4066E 01	0.6801E 04	0.2307E 04	0.2307E 02	FIS.
0.4493E 01	0.7633E 04	0.2523E 04	0.2523E 02	FIS.
0.4966E 01	0.7832E 04	0.2543E 04	0.2543E 02	FIS.
0.5488E 01	0.8088E 04	0.2549E 04	0.2549E 02	FIS.
0.6065E 01	0.7905E 04	0.2380E 04	0.2380E 02	FIS.
0.6703E 01	0.7797E 04	0.2234E 04	0.2234E 02	FIS.
0.7408E 01	0.8222E 04	0.2237E 04	0.2237E 02	FIS.
0.8187E 01	0.8346E 04	0.2151E 04	0.2151E 02	FIS.
0.9048E 01	0.8882E 04	0.2162E 04	0.2162E 02	FIS.
0.1000E 02	0.1085E 05	0.2490E 04	0.2490E 02	FIS.
0.1105E 02	0.1398E 05	0.3027E 04	0.3027E 02	FIS.
0.1221E 02	0.1644E 05	0.3352E 04	0.3352E 02	FIS.
0.1350E 02	0.1879E 05	0.3602E 04	0.3602E 02	FIS.
0.1492E 02				

TABLEAU **III**

SECTIONS EFFICACES DE TRANSFERT D'ENERGIE ET TAUX DE DEPLACEMENT DANS LE CHROME (N=1.15E22 AT/G)

B.INF(MEV)	T EV.CM2/G	D EV.CM2/G	DPG CM2/G	
0.4140E-06	0.3198E 01	0.2672E 01	0.2671E-01	1./E
0.5316E-06	0.2823E 01	0.2359E 01	0.2358E-01	1./E
0.6826E-06	0.2488E 01	0.2078E 01	0.2077E-01	1./E
0.8764E-06	0.2212E 01	0.1848E 01	0.1847E-01	1./E
0.1125E-05	0.2016E 01	0.1684E 01	0.1682E-01	1./E
0.1445E-05	0.1783E 01	0.1490E 01	0.1487E-01	1./E
0.1855E-05	0.1530E 01	0.1279E 01	0.1275E-01	1./E
0.2382E-05	0.1351E 01	0.1129E 01	0.1125E-01	1./E
0.3058E-05	0.1187E 01	0.9917E 00	0.9861E-02	1./E
0.3928E-05	0.1048E 01	0.8759E 00	0.8687E-02	1./E
0.5043E-05	0.9299E 00	0.7775E 00	0.7683E-02	1./E
0.6476E-05	0.8256E 00	0.6906E 00	0.6787E-02	1./E
0.8315E-05	0.7320E 00	0.6127E 00	0.5974E-02	1./E
0.1068E-04	0.6710E 00	0.5620E 00	0.5423E-02	1./E
0.1371E-04	0.6067E 00	0.5087E 00	0.4833E-02	1./E
0.1760E-04	0.5316E 00	0.4464E 00	0.4138E-02	1./E
0.2260E-04	0.4861E 00	0.4090E 00	0.3672E-02	1./E
0.2902E-04	0.4462E 00	0.3765E 00	0.3228E-02	1./E
0.3727E-04	0.4144E 00	0.3511E 00	0.2820E-02	1./E
0.4785E-04	0.3935E 00	0.3350E 00	0.2464E-02	1./E
0.6144E-04	0.3893E 00	0.3332E 00	0.2194E-02	1./E
0.7889E-04	0.3940E 00	0.3395E 00	0.1931E-02	1./E
0.1013E-03	0.4178E 00	0.3623E 00	0.1740E-02	1./E
0.1301E-03	0.4567E 00	0.3985E 00	0.1565E-02	1./E
0.1670E-03	0.5074E 00	0.4457E 00	0.1347E-02	1./E
0.2144E-03	0.5887E 00	0.5190E 00	0.1204E-02	1./E
0.2754E-03	0.6997E 00	0.6182E 00	0.1076E-02	1./E
0.3536E-03	0.8438E 00	0.7467E 00	0.1214E-02	1./E
0.4540E-03	0.1039E 01	0.9186E 00	0.3314E-02	1./E
0.5829E-03	0.1306E 01	0.1151E 01	0.8607E-02	1./E
0.7485E-03	0.1658E 01	0.1457E 01	0.1801E-01	1./E
0.9611E-03	0.2116E 01	0.1851E 01	0.2526E-01	1./E
0.1234E-02	0.2786E 01	0.2423E 01	0.3123E-01	1./E
0.1585E-02	0.3690E 01	0.3193E 01	0.3811E-01	1./E
0.2035E-02	0.5239E 01	0.4518E 01	0.5101E-01	1./E
0.2613E-02	0.9658E 01	0.8282E 01	0.8926E-01	1./E
0.3355E-02	0.2789E 02	0.2378E 02	0.2485E 00	1./E
0.4307E-02	0.4313E 02	0.3656E 02	0.3766E 00	1./E
0.5531E-02	0.4888E 02	0.4118E 02	0.4193E 00	1./E
0.7102E-02	0.5501E 02	0.4604E 02	0.4663E 00	1./E
0.9119E-02	0.3651E 02	0.3035E 02	0.3053E 00	1./E
0.1171E-01	0.2649E 02	0.2186E 02	0.2198E 00	1./E
0.1503E-01	0.2205E 02	0.1805E 02	0.1808E 00	1./E
0.1930E-01	0.2942E 02	0.2389E 02	0.2393E 00	1./E
0.2479E-01	0.4287E 02	0.3448E 02	0.3454E 00	1./E
0.3183E-01	0.5235E 02	0.4176E 02	0.4180E 00	1./E
0.4087E-01	0.1152E 03	0.9089E 02	0.9093E 00	1./E
0.5247E-01	0.1316E 03	0.1032E 03	0.1032E 01	1./E
0.6738E-01	0.6517E 02	0.5060E 02	0.5060E 00	1./E

TABLEAU III(SUITE)

SECTIONS EFFICACES DE TRANSFERT D'ENERGIE ET TAUX DE DEPLACEMENT DANS LE CHROME (N=1.15E22 AT/G)

B.INF(MEV)	T EV.CM2/G	D EV.CM2/G	DPG CM2/G	
0.8652E-01	0.3382E 03	0.2594E 03	0.2594E 01	1./E
0.1111E 00	0.2393E 03	0.1825E 03	0.1825E 01	1./E
0.1228E 00	0.2139E 03	0.1622E 03	0.1622E 01	1./E
0.1357E 00	0.5808E 03	0.4385E 03	0.4385E 01	1./E
0.1500E 00	0.4456E 03	0.3351E 03	0.3351E 01	1./E
0.1657E 00	0.3078E 03	0.2304E 03	0.2304E 01	1./E
0.1832E 00	0.2711E 03	0.2020E 03	0.2020E 01	1./E
0.2024E 00	0.2307E 03	0.1711E 03	0.1711E 01	1./E
0.2237E 00	0.3096E 03	0.2284E 03	0.2284E 01	1./E
0.2472E 00	0.2357E 03	0.1732E 03	0.1732E 01	1./E
0.2732E 00	0.2002E 03	0.1463E 03	0.1463E 01	FIS.
0.3020E 00	0.3772E 03	0.2725E 03	0.2725E 01	FIS.
0.3337E 00	0.3781E 03	0.2711E 03	0.2711E 01	FIS.
0.3688E 00	0.4101E 03	0.2920E 03	0.2920E 01	FIS.
0.4076E 00	0.4924E 03	0.3490E 03	0.3490E 01	FIS.
0.4505E 00	0.5684E 03	0.4008E 03	0.4008E 01	FIS.
0.4979E 00	0.5800E 03	0.4075E 03	0.4075E 01	FIS.
0.5502E 00	0.5042E 03	0.3511E 03	0.3511E 01	FIS.
0.6081E 00	0.7991E 03	0.5527E 03	0.5527E 01	FIS.
0.6721E 00	0.6255E 03	0.4276E 03	0.4276E 01	FIS.
0.7427E 00	0.1049E 04	0.7112E 03	0.7112E 01	FIS.
0.8208E 00	0.1065E 04	0.7143E 03	0.7143E 01	FIS.
0.9072E 00	0.9394E 03	0.6265E 03	0.6265E 01	FIS.
0.1003E 01	0.1005E 04	0.6648E 03	0.6648E 01	FIS.
0.1108E 01	0.1030E 04	0.6738E 03	0.6738E 01	FIS.
0.1225E 01	0.1511E 04	0.9719E 03	0.9719E 01	FIS.
0.1353E 01	0.1347E 04	0.8603E 03	0.8603E 01	FIS.
0.1496E 01	0.1331E 04	0.8488E 03	0.8487E 01	FIS.
0.1653E 01	0.1475E 04	0.9321E 03	0.9321E 01	FIS.
0.1827E 01	0.2098E 04	0.1310E 04	0.1310E 02	FIS.
0.2019E 01	0.2379E 04	0.1472E 04	0.1472E 02	FIS.
0.2231E 01	0.2286E 04	0.1401E 04	0.1401E 02	FIS.
0.2466E 01	0.2444E 04	0.1481E 04	0.1481E 02	FIS.
0.2725E 01	0.2545E 04	0.1526E 04	0.1526E 02	FIS.
0.3012E 01	0.2612E 04	0.1553E 04	0.1553E 02	FIS.
0.3329E 01	0.2761E 04	0.1633E 04	0.1633E 02	FIS.
0.3679E 01	0.2813E 04	0.1657E 04	0.1657E 02	FIS.
0.4066E 01	0.2952E 04	0.1722E 04	0.1722E 02	FIS.
0.4493E 01	0.3123E 04	0.1801E 04	0.1801E 02	FIS.
0.4966E 01	0.3271E 04	0.1864E 04	0.1864E 02	FIS.
0.5488E 01	0.3406E 04	0.1918E 04	0.1918E 02	FIS.
0.6065E 01	0.3602E 04	0.1996E 04	0.1996E 02	FIS.
0.6703E 01	0.3835E 04	0.2087E 04	0.2087E 02	FIS.
0.7408E 01	0.4026E 04	0.2149E 04	0.2149E 02	FIS.
0.8187E 01	0.4242E 04	0.2213E 04	0.2213E 02	FIS.
0.9048E 01	0.4437E 04	0.2258E 04	0.2259E 02	FIS.
0.1000E 02	0.4720E 04	0.2338E 04	0.2338E 02	FIS.
0.1105E 02	0.5075E 04	0.2440E 04	0.2440E 02	FIS.
0.1221E 02	0.5492E 04	0.2564E 04	0.2564E 02	FIS.
0.1350E 02	0.6175E 04	0.2779E 04	0.2779E 02	FIS.
0.1492E 02				

TABLEAU **IV**

SECTIONS EFFICACES DE TRANSFERT D'ENERGIE ET TAUX DE DEPLACEMENT DANS LE FER (N=1.078E22 AT/G)

B.INF(MEV)	T EV.CM2/G	D EV.CM2/G	DPG CM2/G	
0.4140E-06	0.2476E 01	0.2073E 01	0.2071E-01	1./E
0.5316E-06	0.2185E 01	0.1830E 01	0.1827E-01	1./E
0.6826E-06	0.1926E 01	0.1613E 01	0.1610E-01	1./E
0.8764E-06	0.1704E 01	0.1427E 01	0.1423E-01	1./E
0.1125E-05	0.1521E 01	0.1274E 01	0.1269E-01	1./E
0.1445E-05	0.1336E 01	0.1119E 01	0.1113E-01	1./E
0.1855E-05	0.1184E 01	0.9919E 00	0.9839E-02	1./E
0.2382E-05	0.1050E 01	0.8802E 00	0.8699E-02	1./E
0.3058E-05	0.9264E 00	0.7766E 00	0.7633E-02	1./E
0.3928E-05	0.8216E 00	0.6891E 00	0.6721E-02	1./E
0.5043E-05	0.7367E 00	0.6183E 00	0.5965E-02	1./E
0.6476E-05	0.6584E 00	0.5532E 00	0.5252E-02	1./E
0.8315E-05	0.5937E 00	0.4995E 00	0.4635E-02	1./E
0.1068E-04	0.5432E 00	0.4580E 00	0.4117E-02	1./E
0.1371E-04	0.4968E 00	0.4200E 00	0.3606E-02	1./E
0.1760E-04	0.4646E 00	0.3941E 00	0.3179E-02	1./E
0.2260E-04	0.4452E 00	0.3793E 00	0.2814E-02	1./E
0.2902E-04	0.4361E 00	0.3736E 00	0.2478E-02	1./E
0.3727E-04	0.4422E 00	0.3810E 00	0.2195E-02	1./E
0.4785E-04	0.4607E 00	0.3995E 00	0.1921E-02	1./E
0.6144E-04	0.4987E 00	0.4353E 00	0.1692E-02	1./E
0.7889E-04	0.5599E 00	0.4915E 00	0.1500E-02	1./E
0.1013E-03	0.6468E 00	0.5707E 00	0.1326E-02	1./E
0.1301E-03	0.7651E 00	0.6780E 00	0.1170E-02	1./E
0.1670E-03	0.9199E 00	0.8179E 00	0.1023E-02	1./E
0.2144E-03	0.1122E 01	0.9997E 00	0.9070E-03	1./E
0.2754E-03	0.1375E 01	0.1227E 01	0.7952E-03	1./E
0.3536E-03	0.1691E 01	0.1507E 01	0.7074E-03	1./E
0.4540E-03	0.2075E 01	0.1844E 01	0.9336E-03	1./E
0.5829E-03	0.2531E 01	0.2243E 01	0.1352E-01	1./E
0.7485E-03	0.3052E 01	0.2696E 01	0.3289E-01	1./E
0.9611E-03	0.7863E 01	0.6746E 01	0.8077E-01	1./E
0.1234E-02	0.4604E 01	0.4031E 01	0.5556E-01	1./E
0.1585E-02	0.5478E 01	0.4771E 01	0.5973E-01	1./E
0.2035E-02	0.6378E 01	0.5527E 01	0.6343E-01	1./E
0.2613E-02	0.7383E 01	0.6361E 01	0.6957E-01	1./E
0.3355E-02	0.9853E 01	0.8434E 01	0.8906E-01	1./E
0.4307E-02	0.1032E 02	0.8784E 01	0.9076E-01	1./E
0.5531E-02	0.2097E 02	0.1773E 02	0.1811E 00	1./E
0.7102E-02	0.4741E 02	0.3984E 02	0.4038E 00	1./E
0.9119E-02	0.1970E 02	0.1644E 02	0.1655E 00	1./E
0.1171E-01	0.1558E 02	0.1291E 02	0.1300E 00	1./E
0.1503E-01	0.1281E 02	0.1054E 02	0.1056E 00	1./E
0.1930E-01	0.6050E 01	0.4943E 01	0.4947E-01	1./E
0.2479E-01	0.3310E 03	0.2678E 03	0.2684E 01	1./E
0.3183E-01	0.1117E 03	0.8962E 02	0.8973E 00	1./E
0.4087E-01	0.8847E 02	0.7032E 02	0.7036E 00	1./E
0.5247E-01	0.9000E 02	0.7095E 02	0.7096E 00	1./E
0.6738E-01	0.2153E 03	0.1678E 03	0.1678E 01	1./E

TABLEAU **IV** (SUITE)

SECTIONS EFFICACES DE TRANSFERT D'ENERGIE ET TAUX DE DEPLACEMENT DANS LE FER (N=1.078E22 AT/G)

B.INF(MEV)	T EV.CM2/G	D EV.CM2/G	DPG CM2/G	
0.8652E-01	0.1499E 03	0.1159E 03	0.1159E 01	1./E
0.1111E 00	0.8873E 02	0.6809E 02	0.6808E 00	1./E
0.1228E 00	0.1606E 03	0.1226E 03	0.1226E 01	1./E
0.1357E 00	0.3059E 03	0.2326E 03	0.2326E 01	1./E
0.1500E 00	0.1438E 03	0.1090E 03	0.1090E 01	1./E
0.1657E 00	0.2049E 03	0.1546E 03	0.1546E 01	1./E
0.1832E 00	0.3977E 03	0.2983E 03	0.2983E 01	1./E
0.2024E 00	0.2330E 03	0.1740E 03	0.1740E 01	1./E
0.2237E 00	0.2591E 03	0.1925E 03	0.1925E 01	1./E
0.2472E 00	0.2192E 03	0.1620E 03	0.1620E 01	1./E
0.2732E 00	0.2754E 03	0.2026E 03	0.2026E 01	FIS.
0.3020E 00	0.3244E 03	0.2370E 03	0.2370E 01	FIS.
0.3337E 00	0.3155E 03	0.2290E 03	0.2290E 01	FIS.
0.3688E 00	0.5400E 03	0.3895E 03	0.3895E 01	FIS.
0.4076E 00	0.5657E 03	0.4060E 03	0.4060E 01	FIS.
0.4505E 00	0.4695E 03	0.3352E 03	0.3352E 01	FIS.
0.4979E 00	0.4232E 03	0.3008E 03	0.3008E 01	FIS.
0.5502E 00	0.4196E 03	0.2965E 03	0.2965E 01	FIS.
0.6081E 00	0.3717E 03	0.2603E 03	0.2603E 01	FIS.
0.6721E 00	0.6438E 03	0.4471E 03	0.4471E 01	FIS.
0.7427E 00	0.8931E 03	0.6161E 03	0.6161E 01	FIS.
0.8208E 00	0.6123E 03	0.4210E 03	0.4210E 01	FIS.
0.9072E 00	0.5294E 03	0.3637E 03	0.3637E 01	FIS.
0.1003E 01	0.7270E 03	0.4944E 03	0.4944E 01	FIS.
0.1108E 01	0.7801E 03	0.5214E 03	0.5214E 01	FIS.
0.1225E 01	0.9622E 03	0.6379E 03	0.6379E 01	FIS.
0.1353E 01	0.1212E 04	0.7935E 03	0.7935E 01	FIS.
0.1496E 01	0.1223E 04	0.7971E 03	0.7971E 01	FIS.
0.1653E 01	0.1268E 04	0.8184E 03	0.8184E 01	FIS.
0.1827E 01	0.1585E 04	0.1012E 04	0.1012E 02	FIS.
0.2019E 01	0.1786E 04	0.1125E 04	0.1125E 02	FIS.
0.2231E 01	0.1977E 04	0.1236E 04	0.1236E 02	FIS.
0.2466E 01	0.2114E 04	0.1305E 04	0.1305E 02	FIS.
0.2725E 01	0.2012E 04	0.1237E 04	0.1237E 02	FIS.
0.3012E 01	0.2451E 04	0.1493E 04	0.1493E 02	FIS.
0.3329E 01	0.2571E 04	0.1553E 04	0.1553E 02	FIS.
0.3679E 01	0.2734E 04	0.1639E 04	0.1639E 02	FIS.
0.4066E 01	0.2667E 04	0.1598E 04	0.1598E 02	FIS.
0.4493E 01	0.2602E 04	0.1541E 04	0.1541E 02	FIS.
0.4966E 01	0.2800E 04	0.1660E 04	0.1660E 02	FIS.
0.5488E 01	0.3193E 04	0.1858E 04	0.1858E 02	FIS.
0.6065E 01	0.3253E 04	0.1871E 04	0.1871E 02	FIS.
0.6703E 01	0.3202E 04	0.1827E 04	0.1827E 02	FIS.
0.7408E 01	0.3450E 04	0.1926E 04	0.1926E 02	FIS.
0.8187E 01	0.3657E 04	0.2003E 04	0.2003E 02	FIS.
0.9048E 01	0.3841E 04	0.2062E 04	0.2062E 02	FIS.
0.1000E 02	0.0	0.0	0.0	FIS.
0.1105E 02	0.0	0.0	0.0	FIS.
0.1221E 02	0.0	0.0	0.0	FIS.
0.1350E 02	0.0	0.0	0.0	FIS.
0.1492E 02				

TABLEAU V

SECTIONS EFFICACES DE TRANSFERT D'ENERGIE ET TAUX DE DEPLACEMENT DANS LE NICKEL (N=1.026E22 AT/G)

B.INF(MEV)	T EV.CM2/G	D EV.CM2/G	DPG CM2/G	
0.4140E-06	0.6241E 01	0.5176E 01	0.5173E-01	L./E
0.5316E-06	0.5503E 01	0.4563E 01	0.4560E-01	L./E
0.6826E-06	0.4852E 01	0.4024E 01	0.4020E-01	L./E
0.8764E-06	0.4294E 01	0.3561E 01	0.3556E-01	L./E
0.1125E-05	0.3829E 01	0.3175E 01	0.3169E-01	L./E
0.1445E-05	0.3356E 01	0.2783E 01	0.2775E-01	L./E
0.1855E-05	0.2960E 01	0.2455E 01	0.2444E-01	L./E
0.2382E-05	0.2613E 01	0.2168E 01	0.2154E-01	L./E
0.3058E-05	0.2321E 01	0.1926E 01	0.1908E-01	L./E
0.3928E-05	0.2050E 01	0.1702E 01	0.1679E-01	L./E
0.5043E-05	0.1818E 01	0.1510E 01	0.1480E-01	L./E
0.6476E-05	0.1617E 01	0.1344E 01	0.1305E-01	L./E
0.8315E-05	0.1445E 01	0.1202E 01	0.1153E-01	L./E
0.1068E-04	0.1311E 01	0.1092E 01	0.1029E-01	L./E
0.1371E-04	0.1177E 01	0.9821E 00	0.9011E-02	L./E
0.1760E-04	0.1074E 01	0.8980E 00	0.7940E-02	L./E
0.2260E-04	0.9928E 00	0.8331E 00	0.6996E-02	L./E
0.2902E-04	0.9380E 00	0.7903E 00	0.6190E-02	L./E
0.3727E-04	0.9034E 00	0.7652E 00	0.5454E-02	L./E
0.4785E-04	0.8948E 00	0.7626E 00	0.4806E-02	L./E
0.6144E-04	0.9155E 00	0.7856E 00	0.4239E-02	L./E
0.7889E-04	0.9692E 00	0.8376E 00	0.3738E-02	L./E
0.1013E-03	0.1066E 01	0.9277E 00	0.3334E-02	L./E
0.1301E-03	0.1204E 01	0.1054E 01	0.2929E-02	L./E
0.1670E-03	0.1400E 01	0.1232E 01	0.2580E-02	L./E
0.2144E-03	0.1666E 01	0.1473E 01	0.2273E-02	L./E
0.2754E-03	0.2019E 01	0.1791E 01	0.2003E-02	L./E
0.3536E-03	0.2472E 01	0.2195E 01	0.1766E-02	L./E
0.4540E-03	0.3015E 01	0.2675E 01	0.1558E-02	L./E
0.5829E-03	0.3652E 01	0.3234E 01	0.1471E-01	L./E
0.7485E-03	0.4456E 01	0.3935E 01	0.4483E-01	L./E
0.9611E-03	0.5569E 01	0.4900E 01	0.6662E-01	L./E
0.1234E-02	0.7113E 01	0.6232E 01	0.8542E-01	L./E
0.1585E-02	0.9299E 01	0.8107E 01	0.1024E 00	L./E
0.2035E-02	0.1243E 02	0.1078E 02	0.1256E 00	L./E
0.2613E-02	0.1757E 02	0.1516E 02	0.1664E 00	L./E
0.3355E-02	0.3023E 02	0.2593E 02	0.2749E 00	L./E
0.4307E-02	0.4437E 02	0.3783E 02	0.3924E 00	L./E
0.5531E-02	0.3002E 02	0.2544E 02	0.2601E 00	L./E
0.7102E-02	0.2592E 02	0.2182E 02	0.2211E 00	L./E
0.9119E-02	0.5303E 02	0.4430E 02	0.4458E 00	L./E
0.1171E-01	0.2087E 03	0.1733E 03	0.1745E 01	L./E
0.1503E-01	0.3482E 03	0.2873E 03	0.2882E 01	L./E
0.1930E-01	0.1286E 03	0.1053E 03	0.1054E 01	L./E
0.2479E-01	0.1573E 03	0.1276E 03	0.1280E 01	L./E
0.3183E-01	0.8858E 02	0.7132E 02	0.7142E 00	L./E
0.4087E-01	0.7491E 02	0.5974E 02	0.5979E 00	L./E
0.5247E-01	0.1981E 03	0.1562E 03	0.1562E 01	L./E
0.6738E-01	0.2558E 03	0.2005E 03	0.2005E 01	L./E

TABLEAU V (SUITE)

SECTIONS EFFICACES DE TRANSFERT D'ENERGIE ET TAUX DE DEPLACEMENT DANS LE NICKEL (N=1.026E22 AT/G)

B.INF(MEV)	T EV.CM2/G	D EV.CM2/G	DPG CM2/G	
0.8652E-01	0.1980E 03	0.1535E 03	0.1535E 01	1./E
0.1111E 00	0.1961E 03	0.1511E 03	0.1511E 01	1./E
0.1228E 00	0.1465E 03	0.1124E 03	0.1124E 01	1./E
0.1357E 00	0.3828E 03	0.2923E 03	0.2923E 01	1./E
0.1500E 00	0.4388E 03	0.3334E 03	0.3334E 01	1./E
0.1657E 00	0.3247E 03	0.2459E 03	0.2459E 01	1./E
0.1832E 00	0.3063E 03	0.2308E 03	0.2308E 01	1./E
0.2024E 00	0.4463E 03	0.3348E 03	0.3348E 01	1./E
0.2237E 00	0.4293E 03	0.3202E 03	0.3202E 01	1./E
0.2472E 00	0.3901E 03	0.2896E 03	0.2896E 01	1./E
0.2732E 00	0.5100E 03	0.3766E 03	0.3767E 01	FIS.
0.3020E 00	0.4697E 03	0.3449E 03	0.3449E 01	FIS.
0.3337E 00	0.5129E 03	0.3745E 03	0.3745E 01	FIS.
0.3688E 00	0.3940E 03	0.2860E 03	0.2860E 01	FIS.
0.4076E 00	0.5751E 03	0.4146E 03	0.4146E 01	FIS.
0.4505E 00	0.5883E 03	0.4219E 03	0.4219E 01	FIS.
0.4979E 00	0.5273E 03	0.3764E 03	0.3764E 01	FIS.
0.5502E 00	0.4780E 03	0.3381E 03	0.3381E 01	FIS.
0.6081E 00	0.6803E 03	0.4782E 03	0.4782E 01	FIS.
0.6721E 00	0.6479E 03	0.4528E 03	0.4528E 01	FIS.
0.7427E 00	0.7302E 03	0.5052E 03	0.5052E 01	FIS.
0.8208E 00	0.8378E 03	0.5749E 03	0.5749E 01	FIS.
0.9072E 00	0.8212E 03	0.5611E 03	0.5611E 01	FIS.
0.1003E 01	0.8712E 03	0.5894E 03	0.5894E 01	FIS.
0.1108E 01	0.1160E 04	0.7739E 03	0.7739E 01	FIS.
0.1225E 01	0.1386E 04	0.9178E 03	0.9178E 01	FIS.
0.1353E 01	0.1219E 04	0.8054E 03	0.8054E 01	FIS.
0.1496E 01	0.1280E 04	0.8420E 03	0.8420E 01	FIS.
0.1653E 01	0.1365E 04	0.8912E 03	0.8912E 01	FIS.
0.1827E 01	0.1471E 04	0.9528E 03	0.9528E 01	FIS.
0.2019E 01	0.1595E 04	0.1024E 04	0.1024E 02	FIS.
0.2231E 01	0.1727E 04	0.1099E 04	0.1099E 02	FIS.
0.2466E 01	0.1816E 04	0.1148E 04	0.1148E 02	FIS.
0.2725E 01	0.1832E 04	0.1153E 04	0.1153E 02	FIS.
0.3012E 01	0.1832E 04	0.1148E 04	0.1148E 02	FIS.
0.3329E 01	0.1942E 04	0.1209E 04	0.1209E 02	FIS.
0.3679E 01	0.2050E 04	0.1267E 04	0.1267E 02	FIS.
0.4066E 01	0.2134E 04	0.1311E 04	0.1311E 02	FIS.
0.4493E 01	0.2119E 04	0.1305E 04	0.1305E 02	FIS.
0.4966E 01	0.2144E 04	0.1318E 04	0.1318E 02	FIS.
0.5488E 01	0.2299E 04	0.1396E 04	0.1396E 02	FIS.
0.6065E 01	0.2423E 04	0.1453E 04	0.1453E 02	FIS.
0.6703E 01	0.2526E 04	0.1494E 04	0.1494E 02	FIS.
0.7408E 01	0.2621E 04	0.1528E 04	0.1528E 02	FIS.
0.8187E 01	0.2764E 04	0.1586E 04	0.1586E 02	FIS.
0.9048E 01	0.2923E 04	0.1650E 04	0.1650E 02	FIS.
0.1000E 02	0.3108E 04	0.1723E 04	0.1723E 02	FIS.
0.1105E 02	0.3324E 04	0.1809E 04	0.1809E 02	FIS.
0.1221E 02	0.3627E 04	0.1935E 04	0.1935E 02	FIS.
0.1350E 02	0.4034E 04	0.2108E 04	0.2108E 02	FIS.
0.1492E 02				

TABLEAU VI

SECTIONS EFFICACES DE TRANSFERT D'ENERGIE ET TAUX DE DEPLACEMENT DANS LE CUIVRE (N=0.9479E22 AT/G)

B.INF(MEV)	T EV.CM2/G	D EV.CM2/G	DPG CM2/G	
0.4140E-06	0.3341E 01	0.2813E 01	0.2812E-01	1./E
0.5316E-06	0.2782E 01	0.2342E 01	0.2341E-01	1./E
0.6826E-06	0.2478E 01	0.2087E 01	0.2085E-01	1./E
0.8764E-06	0.2169E 01	0.1826E 01	0.1824E-01	1./E
0.1125E-05	0.1958E 01	0.1649E 01	0.1646E-01	1./E
0.1445E-05	0.1724E 01	0.1452E 01	0.1448E-01	1./E
0.1855E-05	0.1470E 01	0.1238E 01	0.1233E-01	1./E
0.2382E-05	0.1290E 01	0.1086E 01	0.1081E-01	1./E
0.3058E-05	0.1123E 01	0.9461E 00	0.9392E-02	1./E
0.3928E-05	0.9782E 00	0.8241E 00	0.8153E-02	1./E
0.5043E-05	0.8523E 00	0.7182E 00	0.7069E-02	1./E
0.6476E-05	0.7411E 00	0.6248E 00	0.6103E-02	1./E
0.8315E-05	0.6445E 00	0.5438E 00	0.5253E-02	1./E
0.1068E-04	0.5784E 00	0.4884E 00	0.4647E-02	1./E
0.1371E-04	0.5096E 00	0.4309E 00	0.4006E-02	1./E
0.1760E-04	0.4289E 00	0.3635E 00	0.3247E-02	1./E
0.2260E-04	0.3773E 00	0.3207E 00	0.2711E-02	1./E
0.2902E-04	0.3334E 00	0.2845E 00	0.2212E-02	1./E
0.3727E-04	0.3045E 00	0.2613E 00	0.1804E-02	1./E
0.4785E-04	0.2889E 00	0.2495E 00	0.1459E-02	1./E
0.6144E-04	0.2879E 00	0.2504E 00	0.1178E-02	1./E
0.7889E-04	0.3018E 00	0.2643E 00	0.9496E-03	1./E
0.1013E-03	0.3347E 00	0.2949E 00	0.7905E-03	1./E
0.1301E-03	0.3879E 00	0.3430E 00	0.7113E-03	1./E
0.1670E-03	0.4972E 00	0.4378E 00	0.1204E-02	1./E
0.2144E-03	0.2334E 01	0.1990E 01	0.1591E-01	1./E
0.2754E-03	0.7004E 00	0.6204E 00	0.1142E-02	1./E
0.3536E-03	0.8481E 00	0.7524E 00	0.1153E-02	1./E
0.4540E-03	0.2660E 02	0.2252E 02	0.2040E 00	1./E
0.5829E-03	0.4122E 01	0.3547E 01	0.2416E-01	1./E
0.7485E-03	0.2197E 01	0.1920E 01	0.1890E-01	1./E
0.9611E-03	0.2210E 01	0.1936E 01	0.2487E-01	1./E
0.1234E-02	0.2372E 01	0.2079E 01	0.2818E-01	1./E
0.1585E-02	0.1223E 02	0.1067E 02	0.1324E 00	1./E
0.2035E-02	0.2576E 02	0.2246E 02	0.2697E 00	1./E
0.2613E-02	0.9445E 01	0.8177E 01	0.9082E-01	1./E
0.3355E-02	0.1251E 02	0.1079E 02	0.1152E 00	1./E
0.4307E-02	0.2946E 02	0.2523E 02	0.2630E 00	1./E
0.5531E-02	0.2156E 02	0.1838E 02	0.1885E 00	1./E
0.7102E-02	0.4261E 02	0.3611E 02	0.3660E 00	1./E
0.9119E-02	0.4993E 02	0.4205E 02	0.4250E 00	1./E
0.1171E-01	0.4226E 02	0.3534E 02	0.3560E 00	1./E
0.1503E-01	0.5273E 02	0.4379E 02	0.4395E 00	1./E
0.1930E-01	0.5764E 02	0.4753E 02	0.4757E 00	1./E
0.2479E-01	0.7401E 02	0.6058E 02	0.6071E 00	1./E
0.3183E-01	0.8268E 02	0.6712E 02	0.6721E 00	1./E
0.4087E-01	0.9700E 02	0.7811E 02	0.7818E 00	1./E
0.5247E-01	0.1565E 03	0.1248E 03	0.1248E 01	1./E
0.6738E-01	0.1786E 03	0.1411E 03	0.1411E 01	1./E

TABLEAU VI (SUITE)

SECTIONS EFFICACES DE TRANSFERT D'ENERGIE ET TAUX DE DEPLACEMENT DANS LE CUIVRE (N=0.9479E22 AT/G)

B.INF(MEV)	T EV.CM2/G	D EV.CM2/G	DPG CM2/G	
0.8652E-01	0.1684E 03	0.1318E 03	0.1318E 01	1./E
0.1111E 00	0.1592E 03	0.1238E 03	0.1238E 01	1./E
0.1228E 00	0.1807E 03	0.1399E 03	0.1399E 01	1./E
0.1357E 00	0.2282E 03	0.1759E 03	0.1759E 01	1./E
0.1500E 00	0.2289E 03	0.1758E 03	0.1758E 01	1./E
0.1657E 00	0.2331E 03	0.1783E 03	0.1783E 01	1./E
0.1832E 00	0.2574E 03	0.1960E 03	0.1960E 01	1./E
0.2024E 00	0.2835E 03	0.2149E 03	0.2149E 01	1./E
0.2237E 00	0.3121E 03	0.2354E 03	0.2354E 01	1./E
0.2472E 00	0.3437E 03	0.2581E 03	0.2581E 01	1./E
0.2732E 00	0.3791E 03	0.2835E 03	0.2835E 01	FIS.
0.3020E 00	0.4091E 03	0.3045E 03	0.3045E 01	FIS.
0.3337E 00	0.4357E 03	0.3228E 03	0.3228E 01	FIS.
0.3688E 00	0.4652E 03	0.3430E 03	0.3430E 01	FIS.
0.4076E 00	0.4988E 03	0.3656E 03	0.3656E 01	FIS.
0.4505E 00	0.5364E 03	0.3908E 03	0.3908E 01	FIS.
0.4979E 00	0.5721E 03	0.4142E 03	0.4142E 01	FIS.
0.5502E 00	0.6049E 03	0.4352E 03	0.4352E 01	FIS.
0.6081E 00	0.6359E 03	0.4548E 03	0.4548E 01	FIS.
0.6721E 00	0.6783E 03	0.4823E 03	0.4823E 01	FIS.
0.7427E 00	0.7331E 03	0.5178E 03	0.5178E 01	FIS.
0.8208E 00	0.7678E 03	0.5391E 03	0.5391E 01	FIS.
0.9072E 00	0.8146E 03	0.5680E 03	0.5680E 01	FIS.
0.1003E 01	0.8554E 03	0.5929E 03	0.5929E 01	FIS.
0.1108E 01	0.9141E 03	0.6293E 03	0.6293E 01	FIS.
0.1225E 01	0.9860E 03	0.6732E 03	0.6732E 01	FIS.
0.1353E 01	0.1030E 04	0.6983E 03	0.6983E 01	FIS.
0.1496E 01	0.1066E 04	0.7183E 03	0.7183E 01	FIS.
0.1653E 01	0.1090E 04	0.7308E 03	0.7308E 01	FIS.
0.1827E 01	0.1130E 04	0.7546E 03	0.7546E 01	FIS.
0.2019E 01	0.1213E 04	0.8042E 03	0.8042E 01	FIS.
0.2231E 01	0.1325E 04	0.8713E 03	0.8713E 01	FIS.
0.2466E 01	0.1406E 04	0.9190E 03	0.9190E 01	FIS.
0.2725E 01	0.1559E 04	0.1011E 04	0.1011E 02	FIS.
0.3012E 01	0.1741E 04	0.1119E 04	0.1119E 02	FIS.
0.3329E 01	0.1840E 04	0.1174E 04	0.1174E 02	FIS.
0.3679E 01	0.2029E 04	0.1282E 04	0.1282E 02	FIS.
0.4066E 01	0.2234E 04	0.1399E 04	0.1399E 02	FIS.
0.4493E 01	0.2333E 04	0.1454E 04	0.1454E 02	FIS.
0.4966E 01	0.2426E 04	0.1503E 04	0.1503E 02	FIS.
0.5488E 01	0.2615E 04	0.1601E 04	0.1601E 02	FIS.
0.6065E 01	0.2788E 04	0.1685E 04	0.1685E 02	FIS.
0.6703E 01	0.2940E 04	0.1753E 04	0.1753E 02	FIS.
0.7408E 01	0.3113E 04	0.1830E 04	0.1830E 02	FIS.
0.8187E 01	0.3277E 04	0.1898E 04	0.1898E 02	FIS.
0.9048E 01	0.3381E 04	0.1928E 04	0.1928E 02	FIS.
0.1000E 02	0.3561E 04	0.1998E 04	0.1998E 02	FIS.
0.1105E 02	0.3811E 04	0.2105E 04	0.2105E 02	FIS.
0.1221E 02	0.4104E 04	0.2225E 04	0.2225E 02	FIS.
0.1350E 02	0.4499E 04	0.2380E 04	0.2380E 02	FIS.
0.1492E 02				

TABLEAU **VII**

SECTIONS EFFICACES DE TRANSFERT D'ENERGIE ET TAUX DE DEPLACEMENT DANS LE ZIRCONIUM (N=0.66E22 AT/G)

B.INF(MEV)	T EV.CM2/G	D EV.CM2/G	DPG CM2/G	
0.4140E-06	0.5846E-01	0.5074E-01	0.5036E-03	1./E
0.5316E-06	0.5184E-01	0.4499E-01	0.4451E-03	1./E
0.6826E-06	0.4651E-01	0.4037E-01	0.3975E-03	1./E
0.8764E-06	0.4027E-01	0.3496E-01	0.3417E-03	1./E
0.1125E-05	0.3663E-01	0.3181E-01	0.3080E-03	1./E
0.1445E-05	0.3286E-01	0.2854E-01	0.2724E-03	1./E
0.1855E-05	0.2904E-01	0.2524E-01	0.2356E-03	1./E
0.2382E-05	0.2740E-01	0.2384E-01	0.2168E-03	1./E
0.3058E-05	0.2552E-01	0.2222E-01	0.1945E-03	1./E
0.3928E-05	0.2311E-01	0.2015E-01	0.1660E-03	1./E
0.5043E-05	0.2171E-01	0.1897E-01	0.1440E-03	1./E
0.6476E-05	0.2153E-01	0.1884E-01	0.1298E-03	1./E
0.8315E-05	0.2135E-01	0.1874E-01	0.1121E-03	1./E
0.1068E-04	0.2237E-01	0.1969E-01	0.1002E-03	1./E
0.1371E-04	0.2423E-01	0.2138E-01	0.8966E-04	1./E
0.1760E-04	0.2677E-01	0.2368E-01	0.7747E-04	1./E
0.2260E-04	0.3108E-01	0.2755E-01	0.7109E-04	1./E
0.2902E-04	0.3683E-01	0.3270E-01	0.6465E-04	1./E
0.3727E-04	0.4421E-01	0.3932E-01	0.5639E-04	1./E
0.4785E-04	0.5400E-01	0.4809E-01	0.4877E-04	1./E
0.6144E-04	0.6724E-01	0.5992E-01	0.4520E-04	1./E
0.7889E-04	0.8426E-01	0.7513E-01	0.4081E-04	1./E
0.1013E-03	0.1084E 00	0.9664E-01	0.5632E-04	1./E
0.1301E-03	0.1821E 00	0.1613E 00	0.4483E-03	1./E
0.1670E-03	0.5651E 00	0.4946E 00	0.3456E-02	1./E
0.2144E-03	0.3097E 00	0.2740E 00	0.8744E-03	1./E
0.2754E-03	0.2824E 01	0.2465E 01	0.1932E-01	1./E
0.3536E-03	0.3906E 00	0.3480E 00	0.2572E-03	1./E
0.4540E-03	0.4584E 00	0.4093E 00	0.3307E-04	1./E
0.5829E-03	0.1111E 01	0.9828E 00	0.3255E-02	1./E
0.7485E-03	0.8109E 00	0.7225E 00	0.6577E-03	1./E
0.9611E-03	0.9354E 00	0.8352E 00	0.5694E-02	1./E
0.1234E-02	0.1950E 01	0.1737E 01	0.2186E-01	1./E
0.1585E-02	0.2043E 01	0.1810E 01	0.2387E-01	1./E
0.2035E-02	0.2513E 01	0.2224E 01	0.2933E-01	1./E
0.2613E-02	0.6918E 01	0.6113E 01	0.7606E-01	1./E
0.3355E-02	0.7938E 01	0.6976E 01	0.7870E-01	1./E
0.4307E-02	0.8385E 01	0.7340E 01	0.7975E-01	1./E
0.5531E-02	0.8847E 01	0.7706E 01	0.8101E-01	1./E
0.7102E-02	0.1013E 02	0.8772E 01	0.9028E-01	1./E
0.9119E-02	0.1337E 02	0.1151E 02	0.1175E 00	1./E
0.1171E-01	0.1728E 02	0.1477E 02	0.1500E 00	1./E
0.1503E-01	0.2230E 02	0.1895E 02	0.1914E 00	1./E
0.1930E-01	0.2872E 02	0.2426E 02	0.2441E 00	1./E
0.2479E-01	0.3691E 02	0.3098E 02	0.3106E 00	1./E
0.3183E-01	0.4725E 02	0.3941E 02	0.3951E 00	1./E
0.4087E-01	0.6019E 02	0.4985E 02	0.4997E 00	1./E
0.5247E-01	0.7629E 02	0.6273E 02	0.6281E 00	1./E
0.6738E-01	0.9635E 02	0.7863E 02	0.7868E 00	1./E

TABLEAU VII (SUITE)

SECTIONS EFFICACES DE TRANSFERT D'ENERGIE ET TAUX DE DEPLACEMENT DANS LE ZIRCONIUM (N=0.66E22 AT/G)

B.INF(MEV)	T EV.CM2/G	D EV.CM2/G	DPG CM2/G	
0.8652E-01	0.1212E 03	0.9814E 02	0.9815E 00	1./E
0.1111E 00	0.1415E 03	0.1137E 03	0.1137E 01	1./E
0.1228E 00	0.1547E 03	0.1239E 03	0.1239E 01	1./E
0.1357E 00	0.1694E 03	0.1352E 03	0.1352E 01	1./E
0.1500E 00	0.1856E 03	0.1476E 03	0.1476E 01	1./E
0.1657E 00	0.2035E 03	0.1613E 03	0.1613E 01	1./E
0.1832E 00	0.2232E 03	0.1765E 03	0.1765E 01	1./E
0.2024E 00	0.2447E 03	0.1928E 03	0.1928E 01	1./E
0.2237E 00	0.2682E 03	0.2105E 03	0.2105E 01	1./E
0.2472E 00	0.2942E 03	0.2301E 03	0.2301E 01	1./E
0.2732E 00	0.3234E 03	0.2520E 03	0.2520E 01	FIS.
0.3020E 00	0.3447E 03	0.2676E 03	0.2676E 01	FIS.
0.3337E 00	0.3701E 03	0.2863E 03	0.2863E 01	FIS.
0.3688E 00	0.4192E 03	0.3232E 03	0.3232E 01	FIS.
0.4076E 00	0.4874E 03	0.3746E 03	0.3746E 01	FIS.
0.4505E 00	0.4978E 03	0.3815E 03	0.3815E 01	FIS.
0.4979E 00	0.5210E 03	0.3980E 03	0.3980E 01	FIS.
0.5502E 00	0.5504E 03	0.4191E 03	0.4191E 01	FIS.
0.6081E 00	0.5401E 03	0.4095E 03	0.4095E 01	FIS.
0.6721E 00	0.5909E 03	0.4461E 03	0.4461E 01	FIS.
0.7427E 00	0.6200E 03	0.4661E 03	0.4661E 01	FIS.
0.8208E 00	0.6443E 03	0.4823E 03	0.4823E 01	FIS.
0.9072E 00	0.6448E 03	0.4806E 03	0.4806E 01	FIS.
0.1003E 01	0.5785E 03	0.4293E 03	0.4293E 01	FIS.
0.1108E 01	0.6147E 03	0.4539E 03	0.4539E 01	FIS.
0.1225E 01	0.6655E 03	0.4886E 03	0.4886E 01	FIS.
0.1353E 01	0.6772E 03	0.4941E 03	0.4941E 01	FIS.
0.1496E 01	0.6903E 03	0.5005E 03	0.5005E 01	FIS.
0.1653E 01	0.7292E 03	0.5251E 03	0.5251E 01	FIS.
0.1827E 01	0.7716E 03	0.5522E 03	0.5522E 01	FIS.
0.2019E 01	0.7755E 03	0.5537E 03	0.5537E 01	FIS.
0.2231E 01	0.7986E 03	0.5685E 03	0.5685E 01	FIS.
0.2466E 01	0.8240E 03	0.5848E 03	0.5848E 01	FIS.
0.2725E 01	0.8523E 03	0.6029E 03	0.6029E 01	FIS.
0.3012E 01	0.9071E 03	0.6386E 03	0.6386E 01	FIS.
0.3329E 01	0.9857E 03	0.6901E 03	0.6901E 01	FIS.
0.3679E 01	0.1072E 04	0.7466E 03	0.7466E 01	FIS.
0.4066E 01	0.1142E 04	0.7913E 03	0.7913E 01	FIS.
0.4493E 01	0.1208E 04	0.8325E 03	0.8325E 01	FIS.
0.4966E 01	0.1271E 04	0.8707E 03	0.8707E 01	FIS.
0.5488E 01	0.1329E 04	0.9052E 03	0.9053E 01	FIS.
0.6065E 01	0.1403E 04	0.9512E 03	0.9512E 01	FIS.
0.6703E 01	0.1502E 04	0.1013E 04	0.1013E 02	FIS.
0.7408E 01	0.1678E 04	0.1124E 04	0.1124E 02	FIS.
0.8187E 01	0.1864E 04	0.1239E 04	0.1239E 02	FIS.
0.9048E 01	0.2036E 04	0.1343E 04	0.1343E 02	FIS.
0.1000E 02	0.2216E 04	0.1447E 04	0.1447E 02	FIS.
0.1105E 02	0.2523E 04	0.1628E 04	0.1628E 02	FIS.
0.1221E 02	0.2922E 04	0.1850E 04	0.1850E 02	FIS.
0.1350E 02	0.3284E 04	0.2038E 04	0.2038E 02	FIS.
0.1492E 02				

TABLEAU **VIII**

SECTIONS EFFICACES DE TRANSFERT D'ENERGIE ET TAUX DE DEPLACEMENT DANS LE MOLYBDENE (N=0.6277E22 AT/G)

B.INF(MEV)	T EV.CM2/G	D EV.CM2/G	DPG CM2/G	
0.4140E-06	0.6300E 00	0.5510E 00	0.5507E-02	1./E
0.5316E-06	0.5393E 00	0.4716E 00	0.4713E-02	1./E
0.6826E-06	0.4836E 00	0.4230E 00	0.4226E-02	1./E
0.8764E-06	0.4201E 00	0.3674E 00	0.3669E-02	1./E
0.1125E-05	0.3968E 00	0.3471E 00	0.3464E-02	1./E
0.1445E-05	0.3787E 00	0.3312E 00	0.3304E-02	1./E
0.1855E-05	0.3554E 00	0.3109E 00	0.3098E-02	1./E
0.2382E-05	0.3256E 00	0.2848E 00	0.2834E-02	1./E
0.3058E-05	0.2872E 00	0.2512E 00	0.2495E-02	1./E
0.3928E-05	0.2380E 00	0.2082E 00	0.2059E-02	1./E
0.5043E-05	0.2123E 00	0.1858E 00	0.1828E-02	1./E
0.6476E-05	0.2150E 00	0.1881E 00	0.1844E-02	1./E
0.8315E-05	0.2869E 00	0.2510E 00	0.2462E-02	1./E
0.1068E-04	0.5890E 01	0.5151E 01	0.5145E-01	1./E
0.1371E-04	0.2418E 00	0.2116E 00	0.2038E-02	1./E
0.1760E-04	0.2168E 00	0.1898E 00	0.1800E-02	1./E
0.2260E-04	0.2946E 00	0.2579E 00	0.2455E-02	1./E
0.2902E-04	0.6767E 00	0.5921E 00	0.5763E-02	1./E
0.3727E-04	0.8297E 02	0.7257E 02	0.7211E 00	1./E
0.4785E-04	0.1561E 01	0.1366E 01	0.1320E-01	1./E
0.6144E-04	0.3973E 01	0.3476E 01	0.3433E-01	1./E
0.7889E-04	0.2154E 00	0.1893E 00	0.1405E-02	1./E
0.1013E-03	0.2452E 01	0.2146E 01	0.2078E-01	1./E
0.1301E-03	0.1871E 02	0.1637E 02	0.1605E 00	1./E
0.1670E-03	0.1876E 00	0.1662E 00	0.5975E-03	1./E
0.2144E-03	0.2604E 00	0.2303E 00	0.1010E-02	1./E
0.2754E-03	0.1358E 01	0.1191E 01	0.1036E-01	1./E
0.3536E-03	0.7257E 01	0.6363E 01	0.5522E-01	1./E
0.4540E-03	0.6260E 01	0.5496E 01	0.4434E-01	1./E
0.5829E-03	0.1847E 01	0.1628E 01	0.9981E-02	1./E
0.7485E-03	0.1787E 01	0.1578E 01	0.8353E-02	1./E
0.9611E-03	0.2152E 01	0.1897E 01	0.1514E-01	1./E
0.1234E-02	0.3195E 01	0.2813E 01	0.2988E-01	1./E
0.1585E-02	0.2988E 01	0.2632E 01	0.3036E-01	1./E
0.2035E-02	0.3102E 01	0.2732E 01	0.3196E-01	1./E
0.2613E-02	0.3445E 01	0.3032E 01	0.3422E-01	1./E
0.3355E-02	0.3938E 01	0.3460E 01	0.3782E-01	1./E
0.4307E-02	0.4592E 01	0.4025E 01	0.4295E-01	1./E
0.5531E-02	0.5494E 01	0.4798E 01	0.4996E-01	1./E
0.7102E-02	0.6859E 01	0.5962E 01	0.6145E-01	1./E
0.9119E-02	0.8795E 01	0.7603E 01	0.7756E-01	1./E
0.1171E-01	0.1142E 02	0.9817E 01	0.9946E-01	1./E
0.1503E-01	0.1501E 02	0.1282E 02	0.1291E 00	1./E
0.1930E-01	0.1993E 02	0.1691E 02	0.1703E 00	1./E
0.2479E-01	0.2648E 02	0.2231E 02	0.2238E 00	1./E
0.3183E-01	0.3469E 02	0.2904E 02	0.2909E 00	1./E
0.4087E-01	0.4486E 02	0.3730E 02	0.3740E 00	1./E
0.5247E-01	0.5798E 02	0.4787E 02	0.4794E 00	1./E
0.6738E-01	0.7543E 02	0.6182E 02	0.6187E 00	1./E

TABLEAU VIII (SUITE)

SECTIONS EFFICACES DE TRANSFERT D'ENERGIE ET TAUX DE DEPLACEMENT DANS LE MOLYBDENE (N=0.6277E22 AT/G)

B.INF(MEV)	T EV.CM2/G	D EV.CM2/G	DPG CM2/G	
0.8652E-01	0.1016E 03	0.8260E 02	0.8261E 00	1./E
0.1111E 00	0.1241E 03	0.1004E 03	0.1004E 01	1./E
0.1228E 00	0.1377E 03	0.1111E 03	0.1110E 01	1./E
0.1357E 00	0.1521E 03	0.1223E 03	0.1223E 01	1./E
0.1500E 00	0.1673E 03	0.1340E 03	0.1340E 01	1./E
0.1657E 00	0.1826E 03	0.1458E 03	0.1458E 01	1./E
0.1832E 00	0.1973E 03	0.1569E 03	0.1569E 01	1./E
0.2024E 00	0.2122E 03	0.1682E 03	0.1682E 01	1./E
0.2237E 00	0.2274E 03	0.1797E 03	0.1797E 01	1./E
0.2472E 00	0.2451E 03	0.1930E 03	0.1930E 01	1./E
0.2732E 00	0.2632E 03	0.2066E 03	0.2066E 01	FIS.
0.3020E 00	0.2823E 03	0.2207E 03	0.2207E 01	FIS.
0.3337E 00	0.3056E 03	0.2381E 03	0.2381E 01	FIS.
0.3688E 00	0.3318E 03	0.2575E 03	0.2575E 01	FIS.
0.4076E 00	0.3508E 03	0.2714E 03	0.2714E 01	FIS.
0.4505E 00	0.3644E 03	0.2811E 03	0.2811E 01	FIS.
0.4979E 00	0.3824E 03	0.2940E 03	0.2940E 01	FIS.
0.5502E 00	0.4066E 03	0.3113E 03	0.3113E 01	FIS.
0.6081E 00	0.4324E 03	0.3298E 03	0.3298E 01	FIS.
0.6721E 00	0.4571E 03	0.3475E 03	0.3475E 01	FIS.
0.7427E 00	0.4744E 03	0.3594E 03	0.3594E 01	FIS.
0.8208E 00	0.4862E 03	0.3674E 03	0.3674E 01	FIS.
0.9072E 00	0.5047E 03	0.3801E 03	0.3802E 01	FIS.
0.1003E 01	0.5419E 03	0.4063E 03	0.4063E 01	FIS.
0.1108E 01	0.5861E 03	0.4370E 03	0.4370E 01	FIS.
0.1225E 01	0.6044E 03	0.4490E 03	0.4490E 01	FIS.
0.1353E 01	0.6299E 03	0.4654E 03	0.4654E 01	FIS.
0.1496E 01	0.6157E 03	0.4546E 03	0.4546E 01	FIS.
0.1653E 01	0.6726E 03	0.4933E 03	0.4933E 01	FIS.
0.1827E 01	0.7289E 03	0.5312E 03	0.5312E 01	FIS.
0.2019E 01	0.7804E 03	0.5649E 03	0.5649E 01	FIS.
0.2231E 01	0.8377E 03	0.6024E 03	0.6024E 01	FIS.
0.2466E 01	0.9008E 03	0.6435E 03	0.6435E 01	FIS.
0.2725E 01	0.9733E 03	0.6906E 03	0.6906E 01	FIS.
0.3012E 01	0.1026E 04	0.7237E 03	0.7237E 01	FIS.
0.3329E 01	0.1082E 04	0.7589E 03	0.7589E 01	FIS.
0.3679E 01	0.1154E 04	0.8045E 03	0.8045E 01	FIS.
0.4066E 01	0.1233E 04	0.8541E 03	0.8541E 01	FIS.
0.4493E 01	0.1309E 04	0.9012E 03	0.9012E 01	FIS.
0.4966E 01	0.1377E 04	0.9427E 03	0.9427E 01	FIS.
0.5488E 01	0.1445E 04	0.9846E 03	0.9846E 01	FIS.
0.6065E 01	0.1529E 04	0.1036E 04	0.1036E 02	FIS.
0.6703E 01	0.1605E 04	0.1081E 04	0.1081E 02	FIS.
0.7408E 01	0.1700E 04	0.1138E 04	0.1138E 02	FIS.
0.8187E 01	0.1798E 04	0.1197E 04	0.1197E 02	FIS.
0.9048E 01	0.1971E 04	0.1301E 04	0.1301E 02	FIS.
0.1000E 02	0.2207E 04	0.1440E 04	0.1440E 02	FIS.
0.1105E 02	0.2424E 04	0.1559E 04	0.1559E 02	FIS.
0.1221E 02	0.2677E 04	0.1693E 04	0.1693E 02	FIS.
0.1350E 02	0.2967E 04	0.1844E 04	0.1844E 02	FIS.
0.1492E 02				

TABLEAU **IX**

SECTIONS EFFICACES DE TRANSFERT D'ENERGIE ET TAUX DE DEPLACEMENT DANS LE TUNGSTENE (N=0.327E22 AT/G)

B.INF(MEV)	T EV.CM2/G	D EV.CM2/G	DPG CM2/G	
0.4140E-06	0.9028E 00	0.8010E 00	0.1485E-01	1./E
0.5316E-06	0.7696E 00	0.6828E 00	0.1266E-01	1./E
0.6826E-06	0.6878E 00	0.6102E 00	0.1131E-01	1./E
0.8764E-06	0.6026E 00	0.5347E 00	0.9909E-02	1./E
0.1125E-05	0.6384E 00	0.5664E 00	0.1050E-01	1./E
0.1445E-05	0.7135E 00	0.6330E 00	0.1173E-01	1./E
0.1855E-05	0.8100E 00	0.7186E 00	0.1332E-01	1./E
0.2382E-05	0.9609E 00	0.8525E 00	0.1580E-01	1./E
0.3058E-05	0.1036E 02	0.9188E 01	0.1703E 00	1./E
0.3928E-05	0.4083E 02	0.3623E 02	0.6715E 00	1./E
0.5043E-05	0.1098E 01	0.9742E 00	0.1804E-01	1./E
0.6476E-05	0.1195E 02	0.1060E 02	0.1966E 00	1./E
0.8315E-05	0.1440E 01	0.1277E 01	0.2365E-01	1./E
0.1068E-04	0.3337E 01	0.2961E 01	0.5486E-01	1./E
0.1371E-04	0.1257E 03	0.1115E 03	0.2067E 01	1./E
0.1760E-04	0.1233E 04	0.1094E 04	0.2027E 02	1./E
0.2260E-04	0.4850E 02	0.4303E 02	0.7975E 00	1./E
0.2902E-04	0.3013E 01	0.2674E 01	0.4947E-01	1./E
0.3727E-04	0.3248E 02	0.2881E 02	0.5340E 00	1./E
0.4785E-04	0.8743E 01	0.7757E 01	0.1436E 00	1./E
0.6144E-04	0.2010E 01	0.1783E 01	0.3286E-01	1./E
0.7889E-04	0.2135E 01	0.1894E 01	0.3485E-01	1./E
0.1013E-03	0.2030E 02	0.1801E 02	0.3335E 00	1./E
0.1301E-03	0.7427E 01	0.6589E 01	0.1217E 00	1./E
0.1670E-03	0.7256E 02	0.6438E 02	0.1193E 01	1./E
0.2144E-03	0.1823E 02	0.1617E 02	0.2991E 00	1./E
0.2754E-03	0.2954E 01	0.2621E 01	0.4768E-01	1./E
0.3536E-03	0.2773E 01	0.2460E 01	0.4445E-01	1./E
0.4540E-03	0.2581E 01	0.2290E 01	0.4096E-01	1./E
0.5829E-03	0.2505E 01	0.2222E 01	0.3928E-01	1./E
0.7485E-03	0.2426E 01	0.2152E 01	0.3744E-01	1./E
0.9611E-03	0.2363E 01	0.2096E 01	0.3596E-01	1./E
0.1234E-02	0.2356E 01	0.2090E 01	0.3578E-01	1./E
0.1585E-02	0.2350E 01	0.2085E 01	0.3559E-01	1./E
0.2035E-02	0.2341E 01	0.2077E 01	0.3535E-01	1./E
0.2613E-02	0.2334E 01	0.2071E 01	0.3498E-01	1./E
0.3355E-02	0.2354E 01	0.2089E 01	0.3393E-01	1./E
0.4307E-02	0.2418E 01	0.2145E 01	0.3271E-01	1./E
0.5531E-02	0.2802E 01	0.2486E 01	0.3377E-01	1./E
0.7102E-02	0.3397E 01	0.3014E 01	0.3613E-01	1./E
0.9119E-02	0.4289E 01	0.3801E 01	0.4159E-01	1./E
0.1171E-01	0.5455E 01	0.4816E 01	0.5127E-01	1./E
0.1503E-01	0.6951E 01	0.6118E 01	0.6393E-01	1./E
0.1930E-01	0.8873E 01	0.7791E 01	0.8019E-01	1./E
0.2479E-01	0.1105E 02	0.9654E 01	0.9848E-01	1./E
0.3183E-01	0.1347E 02	0.1169E 02	0.1188E 00	1./E
0.4087E-01	0.1659E 02	0.1431E 02	0.1448E 00	1./E
0.5247E-01	0.2059E 02	0.1768E 02	0.1782E 00	1./E
0.6738E-01	0.2573E 02	0.2200E 02	0.2211E 00	1./E

TABLEAU **IX** (SUITE)

SECTIONS EFFICACES DE TRANSFERT D'ENERGIE ET TAUX DE DEPLACEMENT DANS LE TUNGSTENE (N=0.327E22 AT/G)

B.INF(MEV)	T EV.CM2/G	D EV.CM2/G	DPG CM2/G	
0.8652E-01	0.3203E 02	0.2728E 02	0.2736E 00	1./E
0.1111E 00	0.3578E 02	0.3035E 02	0.3041E 00	1./E
0.1228E 00	0.3792E 02	0.3208E 02	0.3214E 00	1./E
0.1357E 00	0.4029E 02	0.3399E 02	0.3404E 00	1./E
0.1500E 00	0.4290E 02	0.3610E 02	0.3615E 00	1./E
0.1657E 00	0.4579E 02	0.3844E 02	0.3848E 00	1./E
0.1832E 00	0.4899E 02	0.4102E 02	0.4105E 00	1./E
0.2024E 00	0.5277E 02	0.4406E 02	0.4409E 00	1./E
0.2237E 00	0.5710E 02	0.4755E 02	0.4757E 00	1./E
0.2472E 00	0.6190E 02	0.5141E 02	0.5142E 00	1./E
0.2732E 00	0.6727E 02	0.5573E 02	0.5575E 00	FIS.
0.3020E 00	0.7214E 02	0.5961E 02	0.5962E 00	FIS.
0.3337E 00	0.7677E 02	0.6326E 02	0.6327E 00	FIS.
0.3688E 00	0.8188E 02	0.6729E 02	0.6731E 00	FIS.
0.4076E 00	0.8754E 02	0.7175E 02	0.7177E 00	FIS.
0.4505E 00	0.9379E 02	0.7668E 02	0.7670E 00	FIS.
0.4979E 00	0.1000E 03	0.8155E 02	0.8156E 00	FIS.
0.5502E 00	0.1061E 03	0.8626E 02	0.8628E 00	FIS.
0.6081E 00	0.1128E 03	0.9147E 02	0.9149E 00	FIS.
0.6721E 00	0.1202E 03	0.9723E 02	0.9724E 00	FIS.
0.7427E 00	0.1284E 03	0.1036E 03	0.1036E 01	FIS.
0.8208E 00	0.1375E 03	0.1106E 03	0.1106E 01	FIS.
0.9072E 00	0.1475E 03	0.1184E 03	0.1184E 01	FIS.
0.1003E 01	0.1596E 03	0.1276E 03	0.1276E 01	FIS.
0.1108E 01	0.1737E 03	0.1384E 03	0.1384E 01	FIS.
0.1225E 01	0.1893E 03	0.1503E 03	0.1503E 01	FIS.
0.1353E 01	0.2066E 03	0.1634E 03	0.1635E 01	FIS.
0.1496E 01	0.2244E 03	0.1769E 03	0.1769E 01	FIS.
0.1653E 01	0.2426E 03	0.1907E 03	0.1907E 01	FIS.
0.1827E 01	0.2627E 03	0.2060E 03	0.2060E 01	FIS.
0.2019E 01	0.2808E 03	0.2196E 03	0.2196E 01	FIS.
0.2231E 01	0.2982E 03	0.2325E 03	0.2325E 01	FIS.
0.2466E 01	0.3168E 03	0.2461E 03	0.2461E 01	FIS.
0.2725E 01	0.3363E 03	0.2604E 03	0.2604E 01	FIS.
0.3012E 01	0.3579E 03	0.2761E 03	0.2761E 01	FIS.
0.3329E 01	0.3790E 03	0.2913E 03	0.2914E 01	FIS.
0.3679E 01	0.3873E 03	0.2971E 03	0.2971E 01	FIS.
0.4066E 01	0.3942E 03	0.3019E 03	0.3019E 01	FIS.
0.4493E 01	0.4020E 03	0.3072E 03	0.3072E 01	FIS.
0.4966E 01	0.4220E 03	0.3215E 03	0.3215E 01	FIS.
0.5488E 01	0.4563E 03	0.3463E 03	0.3463E 01	FIS.
0.6065E 01	0.4919E 03	0.3719E 03	0.3719E 01	FIS.
0.6703E 01	0.5370E 03	0.4040E 03	0.4040E 01	FIS.
0.7408E 01	0.5974E 03	0.4467E 03	0.4467E 01	FIS.
0.8187E 01	0.6583E 03	0.4896E 03	0.4896E 01	FIS.
0.9048E 01	0.7488E 03	0.5525E 03	0.5525E 01	FIS.
0.1000E 02	0.8414E 03	0.6160E 03	0.6160E 01	FIS.
0.1105E 02	0.9224E 03	0.6703E 03	0.6703E 01	FIS.
0.1221E 02	0.1002E 04	0.7226E 03	0.7226E 01	FIS.
0.1350E 02	0.1089E 04	0.7805E 03	0.7805E 01	FIS.
0.1492E 02				

TABLEAU X

SECTIONS EFFICACES DE TRANSFERT D'ENERGIE ET TAUX DE DEPLACEMENT
POUR LES NEUTRONS THERMIQUES (E = 0,0253 eV)

Elément	σ th (barn)	N (g^{-1} x 10^{24})	par capture			par gramme		
			T (eV)	E_D (eV)	N_D	T (eV cm^2g^{-1})	D (eV cm^2g^{-1})	DPG (cm^2g^{-1})
Al	0,2303	0,0223	770,6	609,9	6,100	3,957	3,132	0,03132
Zr	0,185	0,0066	201	174,4	1,744	0,2455	0,213	0,00213
Fe	2,548	0,01078	389,2	326,9	3,259	10,69	8,951	0,08951
Cu	2,67	0,009479	381,9	321,5	3,215	9,665	8,137	0,081368
Mo	2,7	0,006277	148,5	129,9	1,299	2,520	2,204	0,02204
W	18,5	0,00327	60,8	53,94	1,000	3,678	3,262	0,06049
Cr	3,12	0,0115	389,1	325,1	3,25	13,96	11,66	0,11661
Ni	4,628	0,01026	567	470,2	4,702	26,92	22,32	0,2232
Si	0,161	0,0214	473,2	381	3,810	1,629	1,312	0,01312

REFERENCES

[1] HONECK H.C., ENDF/B, Specifications for an evaluated nuclear data file for reactor applications, May (1966) BNL 500 66 (T-467).

[2] PARKER, The Altermaston Nuclear Data Library, AWRE report NO 0.70/63.

[3] LINDHARD J., NIELSEN V., SCHARFF M., THOMSEN P., Integral equation governing radiation effects, MAT. fys Medd Dan Vid Selsk 33 10 (1963).

[4] KINCHIN G.H., PEASE R.S., The displacement of atoms in solids by radiation, Rep. Progr.Phys. 18 1 (1955).

[5] SIGMUND P., A note of integral equation on the Kinchin Pease type, Rad. Eff. 1 (1969) 15.

[6] TORRENS I.M., ROBINSON M.T., Computer Simulation of Atomic Displacement Cascades in metals, Proc. of the 1971 Int. Conf. Held at ALBANY, 9.11 June 1971.

[7] WECHSLER M.S., Radiation effects on metal and neutron dosimetry, STP n° 341, p. 86, American Society for Testing and Materials, Philadelphia, Pa (1963).

[8] ROBINSON M.T., Phil. Mag. 17 (1968) 639.

[9] ROBINSON M.T., In nuclear fusion reactor (BNES London) (1970) 264.

[10] NORGETT M.J., ROBINSON M.T., TORRENS I., Une méthode de calcul du nombre de déplacements atomiques dans les matériaux irradiés, Rapport CEA R-4389.

[11] GERVAISE F., Programme ARTUS X, Communication privée.

[12] CANCE M., CHABRY P., GENTHON J.P., Programme SOURCE, note CEA N 1294 (1970).

[13] Specialist's Meeting on Radiation Damage on Graphite and on Ferritic and Austenitic Steel, Battelle Seattle Research Center, Oct. Nov. 1972.

[14] ENGLE W.W., A Users Manual for ANISN, AEC Research and Development Report K 1693.

[15] COLTMAN R.R. et al., Reactor Damage in Pure Metals, Journal of Applied Physics 33 12 (Dec.1962).

[16] DORAN D.G., Neutron Displacement Cross Sections for Stainless Steel and Tantalum based on a LINDHARD model, Nuclear Science and Engeneering 49 (1972) 130-144.

[17] THOMPSON M.W., WRIGHT S.B., A new damage function for predicting the effect of reactor irradiation on graphite in different neutron spectra, J. Nucl. Mat. 16 (1965) 146.

DISCUSSION

D. R. HARRIS: Can a cost analysis be carried out in order to estimate the benefits of nuclear data required for radiation damage analysis as compared with the costs of obtaining the data?

M. LOTT: The precision of the nuclear data appears to be sufficient at present for calculating the irradiation rates as defined in our paper. Hence, the cost of obtaining the data is negligible by comparison with the benefit derived from them. Moreover, further data measurements are probably not required for fission reactors. In the case of fusion reactors, on the other hand, there is a definite lack of data.

Section II
REACTOR TECHNOLOGY

Chairman

W.B. LEWIS (Canada)

ТОЧНОСТЬ ЯДЕРНЫХ ДАННЫХ И ЕЕ ВЛИЯНИЕ НА РАЗРАБОТКУ БЫСТРЫХ РЕАКТОРОВ. ПОДХОД К ВЫРАБОТКЕ ТРЕБОВАНИЙ НА ТОЧНОСТЬ ЯДЕРНЫХ ДАННЫХ

Л.Н.УСАЧЕВ, В.Н.МАНОХИН, Ю.Г.БОБКОВ
Физико-энергетический институт,
Обнинск,
Союз Советских Социалистических Республик

Представлен Г.Б.Яньковым

Abstract–Аннотация

ACCURACY OF NUCLEAR DATA AND ITS EFFECT ON FAST-REACTOR DESIGN. AN APPROACH TO SETTING UP NUCLEAR DATA ACCURACY REQUIREMENTS.

The paper deals with the prediction of fast-reactor parameters, with the accuracy required in obtaining them from neutron calculations and with deliberations concerning error magnitudes. A method of determining the errors of various quantities resulting in a given value of a reactor parameter is described. In addition, the accuracy of nuclear data resulting in an error of ± 2% in the conversion ratio is discussed; the use of integral experiments in relaxing the accuracy requirements for microscopic data is studied.

ТОЧНОСТЬ ЯДЕРНЫХ ДАННЫХ И ЕЕ ВЛИЯНИЕ НА РАЗРАБОТКУ БЫСТРЫХ РЕАКТОРОВ. ПОДХОД К ВЫРАБОТКЕ ТРЕБОВАНИЙ НА ТОЧНОСТЬ ЯДЕРНЫХ ДАННЫХ.

В данной работе обсуждаются предсказания параметров быстрых реакторов, точность их обеспечения нейтронными расчетами, а также из каких соображений следуют величины погрешностей. Описывается метод определения совокупности погрешностей различных величин, обеспечивающей заданную величину погрешности реакторного параметра, идет речь о точности ядерных данных, обеспечивающих ± 2% погрешности в коэффициенте воспроизводства, и исследуется использование интегральных экспериментов для смягчения требований на точность микроскопических ядерных данных.

I. ВВЕДЕНИЕ

Деятельность по ядерным данным для реакторов имеет уже более чем тридцатилетнюю историю. Ее начало, по-видимому, можно исчислять с 1939-1940 года, когда стала ясна возможность получения цепной реакции деления. Знание вероятностей различных взаимодействий нейтронов с различными ядрами определяло тогда путь получения цепной реакции деления. На следующем этапе развития ядерной энергетики изучение ядерных данных определило способность реакторов на быстрых нейтронах к расширенному воспроизводству ядерного горючего. К настоящему времени это обстоятельство привело к общему признанию этого типа реакторов как наиболее перспективного. На настоящем этапе развития ядерной энергетики пускаются опытные промышленные быстрые реакторы, ведутся работы по проектированию энергетики, основанной на реакторах такого типа. На данном этапе требуется дальнейшее уточнение наших знаний ядерных данных, так как имеющиеся неопределенности требуют слишком дорогих запасов. С другой стороны, чрезмерное уточнение ядерных данных также требует чрезвычайно больших вложений в развитие экспериментальной техники. Оценку стоимости эксперимента или совокупности экспериментов в зависимости от требуемой точности обычно

делают по закону обратной пропорциональности квадрату ошибки, т.е., если мы потребуем вдвое меньшую погрешность, то мы должны затратить в 4 раза больше средств для выполнения этого требования. Поэтому и возникает задача об обосновании требуемых точностей ядерных данных. Или, говоря более общими словами, возникает задача выбора оптимальной совокупности экспериментов, как микроскопических, так и интегральных, характеризуемых требуемой погрешностью для каждого типа опыта и обеспечивающих требуемую точность расчета реакторных параметров при минимальных общих затратах.

Очевидно, что совершенно аналогичные задачи возникают при определении необходимых точностей в любых областях применения ядерных данных в науке и технологии, им и посвящен данный Симпозиум. Это же, впрочем, относится и к любым другим числовым данным для науки и технологии. Именно поэтому мы считаем полезным представить данный доклад на настоящем Симпозиуме, имея в виду наибольшую разработанность вопроса о потребностях в данных для реакторов. Подход к вопросу, основные понятия, методы расчета разрабатывались с 1961 года в ряде работ авторов из различных стран [1-19]. Ниже будет охарактеризован вклад некоторых из указанных работ в современное понимание проблемы.

II. ЯДЕРНЫЕ ДАННЫЕ, НЕОБХОДИМЫЕ ДЛЯ РАЗРАБОТКИ БЫСТРЫХ РЕАКТОРОВ

В этом разделе мы ответим на следующие вопросы: предсказания каких параметров быстрых реакторов и с какой точностью должны быть обеспечены нейтронными расчетами, из каких соображений следуют причины погрешностей.

1) Расчет критической массы или эффективного коэффициента размножения.

Погрешность расчета эффективного коэффициента размножения вследствие погрешности ядерных данных должна составлять 1%. В докладе Р.С.Смита [5] обосновывается требование на точность расчета $K_{эфф.}$ в ± 1%, исходя из возможности без переделки конструкции реактора скомпенсировать соответствующую ошибку. С этой оценкой согласны авторы работы [10] на основе примерно тех же соображений. Что же касается дальнейшего уменьшения требуемой погрешности за счет погрешностей ядерных данных, то по мнению авторов работы [10], это не приведет к заметному уменьшению общей погрешности вследствие погрешностей изготовления тепловыделяющих элементов, которые ведут, примерно, к погрешности $K_{эфф.}$ в ± 1%.

Требование на уменьшение этих технологических погрешностей привело бы к необходимости более дорогой технологии. Таким образом, допускается общая погрешность, за счет технологии и ядерных данных, равная $\sqrt{1^2 + 1^2} = 1{,}4\%$.

2) Теплофизические расчеты предельной мощности, снимаемой с реактора, т.е. мощности АЭС, требуют знания коэффициента неравномерности – отношения максимального тепловыделения к среднему.

В докладе [11] показано, что существующая погрешность в ядерных данных приводит к неопределенности в 2,5% в указанной величине. В докладе [14] считается, что из экономических соображений следует потребовать знания этой величины с точностью в 1%.

3) Для безопасной эксплуатации реактора нужно обеспечить расчеты мощностного и температурного коэффициентов реактивности с точностью в ± 20% [5,14].

4) Объемы добычи урана и его обогащения, так же как и объемы переработки топлива, необходимые для обеспечения развивающейся энергетики, основанной на быстрых реакторах, определяются задаваемым темпом развития энергетики и временем удвоения реакторов с расширенным воспроизводством. Время удвоения определяется как время, за которое число реакторов удвоится за счет воспроизводимого горючего без подпитки всей системы реакторов другим горючим, кроме воспроизводимого в них самих.

Время удвоения обратно пропорционально коэффициенту воспроизводства без единицы. В ряде работ [5,10] на погрешность коэффициента воспроизводства налагается требование в ± 2%, что, грубо говоря, соответствует погрешности в 10% во времени удвоения. Дальнейшее уменьшение этой погрешности было бы желательно с точки зрения уменьшения неопределенности времени удвоения, однако его нельзя добиться, не меняя и не удорожая технологии изготовления топлива по причинам, объясненным в п.1.

5) Для определения доступности для обслуживания насосов и другого технологического оборудования надо знать активность натрия после выдержки, которая определяется процессом (n, 2n), активацию компонент стали за счет процессов (n,p), (n,α), (n,2n), (n,np) и др.(вместе со знанием массопереноса этих компонент жидким натрием).

Знание активности облученной стали необходимо и при проектировании заводов по переработке тепловыделяющих элементов.

Указанные активности надо знать, повидимому, с точностью 20%.

Процессы (n,p) и (n,α) ведут к накоплению газов в оболочках твэлов и их надо знать примерно с той же точностью.

6) Перевозка облученного топлива на переработку требует защиты, величина которой определяется нейтронной активностью, накопленной в топливе Cm-242 и Cm-244. Нейтронную активность надо знать, повидимому, с точностью порядка 20%.

7) Технология изготовления топливных элементов из плутония, полученного из химической переработки, определяется количеством накопившихся активных изотопов плутония-236 и плутония-238. В настоящее время неопределенности в уровне нейтронной активности оцениваются [11] фактором 5. Повидимому концентрации указанных изотопов надо знать также с точностью порядка 20%.

8) Расчеты тепловыделения в конструкциях активной зоны требуют знания спектров γ-лучей деления, неупругого рассеяния, захвата.

Во всех этих пунктах говорится о требованиях, вытекающих из технологии, к точностям предсказания некоторых реакторных параметров, а не о точностях ядерных данных, от которых эти параметры зависят.

Непосредственно из технологических требований вытекают требования на точность ядерных констант только в п.5, да и то в очень грубом приближении, так как,строго говоря, числа процессов зависят как от сечений самих интересующих нас процессов, так и от спектра нейтронов в реакторе, который определяется ядерными данными всех присутствующих в реакторе материалов. Поэтому погрешность предсказания определяется не только погрешностью в знании основного интересующего нас процесса (например, (n,p), (n,α) и т.д.), но и погрешностями других

величин. Из этих соображений следует, что точность сечений указанных процессов должна быть лучше требуемых для активации 20%, так как какую-то неопределенность внесут погрешности ядерных данных всех реакторных материалов.

Технологические требования пунктов 6 и 7 связываются с требованиями к величинам погрешностей ядерных данных – сечений ряда изотопов цепочки превращений через уравнения кинетики, описывающие накопления изотопов, существенных для технологии.

Если сначала предполагать спектр нейтронов в реакторе заданным, то можно определить допускаемые погрешности в средних на этом спектре сечениях цепочки изотопов, пользуясь уравнениями кинетики. А затем, имея в виду отмеченный выше эффект неопределенности спектра в реакторе, зависящий от неопределенностей ядерных данных всех входящих в состав реактора веществ, можно поставить задачу о совокупности допустимых погрешностей всех величин, влияющих на величину среднего сечения. Эта задача совершенно аналогична той, которая будет обсуждаться ниже, применительно к п.п.1-4.

III. МЕТОД ОПРЕДЕЛЕНИЯ СОВОКУПНОСТИ ПОГРЕШНОСТЕЙ РАЗЛИЧНЫХ ВЕЛИЧИН, ОБЕСПЕЧИВАЮЩЕЙ ЗАДАННУЮ ВЕЛИЧИНУ ПОГРЕШНОСТИ РЕАКТОРНОГО ПАРАМЕТРА

Для определения погрешностей в ядерных данных, обеспечивающих предсказания реакторных величин п.п.1-4 с заданной точностью, в настоящее время мы имеем метод, учитывающий корреляционные свойства погрешностей в простой, но реалистической модели. Этот метод, по нашему мнению, сожет претендовать на количественное определение требуемых точностей.

Относительная вариация реакторного параметра $\delta C/C$ выражается линейно через относительные вариации $(\delta\sigma/\sigma)_{\alpha ij}$ групповых величин типа α изотопа i в группе j с коэффициентами пропорциональности или чувствительности $S_{\alpha ij}$

$$\delta C/C = \sum_{\alpha ij} S_{\alpha ij} (\delta\sigma/\sigma)_{\alpha ij} \qquad (1)$$

Коэффициенты $S_{\alpha ij}$ вычисляются с помощью обобщенной теории возмущений [3].

Для определения погрешности в реакторном параметре надо сделать предположение о том, как складываются вклады от многих погрешностей, входящих в формулу (1). Если принять во внимание, что эти вклады являются случайными величинами, нескоррелированными между собой, то, в соответствии с правилами математической статистики, дисперсия или иначе квадрат стандартного отклонения реакторного параметра C - D^2 ($D^2 \equiv \overline{(\delta C/C)^2}$) выражается через дисперсии групповых микроскопических величин $d^2_{\alpha ij}$ ($d^2_{\alpha ij} \equiv (\delta\sigma/\sigma)^2_{\alpha ij}$) следующим образом

$$D^2 = \sum_{\alpha ij} S^2_{\alpha ij} d^2_{\alpha ij} \qquad (2)$$

Такое предположение было использовано в работе Мурхэда [1], который вычислял коэффициенты чувствительности прямым расчетом в пятигрупповой модели. Гриблер, Хатчинс и Лимфорд [8] поставили вопрос о

важности учета корреляции в погрешностях. Они высказали мнение, что реально почти каждой ядерной константе можно сопоставить 2-3 корреляционных интервала на всей энергетической оси. Зарицкий и Троянов[9], в своей обстоятельной работе, посвященной этому же вопросу, также подчеркнули роль корреляций. А в работе Зарицкого, Николаева и Троянова [10] была реализована мысль о выработке требований на точности отношений величин к стандартам, таким как ν ^{252}Cf и сечение деления урана-235, а также на точность самих стандартов. В работе Усачева и Бобкова [12] предложено погрешность разбивать на компоненты, различающиеся своими корреляционными свойствами. Чаще всего это три компоненты: 1) статистическая-некоррелированная, 2) компонента ошибки, перенесенная со стандарта при его использовании. Эта компонента присутствует в погрешностях всех величин, измеренных с помощью этого стандарта, 3) предполагаемая ошибка в нормировке кривой, постоянная в пределах выбранного корреляционного интервала и проистекающая от возможной систематической ошибки. Представление $\delta\sigma/\sigma$ в виде трех компонент подставляется в уравнение (1) и члены с одинаковыми компонентами, описывающими коррелированную ошибку, объединяются таким образом, что новые коэффициенты чувствительности Z_β данной корреляционной компоненты погрешности оказываются суммами коэффициентов $S_{\alpha ij}$ по области скоррелированности. Подробно все соответствующие формулы для коэффициентов Z_β расписаны в работе [12]. Теперь $\delta C/C = \sum Z_\beta (\delta\sigma/\sigma)^\beta$, где компоненты погрешности $(\delta\sigma/\sigma)^\beta$ между собой считаются статистически независимыми и на этом основании производится переход к формуле (3), аналогичный переходу от формулы (1) к формуле (2)

$$D^2 = \sum_\beta Z_\beta^2 d_\beta^2 \qquad (3)$$

задавая левую часть – погрешность реакторного параметра –, надо определить совокупность погрешностей отдельных величин d_β^2.

Очевидно, что задача в такой постановке не однозначна – можно по-разному распределить вклады погрешностей разных величин в погрешность реакторного параметра. Однако достаточно наложить условие минимума затрат на совокупность экспериментов, делая одновременно предположения об относительных величинах затрат для измерения различных величин с достигнутыми к данному моменту точностями и экстраполируя стоимость эксперимента в зависимости от величины погрешности Σ, например, по закону $1/\Sigma^2$, как задача становится однозначной и сразу решается. Подробнее об этом написано в докладе [12].

Описанную методику мы проиллюстрируем на примере п.4, т.е. на примере требований к точности расчета коэффициента воспроизводства.

IV. ТОЧНОСТЬ ЯДЕРНЫХ ДАННЫХ, ОБЕСПЕЧИВАЮЩИХ ±2% ПОГРЕШНОСТИ В КОЭФФИЦИЕНТЕ ВОСПРОИЗВОДСТВА

Рассмотрена модель реактора на быстрых нейтронах, состав и размеры которого соответствуют электрической мощности около 1000 МВт. В качестве топлива используется смесь окиси урана-238 с окисью плутония, содержащего высшие изотопы в некоторой "равновесной" концентрации, а также осколки деления.

ТАБЛИЦА I. ОСНОВНЫЕ ХАРАКТЕРИСТИКИ ИССЛЕДУЕМОГО РЕАКТОРА

Объем активной зоны, $м^3$		5
Топливо $PuO_2 + UO_2$		
Средняя плотность топлива, $г/см^3$		8
Объемное содержание, %	топливо	40
	натрий	40
	сталь	20
Обогащение топлива, %		11,3
Коэффициент воспроизводства		1,41
Равновесные концентрации Pu, %	^{239}Pu-61	
	^{240}Pu-30	
	^{241}Pu-6	
	^{242}Pu-3	

Содержание осколков – 4% от количества (Pu + U).

Характеристики реактора приведены в приложениях в табл.I.

Результаты расчета приведены в приложениях в таблицах II и III.

Необходимо сделать некоторые пояснения к модели расчета и результатам.

Принята некоторая упрощенная модель корреляций погрешностей, которая характеризуется следующими чертами.

1) Числа вторичных нейтронов всех делящихся изотопов при всех энергиях первичных нейтронов измеряются относительно калифорниевого стандарта и поэтому погрешность этого стандарта входит наиболее весомо.

Большие усилия во многих странах за последние десять лет и особенно начиная с 1966 года по абсолютному определению ν калифорния-252, привели к результату $\nu_0 = 3{,}733 \pm 0{,}0085$, принятому Вторым совещанием экспертов МАГАТЭ по стандартам (Вена, ноябрь 1972 года). Соответственно этому мы приняли достигнутую погрешность в 0,3%.

2) Считается, что для каждой величины вся область энергий разбита на три корреляционных интервала: 0-0,1 МэВ; 0,1-0,8 МэВ; 0,8-10 МэВ, и погрешность каждой величины имеет компоненту постоянную на протяжении каждого из корреляционных интервалов. Оказывается, что именно эти компоненты погрешности следует принимать в расчет и именно на них следует выставлять требования, так как статистическая компонента погрешности дает значительно меньший вклад в общую погрешность. Квадрат вклада от статистических ошибок всех рассматри-

ваемых величин при наших предположениях об их величинах в пределах от 1-5% составляет всего 0,12 в общий квадрат погрешности, равный четырем.

Таким образом, в табл.II приведены требования на скоррелированные по корреляционным интервалам компоненты погрешности, т.е. на ошибки в нормировке кривых сечений в пределах этих интервалов. Поэтому при сравнении с достигнутыми точностями данных надо исключать статистическую компоненту погрешности.

3) Считается, что поток нейтронов при измерениях всех сечений измеряется единым методом в пределах каждого из корреляционных интервалов. Например, в интервалах выше 0,1 МэВ по сечению деления урана-235, а ниже по сечению бора и лития. Это предположение соответствует рекомендации измерять конкурирующие процессы в наибольшей степени относительно, что, как показывает расчет, уменьшает требования на точность измерения. Поэтому в таблице имеются достигнутые и требуемые точности в измерении потока, которые можно трактовать и как точности сечения деления урана-235, предполагая его использование для измерения потока нейтронов.

Из результатов таблицы хотелось бы отметить большие требуемые уточнения в сечениях захвата урана-238, плутония-239, осколков деления, особенно в области ниже 100 кэВ, но также и до 800 кэВ, в неупругом рассеянии урана-238, особенно в области от 0,8 до 2,5 МэВ, ν плутония-239.

Рассмотрение таблицы дает возможность определить величины, уточнение которых наиболее эффективно. Это те величины, существующие погрешности которых дают наибольшие вклады в дисперсию реакторного параметра, в данном случае КВ, а при достижении требуемых погрешностей их вклад меняется максимально, оставаясь тем не менее определяющим и в новом значении дисперсии реакторного параметра.

Теперь следует обсудить место требований, полученных с точки зрения уточнения предсказания коэффициента воспроизводства среди требований, исходящих из других соображений.

Во-первых, можно отметить сравнительно умеренный характер требований по сравнению с требованиями для уточнения предсказаний $K_{эфф.}$ до погрешности в ± 1% (см.напр.[12]).

Однако далее при рассмотрении роли интегральных экспериментов мы приведем аргументы в пользу этих более умеренных требований.

Во-вторых, надо отметить, что для установления полного списка потребностей для быстрых реакторов, надо привлечь и все другие соображения восьми пунктов раздела II, а также соображения по защите. С точки зрения методики использование указанных соображений проводится точно так же, как описано выше. Мы не будем здесь этого делать, так как такие списки можно найти в изданном МАГАТЭ мировом списке потребностей в ядерных данных RENDA-72. Сравнение же требований таблиц II и III с RENDA-72, особенно с английскими запросами Кэмпбела, показывает довольно хорошее их числовое согласие, хотя смысл этих чисел нельзя считать совпадающим, поскольку он не объяснен достаточно ясно в RENDA-72.

Дальнейшее изложение мы посвятим возможной роли интегральных экспериментов в ослаблении требований на точность микроскопических ядерных данных и общему описанию соответствующего математического аппарата, заимствованного из математической теории планирования эксперимента.

ТАБЛИЦА II. ДОСТИГНУТЫЕ И ТРЕБУЕМЫЕ ПОГРЕШНОСТИ ЯДЕРНЫХ ДАННЫХ И ИХ ВКЛАД В ДИСПЕРСИЮ КВ

Изотоп	Процесс	Интервал энергий, МэВ											
		10,5 > E > 0,8				0,8 > E > 0,1				E < 0,1			
		1	2	3	4	1	2	3	4	1	2	3	4
^{239}Pu	σ_c	50	22	0,35	0,07	15	5	1,15	0,13	10	3,6	3,17	0,42
	σ_F	6	6	0,00	0,00	4	4	0,00	0,00	5	3,8	0,04	0,02
	ν_F	3	1,1	0,75	0,10	1	0,5	0,23	0,06	2	0,75	0,700	0,10
^{241}Pu	σ_c	50	50	0,00	0,00	30	30	0,00	0,00	20	20	0,00	0,00
	σ_F	10	9	0,02	0,02	10	5	0,19	0,05	15	5	1,21	0,14
	ν_F	4	4	0,01	0,01	3	2,5	0,03	0,02	2	1,6	0,04	0,02
^{240}Pu	σ_c	50	37	0,05	0,03	30	15	0,29	0,07	20	10	0,29	0,07
	σ_F	7	4	0,16	0,05	7	7	0,00	0,00	7	7	0,00	0,00
	ν_F	3,0	2,0	0,06	0,03	3	3	0,00	0,00	3	3	0,00	0,00
^{238}U	σ_c	20	10	0,19	0,05	10	3,3	1,42	0,14	15	2,7	13,5	0,43
	σ_F	5	2	0,54	0,09								
	ν_F	3	1,3	0,43	0,08								
	σ_{tr}	20	20	0,00	0,00	20	20	0,00	0,00	20	20	0,00	0,00
Осколки деления	σ_c	50	36	0,05	0,03	30	14	0,27	0,06	30	10	1,1	0,12
^{242}Pu	σ_c	50	50	0,00	0,00	30	30	0,00	0,00	20	20	0,00	0,00
	σ_F	7,0	7,0	0,00	0,00								
	ν_F	4,0	4,0	0,00	0,00								
^{23}Na	σ_c	50	50	0,00	0,00	50	50	0,00	0,00	50	45	0,02	0,02
	σ_{tot}	20	20	0,01	0,01	10	10	0,01	0,01	10	10	0,01	0,01

ТАБЛИЦА II . (продолжение)

Сталь	σ_c	50	22	0,39	0,07	30	16	0,19	0,05	30	13	0,40	0,08
	σ_{tot}	20	20	0,00	0,00	20	20	0,01	0,01	20	20	0,00	0,00
^{16}O	σ_c	15	15	0,00	0,00								
	σ_{tot}	10	9	0,02	0,01	10	6,0	0,07	0,03	10	10	0,00	0,00
^{252}Cf	ν_o	0,3	0,3	0,50	0,50								
Поток		6	1,8	1,61	0,15	3	2,4	0,03	0,02	4,0	2,3	0,13	0,04

ТАБЛИЦА III. ПОГРЕШНОСТИ В НЕУПРУГОМ РАССЕЯНИИ ИЗ ДАННОЙ ГРУППЫ ВО ВСЕ НИЖЕЛЕЖАЩИЕ И ИХ ВКЛАДЫ В ДИСПЕРСИЮ КВ

Изотоп		Интервал энергий, МэВ								
		10,5 - 6,5	6,5 - 4,0	4,0 - 2,5	2,5 - 1,4	1,4 - 0,8	0,8 - 0,4	0,4 - 0,2	0,2 - 0,1	0,1 - 0,04
^{238}U	1	30	20	20	15	10	7	7	7	7
	2	11	14	20	4,5	3,0	7	7	3,4	7
	3	0,71	0,06	0,02	1,98	3,42	0,01	0,01	0,25	0,00
	4	0,10	0,03	0,02	0,17	0,22	0,01	0,01	0,05	0,00
Осколки деления	1	30	30	30	30	30	30	30	30	30
	2	25	30	30	15	13	30	30	24	30
	3	0,03	0,00	0,01	0,22	0,45	0,00	0,00	0,04	0,00
	4	0,02	0,00	0,01	0,06	0,08	0,00	0,00	0,02	0,00
^{239}Pu	1	30	30	30	30	30	30	30	30	30
	2	30	30	30	23	17	30	30	26	30
	3	0,00	0,00	0,00	0,04	0,12	0,00	0,00	0,03	0,00
	4	0,00	0,00	0,00	0,02	0,04	0,00	0,00	0,02	0,00

Примечания к таблицам II и III.

1 – погрешности, имеющие место в настоящее время.

2 – требуемая погрешность, обеспечивающая расчет КВ с точностью 2%.

3 – квадрат вклада погрешности, имеющей место в настоящее время, в дисперсию КВ, равную 37.

4 – квадрат вклада погрешности, которую надо достичь, в дисперсию КВ, равную 4.

Сумма столбцов 3 в таблицах II и III равна 37, что соответствует точности расчета КВ 6%.

Сумма столбцов 4 в таблицах II и III равна 4, что соответствует точности расчета КВ 2%.

V. ИСПОЛЬЗОВАНИЕ ИНТЕГРАЛЬНЫХ ЭКСПЕРИМЕНТОВ ДЛЯ СМЯГЧЕНИЯ ТРЕБОВАНИЙ НА ТОЧНОСТЬ МИКРОСКОПИЧЕСКИХ ЯДЕРНЫХ ДАННЫХ

Интегральные эксперименты использовались с самого начала работ по цепной реакции деления. По их результатам подгонялись ядерные данные. Но в начале это делалось на интуитивном уровне, без выработки соответствующего математического формализма.

В работе Чечини [7], Барре, Равье [13], Пази [21], Роулэндса и др.[14], Хеммент и Пэндлбэри [22], Кэмпбела и Роулэндса [18], Бэллэнса [23], Драгта [24], Усачева и Бобкова [19] применен метод наименьших квадратов для подгонки ядерных данных, с целью наилучшим образом описать всю совокупность имеющихся интегральных экспериментов, не входя в противоречие и с микроскопическими измерениями.

На основе такого подхода были существенно смягчены английские требования на точности ядерных данных, публикуемые в списке запросов RENDA, начиная с 1966 года. Однако это делалось математически неформализованным способом.

В развитие математического алгоритма, выработанного для определения потребностей в точностях совокупности только микроскопических экспериментов [12], кратко изложенного и использованного выше, был выработан и алгоритм для планирования совокупности микроскопических и интегральных экспериментов, позволяющих в частности решить задачу об определении смягчения требований на ядерные данные.

В работе Усачева и Бобкова "Математическая теория эксперимента и обобщенная теория возмущений – эффективный подход к исследованию физики реакторов" [16] было предложено для решения комплекса задач подгонки ядерных данных и планирования наиболее информативных экспериментов использовать метод последовательного планирования эксперимента, изложенный, например, в книге под редакцией Налимова В.В. [20] в статье Федорова В.В.

В рамках метода последовательного планирования эксперимента было введено понятие информативности интегрального эксперимента относительно поставленной цели уточнения определенной реакторной характеристики проектируемого реактора [16]. Информативность

определена как уменьшение дисперсии предсказания интересующей нас реакторной характеристики в результате проведения данного эксперимента. На этой основе развертывается исследование информативности уже проведенных интегральных экспериментов и планируемых вновь. Так в этой же работе исследованы эксперименты на сборках ZPR-III с точки зрения уточнения предсказания $K_{эфф}$ реактора БН-600. Оказалось, что только 5 экспериментов из 20 уменьшают дисперсию предсказания, и особенно информативной оказалась сборка ZPR-III-29.

В этой же работе предложен способ проведения подгонки констант в рамках той же идеологии, что в цитируемых выше работах, но не требующий обращений матриц. Все вычислительные операции сводятся лишь к умножению матрицы на вектор. Все дело в том, что в качестве первого шага выбирается совокупность только микроскопических экспериментов с диагонализованной, благодаря описанному выше способу учета корреляций, ковариационной матрицей.

Вычисление ослабления требований на ядерные данные при использовании интегральных экспериментов производится следующим образом. Задаем набор дисперсий интересующего нас реакторного параметра от требуемого значения, например, четыре для коэффициента воспроизводства соответственно требованию точности – 2%, до значения, имеющего место на данный момент, для КВ-37.

Для выбранных значений дисперсий определяется совокупность требуемых точностей одних микроскопических величин, аналогично представленным в табл.II и III. Принимая за исходные полученные таким образом точности и подключая используемые интегральные эксперименты последовательно по одному, на основе алгоритма, описанного в работе [16], вычисляем дисперсию предсказания реакторной характеристики-цели. Вычисленные значения дисперсии откладываются на графике в зависимости от заданных дисперсий, соответствующих предсказаниям на основе только микроскопических ядерных данных. Интерполяцией определяется точка кривой, в которой дисперсия, вычисленная с учетом интегральных экспериментов, равна заданной дисперсии интересующего нас реакторного параметра, например, четырем в случае коэффициента воспроизводства. Другая координата этой точки определит сниженный уровень точности, требуемый от микроскопических величин.

И для этого нового значения дисперсии интересующего нас реакторного параметра по описанному выше алгоритму, еще раз вычисляются все величины, входящие в таблицы II и III. Это и будут требования к микроскопическим величинам, ослабленные благодаря использованию интегральных измерений.

Первые результаты, полученные на пути применения описанного алгоритма, привели к выводу о том, что существующие интегральные эксперименты на обогащенном уране могут полностью снять требования по уточнению ядерных величин для расчета $K_{эфф}$ с точностью ±1% больших урановых быстрых реакторов. Иными словами, при устанавливаемых в результате подгонки корреляций между константами для экстраполяции расчета в область очень больших реакторов достаточно и существующих точностей ядерных данных.

Исследованные до сих пор интегральные эксперименты не могут полностью снять требований на ядерные данные, если нас интересует предсказание КВ. Это – эксперименты по отношениям чисел процессов в центре активной зоны $\sigma_F 8/\sigma_F 9$, $\sigma_c 8/\sigma_F 9$, $\sigma_c 9/\sigma_F 9$ и $\sigma_F 5/\sigma_F 9$ в сборке

ZPR-III-48 и по $K_{эфф}$ этой сборки. Все указанные эксперименты могут снизить требование к дисперсии в КВ всего с 4-х до 5, т.е. требования на микроскопические ядерные данные для обеспечения расчета КВ с дисперсией 4 можно будет получать по описанному выше алгоритму, исходя из дисперсии 5.

Надо отметить, что выше употреблялись выражения "могут снять или ослабить требования", но не "снимают или ослабляют требования" по той причине, что к интегральным экспериментам надо относиться с очень большой осторожностью, поскольку для указанных целей необходимо полное соответствие эксперимента и его расчетной модели, не говоря уже об отсутствии систематической ошибки самого эксперимента.

Чрезвычайно опасным является невыявленное несоответствие, которое может привести к сдвигу предсказываемых параметров, хотя такой сдвиг и можно обнаружить в процессе подгонки констант, благодаря критерию χ^2. Таким образом, наши утверждения о роли интегральных экспериментов следует понимать как возможности того или иного интегрального эксперимента; что же касается превращения этой возможности в действительность, то здесь требуется большая работа специалистов-реакторщиков по оценке каждого интегрального эксперимента [19], т.е. приведению его в соответствие с расчетной моделью и расчету коэффициентов чувствительности измеряемых величин к изменению ядерных данных.

ЛИТЕРАТУРА

[1] MOORHEAD, T.P., in Physics of Fast and Intermediate Reactors, (Proc. Seminar, Vienna, 1961), 2, IAEA, Vienna (1962) 111.

[2] GANDINI, A., ANL-6608 (1962).

[3] УСАЧЕВ, Л.Н., Атомная энергия 15 (1963) 472.
УСАЧЕВ, Л.Н., ЗАРИЦКИЙ, С.М., Бюллетень Информационного Центра по Ядерным Данным. Вып.2, М., Атомиздат, 1965, стр.242.

[4] GREEBLER, P., HUTCHINS, B.A., Conference on Neutron Cross Section Technology, Washington (1966).

[5] SMITH, R.D., in Nuclear Data for Reactors (Proc.Conf.Paris, 1966) 1, IAEA, Vienna (1967) 27.

[6] УСАЧЕВ, Л.Н., ЗАРИЦКИЙ, С.М., Ядерные Данные для Реакторов, (Труды Конференции, Париж, 1966) МАГАТЭ, Вена 1 (1967) 321.

[7] GANDINI, A. et al., in Fast Reactor Physics and Related Safety Problems (Proc. Symp.Karlsruhe, 1967); CECCHINI, G.et al., Comparison between experimental and theoretical integral data, 1966 (ANL-7320), p.107.

[8] GREEBLER, P., HUTCHINS, B.A., LINFORD, R.B., Nucl.Appl., 4 5 (1968) 297.

[9] ЗАРИЦКИЙ, С.М., ТРОЯНОВ, М.Ф., В сб."Физика ядерных реакторов". Вып.2, М., Атомиздат, 1970, стр.168.

[10] ЗАРИЦКИЙ, С.М., НИКОЛАЕВ, М.Н., ТРОЯНОВ, М.Ф., Доклад на Совещании по Нейтронной Физике, Киев, 1971.

[11] GREEBLER, P., HUTCHINS, B.A., COWAN, C.L., in Nuclear Data for Reactors (Proc.Conf.Helsinki, 1970) 1, IAEA, Vienna (1970) 17.

[12] USACHEV, L.N., BOBKOV, Y.G., Planning of an optimum set of experiments and evaluations, INDC (CCP)-19/V - Vienna, 1972.

[13] BARRE, J.Y., RAVIER, J., in Fast Reactor Physics and Related Safety Problems (Proc.Symp.Karlsruhe, 1967).

[14] Выступление Роулэндс на англо-советском семинаре, 1968.

[15] HÄGGBLOM, Adjustement of Neutron Cross Section Data by a Least Squares Fit. Studswyk, Sweden, 1971.

[16] УСАЧЕВ, Л.Н., БОБКОВ, Ю.Г., Ядерные Константы, Вып.10, М., Атомиздат, 1973.

[17] УСАЧЕВ, Л.Н., БОБКОВ, Ю.Г., Предложение по RENDA – всемирному списку запросов. Доклад на 4-ом заседании МКЯД, Вена, 1972.

[18] CAMPBELL, C.G., ROWLANDS, J.L., The Relationship of Microscopic and Integral Data, in Nuclear Data for Reactors, (Proc.Conf.Helsinki, 1970) 2, IAEA, Vienna (1970) 391.
[19] УСАЧЕВ, Л.Н., БОБКОВ, Ю.Г., О совокупном использовании результатов интегральных измерений в проблеме ядерных данных для реакторов, I Совещание по Нейтронной Физике для Реакторов, Киев, 1971.
[20] Новые Идеи Планирования Эксперимента. Под ред.В.В. Налимова, М., Изд-во "Наука", 1970.
[21] PAZY, Use of Integral Measurements as Supplementary Data in Neutron Cross-Section Evaluations, (ANL-7320), 1966, 270.
[22] HEMMET, P.C.E., PENDLEBURY, E.D., Optimization of Neutron Cross-Section Data. (ANL-7320), 1966, p. 88.
[23] BALLANCE, B.M.O. et al., Optimization of Neutron Cross-Section Data, Proc.BNES, London, 1969, p. 149.
[24] DRAGT, J.B., Statistical Consideration of Techniques for Adjustment 1970. (RCN-122), p. 85.

DISCUSSION

A. M. WEINBERG: The Bromley Report entitled "Physics in Perspective" estimates that uncertainties in cross-sections will cause a cost increment of 0.15 to 0.25 US mill/kW · h in fuel-cycle costs of breeder reactors. This, if extrapolated to the year 2000, would represent a cost of several thousand million dollars/yr. Have you made any similar estimates of how much would be saved in fast-reactor costs by such improvements in breeding ratio as you suggest, and how much the experiments might cost?

G. YANKOV: The paper which I have presented does not include any economic calculations whatever.

J. Y. BARRE: In reply to Professor Weinberg's question, I can say that in France the experience with fast-neutron reactors has been that the cost of reactor physics studies was largely offset by the resulting savings on this type of reactor. However, as mentioned in our paper (IAEA-SM-170/69), these are studies based on integral experiments. The data obtained in these investigations have an important bearing on the optimization of the project, on the safety aspects and on understanding of power plant operations.

W. B. LEWIS: The Bromley Report to which Professor Weinberg referred included, of course, a projection of light-water reactors from the present time and, working from this, one can show what the cost savings would be. To do the same thing for the fast-breeder reactor, we would have to make a projection for the number and total capacity of these reactors, and as yet I think there is hesitation about making any such prediction for the year 2000.

ROLES RESPECTIFS DES EVALUATIONS ET DES EXPERIENCES INTEGRALES POUR LA PHYSIQUE DES REACTEURS RAPIDES

J. Y. BARRE, J. P. CHAUDAT
CEA, Centre d'études nucléaires de Cadarache,
France

Abstract–Résumé

RESPECTIVE ROLES OF EVALUATIONS AND INTEGRAL EXPERIMENTS IN THE PHYSICS OF FAST REACTORS.

Applications of nuclear data to the prediction of fast-power reactor parameters are described. In the integral approach chosen at the Commissariat à l'énergie atomique, differential measurements play, through evaluations, a complementary role with respect to the critical experiments which serve as references. The significance of differential measurements in realizing version 3 of the Cadarache multigroup effective cross-section sets and the most important future needs of the fast-reactor physicists are described.

ROLES RESPECTIFS DES EVALUATIONS ET DES EXPERIENCES INTEGRALES POUR LA PHYSIQUE DES REACTEURS RAPIDES.

Les applications des constantes nucléaires dans les prédictions des paramètres des réacteurs rapides de puissance sont décrites. Dans l'approche intégrale choisie au Commissariat à l'énergie atomique, les mesures différentielles, par l'intermédiaire des évaluations, jouent un rôle complémentaire par rapport aux expériences critiques qui servent de référence. La part donnée aux mesures différentielles dans la mise au point de la version 3 du jeu de sections efficaces multigroupes de Cadarache et les principaux besoins futurs des physiciens de réacteurs rapides sont analysés.

INTRODUCTION

Sur ce problème aussi largement traité [1, 2] que controversé [3] il n'est pas réaliste de penser apporter des arguments nouveaux suffisamment forts pour convaincre aujourd'hui les partisans de l'une ou l'autre des approches utilisées pour la détermination des caractéristiques d'un réacteur à neutrons rapides de puissance. En schématisant à l'extrême le sujet, deux solutions opposées existent sur le plan mondial:

a) Utilisation des études de méthodes de calcul et des mesures différentielles «triées» dans des évaluations: Les résultats des expériences critiques servent uniquement à tester la validité des paramètres calculés. C'est plutôt l'orientation suivie aux Etats-Unis d'Amérique et en République fédérale d'Allemagne, par exemple.

b) Utilisation des études de méthodes de calcul et des résultats des expériences intégrales pour améliorer les prédictions: Les données de base, issues des mesures différentielles, servent essentiellement de point de départ ou d'intermédiaires. Cette approche est retenue en particulier en Grande-Bretagne et en France.

Les positions respectives ne sont évidemment pas aussi tranchées et se situent entre ces deux extrêmes.

Quels sont les arguments du CEA pour retenir la seconde approche, c'est-à-dire se baser sur les expériences intégrales, et dans cette solution, quel rôle incombe aux mesures différentielles et aux évaluations? Enfin, au stade actuel, quels sont les besoins futurs en mesures différentielles des projets rapides en France?

Le moment est bien choisi pour aborder ces problèmes, car la synthèse de quatre ans de programmes d'expériences critiques effectuées au CEA vient de se concrétiser dans la réalisation, au début de cette année, de la version 3 du jeu de sections efficaces multigroupes de Cadarache, utilisé maintenant pour les définitions des projets. Cette nouvelle version représente un gain considérable en précision par rapport à la version précédente [4] grâce aux résultats intégraux obtenus sur Masurca, Ermine et Harmonie.

1. NECESSITE DE L'APPROCHE INTEGRALE

1.1. Buts de la physique des réacteurs

L'orientation retenue découle directement des buts poursuivis: obtenir, avec la précision et dans les délais requis par les projets, les paramètres principaux des réacteurs rapides de puissance. La connaissance de ces quantités, qui sont toutes des valeurs intégrales, est nécessaire, au stade de l'avant-projet pour la sûreté et l'optimisation de la centrale, au stade de l'exploitation pour prévoir et comprendre de manière sûre le comportement du réacteur. Il s'agit principalement:
- des enrichissements critiques
- des distributions de puissance
- des gains de surrégénération
- des valeurs des barres de commande
- des problèmes liés aux blindages.

1.2. Conséquences

Les buts étant définis, il est nécessaire, pour comprendre les raisons des choix faits, de réfuter quelques idées trop souvent reçues et d'insister sur les problèmes de précision et de délai:

- La connaissance des données de base n'est pas un but en soi. Le fait que, par exemple, la section efficace de fission du plutonium-239 soit 1,5 ou 1,6 barn à 100 keV n'apporte rien aux ingénieurs de projet. Ce qui importe, c'est la connaissance de paramètres intégraux, de taux de réactions: ce sont ces quantités qui sont mesurées dans les expériences critiques.

- La classe de paramètres intégraux ou de réacteurs à étudier est limitée à un domaine bien défini: dans le cas du CEA, il s'agit de réacteurs à oxyde mixte de plutonium, refroidis au sodium, à deux zones, réfléchis, dans la gamme de puissance comprise entre 250 et 2000 MW(e). Pour les blindages du cœur, les matériaux et les compositions volumiques possibles sont en nombre restreint: acier inox-sodium ou fer-graphite-sodium.

La quantité d'informations nécessaires pour connaître les paramètres principaux dans le domaine considéré est en réalité très inférieure à celle contenue dans les données différentielles. Les expériences intégrales sont, elles, centrées sur le domaine et les informations intéressants.

- La précision des données de base évaluées, issues des mesures différentielles, est insuffisante actuellement pour satisfaire les demandes de précision des projets: ce point, reconnu unanimement, ne nécessite pas d'exemple supplémentaire, même si la convergence entre laboratoires a été améliorée sur certaines données, ces dernières années [2, 5-7].

- Il est possible d'envisager une amélioration des précisions des mesures différentielles dans les années futures, bien que pour plusieurs données un certain plafond semble atteint dans l'état actuel des techniques (exemple: paramètres de résonance du plutonium-239). Mais, pour ce qui concerne le CEA, respecter les délais des projets impliquait pour Phénix et implique pour 1200 MW(e) de passer par les expériences intégrales.

- En fait, même dans l'hypothèse utopique d'une connaissance parfaite de toutes les données différentielles, le test des approximations de méthode, rendues obligatoires par la complexité des problèmes posés par le découpage énergétique ou les conditions géométriques, serait impératif. L'exemple le plus parlant est probablement le calcul des fuites préférentielles dans les canaux de circulation d'hélium d'un réacteur rapide à gaz.

1.3. Application

Pour atteindre dans les délais voulus les précisions demandées par les projets, les expériences intégrales sont indispensables.

Ces expériences sont conçues au CEA pour mesurer, sur des milieux simples, des grandeurs caractéristiques des milieux étudiés et directement reliées aux paramètres projet. Les résultats servent à la qualification de l'ensemble des méthodes de calcul et des données de base, couramment appelé «formulaire». Le seul problème réside dans la validité des transpositions des résultats des expériences intégrales au cas réel du projet. Si les expériences sont correctement choisies, cette transposition calculée est faible et faite avec le minimum de risques d'erreur.

Le programme qui a servi de base à la réalisation de la version 3 du jeu de sections efficaces multigroupes de Cadarache a déjà été partiellement décrit [8, 9]. Il repose essentiellement sur les trois types de mesures intégrales suivantes:

- laplacien matière;
- rapport production totale sur absorption totale dans des expériences à fuites nulles;
- rapport de taux de réaction moyens:
  par rapport à la fission ^{235}U, fission ^{238}U, capture ^{238}U, fission ^{239}Pu, fission ^{240}Pu, fission ^{241}Pu,
  par rapport à la capture ^{238}U, capture ^{235}U, capture ^{239}Pu, capture ^{240}Pu, capture ^{241}Pu.

Pour ces paramètres, les progrès des méthodes de calcul sont tels que le recalage du formulaire sur les résultats des expériences intégrales revient uniquement à un ajustement des données de base. La méthode utilisée pour cette nouvelle version est identique dans son principe à celle utilisée précédemment [4].

Il importe de préciser que c'est l'ensemble approximations de méthode – données ajustées qui seul conduit aux prédictions correctes des paramètres intégraux, dans la gamme étudiée, mais que chaque donnée individuelle n'est pas nécessairement la valeur vraie: les tendances se dégagent cependant. A la limite, cela n'est pas fondamentalement important puisque les quantités intégrales pour lesquelles le formulaire est qualifié sont prédites avec la précision requise.

Une solution identique est actuellement mise au point pour les paramètres liés aux protections, basée sur des expériences systématiques de propagation dans des milieux de composition variable en sodium et fer.

2. ROLE DES EVALUATIONS DANS CETTE APPROCHE

Dans cette approche intégrale, les mesures différentielles, par l'intermédiaire obligatoire des évaluations, jouent un rôle complémentaire à quatre niveaux:

- fournir les données nucléaires de départ les plus probables,
- définir les marges d'incertitude sur ces valeurs, admissibles pour la physique et la métrologie nucléaires,
- déterminer certaines données pour lesquelles la précision des évaluations est suffisante,
- déterminer les données pour lesquelles les expériences critiques apportent peu d'informations.

2.1. Données de départ

C'est certainement le rôle le plus important joué par les mesures différentielles. Il est cependant évident actuellement que, pour la majorité des besoins prioritaires, les données initiales sont disponibles tant du point de vue sections efficaces à dilution infinie que paramètres de résonance.

Par exemple, au départ de la version 3 Cadarache, les évaluations récentes du ^{240}Pu et du ^{241}Pu (DFN 408 et 403) ont été utilisées [10].

La précision sur ces valeurs absolues est très variable suivant les données. Mais, au stade des valeurs de départ, une connaissance précise des formes des sections efficaces en fonction de l'énergie ou du rapport de deux données à une énergie permet de réduire le nombre d'inconnues dans l'ajustement.

2.2. Incertitudes

La définition des incertitudes admissibles sur les données différentielles est un des éléments fondamentaux de la qualification du formulaire, spécialement pour certaines méthodes d'ajustement [1]. En effet, les ajustements des données de base sur les résultats intégraux ne se font que dans la gamme possible de variation estimée par l'évaluation à partir

de la dispersion des mesures différentielles. Il est important pour les physiciens de réacteurs que les incertitudes soient évaluées avec autant d'attention que les valeurs absolues.

La mise au point de la version 3 Cadarache s'est basée sur les incertitudes évaluées à partir des mesures les plus récentes pour les réactions de production et d'absorption des isotopes ^{235}U, ^{238}U, ^{239}Pu, ^{240}Pu et ^{241}Pu [10 - 14].

2.3. Données connues avec une précision suffisante

Le niveau de précision suffisant est spécifique du problème considéré. Les sections efficaces de capture sont suffisamment bien connues pour les problèmes de blindage, alors que pour les besoins «cœur» la précision doit être encore améliorée. L'inverse est vrai pour les réactions totales.

Un exemple caractéristique de ce genre d'apport des mesures différentielles est le paramètre ν dont l'étude a été approfondie dans deux voies:

- valeur du standard ^{252}Cf,
- variation de ν en fonction de l'énergie.

Etant donné les précisions atteintes par la métrologie nucléaire sur les rapports de ν des divers isotopes fissiles au standard et les variations de ν en fonction de l'énergie pour un isotope, c'est essentiellement la valeur absolue du standard qui devrait être étudiée pour les besoins des réacteurs. En effet, pour le cœur 1 de Phénix par exemple, la valeur moyenne de ν sur le spectre du cœur est très proche de la valeur thermique pour les principaux isotopes fissiles:

^{235}U	$\bar{\nu}/\nu_{th}$	:	1,018
^{239}Pu		:	1,024
^{241}Pu		:	1,013

Une erreur de 0,5% sur la valeur absolue thermique a la même influence qu'une erreur de 25% sur la variation de ν avec l'énergie. Les pentes de ν en fonction de l'énergie sont connues d'après la métrologie à mieux que ± 15% pour ces isotopes.

2.4. Données auxquelles les résultats intégraux sont peu sensibles

Cet apport des évaluations est voisin du point précédent. L'exemple classique concerne les sections efficaces de ralentissement élastique et, mis à part ^{238}U et Fe, les sections efficaces de ralentissement inélastique.

Au niveau de la version 3 du jeu de Cadarache, ce type d'apport s'est concrétisé par un vaste ensemble de données évaluées pour lesquelles un bon ordre de grandeur est nécessaire, par exemple les réactions concernant l'oxygène, le sodium, le plutonium-242, les impuretés des aciers, le bore-11.

En dehors des problèmes liés au cœur, les évaluations des réactions de disparition d'isotopes xénon ou krypton employés comme traceurs pour les détections de rupture de gaine sont directement utilisées.

3. BESOINS FUTURS EN DONNEES EVALUEES

3.1. Généralités

Ces demandes futures doivent tenir compte du progrès des connaissances et de l'évolution des besoins de la filière rapide au CEA.

Les programmes exécutés en physique des réacteurs ont donné les résultats attendus. Le degré de précision atteint dans les prédictions à partir des expériences critiques met en évidence de nouvelles sources possibles d'erreur qui ne peuvent plus être négligées: exemple, capture des aciers. D'autre part, les progrès réalisés dans les mesures différentielles des données de base prépondérantes rendent maintenant difficile une amélioration sensible de la précision: c'est probablement le cas, par exemple, pour les paramètres de résonance de ^{235}U, ^{239}Pu, ^{241}Pu, ^{240}Pu, ^{238}U.

Les besoins de la filière ont évolué vers des puissances supérieures (1200 MW(e)) et des performances plus poussées qui demandent de meilleures précisions. La stratégie, les perspectives et les solutions nouvelles envisagées pour les centrales futures suscitent de nouveaux problèmes. On passe, par exemple, d'une fréquence de rechargement de 56 jours pour Phénix à 1 an pour le réacteur de 1200 MW(e): la connaissance des données concernant l'évolution, en particulier les produits de fission (PF), devient importante.

3.2. Evolution de la puissance des centrales

Cette évolution donne un poids nettement plus important aux basses énergies (inférieures à 25 keV) et aux problèmes d'autoprotection. Par exemple, la part de capture ^{238}U en dessous de 25 keV passe de 0,37 pour un enrichissement de 25% (Phénix) à 0,52 pour un enrichissement de 12% (1200 MW(e)).

De même, le rapport F de la section efficace moyenne autoprotégée de capture ^{238}U à la même section efficace à dilution infinie décroît avec l'enrichissement E:

E = 25%	F = 0,88
18%	0,82
12%	0,73

3.3. Capture des matériaux de structure

C'est la principale inconnue des lois de production et d'absorption qui subsiste actuellement au niveau de la version 3 du formulaire de Cadarache pour obtenir les caractéristiques d'un cœur de démarrage. Pour les principaux isotopes concernés (fer, chrome, nickel), le domaine d'énergie prépondérant est situé entre 1 et 300 keV quel que soit l'enrichissement E (fig.1 et 2):

Pourcentage de capture entre 1 et 300 keV	Fe	Ni
E = 25%	62%	28%
18%	64%	35%
12%	65%	43%

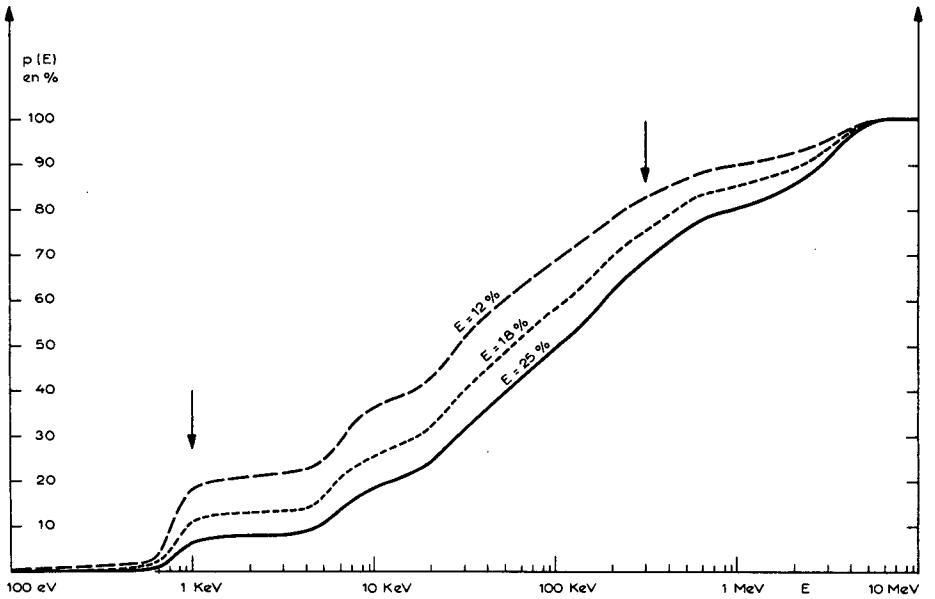

FIG. 1. Fer: pourcentage de capture en dessous de l'énergie E.

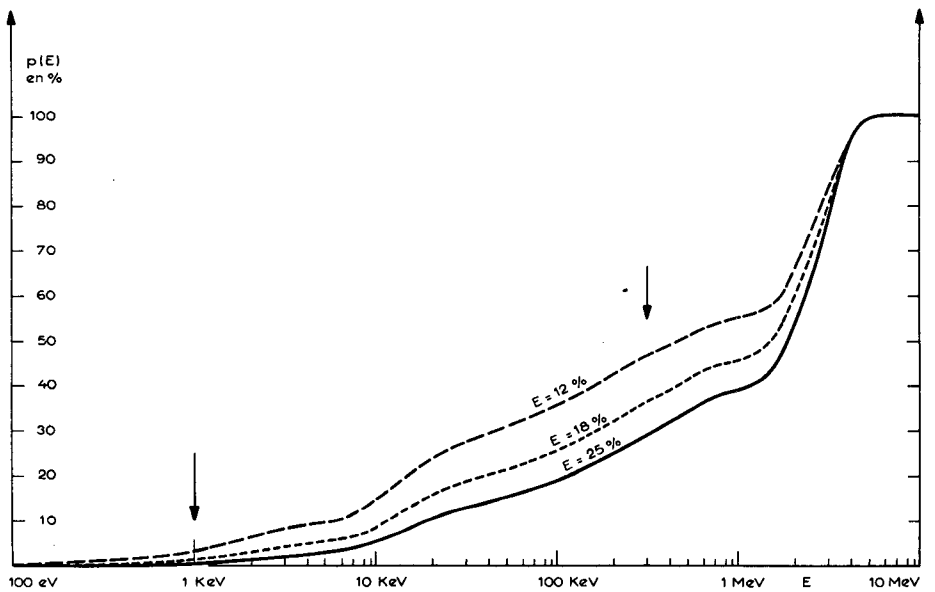

FIG. 2. Nickel: pourcentage de capture en dessous de l'énergie E.

TABLEAU I. MATERIAUX DE STRUCTURE: BILAN EN REACTIVITE

Enrichissement	25%			18%			12%		
f	0,967			0,963			0,957		
dk/k (%)	1,7			2,3			3,4		
Isotope	Fe	Cr	Ni	Fe	Cr	Ni	Fe	Cr	Ni
1/f-1	0,017	0,004	0,007	0,019	0,005	0,008	0,024	0,006	0,008
dk/k (%)	0,8	0,2	0,4	1,2	0,3	0,5	1,8	0,5	0,6

L'importance relative de ces captures «parasites» par rapport aux autres absorptions est définie dans le tableau I par l'intermédiaire du paramètre f défini comme le rapport des absorptions «combustible» aux absorptions totales. Ce paramètre ne décroît que de 1,0% quand l'enrichissement varie de 25 à 12%. En réactivité (dk/k), cette capture «parasite», proportionnelle à 1 - f, varie de 1,7 à 3,4% pour les cas choisis.

La précision globale souhaitée sur la réactivité étant ± 0,5%, pour toutes les sources d'erreur neutronique, il faut connaître la capture des aciers à mieux de ± 10%.

La paramètre (1/f - 1), correspondant au rapport de la capture des structures à l'absorption combustible, met en évidence le rôle prépondérant du fer, puis du nickel (tableau I), pour les acier inox classiques dans la filière rapide (Fe 72%, Cr 18%, Ni 10% en volume).

Les besoins concernent non seulement les sections efficaces de capture à dilution infinie mais également les paramètres de résonance, particulièrement difficiles à déterminer pour les structures. Ces paramètres sont utilisés pour calculer, dans un découpage multigroupe, le rapport de la section efficace de capture autoprotégée à celle à dilution infinie: dans le formulaire de Cadarache actuel par exemple, ces rapports n'existent que pour le fer entre 10 et 500 keV et varient entre 1 et 0,6 pour les cœurs usuels.

La priorité 1 des demandes est actuellement donnée aux sections efficaces de capture à dilution infinie et aux paramètres de résonance des éléments fer, nickel et chrome. Les tests intégraux comportent des réseaux pour lesquels l'influence des structures varie de 1 à 10% en réactivité, mais une transposition au niveau du projet ne peut se faire avec garantie qu'avec des données de départ plus précises.

3.4. Produits de fission

La seconde inconnue actuelle du formulaire version 3 Cadarache concerne, pour le cœur brûlé, les données des produits de fission.

Une évolution caractéristique est représentée sur le tableau II pour deux valeurs d'enrichissements initiaux, 15 et 18%. La variation absolue de réactivité entre le cœur «fin de vie» et le cœur «début de vie», pour un taux de combustion de 50 000 MWj/t, est décomposée entre les

TABLEAU II. EVOLUTION D'UN REACTEUR DE 1200 MW(e) (50 000 MW j/t): contribution des différents isotopes

dk/k (%)	Cœur 1 (E = 15%)	Cœur 2 (E = 18%)
U-235	- 0,3	- 0,2
U-238	- 1,6	- 2,7
Pu-239	- 0,7	- 1,2
Pu-240	- 0,0	- 0,1
Pu-241	+ 0,6	+ 0,6
Produits de fission	- 3,7	- 3,1
Divers	- 1,3	- 2,2
Total	- 7,0	- 8,9

principaux isotopes. Les *prédictions concernant* les effets des isotopes ^{238}U et ^{239}Pu étant actuellement suffisamment précises, l'amélioration de la connaissance des données des produits de fission devient prioritaire.

L'incertitude sur l'effet d'un pseudo-produit de fission moyen doit être inférieure à ± 10%. Cette limite maximale varie en fonction inverse du taux de combustion retenu (50 000 à 100 000 MWj/t) et de la fréquence de rechargement (six mois à 1 an) et sera plus basse pour des enrichissements plus faibles, donc des puissances plus élevées des centrales: la figure 3 montre par exemple l'augmentation du rapport $\bar{\sigma}_{C\ PF} / \bar{\sigma}_{C\ U\text{-}238}$ de la capture moyenne des PF à la capture moyenne de ^{238}U quand l'enrichissement diminue.

Le domaine d'énergie prépondérant est situé entre 1 et 100 keV (fig.4): quel que soit l'enrichissement, 65% des captures des PF ont lieu dans cette gamme d'énergie.

La principale difficulté pour satisfaire ces demandes à partir de la métrologie et de la physique nucléaires réside dans le grand nombre d'isotopes séparés à étudier: il n'y a pas de PF prépondérant pour la filière rapide. En plus des sections efficaces, il faut également connaître les rendements de fission indépendants qui varient suivant l'énergie de fission et l'isotope fissile considéré.

Les données de base évaluées pour les différents produits de fission séparés serviront principalement de point de départ pour la détermination des données d'un pseudo-produit de fission moyen, ayant un effet en réactivité équivalent à celui de l'ensemble des PF, pour un cœur à l'équilibre. Ces données seront ajustées sur des expériences intégrales qui mesurent directement l'effet en réactivité de ce pseudo-produit de fission.

Etant donné les puissances et les performances en taux de combustion envisagées pour les centrales rapides futures, la priorité 2 des demandes est actuellement donnée aux évaluations des produits de fission.

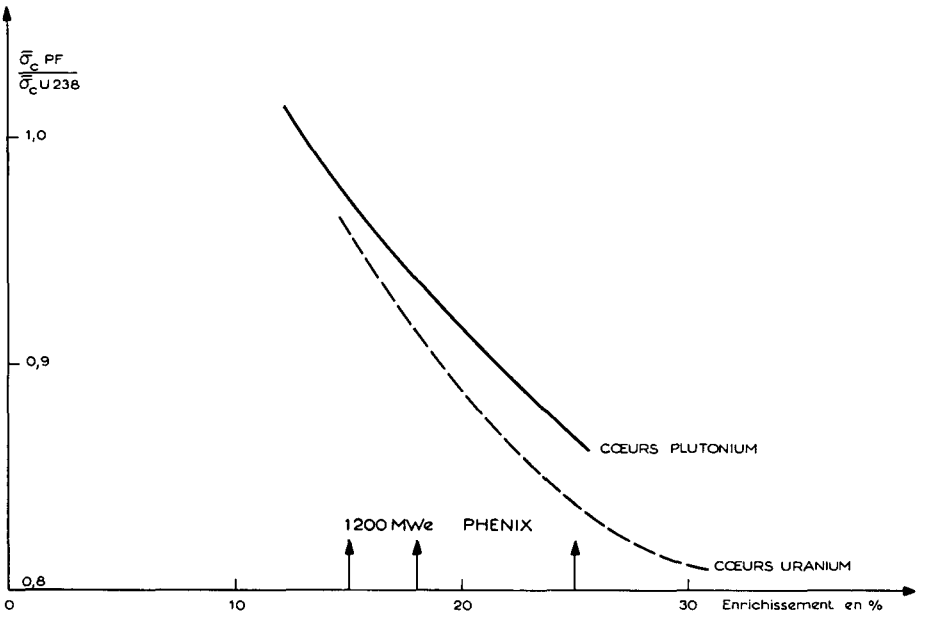

FIG. 3. Capture des produits de fission rapportée à la capture de ^{238}U en fonction de l'enrichissement.

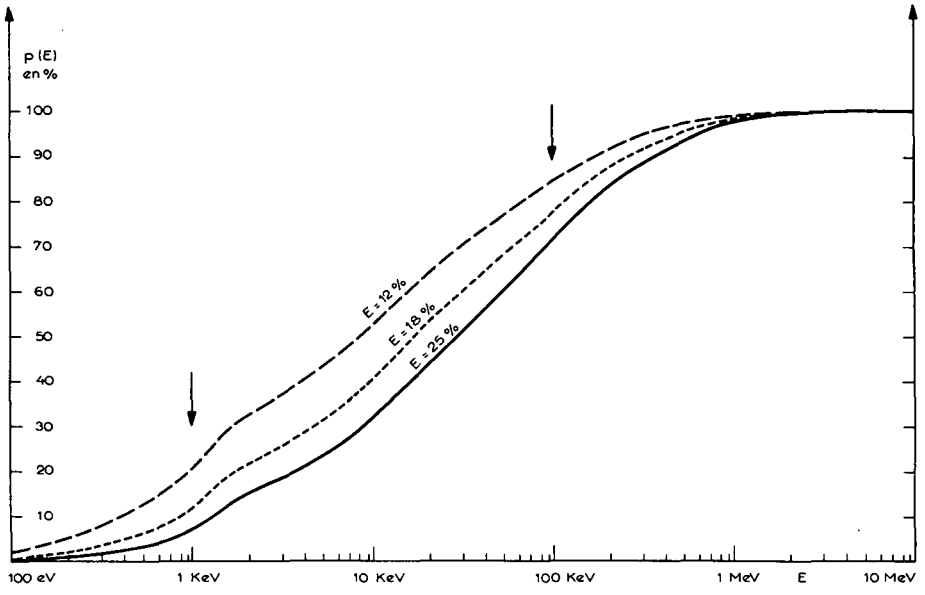

FIG. 4. Produits de fission: pourcentage de capture en dessous de l'énergie E.

3.5. Autres demandes

Il existe d'autres problèmes pour lesquels une amélioration de la connaissance des données de départ, sans être fondamentale comme pour les deux cas précédents, serait actuellement utile. Sans être exhaustif, on peut citer par exemple:
- le ralentissement inélastique de l'uranium-238
- la production et l'absorption des isotopes ^{242}Pu, ^{241}Am, ^{238}Pu.

CONCLUSION

Dans l'approche choisie au CEA pour satisfaire les demandes des projets de réacteurs à neutrons rapides, la base expérimentale de référence est constituée par les résultats des programmes d'expériences critiques. Les évaluations, issues des mesures différentielles, jouent un rôle complémentaire par rapport aux mesures intégrales.

Les résultats accumulés dans les travaux des quatre dernières années en physique des réacteurs et l'évolution des besoins des centrales rapides liée aux performances nouvelles recherchées se traduisent, au CEA, d'une part par une réduction du volume de demandes fondamentales de mesures différentielles, d'autre part par une évolution dans la nature des demandes, enfin par la naissance d'un ensemble de besoins de seconde priorité. Les demandes actuelles d'évaluations sont focalisées sur deux problèmes prioritaires, dans l'ordre: capture des matériaux de structure Fe, Ni, Cr et constantes des produits de fission.

La validité de l'approche retenue, qui s'est concrétisée récemment dans la version 3 du jeu de sections efficaces multigroupes de Cadarache, va pouvoir être testée, en vraie grandeur, sur les mesures prévues au démarrage de Phénix, centrale de 250 MW(e), dont la divergence est attendue pour le milieu de cette année.

REFERENCES

[1] CAMPBELL, C. G., ROWLANDS, J. L., «The relationship of microscopic and integral data», Nuclear Data for Reactors (Compt. Rend. Conf. Helsinki, 1970) 2, AIEA, Vienne (1970) 391.

[2] BARRE, J. Y., BOUCHARD, J., «Rôle complémentaire des expériences intégrales par rapport aux mesures différentielles pour un projet de réacteur à neutrons rapides», Ibid., p. 465.

[3] Table ronde, «The physics of fast reactor operation and design» (Compt. Rend. Conf. Londres, 1969) BNES (1969) 277.

[4] BARRE, J. Y. et al., «Lessons drawn from integral experiments on a set of multigroup cross sections», Ibid., p. 165.

[5] LITTLE, W. W. et al., «Progress in meeting cross sections needs from a fast reactor designer's view», Neutron Cross Sections and Technology (Compt. Rend. Conf. Knoxville, 1971) 1, CONF-710301 (1971) 32.

[6] FRÖHNER, F. H. et al., «On shielding calculations with computer files of neutron data», 4e Conf. Int. sur la protection des réacteurs, Paris, 1972, Compt. Rend. à paraître, mémoire D5.

[7] DUNFORD, C. et al., «A status report on nuclear data for shielding calculations», Ibid., mémoire D6.

[8] BOUCHARD, J. et al., «Experimental study of burn-up in fast breeder reactors», New Developments in Reactor Physics and Shielding II (ANS National Meeting, Kiamesha Lake) 2, CONF-720901 (1972) 888.

[9] BARRE, J. Y. et al., «Reactor physics and fast power breeders: MASURCA core R-Z program», Ibid., p. 822.

[10] L'HERITEAU, J. P., RIBON, P., Examen critique des sections efficaces neutroniques du Pu 240, Note CEA-N-1273 - EANDC (E) 126 AL (mars 1970).

[11] SZABO, I. et al., «Mesure absolue de la section efficace de fission de l'uranium-235 et du plutonium-239 entre 0,025 et 1 MeV», Nuclear Data for Reactors (Compt. Rend. Conf. Helsinki, 1970) 1, AIEA, Vienne (1970) 229;
Ibid., «^{235}U fission cross section from 10 keV to 200 keV», Neutron Cross Sections and Technology (Compt. Rend. Conf. Knoxville, 1971), CONF-710301 (1971) 573.

[12] BLONS, J. et al., «Mesure et analyse des sections efficaces de fission de l'uranium-235 et du plutonium-241», Nuclear Data for Reactors (Compt. Rend. Conf. Helsinki, 1970) 1, AIEA, Vienne (1970) 469;
Ibid., in Neutron Cross Sections and Technology (Compt. Rend. Conf. Knoxville, 1971), CONF-710301 (1971) 829, 836.

[13] RIBON, P., LECOQ, G., Evaluation des données neutroniques de ^{239}Pu, Note CEA-N-1484 (novembre 1971).

[14] SOWERBY, M. G., KONSHIN, V. A., Review of the measurements of alpha for ^{239}Pu in the energy range 100 eV to 1 MeV, At. Energy Rev. 10 4 (1972) 453.

DISCUSSION

W. B. LEWIS (Chairman): I should like to say on my own behalf that I have never been a disbeliever in the neutron physics of fast-breeder reactors. The authors are to be congratulated on the developments which have been achieved through the combination of integral and microscopic data. The advance looks very impressive.

F. RUSTICHELLI: As regards data on fission products, what is more critical, the yields or the neutron capture cross-sections?

J. Y. BARRE: Our requirement in respect of fission products is to obtain the following starting data for the main isotopes separated: capture cross-sections, inelastic slowing-down cross-sections and yields (especially of ^{241}Pu) for fast reactors. These data will be used for defining the constants of a pseudo fission product. The constants will be adjusted on the basis of two types of integral experiments: first, measurement of the reactivity signal of the total fission product obtained by irradiation and, second, irradiation of certain preponderant fission-product isotopes which have been separated. In the last analysis, only the constants of this pseudo fission product are of importance for the project.

CROSS-SECTION UNCERTAINTY EFFECTS ON THE RATIO OF THE HIGH-ENERGY NEUTRON FLUX TO THE POWER AND RESULTING ESTIMATION OF THE IRRADIATION LIMIT ERRORS IN A FAST POWER REACTOR

A. BOIOLI, G.P. CECCHINI
Progettazioni Meccaniche Nucleari, Genoa, Italy

M. COSIMI, M. SALVATORES
Comitato Nazionale per l'Energia Nucleare, Rome, Italy

Abstract

CROSS-SECTION UNCERTAINTY EFFECTS ON THE RATIO OF THE HIGH-ENERGY NEUTRON FLUX TO THE POWER AND RESULTING ESTIMATION OF THE IRRADIATION LIMIT ERRORS IN A FAST POWER REACTOR.

The results of some relevant cross-section uncertainty effects on the ratio φ_H/P of the high-energy neutron flux to the specific power produced in different zones of a fast power reactor are presented. In particular, the uncertainty effects of ^{238}U fission, capture and high-energy inelastic scattering cross-sections, prompt neutron spectrum, high-energy ^{239}Pu fission cross-sections, etc. are considered. The calculations are performed by two-dimensional generalized perturbation methods developed recently by the authors. The structural material swelling is essentially determined by the ratio considered, φ_H/P, as a function of the total energy produced in the reactor. Therefore, the related irradiation limits can be investigated in terms of cross-section uncertainties. The results are discussed, allowing for the different correlations which can be used in the swelling calculations.

1. INTRODUCTION

Stainless-steel swelling was first observed on fuel-element claddings by Cawtorne and Fulton [1], but now the effects of swelling are well known also on fuel-element support and core-structural components. Therefore, core life-time has up to now been considered to be limited only by the swelling phenomenon, which is due to interactions of atoms of the structural materials with fast neutrons. Many investigators have constructed correlations of volume increase against several important parameters, with particular reference to high-energy fluences ($E > 0.1$ MeV) [2-4].

Even if the uncertainties of these correlations are rather high, it is necessary to evaluate and, possibly, to minimize the ratio F = fast flux/power, in order to increase the life of fast reactor fuel elements towards the intrinsic burn-up capability of high-quality elements.

For this reason, it seemed important to assess the uncertainty effects introduced in the F-ratio calculation.

In particular, the confidence in the F-calculation can be based, to some extent, on detailed analyses of the sensitivity to the adopted multigroup cross-section set uncertainties.

Many sensitivity analyses are available [5-7], related to integral parameters, such as K_{eff}, breeding ratio, ℓ_{eff}, Doppler and sodium void reactivity coefficients, but no previous study on the F-ratio seems to have been performed.

This work aims at analysing the influence of the more important cross-section uncertainties on the F-ratio, in order to establish whether the cross-sections are known to such a point as to suggest an effective minimization of the F.

2. TWO-DIMENSIONAL GENERALIZED PERTURBATION METHODS

The generalized Usachev-Gandini (U-G) [8, 9] perturbation theory was used to calculate the abovementioned sensitivities.

As is well known, with the U-G perturbation theory, it is possible to evaluate integral quantity variations as linear functions of the system parameter variations (cross-sections, geometrical parameters, etc.).

The perturbation expressions of the linear function coefficients require generalized importance-function calculations:

$$\Psi^{\dagger} = \sum_{i=1,N} \psi_i^{\dagger} \tag{1}$$

$$\Psi = \sum_{i=1,N} \psi_i \tag{2}$$

where ψ_i and $\psi_i^{\dagger}$ are solutions of the iterative systems

$$\begin{cases} A^{\dagger}\,\psi_1^{\dagger} = G^{\dagger} \\ \cdots\cdots\cdots\cdots \\ A^{\dagger}\,\psi_i^{\dagger} = F^{\dagger}\,\psi_{i-1}^{\dagger} \\ \cdots\cdots\cdots\cdots \end{cases} \qquad i = 2, \ldots, N \tag{3}$$

$$\begin{cases} A\,\psi_1 = G \\ \cdots\cdots\cdots\cdots \\ A\,\psi_i = F\,\psi_{i-1} \\ \cdots\cdots\cdots\cdots \end{cases} \qquad i = 2, \ldots, N \tag{4}$$

A, $A^{\dagger}$ real and adjoint leakage and absorption matrix
F, $F^{\dagger}$ real and adjoint production matrix
G, $G^{\dagger}$ functional-dependent generalized sources [9, 10].

According to the generalized perturbation theory [8, 9], functions $\psi_i^{\dagger}$ and ψ_i satisfy the following conditions:

$$\lim_{i\to\infty} \psi_i^{\dagger} = 0 \tag{5}$$

$$\lim_{i\to\infty} \psi_i = 0 \tag{6}$$

In this work, the multigroup diffusion approximation was used for the solution of the iterative systems described above.

The code used [11] provided a capability for two-dimensional calculations with the correction for the fundamental mode contamination [10].

The sensitivity calculations were carried out by using the generalized perturbation formulas.

Generally, a ratio of real flux functionals defined in regions R_1 and R_2, respectively, can be expressed as

$$\rho = \frac{\int dE \int_{R_1} a_1(\vec{r}, E)\varphi(\vec{r}, E)d\vec{r}}{\int dE \int_{R_2} a_2(\vec{r}, E)\varphi(\vec{r}, E)d\vec{r}} = \frac{Q_1}{Q_2} \qquad (7)$$

If a perturbation $\delta P(\vec{r}, E)$ is introduced in the system, the corresponding perturbation $\delta \rho$ can be expressed as

$$\frac{\delta \rho}{\rho} = \int dE \int_{R_1 + R_2} \delta G(\vec{r}, E)\, \varphi(\vec{r}, E)d\vec{r} + \int dE \int \Psi^{\dagger}(\vec{r}, E)\delta P(\vec{r}, E)\varphi(\vec{r}, E)d\vec{r} \qquad (8)$$

where

$$\delta G(\vec{r}, E) = \frac{\delta a_1(\vec{r}, E)}{Q_1} - \frac{\delta a_2(\vec{r}, E)}{Q_2} \qquad (9)$$

The first term of the right-hand side represents the so-called "direct" effects, the second one the "spectral" effects.

3. REFERENCE REACTOR DESCRIPTION

A mixed-oxide, Pu-and-depleted-U-fuelled, Na-cooled power breeder reactor with an L/D~0.7 was chosen as reference reactor. Depleted-U blankets were considered. A schematization of the reactor is shown in Fig. 1. Cylindrical geometry was adopted in the calculations. The compositions corresponding to the beginning of life are shown in Table I. Core enrichments are expressed as

$$\text{Enr} = \frac{\text{number of fissile nuclei}}{\text{total number of heavy nuclei}}$$

The ratio F was analysed in regions A and B (Fig. 1). F was defined as the ratio of the mean fast flux and the mean fission number (x $cm^{-3} s^{-1}$) in each of the two regions.

The radial dimension of region A corresponds to one and a half central fuel element.

The radial dimension of region B corresponds to one fuel element. The same height was used for the two regions.

TABLE I. COMPOSITIONS (IN NUCLEI $\times$ cm$^{-3} \times 10^{24}$) OF THE REFERENCE FAST POWER REACTOR

	Inferior axial blanket	CORE		Radial blanket	Superior axial blanket
		Low-enrichment region	High-enrichment region		
N^0	0.01422308	0.0132773	0.01327364	0.02142298	0.01311882
N^{Fe}	0.01352275	0.01352275	0.01352275	0.01442028	0.01106951
N^{Cr}	0.003428303	0.003428303	0.003428303	0.003655845	0.002806354
N^{Ni}	0.002095074	0.002095074	0.002095074	0.002234128	0.001714994
N^{Na}	0.009889507	0.009889507	0.009889507	0.005994968	0.01133355
$N^{238}U$	0.007090205	0.00559675	0.0052477	0.01067935	0.006539732
$N^{235}U$	0.0000213346	-----	-----	0.00003213453	0.0000196782
$N^{239}Pu$	-----	0.000698073	0.000930713	-----	-----
$N^{240+242}Pu$	-----	0.000291732	0.000388955	-----	-----
$N^{241}Pu$	-----	0.000052095	0.0000694962	-----	-----

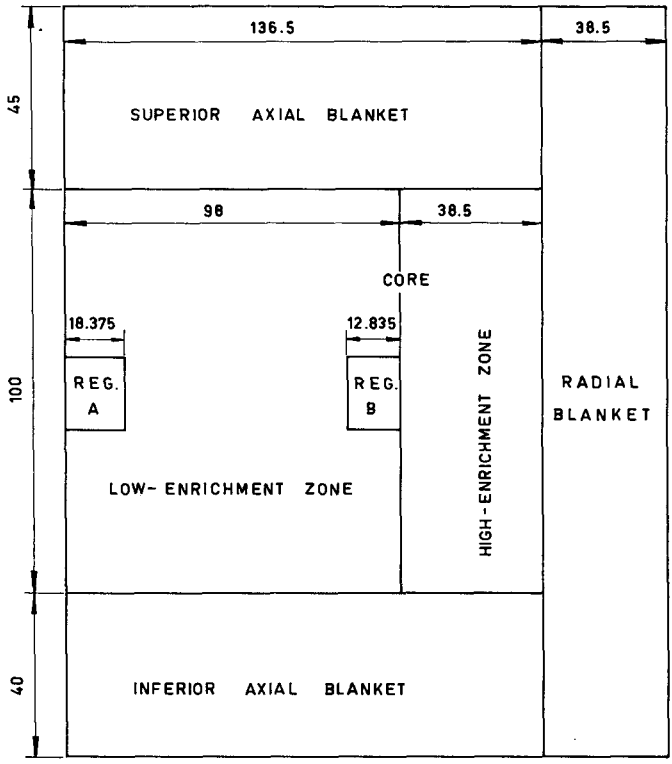

FIG. 1. Axial view of the reactor (all dimensions in cm).

The position of the two regions was chosen to evaluate the F-ratio sensitivity to cross-section uncertainties in regions of the core where the fast flux, or the fast-flux gradient, has a maximum value.

In the first region, therefore, the stainless-steel growth due to the swelling has a maximum value, while in the second region we have the maximum for the differential deformation of the opposite walls of the fuel-element box.

4. NEUTRON CROSS-SECTIONS USED AND THEIR UNCERTAINTIES

The multigroup neutron cross-section set used in this work was recently derived [12] by an optimization procedure based on ENDF/B version-1 data and by the ZPR-6 assembly-7 benchmark integral experiments in support of the LMFBR demonstration program.

We considered the following cross-sections as the main source of error in the calculations of the F-ratio: ^{238}U in inelastic, fission and capture cross-section, ^{239}Pu fission and inelastic cross-sections, ^{240}Pu

TABLE II. CROSS-SECTION UNCERTAINTY LIMITS

Reaction	Energy interval	$\delta\sigma/\sigma$ (in percent)
σ_f^{28}	10 - 0.1 MeV	10.0
σ_c^{28}	10 - 0.1 MeV	10.0
σ_c^{28}	100 - 1.0 keV	20.0
σ_{in}^{28}	Whole range	20.0
σ_f^{49}	10 - 0.1 MeV	10.0
σ_f^{49}	100 - 1.0 keV	15.0
σ_{in}^{49}	Whole range	30.0
χ^{49}	Whole range	10.0
σ_f^{40}	10 - 0.1 MeV	20.0
σ_f^{40}	100 - 1.0 keV	20.0
σ_{in}^{40}	Whole range	30.0

fission and inelastic cross-sections. The assumed energy-dependent uncertainty limits for the cross-section are shown in Table II. These limits are derived by recent works of evaluation [13-18], mainly presented at the Helsinki (1970) and Knoxville (1971) Conferences on nuclear data for reactors.

A ^{239}Pu prompt-fission-spectrum uncertainty was introduced in the analysis, corresponding to an uncertainty of a few percents in the Maxwellian temperature [19].

5. RESULTS

The sensitivity coefficients relative to the F-ratio are shown in Table III. Evidently, all values are very low: only the total effect of the uncertainty of the ^{239}Pu fission cross-section slightly exceeds 10% in the central zone, and this is essentially due to the direct effect.

6. CONCLUSIONS

It follows from the previous results that, taking into account the various correlations which can be used in the swelling calculation, the maximum sensitivity values relative to the swelling may be considered to be twice the values of those relative to the F-ratio [3].

TABLE III. SENSITIVITY VALUES RELATIVE TO THE F-RATIO (IN PERCENT)

Varied parameter	Energy range	Central zone			Peripheral zone		
		Direct	Spectral	Total	Direct	Spectral	Total
σ_f^{28}	Whole range	-1.23	-2.18	-3.41	-0.95	~0.0	-0.95
σ_c^{28}	10 - 1 MeV	---	-2.11	-2.11	---	+0.13	+0.13
	100 - 1 keV	---	+1.02	+1.02	---	+3.60	+3.60
	Whole range	---	-1.09	-1.09	---	+3.73	+3.73
σ_{in}^{28}	Whole range	---	-3.92	-3.92	---	-1.78	-1.78
σ_f^{49}	10 - 1 MeV	-3.23	-2.12	-5.35	-3.42	+0.12	-3.30
	100 - 1 keV	-5.05	-0.74	-5.79	-5.08	+1.39	-3.69
	Whole range	-8.28	-2.86	-11.14	-8.50	+1.51	-6.99
σ_{in}^{49}	Whole range	---	-1.23	-1.23	---	-1.21	-1.21
σ_f^{40}	10 - 1 MeV	-0.98	-2.12	-3.10	-1.06	~0.0	-1.06
	100 - 1 keV	-0.12	-2.16	-2.28	-0.13	+0.03	-0.10
	Whole range	-1.10	-4.28	-5.38	-1.19	+0.03	-1.16
σ_{in}^{40}	Whole range	---	-2.26	-2.26	---	-0.07	-0.07
χ^{49}	Whole range	---	-2.13	-2.13	---	-0.01	-0.01

This means that the errors introduced by the neutronics are negligible in comparison with those due to the uncertainty in the choice of the best correlation to be used.

Another conclusion refers to the minimization of the F-ratio: the very low sensitivity to the cross-section uncertainties seems to indicate that minimization is immediately possible.

ACKNOWLEDGEMENT

The authors would like to thank Mr. V. Viotti for his helpful discussions on the swelling calculation problems.

REFERENCES

[1] CAWTORNE, C., FULTON, E.J., Voids in irradiated stainless steel, Nature 216 (1967) 575.

[2] FINCH, L.M., PETERSON, R.E., Impact of stainless steel swelling on fast reactor core design, Trans. Amer. Nucl. Soc. 12 (1969) 316.

[3] JACKSON, R.J., SUTHERLAND, W.H., METCALF, I.L., Swelling and creep effects upon fast reactor core structural design, Trans. Amer. Nucl. Soc. 13 1 (1970) 112.

[4] RUSSO, S., VIOTTI, V., "LARA – 1 – Analisi del fenomeno del bowing termico e per swelling differenziale nell'ipotesi di non-interazione tra le subassemblies", PMN Report SRV (72) 140 c.
[5] GANDINI, A., SALVATORES, M., "Sensitivity study of fast reactors using generalized perturbation techniques", Fast Reactors (Proc. Symp. Vienna, 1968) 1, IAEA, Vienna (1968) 241.
[6] BITELLI, G., CECCHINI, G.P., GANDINI, A., SALVATORES, M., "Analysis and correlation of integral experiments in fast reactors with nuclear parameters", Physics of Fast Reactor Operation and Design BNES (Proc. Int. Conf. London, 1969) 157.
[7] GREEBLER, P., HUTCHINS, B.A., COWAN, C.L., "Implications of nuclear data uncertainties to reactor design", Nuclear Data for Reactors (Proc. 2nd Int. Conf. Helsinki, 1970) 1, IAEA, Vienna (1970) 17.
[8] GANDINI, A., Perturbation methods in nuclear reactors from the importance conservation principle, Nucl. Sci. Eng. 35 (1969) 141.
[9] GANDINI, A., A generalized perturbation method for bi-linear functionals of the real and adjoint neutron fluxes, J. Nucl. Energy 21 (1967) 755.
[10] CECCHINI, G.P., SALVATORES, M., Advances in the generalized perturbation theory, Nucl. Sci. Eng. 40 (1971) 304.
[11] BOIOLI, A., CECCHINI, G.P., MEDA, N., The GEN-P2 code (to be published).
[12] SALVATORES, M., Adjustment of multigroup neutron cross sections by a correlation method, Nucl. Sci. Eng. (to be published).
[13] PITTERLE, T.A., "Evaluation of ^{238}U neutron cross-sections for the ENDF/B file", in Nuclear Data for Reactors (Proc. 2nd Int. Conf., Helsinki, 1970) 2, IAEA, Vienna (1970) 687.
[14] PITTERLE, T.A., PAIK, N.C., DURSTON, C., "Evaluation of modifications to ENDF/B version-II data", Neutron Cross-Sections and Technology (Proc. Conf. Knoxville, 1971) 1, Knoxville, Tennessee (1971) 461.
[15] HUMMEL, H.H., "Sensitivity studies of the effect of uncertainty in the ^{238}U (n, γ) and in the ^{239}Pu (n, f) and (n, γ) cross-sections", Neutron Cross-Sections and Technology (Proc. Conf. Knoxville, 1971) 1, Knoxville, Tennessee (1971) 65.
[16] OKRENT, D., LOWENSTEIN, W.B., ROSSIN, A.D., SMITH, A.B., ZOLOTAR, B.A., KALLFELZ, J.M., Nucl. Appl. Technol. 9 (1970) 454.
[17] DAVEY, W.G., "Status of important heavy-element nuclear data above the resonance region", Nuclear Data for Reactors (Proc. 2nd. Int. Conf. Helsinki, 1970) 2, IAEA, Vienna (1970) 119.
[18] SUKHORUCHKIN, S.I., ibid., 1 (1970) 309.
[19] CAMPBELL, C.G., ROWLANDS, J.L., The energy spectrum of prompt fission neutrons, EACRP-A-143, 14th Meeting of the European-American Committee, Stockholm (1971).

EL USO DE PARAMETROS NEUTRONICOS DE RESONANCIA Y SECCIONES EFICACES NEUTRONICAS DE CAPTURA RADIATIVA PARA LA EVALUACION DE LA INTEGRAL DE RESONANCIA DE ACTIVACION RESUELTA Y NO RESUELTA

G.H. RICABARRA, R. TURJANSKI, M.D. RICABARRA
Comisión Nacional de Energía Atómica,
Buenos Aires, Argentina

Abstract–Resumen

THE USE OF NEUTRON RESONANCE PARAMETERS AND NEUTRON RADIATIVE CAPTURE CROSS-SECTIONS IN EVALUATING RESOLVED AND UNRESOLVED ACTIVATION RESONANCE INTEGRALS.

The paper reviews the work carried out in the author's laboratory since 1968 on the calculation, evaluation and measurement of activation resonance integrals. The calculation methods used are described, and an analysis is made of the error introduced in the evaluation of the resolved resonance integral as a result of the current uncertainty in neutron resonance parameters. The calculation of the unresolved resonance integral is described, and the neutron radiative capture cross-section data in the region between 1 keV and 10 MeV available for its calculation are considered. The author also describes the use of experimental resonance integral values in evaluating neutron parameters in cases where the neutron parameters obtained by differential time-of-flight measurements show discrepancies. Finally, an account is given of the difficulties that arise in reactor physics and/or activation analysis when inexact or inadequate integral data are used.

EL USO DE PARAMETROS NEUTRONICOS DE RESONANCIA Y SECCIONES EFICACES NEUTRONICAS DE CAPTURA RADIATIVA PARA LA EVALUACION DE LA INTEGRAL DE RESONANCIA DE ACTIVACION RESUELTA Y NO RESUELTA.

En la memoria se pasa revista al trabajo sobre el cálculo de evaluación y medición de integrales de resonancia de activación que los autores realizaron en el laboratorio de la CNEA desde el año 1968. Se describen los métodos de cálculo usados y se analiza el error que la actual incertidumbre de los parámetros neutrónicos de resonancia introducen en la evaluación de la integral de resonancia resuelta. Se examina el cálculo de la integral de resonancia no resuelta, y la disponibilidad de las secciones eficaces neutrónicas de captura radiativa en la zona entre 1 keV y 10 MeV para su cálculo. Se describe igualmente el uso de los valores experimentales de la integral de resonancia para la evaluación de los parámetros neutrónicos en casos donde los parámetros neutrónicos obtenidos por la medición diferencial de tiempo de vuelo son discrepantes. Finalmente se señalan los inconvenientes para la física de reactores y/o análisis por activación de datos integrales evaluados de manera inexacta o inadecuada.

INTRODUCCION

La medición de la integral de resonancia es útil para verificar los parámetros de resonancia de neutrones obtenidos en experiencias de tiempo de vuelo y en ese sentido puede considerarse como una técnica experimental de evaluación. Sin embargo si los datos integrales no se obtienen en un espectro bien definido la comparación entre los datos experimentales y calculados puede resultar incierta.

La mayor parte de las integrales de resonancia de activación, de captura y de absorción se han medido en el espectro de un reactor térmico y se ha supuesto que el espectro es «cuasi» 1/E. La evidencia experimental

de esta hipótesis se basa en el acuerdo obtenido entre los datos experimentales y recomendados de la integral de resonancia de isótopos cuyas principales resonancias están en la zona de baja energía (< 100 eV.). Sin embargo el espectro de un reactor térmico por encima de los 10 keV puede desviarse de la forma 1/E. En reactores compactos de agua liviana y uranio enriquecido se aproxima al espectro de fisión a la energía de 1 MeV y en reactores moderados con agua pesada o grafito podemos tener a alta energía un espectro más blando que el espectro 1/E.

Una hipótesis generalmente aceptada es que la absorción de neutrones a altas energías es despreciable en un reactor térmico y por esto no es necesario tener en cuenta que el espectro en la región de energía de los MeV no es 1/E.

Como se verá en la sección siguiente esta hipótesis puede no ser válida para un buen número de isótopos y en algunos casos puede conducir a serios problemas en la interpretación de las experiencias de medición de la integral de resonancia.

Estas consideraciones muestran que para hacer una comparación correcta de los datos experimentales y calculados de la integral de resonancia es importante evaluar y calcular no solamente la absorción de neutrones de la parte resuelta, sino también de la parte no resuelta.

CALCULO DE LA INTEGRAL EPITERMICA Y DE LA INTEGRAL DE RESONANCIA

Integral epitérmica e integral de resonancia resuelta

Si se conocen los parámetros de resonancia en el intervalo de energía de interés es posible, usando la ecuación de Breit-Wigner y el espectro neutrónico, calcular la integral de captura o absorción epitérmica resuelta, que puede ser definida como:

$$I_e(R) = \int_{E_G}^{E_L} \sigma_A(E)\ \phi_{epi}(E)\ dE/E \qquad (1)$$

donde $\phi_{epi}(E)$ está normalizado a la energía de la resonancia del «standard» Au (4, 5 eV), $\phi_{epi}(E) = E\ \phi(E)/4,5\ \phi(4,5)$, si se supone que el espectro es 1/E, $\phi_{epi}(E) = 1$ y tendremos la integral de resonancia en la zona resuelta:

$$I\ (R) = \int_{E_G}^{E_L} \sigma_A(E)\ dE/E \qquad (2)$$

E_G es la energía de empalme del flujo térmico y epitérmico; en la experiencia la energía de corte, E_L, dependerá del filtro elegido, pero una apropiada corrección permite una comparación consistente entre el cálculo y la experiencia. E_L es la energía de resonancia máxima conocida del isótopo de interés. σ_A es la sección eficaz de absorción, captura o activación.

En un reactor térmico en general se supone que el espectro es aproximadamente 1/E a bajas energías, pero para altas energías se desvía de la forma 1/E y se aproxima al espectro de fisión en la región de los MeV.

La integral resuelta de absorción epitérmica o de resonancia incluye la contribución de: a) resonancias de energía positivas y b) niveles negativos que contribuyen a las capturas 1/v.

Es usual substraer la contribución 1/v de la integral epitérmica o de la integral de resonancia y tenemos:

$$I'_e(R) = \int_{E_G}^{E_L} (\sigma_A(E) - g\,\sigma_0\sqrt{E_0/E})\;\phi_{epi}(E)\;dE/E \qquad (3)$$

y

$$I'(R) = \int_{E_G}^{E_L} (\sigma_A(E) - g\,\sigma_0\sqrt{E_0/E})\;dE/E \qquad (4)$$

que podemos llamar respectivamente integral epitérmica reducida e integral de resonancia reducida en la región de energías resueltas.

Las integrales reducidas en la región resuelta son mucho más sensibles a los parámetros de resonancia positivos y son las que en general se usan para comparar valores experimentales y calculados.

Para bajas energías en general tenemos información detallada de los parámetros de resonancia de neutrones. La parte resuelta de la integral de resonancia puede calcularse sin problemas si se conocen los valores de g_J, $\Gamma_\gamma\Gamma_n/\Gamma$ y E_R para cada resonancia (Γ_n = ancho neutrónico, Γ_γ = ancho radiativo, Γ = ancho total, E_R = energía de resonancia, g_J = factor de peso estadístico).

Como ha sido señalado por Harvey [1] para resonancias de baja energía ($E_R \lesssim 100$ eV), $\Gamma_n \ll \Gamma$, los parámetros de resonancia obtenidos por medidas de transmisión permiten obtener resultados confiables de la integral de resonancia de absorción para cada resonancia estudiada. En consecuencia para isótopos de estas características se observa un buen acuerdo entre los valores calculados y experimentales de la integral de resonancia (ver tabla II en referencia [2]).

Sin embargo para resonancias de alta energía ($E_R >$ keV) o resonancias en que $\Gamma_n \cong \Gamma$ son necesarias medidas de captura por tiempo de vuelo para obtener valores confiables de la integral de captura o absorción para cada resonancia. Además es en esta zona donde resonancias de momento angular superior a 1=0 pueden aparecer y estas capturas pueden ser subestimadas si no existe información sobre su contribución relativa.

En la tabla I se dan los valores experimentales y calculados para isótopos cuyas resonancias más importantes están en la región de energía de los keV.

Se observa una discrepancia sistemática que ha sido explicada parcialmente en un trabajo anterior [3], y a la cual nos referiremos más específicamente en otra parte del trabajo.

En la tabla II también se muestra como los anchos radiativos pueden discrepar fuertemente entre distintas medidas de tiempo de vuelo cuando $\Gamma_n \gg \Gamma_\gamma$, como en las resonancias principales del ^{148}Nd.

TABLA I. COMPARACION DE DATOS INTEGRALES CALCULADOS Y EXPERIMENTALES DE ISOTOPOS CON ESPACIAMIENTO DE NIVELES DEL ORDEN DE LOS keV

Elemento	I' [a] (barn)	I'_e [b] (barn)	Observaciones
^{51}V	0,15	0,48 [23] [c]	Cálculo parámetros ref. [27].
Fe	0,26 [24] 0,32 [4]	1,1 [25] [d]	Medidas de oscilación, los autores suponen espectro 1/E.
Ni	0,16 [4]	1 [25] [d]	Medidas de oscilación, los autores suponen espectro 1/E.
^{64}Zn	0,59 [26]	0,96 [26]	
^{74}Ge	0,22 [3]	0,67 [3]	
^{80}Se	0,56 [7]	1,62 [7]	
^{130}Te	0,17 [6]	0,48 [7]	

[a] Cálculo Breit-Wigner.
[b] Integral epitérmica experimental.
[c] Corregido por desviación espectral a 4 keV (espectro de un acelerador). Por lo tanto el autor supone $I'_e = I'$ [23].
[d] Medido en el centro de un reactor tipo piscina de uranio enriquecido al 20%, $\phi_{epi}/\phi_{th} \cong 0,1$ [25]. Los autores suponen $I'_e = I'$.

TABLA II. PARAMETROS DE RESONANCIA NEUTRONICA DE LAS DOS RESONANCIAS MAS IMPORTANTES DEL ^{148}Nd

E_R (eV)	Γ_γ (meV)	Γ_n (meV)	Γ (meV)	Referencias
	100± 15	1610±240	1710	[19]
155	70± 8	2000	2070	[20]
	40 [a]	2460±200	2500±200	[21]
	250±283 [a]	1850±200	2100±200	[22]
	96± 14	2600±200	2696	[19]
285	58± 6	1980±100	2083	[20]
		3700±370		[21]
	50±224 [a]	3130±100	3180±200	[22]

[a] Obtenido sólo por transmisión, el ancho radiativo tiene un error muy grande debido a que es obtenido por diferencia de magnitudes del mismo orden.

ESTIMACION DE LA PARTE NO RESUELTA DE LA INTEGRAL EPITERMICA Y DE LA INTEGRAL DE RESONANCIA

La integral epitérmica no resuelta puede definirse:

$$I'_e(NR) = \int_{E_L}^{E_{MAX}} (\sigma_A(E) - g\,\sigma_0\sqrt{E_0/E})\,\phi_{epi}(E)\,dE/E \qquad (5)$$

donde E_{MAX} = 10 MeV para nuestros cálculos y si el espectro es 1/E tenemos la integral de resonancia no resuelta:

$$I'(NR) = \int_{E_L}^{E_{MAX}} (\sigma_A(E) - g\,\sigma_0\sqrt{E_0/E})\,dE/E \qquad (6)$$

Esta parte del cálculo tiene en cuenta la contribución a la integral epitérmica o de resonancia de las absorciones neutrónicas en la región no resuelta de alta energía.

En la mayor parte de los trabajos anteriores cuando los parámetros de resonancia a baja energía se conocían con exactitud, se ha supuesto despreciable la contribución de la parte no resuelta en comparación con las absorciones en la zona resuelta [4] o se ha calculado usando la aproximación s [5, 6]. En algunos estudios de las capturas neutrónicas en la región no resuelta en un espectro de un reactor rápido se ha usado la aproximación s y p [8].

Sin embargo si la integral epitérmica no resuelta se estima desde unos pocos keV ($E_{MAX} \gtrsim$ keV) la aproximación s o s más p puede subestimar seriamente las capturas neutrónicas a alta energía en el espectro de un reactor.

En la tabla III se muestra la integral epitérmica no resuelta estimada para el ^{74}Ge, ^{100}Mo y varios isótopos del zirconio y del neodimio, usando la sección eficaz de captura obtenida por ajuste semiempírico del modelo estadístico [10]. Se puede ver que la aproximación s puede subestimar seriamente la integral epitérmica o de resonancia no resueltas.

Las aproximaciones s o s más p no sólo subestiman las capturas a altas energías sino que al describir incorrectamente la forma de la distribución de absorciones en función de la energía pueden enmascarar el efecto del apartamiento de 1/E del espectro a altas energías.

Para algunos isótopos esto afecta no sólo el cálculo de la integral epitérmica que permite una comparación significativa con los datos experimentales, sino también el cálculo del factor de corrección espectral necesario para obtener la integral de resonancia a partir de los datos experimentales.

En la tabla IV mostramos ejemplos de isótopos en que la contribución de la absorción neutrónica a energías del orden de los MeV es significativa para el espectro de nuestro reactor [7, 12]. En reactores de agua pesada y/o grafito como moderador esta fracción puede ser significativamente menor.

Por lo tanto a fin de estimar correctamente (dentro de un 50%) las capturas o absorciones neutrónicas en la parte no resuelta debemos usar secciones eficaces de captura o absorción experimentales o en su defecto secciones eficaces calculadas con un modelo estadístico semiempírico. Estas secciones eficaces deben ser integradas numéricamente en el espectro

TABLA III. CALCULO DE LA INTEGRAL DE RESONANCIA Y DE LA INTEGRAL EPITERMICA NO RESUELTAS DE VARIOS ISOTOPOS .

Isótopo	E_L (keV)	S_γ ($\times 10^3$)	$I'(NR)$ Aproximación s (barn)	$I'(NR)$ Modelo estadístico semiempírico (barn)	$I'_e(NR)$ [a] Modelo estadístico semiempírico (barn)
^{74}Ge	60	0,0471	0,0032	0,058	0,161
^{90}Zr	70	0,0160	0,0009	0,041	0,151
^{91}Zr	10	0,3672	0,1502	0,296	0,537
^{92}Zr	50	0,0396	0,0032	0,070	0,203
^{94}Zr	40	0,0326	0,0033	0,065	0,161
^{96}Zr	60	0,0291	0,0020	0,054	0,148
^{100}Mo	2	0,0865	0,1769	0,650	0,942
^{146}Nd	7	0,181	0,106	0,640	1,16
^{148}Nd	9	0,231	0,105	0,560	1,03
^{150}Nd	4	0,672	0,687	1,21	1,91

[a] Espectro de nuestro reactor (20% uranio enriquecido y agua liviana) [7, 12], calculado con 54 grupos.

TABLA IV. CONTRIBUCION DE LA ABSORCION NEUTRONICA A ALTA ENERGIA[a] A LA INTEGRAL EPITERMICA

Elemento	Δ[a] (barn)	I'_e (barn)	$(\Delta/I'_e) \times 100$
Ni	0,859 [b] (0,798+0,061)	1	86
^{64}Zn	0,350	0,96	36
^{74}Ge	0,108	0,681	16
^{94}Zr	0,123	0,417	30
^{80}Se	0,088	1,62	5
^{100}Mo	0,222	4,20	5
^{146}Nd	0,47	2,58	18
^{148}Nd	0,48	11,7	4

[a] $\Delta = \int_{200\,keV}^{10\,MeV} (\sigma_A(E) - g\,\sigma_0\sqrt{E_0/E})\,\phi_{epi}(E)\,dE/E$ (flujo rápido de nuestro reactor (20% uranio enriquecido y agua liviana) [7, 12], calculado con 54 grupos).

[b] Captura (n, p) = 0,798 b, más captura (n, γ) = 0,061 b.

del reactor calculado a multigrupos. El espectro calculado puede verificarse en algunas regiones de energía importantes mediante detectores de umbral y de resonancia.

Aparece el problema de cuánta exactitud podemos asignar a las secciones eficaces calculadas con el modelo estadístico semiempírico.

Como ha observado Benzi [9] las secciones eficaces de captura calculadas con el modelo estadístico son poco sensibles a las funciones de fuerza neutrónica supuesta pero son fuertemente dependientes de la «función de fuerza radiativa».

Por otro lado es de destacar que para muchos isótopos la sección eficaz de captura o activación a altas energías se conoce solamente en algunos puntos (por ejemplo a 25 keV y a 1 MeV) y a veces se presentan discrepancias notables entre los resultados de distintos laboratorios y por lo tanto los cálculos semiempíricos ajustados con estos datos pueden tener la misma incertidumbre.

Por estas razones es necesario evaluar las secciones eficaces experimentales disponibles en la región de energía mayor de 10 keV e igualmente el ancho radiativo y el espaciamiento promedio a bajas energías obtenidos por mediciones de tiempo de vuelo.

Si las secciones eficaces y el valor de la función de fuerza radiativa concuerdan razonablemente bien con los valores obtenidos o supuestos por el cálculo con el modelo estadístico, se podrán utilizar en forma confiable para la estimación de la integral epitérmica y de resonancia no resuelta. Ejemplos de este tipo de estudio pueden encontrarse en nuestros trabajos anteriores [3, 11].

Finalmente, las consideraciones anteriores se resumen en la figura 1, donde se muestra esquemáticamente el trabajo de evaluación y cálculo necesario para que la comparación con los datos experimentales tenga sentido.

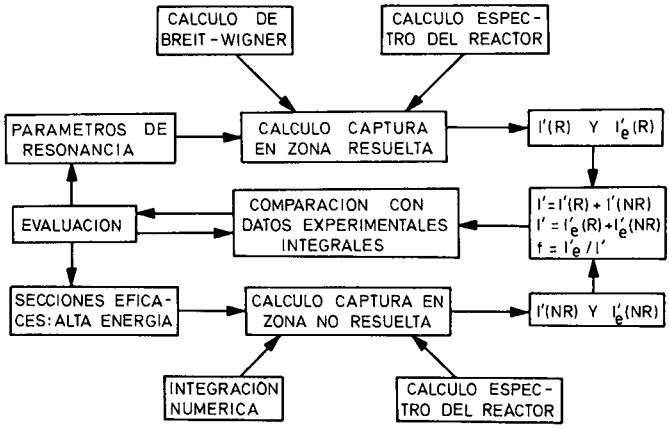

FIG.1. Diagrama de cálculo de la integral epitérmica.

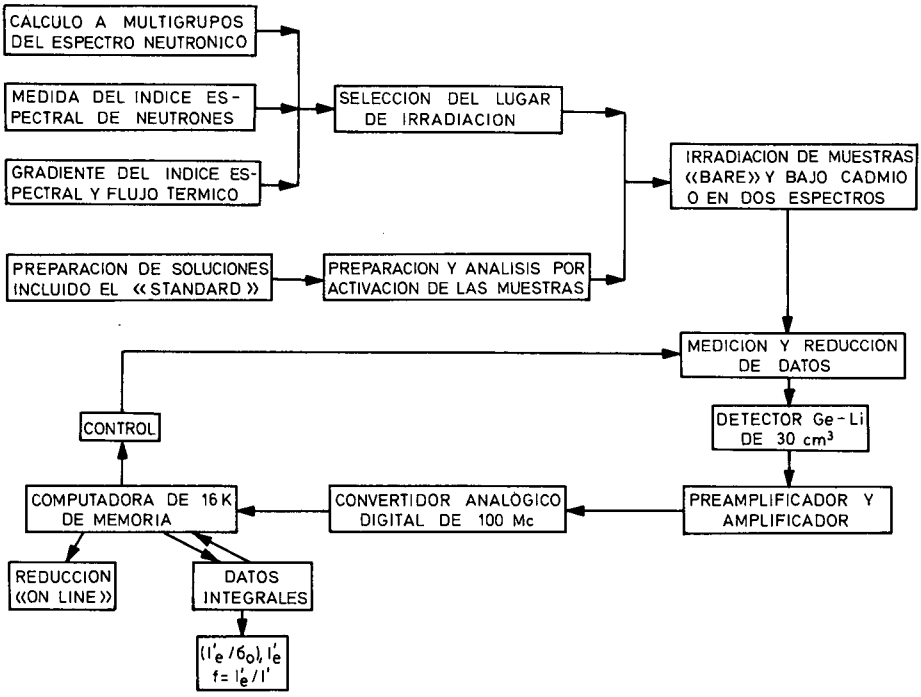

FIG.2. Esquema del sistema experimental usado para determinar la integral epitérmica.

Además, en la figura 2 se muestra el sistema experimental seguido por nosotros en la determinación de la integral de resonancia e integral epitérmica y el procedimiento de evaluación y cálculo aplicado para obtener la integral de resonancia experimental. Los detalles experimentales se han descripto en trabajos anteriores [7, 2].

Para comparar los resultados experimentales obtenidos en distintos reactores es por lo tanto importante disponer de una adecuada descripción del espectro neutrónico y del índice espectral de neutrones. Sin embargo, excepto para unos pocos isótopos, estos datos no son descriptos en la mayoría de los experimentos.

USO DE LOS DATOS INTEGRALES EPITERMICOS EN LA EVALUACION DE LOS PARAMETROS DE RESONANCIA

En esta parte nos limitaremos a dar algunos ejemplos tomados en su mayoría de nuestros trabajos en este tema, que demuestran cómo los datos de experiencias integrales pueden ser útiles en la evaluación.

1) Isótopos del zirconio

El ^{94}Zr y el ^{96}Zr son de interés en física de reactores. Ambos isótopos tienen primera prioridad en Renda 1972; desde el punto de vista de la física nuclear son también interesantes por estar en la región de masa de máxima función fuerza p y mínima función fuerza s. La integral de resonancia medida por nosotros mostró que las capturas p son casi el 100% del total [12]. En particular la resonancia de 302 eV es una resonancia p 100 veces más intensa de los esperados por la sistemática nuclear [13].

Este resultado no se había previsto ni teóricamente ni de las medidas diferenciales y arroja una sombra de duda en la asignación s o p de resonancias de isótopos par del zirconio, basadas solamente en la comparación de los anchos neutrónicos con los previstos por la sistemática nuclear [14].

2) Ejemplo de isótopos con espaciamientos de resonancia del orden de los keV

Las medidas de la integral de resonancia de activación muestran consistentemente que existe una seria discrepancia entre los valores experimentales y los calculados con la formulación de Breit-Wigner. La misma discrepancia se observa en la integral de resonancia epitérmica de absorción determinada con técnicas de oscilación en el espectro de un reactor (tabla II).

Debido a que para el ^{74}Ge se dispone de parámetros de resonancia neutrónica obtenidos por técnicas de tiempo de vuelo de transmisión y captura en muestras enriquecidas [15] y también de medidas de activación de baja resolución entre 10 keV y 2 MeV [16, 17], hemos podido calcular datos integrales de captura en la región de energía mayor que 10 keV por diferentes procedimientos y compararlos [3].

Nosotros llegamos a dos resultados: 1) Una estimación correcta de la integral epitérmica no resuelta debe tener en cuenta que la distribución de secciones eficaces a alta energía no puede ser representada por la aproximación s, en particular, si el espaciamiento promedio de las resonancias es del orden de los keV. 2) El cálculo de la integral epitérmica y de la

integral de resonancia en la zona entre 10 keV y 60 keV a partir de secciones eficaces de activación con baja resolución ($\Delta E \cong 10$ keV) da resultados que concuerdan con la integral epitérmica de activación y discrepan con los obtenidos con los parámetros de resonancia neutrónica que aparentemente subestiman en esta zona las capturas neutrónicas.

3) Ejemplo de los isótopos del neodimio

Los parámetros de resonancia del ^{146}Nd, ^{148}Nd y ^{150}Nd son de interés en la física del quemado [18] y han sido investigados por cuatro experiencias de tiempo de vuelo [19-22].

A pesar de este esfuerzo hay todavía una considerable incertidumbre en los valores del ancho radiativo del ^{148}Nd y del ^{150}Nd presentándose diferencias del doble o más entre los resultados para las resonancias más importantes de estos isótopos.

Nosotros realizamos una medida de la integral epitérmica y de resonancia del ^{146}Nd, ^{148}Nd y ^{150}Nd con un espectrómetro gamma de alta resolución, lo que es especialmente importante para estos isótopos debido al complejo espectro gamma obtenido por activación con neutrones en una muestra de neodimio. Además se realizó un cálculo y evaluación detallados de acuerdo a los procedimientos descriptos en la figura 1 [11].

Hemos llegado a la conclusión de que el valor de la integral de resonancia del ^{148}Nd es aproximadamente la mitad del recomendado anteriormente y en consecuencia el ancho radiativo es también la mitad del valor previamente aceptado.

Por otro lado se obtuvo un buen acuerdo entre los valores experimentales y calculados del ^{146}Nd y del ^{150}Nd. Cabe señalar que la magnitud $\Gamma_n \Gamma_\gamma / \Gamma$ de las principales resonancias del ^{146}Nd y ^{150}Nd presenta un buen acuerdo entre distintas determinaciones de tiempo de vuelo.

ALGUNAS OBSERVACIONES SOBRE LA UTILIZACION DE LAS INTEGRALES EPITERMICAS Y DE RESONANCIA EN EL ANALISIS POR ACTIVACION

Existe actualmente una extensa información sobre parámetros de resonancia neutrónica para calcular la integral epitérmica de muchos isótopos (CINDA 72). Un procedimiento para hacerlo está descripto en la figura 1.

Una pregunta que cabe hacerse es si la gran cantidad de información disponible es utilizada en análisis por activación y si esta información está presentada de manera significativa y utilizable para fines prácticos.

Si esta información estuviera disponible permitiría realizar un análisis semicuantitativo usando muestras cubiertas con diferentes filtros neutrónicos.

Esto sumado a una adecuada descripción del espectro de neutrones en la facilidad de irradiación evitaría la innecesaria determinación de secciones eficaces efectivas para cada campo neutrónico particular.

La combinación de estos procedimientos con un análisis del espectro gamma con un espectrómetro de alta resolución trabajando «on line» con una computadora daría la posiblidad del análisis simultáneo de muchos isótopos en términos semicuantitativos.

La posibilidad de usar diferentes filtros como Rh or B con energía de corte elevada es también muy atractiva para el análisis por activación.

Particularmente el uso de filtros gruesos de boro enriquecido (500 mg/cm^2) daría la posibilidad de medir en la región de alta energía del espectro de un reactor, donde las diferentes activaciones serían aproximadamente proporcionales a la función fuerza radiativa, minimizando el efecto de actividades de contaminación con resonancias intensas de baja energía, que producen una fuerte actividad que dificulta la determinación de isótopos con resonancias de captura débiles.

Los parámetros de resonancias evaluados y secciones eficaces de captura a alta energía podrían usarse para calcular la integral epitérmica y estos datos podrían ser descriptos en tablas de fácil uso para análisis por activación.

Las tablas de que se dispone para análisis por activación son incompletas y no siempre basadas en una adecuada evaluación; además, en general constan los datos experimentales de la integral de resonancia y no usan la información que puede obtenerse de los parámetros de resonancia neutrónica. Aunque existen algunas tablas que siguen las líneas sugeridas [6], no se extienden a todos los isótopos de interés en el análisis por activación.

CONCLUSIONES

Debemos señalar finalmente que un cálculo y evaluación de las absorciones y capturas neutrónicas en función de la energía debe ser hecha en la zona resuelta y no resuelta, si se desea comparar los datos calculados con los datos experimentales de la integral epitérmica obtenida en el espectro de un reactor.

Los parámetros de resonancia deben ser evaluados para calcular la parte resuelta de la integral de resonancia y la integral de resonancia en la región de alta energía del espectro del reactor debe ser estimada usando las secciones eficaces de captura experimentales o calculadas con el modelo estadístico semiempírico.

Una comparación de datos calculados con los experimentos puede resolver discrepancias en los parámetros neutrónicos obtenidos en las mediciones de tiempo de vuelo como lo muestran algunos resultados presentados en este trabajo.

Desde el punto de vista del análisis por activación la posibilidad de usar filtros de alta energía podría extender la aplicabilidad del análisis por activación.

Sin embargo para que el análisis por activación pueda hacerse en forma semicuantitativa, se necesitaría mejorar el conocimiento de las secciones eficaces de captura radiativa para la mayoría de los isótopos.

REFERENCIAS

[1] HARVEY, J.A., Reactor Physics in the Resonance and Thermal Region (GOODJOHN, A.J., POMRANING, G.G., Eds) II, MIT Press, England (1966) 103.

[2] RICABARRA, G.H., TURJANSKI, R., RICABARRA, M.D., Nuclear Data for Reactors (Actas Conf. Helsinki, 1970) II, OIEA, Viena (1970) 589.

[3] RICABARRA, M.D., TURJANSKI, R., RICABARRA, G.H., Can. J. Phys. 50 (1972) 1978.

[4] SCHMIDT, J.J., Neutron Cross Sections for Fast Reactors Materials. Part 1: Evaluation, KFK-120, Karlsruhe (1966).

[5] PERSIANI, P.J., Reactors Physics Constants, P. 163, ANL-5800, Argonne (1963).
[6] WALKER, W.H., Fission Product Data for Thermal Reactors. Part I: Cross Sections, AECL-3037, Chalk River (1969).
[7] RICABARRA, M.D., TURJANSKI, R., RICABARRA, G.H., Can J. Phys. 46 (1968) 2473.
[8] CONNOLLY, T.J., KRUIJF, F., An Analysis of Twenty-Four Isotopes for Use in Multiple Foil Measurements of Neutron Spectra below 10 keV, KFK-718, Karlsruhe (1968).
[9] BENZI, V., Nuclear Data for Reactors (Actas Conf. Helsinki, 1970) II, OIEA, Viena (1970) 379.
[10] BENZI, V., REFFO, G., Newsletter Bulletin 10, CCDN-NW/10, Neutron Data Compilation Centre, France (1969).
[11] RICABARRA, M.D., TURJANSKI, R., RICABARRA, G.H., Measurement and Evaluation of Activation Resonance Integral of ^{146}Nd, ^{148}Nd and ^{150}Nd (presentado al Can. J. Phys.).
[12] RICABARRA, M.D., TURJANSKI, R., RICABARRA, G.H., Can. J. Phys. 48 (1970) 2362.
[13] RICABARRA, M.D., TURJANSKI, R., RICABARRA, G.H., Nucl. Sci. Eng. 48 (1972) 370.
[14] BARTOLOME, J.R., HOCKENBURY, R.W., MOYER, W.R., TATARCZUK, J.R., BLOCK, R.C., Nucl. Sci. Eng. 37 (1969) 137.
[15] MALETZKI, Kh., PIKELNER, L.B., SALAMATIN, I.M., SHARAPOV, E.I., Energie atomique 24 (trad. franc. rev. rusa Atomnaya Energiya) (1968) 80.
[16] DOVBENKO, A.G., KOLESOV, V.E., KOROLEVA, V.P., TOLSTIKOV, B.A., Energie atomique 27 (1969) 41.
[17] TOLSTIKOV, B.A., KOROLEVA, V.P., KOLESOV, V.E., DOVBENKO, A.G., Energie atomique 23 (1967) 114.
[18] Reactor Burn-up Physics (Actas Grupo expertos, Viena, 1971), OIEA, Viena (1973).
[19] KARZHAVINA, E.N., NGUEN NGUEN FONG, POPOV, A.B., TASKAEV, A.I., USSR State Commitee on Utilization of Atomic Energy, Nuclear Data Information Centre, INDC-260 E (1969).
[20] MIGNECO, E., THEOBALD, J.M., PERLMAN, I.J, J. Nucl. Energy 23 (1969) 369.
[21] ALVES, R.N., DE BARROS, S., CHEVILLON, P.L., JULIEN, J., MORGENSTERN, J., SAMOUR, C., Nucl. Phys. A134 (1969) 118.
[22] TELLIER, H., Propriétés des niveaux induits par les neutrons de résonance dans les isotopes stables du néodyme, CEA-N-1459, Saclay (1971).
[23] RYVES, T.B., J. Nucl. Energy 24 (1970) 35.
[24] STORY, J.S., Nuclear Data for Reactors (Actas Conf. Helsinki, 1970) II, OIEA, Viena (1970) 721.
[25] CARRÉ, J.C., VIDAL, R., Nuclear Data for Reactors (Actas Conf. Paris, 1966) I, OIEA, Viena (1967) 479.
[26] RICABARRA, M.D., TURJANSKI, R., RICABARRA, G.H., Can. J. Phys. 47 (1969) 19.
[27] MOXON, M.C., Nuclear Data for Reactors (Actas Conf. Helsinki, 1970) II, OIEA, Viena, (1970) 815.

ASSESSMENT OF METHODS AND DATA FOR PREDICTING INTEGRAL PROPERTIES FOR URANIUM-FUELLED THERMAL-REACTOR PHYSICS EXPERIMENTS*

R. CHAWLA
Indian Institute of Technology,
Kanpur, India

Abstract

ASSESSMENT OF METHODS AND DATA FOR PREDICTING INTEGRAL PROPERTIES FOR URANIUM-FUELLED THERMAL-REACTOR PHYSICS EXPERIMENTS.

The performance of "best" available theoretical methods and differential nuclear data for predicting integral thermal-reactor properties, such as reactivity and reaction rate ratios, is assessed in the light of evidence from a broad range of clean, benchmark experiments. It is shown in the present study that for improving the consistency of calculated integral parameters for D_2O, H_2O and graphite moderated systems, significant modifications to certain currently used nuclear data are desirable. Along with changes in moderator scattering cross-sections, ^{238}U resonance data and the ^{235}U fission energy spectrum, some modification of ^{235}U thermal data has been made which lies within the experimental uncertainties of differential measurements. The "new" data options have been used in various analyses with the WIMS lattice code, and results are presented for the benchmark studies and also for some lattices with more complicated geometries. It is shown that the preferred data generally give more consistent results, for both reactivities and reaction rates over a wide range of conditions, than any previously considered data combinations.

1. INTRODUCTION

In recent years, a high degree of sophistication in representing the physics of thermal reactors has been achieved through the development of detailed computer codes, such as WIMS in the United Kingdom [1] and HAMMER in the United States [2] . Application of these detailed methods and associated nuclear data has been expected to provide a consistent picture for the calculation of integral parameters, such as reactivity and reaction rate ratios, for a wide range of thermal reactor lattices, i.e. for various moderators and fuel enrichments.

Several separate assessments have previously been reported for the performance of WIMS - based methods in analysing simple-geometry lattices moderated by graphite [3] , light water [4] and heavy water [5, 6] . These studies have demonstrated how for experiments where errors due to theoretical approximations are small, it becomes possible to make quantitative inferences on the adequacy of fundamental nuclear data. Thus, for example, earlier analyses have prompted corrections to epithermal data for both ^{238}U [7] and ^{235}U [8] .

In a recent study, Kemshell [9] showed that in spite of the improved differential data embodied in WIMS there have remained certain outstanding inconsistencies in calculations for clean experimental assemblies. For example :

(i) reactivity predictions for D_2O lattices are 1-1.5% low while those for light water and graphite moderated assemblies appear to be correct to within ~0.5%

* Work carried out while author was Research Fellow at Atomic Energy Establishment, Winfrith, Dorchester, Dorset, United Kingdom

(ii) fast fission ratios are significantly (~10%) underpredicted for most lattices.

The present study, following these earlier findings, describes an investigation of WIMS methods and data carried out in the light of evidence from a variety of uranium - fuelled reactor physics experiments. By choosing lattices with simple geometry and accurately documented experimental information, errors of representation in the theoretical methods have been minimised in an effort to focus attention on the effects of existing uncertainties in differential nuclear data. Further, in order to arrive at a consistent set of recommendations, a sufficiently broad range of experiments, in both composition and type, have been considered. These include exponential and critical single-rod assemblies with the three principal moderators, homogeneous experiments with 93% ^{235}U fuel, and British and Canadian heavy-water cluster lattices.

2. METHODS AND DATA

2.1 Resumé of WIMS Methods

Description and earlier validations of the physics methods embodied in the WIMS code have been given by Askew et al [1] and Fayers et al [4] . A brief resumé is presented here.

The basic WIMS library is in 69 energy groups, 14 of these spanning the high energy region from 10 MeV to 9.118 keV, 13 in the resonance region above 4 eV, and 42 thermal groups. In most cases, the group constants are formed from the UKAEA Nuclear Data File [10] using suitable weighting spectra in the GALAXY code [11] . An exception to this rule is the thermal energy transfer matrices which are produced by PIXSE [12] from a variety of thermal scattering laws including the Nelkin model for H_2O, the Effective Width model for D_2O and an improved Egelstaff model for graphite.

Treatment of the resonance region in WIMS is based on the use of equivalence theorems to relate a group resonance integral for the heterogeneous cell to group resonance integrals for various homogeneous mixtures of moderator and resonance absorber. The library of resonance integrals has been compiled via the SDR Code [13] which solves the slowing down equations using some 120,000 energy points. The various procedures embodied in the WIMS resonance treatment have been shown to yield results which compare very favourably with more detailed methods of calculation such as the MOCUP Monte Carlo Code [14] , and it has been concluded that the probable error for ^{238}U captures, for example, is better than 1% at all pitches [4] .

Although solution of the transport equation is possible in the full 69 - group structure, such calculations tend to be unnecessarily elaborate. A special procedure is therefore embodied in WIMS for group condensation. This is based on the use of the "Spectrox" method [15] for producing in the full 69 groups, a condensation flux spectrum for each of the principal regions of the lattice cell, coupled together through collision probability expressions. Following the generation of condensed group cross-sections, a more accurate solution is obtained using either differential (discrete ordinate, DSN) or integral (collision probability) transport theory methods.

Calculations for leakage in WIMS are performed on the homogenised cell in the same group structure as used for the main transport

routine. Allowance for asymmetric diffusion is made using methods due to Benoist [16] . The leakage flux solution is obtained by either diffusion theory or the B_1 method, the latter employing explicit P_1 scattering data for the principal moderating nuclei, viz. hydrogen denterium, oxygen and carbon.

Details of the editing and operating instructions for the WIMS code have been given by Roth et al [17] .

2.2 Data Used

There has been considerable uncertainty in the last few years about the accuracy of epithermal ^{238}U capture data. The original WIMS resonance integral tabulations for ^{238}U were based on differential measurements. Initial comparison of predicted and experimental reaction rate ratios for light water and graphite lattices, however, indicated that these resonance tabulations were too high and a uniform reduction of the ^{238}U microscopic cross-section by 0.2 barn in the resonance region was proposed by Askew [7] . More recently, fresh assessments have been carried out by Kemshell [6, 9] for a wider range of lattices with more accurately documented reaction rate measurements, and it has been concluded that the Askew correction is more than is required for optimum agreement with experiment. An intermediate value of 0.1 barn has been recommended as a suitable uniform adjustment of the original ^{238}U resonance cross-section. This is in line with the results of a recent American study recommending modifications to ENDF/B ^{238}U resonance data [18].

Some uncertainty has also existed on the epithermal data for ^{235}U. The resonance integrals originally contained in the WIMS library for ^{235}U were based on the measurements of Brookes which suggest a value of 0.67 for α_{25}, the infinite dilution ratio of capture to fission above 0.5 eV [4] . As a result of more recent studies [8, 19] , however, opinion has hardened on a much lower α_{25} value of 0.50, and the presently recommended ^{235}U resonance data in WIMS meets this criterion.

The ^{235}U fission spectrum is another item of data on which considerable doubt has been cast recently. The usual representation in the WIMS library is based on the measurements of Bonner and may be approximated by a Maxwellian spectrum with an average temperature of 1.30 MeV. Several different types of integral measurements, however, indicate that the mean energy of the ^{235}U fission spectrum should be 5-10% higher than indicated by the differential measurements. Thus, for example, integral reaction rate measurements by Grundl [20] suggest a Maxwellian temperature as high as 1.5 MeV. Data adjustment studies for fast reactor benchmark experiments have suggested that a 10% increase in the ^{235}U fission temperature is plausible [21] . The use of a fission temperature of 1.43 MeV in the WIMS library has been recently advocated for HTR (High Temperature Reactor) studies, as it leads to considerable improvement in the calculated age of fission neutrons in graphite (Section 3.3). In the light of the above evidence, this 10% hardened fission spectrum has been used for the present study.

The other important recent changes in WIMS data have been those in moderator cross-sections. For deuterium, for example, there have been two alternative UKAEA data files in the past, viz DFN 218 with a cross-section in the slowing down region (σ_p) of 3.4 barns, and DFN 256 with improved high energy data and a σ_p value of 3.2 barns. Recent differential measurements have shown that a value of 3.35 barns is appropriate for the epithermal deuterium scattering cross-section and accordingly a new data file, DFN 905, has been compiled and incorporated into the WIMS library.

Similarly, for hydrogen, a recommended value of 20.3 barns has been used for σ_p instead of the earlier 20.0 barns. For carbon, the presently used WIMS library has revised high energy cross-sections and a σ_p value of 4.74 barns.

3. EXPERIMENTS CONSIDERED

3.1 Natural U/D_2O single-rod lattices

As mentioned in Section 1, an important discrepancy in the analysis of experimental reactor lattices has been the underprediction of reactivity for D_2O systems [6, 22] . As the first stage of the present investigation , WIMS methods and data were applied to two sets of single, natural-uranium rod/D_2O lattices, viz.

(i) a series of exponential experiments carried out in the subcritical assembly MINOR at Würenlingen [23] . The lattices were regular arrays of 10 mm diameter natural uranium metal rods, with square pitches of between 80 and 160 mm.

and (ii) critical lattice studies performed in the Process Development Pile of the Savannah River Laboratory [24] . These were hexagonal lattices with higher moderator-to-fuel volume ratios (V_m/V_f).

WIMS calculations were initially carried out with a view to assessing the effects of simple changes in data and numerical treatment. Most of the calculations were performed in 18 transport groups with 15–20 spatial points. Effects of further reducing the numerical approximations – e.g. using 36 energy groups, doubling the spatial mesh points or using n = 8 instead of n = 4 for the DSN routine – were all found to give $\lesssim 0.1\%$ in reactivity.

Despite the systematic differences between the Würenlingen and Savannah River experiments, the conclusions from the WIMS analyses were similar, viz.

(i) underprediction of k_{eff} was $\sim 1.0\%$ even when using the best numerical approximations and latest recommended moderator data.

(ii) the Kemshell modification to ^{238}U resonance data (Section 2.2) considerably reduced earlier reported trends with lattice pitch.

and (iii) use of the hardened ^{235}U fission spectrum (1.43 MeV temperature) increased fast fissions by 7 – 8%.

3.2 H_2O and graphite moderated single-rod lattices

The reactivity underprediction for D_2O lattices cannot be considered in isolation as any recommended changes in basic nuclear data should be generally applicable, i.e. to H_2O and graphite moderated systems as well. In order to assess the effects of the latest WIMS library data on predictions for light water lattices, the critical single-rod assemblies R/10CH [4] , were reanalysed. Calculations were carried out in 25 transport groups, more detailed high energy treatment being important for these lattices from the standpoint of slowing down in H_2O. The main conclusion drawn from these analyses was that while k_{eff} predictions for R1

TABLE I. "BEST-VALUE" WIMS REACTIVITY ESTIMATES FOR SINGLE-ROD LATTICES

Lattice	Fuel/Moderator	(V_m/V_f)	k_∞	k_{eff}
Wür 8	Nat. U/D_2O	19.4	1.143	0.991
Wür 12	Nat. U/D_2O	44.8	1.221	0.987
Wür 16	Nat. U/D_2O	80.5	1.211	0.985
SRL 1-7-I	Nat. U/D_2O	53.1	1.229	0.989
SRL 1-8-I	Nat. U/D_2O	71.1	1.230	0.990
SRL 1-9-II	Nat. U/D_2O	95.2	1.222	0.993
SRL 1-12-F	Nat. U/D_2O	161.5	1.182	0.991
R1/100 H	3% en. U/H_2O	1.00	1.260	1.000
R2/100 H	3% en. U/H_2O	3.16	1.328	0.993
R3/100 H	3% en. U/H_2O	0.78	1.212	1.000
BICEP 76	Nat. U/C	76.7	1.059	0.994
BICEP EMR 24/5	1.2% en. U/C	26.8	1.172	0.997

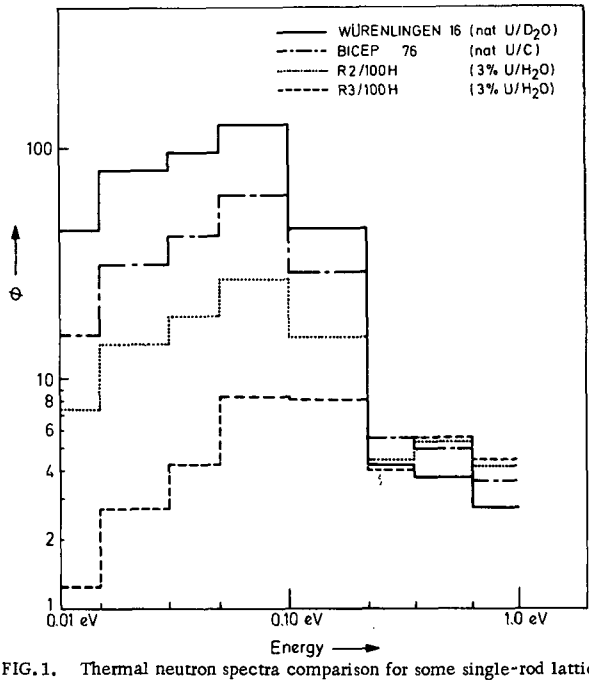

FIG. 1. Thermal neutron spectra comparison for some single-rod lattices.

TABLE II . ENERGY DISTRIBUTION OF CELL ABSORPTIONS FOR SOME SINGLE-ROD LATTICES

Lattice	Absorptions (normalised to total of 1000)							
	10 MeV-5.5KeV	5.5KeV-4.0 eV	4.0 - 0.625eV	0.625-0.100eV	0.100-0.050eV	0.050-0.030eV	0.030-0.015eV	0.015-0.0eV
	Gps.1-15	16-27	28-45	46-56	57-60	61-63	64-66	67-69
Wür 8	52	126	18	103	206	187	181	127
Wür 16	32	33	5	73	235	229	228	165
SRL 1-7-I	42	44	7	81	237	225	216	148
SRL 1-12-F	38	20	3	69	243	235	230	162
R2/100H	45	124	21	112	201	184	179	134
R3/100H	120	323	46	154	127	93	81	56
BICEP 76	54	81	16	110	238	202	180	119
BICEP 24/5	93	197	39	170	203	136	103	59

TABLE III . AGE PREDICTIONS (CM^2) FOR THE PRINCIPAL MODERATORS

Moderator	Present WIMS Value	Value with Earlier Data	Experiment
H_2O	27.3	26.6	27.8 ± 0.2 [25] 26.6 ± 0.3 [26]
D_2O	112	110 (DFN 218)	112 ± 2 [27]
Graphite	311	298	311 ± 2 [1]

TABLE IV . "BEST-VALUE" WIMS RESULTS FOR OAK RIDGE $^{235}U/H_2O$ SPHERES

Expt.	Sphere Radius (mm)	$(H/^{235}U)$ Ratio	k_∞	k_{eff}
1	346.0	1378	1.206	0.987
2	346.0	1177	1.202	0.987
3	346.0	1023	1.195	0.985
4	346.0	972	1.196	0.986
10	610.1	1835	1.065	0.988

and R3/100H were satisfactory, that for R2/100H was low by ~0.7%. As discussed later, this can be attributed to the fact that the neutron energy spectrum for R2/100H is radically different from the spectra for the other lattices.

Calculations for some of the BIGEP single-rod assemblies [3] were repeated using the latest recommended WIMS library data to see the effects on graphite moderated systems with simple geometry. It was found that k_{eff} values were generally underpredicted, though not as much as for the D_2O lattices. Further, the degree of underprediction varied with neutron spectrum for the lattice.

Table I summarises "best-value" WIMS reactivity estimates for the various types of single-rod lattices considered. It is seen that k_{eff} is underpredicted in all cases except for the two low (V_m/V_f) H_2O lattices R_1 and $R_3/100H$. Fig. 1 compares thermal, cell-averaged neutron energy spectra of some of the lattices for which k_{eff} is underestimated with that of $R_3/100H$. The differences indicate that thermal events are much less important in the latter case. A better comparison may be made by considering the energy distribution of neutron absorptions in the various lattice cells. This has been done in Table II, the normalisation being to a total cell absorption of 1000 neutrons. Considering Würr 8, R2/100 H and BIGEP 76, it is seen that although the moderator is different in each case, the distribution of absorption events is quite similar over the entire neutron energy range. One then gets a very consistent picture while noting that WIMS k_{eff} predictions for these single-rod lattices are 0.991, 0.993 and 0.994, respectively. These results indicate that the underprediction of reactivity is a moderator - independent deficiency. The most significant feature appears to be the energy distribution of neutron events, the discrepancies in k_{eff} being greater for the more thermalised lattices. There are no significant trends with resonance capture or with leakage (i.e. k_∞).

3.3 Neutron Age Measurements

Experimental determination of the age of fission neutrons to the 1.45 eV indium resonance is valuable evidence for testing methods and data effecting the calculation of leakage. The present study has involved the use of a considerably hardened fission spectrum, and there have also been significant modifications to moderator cross-sections. It is important to assess the effects of these changes on calculated values of the neutron age in graphite, H_2O and D_2O. Table III summarises WIMS results for the three moderators, obtained using the 1.43 MeV fission spectrum and the latest data files for hydrogen, deuterium and oxygen. Comparisons are made with earlier calculated values and also with the more recent experimental values [1, 25, 26, 27] . It is seen that the present predictions for D_2O and graphite agree very well with experiment but that for H_2O, the large spread in the experimental values prevents any definite conclusion being drawn.

3.4 Oak Ridge $^{235}U/H_2O$ Spheres

The series of critical homogeneous U/H_2O sphere experiments carried out at ORNL [28] is a particularly useful set for the present study, in that the geometry is simple, leakage effects are relatively small, the fuel is highly enriched (~93% ^{235}U) so that ^{238}U data effects are negligible, and finally, the neutron spectra are well thermalised so that any shortcomings in thermal data would be highlighted. Detailed experimental consideration of these ORNL criticals has been given by Staub et

TABLE V. ENERGY DISTRIBUTION OF FISSION YIELD FOR SOME OF THE EXPERIMENTS

Experiment	ORNL Expt. 1	Wür 12	SRL 1-7-I	R2/100H	R3/100H
k_∞	1.206	1.221	1.229	1.328	1.212
k_{eff}	0.987	0.987	0.989	0.993	1.000
$\nu\Sigma_f$ (norm. to 1000)					
0.625 - 0.35 eV	5	5	4	15	37
0.35 - 0.22 eV	8	9	7	23	52
0.22 - 0.10 eV	54	67	68	84	114
0.10 - 0.05 eV	207	233	239	223	173
0.05 - 0.03 eV	221	230	233	205	127
0.03 - 0.015 eV	248	229	227	198	110
0.015 - 0.0 eV	236	165	155	143	77
Net Thermal (< 0.625 eV)	979[a]	938	933	891	690

[a] 975, 972, 970 and 983 for Expts. 2, 3, 4 and 10, respectively.

al [29]. Recently three of the experiments (Nos. 1, 4 and 10) were analysed by Slaggie [30] using ENDF/B data, Versions I and II, and k_{eff} values were found to be consistently underpredicted, by ~0.7% with Version I and ~1.2% with Version II.

In applying WIMS to the analysis of the five ORNL $^{235}U/H_2O$ spheres, several checks were first carried out on the adequacy of the methods. Final "best-value" reactivity estimates obtained using the recommended data options are summarised in Table IV. The k_{eff} values are seen to agree well with the ENDF/B-II results reported by Slaggie, there being a consistent underprediction by ~1.4% for the four small spheres and by ~1.2% for the large one.

From the k_∞ values, it is seen that leakage is ~22% for Experiments 1-4 and only ~8% for Experiment 10. This difference provides a useful check on the adequacy of the leakage calculations for these H_2O moderated experiments. In any event, it is clear that the underprediction of k_{eff} by 1.2% for the large sphere cannot be explained by any discrepancy that may exist between theory and experiment for the age in H_2O (Section 3.3).

The use of ^{10}B as poison in three of the ORNL experiments enables a practical check on the adequacy of moderator absorption cross-sections, absorptions in hydrogen varying between 28% for Experiment 4 and 48% for Experiment 10. The consistent underprediction of k_{eff} for the spheres thus points at shortcomings in fuel cross-sections.

WIMS results for the experiments considered in Sections 3.1 and 3.2 have shown that the only type of single-rod lattice for which eigenvalues are low by more than 1%, is the D_2O moderated assembly, characterised by a well-thermalised neutron spectrum. Table V compares the energy distribution of fission yield, $\nu\Sigma_f$, for ORNL Experiment 1 with those for some of the single-rod lattices and shows that neutron spectra for the ORNL spheres are even more thermalised than for the D_2O lattices. The present results for the spheres thus strengthen the argument presented earlier, viz. that the underprediction of reactivity by WIMS is a moderator-independent deficiency which seems to be linked to shortcomings in thermal data.

4. MODIFICATION OF ^{235}U THERMAL DATA AND ITS EFFECTS

4.1 Discussion of Differential Data and Modifications Considered

The justification and the effects on WIMS predictions of certain simple changes in ^{235}U thermal data are discussed in this section. These have been considered in the light of a recent synopsis, by Westcott [31] , of the various differential measurements at thermal energies of σ_A , σ_f and α for the fissile nuclides. Although an assessment of the relative merits of the different sets of experimental points has not presently been made, it is realised that a least-squares fit is not necessarily the "best" curve especially when there is relatively large scatter among the data points, as is indeed seen to be the case from Figs. 2 and 3. The experimental points for σ_A are seen to have the least spread. This follows from the fact that absolute values are better defined for σ_A, than for either α or σ_f, as systematic errors are smaller in measurements of the former. In comparing different data sets, renormalisation can therefore be justified more easily for α and σ_f measurements than for σ_A sets. Another significant point is that the accuracy of the differential measurements is greatly reduced at very low energies ($E < 0.03$ eV) so that larger changes can be considered in this region.

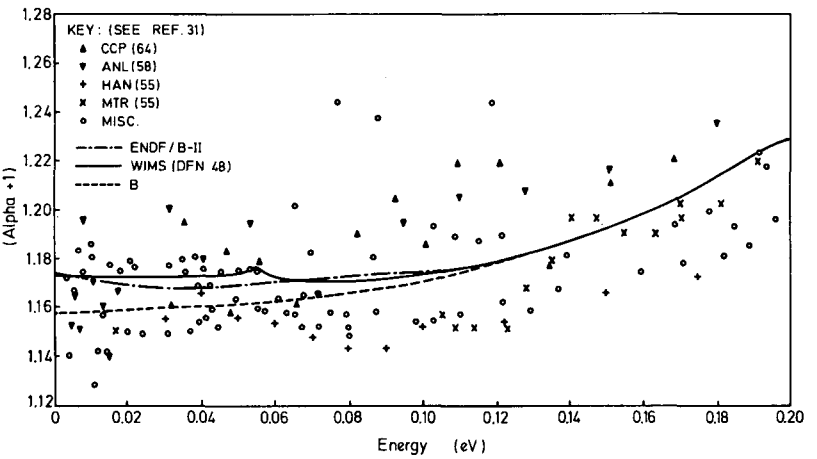

FIG. 2. ^{235}U α between 0.0 and 0.12 eV.

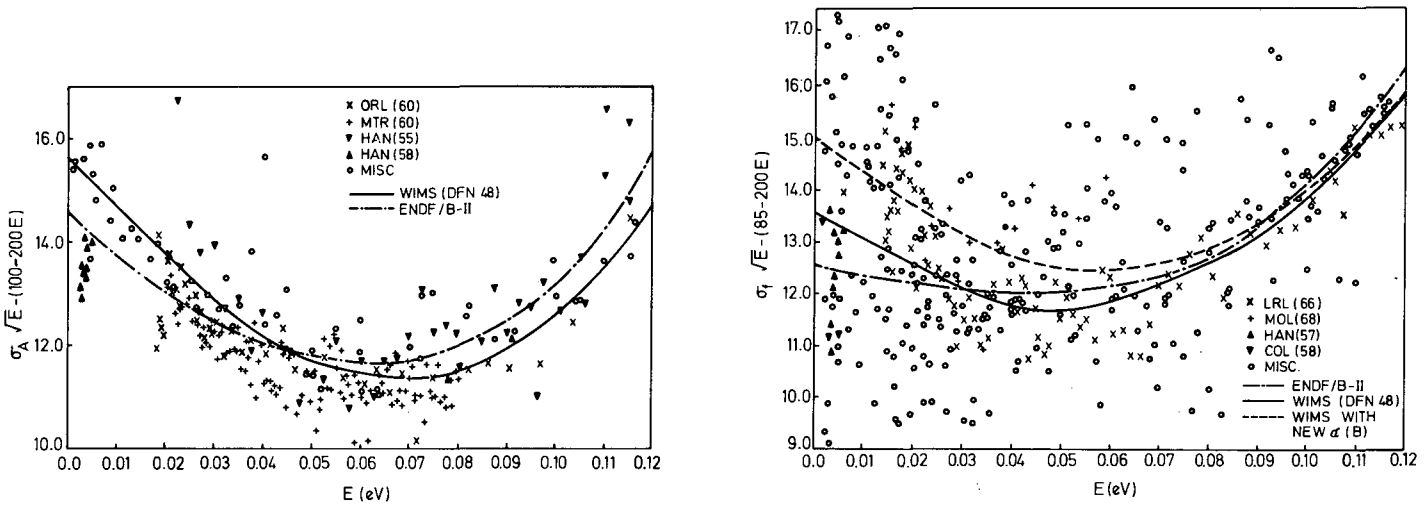

FIG. 3. σ_A and σ_f for ^{235}U between 0.0 and 0.12 eV.

For the discrepancies that have been shown to exist in WIMS reactivity predictions, modifications are sought to the thermal eta for ^{235}U, and the simplest change would be to vary α with absorptions remaining the same. As mentioned above, the measurements of σ_A are more reliable than those of σ_f and α. Hence, considering that the present WIMS data is a fairly good fit to the experimental σ_A points, it is appropriate to assume constancy of ^{235}U absorptions in WIMS and to modify σ_f through α.

The change currently recommended for the thermal ^{235}U α is shown in Fig. 2 as curve B. Instead of a nearly constant value of 0.173 below 0.05 eV, this variation implies an almost linear increase from ~0.157 at 0.0 eV to join smoothly with the earlier curve at 0.12 eV. The resulting variation of σ_f is shown in Fig. 3, the percentage variation (with σ_A remaining constant) being the same as that in $\left(\frac{1}{1+\alpha}\right)$. It is seen that both new curves, i.e. for α and for σ_f, lie well within the scatter of the experimental points.

4.2 Effects on WIMS predictions for benchmark experiments

Table VI summarises the effects, of using variation B for the ^{235}U thermal α, on reactivity predictions for the various sets of experiments considered in Section 3. The mean, unmodified WIMS eigenvalue for each set has been quoted along with the internal consistency, or total spread in the individual k_{eff}'s for that particular set. The values one obtains using the modified ^{235}U thermal data have been tabulated alongside, and it is seen that in this latter case the mean k_{eff} for every set lies in the range 0.996 - 1.003. Further, the internal consistency is improved for each set, particularly for those experiments which cover a relatively wide range of neutron energy spectra (e.g., the R/100H lattices).

TABLE VI. REACTIVITY PREDICTIONS FOR THE VARIOUS SETS OF EXPERIMENTS

Exptl. Set	Fuel (U)	Mod.	No. of Expts. Considered	WIMS K_{eff} predictions			
				Unmodified ^{235}U α		Variation B for α	
				Mean k_{eff}	Spread	Mean k_{eff}	Spread
Würenlingen	Nat.	D_2O	3	0.988	0.6%	0.996	0.5%
SRL	Nat.	D_2O	4	0.992	0.5%	1.001	0.5%
R/100H	3% en.	H_2O	3	0.998	0.7%	1.003	0.4%
BICEP	Nat. & 1.2% en.	C	2	0.995	0.3%	1.002	0.1%
ORNL	93% en. (homog)	H_2O	5	0.987	0.4%	0.997	0.4%

5. FURTHER VALIDATIONS

The satisfactory prediction of reactivity for simple, benchmark experiments is the most important basic criterion in testing a reactor physics code and its associated nuclear data library. However, it is in the analysis of systems with more complicated geometries and under power reactor conditions that a design code finds ultimate application. It was therefore decided to examine the validity of the presently recommended data modifications in the light of experimental evidence from (i) lattices with more complex geometries. e.g. clusters, and (ii) actual power reactor studies.

In view of the fact that earlier reported discrepancies have been largest for heavy water systems, particular attention was given to British and Canadian D_2O - moderated experiments [5, 6] . It was found that, with the presently recommended data modifications, a significant overall improvement is obtained in reactivity predictions for cluster lattices. Furthermore, agreement between theory and experiment was found to be considerably better for reaction rate ratios. Relative conversion ratio (R.C.R) predictions were within 2% of experimental values for a wide range of lattices, and fast fission ratios were underpredicted only by $\sim(3 \pm 2)\%$ compared with earlier errors of over 10%.

As an application to reactors under power conditions, an assessment was made of certain information from the Steam Generating Heavy Water Reactor (SGHWR) Prototype at Winfrith [32] . It was found that reactivity changes with burnup are predicted quite satisfactorily using the modified data in WIMS. However, evidence on the isotopic composition of irradiated fuel was inconclusive. Overall, the presently recommended data, being a more consistent interpretation of available differential and integral information, was thought to be quite acceptable as an interim improvement for reactor design computations.

6. SUMMARY AND CONCLUSIONS

The main aim of this study has been to present a comprehensive comparison between theoretical predictions and integral evidence from thermal reactor physics experiments, in order that a consistent set of recommendations can be made to resolve a range of earlier reported discrepancies. For the most part, the Winfrith-developed code WIMS, has been used. However, reference has been made in places to American methods and data, thereby providing a check on theoretical treatment.

Following Kemshell's recent survey of relative conversion ratio measurements [9] , the recommended modifications to ^{238}U data have been incorporated into the WIMS library, together with the latest changes in moderator scattering cross-sections. Present calculations have confirmed that ^{238}U capture rates are now predicted satisfactorily for various types of reactor lattices. Further, a ^{235}U fission energy spectrum with a temperature of 1.43 MeV has been used in the present analyses, which implies $\sim$10% hardening of the earlier used Bonner spectrum. This modification has significantly improved the prediction of fast fission ratios. The calculation of age in graphite and D_2O has also been improved, but the evidence for H_2O remains somewhat inconclusive.

Using the above modifications in nuclear data, analysis of a range of single-rod uranium lattices with each of the three principal moderators - D_2O, H_2O and graphite - indicated a trend to underpredict reactivity which was found to be related to the energy distribution of thermal neutron events in the fuel, rather than to the type of moderator used. By analysing a series of well thermalised, homogeneous critical sphere

experiments with highly enriched fuel (~93% ^{235}U), any possible residual errors due to uncertainties in ^{238}U data were completely eliminated and attention strongly focused on thermal ^{235}U cross-sections. An energy - dependent variation of the ^{235}U thermal α, based on keeping the more reliably known absorption cross-section unchanged, has been considered within the spread of differential measurements, and it has been shown that this produces considerable improvement in the consistency of reactivity results for the different types of benchmark experiments analysed, the various predicted mean k_{eff} values lying in the range 0.996 - 1.003.

Finally, a limited survey of cluster lattice experiments and power reactor studies has been used to provide some direct evidence of the improvement obtained in reactor design calculations with adoption of the presently recommended data modifications.

ACKNOWLEDGEMENTS

This study was carried out under a Research Fellowship with the United Kingdom Atomic Energy Authority. The author would like to express his gratitude to several people at the Atomic Energy Establishment, Winfrith, in particular to Dr. F.J. Fayers and Dr. D. Hicks, of the S.G.H.W.R. Development Division, for their guidance, advice and encouragement.

REFERENCES

1. ASKEW, J.R., FAYERS, F.J., KEMSHELL, P.B., J. Brit. Nucl. Energy Soc. 5 (1966) 564.

2. SUICH, J.E., HONECK, H.C., Rep. DP - 1064 (1967).

3. BARCLAY, F.R., Rep. AEEW - R473 (1966)

4. FAYERS, F.J., KEMSHELL, P.B., TERRY, M.J., J. Brit. Nucl. Energy Soc. 6 (1967) 161

5. BRIGGS, A.J., JOHNSTONE, I., KEMSHELL, P.B., NEWMARCH, D.A., J.Brit. Nucl. Energy Soc. 7 (1968) 61

6. KEMSHELL, P.B., Rep. AEEW - R549 (1969)

7. ASKEW, J.R., Rep. AEEW - M602 (1965)

8. FOX, W.N., KING, D.C., PITCHER, H.H.W., SANDERS, J.E., J. Brit. Nucl. Energy Soc. 9 (1970) 15.

9. KEMSHELL, P.B., Rep. AEEW - R 786 (1972)

10. STORY, J.S., et. al., Proc. Int. Conf. Peaceful Uses Atom.Energy, Geneva (1964) 168.

11. BELL, V.J., et. al., Rep. AEEW - R379 (1964)

12. MACDOUGALL, J.D., Rep. AEEW - M318 (1963)

13. BRISSENDEN, R.J., DURSTON, C., Rep. ANL - 7050 (1965) 51.

14. BANNISTER, G.W., BASHER, J.C., PULL, I.C., Rep. AEEW - R 243 (1968)

15. LESLIE, D.C., J. Nucl. Energy 17 (1963) 293

16. BENOIST, P., AERE Trans. 842 (1959)

17. ROTH, M.J., MACDOUGALL, J.D., KEMSHELL, P.B., Rep. AEEW-R538 (1967)

18. HARDING, R.S., GAVIN, P.H., HEILENS, R.L., ANS Trans. 1969 Winter Meeting 12 2 744.

19. FEINER, F., ESCH, L.J., Reactor Physics in the Resonance and Thermal Regions, Vol. II, M.I.T. Press (1966) 299.

20. GRUNDL, J.A., Nucl. Sci. Engng. 31 (1968) 191.

21. CAMPBELL, C.G., ROWLANDS, J.L., Proc. IAEA Conf. Nucl. data Reactors, Helsinki (1970) IAEA - CN - 26/116.

22. ROTHENSTEIN, W., Rep. BNL - RP - 1001 (1969)

23. LUTZ, H.R., et al., Proc. IAEA Conf. Exponential and Crit Expts. Vol. II (1964) 85

24. HURLEY, T.J. Jnr., FIKE, H.R., O'NEILL,G.F., Nucl. Sci., Engg. 12 (1962) 341.

25. DOERNER, R.C., et al., Nucl. Sci. Engng. 9 (1961) 221

26. PASCHALL, R.K., Nucl. Sci. Engng. 20 (1964) 436

27. GRAVES, W.E., Nucl. Sci. Engng. 12 (1962) 439

28. GWIN, R., MAGNUSON, D.W., Nucl. Sci. Engng. 12 (1962) 364

29. STAUB, A., et. al., Nucl. Sci. Engng. 34 (1968) 263

30. SLAGGIE, E.L., Rep. Gulf - RT - 10337 (1971)

31. WESTCOTT, C.H., Rep. AECL - 3255 (1969)

32. FAYERS, F.J., J. Brit. Nucl. Energy Soc. 11 (1972) 29

UTILISATION DE RESULTATS DE MESURES INTEGRALES POUR PRECISER LES VALEURS DES CONSTANTES NUCLEAIRES NEUTRONIQUES

P. REUSS
CEA, Centre d'études nucléaires
de Saclay,
France

Abstract–Résumé

USE OF RESULTS OF INTEGRAL MEASUREMENTS IN DETERMINING MORE PRECISELY THE VALUES OF NEUTRON NUCLEAR CONSTANTS.

Integral neutron measurements may – since we now have very precise codes – provide significant information on nuclear constants. Their analysis performed in this spirit is the logical outcome of important experimental research done on reactors. It does not allow testing all data of the calculation, but only those quantities which are already of a global nature. The analysis dealt with in the present paper, concerning measurements of the Laplacian relating to all thermal-neutron-reactor types, has, above all, confirmed the new normalization of the ^{235}U fission cross-section and given rise to a decrease of the ^{238}U effective resonance integral.

UTILISATION DE RESULTATS DE MESURES INTEGRALES POUR PRECISER LES VALEURS DES CONSTANTES NUCLEAIRES NEUTRONIQUES.

Les mesures neutroniques intégrales peuvent conduire, maintenant qu'on dispose de codes très précis, à des renseignements significatifs sur les constantes nucléaires. Leur analyse, faite dans cet esprit, est l'aboutissement logique de l'important travail expérimental fait sur les piles. Elle ne permet pas de tester toutes les données du calcul mais des grandeurs à caractère synthétique. Celle dont le mémoire rend compte, entreprise sur des mesures de laplacien relatives à l'ensemble des filières à neutrons thermiques, a conduit, principalement, à confirmer la nouvelle normalisation de la section de fission de l'uranium-235 et à proposer une diminution de l'intégrale effective de résonance de l'uranium-238.

1. INTERET DES MESURES INTEGRALES

1.1. Mesures intégrales

Les quantités intégrales qu'on mesure dans un massif ou une expérience critique sont souvent obtenues avec une très grande précision. Cette seule remarque incite à penser que ces mesures pourraient être utilement considérées par ceux qui se préoccupent du problème des constantes nucléaires.

Les résultats qu'on obtient ne sont pas des constantes nucléaires : ils en dépendent directement mais de façon complexe. On peut dire qu'on mesure des fonctionnelles des sections efficaces.

Inversement, ce qui intéresse en premier lieu le physicien des réacteurs n'est pas tant les sections efficaces des différents noyaux que les valeurs de quelques paramètres très globaux, tel un facteur de multiplication. On serait logiquement amené à mesurer les quantités intégrales auxquelles on s'intéresse, mais, à cause d'impératifs expérimentaux, ce ne sont, généralement, pas exactement les mêmes : par exemple on s'intéresse au facteur de conversion mais on mesure un indice captures ^{238}U/fissions ^{235}U relatif. Les définitions en sont cependant toujours voisines.

1.2. Intermédiaire du calcul

Que ce soit pour passer des grandeurs mesurées aux grandeurs intéressantes, ou pour tester les constantes de base à partir des mesures intégrales, il y aura un intermédiaire indispensable : le calcul de la fonctionnelle reliant les sections efficaces à la grandeur considérée. Il est donc clair que, si ce calcul n'est pas extrêmement précis et fiable, la précision expérimentale qu'on a au niveau de la mesure devient totalement illusoire, surtout quand on passe au niveau du test des données de base.

1.3. Situation ancienne des codes de calcul

Jusque dans un passé récent le schéma trop simpliste des calculs rendait très critiquable l'utilisation des mesures intégrales pour le test des sections efficaces, à tel point qu'on a souvent adopté une démarche de pensée différente.

La mise au point du code COREGRAF [1] (calcul des réseaux de la filière uranium naturel-graphite-gaz) peut servir d'exemple. On a, a priori, laissé indéterminés quelques paramètres (en l'occurrence les constantes A et B de l'expression classique de l'intégrale effective de ^{238}U : $I_{eff} = A + B\sqrt{S/M}$). En interprétant systématiquement un grand nombre d'expériences (mesures de laplacien) on a déterminé ces paramètres. On voit que l'ajustement fait a eu en réalité deux objectifs: non seulement pallier une méconnaissance des sections efficaces dans le domaine des résonances, mais encore corriger les approximations faites par ailleurs dans le schéma de calcul. Ce deuxième objectif était bien présent comme le montre le fait qu'il a fallu ajuster deux intégrales effectives : l'une pour les calculs critiques, l'autre pour les calculs d'évolution. On a remédié de la sorte, entre autres, à l'hypothèse trop simpliste consistant à négliger la répartition non uniforme au sein du barreau des captures de ^{238}U donc de la formation de ^{239}Pu.

1.4. Situation présente des codes de calculs

Depuis quelques années des outils beaucoup plus perfectionnés ont été mis au point. On peut prendre comme exemple le code APOLLO [2] résolvant dans un grand nombre de groupes (186 ou 99) l'équation de Boltzmann en géométrie à une dimension par la méthode des probabilités de premier choc. On peut penser que maintenant le passage des sections efficaces microscopiques aux quantités intégrales auxquelles on s'intéresse est beaucoup moins hasardeux, au moins dans les cas simples (par exemple, réseau régulier de cellules contenant un barreau cylindrique de combustible).

Une autre remarque très importante doit être faite : non seulement l'outil de calcul s'est perfectionné, mais il s'est aussi généralisé. Ainsi, alors que COREGRAF ne pouvait être utilisé que pour les calculs de réacteurs de la filière UNGG (parce que l'ajustement n'était valable que pour cette gamme étroite de situations), APOLLO peut servir au calcul des réseaux des réacteurs de n'importe quelle filière.

1.5. Nouvel intérêt des mesures intégrales

L'utilisation des mesures intégrales pour tester les sections efficaces devient maintenant intéressante. D'une part les imprécisions dues au calcul nécessaire pour faire la transposition semblent maintenant suffisamment faibles pour ne pas rendre illusoire cette démarche (au sens indiqué et non au sens «ajustement du code de calcul»). D'autre part le fait qu'un même code devient utilisable pour interpréter une bien plus large gamme de situations va rendre ce test beaucoup intéressant : par exemple il est bien évident que c'est le même uranium qu'on met dans tous les réacteurs. Si on utilise des quantités intégrales (qui dépendent de ses sections) mesurées dans des situations très différentes, on aura une information beaucoup plus précise.

1.6. Difficulté de mise en œuvre

Les sections efficaces sont des fonctions, donc sont représentées par une infinité de valeurs numériques. Même si on se limite à un schéma multigroupe, comme dans APOLLO, ce sont des milliers de valeurs numériques qu'on utilise dans les calculs.

D'autre part, même en considérant toutes les mesures intégrales faites dans le monde, il est bien clair que le nombre de renseignements de ce type est bien moindre.

Il n'est, par conséquent, pas question de tester toutes les sections efficaces par les mesures intégrales. Cela signifie qu'il y a un préalable à ce genre d'études : il faut synthétiser l'information que représentent les milliers de sections efficaces en un petit nombre de grandeurs les caractérisant de façon globale.

On a là une étape intermédiaire nécessitant un choix délicat à faire : ces grandeurs doivent d'une part représenter de façon correcte les sections efficaces qu'on veut tester, d'autre part jouer un rôle non négligeable dans le calcul des quantités intégrales qu'on examine et de celles auxquelles s'intéresse le physicien des réacteurs. Pour prendre des exemples extrêmes : la valeur moyenne de la section efficace de ^{235}U dans le domaine des résonances caractérise mieux cette fonction que le maximum dans le même domaine ; la section à 2200 m/s de ^{241}Am joue un rôle moins important que celle de ^{235}U.

2. EXEMPLE DE MISE EN ŒUVRE

2.1. Principes de l'étude qui a été faite

On a cherché à appliquer les idées évoquées plus haut à l'étude critique du code APOLLO. Dans une première étape on s'est limité aux réseaux à combustible en uranium frais, appartenant aux différentes filières à neutrons thermiques. En effet, dans un réacteur à neutrons rapides la situation neutronique est vraiment trop différente et ce serait d'autres grandeurs synthétiques qu'on pourrait tester (et non les mêmes dans un rôle différent).

On est parti des données de la bibliothèque UKAEA [3]. On a caractérisé l'ensemble des sections qu'elle contient par douze grandeurs seulement. En examinant les divergences entre calcul et expérience sur un certain nombre de mesures intégrales soigneusement choisies on a cherché à dégager des tendances à modifier l'une ou l'autre de ces grandeurs. Ces tendances pourront ensuite être utilisées dans deux optiques : soit le choix, pour chaque noyau, de la bibliothèque la mieux en accord avec ces tendances obtenues; soit l'ajustement de la bibliothèque dont on est parti.

2.2. Méthode utilisée pour la recherche de tendances

Désignons par U_n l'une des grandeurs synthétiques retenues et Q_i l'une des quantités intégrales examinées. Au premier ordre, pour une petite modification des U_n, on peut écrire

$$\delta Q_i = \sum_n \alpha_{in}\, \delta U_n \qquad (1)$$

Si on peut trouver un jeu de modifications δU_n tel que les écarts entre expérience et calcul corrigé par (1) soient sensiblement réduits, on aura dégagé les tendances à ces modifications.

Pratiquement on a procédé de la façon suivante :

– On a évalué les coefficients d'influence α_{in} par des formules simples, ce qui a permis d'éviter de passer un grand nombre de fois le code APOLLO.

– Considérant les variations maximales des U_n qu'on peut admettre compte tenu des imprécisions sur les mesures des sections, on a éliminé de l'étude les U_n conduisant à des modifications trop petites des Q_i (une tendance dégagée sur une telle grandeur n'aurait pas été significative).

– Pour les U_n restants on a cherché les modifications améliorant de façon claire la cohérence entre calcul et expérience sans conduire à des variations prohibitives des U_n. Pour cela on a ajusté les δU_n de (1) par moindres carrés en minimisant l'écart quadratique moyen entre mesure et calcul des Q_i, tout en donnant un certain poids aux mesures des sections efficaces (ce qui signifie qu'on suppose plus probable que $|\delta U_n|$ soit petit que grand).

2.3. Mesures utilisées

Deux types de mesures ont été utilisées :

- des mesures de l'âge pour les trois principaux modérateurs (graphite, eau ordinaire, eau lourde),
- des mesures de laplacien et de taux de réaction dans des réseaux appartenant à toutes les filières à neutrons thermiques :

RHT (mesures françaises)
UNGG (mesures françaises)
D_2O (mesures françaises)
H_2O (mesures américaines).

Par ailleurs on a utilisé la valeur de la section de fission de ^{235}U tenant compte de la nouvelle évaluation de la période de ^{234}U et les valeurs recommandées dans [4] pour les sections de diffusion des modérateurs dans le domaine des résonances des noyaux lourds.

2.4. Grandeurs synthétiques conservées dans l'étude et tendances obtenues

Après élimination des grandeurs peu efficaces on a conservé pour la recherche de tendances les U_n suivants :

σ_{f8} – section moyenne de fission de ^{238}U
I_{eff8} – intégrale effective de résonance de ^{238}U
σ_{f5} – section moyenne de fission de ^{235}U
τ – âge dans le modérateur
D – coefficient de diffusion thermique moyen du modérateur.

L'étude a conduit à proposer les modifications suivantes (de la bibliothèque UKAEA) :
- prendre pour τ les valeurs mesurées qui sont un peu supérieures aux valeurs qu'on obtient en utilisant la bibliothèque ;
- ne pas modifier en plus des fuites (τ et D), ou alors très légèrement si on veut recentrer au mieux les résultats ;
- prendre la valeur de σ_{f5} normalisée avec la nouvelle évaluation de la période de ^{234}U. Il est intéressant de noter que la recherche de tendances qui a été faite a confirmé cette nouvelle valeur.
- diminuer I_{eff8} de 0,8 barn.

Ce dernier point est sans doute le plus important. On sait que cette conclusion est classique: elle avait déjà été notée lors de l'ajustement de COREGRAF; elle a également été obtenue par d'autres auteurs.

CONCLUSION

Une fois admis qu'on peut faire confiance au code de calcul on ne peut guère douter de l'intérêt de prendre en compte les mesures intégrales pour préciser les constantes neutroniques. Par contre la mise en œuvre peut être revue : on peut critiquer le choix des grandeurs synthétiques retenues, le choix des mesures intégrales utilisées et la méthode de recherche des tendances. L'application a été faite dans un cadre restreint. On pourrait l'étendre, en particulier, à l'étude du plutonium.

Il nous semble que ce n'est que par une étude critique remontant jusqu'au test des données de base qu'on peut pleinement justifier et valoriser le travail expérimental de longue haleine qui a été accompli et est poursuivi sur les maquettes ou les piles. Un simple constat des divergences entre calcul et expérience est peut-être un renseignement suffisant pour l'exploitant des réacteurs, mais certainement pas pour le physicien qui a besoin de savoir les expliquer.

REFERENCES

[1] COGNE, F., HOFFMANN, A., REUSS, P., COREGRAF 2, code de calculs de réseaux et d'évolution des réseaux à graphite, CEA-N-1344 (1970).

[2] HOFFMANN, A., JEANPIERRE, F., KAVENOKY, A., LIVOLANT, M., LORAIN, H., APOLLO, code multigroupe de résolution de l'équation du transport pour les neutrons thermiques et rapides, CEA-N-1610 (1972).

[3] NORTON, S., The UKAEA Nuclear Data Library, AEEW-M824 (1968).

[4] KEMSHELL, P.B., Some Integral Properties of Nuclear Data Deduced from WIMS Analyses of Well Thermalised Uranium Lattices, AEEW-R786 (1972).

DISCUSSION

J. BOUCHARD: My question is addressed to Mr. Reuss and also to Mr. Barré: what, from your point of view, are the most important integral measurements?

P. REUSS: As far as thermal neutron reactors are concerned, the most important measurements are the following: buckling (or k_{eff}); the ratio ^{238}U fissions/^{235}U fissions; conversion factor, i.e. ^{238}U captures/^{235}U fissions; also, analyses on irradiated fuels.

J. Y. BARRE: In the case of fast neutron reactors, among the most important integral experiments, i.e. measurements of neutron balance parameters which can be carried out very easily (one might say "asymptotically"), mention should be made of the following: material buckling; ratio of production to total absorption, or the "K_∞ parameter"; ratio of average reaction rates, either of fission or capture, especially the average ratio ^{238}U captures/^{239}Pu fissions, which is at present measured with a precision of ± 2 by our techniques and enables us to have very good confidence in the calculated breeding gain.

G. CASINI: I should like to comment on integral experiments, in particular, those relating to burnt lattices. As has been pointed out in the preceding discussion, there are a number of bench-mark experiments with which the reliability of nuclear data can be checked – especially in the case of unirradiated lattices. An effort has been made in the United States to select 12 bench-mark experiments for fast breeders and a similar program for thermal lattices is being undertaken by the European-American Reactor Physics Committee. However, I feel that it would be desirable to devise a number of bench-mark experiments for the case of irradiated lattices, covering in particular isotopic concentrations and, if possible, reactivity values as well. I think an international effort along these lines would be welcome.

Section III
SAFEGUARDS

Chairman

O.J. EDER (Austria)

THE ROLE OF NUCLEAR DATA IN NUCLEAR MATERIAL SAFEGUARDS

C. WEITKAMP, A. v. BAECKMANN, K. BÖHNEL, M. KÜCHLE
Gesellschaft für Kernforschung, Karlsruhe

L. KOCH
European Institute for Transuranium Elements,
Karlsruhe, Federal Republic of Germany

Abstract

THE ROLE OF NUCLEAR DATA IN NUCLEAR MATERIAL SAFEGUARDS.

For the timely detection of a diversion of fissionable material from the nuclear fuel cycle the safeguards system uses material balances based on measurements of material flow and inventory. In addition to classical analytical techniques, various nuclear methods have been developed for this purpose. The general procedure for most of these methods consists in the determination of the mass of the fissile specimen relative to a known standard. The way in which nuclear data are required for the development or efficient use of the methods can be divided into four categories. (A) The very feasibility of the method or its development depend upon data insufficiently known. (B) Data are directly needed for the conversion of measured values into material mass; no standard specimens are used. (C) The use of a sufficiently large set of standards is impossible or impractical; therefore nuclear data are needed for calibration or interpolation. (D) The use of standards provides full calibration possibilities, or existing data are adequate.

For purposes of illustration a few methods are discussed. An extreme example for category A is gamma resonance fluorescence where the accuracy required for the level and transition energies is far beyond present-day capabilities. Calorimetry and α-spectrometry are directly based upon half-lives and energies some of which are inadequately known (case B). Typical methods for which the number of standards can be greatly reduced by calculation are neutron coincidence determination of plutonium, all techniques that use thermal neutron interrogation and different kinds of activation analysis; some of the required nuclear data need improvement (case C). Passive γ-assay and fast-neutron interrogation belong to category D. Spent fuel is generally not amenable to direct measurement of fissile material content. Here isotope correlations as now determined empirically for a number of thermal reactors and within the burn-up range presently obtainable lend themselves to the indirect determination of burn-up parameters including fissile material content. This correlation technique has proved remarkably universal. An extended general application requires quantitative theoretical explanation which is only possible if the integral neutron reaction cross-sections of heavy isotopes and selected fission products are improved.

1. INTRODUCTION

In order to detect and prevent the diversion of fissionable material from the nuclear fuel cycle, a worldwide system has been developed that is generally referred to as nuclear material safeguards. This system is based to a large extent on the closure of material balances. In order to set up the balance accurate measurements of inventory and all input and output of the particular material balance area are necessary. These measurements cannot always be performed, or are impractical to perform, by classical (i.e., non-nuclear) means. So methods for the determination of reactor fuel have been developed that make use of its nuclear properties. It is the purpose of this paper to show in which way the assay of nuclear fuel depends upon the availability and accuracy of nuclear data.

TABLE I. CATEGORIES OF METHODS GROUPED ACCORDING TO THEIR DEPENDENCE UPON NUCLEAR DATA

Category	Dependence upon Data	Examples
A	The feasibility of the method or its development depend upon data insufficiently known.	γ-Ray Resonance Flurescence Neutron Capture γ Spectroscopy
B	Data are directly needed for the conversion of measured values into physical quantities (isotopic ratio, material mass); no standard specimens are used.	α Spectrometry Calorimetry
C	Measurements are made relative to standard samples, but the proper application of corrections requires nuclear data.	Thermal Neutron Interrogation Activation Analysis Neutron Coincidence Techniques
D	The use of standards provides full calibration possibilities, or existing data are adequate.	Passive γ Assay Fast Neutron Interrogation

Instead of presenting a list arranged similarly to the well-known INDC nuclear data request compilation [1] we discuss a few individual methods with respect to their dependence upon nuclear data, trying to group them into four categories as shown in Table I.

2. GAMMA-RAY RESONANCE FLUORESCENCE

An example for a method that is only now being investigated for its use in the assay of nuclear material is γ-ray resonance fluorescence. In this method the sample is irradiated with γ rays, and the resonance-scattered photons are measured with a well-shielded detector. The method utilizes the fact that the elastic scattering cross section which, at a γ-ray energy around 1 MeV, is 1 barn for isotopes of uranium and plutonium, increases by orders of magnitude if the energy of the γ-ray is very close to the energy of a level of the nuclide of interest, e.g. ^{235}U. Emission by an identical system does usually *not*, as it does in optical spectroscopy, fulfill the energy requirement because the energy loss of the γ-ray due to recoil of the residual nucleus exceeds the width of the γ line by a factor of ten. Even if intense sources of radiation that deexcite appropriate levels in ^{235}U were available (which is not the case), other sources of γ radiation would therefore have to be used.

The cross section for γ resonance fluorescence can be shown [2] to be given by

$$\sigma = 1.4\ g\ \gamma^2\ (E^2\ \tau\ \delta)^{-1}\ \exp\{-(\Delta E/\delta)^2\}\ \text{barn} \qquad (1)$$

where E is the energy of the γ ray or of the level in MeV, τ its lifetime in picoseconds, $g = (2J_1+1)/(2J_0+1)$ the statistical factor which accounts for the angular momenta J_0 and J_1 of the ground and excited states, and $\gamma = \Gamma_0/\Gamma$ the branching ratio for deexcitation of the excited state into the ground state. $\Delta E = |E_a - E_e + R|$ is the energy mismatch, i.e. the difference between the level energy E_a and the γ-ray energy E_e minus recoil R (in eV), and δ (also in eV) is a width parameter which, if line shapes are approximated by Gaussians, is given by $\delta^2 = \Delta_a^2 + \Delta_e^2$, Δ_a and Δ_e being the level width of the absorber and line width of the emitter, respectively.

In order to predict the feasibility of an experiment designed to produce a sizeable enhancement of the elastic scattering cross section, an attempt has recently been undertaken [3] to compare energies of known states of ^{235}U with tables of γ-ray energies from radioactive sources and to compute the resonance contribution to the cross section via eq. (1). This work could only yield candidates (pairs of matching γ sources and ^{235}U nuclear states) for an experiment; exact cross sections could not be obtained due to lack of sufficient and sufficiently accurate nuclear data for various quantities, in particular

(1) Energy: state-of-the-art measurements of γ-ray and level energies around 1 MeV are accurate to about 25 eV, with the main contribution of 22 eV from the reference energies and only 13 eV from all experimental errors [4]. As γ-ray widths in excess of 10 eV can be obtained by use of special techniques like Coulomb fragmentation [5], the present

TABLE II. ENERGY E AND PARTIAL PRODUCTION CROSS-SECTION σ FOR THE MOST INTENSE γ-LINES FOLLOWING THERMAL NEUTRON CAPTURE

Isotope	E, keV	σ, barn	Reference	Element	E, keV	σ, barn	Reference
^{235}U	6395.5 ± 0.3	0.32 ± 0.05	[11]	Cr	8881	0.22	[15]
^{238}U	4059.4 ± 2.0	0.30 ± 0.04	[12]	Fe	7646, 7632	0.55 + 0.55	[15]
^{239}Pu	5123.2 ± 0.4	2.05 ± 0.40	[10, 13]	Ni	8996	1.20	[15]
^{241}Pu	5476.9 ± 0.5	7.60 ± 1.90	[14]	Cu	7917	1.52	[15]

state of development of energy measurements is not inadequate. However, few authors go through the tedious procedure of analyzing their measured data to that degree of accuracy, or if they do, fail to publish important details of their work as, e.g., the set of reference energies used. So a consistent comparison of data from different authors is seldom possible.

In the case of ^{235}U, energies of levels around 1 MeV are accurate to 100 - 300 eV if measured by γ-ray spectroscopy (following the reaction $^{234}U(n,\gamma)^{235}U$) or about 2 keV from charged-particle spectroscopy. For the most promising level, however, an energy of (1116.2 ± 0.2) keV has been quoted (computed from cascade deexcitation) whereas the ground state transition energy is given as (1115.6 ± 0.3) keV [6]. A source of 245 d - ^{65}Zn with its strong (1115.518 ± 0.025) keV γ-ray may provide some chance for resonance excitation only if the latter of the two level energies is correct.

(2) Other properties of excited states: for the computation of the cross section from eq. (1) the spin, deexcitation branching ratio and half life of the level of interest are also required. One of the virtues of the 1116 keV state of ^{235}U is that its values for J and Γ_0/Γ are known; the half-life, although not measured, can be computed theoretically within a factor of 10 or so from the spin, parity, and K quantum number which are all known.

The number of candidates for assay by γ resonance fluorescence could be greatly increased if more details were known about the level scheme of ^{235}U. Only then would the start of an experimental program be justified in which the feasibility of the method is proved. So γ ray resonance fluorescence which could offer considerable advantages over existing methods of ^{235}U assay is an example how lack of data can affect a method in its very first stage of development.

3. NEUTRON CAPTURE GAMMA-RAY SPECTROSCOPY

Another method for which data dependence has also been critical at an early stage is γ-ray spectroscopy following neutron capture. The reason for this has been the fact that, after a feasibility study of the method had shown its potential applicability to the assay of individual isotopes in nuclear fuel [7], γ rays from capture had to be identified as such, and partial capture γ-ray production cross sections had to be measured. The first problem was solved using different approaches [8 - 10], and it turned out that, in agreement with expectations, only few low-energy γ rays can be definitely assigned to capture, but in the high-energy part of the spectra (E > 4 MeV) most of the lines observed are indeed primary capture γ rays. Intensity measurements, however, had the somewhat disappointing result that partial production cross sections for the strongest primary γ rays are a factor of 10 to 30 smaller than expected. The most intense capture γ ray of some isotopes of uranium and plutonium and the corresponding production cross section for thermal neutrons are listed in Table II. For comparison the same data are also given for a number of metals that occur in alloys for structural and cladding materials. As Table II shows, γ-ray

energies from capture in fuel are usually lower and production cross sections only of the same order of magnitude as for other materials. Therefore very good statistics is required which can only be obtained by using a reactor neutron beam; due to this fact the method has not matured into a widely-used procedure for in-plant application. If photon production cross sections had been at hand in an early stage a much more detailed prediction of the potential and limitations of the method would have been possible.

4. ALPHA SPECTROMETRY

The measurement of ^{238}Pu which is of great importance for the assay of reactor plutonium by calorimetry (cf. chapter 5) or coincidence counting is usually done by α spectrometry or mass spectrometry. Because mass-238 contaminations from uranium are hard to avoid, α spectrometry is the preferred method, particularly for concentrations <0.3 %, and in some laboratories including our own the cross check of mass spectrometric ^{238}Pu measurements by α spectrometry is current practice.

For the computation of the atomic ratio P_8/P_9 of ^{238}Pu and ^{239}Pu from the measured ratio α of ^{238}Pu activity and the sum of the activities of ^{239}Pu and ^{240}Pu from the relation

$$P_8/P_9 = \alpha\, T_{1/2}(^{238}Pu)\left\{\frac{1}{T_{1/2}(^{239}Pu)} + \frac{P_0/P_9}{T_{1/2}(^{240}Pu)}\right\}$$

the precise knowledge of the half lives $T_{1/2}$ of ^{238}Pu, ^{239}Pu and ^{240}Pu is required, and geometrical factors for the detection of α particles from ^{238}Pu and $^{239,240}Pu$ must be equal. Whereas α spectra of the three isotopes seem to be known with adequate accuracy and the values of the half lives of ^{239}Pu and ^{240}Pu have not changed much in recent years, new measurements of $T_{1/2}(^{238}Pu)$ changed its value from 86.4 years [16] to 87.8 years [17], i.e. by 1.6 %. This accounts perfectly for the systematic deviation of the results of α spectrometric ^{238}Pu determinations which were systematically low as long as the older half life was used. Therefore an independent reinvestigation of all three half lives appears valuable.

5. CALORIMETRY

Half lives of plutonium isotopes are sufficiently short so this material can be determined nondestructively by measurement of the decay heat

$$H = (\Sigma\, s_i p_i)\, M = \frac{1}{\varepsilon}\, M \qquad (2)$$

H is related to the plutonium mass M by a proportionality factor $\frac{1}{\varepsilon}$ given by the sum of the products of the specific power constants s_i and percentages p_i of the isotopes involved. Unlike most other methods, calorimetry relies heavily on precise nuclear data because the determination is usually done by absolute measurement of electric quantities without reference to a set of standard samples. The use of standards would be impractical because too many parameters would have to be varied. Just as α

spectrometry can be considered an absolute method for the determination of isotope *ratios*, calorimetry is often referred to as an absolute method for the measurement of plutonium *quantities*.

The conversion of heat output into plutonium mass via eq.(2) is complicated by the fact that the isotopic composition is usually not measured at the same time. The actual percentages p_i to be used in eq. (2) are therefore functions of the measured values of p_i, of the half lives and of the time t between isotopic analysis and calorimetric measurement.

This means that the error of the plutonium mass M depends *directly* upon the accuracy of the measured power H, of the constants s, of the measured percentages p, of the time lag t and of the half lives $T_{1/2}$ (^{238}Pu) and $T_{1/2}$(^{241}Pu). In addition errors of the half lives enter into the accuracy of some of the measured values of p as discussed in the preceding section and into some of the s as will be shown below and thus *indirectly* influence the accuracy of the result.

A detailed error analysis has been made [18] which shows that the importance of the different parameters depends in a complicated way upon the composition of the material. Instead of giving the lengthy formulae results will be discussed that have been obtained for three typical cases (Table III). Of the variables that determine the proportionality factor ε all but five contribute negligibly (<0.05 %) to the total error of the plutonium mass M. In Table IV the assumed relative uncertainties δ of those five quantities and their contributions σ to the total relative error δM are shown; for comparison the state-of-the-art precision of the heat measurement H is also included. The largest fraction of the total error is clearly due to the error of the percentage of ^{238}Pu for which some improvement can be expected from better half-life values (see section 4). For material with low content of ^{238}Pu the specific power constants of ^{239}Pu and ^{240}Pu play a certain part; the determination of plutonium with high contents in ^{241}Pu suffers to some extent from the poor knowledge of the specific power of ^{241}Pu. A survey of the latest values of s as determined directly (by calorimetry) or indirectly (from energy and half-life measurements) is given in Table V. Where computed and measured values exist, the two values have been compared with each other and with the errors of the individual determination. For ^{239}Pu the agreement is quite good. For ^{240}Pu the difference is larger than the sum of the errors; therefore the larger of the two errors (0.76 %) seems to be more realistic and has been adopted for the calculation of the mass error in Table IV. For ^{241}Am the two errors just overlap, and the smaller of the two has been used.

The question of independence of the errors of the quantities listed in Table IV and of their influence or mutual cancellation for the accuracy of the value of ε, i.e. of the calorimetric plutonium determination, is not a trivial problem because of the following reasons:

(1) Few half-life measurements are absolute, or if they are, impure samples are used. Therefore corrections for the impurity half lives have to be applied which have mostly been determined by the same procedure as the one mentioned. This feedback effect has seldom been properly taken into account.

TABLE III. COMPOSITION OF THREE BATCHES OF PLUTONIUM

Isotope	ALKEM 1968	Yankee V+VI,1	Yankee V+VI,16
^{238}Pu	0.041 %	0.289 %	1.228 %
^{239}Pu	90.517 %	85.050 %	69.309 %
^{240}Pu	8.265 %	10.294 %	16.337 %
^{241}Pu	1.113 %	4.011 %	10.853 %
^{242}Pu	0.064 %	0.356 %	2.274 %

TABLE IV. ADOPTED RELATIVE ERRORS δ AND ERROR CONTRIBUTION σ OF THE MOST IMPORTANT PARAMETERS TO THE TOTAL ERROR OF THE CALORIMETRIC DETERMINATION OF THREE BATCHES OF REACTOR-GRADE PLUTONIUM 180 D AFTER ISOTOPIC COMPOSITION MEASUREMENT

Batch Quantity	ALKEM 1968 δ	ALKEM 1968 σ	Yankee V+VI,1 δ	Yankee V+VI,1 σ	Yankee V+VI,16 δ	Yankee V+VI,16 σ
Heat Output	0.25 %	0.25 %	0.25 %	0.25 %	0.25 %	0.25 %
Percentage of ^{238}Pu	2.00 %	0.18 %	1.00 %	0.39 %	0.75 %	0.52 %
" " ^{240}Pu	0.30 %	0.07 %	0.26 %	0.05 %	0.18 %	0.02 %
Specific Power of ^{239}Pu	0.20 %	0.13 %	0.20 %	0.08 %	0.20 %	0.03 %
" " " ^{240}Pu	0.76 %	0.17 %	0.76 %	0.13 %	0.76 %	0.09 %
" " " ^{241}Pu	5.00 %	0.08 %	5.00 %	0.17 %	5.00 %	0.19 %
Total Error of Pu Mass		0.40 %		0.52 %		0.62 %

TABLE V. DECAY ENERGY Q, HALF-LIFE $T_{\frac{1}{2}}$ AND CALCULATED SPECIFIC POWER s AS WELL AS CALORIMETRIC VALUE OF s FOR FIVE ISOTOPES OF PLUTONIUM AND ^{241}Am. ERRORS OF THE s ALSO GIVEN IN PERCENT AND COMPARED WITH THE DIFFERENCE BETWEEN THE CALCULATED (FROM Q AND $T_{\frac{1}{2}}$) AND MEASURED (CALORIMETRIC) VALUE

Isotope	Decay Energy[a] Q, keV	Half Life[b] $T_{1/2}$, years	Specific Power s, mW/g from Q and $T_{1/2}$	Specific Power s, mW/g by Calorimetry	Difference	Percent Errors of s
^{238}Pu	5593.40 ± 0.20[d]	87.80 ± 0.02[e]	567.17 ± 0.13	-	-	0.023 -
^{239}Pu	5243.6 ± 0.8[f]	24401 ± 40[g]	1.9052 ± 0.0032	1.9142 ± 0.0100[h]	0.52%	0.17 0.47
^{240}Pu	5255.5 ± 0.7[j]	6620 ± 50[k]	7.0088 ± 0.0530	7.1046 ± 0.0150[h]	1.37%	0.76 0.21
^{241}Pu	not applicable	15.10 ± 0.14[ℓ]	-	3.62 ± 0.18[m]	-	- 5.00
^{242}Pu	4982.5 ± 1.2[f]	386900 ± 1600[n]	0.11277± 0.00050	-	-	0.44 -
^{241}Am	5638.05 ± 0.12[d]	436.6 ± 3.0[o]	113.53 ± 0.80	114.50 ± 0.17[p]	0.85%	0.70 0.15

[a] Decay energies not updated or corrected for consistent standards.
[b] Half lives as determined by calorimetric and decay energy measurement not considered.
[c] Values computed from the relation $s = 2119.338\ (Q/MeV)/\{(A/amu)(T_{1/2}\ years)\}$ where A is the mass number on the ^{12}C scale as given, e.g., in Ref. [19].
[d] From Ref. [20].
[e] From Ref. [17].
[f] From Ref. [21].
[g] From Ref. [22, 23].
[h] From a reevaluation of the data published in Ref. [24] using (original values in parentheses) $T_{1/2}(^{238}Pu) = 87.80\ (87.60)$ y, $T_{1/2}(^{241}Pu) = 15.10\ (14.03)$ y, $s_1 = 3.62\ (4.24)$ mW/g and of the data of [50] by use of $s_1 = 567.17\ (567.00)$ mW/g, $s_0 = 7.105\ (7.097)$ mW/g. Results are (for [24]) $s_9 = 1.9054 \pm 0.0040$ mW/g, $s_0 = 7.1046 \pm 0.0150$ mW/g and (for two samples measured in [50]) $s_9 = 1.9235 \pm 0.0039$ mW/g, $s_9 = 1.9136 \pm 0.0039$ mW/g. For s_0 the value so determined has been adopted, for s_9 the average of the three values has been taken. Clearly, the probable s_9 error is larger than the uncertainties quoted.
[j] From Ref. [25].
[k] From Ref. [22].
[ℓ] From Ref. [26]. Note that the new value was added in proof and does not appear in the abstract of [26] nor in the older paper [27].
[m] From Ref. [28].
[n] From Ref. [51].
[o] From Ref. [29].
[p] From Ref. [30].

(2) The influence of errors of nuclear constants upon the amount of plutonium to be measured differs with the application of different measurement and evaluation techniques. An example is the measurement of the ^{238}Pu percentage, p_8. If p_8 is determined by α spectrometry, the error of $T_{1/2}(^{238}Pu)$ enters in both p_8 and s_8 and will partially cancel, provided the α spectrometrist and calorimetrist use the same half-life value. If, on the other hand, p_8 is large so that mass spectrometry is applied for its determination, $T_{1/2}(^{238}Pu)$ enters only in s_8 producing a qualitatively different effect.

Therefore more precise measurements of individual nuclear data involved in the conversion of heat into plutonium mass must be accompanied by a comprehensive evaluation or reevaluation of published measurements with the aim of obtaining a *consistent set of data*, and a systems analytical study of the method with all its ancillary measurements that could go as far as to present a recipe for the *procedure to follow* in the assay of reactor plutonium by calorimetry.

6. ASSAY TECHNIQUES USING NEUTRON INTERROGATION

A widely used nondestructive technique for the assay of nuclear material consists of irradiating the sample with neutrons and counting of the emitted fission neutrons. Their intensity is a measure of the amount of fissile material present. Discrimination between source neutrons and fission neutrons is done either by using a pulsed source and detecting delayed fission neutrons, by using a stationary source of relatively low energy neutrons together with a threshold detector, or by utilizing the multiplicity of fission neutron emission.

In any case reactions and materials are used which also occur in a nuclear reactor and for which all relevant nuclear data are available. They are used for instrument design calculations, optimization studies, and for the determination of corrections such as neutron multiplication in the sample. Because calculations do not give the required accuracy the calibration of the instrument is usually done with a set of standard samples.

Good calibration is relatively easy to obtain for clean material like fresh fuel rods, but is difficult for scrap and waste where the detector response depends greatly upon the matrix material and the location of the fissile material in the sample. Extensive studies of this effect were made, and methods for its reduction proposed [31]. Nevertheless uncertainties in sample composition, e.g. the presence of hydrogen, are still a major source of error. This effect is probably much larger than the influence of nuclear data uncertainties in supplementary calculations.

An area in which nuclear data are of immediate importance is the determination of fissionable material in samples containing mixtures of different fissile and fertile species. The preparation of standards of a large number of compositions is not economic. Therefore calculated values are needed for interpolation. Errors may result from interaction effects; it was,

e.g., observed that predictions of resonance self shielding of ^{235}U - ^{239}Pu mixtures in the slowing-down spectrometer were in error by 15 %. Errors can also result from fast fission and inelastic scattering in ^{238}U. A study of the influence of nuclear data upon these effects has so far not been made.

7. ACTIVATION ANALYSIS

An example for activation analysis is the determination of concentrations of ^{235}U and ^{239} Pu in waste solutions of reprocessing plants as presently under investigation [13, 14, 32]. The method is based on the separation of the fission products ^{88}Kr and ^{138}Xe and γ spectrometry of the daughter nuclides ^{88}Rb and ^{138}Cs. Because of the large differences in yield for the isobars 88 and 138 in fission of ^{235}U and ^{239}Pu the method is suited for the determination of the absolute quantity and of the ratio of the two fissionable nuclides. For the reduction of measured data the following nuclear constants are relevant:

- half lives of ^{88}Kr, ^{88}Rb, ^{138}Xe, ^{138}Cs;
- emission probabilities for the 1426 and 1837 keV γ rays of ^{138}Cs and ^{88}Rb, respectively;
- fission cross sections of ^{235}U and ^{239}Pu;
- cumulative yields of ^{88}Kr and ^{138}Xe.

If the system is carefully calibrated with standard solutions the knowledge of the nuclear data listed is of little importance as long as all experimental conditions remain unchanged. The experience shows, however, that this requirement is impossible to fulfill, and corrections have to be applied that depend most critically upon the half lives and to a lesser extent upon the other data listed. Whereas cross sections and γ intensities are accurately known, no satisfactory values for cumulative yields of ^{88}Kr and ^{138}Xe have so far been published.

8. COINCIDENCE TECHNIQUES

A characteristic of nuclear fission is the fact that in most of the individual events a number of neutrons and photons are emitted simultaneously. To use this effect for assay purposes several coincidence techniques have been developed [33-39] that essentially allow to determine the number of pairs, triples, or higher multiples of correlated particles and therefrom the number of fissions in the sample to be assayed. The measurement of pair coincidences has proven particularly useful in the determination of isotopes that undergo spontaneous fission, e.g. in the nondestructive assay of plutonium.

The net count rate C of two-fold coincidences is related to the masses m_i of the fissioning isotopes i by the relation

$$C = \sum m_i \times (L/A_i) \times (\ln 2/\tilde{T}_{1/2,i}) \times \{\overline{\nu_p(\nu_p-1)}/2\}_i \times I = m \sum \mu_i k_i I \quad (3)$$

where L is Avogadro's number, A the mass number, and I is characteristic of the instrument used and the method applied. Nuclear data of interest are the partial half life for spontaneous fission $\tilde{T}_{1/2}$ and the average number of prompt neutron pairs $\overline{\nu_p(\nu_p-1)/2}$ which may be determined from the first and second moment of the probability distribution $p(\nu_p)$ that ν_p neutrons are

emitted in a fission event. Eq. (3) can be shown to hold for instruments with small dead time losses [40]. Sometimes, however, correction terms must be added which contain higher moments of $P(\nu_p)$. Whether the accuracy of these data is sufficient for practical purposes has never been investigated.

In the following the dependence of the method on the nuclear constants k_i as defined in eq. (3) is discussed under the assumption that I in eq. (3) is determined by calibration with one or more standards. $\mu_i = m_i/m$ denotes the abundance of isotope i relative to the sum of all *spontaneously fissioning* isotopes, i.e. $\Sigma\ \mu_i = 1$, and $m = \Sigma m_i$ is the total mass of *spontaneously fissioning* material. It is shown that the data dependence differs widely as different procedures are followed.

(1) The simplest case is the one in which samples and standards have the same composition, and the coincidence rate C is proportional to m, i.e. I is independent of both mass and composition of the sample. This may, e.g., be the case for fuel rods fabricated from one batch of material. Evidently no nuclear data are needed at all.

(2) In general, however, the composition of the standards differs from that of the unknown samples, and the value of I must be assumed to be a function of both quantity and composition of the spontaneously fissioning fraction. A solution of the problem (at least theoretically) is a sufficiently large set of standards that allows to determine the terms $\mu_i k_i I$ or combinations thereof which enter into eq. (3). No nuclear data are required; if available, however, they provide a valuable consistency check of the experimental results.

(3) In all practical cases few standards are available, and nuclear data are needed for interpolation and extrapolation. Generally speaking the data must be the more accurate the smaller the number of standards and the more their mass and composition differ from those of the samples.

As so many parameters can vary, let us consider the example of one "good standard", i.e. make the restriction that it is so similar to the unknown sample in both composition and mass that I does not differ. Then the mass m of the spontaneously fissioning plutonium in the unknown sample is related to the mass m_S in the standard and the corresponding count rates C and C_S via the relation

$$m = m_S\ C/C_S\ \{1 + y(k_8-k_0)/(\mu_8 k_8+\mu_0 k_0)\}$$

and its relative error is given by

$$\frac{\Delta m}{m} = \frac{1}{\Sigma\mu_i k_i + y(k_8-k_0)} \left\{\left[y(k_8-k_0)\frac{\Delta y}{y}\right]^2 + \left[\frac{yk_0k_8}{\Sigma\mu_i k_i}\right]^2\left[\left(\frac{\Delta k_8}{k_8}\right)^2+\left(\frac{\Delta k_0}{k_0}\right)^2\right]\right\}^{1/2} \quad (4)$$

where $y = \mu_8$ (standard) $-\mu_8$ (sample) is a measure of the difference in composition of the sample and the standard. The μ_i refer to the unknown sample. Uncertainties in the k_i have obviously no effect when y=o, i.e. standard and sample have the same composition. Using nuclear data as listed in Table VI, assuming a composition of 1 % ^{238}Pu, 75 % ^{239}Pu

TABLE VI. RELEVANT DATA FOR ASSAY OF PLUTONIUM BY COINCIDENCE COUNTING OF NEUTRONS FROM SPONTANEOUS FISSION

Isotope	$\overline{\nu_p(\nu_p-1)} / \bar{\nu}_p^2$	$\bar{\nu}_p$	$\tilde{T}_{1/2}$, years
^{238}Pu	0.8 (after [41])	2.21 ± 0.07 [42]	5.0 ± 0.6x10^{10} [43]
^{240}Pu	0.807 ± 0.008 [44]	2.150 ± 0.008 [42]	1.32 ± 0.05x10^{11} [45]
^{242}Pu	0.8 (after [41])	2.141 ± 0.009 [42]	7.00 ± 0.10x10^{10} [52]

and 24 % ^{240}Pu, and taking $y = 0.5\ \mu_8$ (i.e. a standard with twice as much ^{238}Pu), eq. (4) transforms into

$$\frac{\Delta m}{m} = \{(0.035\ \frac{\Delta y}{y})^2 + (0.057\ \frac{\Delta k_8}{k_8})^2 + (0.057\ \frac{\Delta k_0}{k_0})^2\}^{1/2}$$

This means that an error of 1 % in the determination of the ^{238}Pu percentage (which is realistic) contributes negligibly (0.04 %) to the total error $\Delta m/m$, whereas 10 % error in each of the $\Delta k/k$ (which is an arbitrary but not too far-fetched assumption) would result in a mass error $\Delta m/m$ of 0.8 %.

(4) In some cases it can even be advantageous to use well-calibrated standard sources of a different isotope, e.g. ^{252}Cf. Then the constants k_i enter directly into the calculations. Their accuracy is far from sufficient for this purpose.

It may be concluded that the nuclear data needed for some variants of coincidence techniques are not sufficiently accurate. It should be kept in mind, however, that proper preparation of standards usually solves the problem to an accuracy where other effects including plain statistics limit the total accuracy that can be achieved.

9. PASSIVE GAMMA ASSAY

For the passive assay of uranium by gamma spectroscopy no increase in accuracy can be expected from improved nuclear data because self-absorption of the 185 keV γ ray of ^{235}U is the limiting factor and the use of standard samples is mandatory. Where corrections have to be applied, the necessary data (mainly γ-ray interaction cross sections) are usually accurate to 3 % or better [46]. The same applies to the passive γ measurement of plutonium. The situation is somewhat different if plutonium isotope ratios are to be determined. Because different isotopes emit γ rays with very similar energies, some isotope ratios can be determined quickly and nondestructively, although not quite as precisely as by mass or α spectrometry. In order to do so relative γ intensities are needed. Measurements from different authors do, however, not agree very well.

TABLE VII. COMPARISON OF INTENSITIES OF PROMINENT γ RAYS FROM VARIOUS PLUTONIUM ISOTOPES AND ^{241}Am AS MEASURED BY TWO AUTHORS

Isotope	Energy[a] keV	Absolute Intensity[b] /47/	/48/	% Error /48/[c]	Isotope	Energy[a] keV	Absolute Intensity[b] /47/	/48/	%Error /48/[c]
^{238}Pu	43.5	3.80-4	3.92-4	1	^{240}Pu	160.3	1.04-5	4.20-6	1
	99.8	8.00-5	7.40-5	1	(cont'd)	642.5	4.10-7	1.45-7	3
	152.6	1.27-5	1.01-5	1		688.0	8.10-8	3.70-8	4
	766.4	2.80-7	2.40-7	1	^{241}Pu	77.0	1.00-6	2.41-7	3
	786.0	7.20-8	3.53-8	1		103.5	1.01-6	1.04-6	1
^{239}Pu	51.6	1.35-4	2.08-4	1		148.6	2.07-6	1.90-6	1
	129.3	5.60-5	6.20-5	1		160.0	7.45-8	6.45-8	2
	203.6	4.80-6	5.60-6	2	^{241}Am	59.5	3.53-1	3.59-1	1
	375.0	1.50-5	1.58-5	1		125.3	2.65-5	3.95-5	3
	413.7	1.50-5	1.51-5	1		208.0	7.06-6	7.60-6	2
^{240}Pu	45.3	4.50-4	4.50-4	1		335.4	4.83-6	4.70-6	2
	104.2	1.00-4	7.00-5	1		722.0	1.90-6	1.85-6	1

[a] Energies taken from Ref. /47/; as absolute values are relatively unimportant for the purpose, no comparison of energies was attempted.

[b] Intensities in photons per disintegration. The notation 3.80-4 means 3.80×10^{-4}.

[c] For the figures of Ref. /47/ intensity errors are not quoted explicitly. An upper limit of 10 % is estimated even for weak lines at low energies where self-absorption is maximum.

Table VII shows as examples intensities of the most prominent γ lines which occasionally differ by a factor of 2 although the errors quoted for each of the measurements are below 10 %. An improvement of these data is desirable.

10. ISOTOPE CORRELATIONS

Isotope analysis of spent fuel is a key point in the fuel cycle because the burnup and the content of fissile material can be determined more precisely by experimental than by computational methods. However, high expenditures necessary for isotope dilution analysis as presently in use stimulated the search for less expensive methods which may not replace, but can be used for verification of the results of isotope dilution analysis. Isotope correlations frequently observed in post-irradiation examinations of reactor fuel offer such a possibility.

Isotope correlations were found between *ratios* of isotopes and the *concentration* of isotopes in the fuel. The present knowledge is obtained from experimental results of analyses during fuel reprocessing or from post-irradiation analyses of fuel pellets [14,49]. The advantages of isotope correlations are the simplicity and high accuracy of isotope ratio measurements as compared to the cumbersome and less precise determination of isotopic concentrations. Isotope correlations can be grouped into those depending upon heavy isotope ratios and those depending on the ratios of fission products.

Heavy isotopes are measured routinely in reprocessing input analysis or post-irradiation examinations. Therefore no additional analytical effort is required for this method. A few examples are given. The ^{235}U depletion D5 defined as the change of ^{235}U concentration relative to its initial value can be correlated to the $^{240}Pu/^{239}Pu$ ratio (Fig. 1 a). This correlation seems to be independent of the individual reactor and is not sensitive to the initial ^{235}U enrichment. Other correlations, however, do depend upon the initial enrichment. An example is shown in Fig. 1 b.

These two examples illustrate the benefit of correlation methods as well as their limits which result from the sensitivity to the initial fuel composition. This problem will be enhanced in the case of plutonium recycling. Fission products offer a better choice in this respect. E.g. the correlation between burnup and $^{132}Xe/^{131}Xe$ ratio is independent of initial enrichment and of the individual reactor (Fig. 1 c). This is also the case for the correlation of the ^{240}Pu concentration with the $^{145}Nd/^{146}Nd$ ratio (Fig. 1 d). The role of nuclear data in this field is as follows.

In order to understand the reactor physics behind these correlations burnup calculations are required. Predictions with existing codes have so far not given good agreement with experiment. It is not clear, however, to what extent uncertainties of nuclear data contribute to this discrepancy. Therefore the adequacy of details of the computations, such as the energy

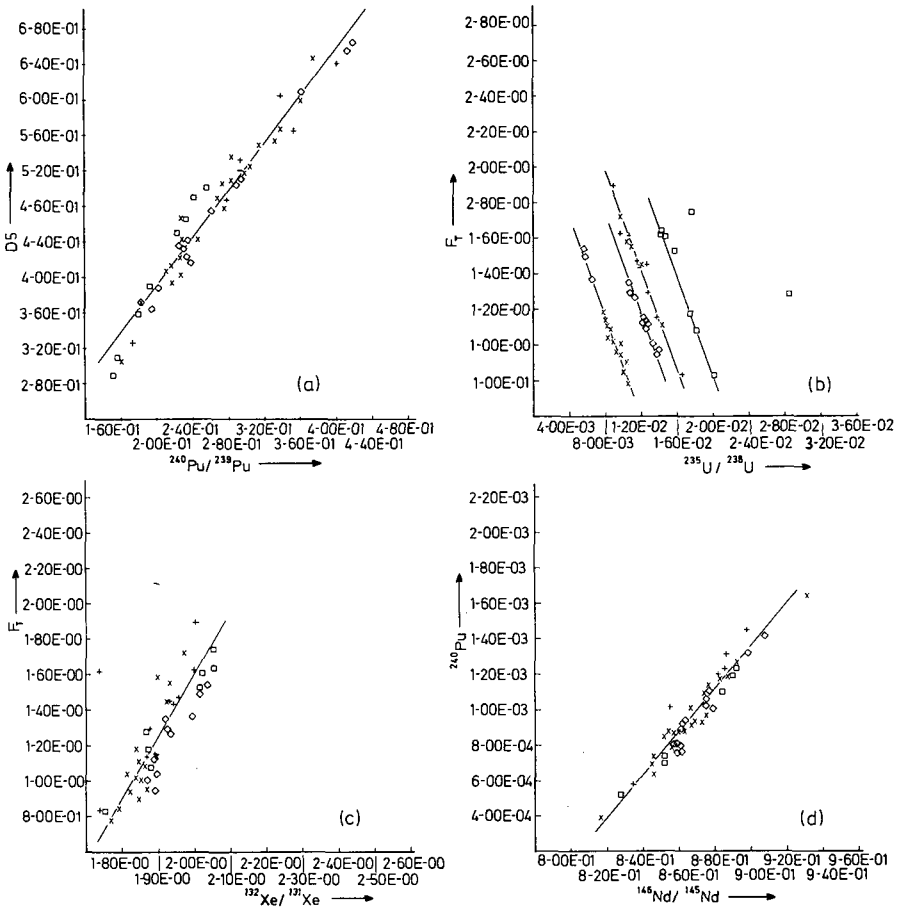

FIG. 1. Correlation between (a) ^{235}U depletion D5 and $^{240}Pu/^{239}Pu$ ratio; (b) burn-up F_T (fissions per 100 heavy nuclei initially present) and $^{235}U/^{238}U$ ratio; (c) F_T and $^{132}Xe/^{131}Xe$ ratio; (d) ^{240}Pu content and $^{146}Nd/^{145}Nd$ ratio. Different symbols refer to different light-water reactors with six different initial enrichments.

group structure, should be checked more carefully, and the dependence of the results upon nuclear data should be investigated. Only then can the requirement for improved or additional nuclear data be assessed.

11. CONCLUSION

Although most methods of nuclear material assay for safeguards are based upon some form of nuclear data, there are few examples where a better or more precise value of a given quantity would result in an immediate and drastic improvement of the performance of a measurement technique for the following reasons:

(1) Even the most accurate nuclear data will not meet the accuracy of classical (i.e., chemical) analytical methods so calibration is and will primarily be done by use of *standards*.

(2) Nuclear Safeguards being a relatively young field few methods have become routine, and second-order effects that can be dealt with by improved nuclear data compete with much larger *uncertainties from other effects* as, for example, insufficient knowledge of matrix material in the sample.

(3) Unlike nuclear data for reactors, nuclear data for safeguards are not directly amenable to cost-benefit calculations because the virtue of a decrease in the amount of material unaccounted for, or MUF, is *hard to quantify*.

(4) Most of the research work done so far has been concentrated on the development of *instruments*, not of *systems* that specify the usage of those instruments for particular applications and help determine problem areas in which nuclear data are most urgently needed.

Therefore studies of this kind are a prerequisite for the efficient improvement of existing nuclear data for safeguards, and more thorough investigations of the quantitative role of nuclear data in every individual method deserve all possible support.

REFERENCES

[1] BYER, T.A., INDC (NDS)-44/G (1972).

[2] METZGER, F.R., in O.R. Frisch ed., Progress in Nuclear Physics 7 (1959) 54.

[3] WEITKAMP, C., KFK 1745 (1973).

[4] HELMER, R.G., GREENWOOD, R.C., GEHRKE, R.J., Nucl. Instr. and Meth. 96 (1971) 173.

[5] METZGER, F.R., Phys. Rev. Letters 18 (1967) 434.

[6] RICKEY, F.A., JURNEY, E.T., BRITT, H.C., Phys. Rev. C 5 (1972) 2072.

[7] MICHAELIS, W., Atomkernenergie 14 (1969) 347.

[8] CHRIEN, R.E., et al., BNL 15698 (1970).

[9] KANE, W.R., Phys. Rev. Letters 25 (1970) 953.

[10] MATUSSEK, P., et al., *Safeguards Techniques* , Vol. II, IAEA, Vienna 1970, p. 113.

[11] MATUSSEK, P., et al.,*Contributions to the Conference on Nuclear Structure Study with Neutrons*, Budapest, July 31 - August 5, 1972, p. 84.

[12] GROSHEV, L.V., et al., Nuclear Data A 5 (1969) 243.

[13] BORK, G., ed., KFK 1429 (1971).

[14] BORK, G., ed., KFK 1618 (1972).

[15] BARTHOLOMEW, G.A., et al., Nuclear Data A 3 (1969) 367.

[16] HOFFMANN, D.C., et al., J. Inorg. Nucl. Chem. 5 (1957) 6.

[17] SMITH, W.H., ROGERS, D.R., SILVER, G.L., Mound Laboratories Report MLM-1691 (1969).

[18] WEITKAMP, C., et al., KFK 1299 (1971).

[19] WAPSTRA, A.H., GOVE, N.B., Nuclear Data A 9 (1971) 265.

[20] GRENNBERG, B., RYTZ, A., Metrologia 7 (1971) 65.

[21] BARANOV, S.A., et al., Yadern. Fiz. 7 (1968) 727; Sovjet Journal of Nuclear Physics 7 (1968) 442.

[22] DOKUCHAEV, Ya. P., Atomnaja Energija 6 (1959) 74; J. Nuclear Energy 11 A (1960) 195.

[23] MARKIN, T.L., J. Inorg. Nucl. Chem. 9 (1959) 320.

[24] OETTING, F.L., *Thermodynamics of Nuclear Materials*, IAEA, Vienna 1970, p. 55.

[25] LEANG, C.F., Comptes Rendus Acad. Sci. 255 (1962) 3155.

[26] CABELL, M.J., *Chemical Nuclear Data, Measurements and Applications*, Proceedings of the International Conference, 20 - 22 September 1971, Canterbury.

[27] CABELL, M.J., WILKINS, M., J. Inorg. Nucl. Chem. 33 (1971) 903.

[28] OETTING, F.L., Phys. Rev. 168 (1968) 1398.

[29] STONE, R.E., HULET, E.K., J. Inorg. Nucl. Chem. 30 (1968) 2003.

[30] OETTING, F.L., GUNN, S.R., J. Inorg. Nucl. Chem. 29 (1967) 2659.

[31] AUGUSTSON, R.H., et al., *Safeguards Techniques*, Vol. II, IAEA, Vienna 1970, p. 53.

[32] HAWA, A.H., Thesis, Karlsruhe, in preparation.

[33] JACQUESSON, J., J. Phys. 24, Suppl. to No. 6 (1963) 112 A.

[34] KEEPIN, G.R., ed., LA-3974-MS (1968) 14.

[35] OMOHUNDRO, R.J., NRL-Memorandum Report 2005 (1969).

[36] GOZANI, T., COSTELLO, D.G., Transactions of the American Nuclear Society 13 (1970) 746.

[37] FOLEY, J.E., THORPE, M.M., LA-4705-MS (1971) 9.

[38] BIRKHOFF, G., et al., *Safeguards Techniques*, Vol. II, IAEA, Vienna, 1970, p. 477.

[39] STRAIN, C.V., NRL-Memorandum Report 2127 (1970).

[40] BÖHNEL, K., Transactions of the American Nuclear Society 15 (1972) 671.

[41] KEEPIN, G.R., *Physics of Nuclear Kinetics*, Addison-Wesley, Reading, 1965, p. 60.

[42] MANERO, F., KONSHIN, V.A., INDC(NDS)-34/G (1972).

[43] ELLIS, Y.A., Nuclear Data B 4 (1970) 635.

[44] DIVEN, B.C., et al., Phys. Rev. 101 (1956) 1012.

[45] SCHMORAK, M.R., Nuclear Data B 4 (1970) 661.

[46] STORM, E., ISRAEL, H.I., Nuclear Data A 7 (1970) 565.

[47] CLINE, J.E., et al., ANCR-1069 (1972).

[48] GUNNINK, R., MORROW, R.J., UCRL-51087 (1971).

[49] KOCH, L., et al., *Analytical Methods in the Nuclear Fuel Cycle*, IAEA, Vienna 1972, p. 523.

[50] OETTING, F.L., *Plutonium 1970 and other Actinides*, Proceedings of the 4th International Conference, Santa Fe, New Mexico, October 5-9, 1970, Part I, p. 154; Nuclear Metallurgy 17 (1970) 154.

[51] BEMIS, C.E., Jr., HALPERIN, J., EBY, R., ORNL-4306 (1968) 31; J. Inorg. Nucl. Chem. 31 (1969) 599.

[52] ELLIS, Y.A., Nuclear Data B 4 (1970) 686.

DISCUSSION

B. GRINBERG: In the oral presentation you showed two tables, the first drawing attention to the differences in the values which have been determined for the half-lives of americium-241 and plutonium and the second giving the recommended values ("best values") for these half-lives. I would like to ask the following questions in this connection:

- By what method was the list of recommended values drawn up?
- Do you think that a thorough evaluation of these half-lives should be undertaken, covering in particular the matter of accuracies?
- Do you feel that in some cases new, high-quality determinations would be desirable?

C. WEITKAMP: The procedures used in compiling the tables of recommended values varied according to the method used for obtaining the data, the number and nature of corrections introduced, and the details given in the original papers. In the most cases the half-lives and the specific decay heats were replaced by the most recent values; for ^{239}Pu and ^{240}Pu a simultaneous analysis was carried out, but since in the case of ^{240}Pu the errors were greater than those given in two earlier publications, the mean of the latter was selected.

As regards improvement of the situation as a whole, I would,in fact, recommend that some new experimental determinations be undertaken and that a thorough analysis of the errors be made beforehand, so that all the problems can be taken into account when the experiments are designed.

THE ROLE OF NUCLEAR DATA IN THE PRACTICAL APPLICATION OF NON-DESTRUCTIVE NUCLEAR ASSAY METHODS*

M. M. THORPE
University of California,
Los Alamos Scientific Laboratory,
Los Alamos, N. Mex.,
United States of America

Abstract

THE ROLE OF NUCLEAR DATA IN THE PRACTICAL APPLICATION OF NON-DESTRUCTIVE NUCLEAR ASSAY METHODS.

Uses of nuclear data in the development of practical nuclear assay techniques fall naturally into three categories. First, there are parameters which can enter directly into the calibration of equipment, such as decay rates, gamma intensities and attenuation coefficients, neutron yields, etc. The second category involves the use of nuclear data in the predictive sense as input to neutron and gamma-ray transport codes which provide calculational support and guidance to the safeguards research and development program. This support is necessary for the detailed understanding of techniques under investigation as well as for design optimization of systems already proven to be worthy of development to the prototype stage. The third category utilizes nuclear data as a reservoir of basic information to aid in the search for new methods and signatures.

To illustrate these three categories of use of nuclear data, the development of several systems from initial research through prototype construction, calibration and final field testing is outlined. Typical of the systems described are: delayed and prompt neutron methods applied to scrap and small sample assay; the application of radioactive sources to the measurement of the fissile content of reactor fuel pins; coincidence counting of fission events, either spontaneous or induced; gamma methods applied to measurement of enrichment, minor isotope composition, and fissile content of feed, product, scrap and waste. An experimental program to evaluate the use of μ-meson capture X-rays is described as an example of the role of basic data in exploring promising elemental and isotopic signatures.

Future challenges for non-destructive assay are: to meet the assay requirements of new chemical and physical forms of nuclear fuels, to reduce the costs while maintaining or increasing the accuracy and precision of the methods, and to establish the rapidly advancing non-destructive assay methods as an independent alternative to traditional chemical analysis. Typical categories and accuracies of nuclear data needed to meet these major challenges are described.

INTRODUCTION

Practical nuclear nondestructive assay methods for fissionable material gaining acceptance today are based mainly on two fundamental signatures. First, the naturally occurring radioactivity characteristic of the nuclides of interest and second, the ability of these same nuclides to be fissioned either by neutrons or gamma rays. With some important exceptions, the basic nuclear data relating to these properties has been available for a number of years. Why then are nuclear data important? The answer lies in the diversity of purpose of the assay methods. The hundred-thousand-dollar machine designed to provide precise assay of several million dollars worth of fuel pins is hardly comparable to the device used for the occasional measurement of a dozen or so waste barrels. Because of this diversity of purpose an array of instrumentation is being developed, each making use of the basic signatures in a different way to satisfy a different set of conditions.

* Work performed under the auspices of the U.S. Atomic Energy Commission

Uses of nuclear data in the development of practical nuclear assay techniques fall naturally into three categories. First, there are parameters which can enter directly into the calibration of equipment, such as decay rates, gamma intensities and attenuation coefficients, neutron yields, etc. The second category involves the use of nuclear data in the predictive sense as input to neutron and gamma-ray transport codes which provide calculational support and guidance to the safeguards research and development program. This support is necessary for the detailed understanding of techniques under investigation as well as for design optimization of systems already proven to be worthy of development to the prototype stage. The third category utilizes nuclear data as a reservoir of basic information to aid in the search for new methods and signatures.

FUEL PIN ASSAY

A number of fuel pin assay systems either complete or under development serve as an illustration of some of these uses of nuclear data. These systems are for the measurement of:

1. Uranium-235 content of LWR fuel.
2. Uranium-235 content of LWR fuel and the detection of out of specification fuel pellets.
3. Plutonium content and isotopic composition of fast breeder reactor (FBR) fuel.
4. Plutonium recycle LWR fuel.
5. Fissile content of irradiated fuel.
6. Uranium-235 content of LWR fuel which also contains burnable poison.

Three properties of the system for measuring LWR pins are most important:

1. High throughput rate to take care of a modern plant capacity of several hundred pins per shift.
2. Sensitivity to all of the fissile material within the pins.
3. Reliability.

These three criteria lead to the choice of thermal neutron interrogation; the thermal flux supplied by a moderated ^{252}Cf source, and the detection of prompt fission neutrons from the thermal fission of ^{235}U furnishing the primary signature and differentiation from ^{238}U, the major constituent of LWR fuel.

The moderator for the neutron source must provide sufficient thermal flux at the fuel channel while providing maximum discrimination between ^{235}U and ^{238}U as well as minimizing the source strength and biological shielding required. The configuration of source, moderator materials and detectors was optimized by modeling the system on the computer using only enough actual experimentation to assure confidence in the computer calculations [1]. The method of optimizing a design by computer calculations illustrates one of the more important uses of nuclear data as input to computer codes which provide the calculational tool necessary to design practical nondestructive assay instrumentation.

The assay of a fuel pin requires a mathematical calibration function which describes as accurately as possible the response for various enrichments and yet is simple enough to permit on-line data reduction. Analysis [2] indicates that the response of a fuel rod having an enrichment less than 4% ^{235}U is adequately described by a function of the form

$$R = A(1 - e^{-BU})$$

R is the measured response, U is the ^{235}U content of the fuel rod, and A and B are parameters determined from measurements of standard fuel pins.

In addition to the ^{235}U content, the response of an actual fuel pin depends on a number of factors: cladding thickness and composition, fuel section length, density, diameter, impurity content, etc. It is important to investigate the sensitivity of the assay system to changes in these various parameters. Here again, the computer and nuclear data are used to obtain the information. These calculations and other considerations provide the basis for a systematic error analysis [3]. The precision of a single fuel rod assay is dominated by propagated counting statistics amounting to ~1.1 to 1.5% (1σ) over the mass range of 30 to 120 g of ^{235}U per rod. After 100 fuel rod assays, the statistical uncertainty in the total mass decreases to less than 0.15%. At this point the error becomes dominated by factors other than counting statistics (e.g., the error in the calibration curve).

In-plant experience has proven the practicality of measuring the entire ^{235}U throughput of a modern plant. The system can be operated by plant personnel with little technical training at a rate of 400- to 600-rod assays per eight-hour shift. This rate includes the time taken for pin identification, handling, and the assay of several standard rods to provide a calibration check. A more detailed description of the construction and operation of the units may be obtained from a paper by R. A. Forster, et al. [4].

A series of Monte Carlo calculations and measurements [5] led to the following modifications of the thermal neutron ^{252}Cf fuel rod system to include measurements of pellet-to-pellet variations: 1) lengthening the moderator assembly in the direction of fuel rod travel, which results in a longer region of high thermal flux; 2) positioning the fuel rod channel closer to the ^{252}Cf source to take advantage of the higher intensity flux near the source while still preserving a high fissile/fertile fission ratio (~10^4) to ensure accurate measurement of fissile content in the presence of much larger amounts of fertile material; 3) replacing the D_2O in the moderator assembly with deuterated water-extended-polyester resin and carbon to decrease cost while simplifying the fabrication and shipping; 4) changing the fuel channel position requires that the ^4He detectors be shortened and displaced to one end of the carbon moderator to give a sufficiently large signal/^{252}Cf background ratio in the ^4He detectors; and 5) the addition of a small (2 by 2 by 3/4 in.) NaI detector near the exit port of each fuel-rod channel to give pellet-to-pellet fissile content by counting fission-induced gamma rays. Figure 1 is a schematic diagram of the Pin and Pellet Assay System (PAPAS). Figure 2 illustrates the system capability for the detection of off-specification pellets.

A complete assay and quality control station for FBR fuel rods has been delivered to Westinghouse-Hanford Engineering Development Laboratory (HEDL). These rods contain mixed oxide fuel with a $^{239}Pu/^{238}U$ ratio of ~1/4, and a total ^{239}Pu mass of ~30 g. The instrumentation has been calibrated and is now in routine operation. The station consists of two units. One unit [6] contains a ^{252}Cf (619 μg) source tailored to provide fast neutron irradiation of the pins. The delayed gamma rays from fission (E_γ > 1.2 MeV) are detected as a measure of the total fissile content. The gamma rays from ^{241}Am, ^{239}Pu

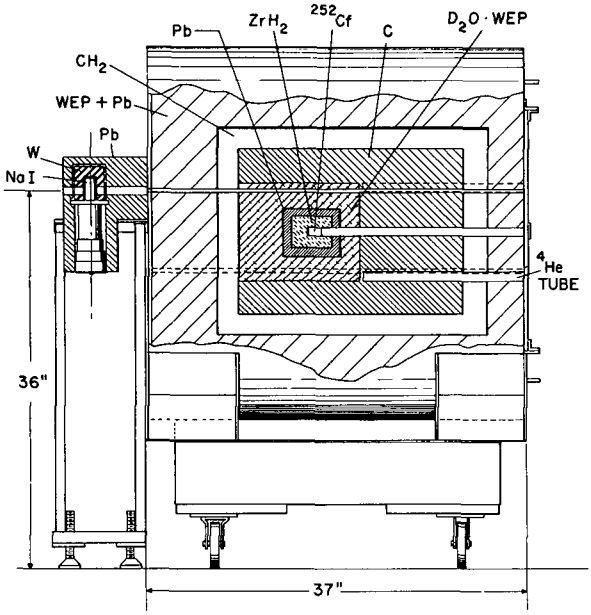

FIG. 1. Thermal-neutron ^{252}Cf fuel-rod assay system with modifications for pellet-to-pellet scan. The ^{4}He neutron detectors in the carbon core count the prompt fission neutrons for total fissile determination, and the NaI detectors near the fuel-rod exit channel count the delayed gamma rays for pellet-to-pellet determination.

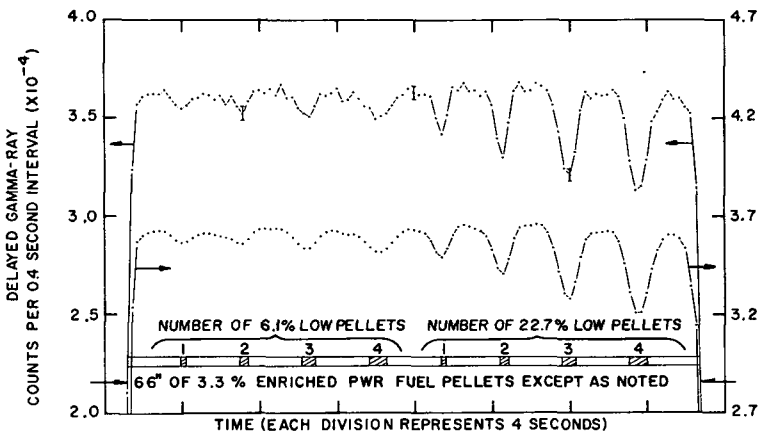

FIG. 2. A typical delayed gamma-ray scan of a 66-in.-long 3.3% PWR fuel rod with pellets of lower enrichments interspersed as shown above. The lower curve is a smoothed version of the raw data in the upper curve (the error bars represent 2σ uncertainties). Each point represents the total counts accumulated in 0.4 s for a rod feed rate of 8 ft/min.

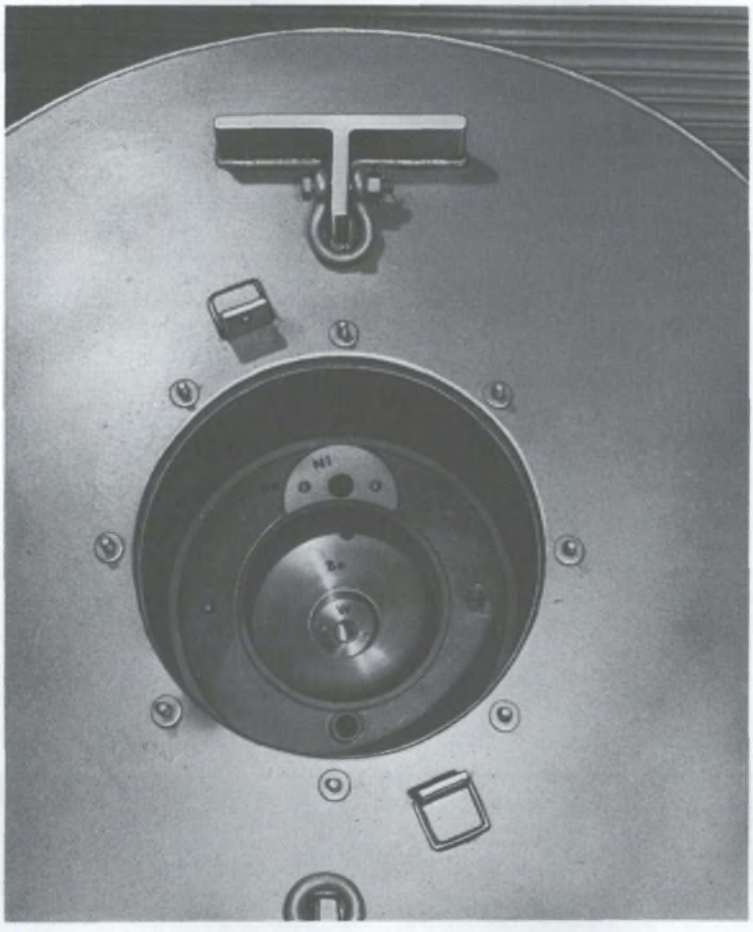

FIG. 3. Photograph of moderator and shield assembly for a fast neutron ^{252}Cf assay system. The ^{252}Cf source is positioned in the centre of the tungsten and the sample is placed in the nickel reflector for the neutron irradiation.

are counted and used to provide pellet-to-pellet information. The second unit measures the ^{240}Pu content by coincidence counting the neutrons emitted from the spontaneous fission of ^{240}Pu [7].

Because of the high fissile loading of FBR fuel pins, thermal neutron irradiation would have yielded an unacceptably nonlinear response curve. Calculations led to the choice of the cylindrical moderator assembly shown in Fig. 3. The assembly has a core of tungsten (2.5 cm radius) surrounded by a 7.5-cm-thick shell of beryllium followed by 5 cm of lead and nickel. The nickel reflector increased the fission rate ~70% over the lead reflector alone. This moderator design resulted in a $^{239}Pu/^{238}U$ fission ratio of ~400/1 for irradiation neutrons above the cadmium cut-off energy (~0.4 eV).

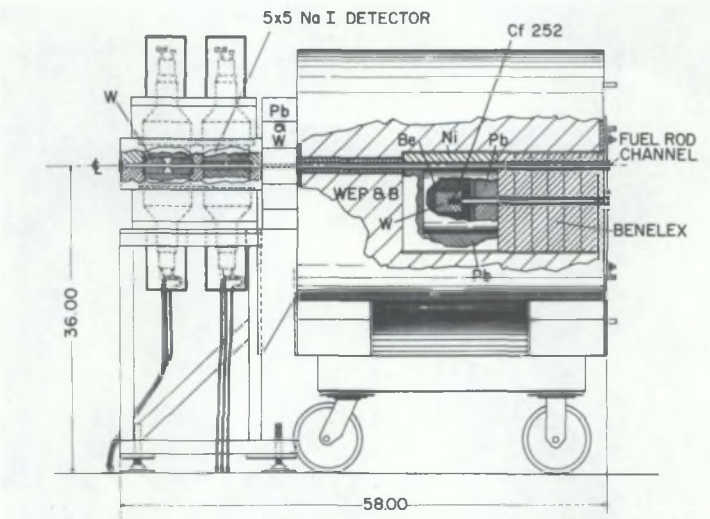

FIG. 4. Schematic diagram of the ^{252}Cf fast-neutron assay system for FBR-type fuel rods. The delayed gamma rays induced by the fast-neutron irradiation are subsequently counted with the two NaI detectors that also measure the passive gamma rays to determine pellet-to-pellet uniformity.

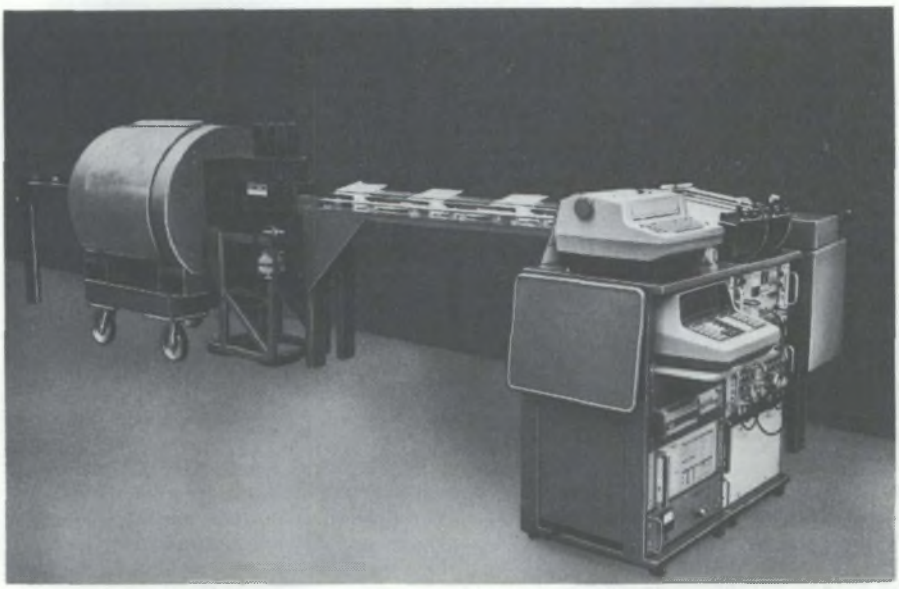

FIG. 5. Fast neutron ^{252}Cf assay system for FFTF fuel rods. System includes 619 μg ^{252}Cf source and shield, two 5 by 5-in. NaI detectors to count the delayed gamma rays, automated fuel-rod handling, and data reduction system.

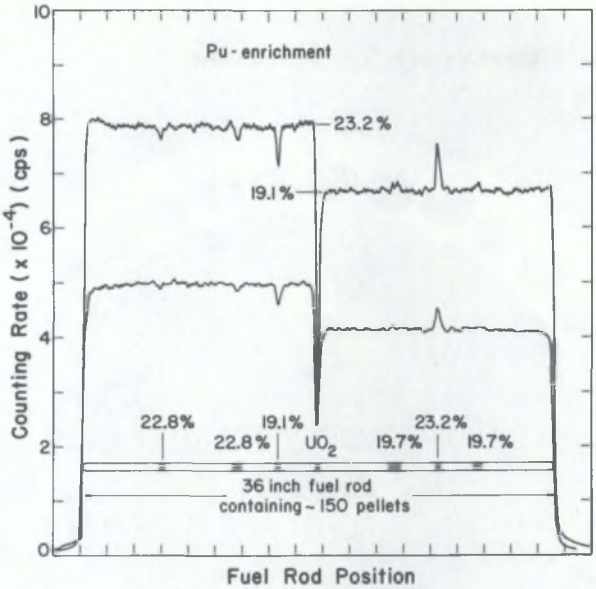

FIG. 6. FFTF fuel pin with various combinations of plutonium enrichments for pellet-to-pellet scanning. Top curve corresponds to 60 KeV energy window and bottom curve corresponds to 100 to 500 keV window.

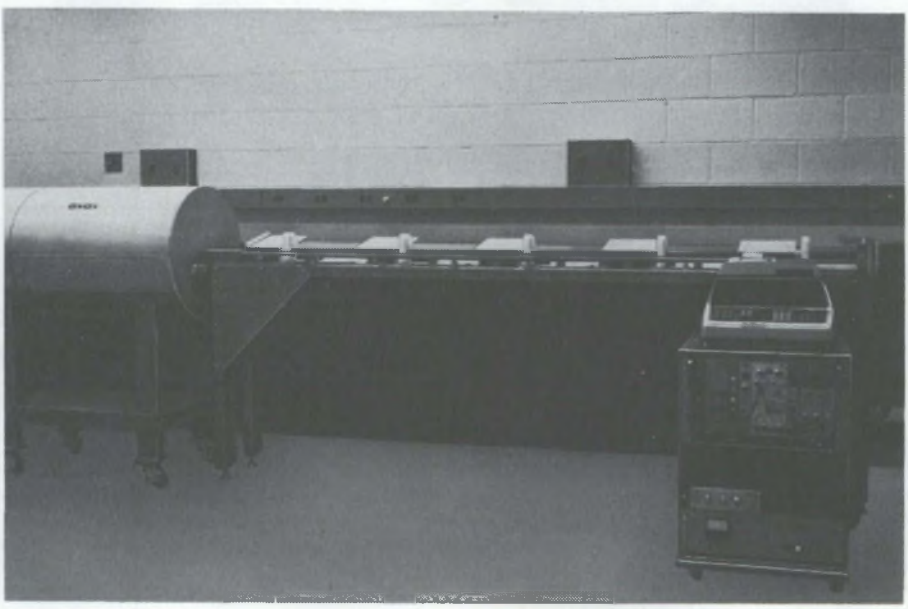

FIG. 7. Passive neutron-coincidence counter for measuring ^{240}Pu content in FBR-type fuel pins. The system includes ^{3}He thermal-neutron detector, automated fuel pin loader and translator, and electronics and data control rack.

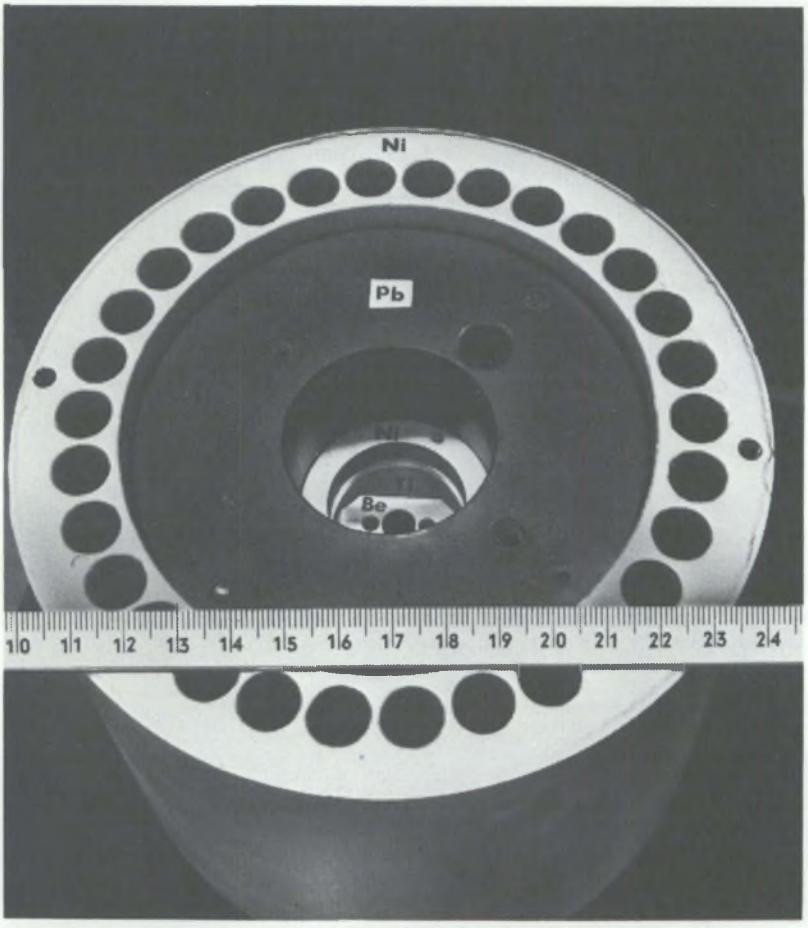

FIG. 8. Photoneutron assay system using either ^{124}Sb or ^{88}Y in the beryllium core surrounded by nickel and titanium neutron reflectors and lead gamma-ray shielding

Figure 4 is a schematic diagram of the unit showing the NaI detectors each having a different degree of collimation, moderator, and shield assembly. Americium-241 doped, NaI seeds embedded in each crystal provide a source of constant amplitude pulses (roughly equivalent to a 3 MeV gamma ray) which are used in conjunction with an electronic stabilizing unit to reduce the effects of long-term photomultiplier and electronic drifts. Figure 5 is a photograph of the entire unit showing the moderator-shield assembly, the pin handling equipment, the programmable calculator and associated electronics. The automated translator picks up the rod to be assayed and moves it through the NaI crystals and the ^{252}Cf assembly at a rate of 2.5 in./sec in order to take a background count of the unirradiated rod. The direction of travel is then reversed and the rod is withdrawn at 0.36 in./sec during

which time the delayed fission gamma-ray data are acquired and the pellet-to-pellet scans are made. The rod is then unloaded in the tray directly below the loading magazine and the cycle is repeated for the next rod. The translator speeds are set to give a 5-min cycle per rod.

Error analysis and measurements indicates that the standard deviation of the measured fissile content of a rod is ~0.2 g. Figure 6 illustrates the sensitivity to pellet-to-pellet changes as observed with a test pin containing various pellet and enrichment combinations. It can be seen that small changes in enrichment (1.7% to 3.1% relative) can be detected. The ^{240}Pu assay system, shown in Fig. 7, contains 32 ^{3}He tubes (1 in. diam by 20 in. long, 4 atm gas pressure). The detector efficiency is ~36% and the neutron lifetime was measured to be 28 μsec. Assay precision is a little greater than 1% (1σ) for a counting time of 100 sec.

Assay units using Sb-Be or ^{88}Y-Be as fast, subthreshold neutron sources are under investigation. A relatively hard nonthermal interrogation flux offers the potential advantage of insensitivity to the presence of fission product or burnable poisons as well as providing good penetrability and linearity of response. Figure 8 is a photograph of an experimental photoneutron system [8]. There is a central cadmium lined assay channel in beryllium with adjacent holes for the gamma sources followed by rings of titanium and nickel. Three inches of lead shield the ^{4}He detectors from the source gamma rays. The ^{4}He detectors are embedded in a thick (2 cm) nickel ring which serves as a fast neutron reflector. The nickel reflector added about 40% to the signal rate. The energy of the neutrons from the photoneutron sources is such that the ^{4}He detectors can be biased to eliminate most of the neutron signal from the source. This in turn permits the addition of sufficient lead to shield the detectors from the intense gamma radiation of either the source or the sample. The photoneutron unit just described is being used to acquire data on optimum detector gas pressure, signal rates and signal-to-background ratios, response linearity, etc. The unit is also being used to determine its suitability for other applications such as small-sample assay [9].

LWR fuel containing recycled plutonium will become important in the near future. The special assay problems associated with this type of fuel are being studied.

NEUTRON METHODS APPLIED TO SCRAP AND SMALL SAMPLE ASSAY

One of the most significant problems associated with the assay of scrap and waste is the lack of control over the extraneous material that might be present within the sample. Assay by means of fast neutron irradiation and detection of delayed or prompt fission neutrons has been found to be relatively insensitive to all matrix materials except hydrogen and other low Z elements which are good neutron moderators. Fission chambers (or other detectors sensitive to low energy neutrons) closely coupled to the sample provide a means of detecting or correcting for the effects of neutron moderation. Gamma-ray assay methods are most suitable for light, hydrogenous matrix materials. Together, the two techniques, gamma-ray and neutron assay methods, provide broad capability for many of the assay problems associated with scrap and waste.

The development of the technique of neutron interrogation with delayed neutron detection is an example of the key role that nuclear data can play. When this method was first being considered it was necessary to undertake an experimental program to measure the delayed neutron yield from fission as a

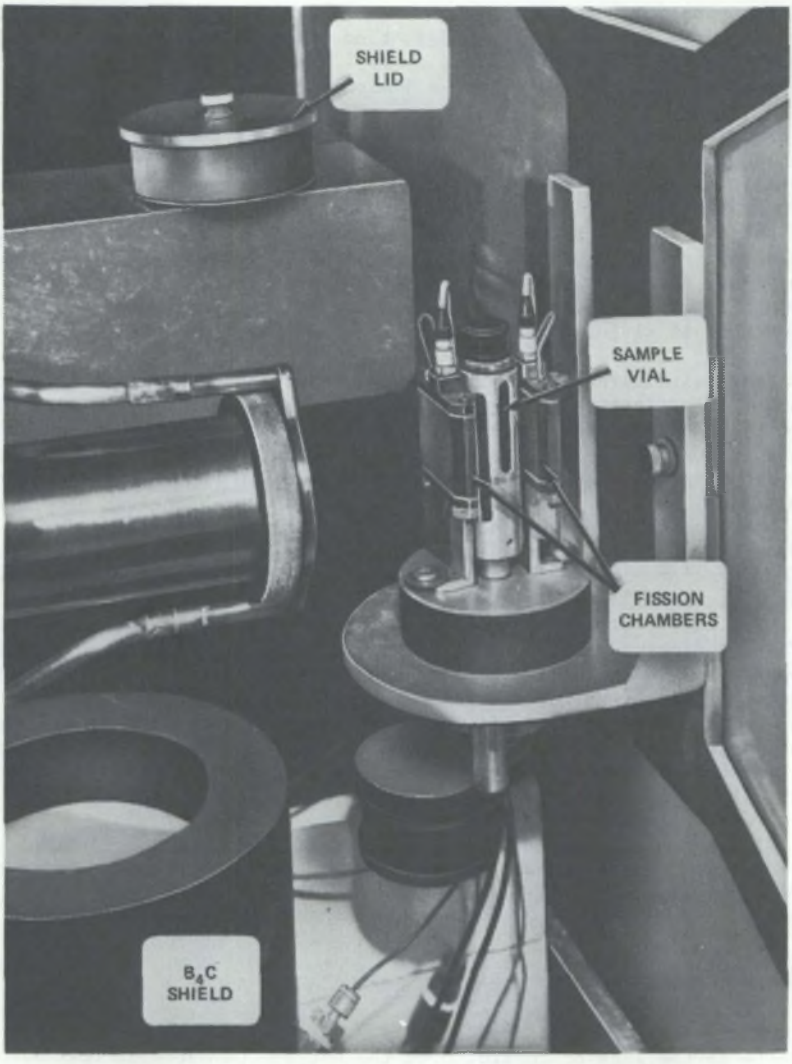

FIG. 9. View of small-sample assay station with B_4C shield removed.

function of incident neutron energy. Initial emphasis was placed on measurements at 14 MeV [10] since 14 MeV neutron generators are a relatively inexpensive, copious source of neutrons. This program was followed by another set of measurements using a Van de Graaff as a variable energy neutron source [11].

These experiments were designed to confirm and extend the available delayed neutron yield data. The results show that the delayed neutron yield is not significantly dependent on the energy of neutrons causing fission for

energies below 5 MeV. Above 5 MeV there is a drop in yield corresponding to the onset of second chance fission. The data obtained so far are in general sufficient to satisfy most immediate practical needs. Nonetheless there is interest in the delayed neutron yield in the energy region 6 to 14 MeV and in data for the higher plutonium isotopes. These basic data are used for computer calculations to explore and define possible technique refinements.

An example of the application of subthreshold neutron interrogation and delayed neutron detection is the fissile assay of small samples [12] taken from various portions of a plant inventory for process control or inventory verification. Several thousand such samples are chemically analyzed yearly. To be generally useful, a small sample assay technique must be able to furnish few percent or less accuracy for a wide variety of chemical forms and concentrations of fissile material. Figure 9 is a photograph of a small sample assay apparatus which utilizes a Van de Graaff accelerator as a pulsed source of few hundred kilovolt neutrons. The delayed neutrons are detected between accelerator pulses by a large, flat efficiency detector. Closely coupled fission chambers monitor the fission rate in the samples. A background equivalent of 15 mg ^{235}U has been achieved.

Assay precision depends on sample fission rate and detector efficiency. It is advantageous to closely couple the detector and to provide neutron reflectors to increase the flux at the sample. The presence of extraneous materials in the vicinity of the sample degrades the incident neutron energy and causes undesirable sample self-absorption and matrix effects. An acceptable compromise, found experimentally, is to use iron reflectors adjacent to the target and sample in conjunction with a 3/4-in.-thick boron carbide sleeve surrounding the sample to eliminate the majority of neutrons below 100 eV. Favorable experience gained to date from several hundred assays has provided the incentive to undertake the following major improvements in the system: automatic sample handling, automated data processing, and a more efficient detector-reflector geometry. Ongoing research effort involves finding methods of increasing precision, reducing the number of standards required, and defining and eliminating sources of bias.

GAMMA METHODS

Gamma-ray spectroscopy, particularly with lithium drifted germanium (GeLi) detectors, is a general purpose method with a wide range of applications. In this instance, nuclear data is not so important in the design of the hardware, but is essential for its application. Usually only a few lines from the complex decay spectra of the nuclides of interest are used for assay. Nonetheless extensive knowledge of gamma spectra is required to provide the assurance that the lines used are specific and that the presence of unusual or unsuspected activity will not yield an erroneous assay. Attenuation corrections for the matrix materials involved are the major sources of uncertainty in the assay. Attenuation corrections are usually obtained through: preparation of standards which are representative of the material being measured; measurement of the transmission of a source [13]; comparison of the relative intensities of two or more characteristic gamma rays [14].

In addition to quantitative assay gamma-ray detection has been applied to the measurement of enrichment, concentration, and isotopic composition. Relatively simple instrumentation, particularly when used by knowledgeable personnel, can be quite effective. Figure 10 shows one of the devices which was used to estimate the holdup in a shutdown diffusion plant cascade. The instruments were also used in the operating cascade to monitor UF_6 retention in NaF traps, measure enrichment and to detect plating or holdup in the main gas pipes [15].

FIG. 10. Cooled, portable NaI gamma spectrometer for assay of ^{235}U inside an operating gaseous-diffusion plant.

COINCIDENCE COUNTING OF FISSION EVENTS

Coincidence detection of the many neutrons and gamma rays from fission provides a convenient method for separating the occurrence of fission from the source producing the fission or from extraneous radiation which might be present [e.g., neutrons from (α,n) reactions]. Neutron coincidence counting of ^{240}Pu spontaneous fission provides a simple method of plutonium assay when the isotopic composition is known. The spontaneous fission rate of ^{238}U can also be used for assay purposes. Both rates are low and high efficiency 4π neutron counters are required for rapid quantitative assay.

Organic scintillation detectors permit the detection of time correlated events, neutrons or gamma rays, using coincidence gate widths of only a few tens of nanoseconds. Since the ratio of accidental coincidence rate to true

coincidence rate is directly proportional to the coincidence gate width, the short gate width allows the detection of fission in the presence of relatively large backgrounds of uncorrelated neutrons and gamma rays. Conversely, an uncorrelated or random source can be introduced to cause fission in the sample. The detected fission rate then is a measure of the fissionable content. Neutron source energies can be changed to increase sensitivity, and to provide both fissile and fertile assay. Figure 11 is a photograph of a system called the "Random Driver" which uses an Am-Li neutron source to cause fission in the sample. This system proved an effective instrument for the assay of uranium [16,17].

BASIC SIGNATURES

Although natural radioactivity and fission have furnished the basic signatures which have proven to be the most utilitarian, there are other characteristics which can be used to identify particular elements or isotopes. A few examples are: neutron capture gamma rays; delayed-neutron and gamma-ray spectra, gamma-ray and x-ray fluorescence; selective neutron and gamma-ray absorption. The gathering of information, particularly basic data, pertaining to any physical phenomenon which might be applicable to materials analysis should be encouraged. This reservoir of basic information can then be used as a basis to continually review the techniques for possible application to the changing and differing needs for quantitative

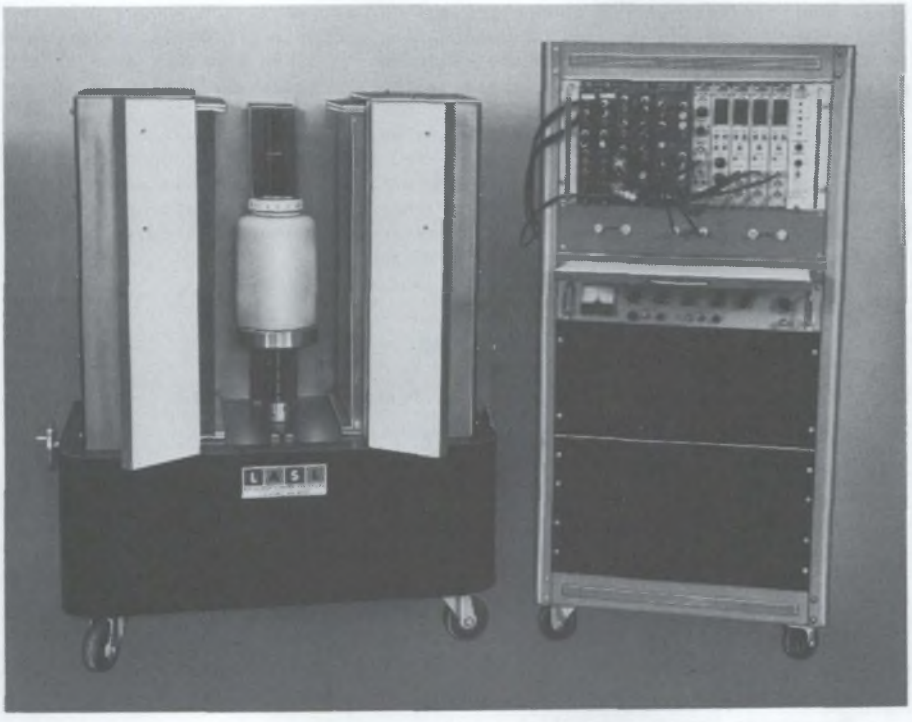

FIG. 11. The random source-interrogation system used to determine the ^{235}U content in containers of up to 5-gal capacity.

assay. These needs range from the detection of trace quantities in effluents to detailed analysis of spent reactor cores. New facilities and improvements in detector characteristics, for example, may render completely practical a technique previously thought not worthy of further development.

An example of the information gathering process is a program that is designed to investigate the application of μ-meson capture x-rays to elemental and isotopic analysis. The objective of this program is to obtain high quality spectra for each fissionable isotope and to obtain information on how the chemical form of the material might affect possible assay applications. Using the facilities at the Space Radiation Effects Laboratory (NASA) data have been taken on metal targets of ^{208}Pb, ^{232}Th, ^{235}U, ^{238}U, and ^{239}Pu. Some data were also obtained for depleted uranium compounds, mainly oxides. The experiments are expected to continue early next year when more intense beams become available at the Los Alamos Meson Physics Facility.

CONCLUSIONS

The number of systems for assay that exist, complete with operations manual, error analysis, and operational history of reliability and effectiveness, is testimony to the growing maturity of nondestructive assay. A more difficult phase is beginning which emphasizes accuracy without undue increase in cost and complexity, the development of standard procedures, and the establishment of nondestructive assay methods as independent alternatives to traditional chemical analysis.

Calorimetry is an example of a technique for which refined nuclear data would have a direct effect on meeting the challenges listed above. The radioactive decay data and methods of determining isotopic composition are not sufficiently accurate to establish the relationship of heat output and quantity of material to an accuracy comparable to the precision available [18].

The value of readily available data which form the basis for design calculations and the foundations from which to explore new concepts can hardly be overemphasized. Routine calibration of equipment is accomplished by means of standards. Improvements of the data and calculational techniques will permit more precise evaluation of system performance which will reduce the number of these costly standards required.

REFERENCES

[1] FORSTER, R. A. and MENLOVE, H. O., LA-4605-MS (1970) 8.

[2] FORSTER, R. A., LA-4994-PR (1972) 9.

[3] FORSTER, R. A., SMITH, D. B., MENLOVE, H. O., Error Analysis of a ^{252}Cf Fuel Rod Assay System (LA report to be published in 1973).

[4] FORSTER, R. A., SMITH, D. B., and MENLOVE, H. O., "^{252}Cf fuel rod assay system: in-plant performance," Proc. Thirteenth Annual Meeting of the Institute of Nuclear Materials Management, Boston, Massachusetts (1972).

[5] FORSTER, R. A. and MENLOVE, H. O., LA-4883-PR (1971) 6.

[6] MENLOVE, H. O., FORSTER, R. A., PARKER, J. L., and SMITH, D. B., ^{252}Cf Assay System for FBR Fuel Pins: Description and Operating Procedures Manual, LA-5071-M (1972).

[7] MENLOVE, H. O., FORSTER, R. A., and SMITH, D. B., LA-5091-PR (1972) 7.

[8] MENLOVE, H. O. and FORSTER, R. A., LA-4994-PR (1972) 6.

[9] MENLOVE, H. O. and MATTHEWS, D., LA-5091-PR (1972) 16.

[10] MASTERS, C. F., THORPE, M. M., SMITH, D. B., The measurement of absolute delayed neutron yields from 3.1 and 14.9 MeV fission, Nucl. Sci. Engng 36 (1969) 202.

[11] KRICK, M. S. and EVANS, A. E., The measurement of total delayed neutron yields as a function of the energy of the neutron inducing fission, Nucl. Sci. Engng 47 (1972) 311.

[12] EVANS, A. E., THORPE, M. M., and MALANIFY, J. J., Fissile assay of small samples by subthreshold neutron interrogation, Trans. Am. Nucl. Soc. 15 2 (1972) 673.

[13] PARKER, J. L., REILLY, T. D., WALTON, R. B., SMITH, D. B., and EAST, L. V., LA-4705-MS (1971) 12.

[14] CLINE, J. E., A Relatively Simple and Precise Technique for the Assay of Plutonium Waste, ANCR-1055 (1972).

[15] LA-4994-PR (1972) 15.

[16] FOLEY, J. E., Random Source Interrogation System (Random Driver) at the Oak Ridge Y-12 Plant - Preliminary Results, LA-5078-MS (1972).

[17] FOLEY, J. E., LA-5091-PR (1972) 14.

[18] O'HARA, F. A., NUTTER, J. D., RODENBURG, W. W., DINSMORE, M. L., Calorimetry for Safeguards Purposes, MLM-1798 (1972).

INFLUENCE OF UNCERTAINTIES IN FISSION-PRODUCT NUCLEAR DATA ON THE INTERPRETATION OF GAMMA-SPECTROMETRIC MEASUREMENTS ON BURNT FUEL ELEMENTS

O.J. EDER, M. LAMMER*
Österreichische Studiengesellschaft
für Atomenergie, Seibersdorf,
Austria

Abstract

INFLUENCE OF UNCERTAINTIES IN FISSION-PRODUCT NUCLEAR DATA ON THE INTERPRETATION OF GAMMA-SPECTROMETRIC MEASUREMENTS ON BURNT FUEL ELEMENTS.

The combination of computer calculations and gamma spectrometric measurements offers new possibilities for investigations on burnt fuel elements. The accuracy of such a method is mainly limited by the accuracy of nuclear data used and uncertainties in the evaluation of measured gamma spectra arising from experimental conditions.

A method is described that combines "forward" calculations and measured activity ratios of fission products and examples of application are given.

The availability of compilations of nuclear data relevant for burnt fuel element analysis is surveyed and improvements are proposed. A set of fuel isotope and fission product nuclear data is presented which resulted from our own compilation efforts.

Finally, uncertainties are reviewed that arise from detector calibration, experimental conditions, nuclear data of fission products and simplifications in calculations. The influence of uncertainties in nuclear data on results of calculations and measurements is demonstrated by some examples.

1. INTRODUCTION

The combination of gammaspectrometric measurements and theoretical calculations provides a powerful tool to gain information about burnup and the history of fuel elements. The possibilities and limitations of this combined method from both the experimental and theoretical point of view have been investigated for about ten years by now [1-7].

Experimentally the development of high resolution semi-conductor detectors, the Compton coincidence spectrometer [2,3] and the summing Compton coincidence spectrometer [5] provided the basis to measure gamma-spectrometrically the activities of a number of isotopes in burnt fuel elements with sufficient accuracy (e.g. ^{137}Cs, ^{134}Cs, ^{95}Zr, ^{95}Nb, ^{103}Ru, $^{106}Ru + ^{106}Rh$, ^{131}I, $^{132}Te + ^{132}I$, $^{140}Ba + ^{140}La$, $^{144}Ce + ^{144}Pr$, ^{233}Pa, ^{239}Np etc.) Model calculations using the well-known build-up and decay formulae and simplified assumptions of the neutron flux distribution together with an iteration matching procedure are the basis for non-destructive fuel element investigations.

---

* Present address: Nuclear Data Section, IAEA, Vienna

In a "forward" calculation fission product activities are calculated from known irradiation conditions, whereas in a "backward" calculation irradiation history and/or fuel composition are derived from measured activities. The parameters which enter such inventory calculations are

- reactor operation conditions (space, energy and time distribution of the neutron flux, integrated neutron flux, fuel element cycling, cooling time)
- fuel element (initial composition, resonance self-shielding etc.)
- nuclear data (fission yields, half lives, neutron capture and fission cross sections, gamma ray energies and absolute intensities)
- experimental conditions (detector efficiency, geometry, gamma ray attenuation, quality and processing of gamma spectra etc.).

The information that can be obtained from gamma spectrometric measurements are (for a detailed discussion see [7]):

- Burn-up: from ^{137}Cs, ^{134}Cs (ratio $^{137}Cs/^{134}Cs$), $^{144}Ce - ^{144}Pr$, $^{106}Ru - ^{106}Rh$ and $^{95}Zr - ^{95}Nb$.
- Cooling time: from ratios $^{140}Ba/^{95}Zr$, $^{140}Ba/^{141}Ce$, $^{141}Ce/^{95}Zr$, $^{95}Zr/^{95}Nb$ and other combinations.
- Integrated neutron flux: from ratio $^{134}Cs/^{137}Cs$.
- Plutonium fissions: from $^{106}Ru - ^{106}Rh$, ratio $(^{144}Ce - ^{144}Pr)/(^{106}Ru - ^{106}Rh)$.
- Breeding rates at shutdown: from ^{233}Pa (^{232}Th as breeding material) and ^{239}Np (^{238}U as breeding material).

Modifications and further combinations of fission products are presently investigated and some will be discussed in the next chapter, preceded by a brief description of the computer programs used for our calculations. After a brief review of the availability of nuclear data and presentation of our own data set we show the influence of nuclear data uncertainties on results from calculations and measurements.

2. SOME DETAILS OF THE PRESENT INVESTIGATIONS

2.1. Principle Considerations

Characteristic dependencies of fission product concentrations on irradiation conditions and fissile material have been observed by several investigators (e.g. [6,8,9]). The use of activity ratios as an interpretation method was, as we believe, for the first time proposed in [7] together with some examples. The ratios shown in [7] as well as other combinations of fission products are presently investigated in more detail. Only interpretations in terms of activity ratios (instead of absolute activities) allow to establish general rules which are independent of the amount of fissile material. Also the use of such ratios has many advantages regarding accuracy and corrections that have to be applied (for a detailed discussion, see chapter 5).

The selection of fission products used for interpretation is guided by several considerations:

- Nuclear data and neutron flux models used in calculations as well as the activity measurements themselves are associated with some uncertainties.
- Depending on their half lives and the irradiation time most of the fission products will only yield information about the later part of the irradiation history.
- Therefore activity ratios have to depend significantly on irradiation parameters of fuel elements in order to enable the derivation of these parameters from the ratio.
- From a practical point of view the fission products used for interpretation have to be suitable for gamma spectrometric measurements.

Bearing these facts in mind fission products were selected considering their nuclear data, modes of production in fission and the possible information they can yield. According to this selection activity ratios of fission produots were calculated for a wide range of irradiation conditions and different fissile isotopes with the aid of computer programs and checked against experimental results.

2.2. Description of computer programs

We used two computer programs with different features for our forward calculations presented in [7]. The results obtained were generally in good agreement.

2.2.1. The computer program IRREL

This program calculates day by day inventories by approximating the differential equation

$$dN_1(t) = [a_2 N_2(t) - a_1 N_1(t)]\,dt$$

by the difference equation

$$\Delta N_1(t_i) = [a_2 N_2(t_{i-1}) - a_1 N_1(t_{i-1})]\Delta t_i$$

Here the symbols used mean:

N_1 ..... number of atoms of isotope 1

N_2 ..... number of atoms of precursor 2 of any kind

a_1 ..... constant giving the rate of decrease in N_1 (decay constant, neutron cross section)

a_2 ..... constant giving the rate of production of N_1 from precursor N_2 (decay, neutron capture, fission).

t_i ..... i-th time interval from start of irradiation (= 1 day)

$$t_{i-1} = \sum_{j=1}^{i-1} tj$$

$a_2 N_2$ stands for all modes of production of fission product N_1.

This approximation is sufficiently accurate for fission products with half lives of several days. Some modifications exist to take account of important shorter lived fission products (e.g. ^{135}Xe). In one version the

decay during each day is calculated exponentially. Other versions use numerical approximation methods or shorter time intervals within one day for such short lived fission products.

The program has the option either to enter the neutron flux as input parameter, or the total core power together with the core fraction of the investigated fuel element. In the latter case the neutron flux is calculated from the energy release per fission of the fissile material present in the fuel element. The neutron flux is represented by

- a maxwellian component, specified by the neutron temperature T,
- an epithermal component, varying with 1/E
- a fission spectrum component,

both of the latter specified by their ratios to the maxwellian flux. Date and time of start and end of each power period complete the description of the irradiation history.

This numerical method is especially well suited for calculations of inventories after varying irradiation conditions as this causes no increase in computer time and the equations involved are rather simple. The program IRREL is presently successfully used for routine calculations of isotope inventories in fuel elements from known irradiation conditions and described in more detail in [10].

2.2.2 The computer program CHAIN

This computer program solves analytically the differential equations that describe the complicated decay and activation processes. Difficulties due to the limited number of digits available have been successfully overcome by expansion of a complete set of exponential functions in one power series. An algorithm could be found which is especially suitable for machine coding. A convergence test of the exponents decides whether the power series or an ordinary exponentiation is to be used.

During the stage of testing the program it proved most convenient to store separately each individual decay and activation chain leading to a certain fission product. Similar chains are used for heavy elements from ^{232}Th to ^{241}Pu. Proceeding chain by chain, the contributions to the inventory of the isotope at the end of each chain are calculated for a given input time interval.

Here only the neutron flux can enter the calculations together with a time interval of constant flux. The input format of the neutron flux is optional:

a) As in IRREL the absolute value of the thermal flux can be given together with the ratios of epithermal and fast component. This is more suitable if the information comes from core calculations.

b) The absolute value of the total flux can be given including maxwellian and epithermal component. The total flux is specified by neutron temperature and an epithermal index. The fast flux is given as ratio to the total flux. This version is more suitable if the flux value is obtained from flux monitors and threshold detectors. [11].

In each case the type of flux representation and epithermal factor has to be specified. All modes of input neutron flux are transferred into Westcott formalism [11] for the calculation of reaction rates. Different

multiplication factors are derived according to whether pile neutron cross sections, maxwellian average cross sections together with reduced resonance integrals or 2200 m/s cross sections together with g and s factors are used.

Various options make this computer program very flexible:

- continuation with the calculated inventory, new start or termination,
- selection of different irradiation parameters or fission products to be calculated,
- continuation with cooling time,
- intermediate or final printout of inventory,
- storage of inventory on disc, which can be recalled repeatedly for further calculations.

In this manner a real irradiation history of varying neutron flux subdivided by cooling periods can be simulated, as the program always returns to this point. A modification is in preparation that allows us to calculate and plot gamma spectra of irradiated fuel elements to facilitate identification of gamma lines in measured spectra. This modification makes use of the advantage that calculated inventory and fission product gamma ray catalogue are both stored on disc. These features and the analytical solution of differential equations make the program CHAIN especially suitable for theoretical studies of different fission products under various conditions. On the other hand it is rather time consuming and less suitable if used for simulation of a complex irradiation history. Therefore it is mainly used for theoretical forward calculations and for small test samples to check the quality of the predictions.

2.3. Examples of application

2.3.1. Irradiation of samples

In order to check the predictions several samples of different fuel compositions were irradiated in different core positions for varying time intervals with and without flux monitors. When the results of these measurements are compared with calculations the agreement is naturally better than in routine examinations of fuel elements. A more precise value for the neutron flux can be obtained and the measurement itself can be performed with great care and high statistical accuracy as it involves only small samples and is not strictly limited in time. An agreement of better than 1% to 5% was obtained, depending in the fission products investigated.

The cooling time could be derived successfully in one case where accidentally the time of discharge of the sample from reactor was unknown. Due to the operation cycle of the reactor it had to be a Saturday and the exact date could be fixed after a half year cooling time by comparison of measured and calculated activity ratios.

2.3.2. Adjustment of irradiation parameters from known operation history

Generally irradiation conditions or at least total core power and time intervals as well as fuel composition are known. However, the neutron flux and contribution of epithermal neutrons within an individual fuel element will generally deviate from that obtained from physical core calculations and operator's data, especially at higher burn-up levels. In this case the comparison of measured and calculated activity ratios can be applied successfully to adjust these parameters in an iterative procedure.

The ratio of final flux to reactor power can be derived from a set of fission products with shorter half lives. If the change of this ratio with time due to burnup and fuel cycling has a noticeable effect on the result, it can be estimated by including a set of fission products which "remember" earlier parts of or the complete irradiation history, all of them being not sensitive on the neutron spectrum. Epithermal index and neutron temperature can be adjusted using the $^{134}Cs/\ ^{137}Cs$ activity ratio. All these independent informations have to be considered simultaneously. Starting with first estimates, the irradiation parameters can be improved in an iterative procedure.

The matching of all calculated activities with the measured ones is, however, rather cumbersome if not done automatically by computer. If less precision is required and a constant neutron flux to core power ratio can be assumed throughout the whole irradiation history within the precision limits, neutron flux, epithermal contribution and neutron temperature can be obtained merely by matching the ^{134}Cs and ^{137}Cs activities. In this case measured and calculated absolute activities have to be compared as they in combination with the initial content of fissile material supply additional information.

2.3.3. Determination of burn-up

Burn-up is determined by gamma spectrometric measurements of ^{137}Cs, $^{144}Ce - {}^{144}Pr$, $^{106}Ru - {}^{106}Rh$ and $^{95}Zr - {}^{95}Nb$ activities successfully on a routine basis. Limits of application of these fission products were already discussed in [7] and other work. The usefulness of ^{137}Cs as burn-up monitor is, however, doubted because of its tendency to migrate. The magnitude of this effect depends on the type of fuel, its temperature and the temperature gradient within the fuel. In many practical cases errors in burn-up determination due to ^{137}Cs migration are not serious.

If we assume that the reactor operation history and fuel composition are known the integrated neutron flux is equivalent to the burn-up (total number of fissions). In this case the $^{134}Cs/\ ^{137}Cs$ activity ratio offers a possibility superior to an absolute measurement of ^{137}Cs. Apart from the advantages of ratios regarding corrections and uncertainties, it can be expected that ^{134}Cs is affected by migration in the same manner as ^{137}Cs. Consequently losses and redistribution of Cs (local concentrations) should have no serious effect on this ratio. Also errors due to absorption corrections assuming a homogeneous radial distribution of Cs in the fuel should cancel.

Not only the axial burn-up profile of a fuel element can be measured with higher accuracy from the $^{134}Cs/^{137}Cs$ activity ratio. Using the matching procedure described in 2.3.2 the neutron flux and the contribution of epithermal neutrons inside a fuel element and its variation can be determined which is not possible by any direct measurement. Radial distributions can only be determined with confidence for fuel types that hinder migration in this direction.

A research co-ordinating meeting on development of gamma spectrometry instrumentation and techniques for safeguards [12] recommended the experimental exploitation of the $^{134}Cs\ /\ ^{137}Cs$ ratio for burn-up determination. Investigations in this direction are in progress. Results of a limited number of comparisons showed that burn-up determined by this ratio agreed with destructive U - Pu analysis within about 1% [13]. In measurements

of the axial burn-up profile the $^{134}Cs/^{137}Cs$ ratio showed a good correlation (factor: 0.993 [14]) and proved to be superior to other ratios or measurements of absolute activities [13,14].

2.3.4. Establishment of fission product inventories.

In some application fields (e.g. fuel element testing and development, fission product release measurements etc.) one might be interested in fission product concentrations that cannot be measured directly. Here the method described in section 2.3.2 can be used together with gamma-spectrometric measurements of fission product activities to adjust the parameters used in calculations. In this manner concentrations of fission products at reactor shut down can be calculated, which cannot be measured because of their low activities, short half lives or the absence of suitable gamma lines. This procedure is already in use on a routine basis [10].

2.3.5. Application in safeguards

The main objectives of safeguards measurements on irradiated fuel elements are the identification of fuel elements and the verification of operators data. In practice this means a check, if the measured content of fissile material, especially Plutonium, and fission products corresponds to the information about initial fuel composition, irradiation history and burn-up given by the plant operator [12]. Here we have the case of known irradiation history and fuel composition, and a forward calculation can be compared with gamma spectrometric measurements for verification. Experiments to check such a verification technique have been performed by IAEA together with Euratom [14] using activity ratios. Among these some ideas presented in [7] were adopted. Correlations between burn-up, cooling time and Pu-fissions on the one hand and activity ratios on the other hand were found to be satisfactory. Details and results can be found in [14].

Significant inconsistencies exceeding experimental error and uncertainties due to nuclear data and simplifications in the calculation (together about 5 - 20%) can easily be detected by this method. In such a case the fuel element can be further investigated by destructive analysis. However, the dependence of activity ratios on certain parameters, as listed in the introduction (1.) and discussed in detail in [7], allow us to derive some limited information about the history and composition of the fuel element with low accuracy. This procedure could be as follows starting with first rough estimates from curves (e.g. from [7] or section 2.4.):

Step 1: The cooling time can be derived roughly from different fission product ratios. If shorter lived fission products can be measured (e.g. ^{131}I, ^{140}Ba, ^{141}Ce) these should be used as first estimates, as they are more likely to be in saturation than fission products with longer half lives. Shutdown activities can then be calculated for all measured fission products.

Step 2: The $^{134}Cs/^{137}Cs$ activity ratio yields a first estimate of the integral neutron flux, assuming ^{235}U fissions only and a typical value for the epithermal neutron flux. With this parameter fixed, the irradiation time can be derived from the $^{95}Zr/^{137}Cs$ activity ratio as shown in figure 4 (see also 2.4.).

Step 3: The number of Pu fissions can be derived from the $^{144}Ce/^{106}Ru$ ratio. The original dependence shown in [7] can be modified by plotting the $^{144}Ce/^{106}Ru$ ratio against the integral neutron flux. Using the initial $^{235}U/^{238}U$ ratio (enrichment) as third parameter several curves are obtained. With the assumption that all Pu fissions result from ^{238}U breeding the initial enrichment of U can be estimated.

Step 4 and further steps: An inventory calculation can be performed with the first estimates and compared with the measured activities. Discrepancies have to be expected as the curves used for first estimates are more or less independent. All parameters can be adjusted, starting again with Step 1. Additional activity ratios can be included to check the initial assumptions of "third" parameters in curves such as epithermal flux or initial fuel composition. So for example the $^{154}Eu/^{137}Cs$ activity ratio (Fig. 6, see also 2.4.3.) cannot be used as a first estimate, as it depends strongly on the fissile isotope and the epithermal flux contribution. But in the adjustment procedure it can be used to check the assumptions of Pu production.

The value and accuracy of such an iterative procedure has to be investigated experimentally.

2.4. Some new results from studies of activity ratios

2.4.1. The $^{134}Cs/^{137}Cs$ activity ratio

The $^{134}Cs/^{137}Cs$ ratio varies linearily with integrated neutron flux over more than 2 decades. Our first calculations [7] showed a strong dependence of this ratio on the epithermal neutron flux contribution and was therefore further investigated. Figure 1 shows the variation of this ratio with irradiation time and total neutron flux (thermal + epithermal) for ^{235}U fissions.

The $^{134}Cs/^{137}Cs$ activity ratio is almost the same for ^{235}U and ^{239}Pu fissions and changes by about 25% when going to ^{233}U fissions (Fig.2). It can also be seen from figure 2 that the variation with neutron temperature is not serious, whereas the strong dependence on the neutron spectrum introduces a large uncertainty.

2.4.2. The $^{95}Zr/^{137}Cs$ activity ratio.

Due to the comparatively short half life of ^{95}Zr (64d) the $^{95}Zr/^{137}Cs$ activity ratio at reactor shut down should vary significantly with irradiation time. This is shown in figure 3 for different values of the total neutron flux (^{235}U only). The dispersion of the curves especially for low values of the ratio (Fig.3) is due to the high ^{235}U depletion which is also indicated in figure 3. In this case ^{95}Zr is no more formed in fission in significant amounts and decays practically. The depletion is equivalent to integrated neutron flux values which can be obtained from $^{134}Cs/^{137}Cs$.

2.4.3. The $^{154}Eu/^{137}Cs$ activity ratio

Due to the low fission yield of ^{153}Eu, ^{154}Eu can only be found in gamma spectra from highly irradiated fuel elements and after rather long cooling times. Calculated ratios are shown in figure 4 and compared to the $^{134}Cs/^{137}Cs$ activity ratio (on different scale). The difference in the $^{154}Eu/^{137}Cs$ ratio for ^{235}U and ^{239}Pu fissions is noticeable. This

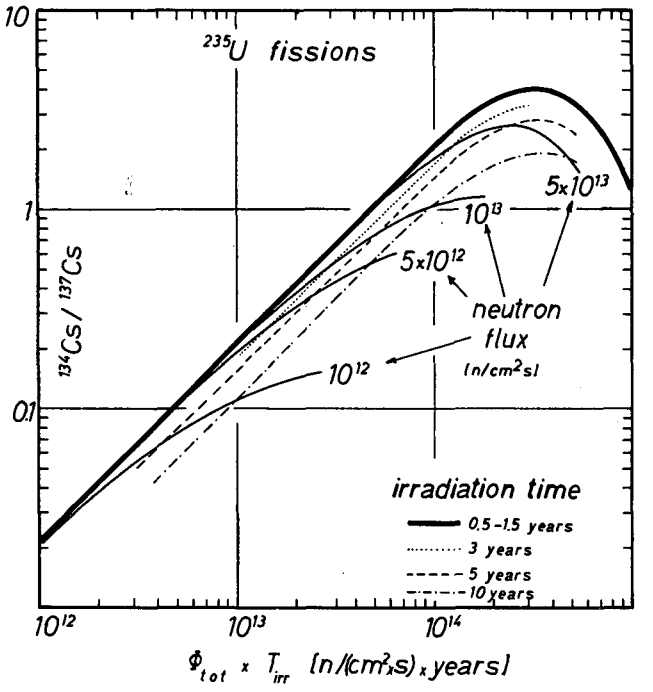

FIG.1. $^{134}Cs/^{137}Cs$ activity ratio at shutdown versus integrated neutron flux for different values of neutron flux and irradiation time.

ratio has another interesting feature: the contributions of lower mass chains to the ^{154}Eu activity increase rapidly with integrated neutron flux as shown in the table below:

Integrated neutron flux [n/cm² s x years]	contributions from masses 153	152	151	149	147
10^{13}	92%	4.4%	3.5%	-	-
5 x 10^{13}	57%	17%	23%	2.6%	-
10^{14}	31%	23%	34%	10%	1.4%
2 x 10^{14}	10%	20%	32%	32%	5.5%
4 x 10^{14}	0.7%	7%	12%	41%	39%
5 x 10^{14}	0.2%	3%	5.5%	36%	53%

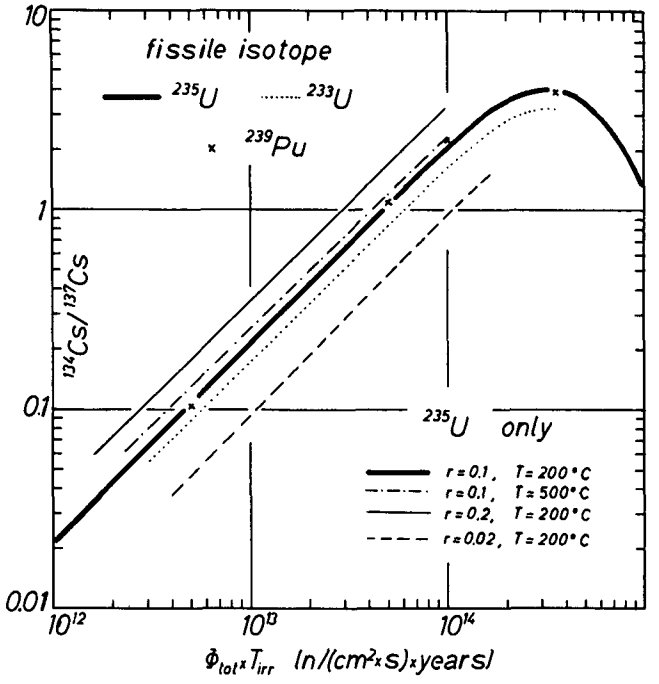

FIG. 2. Dependence of $^{134}Cs/^{137}Cs$ activity ratio at shutdown versus integrated neutron flux on different parameters.

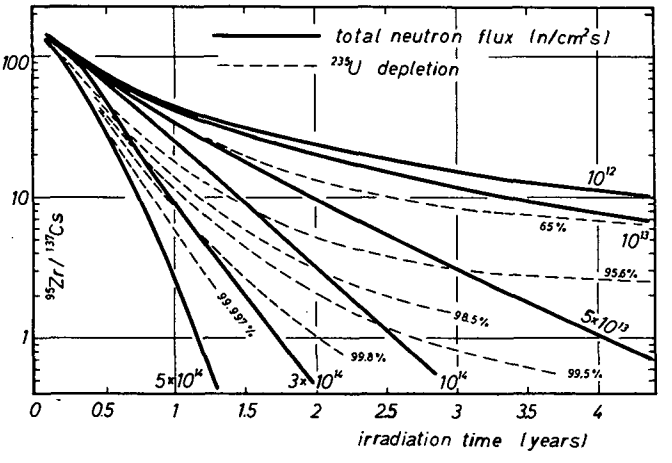

FIG. 3. Dependence of $^{95}Zr/^{137}Cs$ activity ratio at shutdown on irradiation time.

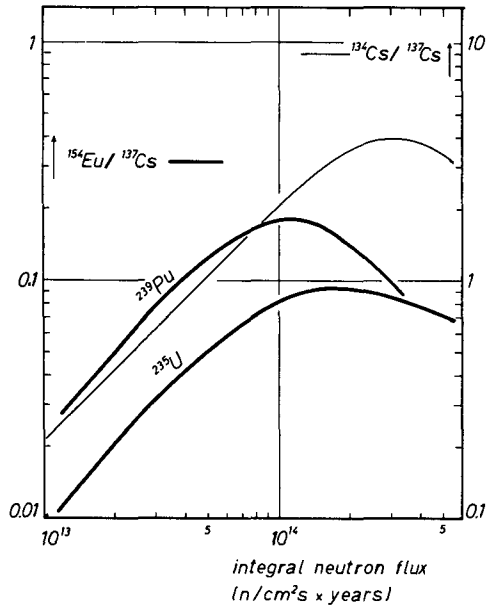

FIG.4. Dependence of $^{154}Eu/^{137}Cs$ activity ratio at shutdown on integrated neutron flux.

This effect has several consequences:

- The slope of the $^{154}Eu/^{137}Cs$ ratio is steeper than that of the $^{134}Cs/^{137}Cs$ ratio at lower integrated fluxes.
- The curve calculated for ^{239}Pu fissions approaches that for ^{235}U fissions at higher integral fluxes as the difference in fission yields is not so pronounced at lower mass numbers.
- The dependence on the fraction of epithermal neutrons is likely to vary with integral neutron flux. This has not yet been investigated.

3. COMPILATIONS WHICH INCLUDE NUCLEAR DATA NEEDED IN THIS WORK

Nuclear data used as input to forward calculations are: half lives, neutron cross sections, branching ratios and fission yields.

Data needed for the evaluation of measured gamma spectra are: gamma ray energies and absolute intensities of calibration standards (detector efficiency) and fission products, half lives and gamma ray attenuation coefficients.

3.1. Fission yields

Existing evaluations and evaluation methods are discussed in another paper at this Symposium [15].

3.2. Decay data and gamma ray properties

The table of isotopes edited by Lederer et al [16] is the last comprehensive compilation of decay data and gamma ray properties that includes all the fission products of interest in our work. However, no

gamma ray measurements with semiconductor detectors are included in this compilation for most of the fission products, as such measurements were not available at that time. Due to the rapid development and increasing application of high resolution semi-conductor detectors these data were of little value to users and superseded by more accurate measurements already shortly after the publication of the last edition of the book.

Decay and level scheme evaluations by the Nuclear Data group are published on a regular basis. However, they still have a large backlog and their last compilations of many important fission products (mass numbers 97, 99, 103, 106, 131, 133, 134, 137, 140) date from 1959 to 1961. The situation is not so bad for half lives and branching ratios as there are not so many measurements performed and the "Recent References" of the Nuclear Data Group helps to find the publications.

More recently a number of evaluations and compilations were published [17 - 19]. Especially the detailed tables of Martin and Blichert-Toft [17] were very valuable for our work, although they do not contain all of the important fission products. However, no up-to-date compilations were available between 1967 and 1970, except for tables of gamma ray energies for detector calibration, and therefore compilation activities started at the reactor center Seibersdorf for internal use.

3.3. Neutron cross sections

As with half lives, measurements of thermal neutron cross sections and resonance integrals are not very frequent. The comprehensive and well known compilation BNL-325 [29,30] contains all pre 1966 measurements. References for later measurements can be found in CINDA [31]. Also a number of other compilations exist due to a world-wide interest in neutron data.

The main problems concerning neutron cross sections are the lack of measurements for a number of nuclides and partially unresolved discrepancies between some measured values. Another striking fact is the lack of information about world-wide compilation activities such as the literature index CINDA [31] or retrieveable computer files of experimental and evaluated data and the services offered by data centers.

3.4. Suggested improvements in compilation efforts

Although a literature index to experimental data may be of great value, a user would preferably not just adopt the result of a most recent measurement. Due to the lack of decay data compilations, especially of gamma ray energies and intensities, several unpublished compilations have been prepared at our and other laboratories for internal use. A number of these compilations have only recently been published or prepared for publication. In order to save world-wide parallel efforts we would strongly support any means to make information about compilation activity and existing compilations commonly available. This could be achieved by issuing periodically a compilation bulletin or by the inclusion of references to compilations and evaluations in indexes to existing literature, even if unpublished. It would then be the responsibility of the compilers to supply this information to indexers.

In many application fields only a limited number of nuclear data types is needed. For example most applications need only gamma ray energies and absolute intensities rather than complete level schemes. During our own compilation work it proved convenient to maintain computer files of experimental data for gamma ray energies and intensities, half lives and branching ratios, which could be updated periodically. A certain selection of

data has to be made but this selection causes not much additional effort. Some care is required on the part of the compiler in calculating absolute gamma ray intensities from supplementary information, but this may not be necessary for every update.

The situation is somewhat different for neutron cross sections and fission yields as these data require careful evaluation. However, these evaluated data could also be maintained in a computer file. We would therefore recommend the investigation of the generation of such computer libraries of important nuclear data which would be readily available to all users.

4. RECOMMENDED NUCLEAR DATA

Tabulations of fission prodcut nuclear data are still rather rare and we have received some requests for our data. Therefore we present a recently updated set of fission product and fuel isotope nuclear data. Details will be published elsewhere.

4.1. Nuclear data of fuel isotopes

Table I contains the preliminary results of a new evaluation of 2200 m/s constants [32] which is a revision of the earlier publication [33]. Only minor changes of these values are expected for the final version, except, perhaps, ^{239}Pu and ^{241}Pu. A careful reevaluation of the half lives of these two isotopes is in progress. The S values were calculated by us from Westcott's data [34] (S_2 values) according to:

$$S_{new} = S_{old} + \sqrt{4T/\pi T_0} \left\{ (RI/\sigma_{2200})_{new} - (RI/\sigma_{2200})_{old} \right\} - b\,(g_{new} - g_{old})$$

The new resonance integrals [33] "RI_{new}" are also shown in Table I.

Table II contains cross sections and half lives of heavy isotopes occuring in nuclear fuel cycles. All publications of these data that could be found in CINDA 72 main volume and supplement [31] were surveyed. The fission spectrum average cross sections shown in Tables I and II should receive special attention. Among these the cross section of ^{238}U was studied most extensively and the absolute values reported had highest precision and consistency. Measured cross section ratios of different isotopes were found to agree for better than absolute values [35]. Therefore the ^{238}U cross section was selected as reference and all other cross sections calculated relative to the ^{238}U value shown in Table II. This selection is reasonable as we deal only with thermal reactors where only ^{238}U and ^{232}Th fast cross sections are of some importance.

4.2. Fission product nuclear data

Half lives and cross section values are shown in Table III. The headings in columns 4 - 6 mean:

maxwellian = maxwellian average cross section $g\,\sigma_0$

res int = reduced infinite dilution resonance integral above 1/v part of cross section

pile = pile neutron cross section .

TABLE I. PRELIMINARY 2200 m/s CONSTANTS

Quantity[a]	^{233}U	^{235}U	^{239}Pu	^{241}Pu
σ_a	579.7±1.4 b	682.2±1.4 b	1011.2±2.9 b	1375.4±7.2 b
σ_f	533.0±1.3 b	584.0±1.3 b	742.7±1.9 b	1010.2±5.9 b
σ_c	46.7±0.3 b	98.2±0.9 b	268.5±2.1 b	365.2±6.7 b
g_a (input)[b]	0.9990±0.0012[d]	0.9787±0.0009	1.0791±0.0031	1.0375±0.0012
g_a (output)[c]	0.9991±0.0009	0.9792±0.0009	1.0788±0.0021	1.0376±0.0012
g_f (input)[b]	0.9966±0.0012[d]	0.9774±0.0012	1.0550±0.0014	1.0505±0.0076
g_f (output)[c]	0.9967±0.0009	0.9762±0.0011	1.0556±0.0013	1.0470±0.0046
g_c (input)[b]	1.0263±0.0070[d]			
g_c (output)[c]	1.0270±0.0049	0.9966±0.0084	1.1428±0.0081	1.0116±0.0126
$g_a \sigma_a$[e]	579.2±1.3 b	668.0 ±1.4 b	1090.8±3.0 b	1427.1±7.5 b
$g_f \sigma_f$	531.2±1.2 b	570.1 ±1.2 b	784.0±2.0 b	1057.7±4.6 b
$g_c \sigma_c$	47.9±0.2 b	97.9 ±0.3 b	306.8±1.5 b	369.4±6.3 b
S_a	1.257	0.1259	2.295	
S_f	1.071	-0.036	1.758	0.8348
S_c	2.827	1.067	3.696	
RI_f[f]	750±20 b	270±10 b	300±10 b	580±40 b
RI_c	140±10 b	140±7 b	181±15 b	160±30 b
σ_f(fiss)[g]	1.70 b	1.174 b	1.74 b	1.6 b

a a = absorption, f = fission, c = capture
b "input" values calculated from cross-section curve
c "output"values from fit of 2200 m/s and maxwellian average cross sections
d Reference [20]
e maxwellian average ($g\sigma$) calculated from "output"values
f RI infinite dilution resonance integral (above 0.5 eV) including 1/v part as used for calculation of S factors
g Fission spectrum average cross section

TABLE II. NUCLEAR DATA OF HEAVY ISOTOPES

	neutron cross sections (barn)[a]						
	capture			fission			
Isotope	maxw	RI	fiss	maxw	RI	fiss	half life
^{232}Th	7.313[b]	82	0.262			0.072	
^{233}Pa	39	860				0.39	27 d
^{234}U	99	600	0.14			1.3	
^{236}U	5.4	415	0.14			0.69	
^{237}U	370[c]		0.07	2		0.68	6.75d
^{238}U	2.73	269	0.085			0.310	
^{237}Np	169	870	0.17	0.019	6	1.28	
^{238}Np	43	10	0.12	2200	510	1.3	50.8 h
^{239}Np	60[c]						2.35 d
^{238}Pu	588	164[d]	0.03	16.3	16.7	2.3	
^{240}Pu	288	8220		0.06		1.5	

a maxw = maxwellian average ($g \times \sigma_0$) cross section,
RI = reduced resonance integral (1/v part subtracted)
fiss = fission spectrum (^{235}U) average cross section.

b $\sigma_0 = 7.3449$ b, $g_0 = 0.99562$ [21].

c pile neutron cross section

d includes 1/v part of cross section

Half lives for many fission products were taken from the evaluation of Martin and Blichert-Toft [17]. "Recent References" issued by the Nuclear Data group in Oak Ridge were scanned regularily for new measurements. A computer fit was made whenever data more recent than those included in [17] were found and use was made of the tables of experimental data in [17]. In some cases, where one value was considered superior to others, this was adopted. Up to now for most of the fission products contained in [17] more recent data were available.

The most extensive compilation of fission product thermal cross sections and resonance integrals is that of Walker [36]. Therefore his values for experimentally determined cross sections were adopted by us and only updated for some new measurements. Stable nuclides, for which no new measurements were found, are not included in our tables and Walker's data [36] are recommended.

For nuclides where no experimental results are available the Australian fission product point cross section library [22,23] is used which is based on more sophisticated calculations than Walker's estimates.

TABLE III. FISSION PRODUCT NUCLEAR DATA[a]

fission product	half-life	cross-sections (barn)			
		2200 m/s	maxwellian	res int.	pile
^{77}As	38.83±0.05 h	12.5 [b]			20 [c]
^{81}Br			2.7±0.2	55 ± 5	
^{82}Br	35.34±0.02 h	18 [b]			40 [c]
^{83}Kr			200±10	150±30	
^{84}Kr			0.1	8	
^{85}Kr	10.73±0.06 a				8
^{86}Rb	18.65±0.02 d	0.49[b]			0.5 [c]
^{89}Sr	50.52±0.05 d				0.42
^{90}Sr	28.6 ±0.4 a				0.8
^{91}Sr	9.48 ±0.02h	0.14[b]			0.15[c]
^{91}Y	58.51±0.12d	1.0 [b]			1.4
^{94}Zr			0.06±0.01	0.37±0.04	
^{95}Zr	63.98±0.12d	0.48[b]			1 [c]
^{95m}Nb	3.61±0.04 d				
^{95}Nb	35.045±0.010d	1.43[b]			4
^{96}Zr			0.006±0.001	5.0±0.5	
^{97}Zr	16.8±0.2 h	0.20[b]			0.4 [c]
^{98}Mo			0.13±0.01	7±1	
^{99}Mo	66.7±0.5 h	1.7[b]			2[c]
^{103}Ru	39.35±0.10 d	7.6[b]			10[c]
^{105}Rh	35.5± 0.2 h		17000±2000	17000±3000	
^{106}Ru	368.3±2.0 d		0.15±0.05	2.0±0.6	
^{109}Pd	13.46±0.02 h				5

Note: for footnotes [a, b, c, d, e, f] see below last portion of this table.

TABLE III (cont.)

fission product	half life	cross-sections (barn)			
		2200 m/s	maxwellian	res int.	pile
^{109}Ag			93±5	1500±200	
^{110m}Ag	252.2±0.3d				82
^{111}Ag	7.45 ±0.01 d		3±2	105±20	
^{112}Pol	20.12±0.06 h				1
^{112}Ag	3.16±0.02h				
^{115m}Cd	44.6± 0.2 d	31 [b]			50 [d]
^{115}Cd	53.38±0.04 h	5.4 [b]			20 [d]
^{121m}Sn	50 ± 10 a	12.4 [b]			13 [c]
^{121}Sn	27.05±0.10 h				
^{121}Sb			6.2±0.1	200±10	
^{122}Sb	64.34±0.06 h	21 [b]			
^{123}Sn	129.3±0.5 d	0.03 [b]			
^{123}Sb			4.2±0.2	120±10	
^{124}Sb	60.20±0.02 d				6.5
^{125}Sn	9.64±0.03 d	0.55 [b]			
^{125}Sb	2.75±0.04 a				1.56
^{125m}Te	58±1 d	11 [b]			20 [d]
^{126}Sn			0.3	0.12	
^{126}Sb	12.4±0.1 d	5.8 [b]			
^{127}Sb	91.2±0.3 h	0.9 [b]			
^{127m}Te	109 ± 2 d	9.4			20 [d]

TABLE III (cont.)

fission product	half life	cross-sections (barn)			
		2200 m/s	maxwellian	res int.	pile
^{129m}Te	33.6±0.2 d	1.1			
^{131m}Te	30 h	0.1			
^{131}I	8.05±0.02 d[e]	0.94[b]		≈8	
^{131m}Xe	11.98±0.05 d				50
^{132}Te	78± 1 h	0.0024[b]			
^{132}I	2.285±0.010 h				
^{133}I	20.9±0.1 h	0.0035[b]			
^{133m}Xe	54±2 h				f
^{133}Xe	5.29±0.01d				190±90
^{133}Cs			29.5±2.0	450±20	
^{134}Cs	2.05±0.02 a	133[b]			140±12
^{135}I	6.585±0.002 h	0.02[b]			
^{135}Xe	9.172±0.005 h	2.65×10^6	3.1×10^6		
^{136}Cs	13.00±0.02 d	1.9[b]			
^{137}Cs	30.0±0.2 a				0.11
^{140}Ba	12.79±0.01d		1.57±0.03	13±2	
^{140}La	40.27±0.05 h		2.7 ±0.3	69±4	
^{141}Ce	32.55±0.02 d				29±3
^{142}Pr	19.1±0.1 h				20±3
^{143}Ce	33 ± 1 h				6

TABLE III (cont.)

fission product	half life	cross-sections (barn)			
		2200 m/s	maxwellian	res.int.	pile
^{143}Pr	13.58±0.03 d		100±10	150±30	
^{144}Ce	284.5±0.4 d		1.0±0.1	2.2±0.3	
^{147}Nd	11.00±0.03 d	50[b]			100[d]
^{147}Pm	2.623±0.001 a		182±20	2400±300	
^{147}Sm			61±7	646±60	
^{148m}Pm	40.9±0.2 d				25000±2000
^{148}Pm	5.37±0.01 d				3000±2000
^{148}Sm			3.5±1.2	27±14	
^{149}Pm	53.08±0.05h				1400±300
^{149}Sm		42100±400			
^{151}Pm	28.4±0.1 h				400
^{151}Sm	93±5 a	15000±1800		(3100)	
^{153}Sm	46.9±0.2 h	335[b]			500[d]
^{153}Eu		450±20			
^{154}Eu	8.5±0.2a				1500
^{155}Eu	4.9±0.1a				4040±125
^{156}Eu	15.16±0.02d	480[b]			500[d]
^{157}Eu	15.15±0.08 h	190[b]			200[d]

a For branching ratios and cross section ratios to metastable states see table VI.

b Interpolated from Australian fission product point cross section library [22,23]. Estimated error 100% [22].

c Rough estimate from 2200 m/s cross section by comparison with nuclei of similar charge and mass number combinations

d Order of magnitude estimated from point cross section library data [22,23]

e More recent measurements quoted in [24 - 26] are not included, as they are either discrepant [24,26] or not yet published [25]

f Cross section not measured nor calculated. Measurements of Reynolds and Emery [27] (on decay schemes) suggest, that this cross section might be of the order of 10^4 b.

0.0253 eV cross sections were obtained from these data by interpolation and pile neutron cross sections estimated as indicated in Table III. In cases where the cross section is insignificant generally only the 2200 m/s value is listed.

Estimated error of the calculated values is ± 100% [22]. The estimated contribution to the pile neutron cross section should have even greater uncertainty and indicate only the order of magnitude. Generally no errors are assigned to measured pile neutron cross sections as the value depends on the neutron spectrum. Other errors shown are from single measurements or assigned according to the dispersion of selected values.

Table IV shows some isomeric ratios for more important fission products with metastable states.

4.3. Table of gamma rays

The complete table of fission product gamma ray energies and absolute intensities cannot be included in this paper. Also, the last update was made in 1971.

Energies and relative intensities are fitted by computer. The conversion of relative to absolute intensities is done by hand and given as input. Examples for two fission products are shown in Table V. The fitted energies and absolute intensities are punched on cards as well as the reference numbers.

These cards are input to another computer program. This program prints out a table of gamma rays sorted by fission products, a table of gamma rays sorted by descending energy and subdivided into three half life groups, and a list of references. Examples are given in Table VI. The half life values shown are superseded now by those in Table III. All these tables are stored on disc and can be recalled for printout by another program. The "Ordered table of energies" serves to facilitate the identification of gamma rays in complex spectra from burnt fuel elements.

5. UNCERTAINTIES IN GAMMA SPECTROMETRIC MEASUREMENTS AND FORWARD CALCULATIONS

The activity of a fission product at the time of measurement, A, is calculated from a measured gamma spectrum from the formula:

$$A = P \cdot \frac{1 + DC}{I_\gamma . EF(E) . T . GA(E)} \qquad (1)$$

P = Photopeak area
DC = Deadtime correction
I_γ = Gamma ray intensity
EF(E) = photopeak efficiency for gamma line with energy E in position of measurement (or scanning efficiency)
T = Measuring time (sec)
GA(E) = Energy dependent gamma ray absorption factor.

TABLE IV. BRANCHING RATIOS

fission product	half life [a]	% β^- decay [b]	branching (%) [c]	precursor	cross section(b) [d] maxw	cross section(b) [d] res.int.
^{82}Br	35 h	100			2.7±0.2 [e]	55±5 [e]
^{85m}Kr	4.4 h	78.8±0.9 [f]	100 [f]	^{85}Br	0.09±0.01	7
^{85}Kr	10.7 a	100	0 [f]	^{85}Br	0.03 [e]	2 [e]
^{95m}Nb	3.6 d	0	1.8±0.5	^{95}Zr		
^{99m}Tc	6 h	0	86.3±1.0	^{99}Mo		
^{110m}Ag	252 d	98.6±0.13			4.67±0.07	70±2
^{125m}Te	58 d	0	22.3	^{125}Sb		
^{127m}Te	109 d	2.4±0.2	17.4	^{127}Sb		
^{129m}Te	33.6 d	36 ± 7	16.6	^{129}Sb	0.016±0.001	0.077±0.005
^{131m}Xe	12 d	0	1.35±0.11	^{131}I		
^{133m}Xe	54 h	0	2.8±0.1	^{133}I	0.04	0.2
^{148m}Pm	41 d	93.2±0.7			86±10	1130±100
^{148g}Pm	5.4 d	100	6.8±0.7	^{148m}Pm	96±2	1270±100

a For exact value see table III. This figure is only given to distinguish between isomeric states.

b Unless otherwise noted, 100% minus the value given is isomeric transition to ground state.

c Percentage of β-decays of radioactive precursor (column 5) to the fission product listed in column 1.

d Cross section of isotope with mass number A-1 for production of fission product with mass number A (column 1).

e Short lived isomeric state neglected. Production cross section listed includes fraction from isomeric transition.

f If a 100% decay of ^{85}Br to ^{85m}Kr is assumed, this value is slightly higher compared to the fraction of ^{85g}Kr observed in fission yield measurements (21.6% - 22% [28]). This might be due to direct formation of ^{85}Kr isomers in fission, but is unlikely for ^{235}U fission. The possibility of a fraction of ^{85}Br decaying directly to ^{85g}Kr should be investigated. The ratios of fission yields [15,28] are recommended for use in calculations.

TABLE V. EXAMPLES OF EVALUATED GAMMA-RAY ENERGIES AND INTENSITIES

58 CE 141

32.38 (+/- 0.02) DAYS HALFLIFE

100 PERC. REL = 100. (+/- 0.) PERC. ABS.

NR	ENERGY (KEV)			INTENSITY (PERC.)		REF
	145.49	+/- 0.03				3
	145.43	+/- 0.02				125
	145.443	+/- 0.006				125
	145.44	+/- 0.05				148
	145.41	+/- 0.03				149
	145.450	+/- 0.005				150
	145.4498	+/- 0.0049				156
	145.441	+/- 0.003				193
				49.	+/- 1.	73
	ADOPTED VALUE					
1	145.444	+/- 0.002	REL	49.	+/- 1.	
			ABS	49.	+/- 1.	

ABSOLUTE VALUE FOR 100 PERC. REL. INTENSITY

SEE REF. 73

LIST OF REFERENCES

3 NUCL.PHYS., A107(1968)177
73 NUCL.DATA, A8/1-2(1970)
82 J.NUCL.SCI.TECHN.,3/5(1966)200
125 NUCL. DATA, A4-3-301 (1968)
148 NUCL.PHYS., A90(1967)650
149 NUCL.PHYS., A91(1967)453
150 NUCL.PHYS., A129(1969)1
156 COO-1112-167 (1967)50
193 NUCL.INSTR.METH., 77(1970)141

TABLE V (cont.)

63 EU 155

1770. (+/- 36.) DAYS HALFLIFE

100 PERC. REL = 32.58 (+/- 1.03) PERC. ABS.

NR	ENERGY (KEV)		INTENSITY (PERC.)	REF
	18.776 +/- 0.035		0.162 +/- 0.038	212
	ADOPTED VALUE			
1	18.776 +/- 0.035	REL	0.162 +/- 0.038	
		ABS	0.053 +/- 0.012	
	* 26.53		1. +/- 1.	79
	26.513 +/- 0.021		1.03 +/- 0.04	212
	ADOPTED VALUE			
2	26.513 +/- 0.021	REL	1.03 +/- 0.04	
		ABS	0.34 +/- 0.02	
	31.55 +/- 0.10	*	0.03 +/- 0.02	99
	31.43 +/- 0.05		0.023 +/- 0.005	212
	ADOPTED VALUE			
3	31.45 +/- 0.05	REL	0.023 +/- 0.005	
		ABS	0.0075 +/- 0.0016	
	* 45.29	*	2.8 +/- 0.7	79
	45.299 +/- 0.002		3.6 +/- 0.7	99
	45.2972 +/- 0.0013			192
	45.299 +/- 0.013		4.18 +/- 0.17	212
	ADOPTED VALUE			
4	45.2977 +/- 0.0011	REL	4.1 +/- 0.2	
		ABS	1.35 +/- 0.07	
	* 58.		0.20 +/- 0.03	79
	57.970 +/- 0.026		0.22 +/- 0.05	99
	57.9805 +/- 0.0020			192
	57.983 +/- 0.030		0.217 +/- 0.011	212
	ADOPTED VALUE			
5	57.980 +/- 0.002	REL	0.215 +/- 0.010	
		ABS	0.070 +/- 0.004	

* NOT USED FOR AVERAGE

TABLE V (cont.)

NR	ENERGY (KEV)		INTENSITY (PERC.)		REF
	* 60.		3.8	+/- 0.2	79
	60.006 +/- 0.004	*	4.3	+/- 0.3	99
	60.0100 +/- 0.0018				192
	60.019 +/- 0.015		3.60	+/- 0.04	212
	ADOPTED VALUE				
6	60.0094 +/- 0.0016	REL	3.61	+/- 0.04	
		ABS	1.18	+/- 0.04	
	* 86.05		0.50	+/- 0.05	79
	86.062 +/- 0.023		0.49	+/- 0.05	99
	86.0621 +/- 0.0051				192
	ADOPTED VALUE				
7	86.062 +/- 0.005	REL	0.50	+/- 0.04	
		ABS	0.16	+/- 0.01	
	86.541 +/- 0.003		100.		99
	86.5452 +/- 0.0033				192
	86.539 +/- 0.015		100.		212
	ADOPTED VALUE				
8	86.5428 +/- 0.0022	REL	100.		
		ABS	32.58	+/- 1.03	
	* 105.3		65.7	+/- 6.5	76
	* 105.32		67.9	+/- 3.4	79
	105.302 +/- 0.004		68.3	+/- 2.7	99
	105.308 +/- 0.003				192
	105.315 +/- 0.015		66.8	+/- 1.3	212
	ADOPTED VALUE				
9	105.306 +/- 0.002	REL	67.1	+/- 1.1	
		ABS	21.9	+/- 0.8	
	146.2 +/- 0.2		0.16	+/- 0.05	76
	146.061 +/- 0.015		0.19	+/- 0.02	99
			0.167	+/- 0.060	254
	146.05 +/- 0.09		0.169	+/- 0.008	212
	ADOPTED VALUE				
10	146.06 +/- 0.01	REL	0.172	+/- 0.007	
		ABS	0.056	+/- 0.003	

* NOT USED FOR AVERAGE

TABLE V (cont.)

ABSOLUTE VALUE FOR 100 PERC. REL. INTENSITY

GROUND STATE BETA TRANSITION OF 13 PRC. ABS. WAS TAKEN FROM
B.N. SUBBA RAO, NUOVO CIM., 16(1960)283
AS THE BETA INTENSITIES GIVEN THERE AGREE BEST WITH THOSE CALCULATED
IN REF 212 FROM REL. GAMMA INTENSITIES AND CONVERSION COEFFICIENTS.
THEREFORE THE GROUND-STATE TRANSITIONS OF 60,86.5,105 AND 146 KEV HAVE TO
TOTAL 87 PERC. THE CONV. COEFF. USED WERE THOSE GIVEN IN REF. 212,WHICH
WERE CALCULATED FROM THE REL. K AND L CE-INTENSITIES OF REF. 254 NORMALIZED
TO THE THEORET. VALUE OF ALPHA-K FOR THE 105 KEV TRANSITION (PURE E1).
THE REL. M AND N CE-INTENSITIES WERE TAKEN FROM NUCL. DATA SHEETS.

LIST OF REFERENCES

76 NUCL.PHYS., A 96(1967)190
79 NUCL.PHYS.,A 108(1968)145
99 IS-T-290 AND NUCL.PHYS., A153(1970)109
192 NUCL.INSTR.METH., 87(1970)7
212 NUCL.PHYS., A132(1969)177
254 J.PHYS.(PARIS), 28(1967)861

TABLE VI. EXAMPLES FROM GAMMA LINE TABLE

55 CS 134 749 (+/- 10) DAYS HALFLIFE

KEV		PERCENT	
242.694	(+/- 0.041)	0.02	(+/- 0.01)
326.512	(+/- 0.095)	0.02	(+/- 0.01)
475.342	(+/- 0.034)	1.54	(+/- 0.05)
563.20	(+/- 0.07)	8.56	(+/- 0.24)
569.35	(+/- 0.02)	14.7	(+/- 0.3)
604.62	(+/- 0.05)	97.5	(+/- 0.1)
795.84	(+/- 0.03)	85.4	(+/- 0.9)
802.06	(+/- 0.08)	8.73	(+/- 0.15)
1038.38	(+/- 0.08)	1.02	(+/- 0.03)
1167.69	(+/- 0.07)	1.93	(+/- 0.06)
1365.19	(+/- 0.05)	3.31	(+/- 0.09)

LIT.REF.
8 9 11 12 13 129 196

---

55 CS 136 12.9 (+/- 0.5) DAYS HALFLIFE

KEV		PERCENT	
66.8	(+/- 0.5)	10	(+/- 1)
86.1	(+/- 0.5)	5.2	(+/- 0.5)
109.5	(+/- 1.0)	0.4	(+/- 0.2)
152.8	(+/- 0.5)	7.3	(+/- 0.7)
163.7	(+/- 0.5)	4.1	(+/- 0.4)
176.2	(+/- 0.5)	12.6	(+/- 1.5)
187	(+/- I)	0.5	(+/- 0.2)
273.3	(+/- 0.5)	11.3	(+/- 1.5)
320	(+/- 2)	0.5	(+/- 0.3)
340.0	(+/- 0.5)	43	(+/- 3)
818.3	(+/- 0.5)	100	(+/- 5)
1047.7	(+/- 1.0)	80.5	(+/- 4.0)
1235.1	(+/- 1.0)	20.5	(+/- 1.0)

LIT.REF.
39 40

---

55 CS 137 10990 (+/- 42) DAYS HALFLIFE

KEV		PERCENT	
32.1	(+/- 0.1)	5.7	(+/- 0.2)
36.5	(+/- 0.1)	1.3	(+/- 0.1)
661.633	(+/- 0.012)	84.6	(+/- 0.4)

LIT.REF.
4 29 45 53 73 233

TABLE VI (cont.)

HALFLIFE BETWEEN 10 AND 100 DAYS

ORDERED TABLE OF ENERGIES

KEV					DAYS	PERCENT
818.3000	55	CS	136		12.900	100.0000
817.2000	52	TE	129	G M	33.000	0.1470
816.5900	51	SB	124		60.200	0.0700
815.7680	56	BA	140	D	12.800	23.3000
811.7000	63	EU	156		15.110	9.8000
802.1700	52	TE	129	G M	33.000	0.2120
794.9000	52	TE	129	G M	33.000	0.0023
790.7600	51	SB	124		60.200	0.7400
768.9000	52	TE	129	G M	33.000	0.0090
765.8300	40	ZR	95	D	65.500	99.8000
765.8300	41	NB	95		35.108	99.8000
756.7800	40	ZR	95		65.500	54.5000
751.7700	56	BA	140	D	12.800	4.3800
741.1000	52	TE	129	G M	33.000	0.0810
735.7000	51	SB	124		60.200	0.1300
729.6200	52	TE	129	G M	33.000	1.1800
725.6500	61	PM	148	M	41.800	31.0000
724.2300	40	ZR	95		65.500	44.2000
723.4000	63	EU	156		15.110	5.4000
722.7800	51	SB	124		60.200	11.1000
716.8000	52	TE	129	G M	33.000	0.0016
713.8200	51	SB	124		60.200	2.5000
709.9000	63	EU	156		15.110	1.0000
709.3400	51	SB	124		60.200	1.3700
705.6000	52	TE	129	G M	33.000	0.0080
701.8000	52	TE	129	G M	33.000	0.0300
695.9800	52	TE	129	G M	33.000	4.9600
695.0000	51	SB	126		12.500	100.0000
685.8000	60	ND	147		11.020	0.5600
679.4000	60	ND	147		11.020	0.0000
672.0300	52	TE	129	G M	33.000	0.0390
665.0000	51	SB	126		12.500	100.0000
646.2500	63	EU	156		15.110	6.9000
645.8400	51	SB	124		60.200	7.3000
632.2600	51	SB	124		60.200	0.1300
629.9000	61	PM	148	M	41.800	87.5000
624.4000	52	TE	129	G M	33.000	0.0930
618.2000	56	BA	140	D	12.800	0.0400
611.5300	44	RU	103		39.600	
611.2600	61	PM	148	M	41.800	6.0000
610.3700	44	RU	103		39.600	5.5000
602.7100	51	SB	124		60.200	98.2000
599.5000	61	PM	148	M	41.800	8.5000
599.5000	63	EU	156		15.110	2.8700
594.7000	60	ND	147		11.020	0.1680
589.3000	60	ND	147		11.020	0.0290
559.7000	52	TE	129	G M	33.000	0.0080
557.1000	44	RU	103		39.600	0.7900
556.6500	52	TE	129	G M	33.000	0.1780
551.5000	52	TE	129	G M	33.000	0.0120

In a forward calculation the activity A_i (Tm) of a fission product i (neglecting all short lived precursors) at time of measurement T_m is given by the following formula:

$$A_i(T_m) = \lambda_i \sum_j \sum_k Y_{ijk} \int_{t=0}^{T_{irr}} N_j(t) . \sigma^f_{jk} . \phi_k(t) . \exp[-(\lambda_i - \sum_k \sigma^c_{ik} . \phi_k) . (T_m - t)] \, dt$$

$\lambda_i = 0.693/T_i$ ....decay constant

T_i ..... half life of fission product i

N_j (t) .... number of atoms of fissile isotope j at time t.

σ^f_{jk} ..... fission cross section of fissile isotope j in neutron group k

ϕ_k ..... neutron flux in group k

σ^c_{ik} .... capture cross section of fission product i in neutron group k

Y_{ijk} ... cumulative fission yield of fission product i for fissile isotope j in neutron group k.

(1) and (2) illustrate how different sources of error enter the equations used for calculation. The requirement for nuclear data uncertainties is that they should not exceed unavoidable errors arising from measurement conditions on the one hand and simplified neutron flux representation in calculations on the other hand. In the following sources of errors are discussed and the advantage of ratio measurements is shown.

5.1. Sources of error in measurements

Sources of errors in gamma spectrometric measurements are discussed below and summarized in Table VII.

5.1.1. Detector calibration

Energy calibration of the detector serves only for identification of fission product gamma lines. The gamma ray energies of calibration standards and main fission products are sufficiently well known for this purpose and their uncertainties have a negligible effect on the energy dependence of detector efficiency.

The photopeak efficiency of a detector(counts in the photopeak per γ-quant emitted from the source) is calibrated with the aid of gamma emitting standards. Primary standards with well known decay schemes and known desintegration rates are used to determine the absolute detector efficiency for different energies. Absolute gamma ray intensities are known to better than 1% for the majority of primary standards.

The specified absolute disintegration rates of standard sources are generally determined independent of a knowledge of decay schemes. The accuracy of available standards ranges from better than 1% (very thin sources) up to several percent.

The energy dependence of the detector efficiency can be determined with the aid of secondary standards emitting a number of strong gamma rays with accurately known relative intensities (better than 1% for a number of

TABLE VII. ERRORS OF MEASUREMENTS OF FISSION PRODUCT ACTIVITIES

	Minimum	Average
Absolute efficiency calibration (standard source)	< 1%	1 - 5%
* Energy dependence of efficiency	< 1%	< 1 - 2%
Geometry	0	0 - 2%
Dead time correction	0	~ 0 - 5%
Gamma ray self absorption within fuel	< 1 %	1 - 20%
* Peak area determination	~ 0.1%	1 - 3%
Total Error: absolute activities	< 1%	3 - 25%
* activity ratios	< 1%	< 2 - 5%

* Only sources of error in activity ratios

radionuclei). The shape of the efficiency curve can be established by normalizing the relative intensities of secondary standards to a set of accurate primary standards. This procedure helps to reduce errors arising from interpolation of the efficiency. The efficiency for photons emitted from the measured samples can be determined with a strong standard source (generally of lower accuracy) in the same arrangement, using the predetermined relative efficiency.

5.1.2. Geometry and scanning error

Errors due to finite size of sample and detector can be kept negligible if the source to detector distance is sufficiently large.

The efficiency of the detector for photons emitted by a measured sample is also determined by the distance and the collimators. For a point source the calibration with one standard in the sample position to normalize the relative efficiency is sufficient.

In scanning measurements of fuel rods one is dealing with extended sources. In this case the intensity of the beam that reaches the detector varies with the distance from the collimator axis and edge transmission effects influence the energy dependence of the efficiency. These changes have to be determined experimentally with standard sources rather than corrected by calculation.

Further errors can erise, if scanning speed and scanning length are not constant, as this means a change in the effective specific activity (per unit length) of the source. Typical errors are about 2 % [37].

5.1.3. Dead time correction

Serious errors can be introduced in scanning measurements of fuel rods, if the activity varies strongly along the rod and dead time corrections are large at points of high activity. As also areas of low activity are measured the measured total activity of the fuel rod will be too low. Errors in dead time corrections are estimated to be less than 1% to 5% [12, 37], depending on the magnitude and variation of dead time.

5.1.4. Gamma ray absorption

The absorption of gamma rays is energy dependent. Tabulated gamma ray absorption coefficients are derived mainly theoretically and have an uncertainty of about 10% [38,39]. Additional errors arise from inhomogenity of absorbing material in fuel elements. The magnitude of the error depends on size and type of the fuel element as well as on the way the correction is calculated (computer or by hand) and is about 2 - 20% [12]. It should be possible to reduce this error by determining the absorption experimentally with unirradiated fuel elements as absorbers.

5.1.5. Determination of peak area.

The accuracy of the determination of peak areas depends mainly on the number of counts accumulated (which in turn depends entirely on the time available for a measurement), the background corrections and the interference of other peaks.

The background is increased by scattering of photons in collimator and surrounding. It can be greatly reduced by application of compton supressed spectrometers or Compton coincidence spectrometers. Best results are obtained by peak shape and background fit with computers, which is indispensable for resolution of composite peaks.

5.1.6. Advantages of activity ratios

The advantages of the use of activity ratios for interpretation become obvious from the sources of error discussed above. First of all activity ratios depend only on the accuracy of the relative efficiency of the detector. The combined effect of gamma ray absorption and edge effect of collimators needs only to be accounted for as change of the relative efficiency and can be determined by intercomparison of activities calculated from gamma rays of the same fission product, which are different in energy (multiline evaluation). Uncertainties can be further reduced by comparison of gamma lines with similar energies. Further all errors cancel, that are common to both fission products such as finite source area or dead time correction.

5.2. Uncertainties in nuclear data

In the following we consider the influence of each type of nuclear data separately and assume that the other nuclear data involved in the same equation contribute no error. Further we assume optimal experimental conditions.

5.2.1. Gamma ray intensities

It can be seen from equation (1) that any arror in the gamma ray intensity has a linear effect on the result. Minimum errors in the other factors of equation (1) contributing to the determination of absolute activities are:

(see also Table VII)

a) Less than 1% for small samples
b) In routine measurements of fuel elements:
   - 1+DC: less than 1%
   - EF (E): 1% if close to gamma energy of calibration standard with accuracy ≦ 1%. Otherwise 2-3%.
   - GA(E): 1% for multiline evaluation, 2% for calculation [12].
c) Activity ratios:
   - EF(E): less than 1% to 2% for the cases listed in b)
   - GA(E) may cancel, other factors cancel.

Therefore the gamma ray intensities should be known to 1% better. This is fulfilled only for the most intense gamma rays of ^{95}Zr, ^{95}Nb, ^{131}I, ^{134}Cs, ^{137}Cs and partially ^{140}La. The error of I_γ disappears, if standard sources of the fission products measured in gamma spectra of fuel elements are used for calibration.

Equation (2) is linear in the fission yields. Therefore the relative error of the fission yield, weighted by $N_j(t)\,\sigma^f_{jk}\,\phi_k(t)$, appears in the same amount as error of the result, which is $A_i(T_m)$ in a forward calculation and $N_j(0)$, $\phi(t)$ or burnup $(\int N(t)\,\sigma^f\,\phi(t))$ in a backward calculation. Except for $A_i(Tm)$, $N_j(t)$ and $\phi_k(t)$ all factors in equation (2) are nuclear data. The accuracy required for the fission yields depends on the knowledge of irradiation history, neutron flux and fuel composition, whether activity ratios are considered and what the aim of the interpretation is.

If we consider activity ratios and assume that fast fissions are negligible and the fission yield ratio is the same for thermal and epithermal neutrons, the uncertainty of the calculated activity ratio depends only on the accuracy of the fission yields (known irradiation and fuel parameters).

If one wants to deduce information from measurements, the minimum error of an activity ratio is less than 1% to 2%, of absolute activities (routine measurements) 1-3 %.

- If the information is deduced from known irradiation history and fuel composition, the uncertainties of fission yields should not exceed the error of measurements.
- If the information has to be deduced from unknown irradiation history, the uncertainties involved exceed experimental errors.

Uncertainties of available fission yield data are not clear and should be subject of a careful assessment. There are discrepancies among experimental and among evaluated data and the philosophy in assigning errors is not unique.

5.2.3. Neutron cross sections and half lives

For the fission cross sections that appear in equation (2), the same arguments are valid as for fission yields, except that their values cancel in ratio measurements.

Absorption cross sections and half lives appear in exponential functions. The influence of their uncertainties on results is therefore a function of time and will be illustrated by some examples.

5.3. Examples of calculated errors

5.3.1. Errors due to incorrect half life.

For some of the most important fission products errors in forward and backward calculation arising from errors in half lives were calculated for typical irradiation conditions and cooling time. The errors were calculated relative to the half lives shown in Table III.

Errors in forward calculation are given in Table VIII a. They are total errors including irradiation time. Table VIIIb lists the errors of decay corrections from the cooling time shown to reactor shutdown. The errors listed under zero cooling time arise only from correction for decay during irradiation and were calculated only for fission products, that serve as burnup monitor. The error of the calculated burnup is then the combined error from cooling time and irradiation time.

All errors listed in Table VIIIa and b are relative to our recommended half lives or relative to activities calculated from these values. The half life values shown in these tables are either previously adopted values (^{95}Zr, ^{103}Ru, ^{141}Ce) or discrepant values included in the average (^{106}Ru, ^{137}Cs) or from a recent experiment (^{131}I). For ^{134}Cs the uncertainty of our recommended half life (Table III) was used. These half lives were selected to illustrate what errors can arise from their use or if some of these values were correct and not those shown in Table III. For Ce^{144} measured half lives are consistent and errors calculated in the same manner are well below 1%. The errors listed for ^{95}Nb are only due to the ^{95}Zr half life.

Errors in shutdown activities do not change in magnitude from those listed in Table VIIIa, if the irradiation time is 1 year and approaches zero for longer irradiation time (equilibrium). Errors in correction for decay during cooling time can be estimated from a more general relationship. The ratio of the error in the result to the error in the half life varies linearily with the ratio of cooling time to half life for small ratios. This relationship holds approximately also for larger values of these ratios. The line goes through zero and the error of the result is equal to the error of the half life if the cooling time is about 1.5 half lives.

The percent uncertainties of our recommended half lives are:

0.2 (^{95}Zr), 0.25 (^{103}Ru), 0.55 (^{106}Ru), 0.25 (^{131}I), 1 (^{134}Cs), 0.67 (^{137}Cs), 0.06 (^{141}Ce) and 0.14 (^{144}Ce). A comparison with Tables VIII a and b shows that they introduce no serious uncertainties at reasonable cooling times. However, some of these half lives have to be confirmed by further measurements (^{95}Zr, ^{103}Ru, ^{141}Ce) or might change after new measurements (^{106}Ru, ^{131}I).

5.3.2. Errors due to incorrect neutron capture cross section.

For most of the fission products measured gamma spectrometrically neutron capture is negligible under normal irradiation conditions. The only exceptions are ^{134}Cs and ^{154}Eu which yield information about the neutron flux. For illustration we calculated the uncertainty of the $^{134}Cs/^{137}Cs$ activity ratio at shutdown arising from the 7% uncertainty of the thermal neutron cross section of ^{133}Cs. The results for a neutron flux of 5×10^{13} n/cm^{2}s are:
Error of ratio 1.6% after 1 year irradiation, 1.5% after 2 year irradiation.

TABLE VIIIa. ERRORS IN "FORWARD" CALCULATION

Fission product	Half Life		errors in result (%) after cooling time of					
	value	error%	0	10 d	30 d	½ a	1 a	2 a
^{95}Zr	65.5 d	2.4	0.8	1.1	1.6	5.6	10.5	21
^{95}Nb	from	^{95}Zr	0.8	0.8	1	3.5	7.7	18
^{103}Ru	39.6 d	0.64	0.12	0.23	0.5	2.2	5.6	
^{106}Ru	371 d	0.7	-0.16	-0.15	-0.13	+0.07	+0.3	+0.8
^{131}I	7.97 d	1.1	0.04	1	2.9			
^{134}Cs		1	0.8	0.8	0.8	0.6	0.4	0.1
^{137}Cs	29.2 a	2.7	2.7			2.6		2.5
^{141}Ce	32.38d	0.5	0.08	0.2	0.4	2		

TABLE VIIIb. ERRORS IN "BACKWARD" CALCULATION

Fission product	Half Life		errors in result (%) after cooling time of					
	value	error%	0	10d	30d	½a	1a	2a
^{95}Zr	65.5 d	2.4	3.1	0.25	0.75	4.5	8.8	17
^{95}Nb	from	^{95}Zr		0.01	0.16	2.6	6.4	14.5
^{103}Ru	39.6 d	0.64		0.11	0.33	2	4	
^{106}Ru	371 d	0.7	0.5	0.01	0.04	0.23	0.46	0.9
^{131}I	7.97 d	1.1		1	2.9			
^{134}Cs		1		0.01	0.07	0.17	0.35	0.7
^{137}Cs	29.2 a	2.7	0.08	0	0	0.03	0.06	0.13
^{141}Ce	32.38 d	0.5		0.11	0.34	2.1	4.2	

$\phi_{tot} = 5 \times 10^{13}$ n/cm^2 s, irradiation time = 2 years

The error of this ratio increases with decreasing integrated neutron flux and approaches 7% for (almost) zero irradiation time. The uncertainty of the resonance integral should have the same effect on the ratio but the magnitude depends in addition on the neutron spectrum.

Generally uncertainties in neutron cross-sections are rather large. Results of calculations depend on the neutron spectrum and thus on the flux model used. Here a comparison of calculations using point cross section data with integral measurements of fission product absorption in different neutron spectra should help to clarify what flux representations are to be used in calculations. Work in this drection is in progress at Petten, Studsvik and Idaho.

REFERENCES

[1] HIGATSBERGER, H.H., HICK, H., WEINZIERL, P., 3rd Int. Conf. peaceful Uses Atomic Energy (Proc. Conf. Geneva, 1964) UN, New York (1964), paper P/399.
[2] HICK, H., RUMPOLD, K., WEINZIERL, P., Nucl. Instr. Meth. 24 (1963) 327.
[3] HIGATSBERGER, M.J., HICK, H., RUMPOLD, K., WEINZIERL, P., BURTSCHER, A., Int. Sympos. nuclear Materials Management (Proc. Sympos. Vienna, 1965) IAEA, Vienna (1966) 817.
[4] BUBA, L., HICK, H., RUMPOLD, K., Atomkernenergie II (1966) 167.
[5] PEPELNIK, R., HICK, H., Nucl. Instr. Meth. 68 (1969) 240
[6] HIGATSBERGER, M.J., BRUNEDER, H., Acta Phys. Austriaca 28 (1968) 94.
[7] HICK, H., LAMMER, M., Int. Conf. Progress in Safeguards Techniques (Proc. Sympos. Karlsruhe, 1970) 1, IAEA, Vienna (1970) 533, also OESGAE Report SGAE-PH-98 (1970).
[8] FORSYTH, R.S., BLACKADDER, W.H., Int. Conf. Progress in Safeguards Techniques (Proc. Sympos. Karlsruhe, 1970) 1, IAEA, Vienna (1970) 521.
[9] SCHAECHTER, L., HACMAN, D., POPA, P., Rev. Roum. Phys. 17 (1972) 729.
[10] HICK, H., LAMMER, M., NABIELEK, H., YORK, J., The Establishment of complete Fission Product Inventories for Irradiated Fuel Elements, Dragan Project report DP-754 (1971)
[11] WESTCOTT, C.H., WALKER, W.H., ALEXANDER, T.K., Int. Conf. peaceful Uses atom. Energy (Proc. Conf. Geneva, 1958) 16, UN, New York (1958) 70.
[12] Report of the Research co-ordination Meeting on Development of Gamma Spectrometry Instrumentation and Techniques for Safeguards, IAEA, Vienna (1971).
[13] DRAGNEV, T., IAEA, Div. Safeguards Inspection, private communication (January 1973).
[14] DRAGNEV, T., BEETS, C., "Identification of Irradiated Fuel Elements", Ch. 3, Joint Integral Safeguards Experiment (JEX70) at the Eurochemic Reprocessing Plant, Mol Belgium (KRAEMER, R., BEYREICH, W., Eds.), published as EURATOM report EUR-4576 e (1971) (= KFK-1100 (1971)).
[15] LAMMER, M., EDER, O.J., this Symposium, paper SM-70/13.
[16] LEDERER, C.M., HOLLANDER, J.M., PERLMAN, I., Table of Isotopes (6th edition), Wiley, New York (1967).
[17] MARTIN, M.J., BLICHERT-TOFT, P.H., Radioactive Atoms, Auger-Electron, α-, β-, γ-, and x-Ray Data, Nucl. Data Tables A 8, (1970) 1.
[18] LARGE, N.R., BULLOCK, R.J., Table of Radioactive Nuclides Arranged in Ascending Order of Half-Life, Nucl. Data Tables A 7 (1970) 477.
[19] WAKAT, M.A., Catalogue of γ-Rays Emitted by Radionuclides, Nucl. Data Tables A 8 (1971) 445.
[20] STEEN, N.M., USAEC rep. WAPD-TM-1052 (1972).
[21] STEEN, N.M., USAEC rep. WAPD-TM-971 (1970).
[22] COOK, J.L., Australian AEC rep. AAEC/TM-549 (1970). (Description of calculation only, point cross section data available on magnetic tape).
[23] ROSE, E.K., Australian AEC rep. AAEC/TM-587 (197). (Description of computer programs and library format).
[24] ZOLLER, W.H., HOPKE, P.K., FASCHING, J.L., MACIAS, E.S., WALTERS, W.B., Phys. Rev. C 3 (1971) 1699.
[25] GLEASON, G.I., REYNOLDS, S.A., unpublished, quoted in [24] and in USAEC rep. ORNL-TM-2878 (1970)5.
[26] CHACKETT, G.A., CHACKETT, K.F., WELBORN, J.B., Int. J.Appl.Rad.Isot. 22 (1971) 715.
[27] REYNOLDS, S.A., EMERY, J.F., USAEC report ORNL-4466 (1970) 75.
[28] LISMAN, F.L., ABERNATHEY, R.M., FOSTER, R.E., Jr., MAECK, W.J., J. inorg. nucl. Chem. 33 (1971) 643.

[29] HUGHES, D.J., SCHWARTZ, R.B., USAEC report BNL-235 second edition (1958), Supplement 1 (1960).
[30] STEHN, J.R., GOLDBERG, M.D., WIENER-CHASMAN, R., MUGHABGHAB, S.F., MAGURNO, B.A., MAY, V.M., USAEC report BNL-325 second edition, supplement 2 (1965).
[31] CINDA72, main volume + supplement, Index to the literature on Microscopic Neutron Data, IAEA, Vienna (1972).
[32] LEMMEL,H.D., AXTON, E.J., DERUYTTER, A.J., LEONARD, B.R., Jr. STORY, J.S., DUNFORD, C.H., Third Evaluation of the 2200 m/s Neutron Constants for four fissile Nuclides.
LEMMEL,H.D., IAEA, private communications December 1972 and February 1973.
[33] HANNA, G.C., WESTCOTT, C.H., LEMMEL, H.D., LEONARD, B.R., Jr. STORY, J.S., ATTREE, P.M., Atom. Energy Review 7 (1969) 3.
[34] WESTCOTT, C.H., A.E. of Canada report AECL-1101 (1960).
[35] FABRY, A., DE COSTER, M., MINSART, G., SHEPERS, J.C., VANDEPLAS, P., Int. Conf. Nuclear Data for Reactors (Proc. Sympos. Helsinki, 1970) 2, IAEA, Vienna (1970) 535.
[36] WALKER, W.H., A.E. of Canada report AECL-3037, Part I (1969).
[37] HICK, H., private communication.
[38] DAVISSON, C. M., "Gamma-Ray Attenuation coefficients", App. 1, Alpha-, Beta- and Gamma-ray Spectroscopy (SIEGBAHN, K., Ed), 1, North-Holland, Amsterdam (1965) 827.
[39] STORM, E., ISRAEL, H.I., Nuclear Data Tables A 7 (1970) 565.

DISCUSSION

D. J. HOREN: Of the radioisotopes that you consider in your work, how many have absolute normalizations known to < 1%?

M. LAMMER: The absolute intensities of the strongest gamma rays of ^{95}Zr, ^{95}Nb, ^{106}Ru-^{106}Rh, ^{134}Cs, ^{137}Cs and ^{140}Ba-^{140}La are known to better than 1%, but not those of ^{141}Ce and ^{144}Ce-^{144}Pr.

B. GRINBERG: I think you are right in emphasizing that the accuracies claimed by the authors of published material should be subjected to serious critical examination, since the erros are generally considerably greater than stated.

M. LAMMER: What I said was that the errors as quoted by the authors are very often much smaller than they really are, so the matter, indeed, needs investigation.

D. J. HOREN: As Professor Grinberg has pointed out, the experimentalists are sometimes overly optimistic, and this optimism may extend to their half-life measurements. However, the critical evaluation of half-lives is often very difficult because authors usually do not give sufficient information in their papers to permit such an evaluation to be made.

D. BERÉNYI: What is the origin of the half-life data in Table II, and what data were included?

M. LAMMER: We used all available references included in Nuclear Data, Part B "Recent References", published up to the autumn of 1972.

C. BEETS: I would merely like to emphasize the value of the method presented from the point of view of safeguards. Its possibilities are being analysed at present in an experiment on irradiated power reactor fuel for the purpose of extending the correlation technique to a more important part of the fuel cycle, namely, from the end of irradiation (storage pool for irradiated assemblies at the reactor site) to the dissolver of the reprocessing plant. This experiment, which is known as MOL IV, is being

carried out by the European Association for Safeguards in collaboration with the Agency, the Batelle Memorial Institute and the United States Arms Control and Disarmament Agency (ACDA).

C. WEITKAMP: In compiling Table II of your paper, did you merely adopt figures from the literature, or did you make a critical evaluation of your own? In the latter case, how far did you go in the evaluation or re-evaluation of published half-lives?

M. LAMMER: For all pre-1970 measurements, we relied on the selection of Martin and Blichert-Toft, as indicated in the full text of the paper. We subjected all subsequent publications to a critical examination and made certain selections. We took weighted averages where appropriate and assigned higher uncertainties in cases of discrepancies.

AN ANALYSIS OF CLAIMS AND AVAILABLE RADIOACTIVE DATA FOR SAFEGUARDS

D. BERÉNYI
Institute of Nuclear Research
of the Hungarian Academy of Sciences,
Debrecen, Hungary

Abstract

AN ANALYSIS OF CLAIMS AND AVAILABLE RADIOACTIVE DATA FOR SAFEGUARDS.

On the occasion of the First Meeting of the International Working Group on Nuclear Structure and Reaction Data at the IAEA, a number of requests and priority lists were presented from the different application fields of nuclear data. Of these, one of the relatively most detailed and concrete ones was the list of non-neutron nuclear data needs for safeguards development purposes, which was published during the year in a more concise and modified form, as an IAEA Report.

On the basis of the above lists, a comparison of the requested and available data has been carried out. The most strongly expressed claims are for the half-lives of ^{95}Zr, ^{106}Ru, ^{134}Cs, ^{137}Cs, ^{140}Ba and ^{144}Ce as well as the gamma yield per beta decay for ^{95}Zr, ^{106}Ru, ^{134}Cs, ^{137}Cs, ^{140}La and ^{144}Ce with an accuracy of one per cent, in general.

The results of the analysis are given in tables. Conclusions are drawn and some suggestions are given for further experimental tasks, for the use of the facilities of the Oak Ridge Nuclear Data Center (Recent References, Nuclear Data Sheets, tables of selected radioactive isotopes, computerized file of references) and for the request lists.

1. Introduction

As is well known, an International Working Group on Nuclear Structure and Reaction Data was convened by the IAEA in March, 1972, with the aim of promoting the compilation, evaluation and dissemination of nuclear structure and reaction data. During the first session of this group, a number of requests and priority lists were presented from the different fields of application of nuclear data. The relatively most detailed and concrete among these was the list of non-neutron nuclear data needs for safeguards [1]. In June, 1972, an even more clearly arranged but shorter list of the above claims was published [2], and this latter one is, first of all, the basis of the present analysis.

The main goal is here to test the utility of the Nuclear Data Group /Oak Ridge, Tennessee/ data accumulation systems /data sheets, data tables, recent references, data file of references/ for safeguards purposes and to compare the accuracy

claims for radioactive data with the accuracy of the recent experimental data. At the same time we compile the recent radioactive data necessary for safeguards.

2. Results of the analysis

The results of the present analysis are summarized in Tables I and II for the half-lives and gamma yields, respectively, of the radioactive nuclides in question. When compiling the tables, the Recent References issues of Nuclear Data Sheets published in the last two years [3-10], the Nuclear Data Sheets /for ^{95}Zr/ [11], the computerized data file of the Oak Ridge Nuclear Data Center /for ^{134}Cs/ [12] and the Nuclear Data Tables for 105 radioactive atoms published by the Oak Ridge Nuclear Data Group [13] were used. In the last tabulation, the "best" values for half-lives, intensities etc. for each of the atomic and nuclear radiations emitted by the chosen 105 radioactive atoms are given in tabular form. The "best" values mentioned above are partly adopted, partly averaged data.

In the present tables, besides the data and references, the priority assignment from ref. [2] and the relative experimental and claimed accuracy are also indicated. Where more than one datum is available for the requested quantity, the most accurate experimental value is underlined.

3. Discussion and conclusions

As can be seen from the tables, the claimed radioactive decay data are available in the recent literature with the necessary accuracy in the case of the half-lives. As regards the gamma yields, the situation is definitely worse. Especially for ^{134}Cs and ^{144}Ce, more accurate measurements are needed. The data, however, are nearly satisfactory in the case of ^{95}Zr, ^{106}Ru(^{106}Rh) and ^{140}La /as to the most intensive gamma rays here/. The experimental gamma yield value perfectly meets the claims for ^{137}Cs.

On the basis of the present analysis, we can state the good utility of the facilities of the Oak Ridge Nuclear Data Group. The data obtained by this way are, in general, more recent and accurate or reliable /in the cases in which I was

able to check them/ than those suggested in the recent safeguards publication [2]. E. g. the gamma yield for the 661.64 keV gamma ray of ^{137}Cs is 84.2 /without any error/ in one of the suggested literature [33] and 85.7±0.9 in the other [34]. Our corresponding value is 84.6±0.4 /see Table II/. The same quantity is 41.7 in [33], 43.7±1.0 in [34] and our datum is 43.5±0.5 /in Table II/. In the case of ^{134}Cs there is no reference to the 98.4±1 value in [34] and, in this way, the reliability of the accuracy of this datum is doubtful.

Summing up the experiences in connection with the nuclear data accumulation system of the Oak Ridge Nuclear Data Group, from the point of view of the safeguards claims, one can say the following: The most complete and recent information in connection with the decay data of an actual nuclide can be obtained if the computerized file of references of the Group is used /in the present analysis e. g. for ^{134}Cs/. In these files all the post-1959 literature is included. These practically do not contain more information than the Recent References issues of the Nuclear Data Sheets periodical except that the files are more concise and easy to survey. It means that the Recent References issues are usable in every respect beside the Oak Ridge file. If there exists a similar evaluated compilation of data as [13] or a recent Nuclear Data Sheets for the actual A-chain, then the use of the Recent References or the files is necessary only for the period after the completion of the compilation in question, i. e. the actual Sheets or specified tabulations.

This is a reason why the following sources of information were used during the present analysis in detail. For $^{106}Ru(^{106}Rh)$, ^{137}Cs, ^{140}Ba, ^{140}La and ^{144}Ce the Martin and Blichert-Toft [13] table and the Recent References issues from 1970-72 [3-10] were used, for ^{134}Cs the computerized file of references from Oak Ridge [12], for ^{95}Zr the tabulation [13], and the just published Nuclear Data Sheets issue for the A=95 mass chain [11].

As a last remark for the future, I should like to suggest to publish not only the relative gamma intensities but also the gamma quanta per decay data in the Nuclear Data Sheets. An even more important suggestion, but certainly for the more distant

TABLE I. HALF-LIFE OF RADIOACTIVE NUCLIDES FOR SAFEGUARDS

Radioactive nuclide, Priority assignment	Recent experimental data[a]			Claimed accuracy, %
	Half-life	Reference	Experimental accuracy, %	
^{134}Cs I.	2.058 ± 0.012 y	1972 [14]	0.6	1
^{137}Cs I.	30.0 ± 0.5 y	1970 [13]	1.7	1
	30.64 ± 0.43 y	1970 [15]	1.4	
	29.901 ± 0.045 y	1970 [16]	0.15	
^{95}Zr II.	65.5 ± 0.5 d	1970 [13]	0.8	1
	63.98 ± 0.06 d	1971 [17]	0.09	
$^{106}Ru(^{106}Rh)$	369 ± 2 d (Ru)	1970 [13]	0.5	1
	30.4 ± 0.5 s (Rh)	1970 [13]	1.6	1

[a] Data with the smallest error are underlined.

TABLE I. CONTINUATION

Radioactive nuclide, Priority assignment	Recent experimental data[a]			Claimed accuracy, %
	Half-life	Reference	Experimental accuracy, %	
^{140}Ba	12.8 ± 0.1 d	1970 [13]	0.78	1
II.	<u>12.789 ± 0.006</u>	1971 [18]	0.05	
^{144}Ce	287.5 ± 3.5 d	1967 [19]	1.2	1
II.	<u>284 ± 1 d</u>	1970 [13]	0.35	

[a] Data with the smallest error are underlined.

TABLE II. YIELD OF GAMMA QUANTA PER BETA DECAY EVENT FOR SAFEGUARDS[a]

Radioactive nuclide, Priority assignment	Recent experimental data[c]				Claimed accuracy, %
	Energy of the gamma rays (keV)[b]	Gamma ray intensity (qu/100 d)	Reference	Experimental accuracy, %	
^{134}Cs I.	475,355 ± 0.038	1.51 ± 0.16	1967 [20]	10.6	1
		1.4 ± 0.2	1968 [21]	14.3	
		1.57 ± 0.08	1970 [22]	5.1	
	563.325 ± 0.041	8.96 ± 0.84	1967 [20]	9.4	
		8.7 ± 1.0	1968 [21]	11.5	
		8.86 ± 0.45	1970 [22]	5.1	
	569.371 ± 0.047	15.81 ± 1.1	1967 [20]	7.0	
		15.0 ± 1.6	1968 [21]	10.7	
		16.0 ± 1.0	1970 [22]	6.3	
	604.744 ± 0.027	98.04	1967 [20]		
		98.0	1968 [21]		
		98.1 ± 6.0	1970 [22]	6.1	
	795.806 ± 0.050	87.79 ± 6.6	1967 [20]	7.5	
		88.4 ± 9.1	1968 [21]	10.3	
		86.0 ± 4.3	1970 [22]	5.0	

[a] Only gamma rays with an intensity higher than 1 percent are included.

[b] The energy values are, in general, taken from Martin and Blichert-Toft [13], except for ^{134}Cs and ^{95}Zr where the data of Raeside et al. [20] and Brahmavar and Hamilton [24] are used, respectively.

[c] Data with the smallest error are underlined.

TABLE IIa. CONTINUATION

Radioactive nuclide, Priority assignment	Recent experimental data[a]				Claimed accuracy, %
	Energy of the gamma rays (keV)[b]	Gamma ray intensity (qu/100 d)	Reference	Experimental accuracy, %	
	801.86 ± 0.28	8.94 ± 0.8	1967 [20]	8.9	
		9.2 ± 1.0	1968 [21]	10.9	
		8.7 ± 0.44	1970 [22]	5.1	
	1038.61 ± 0.49	1.02 ± 0.08	1967 [20]	7.8	
		1.1 ± 0.6	1968 [21]	54.5	
		0.99 ± 0.06	1970 [22]	6.1	
	1167.99 ± 0.39	1.96 ± 0.22	1967 [20]	11.2	
		1.8 ± 0.2	1968 [21]	11.1	
		1.86 ± 0.10	1970 [22]	5.4	
	1365.08 ± 0.32	3.25 ± 0.32	1967 [20]	9.8	
		3.3 ± 0.3	1968 [21]	9.1	
		3.23 ± 0.17	1970 [22]	5.3	
^{137}Cs I.	661.64 ± 0.8	85.1 ± 0.4	1969 [23]	0.5	1
		84.6 ± 0.4	1970 [13]	0.5	

[a] Data with the smallest error are underlined.

[b] The energy values are, in general, taken from Martin and Blichert-Toft [13], except for ^{134}Cs and ^{95}Zr where the data of Raeside et al. [20] and Brahmavar and Hamilton [24] are used, respectively.

TABLE IIb. CONTINUATION

Radioactive nuclide Priority assignment	Recent experimental data[a]				Claimed accuracy, %
	Energy of the gamma rays (keV)[b]	Gamma ray intensity (qu/100 d)	Reference	Experimental	
^{95}Zr	724.23 ± 0.04	44.2 ± 0.7 [c]	1969 [24]	1.6	1
II.		<u>43.5 ± 0.5</u>	1970 [13]	<u>1.1</u>	
	756,74 ± 0.04	54.6 ± 0.5 [c]	1969 [24]	0.9	
		<u>54.3 ± 0.5</u>	1970 [13]	<u>0.9</u>	
$^{106}Ru(^{106}Rh)$	511.8 ± 0.2	<u>20.6 ± 0.6</u>	1969 [25]	<u>2.9</u>	3
II.		20.6 ± 0.9	1970 [13]	4.3	
	622.1 ± 0.2	9.89 ± 0.48 [d]	1968 [26]	4.9	
		9.80 ± 0.53 [d]	1969 [27]	5.4	
		9.83 ± 0.30	1969 [25]	3.1	
		<u>9.94 ± 0.11</u>	1970 [13]	<u>1.1</u>	
	1050.1 ± 0.2	1.48 ± 0.11 [d]	1968 [26]	7.1	
		1.45 ± 0.09 [d]	1969 [27]	6.0	
		1.51 ± 0.08	1969 [25]	5.0	
		<u>1.48 ± 0.04</u>	1970 [13]	<u>2.7</u>	

[a] Data with the smallest error are underlined.

[b] The energy values are, in general, taken from Martin and Blichert-Toft [13], except for ^{134}Cs and ^{95}Zr where the data of Raeside et al. [20] and Brahmavar and Hamilton [24] are used, respectively.

[c] Computed from the published value accepting (54.6 ± 0.5) per cent [24] for the relative intensity of the beta group to the 756.74 level.

[d] Computed from the published value accepting (20.6 ± 0.9) quanta per decay intensity [13] for the 511.8 keV gamma rays.

TABLE IIc. CONTINUATION

Radioactive nuclide, Priority assignment	Recent experimental data[a]				Claimed accuracy, %
	Energy of the gamma rays (keV)[b]	Gamma ray intensity (qu/100 d)	Reference	Experimental	
^{140}La II.	328.77 ± 0.02	21 ± 2	1970 [13]	9.5	1
		<u>18.5 ± 0.07</u> [c]	1970 [28]	<u>0.4</u>	
		19.0 ± 1.2 [c]	1971 [29]	6.0	
	432.55 ± 0.03	3.3 ± 0.2	1970 [13]	6.1	
		<u>2.7 ± 0.16</u> [c]	1970 [28]	<u>5.3</u>	
		2.9 ± 0.20 [c]	1971 [29]	7.0	
	487.03 ± 0.02	45 ± 2	1970 [13]	4.4	
		<u>43.0 ± 0.22</u> [c]	1970 [28]	<u>0.5</u>	
		46.8 ± 2.9 [c]	1971 [29]	6.1	
	751.79 ± 0.06	<u>4.4 ± 0.1</u>	1970 [13]	<u>2.3</u>	
		4.2 ± 0.20 [c]	1970 [28]	4.6	
		4.1 ± 0.29 [c]	1971 [29]	7.1	
	815.83 ± 0.06	<u>23.1 ± 0.4</u>	1970 [13]	<u>1.7</u>	
		22.5 ± 0.67 [c]	1970 [28]	3.0	
		21.4 ± 1.3 [c]	1971 [29]	6.3	

[a] Data with the smallest error are underlined.

[b] The energy values are, in general, taken from Martin and Blichert-Toft [13], except for ^{134}Cs and ^{95}Zr where the data of Raeside et al. [20] and Brahmavar and Hamilton [24] are used, respectively.

[c] Computed from the published value accepting (95.6 ± 0.3) quanta per decay intensity [13] for the 1596.6 keV gamma rays.

TABLE IId. CONTINUATION

Radioactive nuclide Priority assignment	Recent experimental data[a]				Claimed accuracy, %
	Energy of the gamma rays (keV)[b]	Gamma ray intensity (qu/100 d)	Reference	Experimental	
	867.84 ± 0.10	5.5 ± 0.3	1970 [13]	5.5	
		5.4 ± 0.3 [c]	1970 [28]	5.4	
		5.4 ± 0.38 [c]	1971 [29]	7.1	
	919.6 ± 0.2	2.5 ± 0.2	1970 [13]	8.0	
		2.5 ± 0.15 [d]	1970 [28]	6.1	
		2.9 ± 0.26 [d]	1971 [29]	9.1	
	925.2 ± 0.8	6.9 ± 0.3	1970 [13]	4.3	
		6.8 ± 0.29 [d]	1970 [28]	4.2	
		7.5 ± 0.55 [d]	1971 [29]	7.4	
	1596.6 ± 0.2	95.6 ± 0.3	1970 [13]	0.3	
			1970 [28]		
			1971 [29]		
	2522.0 ± 0.4	3.3 ± 0.2	1970 [13]	6.0	
		3.4 ± 0.17 [d]	1970 [28]	5.0	
		3.6 ± 0.21 [d]	1971 [29]	5.8	

[a] Data with the smallest error are underlined.

[b] The energy values are, in general, taken from Martin and Blichert-Toft [13], except for ^{134}Cs and ^{95}Zr where the data of Raeside et al. [20] and Brahmavar and Hamilton [24] are used, respectively.

[c] Computed from the published value accepting (95.6 ± 0.3) quanta per decay intensity [13] for the 1596.6 keV gamma rays.

[d] Computed from the published value accepting (20.6 ± 0.9) quanta per decay intensity [13] for the 511.8 keV gamma rays.

TABLE IIe. CONTINUATION

Radioactive nuclide Priority assignment	Recent experimental data[a] Energy of the gamma rays (keV)[b]	Gamma ray intensity (qu/100 d)	Reference	Experimental	Claimed accuracy, %
^{144}Ce	80.12 ± 0.3	2.38 ± 0.24 [c]	1969 [30]	10.2	
II.		1.54 ± 0.15	1970 [13]	9.7	
		1.60 ± 0.11 [c]	1970 [31]	6.9	
		1.73 ± 0.11 [c]	1970 [32]	6.4	
	133.53 ± 0.3	10.8 ± 0.5	1970 [13]	4.6	

[a] Data with the smallest error are underlined.

[b] The energy values are generally taken from Martin and Blichert-Toft [13], except for case of ^{134}Cs and ^{95}Zr where the data of Raeside et al. [20] and Brahmavar and Hamilton [24] are used, respectively.

[c] Computed from the published value accepting (10.8 ± 0.5) quanta per decay intensity [13] for the 133.53 keV gamma rays.

future: it would be very useful, in view of the various applications, if the file of references in Oak Ridge would be the file of nuclear data.

Finally, I should like to summarize our experiences in connection with the request lists for safeguards purposes [1-2]. First of all, the real claims are much more numerous than they could be analysed now here, but these requests are not concrete enough, e. g. there is no figure about the requested accuracy / cf. [1]/. Even in the case of the second, more precise request list [2] there are some insufficiencies. Thus, there is no hint for the intensity limit up to which the gamma quanta per decay data are necessary. /It is obvious, that the gamma rays of low intensity are of no interest for safeguards./ In the present analysis this limit was arbitrarily chosen as 1 % /i. e. 1 quantum per 100 decays/.

Furthermore, in the request list [2] only ^{95}Zr, ^{106}Ru, etc. are indicated, although it is very probable that the gamma rays from the corresponding daughter nuclides /^{95}Nb, ^{106}Rh etc./ are also important. E. g. in the case of ^{106}Ru we were obliged to include the decay of ^{106}Rh in the analysis because the ^{106}Ru itself is only a beta decaying nuclide without any monoenergetic gamma rays. Some of the nuclides in question have an isomer state too /e. g. ^{106m}Rh/, the decay characteristics of which might be important in safeguards tasks, but such claims are not indicated in the lists.

As a final conclusion, it can be stated that further thorough and detailed request lists are badly needed.

The author is obliged to Professor D. J. Horen, Director, Nuclear Data Project, Oak Ridge, Tennessee, for sending the necessary list from the computerized file of references and the Nuclear Data Sheets for A=95 mass chain before the official publication.

REFERENCES

[1] BYER, T. A., „Draft Working Paper for IWGNSRD on Non-Neutron Nuclear Data Needs for Safeguards Development Purposes." 1st Meeting of IWGNSRD, Working Paper No. 20, March, 1972

[2] BYER, T. A., INDC(NDS)-44/G, IAEA, Vienna, June 1972

[3] Nuclear Data Sheets, 4B 1-2 (1970)

[4] Nuclear Data Sheets, 4B 5 (1970)
[5] Nuclear Data Sheets, 5B 1 (1971)
[6] Nuclear Data Sheets, 5B 4 (1971)
[7] Nuclear Data Sheets, 6B 2 (1971)
[8] Nuclear Data Sheets, 6B 5 (1971)
[9] Nuclear Data Sheets, 7B 3 (1972)
[10] Nuclear Data Sheets, 7B 6 (1972)
[11] MEDSKER, L. R. and HOREN, D. J., Nuclear Data Sheets B8 (1972) 29
[12] Computerized data files for ^{134}Cs, Oak Ridge Nuclear Data Group, Oak Ridge, Tennessee, USA.
[13] MARTIN, M. J. and BLICHERT-TOFT, P. H., Nuclear Data Tables 8A (1970) 1
[14] LAGOUTINE, F., LEGRAND, J., PERROT, C., BRETHON, J. P. and MOREL, J., Int. J. Appl. Rad. Isotope, 23 (1972) 219
[15] HARBOTTLE, G., Radiochim. Acta 13 (1970) 132
[16] WALZ, K. F. und WEISS, H. M., Zeits. Naturf. 25a (1970) 921
[17] DEBERTIN, K., Zeits. Naturf. 26a (1971) 596
[18] BABA, S., BABA, H., NATSUME, H., J. Inorg. Nucl. Chem. 33 (1971) 589
[19] WALKER, D. A. and EASTERDAY, H. T., Nucl. Instr. Meth. 48 (1967) 277
[20] RAESIDE, D.E., REIDY, J. J. and WIDENBECK, M. L., Nucl. Phys. A98 (1967) 54
[21] ABDUL-MALEK, A. and NAUMANN, R.A., Nucl. Phys. A106 (1968) 225
[22] HOFMANN, H., WALTER, H.K., WEITSCH, A., Z. Physik, 230 (1970) 37
[23] HANSEN, H.H., LÖWENTHAL, G., SPERNOL, A., EIJK,van der W., and VANINBROUKX, Zeits. Phys. 218 (1969) 25
[24] BRAHMAVAR, S.M. and HAMILTON, J. H., Phys. Rev. 187 (1969) 1487
[25] ODRU, P., Radiochim. Acta 12 (1969) 64
[26] HATTULA, J. and LIUKKONEN, E., Ann. Acad. Sci. Fennicae, Ser. A. VI. No. 274 (1968)
[27] STRUTZ, Kl.-D. and FLAMMERSFELD, A. Zeits. Phys. 221 (1969) 231
[28] KALINNIKOV, V. G., RAVN, K. L., HANSEN, H. G., LEBEDEV, N. A., Izv. AN SSSR, Ser. Fiz. 34 (1970) 916

[29] ARDISON, G. et MARSD, C., Rev. Roum. Phys. 16 (1971) 1043
[30] MANGAL, P. C. and TREHAN, P.N., Journ. Phys. Soc. Japan, 27 (1969) 1
[31] ANTTILA, A. and PIIPARINEN, M. Zeits. Phys. 237 (1970) 126
[32] POTNIS, V. R., AGIN, G.P., MANDEVILLE, C.E., J. Phys. Soc. Jap. 29 (1970) 539
[33] HILLER, S., Kerntechnik 12 (1970) 485
[34] MILLER, O. A., DEMIDOV, A. M., OVCSINIKOV, F. Ja., GOLUBEV, L. I. and SUNCSUGASHEV, M. A., Atomnaya Energiya 27 (1969) 281

DISCUSSION

C. WEITKAMP: In connection with your statement that half-lives are usually well enough known for safeguards purposes, I should like to give an example of a case in which they are not. The accuracies of specific power values of ^{239}Pu, ^{240}Pu and ^{241}Pu for colorimetric plutonium assay are at present inadequate, and better half-lives for the first two would greatly improve the situation. Improvements can, of course, also come from other measurements, such as direct (i.e. calorimetric) determination.

D. J. HOREN: First, I would like to thank Mr. Berényi for making such good use of our output. I would also mention that these types of specialized reference lists are available to anyone on request. The idea of publishing cumulative reference lists instead of Recent References has been under consideration for the past year and a half but we feel that it is more economical to respond to individual requests.

You started to get down to some of the details of the handling of these data. I think this would lead to a very lengthy discussion if we were to pursue it. However, I would like to make a couple of comments on the subject. We agree that it would be helpful for us to tabulate absolute gamma intensities and we hope with some of the computer programming that we are now doing, to set up a system by which we will be able to calculate the whole decay scheme and then produce tabulations of absolute gamma intensity, total transitions intensity or conversion electrons. These programs have not yet been completed, but we are working in that direction.

K. WAY: Did you mean to suggest a data file of experimental data or recommended data?

D. BERÉNYI: I think the main task of a data centre is to collect data and that is why a file of experimental nuclear data is the most important requirement. The evaluation of the data according to different points of views is, of course, also very important and necessary but it is possible only if we have as complete a collection (data file) of the original experimental data as possible.

D. J. HOREN: I would like to follow up Miss Way's question. I think, when it is a matter of a raw data file, i.e. data put into a computer file directly from experimental papers, that until the experimentalists adopt some of the ideas advocated by Miss Way for many years now, the real value of such a file is somewhat questionable.

C. BEETS: The importance of the various safeguards requirements has been specified in greater detail, as far as gamma measurements of irradiated fuel are concerned, in a paper presented at the 1972 ANS meeting in Washington by C. Beets, T. Dragnev et al.

Section IV
LIFE SCIENCES

Chairman

A.H.W. ATEN (CCE)

LE ROLE DES DONNEES NUCLEAIRES DANS L'UTILISATION DES INDICATEURS RADIOACTIFS EN MEDECINE

C. KELLERSHOHN, D. COMAR
CEA, Département de biologie,
Service hospitalier Frédéric Joliot,
Orsay, France

Abstract–Résumé

THE ROLE OF NUCLEAR DATA IN THE USE OF RADIOACTIVE TRACERS IN MEDICINE.

The nuclear data, knowledge of which is fundamental for the use of radioelements in medical diagnostics, are reviewed. After an introductory part on the production of radioelements problems concerning functional exploration, as, e.g., kinetic studies and dosimetry, are considered. The last part of the paper deals with the analysis of the elementary composition of biological materials using radioactivation analysis in vitro et in vivo, the latter also concerning dosimetric problems connected with the nature of the particles used for irradiation.

LE ROLE DES DONNEES NUCLEAIRES DANS L'UTILISATION DES INDICATEURS RADIOACTIFS EN MEDECINE.

Les auteurs passent en revue les données nucléaires dont la connaissance est fondamentale pour l'utilisation des radioéléments dans le diagnostic médical. Après un exposé sur la production des radioéléments ils étudient les problèmes relatifs à l'exploration fonctionnelle, tels que les études cinétiques et la dosimétrie. La dernière partie du mémoire traite de l'analyse de la composition élémentaire des matériaux biologiques par analyse par radioactivation in vitro et in vivo, cette dernière faisant également appel à des problèmes dosimétriques liés à la nature des particules utilisées pour l'irradiation.

Les données nucléaires dont la connaissance est fondamentale pour l'utilisation des radioéléments en diagnostic médical s'appliquent à trois domaines principaux :

- la production des radioéléments,
- l'exploration fonctionnelle comportant les études cinétiques, l'imagerie, et leurs conséquences dosimétriques,
- l'analyse de la composition élémentaire des matériaux biologiques par analyse par radioactivation in vitro et in vivo, cette dernière faisant également appel à des problèmes dosimétriques liés à la nature des particules utilisées pour l'irradiation.

1. PRODUCTION DES RADIOELEMENTS

Quoique le nombre des radioéléments connus à l'heure actuelle soit voisin de 1300, bien peu sont utilisés en médecine diagnostique soit en raison de la difficulté de leur production soit que leurs caractéristiques nucléaires ne sont pas souvent convenables.

L'irradiation par les neutrons dans les réacteurs nucléaires est la méthode de choix de production d'un certain nombre d'entre eux. A côté du rendement de fission qu'il est utile de

connaître pour déterminer la proportion des radioéléments produits au cours de la fission de l'uranium-235, les deux paramètres nucléaires qui gouvernent les réactions avec les neutrons sont la section efficace et la période.

A partir des neutrons thermiques les réactions par capture radiative sont les plus fréquentes conduisant à l'isotope radioactif d'une unité de masse supérieure. La quantité de radioactivité produite sera, à flux de neutrons constant et pour un temps d'irradiation long par rapport à la période, directement proportionnel à la section efficace d'activation. Sa connaissance est donc fondamentale si l'on veut prévoir la radioactivité spécifique du produit fabriqué. Il est important que la masse d'entraîneur associée aux radioéléments soit aussi faible que possible, sinon nulle. En effet les études cinétiques fondées sur l'emploi des indicateurs supposent au préalable que la masse de produit injectée soit négligeable par rapport à celle contenue dans le système.

La toxicité de l'espèce chimique utilisée est également un facteur limitant de l'emploi des indicateurs nucléaires en diagnostic médical et ici aussi la connaissance de la section efficace permettra de décider de la possibilité d'utilisation du radioélément chez l'homme. Les éléments lourds en sont un bon exemple : le ^{197}Hg produit par réaction (n,γ) à partir du ^{196}Hg malgré sa grande section efficace d'activation suppose pour avoir une radioactivité spécifique suffisante, l'enrichissement de l'isotope stable et l'irradiation dans un flux de neutrons important.

Un autre élément lourd, le thallium, dont l'intérêt pour l'exploration fonctionnelle du rein a récemment été mis en évidence, ne possède qu'un seul radioisotope (^{204}Tl) produit par capture radiative. La faible section efficace d'activation, associée à la période de ^{204}Tl (38 ans) et du schéma de désintégration défavorable pour la détection "in vivo" rendent ce radioélément inutilisable chez l'homme.

La connaissance des données nucléaires relatives aux paramètres d'activation en fonction de l'énergie des neutrons sont également très utiles pour déterminer les conditions les meilleures de production. Ainsi le cuivre-67 de période 2,44 j et émetteur d'une raie gamma à 184 keV est produit par réaction n,p sur le zinc enrichi. Il constituera donc un radioélément sans entraîneur d'intérêt beaucoup plus grand en médecine que n'est le ^{64}Cu T = 12,8 h et émetteur de positrons produit avec entraîneur lors de l'irradiation du cuivre naturel par les neutrons thermiques.

Dans la plupart des cas où le radioélément a une période suffisamment longue pour être transporté du lieu de sa production à celui de son utilisation, le médecin connaissant la radioactivité indiquée par le fabricant doit à partir de la période du radioélément calculer la radioactivité réelle qu'il sera amené à injecter au patient. Il pourra également comparer la radioactivité de la source à celle d'un standard commercial.

Le cas particulier des générateurs de radioéléments plus communément appelés "vaches à radioéléments" suppose la connaissance simultanée de la part du médecin de la période et du schéma de désintégration. Le générateur de radioélément le plus généralement utilisé à l'heure actuelle est la "vache à technétium" dont le fonctionnement se déduit facilement du schéma de désintégrations du ^{99}Mo et ^{99m}Tc présenté sur la figure 1. De la radioactivité connue en ^{99}Mo à un instant donné, l'application des équations de la filiation radioactive permet à chaque instant

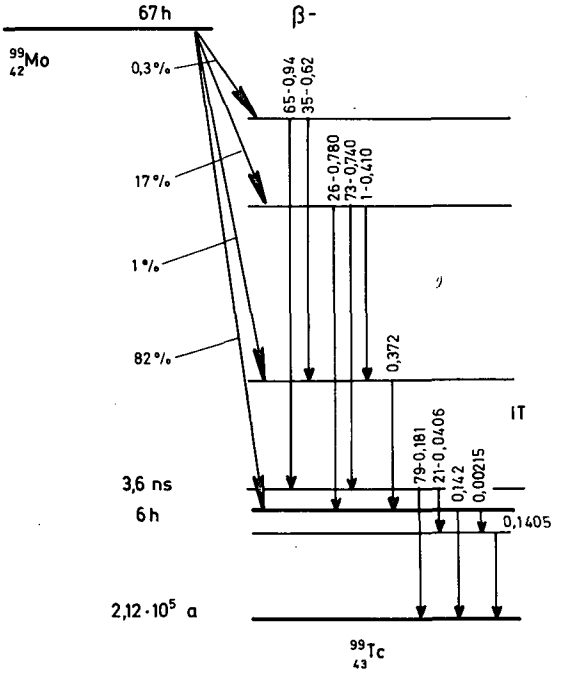

FIG. 1. Schéma de désintégration du molybdène-99 (67 h) et du technétium-99m (6 h).

de déterminer la radioactivité en produit fils ^{99m}Tc à condition de connaître avec précision les périodes physiques des deux radioéléments.

Une alternative consiste bien entendu à mesurer la radioactivité du ^{99m}Tc séparé du ^{99}Mo à l'aide d'un détecteur spectromètre gamma convenablement étalonné et de déduire du taux de comptage le taux de désintégrations, donnée pour laquelle le pourcentage d'émission par désintégration de la raie gamma mesurée est le paramètre nécessaire.

Depuis quelques années l'apparition sur le marché de cyclotrons compacts à usage médical ouvre des perspectives nouvelles quant à la disponibilité des radioéléments (1). Une dizaine de cyclotrons de ce type sont installés à l'heure actuelle dans différents instituts médicaux ; une de leurs principales caractéristiques est de pouvoir produire des isotopes radioactifs de période très brève inaccessibles par d'autres méthodes. Les trois principaux sont l'^{15}O (T = 2,05 min), le ^{11}C (T = 20,4 min) et l'^{13}N (T = 10 min). Utilisés directement sous forme gazeuse (O_2, CO_2, CO, N_2) ces radioéléments sont particulièrement intéressants pour l'étude de la ventilation pulmonaire. Combinés à des molécules plus complexes ils permettent d'étudier les composantes rapides de certains métabolismes (médicaments ou produits naturels). Ces études doivent dans certains cas se poursuivre pendant un temps correspondant à plusieurs périodes de désintégration du radioélément. La précision avec laquelle cette période sera connue conditionnera la précision des données biologiques mesurées.

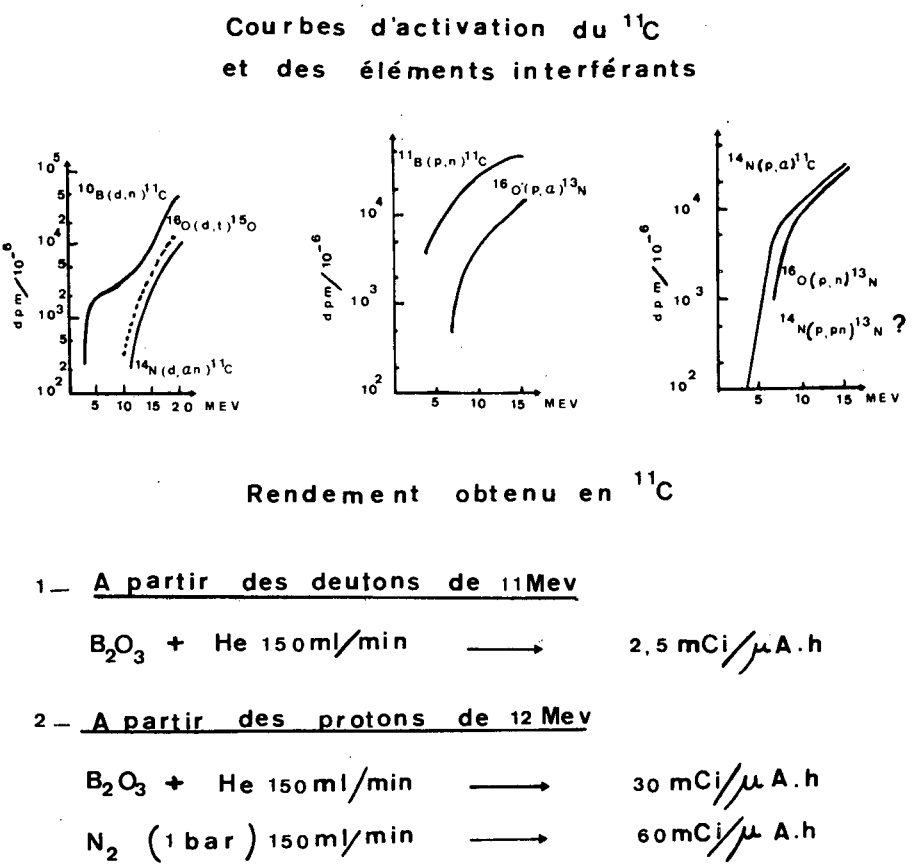

FIG. 2. Production de ^{11}C à partir des réactions $^{10}B(d,n)^{11}C$, $^{11}B(p,n)^{11}C$ et $^{14}N(p,\alpha)^{11}C$.
En haut: courbes d'activation du ^{11}C et des éléments interférants pour les trois réactions considérées sous forme de la radioactivité exprimée en fonction de l'énergie.
En bas: rendement des trois réactions en millicuries par microampère-heure.

En ce qui concerne la production de ces radioéléments un des paramètres fondamentaux qu'il est nécessaire de connaître et qui malheureusement fait encore défaut dans bien des cas est la variation de la section efficace en fonction de l'énergie des particules. Celle-ci permettra de prévoir l'énergie optimale pour obtenir le meilleur rendement tout en évitant certaines réactions parasites conduisant à la fabrication d'un autre radioélément.

La figure 2 illustre les problèmes posés par la fabrication du ^{11}C ainsi que quelques résultats préliminaires obtenus dans notre service.

Les courbes d'activation du ^{11}C à partir des réactions ^{10}B (d,n) ^{11}C, ^{11}B (p, n) ^{11}C et ^{14}N (p,α) ^{11}C sont empruntées à Engelmann (2). Pratiquement la méthode la plus intéressante consiste à irradier par des protons d'énergie voisine de 12 MeV de

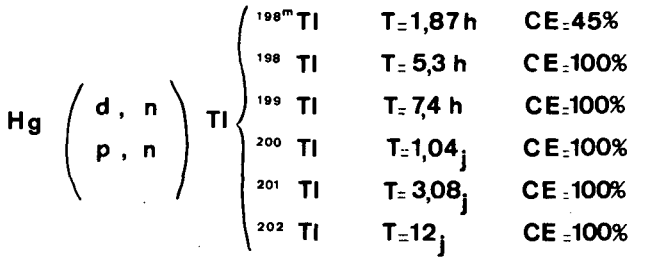

CIBLE	PARTICULES	RENDEMENT μCi/μA·heure				
		^{198}Tl	^{199}Tl	^{200}Tl	^{201}Tl	^{202}Tl
HgO	d (15 Mev)	365	410	233	84	21
HgO	p (50Mev)	5450	2600	730	123	7,6
HgO	p (16Mev)	-	250	60	45	-
Hg	p(16Mev)	660	900	230	180	7

FIG. 3. Radioisotopes du thallium produits par cyclotron.
En haut: Radioisotopes produits avec leur période et leur mode de désintégration.
En bas: Rendement de production en fonction de la nature des particules, de leur énergie et de la nature de la cible.

l'azote gazeux contenant 2 à 3 % d'oxygène, ce dernier ayant pour effet de réagir directement avec les atomes de ^{11}C pour donner du $^{11}CO_2$. Les courbes présentées en haut et à droite de la figure mettent bien en évidence que l'oxygène présent dans le gaz cible conduira à la formation d'azote-13 contaminant le ^{11}C. La conséquence logique d'une telle observation aboutira soit à modifier le mode de préparation, soit à effectuer une séparation chimique des deux gaz radioactifs.

Dans la plupart des cas la fonction d'excitation étant inconnue, seule l'expérience permettra de déterminer le rendement de fabrication d'un radioélément et la contamination par les radioisotopes voisins, s'ils existent. La figure 3 illustre un tel cas. Il concerne la fabrication des thallium 198m à 202 par bombardement du mercure par les protons ou les deutons. La partie supérieure indique les radioisotopes produits ainsi que leur période et le mode fondamental de désintégration. Le tableau inférieur illustre les rendements de fabrication en fonction de la nature chimique de la cible de la particule incidente et de son énergie. Il apparaît que le bombardement par les protons conduit à un mélange de radioisotopes plus riche en radioéléments de courte période.

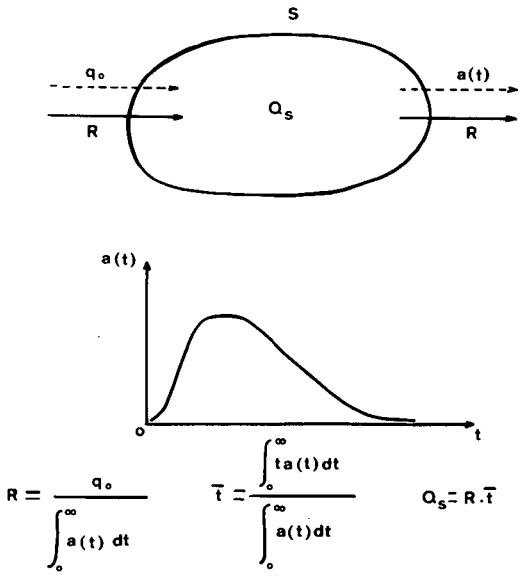

FIG. 4. Schéma du principe de Stewart-Hamilton.
S: Système biologique étudié
q_0: Radioactivité injectée
a(t): Radioactivité spécifique à l'instant t de la substance étudiée à la sortie de S
R: Diète ou flux d'entrée de la substance étudiée dans S
$\bar{t}$: Temps moyen de transit de la substance étudiée à travers S
Q_S: Masse ou pool de la substance étudiée dans le système.

2. DONNEES NUCLEAIRES DANS LE CADRE DES ETUDES CINETIQUES ET DE L'EXPLORATION FONCTIONNELLE

2.1. Procédures

Que ce soit pour l'exploration fonctionnelle d'un organe, l'étude d'une fonction physiologique et de ses anomalies ou plus généralement l'étude du métabolisme d'un élément ou d'une substance à différents niveaux d'une structure vivante en état stationnaire vis-à-vis de cet élément ou de cette substance, l'utilisation des indicateurs nucléaires se ramène à trois types de procédures :

2.1.1. Le principe de Stewart-Hamilton

La figure 4 schématise ce principe dans le cas où l'excrétion de l'indicateur se fait par une seule voie. C'est par exemple le cas de toutes les substances qui sont excrétées par la seule voie urinaire. Le flux de substances à travers l'organisme

ou système S considéré, la diète quotidienne R, est égale au quotient de la radioactivité injectée q_0 par la surface limitée par la courbe représentant la variation de la radioactivité spécifique de l'excréta en fonction du temps a(t)

$$R = \frac{q_0}{\int_0^\infty a(t)\,dt}$$

L'application la plus connue de cette procédure est la mesure du débit cardiaque F au moyen de l'expression

$$F = \frac{q_0}{\int_0^\infty c(t)\,dt}$$

où q_0 est la radioactivité injectée en amont du coeur et c(t) la concentration radioactive à l'instant t d'échantillons sanguins prélevés en aval du coeur.

L'injection de la radioactivité étant effectuée en "equivalent supply", c'est-à-dire que dans le cas où la substance étudiée pénètre dans l'organisme par plusieurs portes d'entrée, la radioactivité de l'indicateur est injectée simultanément dans chaque porte d'entrée dans les mêmes proportions que les flux de substance-mère, le temps moyen de transit $\bar{t}$ de la substance considérée à travers le système S est donné par l'expression

$$\bar{t} = \frac{\int_0^\infty ta(t)\,dt}{\int_0^\infty a(t)\,dt}$$

valable si la durée de l'injection est brève par rapport à $\bar{t}$.

La masse totale ou pool Q_S de la substance considérée dans le système est alors donnée par la relation

$$Q_S = R.\bar{t}$$

2.1.2. Le principe d'occupation

Il constitue au fond une généralisation du principe de Stewart-Hamilton. Si q_0 représente la radioactivité totale injectée, $q_{S'}(t)$ la radioactivité, à l'instant t après le début de l'injection, dans une portion arbitraire S' du système S et $Q_{S'}$ la masse totale ou pool de la substance considérée dans S', le flux constant R de cette dernière dans S (Figure 5) est donnée par l'expression

$$R = \frac{Q_{S'}}{\int_0^\infty \frac{q_{S'}(t)}{q_0}\,dt}$$

Elle a été établie pour la première fois par Bergner (3) qui désignait le temps $(-)_{S'} = \int_0^\infty \frac{q_{S'}(t)}{q_0}\,dt$ sous le vocable de temps moyen de séjour de la substance considérée dans la

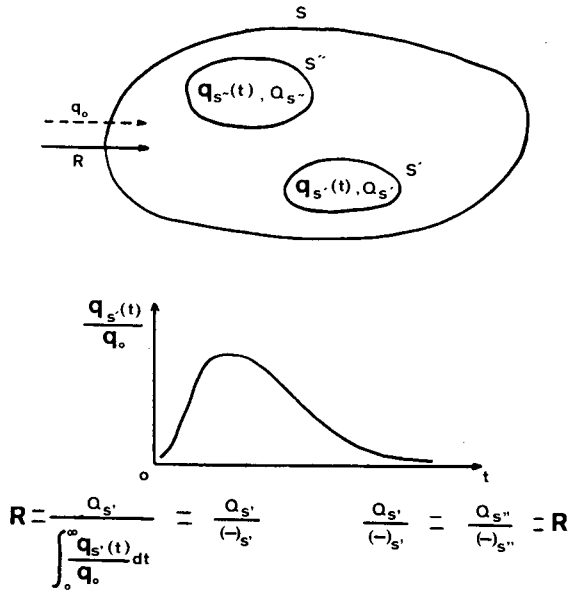

FIG. 5. Schéma du principe d'occupation.
S: Système biologique étudié
S', S": Portions arbitraires de S
q_0: Radioactivité injectée dans S
$q_{S'}(t)$, $q_{S''}(t)$: Radioactivité à l'instant t dans S' et S"
R: Diète ou flux d'entrée de la substance étudiée dans S
$(-)_{S'}$, $(-)_{S''}$: Occupation de S' et S" par la substance étudiée.
$Q_{S'}$, $Q_{S''}$: Capacité de S' et S" pour la substance étudiée.

région arbitraire S'. Elle a été reprise et largement développée dans ses applications pratiques par Orr et Gillespie (4) sous le nom de principe d'occupation. Ces auteurs appellent le temps $(-)_{S'}$ occupation de S' par la substance étudiée et le pool $Q_{S'}$ capacité de S' pour cette substance. Ils énoncent alors le principe : le quotient de la capacité d'une région arbitraire d'un organisme S en état stationnaire par l'occupation de cette dernière, est égal au flux ou diète de la substance considérée pour cet organisme.

$(-)_{S'}$ est mesuré par l'étude de la cinétique de la radioactivité dans S'. Si d'autre part $Q_{S'}$ peut être déterminé par une quelconque technique analytique, on en déduit la diète quotidienne moyenne R du sujet S. La région arbitraire S' est souvent constituée par un certain volume, un litre par exemple, de plasma. S'il est possible expérimentalement de mesurer la radioactivité au niveau d'un organe S", on détermine son occupation $(-)_{S''}$ et par suite son pool $Q_{S''}$ pour la substance étudiée puisque :

$$\frac{Q_{S'}}{(-)_{S'}} = \frac{Q_{S''}}{(-)_{S''}} = R$$

Si on prend pour région S' le système S lui-même, l'occupation se confond avec le temps de transit moyen $\bar{t}$.

Le principe d'occupation est une méthode très puissante pour l'étude des métabolismes dans un organisme en état stationnaire. Il a été notamment utilisé dans le cas du métabolisme de l'iode (5), du brome (6), du rubidium (7), du calcium (8), du sélénium (9).

2.1.3. L'analyse compartimentale

Elle constitue un mode de représentation bien connu du métabolisme d'un élément ou d'une molécule dans un organisme en état stationnaire. Sur la base de données anatomiques, physiologiques et biochimiques, ce dernier est divisé en "compartiments" représentant l'ensemble des atomes ou molécules étudiés se trouvant dans un même volume spatial, un même organe, ou un même état chimique. Les paramètres d'un tel système compartimental sont constitués par les pools des compartiments, ainsi que les taux d'échange et de transfert entre eux. Après injection d'une radioactivité q_0 d'un indicateur dans l'un de ces compartiments, en général celui

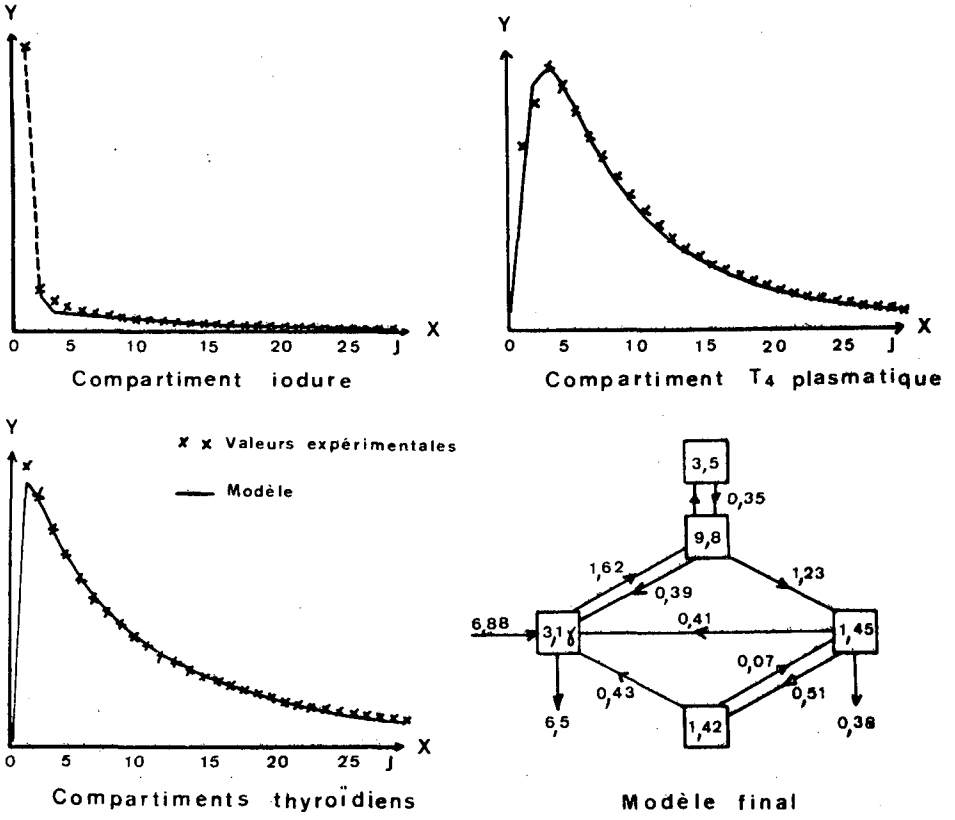

FIG. 6. Analyse compartimentale du métabolisme de l'iode chez le rat normal.
Diète: 6,88 µg/j. Pool iodure: 3,1 µg. Pool thyroïdien formé de 2 compartiments de pools 3,5 et 9,8 µg. Pool d'iode organique formé de 2 compartiments de pools 1,45 et 1,42 µg. Les taux de transfert entre compartiments sont exprimés en µg/j.

auquel appartient le plasma, la radioactivité $q_i(t)$ ou la radioactivité spécifique $a_i(t)$ du ième compartiment sont des fonctions du temps obéissant à un système de n équations différentielles linéaires du premier ordre dont les coefficients constants s'expriment en fonction des paramètres du système. Il est possible dans certaines conditions de déterminer ces paramètres en résolvant le système de façon que l'une ou plusieurs des fonctions $q_i(t)$ ou $a_i(t)$ correspondent à leur valeur expérimentale. Ceci est aujourd'hui effectué sur ordinateur au moyen de programmes convenables.

La figure 6 représente les courbes expérimentales de radioactivité dans les compartiments thyroïdiens, iodure plasmatique et thyroxine plasmatique chez le rat normal recevant une diète quotidienne de 5 µg d'iode, après injection plasmatique d'iode-125 sous forme d'iodure, ainsi que le schéma compartimental qui s'adapte le mieux à ces courbes. De tels schémas compartimentaux sont très utiles pour mettre en valeur le caractère normal ou pathologique d'un métabolisme. Ils permettent notamment de classer différents états pathologiques suivant ceux des paramètres du système (pool et taux de transfert) qui présentent des valeurs anormales. Une telle méthode d'analyse est employée pour de nombreux éléments tels que l'iode, le calcium, le fer, etc... etc...

Finalement les trois procédures qui viennent d'être passées en revue et qui représentent l'essence actuelle des applications biologiques et médicales de la méthode des indicateurs se ramènent à des mesures de radioactivité en valeur relative à la radioactivité injectée $\frac{q(t)}{q_0}$ et à leurs variations en fonction du temps. Ces dernières bien entendu doivent être corrigées de la perte de radioactivité par le mécanisme de désintégration, de façon à ce que les variations observées correspondent aux seuls processus métaboliques. La seule donnée proprement nucléaire nécessaire est en toute rigueur la constante radioactive, ou la demi-vie de l'indicateur utilisé. Encore est-il que, eu égard au caractère aléatoire des processus métaboliques, une très grande précision n'est pas nécessaire sur cette donnée. Ajoutons d'ailleurs que dans la plupart des cas cette correction est effectuée automatiquement par comparaison des activités des échantillons à une partie aliquote de la dose injectée et qu'alors cette unique donnée nucléaire n'est même plus nécessaire. Font exception les cas d'emploi d'éléments à vie très courte comme l'oxygène-15 (T = 2,5 min) et le baryum-137m (T = 2,5 min) pour lesquels la mesure alternée sur un échantillon et un standard est difficilement réalisable.

Une connaissance détaillée du spectre de rayonnement du radioélément utilisé n'est pas nécessaire si les mesures sur les échantillons et le standard sont effectuées dans les mêmes conditions de géométrie et de détection. Les données d'un schéma de désintégration simplifié donnant les énergies maxima des spectres bêta et leur pourcentage ainsi que la répartition des principales raies gamma ou X et leur pourcentage par 100 désintégrations sont suffisantes. Ces dernières données sur les rayonnements électromagnétiques sont particulièrement importantes pour la détection externe et les techniques d'imagerie (scintigraphie, caméra) qui jouent un rôle majeur dans les applications cliniques.

2.2. Dosimétrie

Si l'on met à part certaines techniques d'avant-garde, qui appartiennent essentiellement à des perspectives d'avenir et que

nous examinerons plus loin, nous voyons que les résultats que l'on peut obtenir dans le domaine du diagnostic médical au moyen des indicateurs nucléaires ne nécessitent que peu de données nucléaires précises. Il n'en va pas du tout de même de l'appréciation des doses de radiation délivrées à l'organisme au cours de leur utilisation, appréciation de première importance dans le cas des applications sur l'homme.

Le formalisme actuellement employé en dosimétrie (10) repose sur l'emploi d'un "modèle isotropique uniforme" pour lequel la source de rayonnement et la cible sur laquelle elle agit sont plongées dans un matériau absorbant homogène de dimensions suffisamment grandes pour négliger les effets de bord et tel que la radioactivité est distribuée uniformément dans la source. La dose absorbée moyenne $\bar{D}$ (v⟵r) dans le volume v de la cible à partir de la radioactivité répartie dans la région r est alors fournie par l'une ou l'autre des expressions :

$$\bar{D}\ (v \longleftarrow r) = \tilde{A}_r \sum \Delta_i \ \Phi_i\ (v \longleftarrow r)$$

$$\bar{D}\ (v \longleftarrow r) = \frac{\tilde{A}_r}{m_v} \sum \Delta_i \ \varphi_i\ (v \longleftarrow r)$$

$\tilde{A}_r$ représente la radioactivité intégrée en μCi-h dans la région r, m_v la masse de la cible de volume v en grammes, et Δ_i la constante de dose absorbée à l'équilibre de la ième composante du rayonnement du radioélément utilisé, c'est-à-dire, exprimée en g-rad/μCi-h, l'énergie totale émise par cette composante. Elle est donnée par l'expression :

$$\Delta_i = 2{,}13\ n_i\ \bar{E}_i$$

$\bar{E}_i$ étant l'énergie moyenne des particules de la ième composante en MeV
n_i le nombre de celles-ci émises par désintégration.

φ_i représente la fraction absorbée (11) c'est-à-dire la fraction de l'énergie émise par la ième composante dans la région r qui est absorbée dans le volume de la cible v.

$\Phi_i = \frac{\varphi_i}{m_v}$ représente la fraction absorbée spécifique (12) qui a l'avantage de conserver un sens quand la cible est à une ou deux dimensions.

En pratique on considère que les électrons de toute origine émis au cours de la désintégration nucléaire ont dans les tissus un parcours suffisamment faible pour être classés comme particules "non pénétrantes". Pour de telles particules si la région r de la source et le volume v de la cible n'ont pas de points communs φ_i (v ⟵ r) = 0 et si au contraire la région r et le volume v se superposent φ_i (v ⟵ V) = 1 ou $\Phi_i = m_v^{-1}$. Ce résultat est considéré également comme valable pour des photons d'énergie inférieure à quelques keV.

Pour des photons d'énergie supérieure à quelques keV φ_i et Φ_i sont compris entre 0 et respectivement 1 et m_v^{-1}. Leur valeur dépend de l'énergie des photons, de la forme, des dimensions et des relations géométriques de la source et de la cible. De nombreux travaux ont été effectués pour déterminer par la méthode de Monte Carlo ou la méthode des moments (13, 14, 15, 16, 17, 18) φ_i et Φ_i pour des formes simples de la source et du volume cible: point, sphère, cylindre, ellipsoïde utilisables pour représenter différentes régions du corps humain.

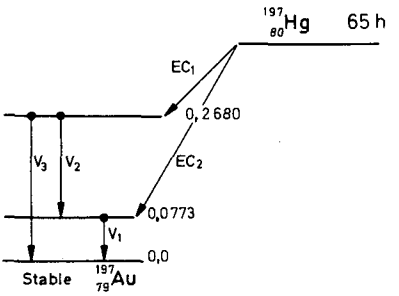

Rayonnement	% par désintégration	Energie de transition (MeV)	Autres paramètres
Capture électronique-1	2	0,15	Première interdite
Capture électronique-2	98	0,34	Première interdite
Gamma-1	99,8	0,0773	$M_1 + 10\ \% E_2$
Gamma-2	1,8	0,1915	$\alpha_K = 0,0$ $\alpha_L = 3,27$ $M_1 + 30\ \% E_2$ $\alpha_K = 0,80$ $K/(L+M) = 4,0$
Gamma-3	0,14	0,2680	$M_1, \alpha_K = 0,375$ (T) $\alpha_L = 0,0643$ (T)

D'après - L.T. DILLMAN, MIRD Pamphlet N° 4, J. Nucl. Med 10, supplement-2

FIG. 7. Schéma de désintégration du mercure-197.

TABLEAU Ia. NOMBRE PAR DESINTEGRATION ET ENERGIE DES PHOTONS GAMMA ET ELECTRONS DE CONVERSION DE ^{197}Hg

Rayonnement (i)	Nombre moyen par désintégration (n_i)	Energie moyenne ($\bar{E}_i$)	$\left(\frac{\text{g-rad}}{\mu\text{Ci-h}}\right)$ Δ_i
Capture électronique-1	—	—	*
Capture électronique-2	—	—	*
Gamma-1	0,186	0,0773	0,0306
Electron con. int. L, gamma-1	0,609	0,0640	0,0830
Electron con. int. M, gamma-1	0,203	0,0746	0,0323
Gamma-2	0,0090	0,1915	0,0037
Electron con. int. K, gamma-2	0,0072	0,1108	0,0017
Electron con. int. L, gamma-2	0,0014	0,1782	0,0005
Electron con. int. M, gamma-2	0,0005	0,1888	0,0002
Gamma-3	0,0010	0,268	0,0006
Electron con. int. K, gamma-3	0,0004	0,1873	0,0002

TABLEAU Ib. NOMBRE PAR DESINTEGRATION ET ENERGIE DES PHOTONS X DE ^{197}Hg

^{197}Hg (RAYONS X)			
Rayonnement (i)	Nombre moyen par désintégration (n_i)	Energie moyenne $(\bar{E}_i)$	$\left(\frac{g\text{-rad}}{\mu Ci\text{-}h}\right)$ Δ_i
Rayons X K2-1	0,363	0,0688	0,0532
Rayons X K2-2	0,199	0,0670	0,0284
Rayons X Kβ-1	0,126	0,0780	0,0209
Rayons X Kβ-2	0,0338	0,0807	0,0058
Rayons X $L_1\alpha$	0,252	0,0097	0,0052
Rayons X $L_1\beta$	0,236	0,0115	0,0058
Rayons X $L_1\gamma$	0,0317	0,0134	0,0009

TABLEAU Ic. NOMBRE PAR DESINTEGRATION ET ENERGIE DES ELECTRONS AUGER DE ^{197}Hg

^{197}Hg (ELECTRONS Auger)			
Rayonnement (i)	Nombre moyen par désintégration (n_i)	Energie moyenne $(\bar{E}_i)$	$\left(\frac{g\text{-rad}}{\mu Ci\text{-}h}\right)$ Δ_i
Electron Auger KLL	0,0191	0,0540	0,0022
Electron Auger KL_1X	0,0108	0,0646	0,0015
Electron Auger KXY	0,0018	0,0752	0,0003
Electron Auger L_1MM	0,903	0,0079	0,0152
Electron Auger MXY	2,72	0,0027	0,0156

Quoi qu'il en soit la fraction absorbée et la fraction absorbée spécifique ne sont pas des données nucléaires. Ce sont essentiellement les valeurs de n_i et $\bar{E}i$ pour chaque composante qui représentent les données nucléaires nécessaires au calcul des doses de radiation. Leur détermination exige une connaissance extrêmement précise du schéma de désintégration du radioélément utilisé sous peine d'erreurs d'appréciation sur les valeurs des doses absorbées qui peuvent être importantes.

A titre d'exemple la figure 7 représente le schéma de désintégration du mercure-197, radioélément assez utilisé en médecine nucléaire notamment pour l'exploration du rein et le diagnostic

des tumeurs. Ce schéma est emprunté à une monographie de Dillman (19) sur l'usage des schémas de désintégration et des paramètres nucléaires pour l'estimation des doses de radiation. Cet auteur a établi un programme d'ordinateur permettant d'obtenir à partir des données d'entrée les différentes valeurs de n_i et E_i pour les radionuclides d'intérêt médical. Les données des schémas de désintégration telles que celles présentées sur la moitié inférieure de la figure 7 pour le mercure comprennent le nombre, le pourcentage par désintégration, l'énergie et la nature des différentes transitions β^-, β^+ et par capture électronique, le nombre, le pourcentage par désintégration, l'énergie, la nature multipolaire magnétique ou électrique, les coefficients de conversion K, L, M... des différentes transitions gamma.

Les Tableaux Ia Ib et Ic représentent dans le cas du mercure-197 les données de sortie, c'est-à-dire les valeurs de n_i et E_i respectivement, pour les photons γ et les électrons de conversion, les photons X et les électrons Auger. On voit que 21 composantes sont à considérer, 9 pour les γ et les électrons de conversion, 7 pour les photons X et 5 pour les électrons Auger. La désintégration se faisant par capture électronique, il n'y a pas de particules β en jeu.

Si nous considérons la seule dose délivrée au rein par les particules non pénétrantes, c'est-à-dire en l'occurrence les électrons de conversion et les électrons Auger, nous avons pour ces deux types de particules :

$$\sum_i \varphi_i \Delta_i = \sum \Delta_i,$$ soit respectivement 0,1179 et 0,0348 puisque $\sum_i \varphi_i = 1$.

On voit que les électrons Auger représentent alors $\frac{0,0348}{0,1179 + 0,0348}$ soit 23 % de la dose due aux radiations non pénétrantes, fraction dont la plus grosse partie est due aux électrons Auger LMM et MXY de très faible énergie par suite de leur nombre par désintégration élevé. Une appréciation précise de ces derniers exige une connaissance très détaillée des données nucléaires caractérisant le schéma de désintégration. Il faut dire qu'elle est surtout importante dans le cas des radionuclides décroissant par

TABLEAU II. CARACTERISTIQUES DES GROUPES D'ELECTRONS PRODUITS AU COURS DE LA DESINTEGRATION DE ^{125}I
(D'après Feige et al. [20])

Rayonnement	Energie (KeV)	Abondance A(%)	Parcours R(μm)	TEL = E/R KeV/μm	TEL_{In} KeV/μm
Conversion interne M Conversion interne L+Auger	32,4	19,6	20,9	1,55	0,93
Electron Auger K.L.X Electron Auger K.L.L	23,8	19,5	12,1	1,96	1,12
Conversion interne K Electron Auger L.M.M	3,2	220	0,44	7,2	4,8
Electron Auger M.X.Y	0,8	360	0,056	14,2	11,4

capture électronique. Pour les émetteurs β^- ou β^+, le nombre de particules β par désintégration est en général plus élevé que celui des électrons Auger et surtout leur énergie est incomparablement plus grande. Aussi la fraction de la dose due aux électrons Auger est-elle beaucoup plus faible pour ces nuclides.

Un autre exemple de l'importance de l'appréciation précise des électrons Auger de faible énergie est fourni par l'iode-125, radionuclide décroissant par capture électronique, très utilisé en biologie et en médecine.

Le Tableau II dû à Feige et al. (20) donne les caractéristiques des groupes d'électrons produits au cours de la décroissance de ^{125}I : énergie, abondance, parcours et transfert linéaire d'énergie. Les électrons Auger LMM et MXY de très faible énergie ont une très grande abondance et présentent un transfert d'énergie linéique élevé pour un parcours très faible. On conçoit que ceci peut entraîner un dépôt d'énergie sur des structures subcellulaires comme l'interface colloïde-cellule de la vésicule thyroïdienne très supérieur à celui que la dose moyenne de radiation délivrée au tissu thyroïdien laisserait prévoir. D'autre part, il est possible que les ions à charges multiples consécutifs aux cascades d'électrons Auger aient quelque importance biologique (21).

L'ensemble des considérations développées dans ce paragraphe montre que si des données nucléaires précises ne sont pas nécessaires pour étudier une fonction physiologique ou un métabolisme, une connaissance détaillée des caractéristiques nucléaires est indispensable pour apprécier les doses de radiation délivrées par les radionuclides utilisés chez l'homme à cette fin.

3. DONNEES NUCLEAIRES DANS LE CADRE DE LA MESURE DE LA COMPOSITION ELEMENTAIRE DES MATERIAUX BIOLOGIQUES

L'analyse des milieux biologiques a considérablement profité des propriétés particulières des radioéléments, en particulier grâce au concept de dilution isotopique. Celui-ci, d'ailleurs connu avant la découverte des radioéléments, n'a pu trouver sa généralisation qu'à partir du moment où n'importe quelle espèce chimique a pu être reconnue et mesurée après marquage par un indicateur nucléaire. Qu'il s'agisse de la dilution isotopique simple, double, de l'analyse par substoiechiométrie, par compétition, ou radioimmunologique, le concept utilisé obéit à la formule générale

$$M = \frac{A}{a_s}$$

M = masse de la molécule ou de l'élément à mesurer,
A = radioactivité totale de la molécule ou de l'élément dans l'échantillon,
a_s = radioactivité spécifique de l'espèce chimique dans l'échantillon après dilution homogène de l'indicateur.

La radioactivité spécifique, lorsqu'elle est définie comme étant le rapport du nombre de noyaux radioactifs au nombre total de noyaux présents suppose pour être mesurée la connaissance du schéma de désintégration de l'indicateur nucléaire. En fait, le chimiste n'a pas besoin de cette donnée car toutes les mesures qu'il pratique sont comparatives. A la rigueur il peut lui être utile de connaître le mode de désintégration (bêta et gamma) du radioélément concerné surtout si travaillant à la limite de sensibilité de son détecteur il cherche à obtenir le meilleur rapport signal/bruit de fond.

Il en est de même pour les méthodes de radioactivation appliquées à l'analyse des milieux biologiques "in vitro". Dans son principe cette méthode permet, à partir de la mesure de la radioactivité induite à la suite d'une réaction nucléaire, de déterminer la masse de l'élément présent dans l'échantillon soumis à l'irradiation. La loi gouvernant la production de cette radioactivité s'exprime par la relation suivante :

$$M = \frac{A.des/s}{\Phi \cdot \sigma \cdot f\ (1-e^{-\lambda t_1})\ (e^{-\lambda t_2})}$$

dans laquelle
M = masse à mesurer
A = masse atomique de l'élément
des/s = taux de désintégration du radioélément produit au moment de la mesure
Φ = flux de particules induisant la radioactivation
σ = section efficace de la réaction nucléaire
f = abondance isotopique de l'élément stable ayant subi la réaction nucléaire
λ = constante radioactive du radioélément produit
t_1 et t_2 = durée de l'irradiation et temps séparant la fin de celle-ci de la mesure de la radioactivité.

Dans la plupart des cas cette formule approchée n'est pas utilisée pour convertir le taux de désintégration en masse de l'élément dans l'échantillon car les données nucléaires qu'elle contient, et en particulier la section efficace, ne sont pas connues avec suffisamment de précision.

Le chimiste préfère éliminer tous ces paramètres en irradiant simultanément l'échantillon et un étalon contenant une quantité connue de l'élément à doser.

La connaissance précise des données nucléaires de section efficace, de période et de schéma de désintégration permettrait de s'affranchir de cet étalon et présenterait un gros avantage en particulier au cours des analyses multiélémentaires lorsque l'on ne connaît pas au préalable la composition de l'échantillon. Ces remarques valables pour l'activation par les neutrons thermiques s'appliquent bien évidemment aux irradiations par les neutrons épithermiques pour lesquels les sections efficaces de résonance permettent des activations sélectives ainsi qu'aux neutrons rapides.

Un deuxième aspect de l'analyse par radioactivation neutronique qui s'apparente plus au domaine de la recherche qu'à celui de la routine concerne les analyses "in vivo". Celles-ci pratiquées depuis 5 ou 6 ans par quelques laboratoires spécialisés (22) utilisent l'irradiation par des neutrons de réacteurs lents ou épithermiques ou produits à partir d'accélérateurs. Le Tableau III indique les principaux éléments constituant les organismes vivants susceptibles d'être dosés par activation "in vivo", leur abondance respective, les éléments résultant des réactions, les réactions nucléaires qui leur ont donné naissance et les caractéristiques nucléaires utilisées pour leur mesure. Il apparaît que celles-ci peuvent être soit le résultat de la connaissance du schéma de désintégration du radioélément produit (gammas de désintégration), soit le résultat de la connaissance de la réaction nucléaire (gammas de capture).

TABLEAU III. CARACTERISTIQUES D'INTERET POUR LA RADIOACTIVATION "IN VIVO" DES ELEMENTS SUSCEPTIBLES D'ETRE DOSES PAR CETTE METHODE

Elément stable	% du poids du corps	Radioélément produit	Réaction neutronique	Raie γ à mesurer
H	10	^{2}H	n, γ	capture
N	3	13N	n,2n	désintégration
Ca	1,5	^{49}Ca	n, γ	désintégration capture
P	1	^{28}Al	n, α	désintégration
		^{32}P	n, γ	capture
Na	0,15	^{24}Na	n, γ	désintégration
Cl	0,15	^{38}Cl	n, γ	désintégration
		^{37}S	n,p	capture
Mg	0,05	^{26}Mg	n, γ	désintégration
		^{24}Na	n,p	désintégration
I	0,03 thyroïde	^{128}I	n, γ	désintégration

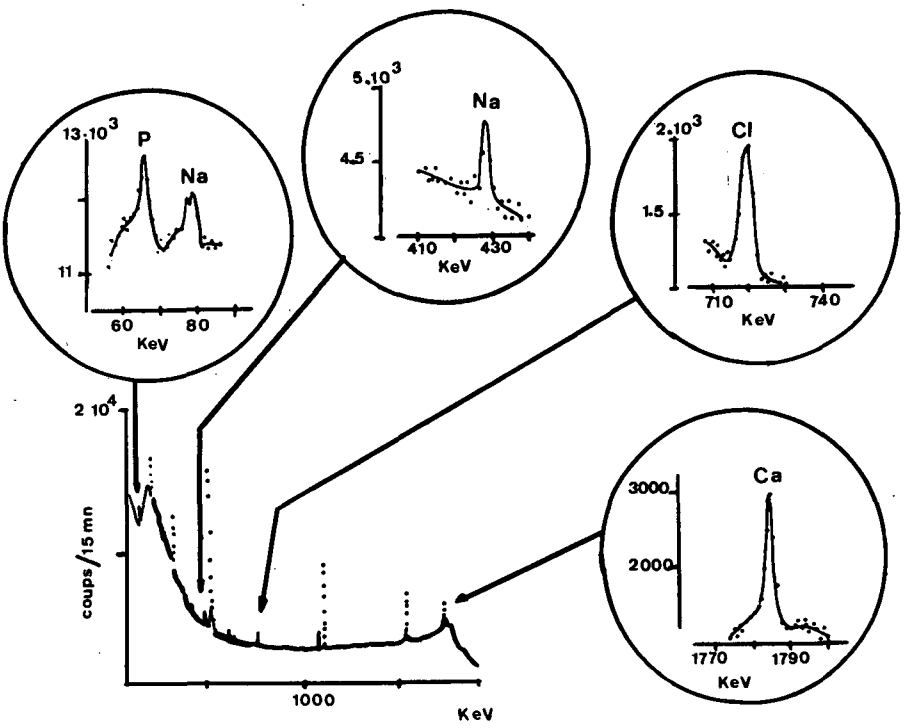

FIG. 8. Spectres des gammas de capture d'un tibia humain irradié par des neutrons thermiques, montrant des raies caractéristiques du phosphore, du sodium, du chlore et du calcium.

Il apparaît dans ce Tableau deux éléments, l'hydrogène et le phosphore, qui après activation par les neutrons thermiques, conduisent à des éléments soit stable (^{2}H) soit radioactif (^{32}P) n'émettant aucun gamma de désintégration, seuls les gammas de capture permettront de les mesurer.

Le spectre présenté sur la figure 8, obtenu au cours de l'irradiation "in vivo" par des neutrons thermiques, du tibia d'un sujet normal, montre les différents γ de capture caractéristiques du phosphore, du sodium, du chlore et du calcium. L'identification de ces raies, si elle peut être faite par comparaison avec des étalons de composition connue, suppose cependant une connaissance préalable des données nucléaires de la réaction de capture. Les raies non identifiées sur le spectre correspondent aux pics d'échappement par production de paires de la raie de capture à 2,2 MeV de l'hydrogène.

En raison de leur faible pouvoir de pénétration dans les tissus biologiques, les neutrons thermiques ne peuvent assurer l'irradiation homogène de la totalité d'un organisme humain. C'est la raison pour laquelle l'application de ce type d'activation est réduite aux irradiations localisées, desquelles on peut déduire cependant des paramètres biologiques intéressants tels les rapports en masse des éléments activés (23). Il est un exemple cependant où la masse totale d'un élément contenu dans un organe a pu être dosé par irradiation par les neutrons thermiques. Il s'agit de l'iode intrathyroïdien pour la mesure duquel la méthode de l'étalon interne a été employée (24). Une quantité connue d'iode-129 ($T = 1{,}7.10^{7}$ ans) ayant été fixée dans la thyroïde et étant supposée avoir la même répartition anatomique que l'iode stable natif a été utilisée comme moniteur de flux. Des calculs

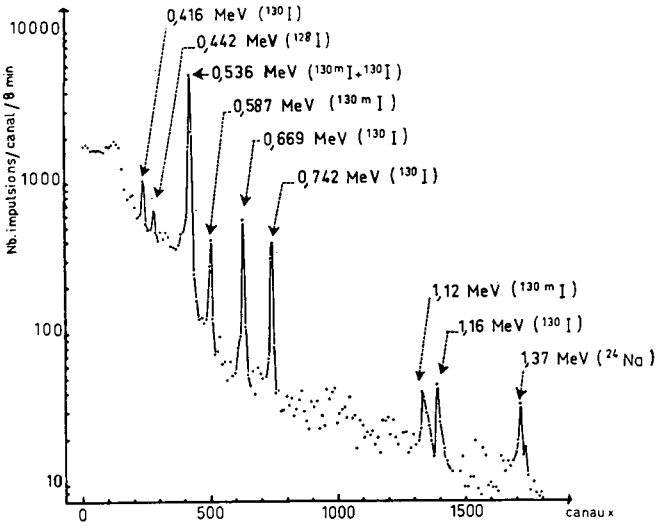

FIG. 9. Spectre gamma effectué avec un détecteur Ge(Li) obtenu 6,5 minutes après une irradiation de 3 minutes aux neutrons thermiques de ^{129}I (origine du comptage: 6,5 min). Les raies à 0,587 et 1,12 MeV sont caractéristiques de l'état isomérique ^{130m}I.

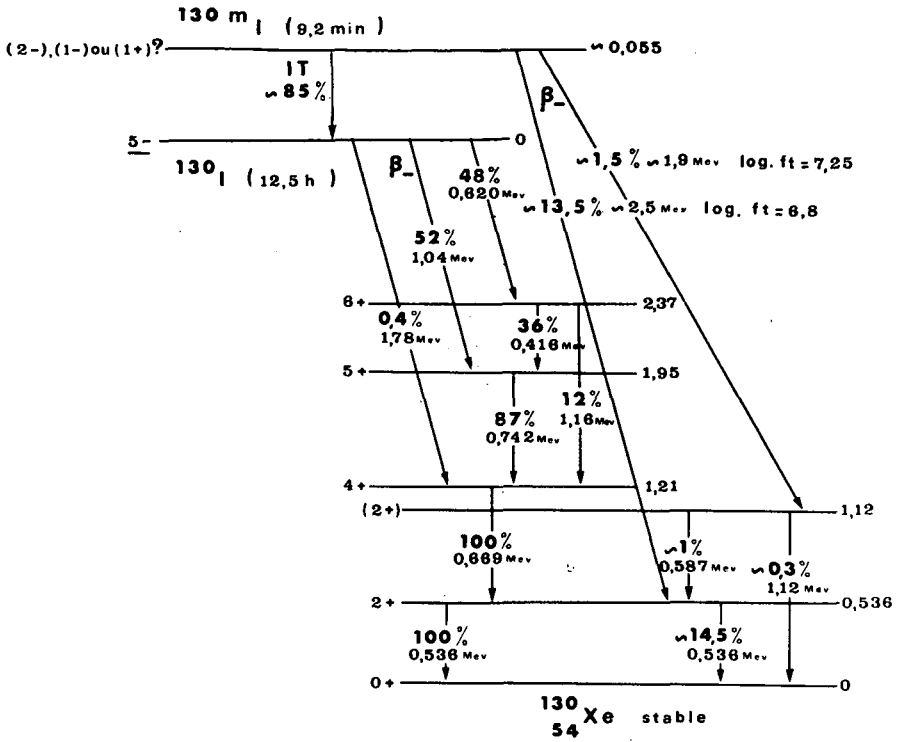

FIG. 10. Schéma de désintégration proposé pour l'iode-130m.

préliminaires utilisant les caractéristiques de la réaction ^{129}I (n, γ) ^{130}I et le flux de neutrons disponible avaient permis de déterminer la quantité d'iode-129 nécessaire à administrer pour obtenir une radioactivité de l'iode-130 mesurable dans les conditions expérimentales imposées. L'activation "in vivo" ayant été pratiquée, le spectre γ enregistré quelques minutes après la fin de l'irradiation a montré une raie γ d'amplitude et de période très différentes de ce qui était attendu. Les analyses détaillées de ce spectre et d'autres tels que celui présenté sur la figure 9 ont permis de mettre en évidence un nouveau radioélément, ^{130m}I de période 9,2 min isomère de ^{130}I non encore décrit dans la littérature (25, 26). Le schéma de désintégration de ce nouveau radioélément (figure 10) montre que 85 % des désintégrations conduisent par transition isomérique au niveau fondamental de l'iode-130, et que 13,5 % se font par émission β^- aboutissant à un niveau excité du ^{130}Xe à 536 keV. C'est en fait cette raie qui a été mise en évidence sur les spectres enregistrés "in vivo".

Un deuxième aspect de l'analyse par radioactivation "in vivo" concerne l'irradiation totale d'un individu en vue d'y doser la masse de calcium, de sodium, de phosphore, d'azote et de chlore qu'il contient. L'homogénéité de l'irradiation est obtenue en utilisant un flux de neutrons rapides émis par une cible de

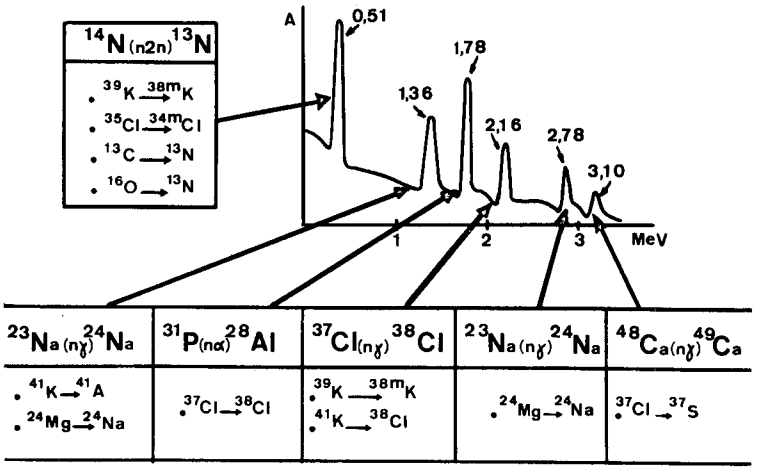

FIG. 11. Spectre gamma d'un rat après radioactivation in vivo au moyen de neutrons de 14 MeV partiellement ralentis. Il permet de déterminer le contenu de l'animal en azote (raie d'annihilation à 0,511 keV de ^{13}N), phosphore (raie gamma à 1,78 MeV de ^{28}Al), chlore (raie gamma à 2,16 MeV de ^{38}Cl), sodium (raies gamma à 1,36 et 2,78 MeV de ^{24}Na) et calcium (raies gamma à 3,10 MeV). Pour chacune des raies sont indiquées les réactions d'interférence. Par exemple le ^{38}Cl présente à 1,60 MeV une raie indiscernable par spectrométrie de scintillation de la raie à 1,78 MeV de Al.

béryllium ou de tritium bombardée par des deutons. Selon l'énergie des neutrons incidents, il est nécessaire de les ralentir partiellement par des matériaux hydrogénés avant leur pénétration dans le milieu biologique. Les radioéléments produits au cours d'une telle irradiation sont plus abondants que ceux obtenus dans le cas de l'irradiation par des neutrons thermiques, du fait du spectre neutronique complexe comme en témoigne le spectre γ présenté sur la figure 11. Ce spectre a été obtenu après irradiation "in vivo" d'un rat par des neutrons de 14 MeV partiellement ralentis. Sous la réaction nucléaire principale conduisant au radioélément responsable des pics d'absorption totale présentés, ont été indiquées les différentes réactions d'interférence dont la connaissance a été nécessaire pour corriger le spectre (27).

Les résultats obtenus à l'heure actuelle par la méthode d'activation "in vivo" sont suffisamment intéressants du point de vue médical pour que l'appréciation de la dose absorbée au cours d'un tel examen soit appréciée avec une grande précision. Nombreux d'ailleurs sont les auteurs qui l'ont calculée théoriquement et dans certains cas mesurée expérimentalement aussi bien lors de l'irradiation par des neutrons rapides (22) que par des neutrons thermiques (28). Ces calculs généralement extrêmement complexes pour la résolution desquels les calculateurs sont nécessaires supposent la connaissance des sections efficaces de diffusion des neutrons dans la matrice biologique.

Dans le cas du bombardement par les neutrons thermiques les deux sources principales responsables de la dose absorbée sont d'une part les γ de capture provenant de la réaction n, γ sur l'hydrogène et les protons de recul issus de la réaction n, p

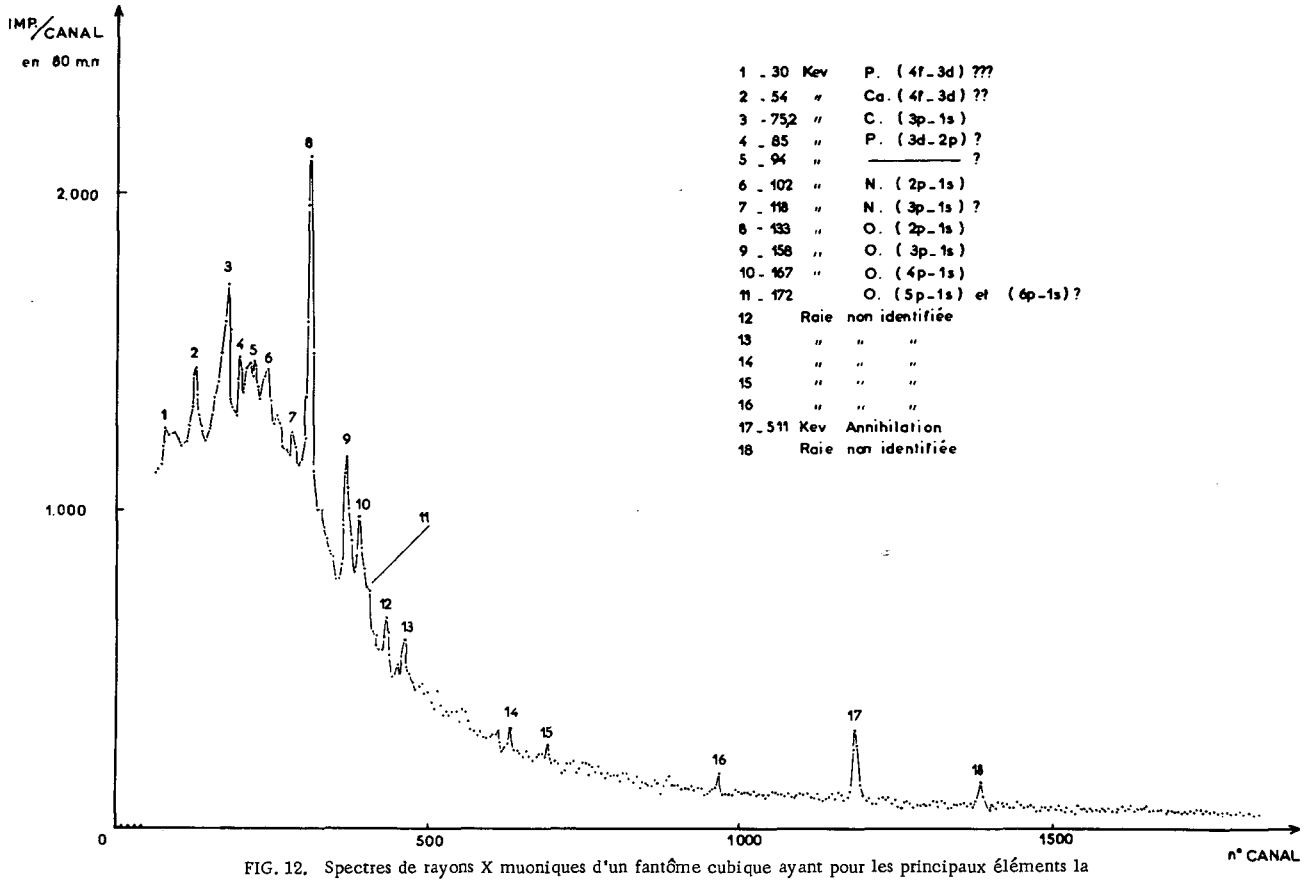

FIG. 12. Spectres de rayons X muoniques d'un fantôme cubique ayant pour les principaux éléments la composition du corps humain. Flux de muons: $5 \cdot 10^3/s \cdot 10\ cm^2$. Durée d'enregistrement: 1 h. Différentes transitions muoniques de O, C et N sont bien visibles. Des raies muoniques appartenant au phosphore et au calcium sont probablement présentes.

sur l'azote-14 (29). Il a été montré que pour un tissu biologique de composition moyenne en azote, oxygène, carbone et hydrogène, la contribution des γ de capture à la dose totale est de 20 %. Dans le cas des irradiations par neutrons rapides le processus principal de transfert d'énergie des neutrons au tissu biologique se fait par les protons de recul dont l'énergie est fonction de celle des neutrons incidents.

Une méthode d'analyse élémentaire "in vivo" potentiellement très intéressante a été proposée récemment par L. Rosen et ses collaborateurs du Laboratoire Scientifique de Los Alamos (30, 31, 32), ainsi que par Daniel au C.E.R.N. (33). Il s'agit de l'observation des rayons X muoniques produits au cours de l'irradiation d'un organisme par un faisceau de muons négatifs. Ces particules ayant une masse 207 fois plus grande que celle de l'électron, forment, quand elles sont stoppées dans la matière, des atomes muoniques d'une durée de vie de moins d'une nanoseconde et qui disparaissent en produisant des rayons X muoniques d'énergies discrètes 200 fois plus élevées que celles de leurs homologues ordinaires. Par exemple pour le carbone la raie X_K muonique est à 75 keV. On conçoit qu'à ces énergies les rayons X muoniques de tous les éléments puissent faire aisément l'objet d'une détection externe dans un organisme. D'autre part le rendement de production est très élevé, c'est-à-dire que 90 % des muons stoppés dans les tissus doivent donner un photon X_K.

La figure 12 montre le spectre de rayons X muoniques que nous avons obtenu au cours d'une expérience préliminaire à l'Accélérateur Linéaire de Saclay sur un fantôme cubique de 10 cm de côté ayant la composition du corps humain pour les principaux éléments. L'intensité du faisceau de muons était de 5.10^3 μ^-/s sur une surface de 10 cm^2 normale au faisceau. Il était produit par un faisceau d'électrons de 300 MeV de 27 mA de courant de crête à une fréquence d'impulsion de 2000 hertz et un cycle utile de 1 %. Tous les muons sont stoppés dans le fantôme. La détection était effectuée au moyen d'un détecteur Ge(Li) de 30 cm^3 de volume utile et la durée d'enregistrement de une heure. Les raies du carbone de l'oxygène de l'azote et ce qui est plus intéressant une raie du phosphore et peut-être du calcium sont visibles. Si on dispose un jour de flux de μ^- 100 à 1000 fois plus élevé, la méthode peut devenir applicable pour l'analyse élémentaire "in vivo", mais nécessitera des données nucléaires plus précises sur la production des muons négatifs et de leur interaction avec la matière.

Terminons en disant que nous avons éliminé systématiquement de cet exposé certains phénomènes nucléaires tels que la RMN, l'effet Mössbauer (34,35) et la corrélation angulaire (36) qui peuvent présenter de l'intérêt dans certains domaines biologiques et médicaux étroits.

REFERENCES

(1) GLASS, H.I., New applications of radiopharmaceuticals labelled with cyclotron-produced radionuclides. Symp. on medical radioisotope scintigraphy, IAEA Monte-Carlo Oct.1972, sous presse.

(2) ENGELMANN, Ch., Contribution à l'étude de la détermination de Be, B, L, N, O et F par activation au moyen de p, d, ^{3}He et . I. Courbes d'activation et sensibilité de détection, J. of Radioanal. Chem. 7 (1971) 89.

(3) BERGNER, P.E.E., Tracer dynamics and the determination of pool-sizes and turnover factors in metabolic systems, J. Theoret. Biol. 6 (1964) 137.
(4) ORR, J.S., GILLESPIE, F.C., Occupancy principle for radioactive tracers in steady-state biological systems, Science 162 (1968) 138.
(5) RIVIERE, R., COMAR, D., KELLERSHOHN, C., ORR, J.S., GILLESPIE, F.C., LENIHAN, J.M.A., Estimation of thyroid iodine content by the occupancy principle, Lancet (1969, 22 Feb.) 389.
(6) GILLESPIE, F.C., SHIMMINS, J., LENIHAN, J.M.A., Total body bromine : estimation by occupancy principle and neutron activation analysis, Radiochem. Radioanal. Letters 4 (1970) 43.
(7) COMAR, C., LOC'H, C., RIVIERE, R., KELLERSHOHN, C., Utilisation de l'analyse par radioactivation et du comptage sur corps entier pour l'étude du métabolisme du rubidium chez l'homme normal, p. 245, Radioaktive Isotope in Klinik und Forschung (FELLINGER, K., HOFER, R., Eds), Urban & Schwarzenberg, Münich-Berlin-Vienne (1970).
(8) SHIMMINS, J., SMITH, D.A., AITKEN, M., LINSLEY, G.P., ORR, J.S., GILLESPIE, F.C., The measurement of calcium absorption using an oral and intravenous tracer, Calc. Tiss. Res. 6 (1971) 301.
(9) MAZIERE, B., MAZIERE, M., COMAR, D., Quelques aspects du métabolisme du sélénium chez le rat, Nuclear Activation Techniques in the Life Sciences IAEA, Vienna (1972) 359.
(10) LOEVINGER, R., BERMAN, M., A schema for absorbed-dose calculations for biologically-distributed radionuclides, MIRD Pamphlet n° 1, J. Nucl. Med. 9 Suppl.1 (1968) 9.
(11) ELLETT, W.H., CALLAHAN, A.B., BROWNELL, G.L., Gamma-ray dosimetry of internal emitters Monte Carlo calculations of absorbed dose from point sources, Brit. J. Radiol. 37 (1964)45.
(12) LOEVINGER, R., BERMAN, M., A formalism for calculation of absorbed dose from radionuclides, Phys. Med. Biol. 13 (1968) 205.
(13) ELLETT, W.H., CALLAHAN, A.B., BROWNELL, G.L., Gamma-ray dosimetry of internal emitters : Monte Carlo calculations of absorbed dose from uniform sources, Brit. J. Radiol. 38 (1965) 541.
(14) REDDY, A.R., ELLETT, W.H., BROWNELL, G.L., Gamma-ray dosimetry of internal emitters : Absorbed fractions for low energy gamma rays, Brit. J. Radiol. 40 (1967) 512.
(15) ELLETT, W.H., BROWNELL, G.L., REDDY, A.R., An assessment of Monte Carlo calculations to determine gamma ray dose from internal emitters, Phys. Med. Biol. 13 (1968) 219.
(16) ELLETT, W.H., HUMES, R.M., Abosrbed fractions for small volumes containing photon emitting radioactivity, MIRD Pamphlet n° 8, J. Nucl. Med. 12 Suppl.5 (1971) 25.
(17) SNYDER, W.S., FORD, M.R., WARNER, G.G., FISHER, H.L., Estimates of absorbed fractions for monoenergetic photon sources uniformly distributed in various organs of a heterogeneous phantom, MIRD Pamphlet n° 5, J. Nucl. Med. 10 Suppl.3 (1969)5.
(18) BERGER, M.J., Energy deposition in water by photons from point isotropic sources, MIRD Pamphlet n° 2, J. Nucl. Med. 9 Suppl.1 (1968) 15.
(19) DILLMAN, L.T., Radionuclides decay schemes and nuclear parameters for use in radiation-dose estimation, Part 1 Pamphlet n° 4, J. Nucl. Med. 10 Suppl.2 (1969) 5 et Part 2 Pamphlet n° 6, J. Nucl. Med. 11 Suppl.4 (1970) 5.

(20) FEIGE, Y., GAVRON, A., LUBIN, E., LEWITUS, Z., BEN-PORATH, M., GROSS, J., LOEWINGER, E., Local energy deposition in thyroid cells due to the incorporation of ^{125}I, Biophysical Aspects of Radiation Quality IAEA, Vienna (1971) 383.
(21) FEINENDEGEN, L.E., ERTL, H.H., BOND, V.P., Biological toxicity associated with the Auger effect, Biophysical Aspects of Radiation Quality IAEA, Vienna (1971) 419.
(22) Panel on "in vivo" activation analysis, I.A.E.A. Vienna (april 1972) sous presse.
(23) COMAR, D., RIVIERE, R., RAYNAUD, C., KELLERSHOHN, C., Recherches préliminaires sur la composition et le métabolisme de l'os étudiés par radioactivation neutronique "in vivo" chez l'homme, p. 186, Radioaktive Isotope in Klinik und Forschung (FELLINGER, K., HOFER, R., Eds), Urban & Schwarzenberg, Münich-Berlin-Vienne (1968) vol.8.
(24) LENIHAN, J.M.A., COMAR, D., RIVIERE, R., KELLERSHOHN, C., Estimation of thyroid iodine "in vivo" by activation analysis, Nature 214 (1967) 1221.
(25) KELLERSHOHN, C., COMAR, D., RIVIERE, R., L'Isomère ^{130m}I. Mise en évidence et étude du rayonnement émis, C.R. Acad. Sc. Paris t.264 (26.6.1967) 1836.
(26) KELLERSHOHN, C., COMAR, D., RIVIERE, R., L'isomère ^{130m}I. Recherche d'un schéma de désintégration, C.R. Acad. Sc. Paris t.265 (3.7.1967) 88.
(27) CHASTELAND, M., COMAR, D., Dosage par radioactivation neutronique "in vivo" de quelques éléments contenus dans l'organisme du rat, Int.J. Appl. Radiat.Isotopes 23 (1972) 209.
(28) FAIRCHILD, R.G., GOODMAN, L., Development and dosimetry of an epithermal neutron beam for possible use in neutron capture therapy, J. Phys. Med. Biol. 11 (1966) 15.
(29) SKLAVENITIS, H., DEVILLERS, C., COMAR, D., KELLERSHOHN, C., Etude dosimétrique d'un faisceau collimé de neutrons thermiques destiné à l'analyse par radioactivation "in vivo", Int. J. Applied Radiat. Isotopes 20 (1969) 585.
(30) ROSEN, L., "Status of Los Alamos meson physics facility", Proc. of the IVth Int. Conf. on High Energy Physics and Nuclear Structure, Dubna (1972) 589.
(31) LUNDY, A.S., Possible diagnostic uses of muons, Proc. of the Biomedical sessions of the IVth LAMPF Users Meeting (compiled by GROCE, D.E., HARPER, K.H.) Los Alamos Scientif. Lab. of the Univ. of California, Los Alamos, New-Mexico (1970) 41.
(32) LUNDY, A.S., HUTTON, R.L., Can negative muons provide unique or better diagnostic information ?, Summary of a talk given at the 13th Annual Meeting of the Am. Ass. of Physicists in Medicine, Houston, Texas, (July 7-9 1971). Private communication.
(33) DANIEL, H., The muon as a tool for scanning the interior of the human body, Nuclear Medizin 8 (1969) 311.
(34) MOSHKOVSKII, Y.S., Applications of the Mössbauer effect in biology, Chap. 10, p.524 Chemical Applications of Mössbauer spectroscopy (GOLDANSKII, V.I., HERBER, R.H., Eds) Academic Press, New-York-London (1968).
(35) MALING, J.E., WEISSBLUTH, M., The application of Mössbauer spectroscopy to the study of iron in heme protein, Chap. 10 p. 327 Solid State Biophysics (WYARD, F.J.,Ed.) Mc Graw Hill Book Comp., New-York (1969).
(36) GOODWIN, D.A., MEARES, C.F., SONG, C.H., The study of ^{111}In-labeled compounds in mice, using perturbed angular correlations of gamma radiations, Radiology, 105 (1972) 699.

DISCUSSION

G.A. KOLSTAD: This is a question that bears on the status of biomedical theory. As you know, we have thus far discovered only about 1600 of the 6000 radioisotopes predicted to exist between the proton and neutron drip-lines that bound the valley of stability. Can you specify, on the basis of theoretically optimum models (e.g. for the liver, kidney, bone, brain, thyroid, etc.) the character of the radiation you need for the different biomedical applications and thus send off the nuclear physicists to seek the particular isotopes you need for these various applications?

C. KELLERSHOHN: Specialists in nuclear medicine are fully aware of the problem which you raise. Thus far, their criteria for deciding what constitutes the favourable characteristics of a radioelement have been based on the possibility of reducing the radiation dose to the organisms or of increasing the activities injected, for equivalent doses, in order to improve the accuracy of measurements, or else on the emission of gamma photons of energy especially favourable for external detection, due allowance being made for tissue absorption and for the properties of the detectors used. This is the reason why an element like ^{99m}Tc, which was developed by Paul Harper, and which emits an intense gamma line at 140 keV and very little energy in the form of charged particles, is so widely used in nuclear medicine even though it is not a natural constituent of the body. Disregarding the matter of metabolic specificity, it does not appear that the nature of the organ under study has played an important role in their concerns. For example, it seemed to us, in the case of the thyroid gland, which is an organ of small volume close to the cutaneous planes, that it might be advantageous to use an electromagnetic radiation of low energy for obtaining images, since use can then be made of collimators with very fine septa, which enable one to get excellent resolution. In this way, we get pictures of the thyroid in our laboratory with X_k photons of ^{125}Te emitted by ^{125}I by means of a spark chamber permitting a resolution of 1 mm.

Whatever the case may be, I agree with you in feeling that in the case of radioisotopes which are still unknown, we have to select several of those which are likely to present more favourable characteristics with respect to these problems than the nuclides known at present.

R. NICKS: In the paper you use the Monte-Carlo method and the method of moments calculations to deal with the problem of transport of radiation (photons, electrons) in the organ under study. The latter technique, however, is applied only in an infinite homogeneous medium and therefore is not directly applicable to organs of finite dimensions. How do you make allowance for finite dimensions?

C. KELLERSHOHN: The use of the Monte-Carlo methods in connection with this problem has been the subject of a number of studies by the Brownell group for over ten years, while the moments method (Spencer and Fano) has been developed along these lines mainly by Berger. The two methods are complementary to some extent, since they can be used for keeping a relative check on one another.

Of course, I agree with you that the moments method is applicable only to infinite media. It is for this reason that the present trend in photon dosimetry in man is to use the results obtained by the Monte-Carlo method, which afford a means of taking boundary effects into account.

NUCLEAR DATA REQUIREMENTS IN RADIOLOGICAL PROTECTION AND RADIOTHERAPY

J. A. DENNIS,
Head of Physics Department,
National Radiological Protection Board,
Harwell, Berks,
United Kingdom

Abstract

NUCLEAR DATA REQUIREMENTS IN RADIOLOGICAL PROTECTION AND RADIOTHERAPY.

The estimates of somatic and genetic risks arising from exposure to low levels of ionizing radiation are derived by linear extrapolation from the effects which have been observed when humans and animals were exposed to large acute doses of radiation for therapeutic or other reasons; this undoubtedly results in an overestimate of the risks, but no adequate theoretical basis exists for any other form of extrapolation. The dependence of the risk on the quality and type of the radiation is based by convention on the linear energy transfer (i.e. specific energy loss) of the ionizing particles in water. This convention is undoubtedly incorrect. While it must be considered that the present levels of allowable exposure to radiation give adequate protection to the individual and society, the existing uncertainties generate some unease. Although the main obstacle to the resolution of these uncertainties in the absence of a detailed understanding of the biological processes involved, an additional obstacle is the lack of adequate physical data and theories to fully describe the interaction of radiation with matter. This inadequacy effects the accuracy of radiation dosimetry and also makes it difficult to develop theoretical explanations to account for the dependence of biological effects on radiation quality.

Similar difficulties exist in the field of radiation therapy, where there is a growing awareness of the advantages of using fast neutrons and accelerated heavy ions for the treatment of tumours. The absence of an adequate theoretical explanation for the dependence of effect on radiation quality makes it difficult to fully evaluate the advantages of using alternative types of radiation other than experimentally.

Some of the current attempts at developing theoretical explanations of the dependence of biological effects on radiation dose and quality are described briefly in order to delineate those areas where additional physical data are required.

1. INTRODUCTION

The need for nuclear data arises in several different ways in Radiological Protection and Medicine. The most obvious which comes to mind is that for cross-section and build-up data for the calculation of the shielding of radiation sources, but this is no different from the present needs of the Nuclear Industry. Less obvious is the need for data on methods of producing different isotopes, and their half-lives and decay schemes. This data is required in the growing field of Nuclear Medicine for the use of isotopes in diagnostic techniques for various diseases and metabolic misfunctions of the human body; it is also required for radiological protection specification in the chemical plants of the Nuclear Fuel industry. Not only is the data required to be available, it also needs to be presented in a manner that is useful to the practical user who may not understand and care even less about theories of nuclear and atomic structure.

However, these aspects are not further discussed in this paper which is concerned with the nuclear data required to further our understanding of the dependence of the biological effects produced by radiation upon the quality of the radiation. One reason for concentrating on this requirement is that it throws up a demand not merely for an extension of the data on cross-sections to a much wider range of energies, but also for an extension of the way in which this data is provided.

2. BIOLOGICAL EFFECTS OF RADIATION

An obvious point to start an investigation of the fundamentals of the biological effects of radiation is by the irradiation of artificially cultured mammalian cells [1]. The aim of such investigations being to uncover any general physical and biological effects which are relevant to radiation-therapy for cancer or to the prediction of the risks of somatic and genetic effects from low levels of radiation.

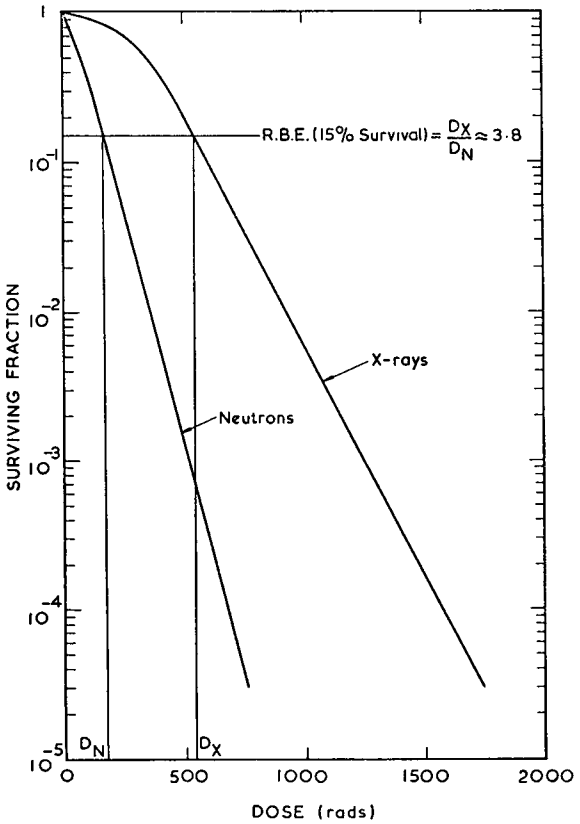

FIG. 1. Survival of chinese hamster cells (H1) after exposure to fast neutrons and X-rays after SCHNEIDER, D.O., WHITMORE, G.F., Radiat. Res. 18 (1963) 286 illustrating the RBE concept.

The typical results of such experiments are shown in Figure 1. Surviving cells are defined in this type of experiment as those which are capable of producing at least 50 daughter cells by further division. If instead of plotting the logarithm of the number of surviving cells against absorbed energy, the number of cells killed by the radiation had been plotted on a linear scale the result would have been that shown in Figure 2. It is this latter type of plot which encourages the belief that the risk estimates for occupation exposure to low doses of radiation derived [2] from the exposure of human beings to large doses of gamma radiation for therapeutic reasons by linear extrapolation are over estimates. The therapist using radiation to cure a malignant disease has always to balance, of course, the risk of inducing further malignancies by his treatment against the possibility of a cure.

Two further points must be made about dose-effect curves.

Firstly, as shown in Figure 3, the efficiency for producing an effect increases as the specific energy loss or linear energy transfer, LET, of the radiation increases.

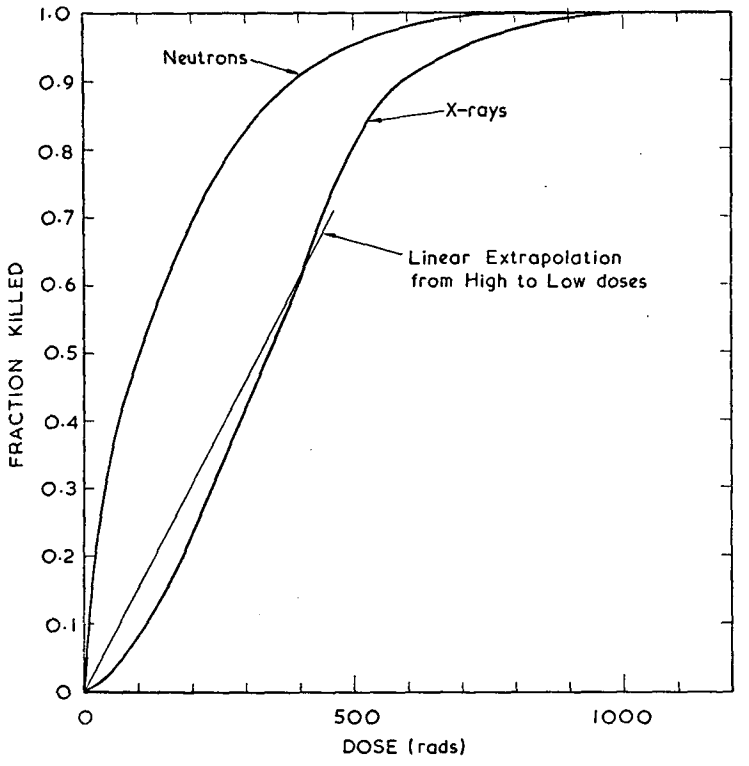

FIG.2. Killing of chinese hamster cells (H1) after exposure to fast neutrons and X-rays, illustrating the effect of linear extrapolation to low doses from the high results.

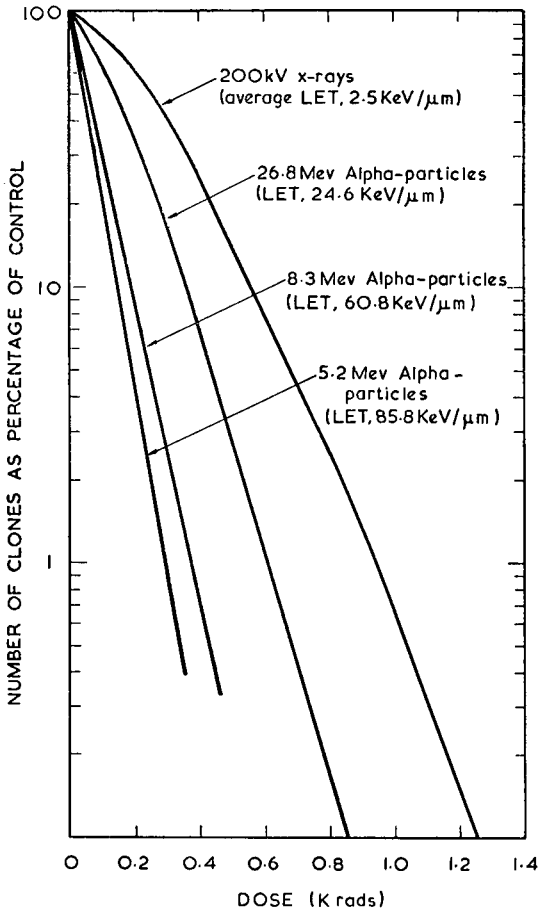

FIG.3. Effect of using radiations with different specific energy loss (LET) to irradiate cultured human kidney cells after BARENDSEN, G.W., WALTER, H.M.D., FOWLER, J.F., BEWLEY, D.K., Radiat. Res. 18 (1963) 106.

Moreover, relative to the effect produced by X-radiation the efficiency of high LET is greater at low levels of effect and small doses of radiation, Figure 4. The relative biological effectiveness, RBE, of a radiation is defined as the ratio of the dose of from X-radiation to the dose from the specified radiation to produce the same level of effect, Figure 1.

Secondly, the protection against damage afforded by depriving the biological material of oxygen decreases as the specific energy loss of the radiation increases, Figure 5. Since it is thought that many tumours are starved of oxygen due to a poor blood supply, this observation is one basis for proposals to use neutrons for

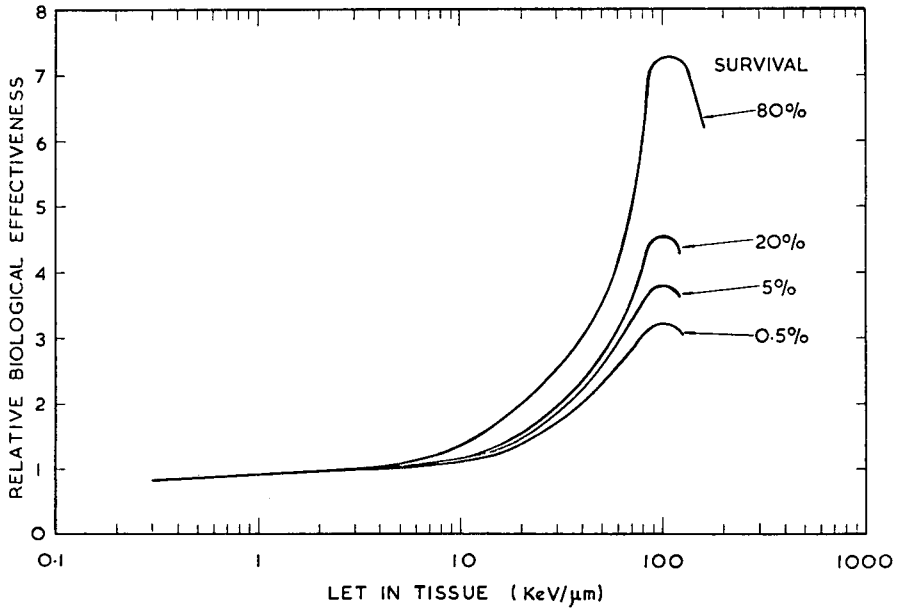

FIG.4. Effect of estimating the RBE at different levels of effect, showing the increase in RBE for low levels of effect after BARENDSEN, G.W., WALTER, H.M.D., FOWLER, J.F., BEWLEY, D.K., Radiat. Res. 18 (1963) 106.

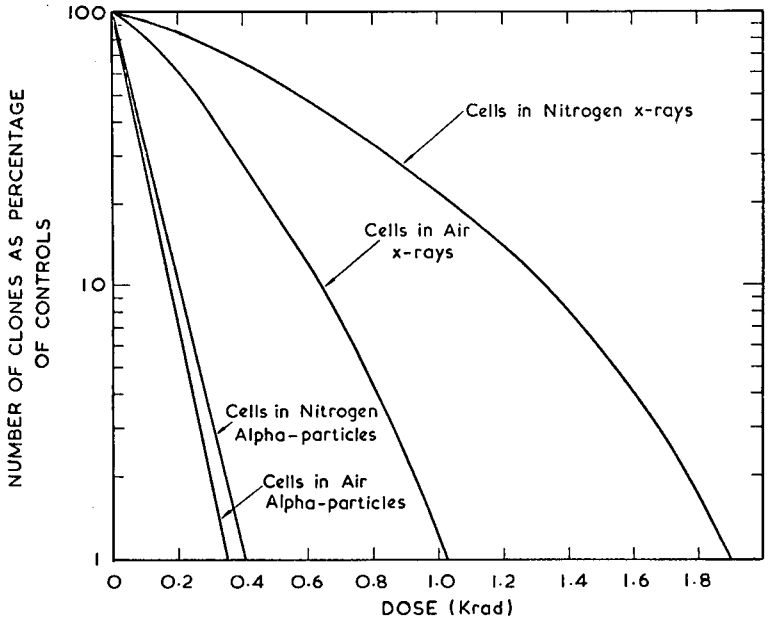

FIG.5. Effect of oxygen deprivation in protecting cells against the effects of radiation, illustrating the decrease in protection as the specific energy loss of the radiation increases.

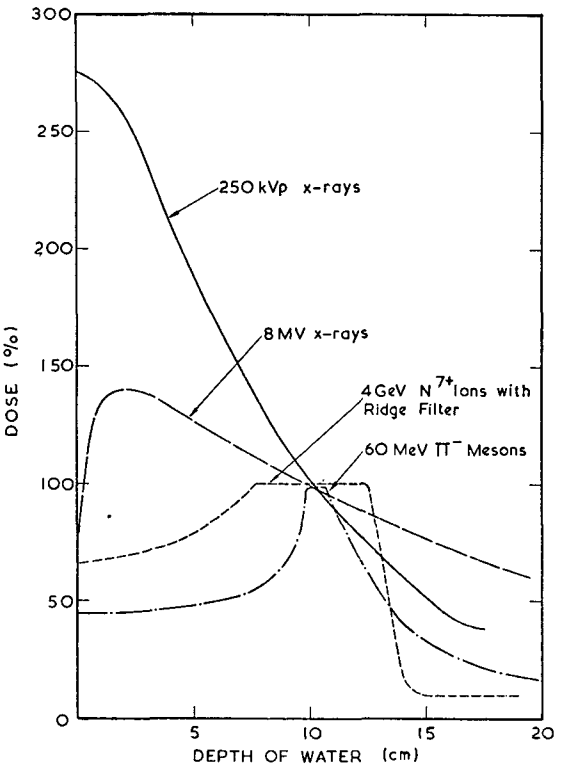

FIG.6. An illustration of the better depth dose characteristics of accelerated heavy ions and negative π-mesons for the treatment of deep tumours after Ref. [4].

radiation therapy, the other is that tumours may exhibit higher RBE values than normal tissues [3] and therefore be more susceptable to treatment with neutrons than with X-radiation.

One of the difficulties of treating deep lying tumours with X-rays, electron beams or neutrons is that the overlying healthy tissue receives greater doses than the tumour, and this can only be overcome to some extent by using multi-directional beams and higher energies. For this reason accelerated heavy ions beams have been used and negative pi-mesons are proposed for use in radio-therapy, since the depth dose charactaristics are more favourable [4], Figure 6.

Now the dependence of biological effect on the specific energy loss demonstrated in Figure 4 has encouraged the belief that the RBE of radiation depends directly on the specific energy loss. This belief is now embodied in the Quality Factor which is used in radiological protection, Figure 7. The quantity used to estimate the hazards from radiation is the dose-equivalent of which the unit is the rem.

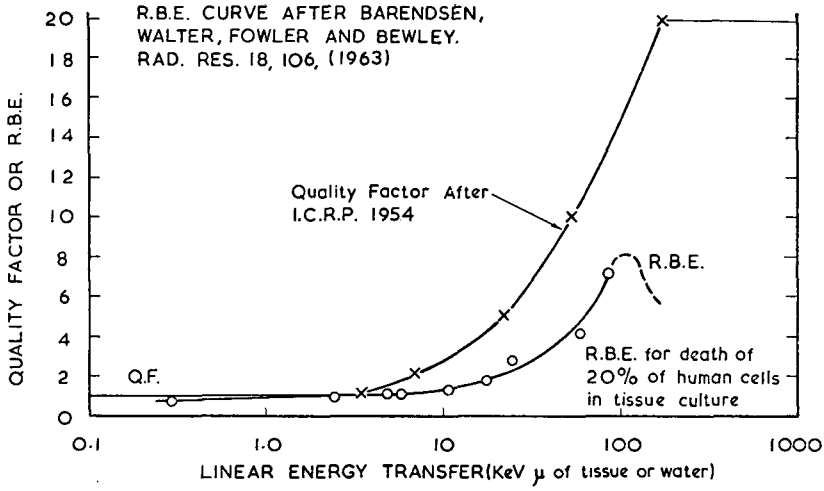

FIG.7. A comparison of the conventional quality factor with an experimentally determined RBE.

Dose-equivalent in rem = Absorbed dose in rads x Quality Factor

The ICRP recommendations for maximum permissible levels of dose-equivalent to guard against both somatic and genetic risks are given in Table I.

The Quality Factor is most commonly involved in estimating the hazards from neutron and high energy accelerator radiations.

Neutrons do not produce a single defined value for the specific energy loss in tissue, instead they produce distributions such as that shown in Figure 8. This distribution must be calculated from a detailed knowledge of the reactions produced by neutrons in the common elements of the body i.e. hydrogen, carbon, nitrogen, oxygen and calcium. At high neutron energies (>5MeV) not only are the details of the non-elastic and in-elastic reactions often uncertain but so are the cross-sections. Also involved in these calculations is the specific energy loss in biological tissue of the secondary particles produced and this is an additional source of uncertainty.

If the calculated specific energy loss distributions from neutrons are combined with the apparent dependence of RBE upon specific energy loss determined experimentally, then it should be possible to predict the RBE of neutron radiation. Attempts to make this prediction have been unsuccessful [5].

TABLE I. SUMMARY OF I.C.R.P. RECOMMENDATIONS FOR MAXIMUM PERMISSIBLE LEVELS OF DOSE EQUIVALENT (I.C.R.P. PUBLICATION 9, PERGAMON PRESS, OXFORD (1966)

Organ	Maximum Permissible Yearly Dose-Equivalent for adults exposed in the course of their work. Rem	Maximum Permissible Yearly Dose-Equivalent for members of the public. Rem
Gonads	5	0.5
Skin, bone and thyroid	30	3
Hands, forearms, feet and ankles	75	7.5
Other single organs	15	1.5

Notes:

1. One half the yearly permissible dose-equivalent may be accumulated in any period of a quarter of a year; with the limitation that the total accumulated dose at any age over 18 should not exceed 5(N - 18) rem, where N is the age in years.

2. Women of reproductive age exposed in the course of their work should not accumulate dose-equivalent at a rate exceeding 1.3 rems in a quarter of a year.

3. To guard against long term genetic consequences the total average dose to members of a population should not exceed 5 rems in a period of 30 years.

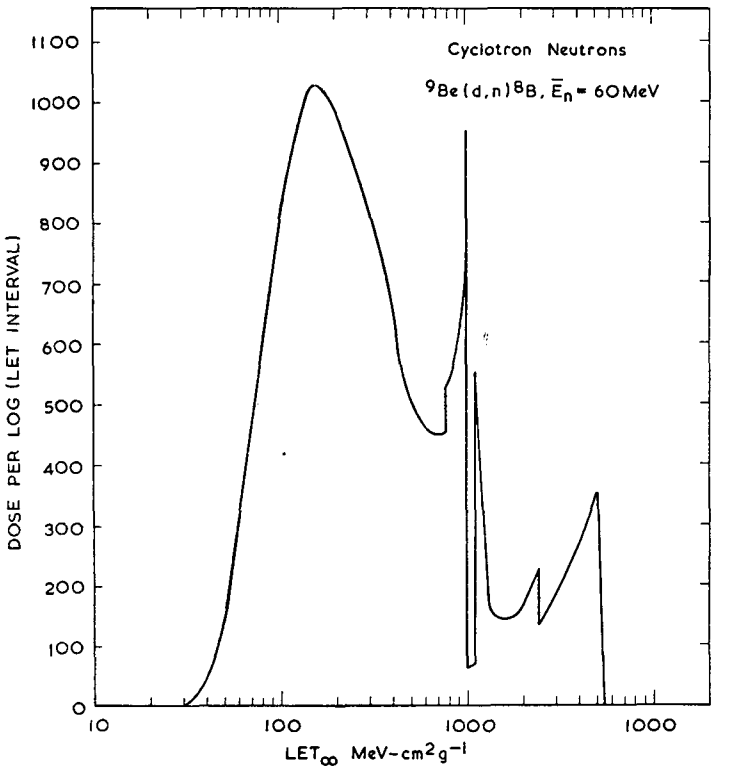

FIG.8. Specific energy loss spectrum in fast-neutron-irradiated tissue after BEWLEY, D.K., in Biophysical Aspects of Radiation Quality (Proc. Panel Vienna, 1967), IAEA, Vienna (1968) 65.

The specific energy loss for a heavy ion, Figure 9, is not a single-valued function of the ion energy, moreover the energy loss processes may be quite different for the same specific energy loss value obtained at different energies. Intuitively it seems inherently unlikely that the different modes of energy loss should produce equal biological effects. When different ions are considered it seems even less likely that specific energy loss is an adequate parameter, since ions of the same energy loss may produce quite different distributions of delta-ray energies and energy deposition about their tracks.

3. DOSE-EFFECT RELATIONSHIPS

Perhaps the most obvious way of explaining the observed relationships between the dose to the tissue and the observed effect is in terms of hits on targets, in a conceptual framework that originated in the 1920's. The most widely used idea from this framework is that of $\underline{m}$ sensitive targets in the cell each of which must be hit in

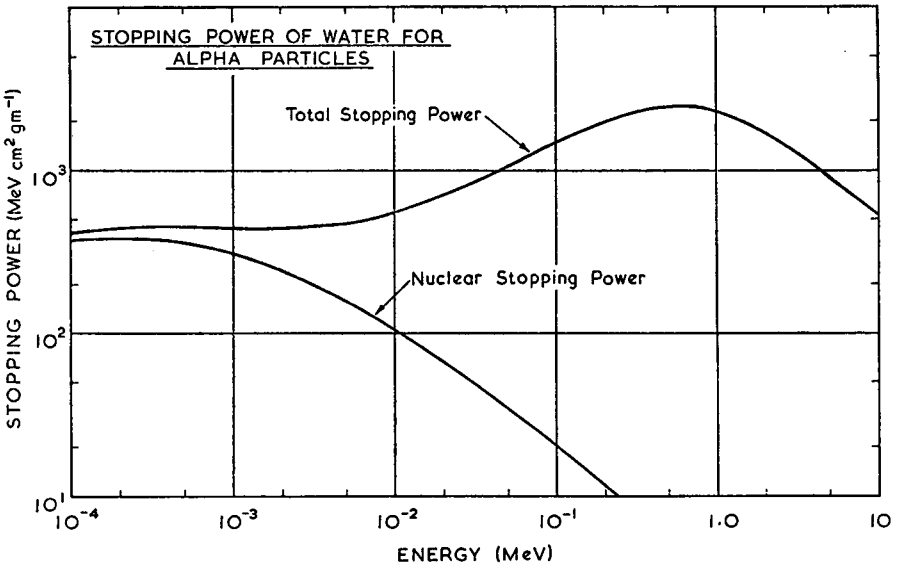

FIG. 9. Specific energy loss of alpha particles in water. (DENNIS, J. A., private compilation.)

order to kill the cell, and the dose Do required to produce an average of one hit on each target. This gives rise to the following formula relating the N survivors of an original population No to the dose D.

$$\frac{N}{N_0} = \left\{1 - \left[1 - \exp\left(- D/D_0\right)\right]^m\right\} \qquad (1)$$

Apart from the study of cell killing, the other major study is that of chromosome aberrations. These are gross visible distortions in the genetic material of the cell. The relationship between the number of aberrations, A, observed in the population No, and the dose can very often be represented by a combination of single and two target models i.e.

$$\frac{A}{N_0} = \left\{1 - \exp\left(- D/{}_1D_0\right)\left[1 - \left(1 - \exp\left(- D/{}_2D_0\right)\right)^2\right]\right\} \qquad (2)$$

which for very low doses can be usefully expanded as

$$\frac{A}{N_0} = \frac{D}{{}_1D_0} - \left(\frac{1}{{}_1D_0{}^2} - \frac{2}{{}_2D_0{}^2}\right)\frac{D^2}{2} + \ldots \text{ etc.} \qquad (3)$$

It must be said at this point that the problem is ill-conditioned in the sense that a large number of different expressions can be made to fit the experimental results

equally well [6]. In fact some biologists reject the whole hit and target concept in favour of explanations based on metabolic factors [7]. It is certainly true that the dose-effect curves are changed by metabolic factors such as temperature, absence or presence of oxygen and the position of the cell within its cycle of growth and division at the time of irradiation. Also the ability of some cell systems to repair the damage caused by radiation has been demonstrated [1]. On the other hand it seems unlikely that purely metabolic factors can account for the dependence on radiation quality.

4. MICRODOSIMETRY AND TRACK STRUCTURE

The work of Lea [8] in the late 1930's and early 1940's is seminal in attempts to provide a physical explanation for biological effectiveness, and in many ways his work anticipated the two current and contending theories. These theories are known as microdosimetry and track structure.

4.1 Microdosimetry

The basis of microdosimetry is the calculation or more often the measurement [9] of the energy event size distribution, $f_1(\varepsilon)\, d\varepsilon$, in spherical volumes with effective dimensions of about 10^{-4} gram cm^{-2} Several considerations [10] lead to the conclusion that there exist one or more loci or targets of dimensions about 0.6 nanometers which must be activated in order to cause a chromosome aberration or kill a cell, and these locii must exist within a site of dimensions about 1.0 micrometer (i.e. 10^{-4} gram cm^{-2} in tissue).

It is assumed [10] in microdosimetry that the probability of activating a locus is proportion to the size of the energy deposited in the site i.e.

$$p = \mu\epsilon \qquad (4)$$

where μ is a constant of proportionality.

These assumptions lead to the following expression for chromosome aberrations:

$$A_0 = \frac{\mu^2\overline{\epsilon}}{2} D - \left\{\frac{\mu^4}{2}\overline{\epsilon}_D^2 - 2\mu^2\right\}\frac{D^2}{2} + \ldots \text{ etc.} \qquad (5)$$

$\overline{\epsilon}_D$ is the dose average event size.

This theory has yet to be vigorously tested by exploration with a range of different radiations and biological systems.

A difficulty in testing the theory is that of calculating the energy even size distribution, $f_1(\varepsilon)\, d\varepsilon$, as this requires a detailed knowledge of neutron cross-sections and reaction kinetics, as well as details of the energy loss in tissue by the secondary particles produced.

Similar details are required for X-rays and electrons, and a point of investigation here is the influence of K and L shell effects and molecular binding on the energy loss processes of low energy electrons [11].

One might anticipate at this stage that the coefficient μ will not be independent of the mode of energy loss that produces the energy deposition $\mathcal{E}$. This will open a new field of investigation requiring data on charge exchange processes, inner shell ionization [12] and quasi-elastic nuclear scattering [13].

4.2 Track Structure

Because of the ultimate influence of metabolic factors in governing the repair and recovery of cell populations that have suffered a large radiation insult it seems unlikely that the theory of microdosimetry can usefully be employed at this time in the field of radiotherapy. It is in this field that the track structure theory being developed by Prof. Katz [14] may prove applicable.

Briefly Katz takes the multi-target dose-effect survived curves, equation 1 above, obtained with X-radiation to represent the response function of the cells to electrons. From this response function he derives the dose-effect curves for heavy ions by regarding them as generating non-uniform distributions of electrons within tissue.

After some manipulation a theoretical expression is obtained for the expected dose-effect relationship which has the plausible form for tissue irradiated by a fluence $\phi(E)$ of heavy ions with specific energy loss $S(E)$ of

$$\frac{N}{N_0} = \exp\left(-\phi(E)\delta\right)\left\{1 - \left[1 - \exp\left(-\left(1 - \delta/\delta_0\right)\phi(E)\,S(E)/D_0\right)\right]^m\right\} \quad (6)$$

The constants m and D_o are related to the X-ray dose-effect relation, and the cross-sections δ and δ_o are related to the distribution of δ-rays about the track of the particle and the dimensions of the sensitive site within the cells.

The data requirements for testing this theory are identical for those required for testing the theories of microdosimetry i.e. details of the kinetics and cross-sections for neutron reactions on the elements hydrogen, carbon, oxygen, nitrogen and calcium over the energy range 10 KeV to 40 MeV and particularly in the region 1 MeV to 20 MeV, details of the specific energy loss of ions of mass numbers from 1 to 16 in the energy range from 0.1 KeV to 40 MeV, details of the δ-ray spectra produced by heavy ions, details of the energy loss processes by electrons down to 100 eV.

5. DISCUSSION AND CONCLUSION

The importance of the theoretical explanations for the dependence of biological effect on radiation quality should not be over emphasized. One must assume that any responsible radiotherapist proposing to use something other than the conventional radiations will first have satisfied himself by means of a series of biological experiments that his treatment will be beneficial to his patient. On the other hand a 10% uncertainty in the level effect produced, or in the dosimetry, may make a significant difference to the cure rate in radiotherapy [15].

There is no evidence either from studies with plants, insects and animals or from the long term follow-up of the victims [16] of the atomic bombing of Japan that the Quality Factors are seriously in error. Never-the-less any uncertainties in our understanding of the connection between radiation quantity and quality and the biological effects produced can be used to create public unease by those who are so minded [17].

The full understanding of the biological effects of radiation has been likened to digging a tunnel under a high mountain, not by starting at the ends and working towards the centre, but by sinking a series of vertical shafts and working outwards from the bottom of each. At one end are the biologists and medical practioners studying the somatic and genetic effects of irradiating animals and human beings, at the other end are the physicists studying the primary features of the interaction of radiation with matter. In between come the biologists studying the effects on cultured mammalian cells, bacteria and viruses; the radio-chemists studying radiation damage to and energy transfer within large micro molecules and enzymes; and the physicists concerned with energy deposit in processes within tissue. It is the latter group that are now extending their requirements for nuclear data; I hope that resulting from this symposium will be data that is of some assistance to them in the next stage of investigation.

REFERENCES

[1] ELKIND, M.M., WHITMORE, G.F., The Radiobiology of Cultured Mammalian Cells. Gordon and Breach, New York (1967).

[2] ICRP Publication 14, Radiosensitivity and Spatial Distribution of Dose, Pergamon Press, Oxford (1969).

[3] BROERSE, J.J., BARENDSEN, G.W., FRERIKS, G., VAN PUTTEN, L.M., Europ. Journ. Cancer 7 (1971) 171.

[4] BEWLEY, D.K., Nature 237 (1972) 17.

[5] BEWLEY, D.K., Radiat. Res. 34 (1968) 446

[6] ZIMMER, K.G., Studies on Quantitative Radiation Biology. Oliver and Boyd, Edinburgh (1961).

[7] LAURIE, J., ORR, J.S., FOSTER, C.J., Brit. Journ. Radiol. 45 (1972) 362.

[8] LEA, D.E., Actions of Radiation on Living Cells. Cambridge University Press (1946).

[9] ROSSI, H.H., Radiation Dosimetry. Vol. I (Ed. Attix, F.H., Roesch, W.C.) Academic Press, New York (1968) 43.

[10] KELLERER, A.M., ROSSI, H.H., Radiation Research 47 (1971) 15.

[11] ARAKAWA, E.T., BIRKHOFF, R.D., et. al. Oak & Ridge National Lab. Report ORNL - 4811 (1972).

[12] METZ, W.M., Science 177 (1972) 156.

[13] WATT, D.E., Phys. Med. Biol. 17 (1972) 409.

[14] KATZ, R., SHARMA, S.C., HOMAGOONFAR, M., Chapter 6. Progress in Radiation Dosimetry Ed. Attix F.H. - to be published.

[15] BARENDSEN, G.W., BROERSE, J.J., First Sumposium on Neutron Dosimetry in Biology and Medicine. Commission of the European Communities. Luxemburg 1 (1972).

[16] ICRP Publication 18. The RBE for High-LET Radiations with respect to Mutagenesis. Pergamon Press, Oxford (1972).

[17] GOFMAN, J.W., TAMPLIN, A.R., Poisoned Power. Rodale Press. Emmaus (1971).

DISCUSSION

L. HJÄRNE: We have sometimes been given the impression that, of all nuclear data, the neutron data are in fairly good shape. Therefore it is perhaps surprising to many of us that the attempts to predict RBE have not been very successful. Regarding the elastic and inelastic data for neutrons above 5 MeV, the reactor physicists, too, would agree that there is still a lot to be desired. However, the fact that the situation is not good enough for dose calculations is disturbing. I would therefore like to ask for your opinion on where the greatest difficulties lie. Is it a matter of the cross-sections and the angualr or energy (secondary) distributions or does it have to do with the calculational methods?

J.A. DENNIS: Particular difficulties arise in the non-elastic reactions, more specifically the (n, α) reactions with carbon and oxygen. Oxygen is a major constituent of biological tissue. Above a neutron energy of 5 MeV virtually all we have is the total cross-section for the (n,α) reactions with this element. We know that there are, at least, five or six alpha groups from this reaction, and without details of the cross-sections for each alpha group the dose estimates can be as much as 20% in error. When calculations

of linear energy transfer distributions are to be made, we require even greater detail, since the exact alpha spectrum provided in each alpha group must be known.

It is my impression that compilations of cross-sections have in the past been concerned only with the fate of the neutron in reactor applications. In biology and medicine we are concerned with the secondary particles as a result of the neutron reactions.

PROBLEMES POSES PAR LA FABRICATION DE PLUTONIUM-238 DE QUALITE BIOMEDICALE

R. BERGER*, C. DEVILLERS*, F. GERVAISE*, G. LE COQ**
Commissariat à l'énergie atomique,
France

Abstract–Résumé

PROBLEMS OF FABRICATING ^{238}Pu OF BIOMEDICAL QUALITY.

The biomedical quality of ^{238}Pu presupposes the lowest possible ^{236}Pu concentration, this being determined by irradiation methods. The results of the chemical analysis of ^{237}Np samples irradiated in reactors have been compared with the results of calculation. A good knowledge of the cross-sections $\sigma_{\gamma,n}$ et $\sigma_{n,2n}$ of ^{237}Np is necessary for calculating the ^{236}Pu concentration and for optimizing the irradiation conditions. Evaluations having shown that it was difficult to estimate these data correctly in the present state of knowledge, $\sigma_{\gamma,n}$ was measured. By slightly adjusting the calculated results for the experimental results it may be possible to produce ^{238}Pu of satisfactory quality.

PROBLEMES POSES PAR LA FABRICATION DE PLUTONIUM-238 DE QUALITE BIOMEDICALE.

La qualité biomédicale du ^{238}Pu exige la plus faible teneur possible en ^{236}Pu, celle-ci étant déterminée par les méthodes d'irradiation. L'analyse chimique d'échantillons de ^{237}Np irradiés dans des réacteurs a pu être comparée avec les résultats de calcul. Une bonne connaissance des sections efficaces $\sigma_{\gamma,n}$ et $\sigma_{n,2n}$ du ^{237}Np est nécessaire pour le calcul de la teneur en ^{236}Pu et l'optimisation des conditions d'irradiation. Les évaluations ayant montré qu'il était difficile d'estimer correctement ces données avec les connaissances actuelles, une mesure de $\sigma_{\gamma,n}$ a été effectuée. Un léger ajustement des résultats de calcul sur les résultats expérimentaux permet d'envisager la production de ^{238}Pu de qualité satisfaisante.

INTRODUCTION

Le plutonium-238 est utilisé comme source thermique du convertisseur thermo-électrique du stimulateur cardiaque [1]. Cette application nécessite certaines propriétés de pureté du ^{238}Pu. En effet, certaines traces contenues dans les descendants du ^{238}Pu contribuent aussi à l'activité radiologique soit en γ pour le ^{236}Pu, soit en neutrons par réaction (α, n) sur les éléments légers tels que F, O, Al, Ca. La fabrication du ^{238}Pu par irradiation en pile de ^{237}Np peut produire du ^{236}Pu par réaction (γ, n) et réaction $(n, 2n)$ sur le ^{237}Np. La connaissance des sections efficaces de ces deux réactions est nécessaire au calcul de la teneur en ^{236}Pu fabriqué compte tenu des conditions d'irradiation.

1. DOSE INDUITE PAR LES NEUTRONS ET LES RAYONNEMENTS GAMMA

Nous rappellerons ici les données nécessaires au calcul de la dose d'une source de 155 mg de ^{238}Pu dont la teneur isotopique est de 90%. L'activité due aux neutrons et aux gammas provenant des isotopes supérieurs au ^{238}Pu est négligeable.

---

* Centre d'études nucléaires de Fontenay-aux-Roses.
** Centre d'études nucléaires de Saclay.

1.1. Neutrons

Pour chaque fission spontanée le ^{238}Pu émet en moyenne $\nu = 2,29$ neutrons; la période de fission étant d'environ $5,0 \cdot 10^{10}$ ans, la source considérée émet $S_n = 355$ n/s, le spectre énergétique étant de la forme $N(E) = C \cdot E^{0,5} \exp(-E/1,23)$, E exprimé en MeV. Ce sont des neutrons rapides, donc ils ne sont pratiquement pas arrêtés par les matériaux constituant le stimulateur; la seule manière de réduire la dose due aux neutrons est d'éloigner au maximum la source de la paroi.

La dose maximale moyennée sur un élément de surface due à ces neutrons est égale à 0,9 mrem/h [2]. Le nombre de neutrons émis par réaction (α, n) sur les éléments légers dépend de la concentration de ces éléments dans le ^{238}Pu (voir paragr. 3).

1.2. Rayonnement gamma

Les gammas provenant du ^{238}Pu sont émis au cours de la désintégration α de période T = 87,5 ans. Ces gammas sont principalement de faible énergie. Pour une désintégration α il y a moins de $2 \cdot 10^{-5}$ gamma d'énergie supérieure à 150 keV. Pour le ^{236}Pu, l'activité gamma est principalement due aux gammas provenant de la désintégration β^- des noyaux de fin de chaîne. Cette activité est donc variable dans le temps et présente un maximum à 18 ans. Ces gammas émis sont plus énergétiques; par rapport à une désintégration β, 60% des γ ont une énergie supérieure à 200 keV, dont 14% ont une énergie de 583 keV et 17% une énergie de 2,6 MeV [2]. Pour la source de ^{238}Pu contenant 0,5 ppm de ^{236}Pu, l'activité gamma est la suivante (en désintégrations par seconde):

T (ans)	0	1	2	5	10	20
Pu-238	$8,9 \cdot 10^{10}$	$8,8 \cdot 10^{10}$	$8,8 \cdot 10^{10}$	$8,5 \cdot 10^{10}$	$8,2 \cdot 10^{10}$	$7,6 \cdot 10^{10}$
Pu-236	0	$4,2 \cdot 10^{3}$	$1,3 \cdot 10^{4}$	$5,0 \cdot 10^{4}$	$8,8 \cdot 10^{4}$	$1,0 \cdot 10^{5}$

Quelques millimètres de platine ou de titane suffisent à ramener la dose biologique des gammas provenant du ^{238}Pu au même ordre de grandeur que la dose biologique due aux neutrons. Dans les mêmes conditions une concentration d'environ 0,5 ppm de ^{236}Pu correspond à une dose moyenne sur 10 ans du même ordre de grandeur que la dose moyenne γ due au ^{238}Pu. Une réduction de 0,5 ppm à 0,3 ppm de la teneur en ^{236}Pu ne réduirait la dose totale que de 17%. Une teneur en ^{236}Pu de 0,5 ppm semble donc une pureté raisonnable du point de vue des dommages biologiques.

2. PRODUCTION DE ^{238}Pu DE QUALITE BIOMEDICALE

Par irradiation en pile de ^{237}Np on souhaite obtenir du plutonium dont la composition isotopique est la suivante: $\geq 90\%$ de ^{238}Pu, environ 9% de ^{239}Pu et 0,5 ppm de ^{236}Pu. Les irradiations faites, sans conditions particu-

lières, dans des réacteurs à eau lourde fournissent un ^{238}Pu contenant plus de 0,7 ppm de ^{236}Pu. On a donc cherché à simuler par calcul la production de ^{236}Pu.

La production de ^{238}Pu et de ^{239}Pu est donnée par des codes éprouvés d'évolution de cœur de pile [3], mais la production de ^{236}Pu par décroissance β^- de ^{236}Np obtenu par réaction (n, 2n) et (γ, n) ne peut être prise en compte dans ces codes.

Des codes de transport de neutrons rapides et de gammas ont dû être utilisés spécialement pour cette étude.

2.1. Etude de la réaction (n, 2n)

Supposons une géométrie cylindrique, la quantité de ^{236}Pu produite par centimètre de hauteur est donc:

$$N_{Pu-236} = 2\pi \int_0^R \int_0^\infty \int_0^T \sigma(E)\, N_{Np-237}(t)\, \phi(E, r, t)\, dr\, dE\, dt \qquad (1)$$

où T = temps d'irradiation

$\sigma(E)$ = section efficace (n, 2n) du ^{237}Np

N_{Pu-236} et $N_{Np-237}(t)$ = nombre de noyaux par cm^3 de ^{236}Pu et de ^{237}Np respectivement.

$\phi(E, r, t)$ = flux de neutrons, il dépend de la géométrie du cœur de pile et il est fourni par un code de transport de neutrons.

2.2. Etude de la réaction (γ, n)

Le calcul de la propagation gamma susceptible de provoquer une réaction (γ, n) est presque rigoureux car il peut être fait, sans grande erreur, en négligeant les photons ayant subi une diffusion.

La formule (1) peut s'appliquer pour le calcul de la quantité de ^{236}Np produite par réaction (γ, n) en prenant le flux de gammas et la section efficace $\sigma_{(n,\gamma)}$. Il faut tenir compte de toutes les sources de gammas: soit de fission, soit provenant des matériaux de structure, tels que bouchon, cuve et composé de l'alliage de l'éprouvette. Un calcul a été effectué sur une éprouvette NpO_2Al irradiée dans le réacteur EL3: le tiers du ^{236}Np fabriqué était dû aux gammas de capture dans l'aluminium du composé [4].

2.3. Ajustement des sections efficaces

L'analyse des irradiations faites en pile de cibles de ^{237}Np avec ou sans matrice d'aluminium nous a permis de choisir la section efficace ENDF-3 pour $\sigma_{(n, 2n)}$ (voir paragr. 3) et ainsi de calculer les contributions relatives des différents milieux environnants. Ceci a permis de fixer à environ 0,014 b la section efficace $\sigma_{(\gamma, n)}$ du ^{237}Np à 7,72 MeV, énergie de la raie principale des gammas provenant de la capture d'un neutron par l'aluminium. Le but de l'étude étant d'éliminer les sources principales de formation de ^{236}Pu, il est donc nécessaire d'avoir plus de renseignements sur la section efficace $\sigma_{(\gamma, n)}$.

3. MESURE ET EVALUATION DES CONSTANTES NUCLEAIRES

3.1. Données nucléaires nécessaires au calcul de la formation de ^{236}Pu à partir de l'irradiation en pile de ^{237}Np

a) Section efficace de réaction (n, 2n) sur le ^{237}Np. Une étude comparative des évaluations de la section efficace $\sigma_{(n,2n)}$ contenues dans les deux bibliothèques KEDAK et ENDF/B III a permis de recommander la section efficace contenue dans les bibliothèques ENDF/B III [5], résultat confirmé par les irradiations en pile.

b) Section efficace de réaction (γ, n) sur le ^{237}Np. Une première évaluation de la section efficace $\sigma_{(\gamma,n)}$ effectuée en septembre 1971 n'a pas permis de répondre d'une manière satisfaisante aux besoins. Aucune mesure expérimentale n'avait été faite et les valeurs proposées avaient été calculées à partir de modèles assez grossiers; ces valeurs avaient donc des barres d'erreurs importantes.

Le groupe d'expérimentateurs spécialistes des mesures photonucléaires a effectué la mesure de la section efficace $\sigma_{(\gamma,n)}$ auprès de l'accélérateur linéaire de 60 MeV de Saclay. Les mesures n'ont pu être faites qu'à des énergies de photons γ quasi monochromatiques supérieures à 9 MeV, ceci étant dû essentiellement à la radioactivité de l'échantillon de ^{237}Np utilisé [6]. A partir des mesures, il a été possible de décrire la section efficace totale d'absorption photonique à toute énergie

$$\sigma_{\gamma t} = \sigma_{\gamma,n} + \sigma_{\gamma,f} + \sigma_{\gamma,2n} + \ldots .$$

Le rapport $\sigma_{\gamma,n}/\sigma_{\gamma,f} = \Gamma_n/\Gamma_f$ a été étudié pour des énergies de γ proches du seuil d'émission de neutrons. Par réaction (γ, n) ou (n, 2n) il y a formation de deux états du ^{236}Np, l'un de période T > 5000 ans et de spin élevé (probablement 6^-), l'autre de période T = 22 h et de spin 1^-; seul celui-ci contribuera à la formation du ^{236}Pu par émission β^-. Le rapport de formation de l'état 1^- du ^{236}Np varie avec les énergies des γ incidents et est égal à environ 0,7 - 0,6 [7]. Les valeurs de $\sigma_{(\gamma,n)}$ en fonction de l'énergie des γ sont les suivantes:

E (MeV)	6,62	6,7	6,8	7	7,5	7,72	8	8,5	9	10
$\sigma_{\gamma,n}$ (mb)	0	3	4	6	14	18	24	40	60	116
$\sigma_{\gamma,n}$ (mb)*	0	3	3	4	8,5	11	14	24	36	70

* Section efficace de formation de l'état 1^-.

3.2. Données nucléaires nécessaires au calcul de la dose

Outre l'évaluation du nombre moyen $\bar{\nu}$ de neutrons émis par fission spontanée et le spectre énergétique de ces neutrons, nous avons étudié les neutrons et les rayons γ émis par un échantillon de ^{238}Pu contenant des traces de fluor [8]. Le fluor peut émettre des neutrons et des rayons γ par réaction α sur ce noyau: (α, $\alpha'\gamma$), (α, pγ) et (α, nγ).

Le rendement neutronique, en cible épaisse de fluor, a été déterminé égal à 10 neutrons par million de α pour des énergies de α de 5,3 MeV provenant du ^{210}Po [9].

Pour le ^{238}Pu (E_α = 5,5 MeV) nous avons pris: $R_0 = 14 \pm 1$ n/10^6. Pour un mélange composé de n éléments, le rendement neutronique R_n est défini par:

$$R_n = \sum_{k=1}^{n} R_{0k} \frac{N_k \; S_k}{\sum_{i=1}^{n} N_i \; S_i}$$

où R_{0k} est le rendement en cible épaisse du kième élément, N_k est le nombre relatif d'atomes et S_k son pouvoir d'arrêt atomique relatif à l'air. Pour une source de ^{238}Pu contenant des traces de fluor, nous avons avec S_{Pu} = 4,6 et S_F = 1,14

$$R = 13 \cdot 10^{+4} \quad \frac{N_F}{N_{Pu}} \text{ (n/s)/Ci}$$

Si nous avons une concentration de fluor de un ppm en masse, la source de 155 mg de ^{238}Pu émettra 4,3 n/s. L'énergie moyenne de ces neutrons est de l'ordre de 1,5 MeV, voisine de l'énergie moyenne des neutrons de fission.

CONCLUSION

Cette étude a permis de sélectionner les conditions d'irradiation dans un réacteur afin d'obtenir un plutonium-238 de qualité isotopique biomédicale:

- utilisation d'un réacteur qui possède un flux bien thermalisé: réacteur à eau lourde ou éventuellement à graphite, ceci afin de diminuer les réactions (n, 2n);
- optimisation de la place de l'échantillon de ^{237}Np dans le réacteur, assez loin des éléments combustibles et surtout assez loin de la cuve du réacteur afin de diminuer les réactions (γ, n);
- définition de la géométrie et de la composition des cibles; un composé Np O_2C semble préférable à un composé NpO_2Al.

En outre, il est important de considérer le problème des traces des éléments légers dans le plutonium-238 et particulièrement les traces de fluor dans l'évaluation de la dose neutronique.

REFERENCES

[1] ALAIS, M., BERGER, R., BOUCHER, R., LAURENS, P., Générateur isotopique au plutonium-238 pour stimulateur implantable électro-systolique (G.I.P.S.I.E.), Bull. Inf. Sci. Tech. (Paris) N° 142 (nov. 1969) 31-38.

[2] DEVILLERS, C., HOT, M., «Dose biologique autour d'un stimulateur cardiaque», Compt. Rend. 2e Symp. Int. sur l'énergie d'origine radioisotopique (Madrid, 1972), OCDE (21 janv. 1973) 859-73.

[3] BERGER, R., DUCASSE, G., KOEHLY, G., PARADIS, G., «Le programme de production du ^{238}Pu et du ^{244}Cm au Commissariat à l'énergie atomique», Ibid., p.31-47.

[4] GERVAISE, F., DE SCHEEMAECKER, J., Production de ^{238}Pu de qualité médicale, Interprétation des expériences EL3 1972, CEA, Rapport interne DPRMA/SERMA/R n° 89 (sept. 1972).
[5] RIBON, P., Sections efficaces de la réaction ^{237}Np (n, 2n) ^{236}Np, CEA, Rapport interne DPhN/MF n° 533/72 (déc. 1972).
[6] VEYSSIERE, A. et al., Nucl. Phys. A199 (1973) 45.
[7] LE COQ, G., VEYSSIERE, A., Mesure des sections efficaces photonucléaires pour le ^{237}Np et évaluation de la section efficace de formation de l'état 1- du ^{236}Np, CEA, Rapport interne DPhN/MF n° 532/72 (déc. 1972).
[8] KREBS, J., Neutrons et rayons gamma émis par un échantillon de ^{238}Pu contenant des traces de fluor, CEA, Rapport interne DPhN/MF n° 880/71 (oct. 1971).
[9] SEGRE, E., WIEGAND, C., Los Alamos Scientific Laboratory Report MDDC-185 (1944).

DISCUSSION

A.H.W. ATEN (Chairman): How long will the production of ^{230}Pu from ^{237}Np be important and when will the production from ^{242}Cm take over?

G. LE COQ: I shall ask Mr. Berger, one of the co-authors of our paper, to reply to this question.

R. BERGER: The production of ^{238}Pu by disintegration of ^{242}Cm, which is itself formed by neutron irradiation of ^{241}Am, is still only in the experimental stage. Several years will be required before it reaches the semi-industrial stage and it is not obvious that it will be able to meet all future ^{238}Pu requirements. Moreover, it is likely that the ^{238}Pu so obtained will be considerably more expensive than that provided by neutron irradiation of ^{237}Np.

NUCLEAR DATA AND NEUTRON ACTIVATION ANALYSIS OF BIOLOGICAL SAMPLES

N. M. SPYROU
Radiation Unit, Department of Physics,
University of Surrey,
United Kingdom

Abstract

NUCLEAR DATA AND NEUTRON ACTIVATION ANALYSIS OF BIOLOGICAL SAMPLES.

The application of activation analysis in the life sciences, environmental studies and industry has increased to such an extent that the technique has been introduced to undergraduates at this University in the form of short-term inter-disciplinary projects. Further it is predicted that the growth area of routine application will be in the bio-medical field and therefore activation analysis is included in certain postgraduate courses, e.g. Clinical Biochemistry, Radiation Studies and Medical Physics. However, this has highlighted several problems which arise mainly from the short period of time available for training in the technique and the multidisciplinary background of the students.

It is suggested that part of the solution lies in a more suitable presentation of nuclear data which will enable the untrained analyst to reach a quick decision as to the procedure he is to follow for the determination of the required elements in a sample.

An illustration is given in which nuclear data are used with particular reference to the analysis of biological material. Comments are included on the specific areas where uncertainties exist or greater accuracy is required in nuclear data.

This paper therefore attempts, by looking to the future, where, for example, in a hospital department routine analyses are undertaken, to provide an approach which will facilitate use of the technique by those who are not radiation scientists.

Introduction:

The application of activation analysis in the life sciences, environmental studies and industry, has increased to such an extent over the past few years that an attempt is being made at this University to introduce the technique to students in several disciplines, at both undergraduate and postgraduate levels. The short period available for training and the multidisciplinary background of the students has highlighted several problems. The accessibility and presentation of nuclear data is one.

Although the remarks below are general, emphasis is laid on the application of activation analysis to biological samples. It is our belief that this is going to be the main growth area in the field and, in particular, stimulated by concern with the problems of environmental health, the measurement of trace elements will be predominant.

The majority of the work with biological media in neutron activation analysis has been concerned, from early days [1,2], with evaluation of the role of trace elements in biological metabolism and their relationship with deficiency diseases and toxicity effects. Schwarz has recently indicated [3] the elements which are likely to come under consideration for essentiality and thus require determination in biological matrices, table I. From a bibliographical survey compiled by J. De Donder [4], using published

TABLE I. TRACE ELEMENTS UNDER CONSIDERATION FOR ESSENTIALITY IN THE MAMMALIAN ORGANISM AND THE NUMBER OF REFERENCES IN NEUTRON ACTIVATION ANALYSIS ASSOCIATED WITH THEIR DETERMINATION (TO 1968)[a]

Bulk elements	H 4/16	C 10/102	N 22/102	O 64/84	Na 134/381	Mg 37/121	P 91/256
	S 37/146	Cl 103/313	K 61/173	Ca 58/148			
Essential trace elements (1972)	F 21/121	Si 15/185	V 58/190	Cr 57/257	Mn 144/452	Fe 78/325	Co 96/416
	Cu 168/647	Zn 127/357	Se 59/187	Mo 49/207	Sn 12/85	I 64/145	
Under special consideration	Li 1/55	Be 0/87	B 6/111	Al 45/128	Ti 20/99	Ge 2/27	As 113/433
	Br 95/205	Rb 47/116	Sr 64/140	Ag 38/256	Cd 36/161	Sb 63/335	Cs 32/109
	Ba 47/139	W 29/189	Au 84/344	Hg 69/146	Pb 3/34		Ni* 27/217

* effects demonstrated 1972

[a] figures indicate the numbers of references the element has been determined in a biological matrix to that in all other matrices.

sources up to 1968, the number of references associated with these elements in biological and other matrices have been counted and included in the same table. Table IIa shows a more recent survey (1969-1971), presented by Bowen [5], of papers on activation analysis in Biology and table IIb gives a breakdown of these into the number of elements studied per paper.

In the period 1969 to 1972, as we have reported elsewhere [6], 27 projects, varying in length from a term's work to over three years, have been carried out by our students; these can be divided into subjects as shown in table III. A similar pattern emerges, in a wider context, when irradiation certificates, issued at the University of London Reactor Centre over the past six years, are examined (see table IVa). The upsurge in the use of irradiation facilities at the Reactor Centre for activation analysis (as opposed to say radiation damage studies), has created a demand which, despite plans for another fast irradiation tube, may be difficult to meet if a substantial proportion of the time available for in-core irradiations continues to be allocated to "long irradiations". This surprisingly to me is the trend as seen in table IVb. The need for neutron irradiation facilities will not diminish. Therefore, we have decided to concentrate our efforts in measuring quantitatively short-lived isotopes of the elements of interest, wherever possible. This suggests the closer examination of both rapid radiochemical and instrumental techniques of analysis. We have gravitated preferentially towards the latter and one facet we are in the process of investigating [7] further is the technique of cyclic activation [8,9].

TABLE IIa. ACTIVATION ANALYSIS IN BIOLOGY, 1969-1971

Subject	No. of papers
Animal tissues	47
Plant tissues	18
Toxicology	9
Clinical Medicine	9
In vivo analysis	3
Biochemistry	4
Reviews	3

Content of 71 papers

TABLE IIb. NUMBER OF ELEMENTS STUDIED PER PAPER

No. of elements	0	1	2	3	4-24	total
No. of papers	3	44	10	2	12	71

TABLE III. NUMBER OF PROJECTS IN NEUTRON ACTIVATION AT THE UNIVERSITY OF SURREY (1969-1972)

Subject	No. of projects
Basic neutron physics	2
Instrumentation	3
Dosimetry	3
Industrial material analysis	3
Geology survey	2
Environmental pollution (air + water)	2
Trace elements in food	3
Toxicology	1
Mammalian (tissue, blood, excreta)	8
Total	27

TABLE IVa. NUMBER OF IRRADIATION CERTIFICATES ISSUED BETWEEN 1967-1972[a] AT THE UNIVERSITY OF LONDON REACTOR CENTRE

Year	1967	1968	1969	1970	1971	1972	total
No. of Irradiation Certificates	8	11	9	34	70	71	203
No. in Biological Work	3	2	1	11	24	29	70
% in Biological Work	37	18	11	32	34	41	34.5

[a] Year ending January 1973

TABLE IVb. DISTRIBUTION OF IRRADIATIONS REQUIRING LONG AND SHORT PERIODS 1971 and 1972

Long irradiations $\geq$ 1 day or 8 hours; short irradiations $\leq$ 1 hour

	All irradiations		in Biological Work	
Year	% long	% short	% long	% short
1971	40	60	54	46
1972	57	43	59	41

The Sensitivity Factor:

Introduction to activation analysis is "simple", the student, together with lectures, is given a list of references from which he can unearth nuclear data information which might prove useful, retrospectively, for the accomplishment of his project. Over the years the most popular sources have been the following:

(i) The Nuklidkarte [10]
(ii) The Table of Isotopes [11]
(iii) The Activation Analysis Handbook by Koch [12]

Further since irradiation in the majority of the projects is by neutrons and isotope identification by gamma-ray spectrometry, the following compilations are used:

(iv) The catalogues on Scintillation Spectrometry by Heath [13]
(v) The catalogues on Neutron Cross-Sections by the Brookhaven National Laboratory [14]
(vi) The 2nd edition of Applied gamma-ray spectrometry (1970) [15], mainly for its Ge(Li) spectra but to a lesser extent as we have been building our own library of these.

At this stage most students have collated their own reference manual from the above and other sources, for ease of accessibility to the relevant nuclear data. Such a document would then, possibly, include (assuming gamma-ray spectrometry):

(a) Tabular (or graphical) distribution of radioisotopes with increasing half-life ($\tau_{\frac{1}{2}}$),
(b) Tabular (or graphical) distribution of radioisotopes with increasing gamma-ray energy (E_γ), and usually
(c) A nomogram (or nomograph) [16,17], for the calculation of saturation activities of each isotope, achieved after thermal neutron irradiation.

(Note: graphical distributions of (a) and (b) have on occasion been very effective in indicating quickly whether "bunching" and "interference" from other radionuclides occurs in the areas of interest.)

However, it is felt that, with some modification in parameters, (a), (b) and (c) can be combined into one table (or figure) which would cut out a lot of cross-referencing when finer detail is not required. The first steps towards this have been taken by Aliev et al [18] where the distribution of radionuclides is plotted on a $\tau_{\frac{1}{2}} \times E_\gamma$ frame of reference (this combines (a) and (b)).

To introduce the third parameter we should go to the equation representing the observed disintegration rate of a radionuclide, after neutron irradiation,

$$D = \varepsilon\phi m. \frac{N_o f}{A} \sigma \frac{[1 - e^{-\lambda ti}]\ [e^{-\lambda tw} - e^{-\lambda(tw + tc)}]}{\lambda tc}$$

where ε is the absolute detector efficiency
ϕ is the neutron flux (neutrons $cm^{-2}s^{-1}$)
m is the mass of the element (g) in the specimen
N_o is Avogadro's number
f is the fractional isotopic abundance of the target nuclide
A is the atomic weight of the element (g/g- atom)
σ is the reaction (activation) cross-section (cm^2)
λ is the decay constant of the nuclide (s^{-1})
ti is the irradiation time (s)
tw is the period between the end of irradiation and commencement of counting (s)
tc is the counting period (s)

and $\sum = \frac{N_o f}{A} \sigma(cm^2\ g^{-1})$ is the macroscopic cross-section of the target nuclide (or equivalent to the saturation activity per unit mass, per unit flux for a 100% efficient detector).

The parameter $\sum$ is not usually tabulated, the reasons are obvious when one considers the variation of reaction cross-section with neutron energy and therefore the necessary correction to be made for the particular neutron spectrum used in the irradiation. Aliev et al. do compute a macroscopic cross-section for thermal neutrons (2200 ms^{-1}) fission neutrons and 14 MeV neutrons.

TABLE Va. ISOTOPIC SENSITIVITIES FOR ELEMENTS IN MAMMALIAN BLOOD

MeV / $\tau_{\frac{1}{2}}$	0.02 - 0.04	0.04 - 0.06	0.06 - 0.08	0.08 - 0.1	0.1 - 0.2
0.1s - 1m					^{19}O 1.61(-9) ^{77m}Se 6.88(-3)
1 - 10m		^{82m}Br 3.12(-5)		^{79m}Se 5.33(-5)	^{27}Mg 5.07(-7) ^{71}Zn 4.52(-8)
10m - 1h		^{60m}Co 4.08(-3)	^{113m}Sn 8.77(-8)		^{101}Mo 3.02(-5) ^{81m}Se 2.43(-5) ^{111m}Cd 1.99(-5) ^{123m}Sn ? ^{199m}Hg 2.87(-6) ^{125m}Sn 4.09(-5)
1 - 10h	^{80m}Br 4.15(-3)	^{80m}Br 1.38(-5)			^{71m}Zn 4.22(-8)
10h - 1d					^{42}K 2.87(-5) ^{197m}Hg 2.15(-4)
1 - 10d		^{99}Mo 1.52(-5)	^{197}Hg 2.31(-3)		^{47}Ca 2.53(-7) ^{99}Mo 5.32(-5) ^{197}Hg 2.56(-4)
10 - 100d					^{59}Fe 1.20(-6) ^{117m}Sn 3.77(-6)

? indicates data incomplete or only relative intensity known, * isotope produced by reaction other than (n,γ)

Sensitivity is followed by the power of ten in parenthesis

When more than one gamma-ray for the same isotope falls in the same box, the most intense is always quoted.

TABLE Vb. ISOTOPIC SENSITIVITIES FOR ELEMENTS IN MAMMALIAN BLOOD

MeV / $\tau_{\frac{1}{2}}$	0.2 - 0.4	0.4 - 0.6	0.6 - 0.8	0.8 - 1.0
0.1s-1m		^{207m}Pb*	^{38m}Cl 2.08(-5)	
	^{71}Zn 6.53(-8) ^{88}Se ? ^{125m}Sn 4.09(-5) ^{205}Hg ?	^{71}Zn 6.53(-7) ^{86m}Rb 3.05(-4)	^{82m}Br 1.56(-5) ^{83m}Se ?	^{27}Mg 5.64(-5) ^{71}Zn 1.51(-7)
10m-1h	^{81}Se 1.09(-5) ^{111m}Cd 6.24(-5) ^{83}Se 2.90(-6) ^{199m}Hg 8.12(-7)	^{81}Se 6.04(-6) ^{128}I 4.12(-3) ^{101}Mo 1.81(-5) ^{128}I 4.12(-4) ^{101}Mo 2.54(-5)	^{80}Br 2.69(-3) ^{81}Se ? ^{101}Mo 1.33(-5) ^{128}I 5.89(-5)	^{80}Br 1.15(-5) ^{81}Se 4.03(-6) ^{88}Rb 3.06(-5) ^{101}Mo 1.81(-5)
1-10h	^{71m}Zn 4.40(-7) ^{117m}Cd 2.19(-6) ^{93m}Mo 3.46(-6)	^{107}Cd 3.66(-5)	^{71m}Zn 3.04(-7) ^{107}Cd 5.23(-8)	^{56}Mn 1.44(-1) ^{71m}Zn 3.75(-8)
10h-1d	^{69m}Zn 1.28(-4) ^{197m}Hg 3.59(-5)	^{64}Cu 1.17(-2)		
	^{99}Mo 7.60(-6) ^{125}Sn 3.62(-11) ^{115}Cd 2.78(-6) ^{197}Hg 1.92(-5) ^{115}Cd 9.28(-6) ^{203}Pb*	^{47}Ca 2.00(-8) ^{115}Cd 4.64(-5) ^{82}Br 7.36(-4) ^{115}Cd 1.21(-4) ^{99}Mo 9.12(-5) ^{198}Au 2.87(-1) ^{125}Sn 4.82(-11) ^{203}Pb*	^{82}Br 9.25(-4) ^{198}Au 3.02(-3) ^{203}Pb*	^{47}Ca 2.00(-8) ^{82}Br 2.79(-4) ^{125}Sn 1.81(-10)
10-100d	^{51}Cr 7.25(-5) ^{59}Fe 1.41(-7) ^{203}Hg 2.76(-4)	^{115m}Cd 1.92(-7)		^{115m}Cd 1.18(-6)

TABLE Vc. ISOTOPIC SENSITIVITIES FOR ELEMENTS IN MAMMALIAN BLOOD

MeV / $\tau_{\frac{1}{2}}$	1.0 - 1.2	1.2 - 1.4	1.4 - 1.8	1.8 - 2.5	>2.5
0.1s-1m	^{207m}Pb*	^{19}O 9.51(-10)	^{20}F 3.17(-4)		^{16}N 3.77(-11)
1-10m	^{27}Mg 2.48(-5) ^{66}Cu 5.00(-4) ^{71}Zn 6.53(-8) ^{83m}Se ?		^{52}V 5.78(-2) ^{82m}Br 9.36(-8)	^{83m}Se ?	^{37}S 3.46(-7) ^{49}Ca 2.72(-5) ^{49}Ca 3.06(-6)
10m-1h	^{101}Mo 3.02(-5) ^{101}Mo 1.33(-5)	^{60m}Co 4.85(-4) ^{80}Br 1.92(-5) ^{88}Rb 3.23(-6)	^{38}Cl 1.07(-3) ^{101}Mo 1.33(-5)	^{38}Cl 7.15(-4) ^{88}Rb 4.95(-5) ^{101}Mo 1.81(-5)	^{88}Rb 2.47(-6) ^{88}Rb 5.42(-5) ^{88}Rb 7.54(-7)
1-10h	^{71m}Zn 1.87(-8)	^{31}Si 4.64(-8)	^{117m}Cd 7.31(-7) ^{93m}Mo 5.97(-6)	^{56}Mn 2.19(-2) ^{117m}Cd 1.83(-6)	^{56}Mn 1.46(-3)
10h-1d		^{24}Na 3.41(-3) ^{64}Cu 1.54(-4)	^{42}K 2.87(-3)	^{42}K 7.98(-6)	^{24}Na 3.41(-3)
1d-10d	^{82}Br 3.23(-4) ^{125}Sn 1.69(-9) ^{198}Au 6.04(-8)	^{47}Ca 2.57(-7) ^{82}Br 2.90(-4)	^{82}Br 1.90(-4) ^{125}Sn 1.69(-11)	^{125}Sn 7.23(-11) ^{82}Br ?	^{125}Sn 6.03(-12)
10-100d	^{59}Fe 2.39(-5) ^{86}Rb 1.79(-4)	^{59}Fe 1.88(-5)			

TABLE VI. ELEMENTS PRESENT IN MAMMALIAN WHOLE BLOOD [19] INCLUDING NON-ESSENTIAL ELEMENTS WITH TOXIC EFFECTS, SOMETIMES FOUND IN BIOLOGICAL MEDIA

Bulk mgl^{-1}	O 775000	C 94200	H 98000	N 33000	Cl 2900	S 2040	Na 1990
Bulk mgl^{-1}	K 1690	P 370	Ca 62	Mg 41			
Trace $>mgl^{-1}$	Fe 475	Zn 6.5	Si 4.0	Cu 1.07	Other $>mgl^{-1}$	Br 4.6	Rb 2.7
Trace $<mgl^{-1}$	I .063	Mn .026	Mo .0041	Co .00033	Cr .026?	V .017?	F .36
Trace $<mgl^{-1}$	Se .27	Sn .13?					
Toxic $<mgl^{-1}$	Hg .0065	Pb .27	Au .00004	Cd .0074			

In the case of a radionuclide with more than one gamma-ray then the observed counts in the photopeak area per unit counting time (tc), for each gamma-ray energy will be given as:

$$D_p = \varepsilon\phi m. \frac{N_o f}{A} \sigma I (1 - e^{-\lambda ti}) \left\{ \frac{e^{-\lambda tw} - e^{-\lambda(tw + tc)}}{\lambda tc} \right\}$$

where I is the absolute intensity of the gamma-ray i.e. the number of photons/100 disintegrations of the radionuclide. Therefore the isotopic sensitivity for that particular energy

$$S = \frac{N_o f \sigma . I}{A} = \sum I \quad .$$

The isotopic sensitivity, S, is the third parameter we feel should be included in tabulations together with $\tau_{\frac{1}{2}} \times E_\gamma$ for each radionuclide and the format may follow that shown in tables Va,b, and c. Although we expect to prepare such tabulations in the future, here, only a small number of elements, commonly found in biological samples and specifically those of interest in mammalian blood are considered.

Data for mammalian blood samples:

Table VI shows the elements in mammalian whole blood, together with trace elements which may be present and other non-essential elements with toxic effects which are sometimes found in biological media [19].

TABLE VII. DATA FOR THERMAL NEUTRON ACTIVATION ANALYSIS: AN EXAMPLE

Isotope	f%	σ(barns)	$\sum(cm^2 g^{-1})$	Daughter	$\tau_{\frac{1}{2}}$	E_γ(keV)	$\simeq I_\gamma$ %	S_γ	E_e(keV)	$\simeq I_e$%
$^{58}_{26}Fe$	0.33	1.2	4.27(-5)	^{59}Fe	45d	143	0.8	3.42(-7)		
						192.5	2.8	1.20(-6)		
						335	0.3	1.41(-7)		
						1098.6	56	2.39(-5)		
						1291.5	44	1.88(-5)		
$^{59}_{27}Co$	100	19	1.94(-1)	^{60m}Co	10.47m	58.5	2.1	4.08(-3)	51	86
				99%↓		1332.4	0.25	4.85(-4)	58	19
		18		^{60}Co	5.258a	1173.1	100			
						1332.4	100			

Note: Only (n,γ) reactions have been considered

E_e is the internal conversion electron energy

I_γ and I_e are the approximate absolute intensities of gamma-rays and conversion electrons

Sensitivities for gamma-spectrometry, S_γ, are not calculated for "long lived" isotopes.

The following points have been taken into account in drawing up the data sheets for the radionuclides formed by neutron capture.

(i) The tables are for (n,γ) produced radionuclides and the thermal neutron cross-sections quoted are for neutrons with a velocity of 2200 ms^{-1}, unless otherwise indicated.

(ii) The main gamma-ray energies of the radionuclide as well as those of less intense gamma-rays are listed and the criteria for inclusion of a particular gamma-ray energy is its isotopic sensitivity, S, and its position in the $E_\gamma \times \tau_{\frac{1}{2}}$ frame of reference. (Under certain conditions the signal to background ratio may be more favourable for the less intense gamma-ray.)

(iii) Although we expect the data to be used with Ge(Li) and NaI detectors, the recent emergence of low-energy photon detectors has allowed us to include certain energies which may be more suitably measured by the latter thus extending the range of instrumental analysis, despite special requirements in the preparation of samples to overcome self-absorption. (Perhaps one should start constructing tables for low energy gamma-rays and X-rays arising from neutron activation.)

(iv) Due to reasons set out in the introduction, very long-lived isotopes are excluded unless the product of isotopic sensitivity, corrected for saturation, and concentration in the biological matrix is significant.

(v) Gamma-rays of radioactive species with unknown intensities or only relative intensities are if considered important clearly identified, otherwise they are excluded.

The following references were used for the compilation in addition to [11], [12], [14] and [18]:

(a) Neutron Activation Analysis by D. De. Soete et al. [20]
(b) (i) Table of principal gamma-rays from radioactive species.

(ii) Table of radioactive species arranged according to half-life. Both listed by Tannila and Kantele [21], [22].

The format of the information required for neutron activation analysis is illustrated in table VII. Here only iron and cobalt are used as examples. Tables V a,b and c indicate on a $E_\gamma \times \tau_{\frac{1}{2}}$ matrix the radioactive species formed and their isotopic sensitivities. Finally in table VIII we have listed those radioactive isotopes which emit internal conversion electrons. The reason for this is twofold: (1) this provides an alternative spectrometric method of measuring radioactive species and (2) since some gamma-ray intensities are indirectly determined from the measurement of the internal conversion electrons, this may highlight an area for improvement in the search for greater accuracy in the data. We have measured with a modest silicon, lithium drifted, semiconductor detector of 50 mm^2 sensitive area and thickness 3 mm, low level activities of ^{137}Cs on filter paper down to about 8pCi for a 30 hour run [23], which compares very favourably with more complex Ge(Li) -NaI coincidence systems.

Discussion:

Although the introduction of isotopic sensitivity, S, will facilitate the reading of nuclear data in activation analysis, the logical extrapolation is to replace this factor by a detection limit for each gamma-ray

TABLE VIII. ISOTOPES EMITTING INTERNAL CONVERSION ELECTRONS. (ELEMENTS IN TABLE VI ONLY CONSIDERED WITH $\tau_{\frac{1}{2}} < 100d$)

Isotope	$\tau_{\frac{1}{2}}$	Ee(keV)	Ie%	Isotope	$\tau_{\frac{1}{2}}$	Ee(keV)	Ie%
^{51}Cr	27.8d	315	<<1	^{113m}Sn	20m	50	57
^{60m}Co	10.47m	51	86			75	34
		58	19	^{117m}Sn	14.0d	130	>8
^{64}Cu	12.75h	1330	<<1			155	>4
^{69m}Zn	13.7h	429	5	^{123m}Sn	40.3m	130	?
^{77m}Se	17.7s	148	40				
		160	10	^{198}Au	2.696d	329	3
^{79m}Se	3.5m	83	63			398	1
		95	22	^{197m}Hg	23.8h	51	21
^{81m}Se	57m	90	72			82	52
		102	20			120	
^{80m}Br	4.42h	24	58	^{197}Hg	64.1h	64	?
		36	?			74	?
		47	?	^{199m}Hg	43m	75	21
^{82m}Br	6.1m	33	80			144	36
		44	35			285	
^{93m}Mo	6.95h	244	29			354	
		261	10	^{203}Hg	46.6d	194	13
^{100m}Mo	14.6m	170	9			264	5
^{111m}Cd	48.6m	123	50			275	
		146	24	$^{203}Pb^{*}$	52.1h	193	14
						264	3

? either insufficient data or only relative intensities known
* isotope produced by reaction other than (n,γ)

energy of the radionuclides in question. There are various interpretations of the term detection limit [24] but none should be considered unless the background matrix due to gamma-rays from other radioactive species present (and other gamma-rays from the same radionuclide) are taken into account.

The main background matrix when measuring trace elements in biological samples (blood, urine, tissue etc.) arises from the radiations of sodium and chlorine (to a lesser extent from phosphorus). These bulk elements have concentrations in biological samples which are well known. "Background spectra" (either generated by computer or recorded in a practical situation)

TABLE IX. DETECTION CHARACTERISTICS OF A 100 cm^3 Ge(Li) AND A 7.5 cm BY 7.5 NaI (Tl) INSIDE A 15 cm STEEL SHIELD

Characteristic	Energy Resolution (keV)	Absolute Efficiency	Background 500-2500 keV	Minimum Detectable Activity
Ge(Li) 662 keV	2.2	0.014	108 counts	9.5 cpm
1333 keV	2.8	0.0071	24 counts	14.5 cpm
NaI(Tl) 662 keV	49	0.118	9920 counts	10.5 cpm
1333 keV	99	0.063	3600 counts	12.1 cpm

tc = 600 minutes and precision 0.2

can then be constructed, for the specific irradiation and counting conditions, and used for the determination of detection limits. A useful definition for the latter is the one suggested by Walford and Gilboy [25] called the minimum acceptable activity which is that source activity which just allows the desired precision to be achieved in a given counting time. The quantity is obviously both background dependent and energy dependent. This can be seen in table IX where a 100 cm^3 Ge(Li) and a 7.5 cm dia by 7.5 cm NaI(Tl) are compared, albeit for a low level counting experiment inside a 15 cm steel shield with long counting times, 600 min, and 0.2 precision. (Precision is defined as the ratio of the standard deviation of the net peak counts of interest to the net peak counts.) This result applies only to isolated peaks on a smooth background continuum and any increase in spectral complexity or variation of background matrix with time would alter significantly the value of minimum acceptable activity.

Conclusions:

In conclusion therefore the following points are made:

(i) University students are being trained in techniques of activation analysis because application of these has become common in biomedical and environmental fields. There is a need therefore for a manual which incorporates the salient features of present publications in a more accessible form. This publication must be directed at the user who is not interested in nuclear data per se.

(ii) Economic necessity demands the determination of elements, wherever possible, by the measurement of short-lived isotopes. Long irradiations and handling will still be necessary and important in specific areas of research but for routine analyses one must be realistic and set practical detection limits and turn-around times for each sample.

(iii) The sensitivity factor has been calculated here for a small number of isotopes undergoing (n,γ) reactions. Sensitivities for other neutron reactions and other neutron energies should be computed wherever these are significant.

(iv) Detection limits for less intense radiations may be lower than for those for the main radiation energy. Thus it is important to have accurate data for absolute intensity of both gamma-rays and internal conversion electrons.

(v) A likely development in the future with the advent of mini-reactors, greater quantities of ^{252}Cf and larger numbers of accelerating machines used in hospitals is the provision of routine analytical services by regional hospital centres. Here with a section specifically treating the activation analysis of biological samples a manual of the type mentioned above will come into its own.

Finally it is to examine, amongst other things, such topics that a Nuclear Activation Group is being formed in the U.K., constituted of members from universities, medical schools and other institutions of higher education.

Acknowledgements:

I would like to thank my colleague, Dr. W.B. Gilboy, for his willingness to be drawn into lengthy discourses and his critique of the work; Mr. G. Burholt, Reactor Manager, for supplying the reactor users' raw data of the University of London Reactor Centre; and all the students, too numerous to mention, who one way or another influenced the content of this paper.

References:

[1] SMALES, A.A., Neutron activation analysis, Symposium on Trace analysis, New York Academy of Medicine, ed. J.H. Yoe and J.H. Koch, John Wiley and Sons, Inc. (1955).

[2] MEINKE, W.W., Trace element sensitivity: comparison of activation analysis with other methods, ibid.

[3] SCHWARZ, K., The role of trace elements in health and disease processes in man and animals, IAEA Symposium on Nuclear Activation techniques in the Life Sciences, Bled, Yugoslavia (April, 1972).

[4] DE DONDER, J., Bibliographical Survey of Neutron Activation Analysis, Chapter 12, Neutron Activation Analysis - D. De Soete, R. Gijbels and J. Hoste, Wiley-Interscience (1972).

[5] BOWEN, H.J.M., The biochemistry of trace elements, IAEA Symposium on Nuclear Activation techniques in the Life Sciences, Bled, Yugoslavia, (April, 1972).

[6] GILBOY, W.B. and SPYROU, N.M., Applications of Neutron Activation Analysis, Reactor Technology and Training Conference, University of Aston, Birmingham (April, 1972).

[7] OZEK, F., Cyclic activation and its applications, M.Sc. thesis, University of Surrey (January, 1973).

[8] CALDWELL, R.L., MILLS, W.R., ALLEN, L.S., BELL, P.R. and HEATH, R.L., Science, 152, 457 (1966).

[9] CALDWELL, R.L., MILLS, W.R. and GIVENS, W.W., Nuclear Instruments and Methods, 80, 95 (1969).

[10] SEELMANN-EGGEBERT, W., PFENNIG, G. and MÜNZEL, H., Chart of the Nuclides, Der Bundesminster für Wissenschaftafliche Forsehung, Bonn, 2nd edition (1968).

[11] LEDERER, C.M., HOLLANDER, J.M. and PERLMAN, I., Table of Isotopes, Sixth edition, John Wiley and Sons, Inc. (1968).

[12] KOCH, R.C., Activation Analysis Handbook, Academic Press (1960).

[13] HEATH, R.L., Scintillation Spectrometry, gamma-ray spectrum catalogue, Vols. I and II, 2nd edition, USAEAC Rep, IDO-16880-1, (1964).

[14] STEHN, J.R. et al., Neutron Cross Sections, USAEAC Rep. BNL-325, 2nd edition (1965).

[15] CROUTHAMEL, C.E., Applied gamma-ray spectrometry, Pergammon Press, Oxford, 1960; 2nd edition by F. Adams and R. Dams, 1970.

[16] FREILING, E.C., Nomogram for radioactivity induced in irradiation Nucleonics, Nucleonics, 18, 12 (1966).

[17] ROUTTI, J.T., Graphical technique for estimating activity levels produced in thermal and fission neutron irradiations, Analytical Chemistry, 40, 3, p.593, (March, 1968).

[18] ALIEV, A.I., et al. Handbook of Nuclear Data for Neutron Activation Analysis, Israel Program for Scientific Translations, Jerusalem (1970).

[19] BOWEN, H.J.M., Trace elements in biochemistry, Academic Press (1966).

[20] DE SOETE, D., et al., Neutron Activation Analysis, Vol. 34 on Chemical Analysis, ed. P.J. Elving and L.M. Kolthoff, Wiley-Interscience (1972).

[21] TAMILA, O., and KANTELE, J., Table of Principal Gamma-rays from Radioactive species, University of Jyväskylä, Research Report 3/1969 (August, 1969).

[22] TAMILA, O., and KANTELE, J., Table of Radioactive Species, Increasing half-life, University of Jyväskylä, Research Report, 2/1969 (February, 1969).

[23] LAMBERT, R.A. and GILBOY, W.B., private communication.

[24] CURRIE, L.A., Limits for qualitative detection and quantitative determination, Analytical Chemistry, 40, 3, (March, 1968).

[25] WALFORD, G., and GILBOY, W.B., Fundamentals of sensitivity limits in low level counting, International Conference on the Natural Radiation Environment II, Houston, Texas (August, 1972).

LES CONSTANTES NUCLEAIRES DANS LES PHARMACOPEES

Leur utilité pour la normalisation des substances pharmaceutiques

Y. COHEN
CEA, Centre d'études nucléaires
de Saclay, France

Abstract–Résumé

NUCLEAR CONSTANTS IN PHARMACOPOEIAS; THEIR USEFULNESS IN THE STANDARDIZATION OF PHARMACEUTICAL SUBSTANCES.

The radioelements administered to man are considered by national and international authorities (Council of Europe, World Health Organization) to be medicinal preparations. As such, they appear in national, regional and international pharmacopoeias under the heading "radiopharmaceutical substances". The preparation of monographs by groups comprising physicists, doctors and pharmacists has shown that it is often necessary to refer to precise nuclear constants, for pharmacopoeias are acquiring regulatory and legislative force, whereby they may be quoted in courts of law. Mention is made in such monographs of national radioactivity metrology laboratories which provide standards to which reference is made in the standardization of "radiopharmaceutical substances" as regards the radionuclide purity, concentration of the principal radionuclide and radioactive concentration. These monographs indicate the radioactive half-life, the nature of the radioactive emissions and the most characteristic radiations (with their energies). They also indicate what parasitic radionuclides accompany the principal radionuclide and establish upper limits for the concentration of such parasites. Such information requires the establishment of tables of generally accepted nuclear constants, which will be possible only if metrology laboratories collaborate. Such laboratories could furnish the authors of monographs with physical data for inclusion in the pharmacopoeias when periodic revisions are made. A standardization of nuclear constants and co-ordination of the work of different laboratories would be useful in the case of all radionuclides.

LES CONSTANTES NUCLEAIRES DANS LES PHARMACOPEES; LEUR UTILITE POUR LA NORMALISATION DES SUBSTANCES PHARMACEUTIQUES.

Les radioéléments administrés à l'homme sont considérés par les autorités nationales et les instances internationales (Conseil de l'Europe, Organisation mondiale de la santé) comme des médicaments. A ce titre, ils sont inscrits aux pharmacopées nationales, régionales ou internationales sous la rubrique de «substances radiopharmaceutiques». L'élaboration des monographies par des groupes réunissant des physiciens, médecins, pharmaciens, a montré la nécessité de se référer à des constantes nucléaires précises car les textes des pharmacopées acquièrent un caractère réglementaire et législatif, susceptible d'une utilisation devant les tribunaux. Il est fait mention, dans les monographies, de laboratoires nationaux de métrologie de la radioactivité qui fourniraient les étalons auxquels se référeraient les praticiens lors de la normalisation des «substances radiopharmaceutiques» quant à la pureté radionucléidique, la teneur en radionucléide principal, la concentration radioactive. Les monographies indiquent la période radioactive, la nature des émissions et les rayonnements les plus caractéristiques ainsi que leur énergie. Elles signalent les radionucléides parasites qui accompagnent le radionucléide principal et établissent une limite à leur présence. Ces précisions ne se conçoivent pas sans l'établissement de tableaux de constantes nucléaires généralement acceptées et dont la mise à jour demande un travail de concertation entre les laboratoires de métrologie. Ces derniers fourniraient aux rédacteurs des monographies les données physiques qui seraient alors introduites dans les pharmacopées lors des révisions périodiques. Pour tous les radionucléides une homogénéisation des constantes nucléaires et une coordination entre les divers laboratoires paraissent utiles.

Les radioéléments destinés à l'usage médical sont considérés comme des médicaments et à ce titre doivent présenter des critères de qualité définis par les pharmacopées. Celles-ci constituent des recueils de monographies dans lesquelles sont indiquées les propriétés physico-chimiques et les méthodes de vérification de ces propriétés.

La pharmacopée internationale publiée par l'Organisation mondiale de la santé, la pharmacopée européenne rédigée par des groupes de travail du Conseil de l'Europe, les pharmacopées nationales: américaine, britannique, française, etc..... décrivent plusieurs substances radio-pharmaceutiques. On désigne par substance radiopharmaceutique les molécules minérales ou organiques qui contiennent un ou plusieurs atomes radioactifs. Ainsi, alors que l'iodure de sodium ^{131}I est un exemple de molécule minérale relativement simple, la sérum-albumine humaine marquée à l'iode radioactif est une molécule organique de grande complexité. L'iode radioactif devra présenter dans les deux cas des constantes nucléaires identiques, ne pas être souillé par un autre radioisotope ou même par un radionucléide de nature chimique différente.

Nous avons réuni dans le tableau I les substances radiopharmaceutiques les plus utilisées et qui de ce fait ont été inscrites à plusieurs pharmacopées. Tel est le cas du chromate de sodium ^{51}Cr, de la cyanocobalamine au cobalt-57 ou 58, du citrate de fer ^{59}Fe, de la sérum-albumine marquée à l'iode-125 ou à l'iode-131, de l'iodohippurate ^{131}I de sodium, du rose bengale marqué à l'iode-131, des solutions d'iodure ^{125}I ou ^{131}I, de la chlormérodine marquée au mercure-197, du phosphate ^{32}P de sodium et de l'or colloïdal ^{198}Au.

Lorsque l'on relève dans les monographies les constantes nucléaires citées on en trouve en général deux: la période radioactive et l'énergie du photon gamma le plus caractéristique. Les chiffres cités dans les pharmacopées que nous avons examinées (tableau II) sont en bonne concordance pour le chrome-51, le cobalt-57, le cobalt-58 et l'or-198. On constate une légère différence pour la période radioactive de l'iode-131 qui est de 8,0 j ou de 8,08 j suivant les monographies, pour le photon gamma le plus caractéristique de l'iode-125 qui est de 0,028 MeV dans la pharmacopée européenne et la pharmacopée internationale et de 0,0355 MeV pour la pharmacopée américaine U. S. P. XVIII. On observe également une légère différence dans l'énergie maximale du rayonnement bêta du phosphore-32 qui est de 1,70 MeV dans la pharmacopée française et de 1,71 MeV dans la pharmacopée américaine ainsi qu'une différence dans la période radio-active: 14,2 j pour les pharmacopées britannique et internationale et 14,3 j pour les autres.

Il est heureux que les divers rédacteurs de pharmacopées se soient accordés sur le choix des données fournies par la littérature scientifique, mais leurs difficultés pour rédiger les nouvelles monographies sont grandes. En effet, on trouve dans la littérature au moins une dizaine de sources différentes de constantes nucléaires qui ne sont pas toujours d'accord non seulement sur l'énergie des rayonnements émis mais également sur leur pourcentage, ce qui explique d'ailleurs que les monographies soient si discrètes à ce sujet.

La détermination d'un spectre à partir de la seule donnée de la monographie est insuffisante pour identifier le radionucléide et a fortiori, pour rechercher les impuretés radionucléidiques qui peuvent se trouver mélangées au radionucléide principal, soit par suite de l'irradiation

TABLEAU I. RADIOELEMENTS INSCRITS DANS LES PHARMACOPEES

	Pharmacopée britannique (1968)	Pharmacopée internationale (1967 et 1971)	Pharmacopée européenne (à paraître)	Pharmacopée française (1965)	U.S.P. XVIII (1970)
Chrome-51					
(chromate)	+	+	+		+
Cobalt-57					
(cyanocobalamine)	+	+	+		+
Cobalt-58					
(cyanocobalamine)	+	+	+		
Fer-59					
(citrate)		+			
Iode-125 (iodure)		+	+		+
sérum-albumine		+	+		+
Iode-131 (iodure)	+	+	+	+	+
iodohippurate	+	+	+		+
sérum-albumine	+	+	+		+
rose bengale		+			+
Mercure-197					
chlormérodine					+
Or-198 (colloïde)	+	+	+	+	+
Phosphore-32 (phosphate)	+	+	+	+	+

TABLEAU II. CONSTANTES NUCLEAIRES CITEES DANS LES MONOGRAPHIES DES PHARMACOPEES

	Pharmacopées				
	britannique	européenne	internationale	française	U.S.P. XVIII
Chrome-51					
Période (j)	27,8	27,8	27,8	-	27,8
Energie (MeV)	γ : 0,32	0,32	0,32	-	0,320
Cobalt-57					
Période (j)	270	270	270	-	270
Energie (MeV)	γ : 0,122	0,122	0,122	-	0,122
Cobalt-58					
Période (j)	71	71	71	-	-
Energie (MeV)	γ : 0,51	0,51	0,51	-	-
	0,81	0,81	0,81	-	-
Iode-125					
Période (j)		60	60	-	60
Energie (MeV)		γ : 0,028	0,028	-	0,0355
Iode-131					
Période (j)	8,0	8,0	8,08	8,0	8,08
Energie (MeV)	γ : 0,36	0,36	0,36	0,364	0,364
Phosphore-32					
Période (j)	14,2	14,3	14,2	14,3	14,3
Energie (MeV)	-	-	-	β : 1,70	1,710
Or-198					
Période (j)	2,7	2,7	2,7	2,7	2,70
Energie (MeV)	γ : 0,41	0,41	0,41	0,41	0,412

neutronique de la cible par réaction nucléaire supplémentaire comme dans le cas de l'or-198 associé à l'or-199, soit par insuffisance d'enrichissement de la cible comme dans le cas du fer-59 associé au fer-55.

Les données relatives à certains radionucléides tel le sélénium-75 mettent les rédacteurs de monographies dans l'embarras. A titre d'exemple nous avons réuni dans le tableau III les constantes nucléaires du mercure-197 et du sélénium-75, relevées dans «Radionuclides in Pharmacology» [1] et dans «Nuclear Data» [2]. On remarque une grande différence: l'une des sources bibliographiques ne donne pas l'abondance en électrons de conversion interne; l'énergy γ et l'abondance en rayonnement gamma ne concordent pas pour le sélénium-75.

TABLEAU III. CONSTANTES NUCLEAIRES DU MERCURE-197 ET DU SELENIUM-75

	Période	Mode de décroissance	Abondance (%)	Energie γ (MeV)	Abondance γ (%)	Abondance en électrons de conversion interne
Mercure						
Référence [1]	65 h	C.E.	100	0,077	19,3	
				0,069	74,5	
Référence [2]	64 h	C.E.	100	0,077	19,3	80,7
				0,069	74,5	
Sélénium-75				0,19	0,5	1,2
Référence [1]	120 j	C.E.	100	0,096	3	
				0,12	15	
				0,14	54	
				0,20	1,5	
				0,27	56	
				0,28	23	
				0,31	1,4	
				0,40	12,5	
Référence [2]	120 j	C.E.	100	0,024	0,03	5,6
				0,066	1,0	0,3
				0,097	3,1	2,7
				0,121	16,4	0,7
				0,136	55,5	1,6
				0,197	1,3	0,03
				0,265	58,6	0,4
				0,280	25,2	0,2
				0,304	1,3	0,1
				0,401	12,9	

On peut penser que les travaux de compilation ont été dans les deux cas menés très sérieusement et cependant ces divergences sont embarrassantes, car les monographies nationales ont, le plus souvent, une valeur juridique contraignante et les données qui y sont inscrites ne devraient pas prêter à discussion.

Les pharmacopées font référence aux laboratoires nationaux de métrologie de la radioactivité qui doivent fournir des étalons pour lesquels sont précisées la pureté radionucléidique et la concentration radioactive.

Ces étalons servent à établir la conformité aux normes de pharmacopée des productions commerciales de radioéléments.

Il serait utile que les méthodes de mesure soient minutieusement décrites pour quelques radioéléments délicats à doser et que les limites d'erreur soient uniformisées grâce à un compromis entre la précision scientifique et l'utilisation pratique. A ce titre un premier effort pourrait consister dans la rédaction d'un ouvrage réunissant les schémas de décroissance, les spectres gamma et les constantes nucléaires des radioéléments inscrits dans les pharmacopées et ceux dont l'utilisation médicale est moins fréquente. L'action qui a été entreprise pour l'aspect chimique de la production des radioéléments et a conduit à la publication par l'AIEA de «Radioisotope production and quality control» [3] devrait être étendu aux constantes nucléaires. Les caractéristiques ainsi décrites autoriseraient un calcul plus précis des doses d'irradiation reçues par les tissus biologiques lors de l'administration des substances radiopharmaceutiques en vue d'une thérapeutique ou d'un diagnostic.

REFERENCES

[1] GLENN, H.J., LAMB, J.F., Radionuclides in Pharmacology, Section 78 of the International Encyclopedia of Pharmacology and Therapeutics (Cohen, Y., Ed.), Pergamon Press (1971) 949.

[2] Nuclear Data 131, 5 (1966); Nuclear Data B 1, 6 (1966).

[3] IAEA, Radioisotope Production and Quality Control, TRS No. 128, IAEA, Vienna (1971).

DISCUSSION

D.J. HOREN: I would like to make a comment and then ask a question of Dr. Cohen. This might be the appropriate session in which to point out that many isotopes used in medicine are contained in the compilation entitled "Radioactive atoms, Auger electrons, alpha, beta, gamma and X-ray data" by M.J. Martin and P.H. Blichert-Toft (Nuclear Data, Part A, 8 1 (1970)). In addition, we have some other isotopes evaluated in the same manner, which are not contained in that publication. I can say that we would welcome any inquiries from medical people on other isotopes which are not so covered, as well as comment on the quality and usefulness of the tabulations in question.

My question to Dr. Cohen is as follows: Is there a problem in the use of these radioisotopes as far as ensuring homogeneity of the actual injected dosage of the isotope is concerned, i.e. once you have it in the solution?

Y. COHEN: The accuracy of the volume withdrawn from the vial is, I would say, ± 10.

D.J. HOREN: But does the radioactivity remain homogeneously distributed throughout the volume? Does it ever plate on to the walls of the container?

Y. COHEN: With carrier-free radionuclides you do have a quantity of the radionuclides which stick to the walls of the container. However, a radiopharmaceutical is for the most part a compound to which a carrier has been added, so you do not have to cope with this question. Accordingly, the solution is homogeneous throughout its volume. The problems are, first, that from one country to another the curie does not always refer to the same quantity of radioactivity. Second, there are a number of radionuclidic impurities that can accompany radiopharmaceuticals. Third, the literature gives different values for various data. So I think it would be necessary for the Agency to issue a compilation of the most widely accepted data in this field, for the use not of physicists but of medical people.

D.J. HOREN: I would agree with this. Such a compilation would be a very useful thing.

M. LEDERER: Where data have important legal implications, or where their accuracy is extremely important, it might be useful to devote a conference (or part of a conference) to establishing "authoritative" best values. Examples of cases for which this has been done are the half-life of ^{14}C and the isotopic abundances of the elements.

Y. COHEN: An example of the legal implications of scientific accuracy is the situation which arises when someone applies to the United States Food and Drug Administration for authorization to use a new radiopharmaceutical. The FDA requires a radiotoxicological assay, which means that he has to calculate the dose delivered to the body. As Professor Kellershohn mentioned in the presentation of his paper (IAEA-SM-170/97), this calculation is related exactly to the percentage and energy of the gamma-rays and electrons being administered. However, when the applicant makes his calculation on the basis of different tables, he ends up with different results and different answers.

The accuracy of data on radiopharmaceuticals depends on the radionuclide involved. One per cent accuracy, which is quite easy to attain, is generally sufficient when you have an impurity. But it might happen that one per mille is required (i.e. 0.1%). This would be the case, for example, with technetium from molybdenum made from fission products. Here the need for accuracy is much greater than with technetium made from irradiated molybdenum and not from fission products. The question is very intricate and there are no simple answers.

APPLICATION OF NUCLEAR DATA IN THE PREPARATION OF RADIONUCLIDES FOR USE IN MEDICINE AND BIOLOGY

R. B. R. PERSSON
Radiation Physics Department,
Lasarettet, Lund,
Sweden

Abstract

APPLICATION OF NUCLEAR DATA IN THE PREPARATION OF RADIONUCLIDES FOR USE IN MEDICINE AND BIOLOGY.

At he IAEA Consultants' Meeting held December 11, 1972, at Studsvik, Sweden, nine experts in various fields of experience gathered in order to exchange information on the application of nuclear data in the preparation of radionuclides for use in medicine and biology. For reactor-produced radionuclides, it was concluded that the averaged thermal neutron cross-sections for the production of all useful radionuclides are required with an accuracy within a few per cent. Accurate decay-scheme data are also needed. Furthermore, cross-section data for the resonance region 5 eV - 1 MeV are not well known for many materials and better information is required. For radionuclide generators, the main problem is to evaluate the best production-techniques for the parent radionuclide and to obtain a daughter nuclide with high radionuclide purity. The data needs to meet these requirements were discussed. Similar data needs for the production of radionuclides by accelerators were discussed. Furthermore, it was suggested to use the number of transformations per particle (R) or its inverse as a standard to express the production yield of radionuclides by charged-particle reactions. Radionuclide production with fast neutrons and photons was also discussed as well as some general problems concerning production-parameters, toxicology etc.

1. INTRODUCTION

In preparation for the IAEA Symposium on Applications of Nuclear Data in Science and Technology to be held in Paris 12 - 16 March, 1973, a preparatory meeting was held on the 11th of December, 1972, at Studsvik, Sweden.

The object of this meeting was to enable the exchange of information on the applications of nuclear data in the preparation of radionuclides for use in medicine and biology.

Nine experts in various fields of experience participated in the meeting[1]. The following subjects were discussed:

Reactor-produced radionuclides,
Generator-produced radionuclides,

[1] Participants:

R. Bergman, Gustaf Werners Institute, Uppsala, Sweden
R. Bodh, AB Atomenergi, Studsvik, Sweden
Y. Cohen, Dept of Radioelements, Saclay, France
H. Condé, Research Institute of National Defence, Stockholm, Sweden (INDC representative)
B. Jung, Radiation Physics Department, Akademiska Sjukhuset, Uppsala, Sweden
B. Persson, Radiation Physics Department, Lasarettet, Lund, Sweden (Scientific Secretary of the meeting)
P. Schmeling, AB Atomenergi, Studsvik, Sweden
K. Svoboda, Nuclear Research Institute, Rez, Prague, Czechoslovak Socialist Republic
T. Wiedling, Institute of Neutron Physics, Studsvik, Sweden

Accelerator-produced radionuclides,
Radionuclide-production with fast neutrons,
Use of medical betatrons for photon-activation,
Other data important for the preparation and use of radionuclides in medicine and biology,
Summary, conclusion and requests.

2. REACTOR-PRODUCED RADIONUCLIDES

The most commonly used reactor-produced radionuclides for medical and biological research are ^{14}C, ^{3}H, ^{32}P, ^{125}I, ^{35}S, ^{131}I, ^{51}Cr, ^{59}Fe, ^{203}Hg, ^{45}Ca and, for clinical applications, ^{131}I, ^{125}I, ^{14}C, ^{51}Cr, ^{198}Au, ^{133}Xe, ^{32}P, ^{3}H, $^{99}Tc^{m}(^{99}Mo)$, ^{59}Fe, ^{75}Se, ^{58}Co, ^{85}Sr, ^{197}Hg, $^{113}In^{m}$, ^{47}Ca.

The following parameters must be considered when producing radionuclides in a reactor:

2.1. Target

It is important to know the isotopic abundance of the different nuclides in the target. It can sometimes be advantageous to irradiate enriched material. For example normal iron has abundances of 5.8% ^{54}Fe, 91.7% ^{56}Fe, 2.2% ^{57}Fe and 0.3% ^{58}Fe. If the Fe-target is enriched to 98% ^{54}Fe, almost pure ^{55}Fe can be produced. On the other hand if the target is enriched to 85% ^{58}Fe, the ^{55}Fe-contamination of the ^{59}Fe produced is only about 5% [1].

2.2. Production cross-sections and reactor-neutron spectra

The most important of the neutron reactions commonly used for activation involve the capture of a thermal neutron with the coincident emission of a gamma ray. The cross-sections at thermal energy of the (n, γ) reactions are fairly well-known. The reactor-neutron spectrum also contains epithermal and fast neutrons which often induce nuclear reactions giving secondary particles other than photons, e.g. $^{32}S(n,p)^{32}P$, $^{14}N(n,p)^{14}C$, $^{40}Ca(n,\alpha)^{37}Ar$, $^{6}Li(n,\alpha)^{3}H$ for which the cross-sections are not well known.

Thus, for radionuclide-production in a reactor, we need neutron-reaction cross-sections as a function of energy for the naturally occurring isotopes and elements, and, in some cases, also for radionuclides. Average cross-sections and yields for reactor-neutron spectra would be helpful as well as information on resonance integrals and yields with and without cadmium covers. Information on flux-density depression corrections is also needed [2]. However, the accuracy in the calculation of the production rate is limited by uncertainties in the shape of the reactor neutron spectrum and in the cross-sections for epithermal and fast neutrons.

2.3. Side products

There are very often resonances in the neutron-capture cross-section and information on resonance-structure is extremely important from the standpoint of radionuclide production. For example, the $^{197}Au(n, \gamma)^{198}Au$-reaction has a resonance at 5 eV and one can prevent the contamination from the secondary thermal neutron-induced reaction $^{198}Au(n, \gamma)^{199}Au$ by wrapping the target with a cadmium foil which absorbs thermal neutrons [1].

The problems of secondary neutron-capture are very important in the production of radionuclides. For example, in the production of ^{125}I(60d) through $^{124}Xe(n,\gamma)^{125}Xe \xrightarrow{EC} {}^{125}I$, the cross-section for the reaction $^{125}I(n,\gamma)^{126}I$(14d) is fairly high 900 b and ^{126}I is an undesirable contamination which should be minimized. It was reported that the production of ^{126}I sometimes is unexpectably high which may indicate a higher cross-section for epithermal neutrons. Secondary capture reactions seriously limit the quality of many radionuclide products.

3. GENERATOR-PRODUCED RADIONUCLIDES

A radionuclide-generator is understood to be a system which periodically makes available a particular radionuclide from a parent radionuclide of longer half-life. About 10 - 15 such radionuclide generators have been designed and constructed for use in medicine and biology [3-6].

The most important nuclear data for production and use of these radionuclide generators are:

Half-lives of parent and daughter radionuclides;
Decay schemes of parent and daughter radionuclides;
Production cross-section for parent and interfering radionuclides.

Nuclear data defining the usefulness of the daughter radionuclide in question for medical scintigraphy and nuclear medicine in general are:

The photon spectrum of the daughter radionuclide, including both γ-energy and emission rates, must be suitable for good detection with fixed and/or mobile systems. The half-life of the parent must be long enough in comparison with the half-life of the daughter to permit a notably longer use of the daughter nuclide.

The electron spectrum of the daughter nuclide must be known and it must enable delivery of a low absorbed dose to the patient per unit of activity.

The following generator systems are most used at present in medical scintigraphy (daughter parent):

$^{99}Tc^{m}(^{99}Mo)$, $^{113}In^{m}(^{113}Sn)$, $^{87}Sr^{m}(^{87}Y)$, $^{68}Ga(^{68}Ge)$, $^{81}Kr^{m}(^{81}Rb)$, $^{137}Ba^{m}(^{137}Cs)$, $^{132}I(^{132}Te)$, $^{188}Re(^{188}W)$.

As an example, $^{99}Tc^{m}$ has the following very favourable nuclear characteristics for use in medical scinitgraphy:

The half-life of 6 h is suitable for most scintigraphic examinations and allows a daily elution of the generator. The gamma-ray energies are almost exclusively 0.14 MeV (0.1405 (94%) and 0.1426 (6%) which make $^{99}Tc^{m}$ very usable) both for scanning devices and gamma cameras. The decay of $^{99}Tc^{m}$ through internal transition does not cause the emission of any corpuscular radiation except conversion and Auger electrons and the internal conversion coefficient is low: $e_K = 0.10$. The radiation-absorbed dose per activity unit is therefore low.

Other examples can also be given to point out different aspects of the use of generator-produced radionuclides. For departments of nuclear

medicine far removed from production and distribution centres, the half-life of 67 h for the parent ^{99}Mo is an important disadvantage.

$^{113}In^{m}$(Sn) generators are much more suited for use in distant areas because the parent ^{113}Sn has a half-life of 115 days. The nuclear data for $^{113}In^{m}$ are not so favourable for scintigraphy as for $^{99}Tc^{m}$ because of the shorter half-life 99.8 min and the higher gamma-energy 0.393 MeV. The gamma energy is, however, very close to that of ^{131}I – 0.364 MeV – so that the same collimator and detection equipment can be used for both radionuclides.

The other radioisotope generators are still at development stage and not widely used in clinical practice. Their use is, however, increasing. For the near future the following generator systems were suggested: $^{72}As(^{72}Se)$, $^{82}Rb(^{82}Sr)$, $^{109}Ag^{m}(^{109}Cd)$, $^{191}Ir^{m}(^{191}Os)$.

The development and use of radionuclide generators can be based on standard nuclear tables such as the Table of Isotopes [7]. The production parameters of most of the parent radionuclides are, however, not well known. Detailed cross-section data and excitation functions for different alternative nuclear reactions for production of the parent radionuclides and eventual contaminants are therefore greatly needed.

4. CYCLOTRON-PRODUCED RADIONUCLIDES FOR BIOLOGICAL AND MEDICAL USE

During the past few years a number of cyclotrons have been installed more or less exclusively for biological and medical purposes. Several medical, biological and biophysical institutions are engaged in projects in which cyclotrons are used for radionuclide-production, activation analysis and radiobiological research. The number of cyclotrons for this purpose will be about 30 by 1975 (Table I) [8, 9].

The characteristics of currently available medical cyclotrons are shown in Table II [9]. As can be seen in this table most of these cyclotrons accelerate protons, deuterons and helium ions up to energies of 15 - 30 MeV and several have capabilities over 50 MeV. Future constructions will probably also accelerate ^{7}Li, ^{12}C, ^{16}O and other heavy ions to useful energies and flux-densities [2].

A summary of cyclotron-produced radionuclides in current use are given in Table III.

To this list can be added a number of radionuclides, which are parents of potential radionuclide-generators.

The use of heavy ions like ^{12}C and ^{16}O will open a quite new and interesting field for both radionuclide-production and activation-analysis.

A particular radionuclide may be produced by several different reactions involving p, d, ^{3}He, α, etc. As an example, ^{18}F can be produced by any of the following reactions:

1. $^{19}F(p, pn)^{18}F$

   $^{19}F(p, 2n)^{18}Ne \ \beta^{+} \rightarrow {}^{18}F$

2. $^{18}O(p, n)^{18}F$

3. $^{22}Ne(p, \alpha n)^{18}F$

4. $^{20}Ne(p,\alpha)^{18}F$
5. $^{16}O(\alpha, 2n)^{18}Ne \ \beta^+ \rightarrow {}^{18}F$
   $^{16}O(\alpha, pn)^{18}F$
6. $^{16}O(^3He, n)^{18}Ne \ \beta^+ \rightarrow {}^{18}F$
   $^{16}O(^3He, p)^{18}F$

Before a decision can be reached about which type of reaction should be used with a certain type of cyclotron or accelerator the excitation functions for all the different reactions are needed. The most important nuclides in this respect are underlined in Table III.

The most commonly used quantity expressing the amount of radionuclides produced by charged-particle bombardment is the so called "thick-target yield" (Y). This is described as the activity produced in a target the thickness of which is greater than that needed for attenuation of the particle energy to values below the threshold energy of the nuclear reaction in question and is usually expressed in mCi/mAh or μCi/μAh.

The quantity Y, involves a "saturation factor" $(1-\exp(-\lambda t))$ which must be taken into account if one wishes to use Y to compare yields obtained at different irradiation times and flux densities.

Because of effects such as loss of radioactive material by evaporation during bombardment, the quantity Y also includes an "irradiation effectiveness" coefficient ϵ [10] which is strongly dependent upon the target conditions and, in particular, upon the beam-current.

It has been suggested that a better defined quantity should be used to express the amount of radionuclide produced by charged-particle production [11].

This quantity could be the production rate R expressed as

$$R = k_i \, n \int_{E_m}^{0} \frac{\sigma(E)}{S/\rho} \, dE$$

or its inverse, R^{-1},

where $\sigma(E)$ = nuclear cross-section as a function of particle energy, E,
S/ρ = mass stopping power of the target material (a function of particle energy, E),
E_m = energy of the incident bombarding particles,
n = number of atoms per kg of target-material,
k_i = conversion factor which determines the unit of R.

The meeting concluded that it was preferable to express R as nuclear transformations per particle, i.e. as a dimensionless quantity. If SI-units are used throughout, k is then equal to 1.

It was also suggested that the inverse of R which is equal to particles per nuclear transformation would be the more practical quantity.

TABLE I. CYCLOTRONS USED IN ISOTOPE PRODUCTION FOR MEDICAL PURPOSES

Location	Type of machine	Manufacturer
USA		
1. Washington University Medical School, St. Louis, Mo.	Fixed energy 7.5 MeV D	Allis Chalmers 1965
2. Massachusetts General Hospital, Boston, Mass.	Variable energy D	Allis Chalmers 1967
3. Sloan-Kettering Institute for Cancer Research, New York, N.Y.	Fixed energy CS-15	Cyclotron Corp. 1967
4. Argonne Cancer Hospital, Chicago, Ill.	Fixed energy CS-15	Cyclotron Corp. 1969
5. New England Nuclear Corp., Billerica, Mass.	Fixed energy CS-22	Cyclotron Corp. 1969
6. Mt. Sinai Hospital, Miami Beach, Florida	Fixed energy CS-22	Cyclotron Corp. 1970
7. University of California at Los Angeles, Los Angeles, Calif.	Fixed energy CS-22	Cyclotron Corp. 1971
8. Mediphysics, Emeryville, Calif.	Fixed energy CS-22	Cyclotron Corp. 1971
9. University of Southern California-County of Los Angeles, Los Angeles, California	Fixed energy CS-22	Cyclotron Corp. 1971
10. Brookhaven National Laboratory, Upton, N.Y.	Variable energy 60"	Research machine
11. Donner Laboratory, UCRL, Berkeley, California	Variable energy 88"	Research machine
12. NASA Lewis Research Center, Cleveland, Ohio	Variable energy 88"	Research machine

TABLE I. (continued)

Location	Type of machine	Manufacturer
13. Oak Ridge National Laboratory, Oak Ridge, Tenn.	Variable energy 86"	Production machine
EUROPE		
14. Hammersmith Hospital, London, Great Britain	Fixed energy	– (1955)
15. German Cancer Research Center, Heidelberg, Fed. Rep. of Germany	Fixed energy	A.E.G. 1972
16. Nuclear Research Center, Jülich, Fed. Rep. of Germany	Variable energy	A.E.G. 1972
17. CEA, Department of Biology, Orsay, France	–	Thompson-CSF 1971
18. IKO, Amsterdam and University of Groningen, Groningen, Netherlands	–	(Philips)
19. Medizinische Hochschule Hannover, Fed. Rep. of Germany	MC-20	Scanditronix 1973
20. Univeristy of Liège, Belgium	–	Thompson-CSF 1974
21. Nuclear Research Institute Prague, Czechoslovakia		

TABLE I. (continued)

Location	Type of machine	Manufacturer
ASIA		
22. IPCR, Saitama, Japan	Variable energy 63"	IPCR-NAIG and TOSHIBA
23. University of Tokyo, Japan	CS-30	Cyclotron Corporation
24. Institute of Radiological Science Chiba, Japan		Thompson-CSF 1974
SOUTH AMERICA		
25. Instituto de Engenharia Nuclear Rio de Janeiro, Brazil	CV-28	Cyclotron Corporation

TABLE II. SPECIFICATIONS OF CURRENTLY AVAILABLE MEDICAL CYCLOTRONS [9]

		CS-22*	Cs-30*	CV-28*	Actitron**	Th-CSF (70)**	MC-20***
Beam Energy	p	22	26	2 - 24	6 - 19	8 - 70	2.5 - 20
(MeV)	d	12	15	2 - 14	3 - 11	11 - 35	1.5 - 10
	^{3}He	31	39	5 - 36	3 - 28	18 - 93	3.0 - 27
	α	24	30	6 - 28	6 - 22	22 - 70	2.5 - 20
External	p	50	60	70	70	20	100
Beam	d	50	100	100	70	40	100
Current	^{3}He	50	70	70	50	-	50
(μA)	α	50	50	50	50	-	50
Internal	p	100	500	500	-	-	-
Beam	d	100	500	500	-	-	-
Current	^{3}He	100	150	150	-	-	-
(μA)	α	100	100	100	-	-	-

* The Cyclotron Corporation ** Thompson-CSF *** Scanditronix

TABLE III. CYCLOTRON-PRODUCED RADIONUCLIDES IN CURRENT USE [9]. The most important nuclides in this respect are underlined.

Radionuclide	Half-life	Principal radiation (keV)	Chemical form of the radiopharmaceutical
^{11}C	20.4 min	511	CO, CO_2, Haemoglobin
^{13}N	10.0 min	511	N_2, NH_4^+
^{15}O	2.1 min	511	O_2, Co, CO_2, H_2O
^{18}F	110 min	511	Complex, Amino Acids
^{43}K	22.4 h	373, 619	KCl
^{52}Fe	8.2 h	165, 511	Ferric citrate
^{67}Ga	78 h	93, 184, 296	Gallium citrate
^{77}Br	57 h	242, 522	NaBr
^{81}Rb	4.7 h	450, 511	RbCl
$^{81}Kr^m$	13 s	190	Kr
^{84}Rb	33 d	511, 880	RbCl
$^{87}Sr^m$	2.8 h	388	Strontium citrate
^{111}In	67.2 h	173, 247	$InCl_3$, Transferrin, Globulin
^{123}I	13.3 h	159	NaI, Hippuran, Albumin
^{129}Cs	32.4 h	375	CsCl
^{131}Cs	9.7 d	29	CsCl
^{157}Dy	8.1 h	326	HEDTA-complex
^{201}Tl	73.5 h	170, 140	TlCl
^{203}Pb	52.1 h	280, 400	Pb-citrate

5. RADIONUCLIDE-PRODUCTION WITH FAST NEUTRONS

Cyclotrons can be used as neutron-generators through the reaction $^7Be(p,n)^7Li$.

Another and less expensive method for fast-neutron production utilizes the $^3H(d,n)^4He$ reaction.

Deuterons are accelerated by an electrostatic accelerator of 150 - 400 kV and focused on a cooled tritium target where the $^3H(d,n)$-reaction takes place. The neutrons are almost monoenergetic with an energy in the range of 14 - 15 MeV, depending on the deuteron energy and the neutron direction.

The neutron-production rates obtained in these machines are about 10^{10} - 10^{12} neutrons per second. These machines are mostly used for therapy and radio-biological experiments, and for activation-analysis of macroelements in biological tissues. They are not very useful for radionuclide production of high specific activity.

Neutrons produced by high-energy proton accelerators could be used for production of labelled biopolymers.

Neutrons with energies higher than 20 MeV can be used for production of ^{11}C, ^{13}N, ^{15}O, ^{30}P and ^{53}Fe (with $T_{\frac{1}{2}}$ of 20, 10, 2, 2.5 and 8.5 minutes, respectively).

There is a need for calculations of an optimum production rate in which the radiolysis of the irradiated substances would also be considered.

6. USE OF MEDICAL BETATRONS FOR PHOTON-ACTIVATION

Betatrons are available at many hospitals for radiotherapy. These accelerators produce electron beams of typical 40 MeV energy with a current of about 1 μA. The electrons strike a platinum target and produce "bremsstrahlung" photons distributed in energy up to the maximum electron energy.

The fluence-rate of photons with energies greater than 10 MeV is in the order of 10^{14} photons m^{-2} s^{-1} at a point about 0.2 - 0.3 m from the target in the forward beam direction.

In the energy region 10 - 35 MeV, the dominant feature of photo-nuclear absorption is electric dipole absorption observed as the giant resonance in the absorption cross-section spectrum. The resonance has its maximum value at about 22 MeV for light nuclei and at about 13 MeV for heavy nuclei. The width of the resonance is about 4 MeV for spherical nuclei and about 8 MeV for strongly deformed ones [12].

The production-yield is given by the expression

$$Y(t_i) = k_j\, n \left\{1 - \exp(-\lambda t_i)\right\} \int_{E_{thr}}^{E_0} \sigma(E)\varphi_E\, dE$$

where k_j = conversion factor,
n = number of target-nuclei per kg,
$\sigma(E)$ = cross-section for the (γ, n) reaction,
φ_E = photon fluence rate m^{-2} s^{-1} per energy-unit interval,
E_0 = maximum energy of the electron,
E_{thr} = threshold energy of the reaction in question.

From existing data it is obvious that it is possible to produce biologically important positron emitters such as ^{11}C, ^{13}N, ^{30}P, $^{31}S(T_{\frac{1}{2}}$ 2.7 s) in activities of the order of 10 - 100 μCi per g of irradiated element. However, for ^{15}O it is possible to produce about 1 - 40 mCi per g of irradiated element [13]. It was also suggested that the possibility of producing labelled biopolymers with short-lived radioisotopes should be considered.

A useful compilation of photonuclear cross-sections in the energy range in question has been made by BÜLOW and FORKMAN [12].

It would also be of value to have tables of $\int \sigma(E)\varphi_E dE$ for different elements, where φ_E is the "bremsstrahlung"-spectrum of platinum.

7. OTHER IMPORTANT DATA

Besides the nuclear data some production parameters which are important for the use of radioisotopes in medicine and biology were also discussed.

There is a great lack of dependable and systematically presented information about the radiolysis of the target material during irradiation with both neutrons and charged particles. Gas production can take place and other unwanted chemical species can be formed which influence the radiochemical treatment which is to follow [14-16].

The request for both the volumic radioactivity Ci/litre and the concentration of the chemical element in question in g/litre or atom/litre or mol/litre (M) was stressed. The specific activity is then easily obtained by taking the quotient of volumic radioactivity and chemical concentration.

It was also proposed by SVOBODA [17] that it might be even more useful to introduce a term defining "the degree of deviation from carrier-free state": this is D_{CF}, the negative logarithm of the specific activity, where

$$D_{CF} = - {}^{10}\log \frac{N_A}{N_A + N_S} = - {}^{10}\log \frac{N_A}{N_T}$$

where N_A = number of radioactive atoms,
N_S = number of stable atoms of the same element,
N_T = total number of atoms of the same element.

For total carrier-free solution:

$$N_S = 0 \text{ and, thus, } D_{CF} = 0$$

It was stressed that further information is needed about the toxicology of many of the elements used as radioactive tracers in medicine and biology.

8. CONCLUSIONS

8.1. Reactor production

The demand made on nuclear data for reactor-produced radionuclides are the following:

Averaged thermal-neutron cross-sections relevant for the production of useful radionuclides (See section 2) are required with an accuracy within a few per cent. Accurate decay-scheme data are also needed.

The neutron cross-section in the resonance-region 5 eV - 1 MeV is not well known for many materials and better information is required. Information is needed on resonance integrals and yields with and without cadmium covers. Information on neutron-fluence depression corrections is also needed [2]. However, the accuracy in the calculation of the production rate is limited by uncertainties in the shape of the reactor neutron spectrum, the irradiation geometry and position.

8.2. Generator production

The main problem is to evaluate the optimum production techniques for present and potentially useful parent nuclei.

The contamination of the daughter nuclide with undesirable radionuclides is a problem which also must be considered seriously.

8.3. Accelerator production

For the calculation of R for charged-particle accelerators used for production of radionuclides there is a need to know cross-sections as a function of energy, $\sigma(E)$, for all nuclear reactions leading to useful radionuclides (See Table III) and for all commonly accelerated particles, e.g. ^{1}H, ^{2}H, ^{3}H, ^{3}He, ^{4}He and, possibly, also ^{7}Li, ^{12}C and ^{16}O.

The mass-stopping power S/ρ and the range of charged particles in various materials are also needed, but are already well known and quite readily available [18].

It was concluded that there is an urgent need for experimental determinations and tabulations of R. The measurement of R might at present be an easier task than detailed studies of $\sigma(E)$ and theoretical calculations.

8.4. Radionuclide production with fast neutrons

Neutrons of energies above 20 MeV can be used for production of ^{11}C, ^{13}N, ^{15}O, ^{30}P and ^{53}Fe.

There is a need for calculations of an optimum production rate in which the radiolysis of the irradiated substances would also be considered.

8.5. Radionuclide production with betatrons

It was concluded that positron emitters such as ^{11}C, ^{13}N, ^{30}P and ^{31}S in activities of the order of 10 - 100 μCi per g and ^{15}O 1 - 40 mCi per g could be produced in biological materials with betatrons. The production yields are known with sufficient accuracy. It was suggested that the possibility of producing labelled biopolymers with short-lived radioisotopes should be considered.

8.6. General remarks

It would be very useful for the producers and users to have an annually revised manual for production data, nuclear data and gamma spectra for all radionuclides which are in current use in medicine and biology. IAEA might be the organization which would best be able to meet this need.

ACKNOWLEDGEMENT

Many thanks are due to AB Atomenergi in Studsvik, who acted as host for the meeting.

REFERENCES

[1] BAKER, P.S., "Radioactive Pharmaceutical", Ch. 8, Reactor-produced Radionuclides (ANDREWS, G.A., KNISELEY, R.M., WAGNER, H.N., Jr., Eds), US Atomic Energy Commission CONF-651111, Oak Ridge (1966).

[2] TILBURY, R.S., private communication, Sloan-Kettering Institute, N.Y. (1972).

[3] RICHARDS, P., "Radioactive Pharmaceuticals", Ch. 10, Nuclide Generators, (ANDREWS, G.A., KNISELEY, R.M., WAGNER, H.N., Jr., Eds), US Atomic Energy Commission CONF-651111, Oak Ridge (1966).

[4] BERNHARD, H., LIESER, K.H., Isotopengeneratoren – ein Überblick über den Stand der Entwicklung, Euro-Spectra 9 Nr 1 (1970) 20.
[5] HENRY, R., Isotope generators, J. Nucl. Biol. Med. 15 (1971) 105.
[6] TOUYA, J.J., New applications of radiopharmaceuticals labelled with generator-produced radionuclides, in Medical Radioisotope Scintigraphy 1972 2 (Proc. Symp. Monte Carlo, 1972) in press.
[7] LEDERER, C.M., HOLLANDER, J.M., PERLMAN, I., Table of Isotopes (6th Edn), John Wiley (1968).
[8] LAMBRECHT, R.M., WOLF, A.P., "Accelerator-Produced Nuclides and Radiopharmaceutical Production", presented at an IAEA panel meeting, Amsterdam (1971).
[9] GLASS, H.I., New applications of radiopharmaceuticals labelled with cyclotron-produced radionuclides, in Medical Radioisotope Scintigraphy 1972 2 (Proc. Symp. Monte Carlo, 1972) in press.
[10] SVOBODA, K., "The Uses of Cyclotrons in Chemistry and Biology", Buttwerworths London (1970) 383.
[11] SVOBODA, K., SILVESTER, D.J., Quantities and units used in the production of radionuclides by charged particle bombardment, Int. J. Appl. Radiat. Isot. 22 (1971) 269.
[12] BÜLOW, B., FORKMAN, B., Photonuclear cross-sections, Nuclear Physics Report, Lund 7208, University of Lund, Sweden.
[13] BRUNE, D., MATTSSON, S., LIDÉN, K., Application of a betatron in photonuclear activation analysis, Anal. Chim. Acta 44 (1969) 9.
[14] LINARCRE, J.K., A list of materials which may be accepted for irradiation in BEPO by the shift manager, without reference to the reactor manager AERE-M 1535 (1965).
[15] TRUSWELL, A.E., Irradiation of small samples in the reactor DIDO and PLUTO, AERE-M1563 (1965).
[16] Sicherheitsbetrachtungen für einfache Bestrahlungen in FR 2. Internbericht RB 3/65, Kernforschungszentrum Karlsruhe, Germany (1965).
[17] SVOBODA, K., On terms defining the specific activity of accelerator-produced radioisotopic preparations, Report Ú.J.V. 2712-Ch Rez, Czechoslovakia (1971).
[18] BARKAS, W.H., BERGER, M.J., Tables of Energy Losses and Ranges of Heavy Charged Particles, Report NASA SP-3013, National Aeronautic and Space Administration, Washington D.C. (1964).

DISCUSSION

M. LEDERER: This is not the first time that the need for more "data" on production has been mentioned. Perhaps a general reference on the subject would be desirable. Such a reference would be a combination of useful measured data (e.g. neutron cross-sections), systematics for other quantities which can be calculated (e.g. cross-sections for charged-particle reactions), and "cook-book"-type knowledge, often essential for dealing with the many problems that arise from the presence of impurities.

R.B.R. PERSSON: The meeting concluded that there is a great need for a general reference work or "cook book" of the type you mention. This would, however, not only cover production data (such as cross-sections, target materials, impurities etc.) and decay schemes of the radionuclides, but also include tables of γ-ray energies and emission rates as well as figures of γ-spectra recorded by a standardized technique.

G.A. KOLSTAD: This question pertains to your last recommendation. The range of particle accelerators you have discussed is rather limited. Have you considered the use of heavy-ion bombardments (i.e. $M > 4$) or higher-energy bombardments (i.e. 200-800 MeV) for the production of proton-rich nuclides with different nuclear properties? For example ^{123}I can be produced at the 200 MeV Brookhaven Linac for Isotope Production (BLIP) or at the 800 MeV Clinton P. Anderson Meson Physics Facility at Los Alamos (LAMPF) at rather low cost. It is not always necessary for the accelerators to be located at the hospitals – only near enough for shipment of the products.

R.B.R. PERSSON: Our discussions concerning the so-called medical cyclotrons were mainly limited to small machines operated by a small organization. We did not devote much attention to large machines like those at Brookhaven and the Lawrence Radiation Laboratory in Berkeley, which we considered to be something very special. Of course, there are extensive uses for such machines in producing radionuclides of interest.

G.A. KOLSTAD: I should point out that both the BLIP and the LAMPF have facilities associated with them for the production of radioisotopes and chemical fabrication of the desired products.

Section V

RADIOISOTOPES IN CHEMISTRY

Chairman

K.H. LIESER (Federal Republic of Germany)

RADIOISOTOPE APPLICATIONS IN CHEMISTRY – A REVIEW

L. GÓRSKI
IAEA, Laboratory Seibersdorf,
Vienna, Austria

Abstract

RADIOISOTOPE APPLICATIONS IN CHEMISTRY – A REVIEW.

Various methods of application of radioisotopes in chemistry – the most important use of the latter being that as tracers – are characterized; the necessity of knowledge of nuclear data for the individual applications is briefly discussed.

The discovery of radioactivity, 77 years ago, by Becquerel in Paris, was due to an effect which should now rather be classified as a new branch of radiochemistry, i.e. radiation chemistry. The chemical aspects of radioactivity were, however, later covered up by the physical face of this phenomenon. It is only with the discovery of induced radioactivity, that the use of radioisotopes for chemical investigation could be applied in a wider framework. The next great discovery in nuclear physics – fission of uranium-235 – was also proved experimentally for the first time with the help of some radiochemical techniques.

It is not possible to describe all chemical applications of radioisotopes in this short contribution. Some applications of great importance are discussed in papers on activation analysis and hot atom chemistry, in these Proceedings.

The most important use of radioisotopes in chemistry is their application as tracers. The use of radiotracers can be of interest in cases in which we wish to investigate the transfer or movement of atoms, molecules, chemical compounds, substances or any other masses. Most of the physico-chemical phenomena are connected with such transfers of matter from one phase to another or from one place to another. Such processes as evaporation, dissolution, partition between two different phases, adsorption on the surface, chemical reactions, analytical separations, etc. are examples of physico-chemical occurrences related to mass transfer on a molecular or on a large-scale level. If the molecules or masses in the movement can be labelled in some way – which permits them to be distinguished from other similar molecules or masses not taking part in the process investigated – the study of this particular process is easy to perform. If the labelling is recognized easily and quickly, then also the kinetics of the considered process can be observed. There are many ways of tagging molecules or substances: colouring, mixing with some easily recognizable substances (e.g. fluorescent compounds) or introducing slightly different atoms into the molecules. Two ways of molecular tagging are now in use: labelling with non-natural composition of stable isotopes and labelling with radioactive isotopes. These two labelling modes operate on a molecular level, but can also be used on large-mass level. Other labelling systems (e.g. colouring substances) can only be applied to large-scale experiments with larger masses involved.

Unfortunately, the labelling with non-natural composition of stable isotopes can only be recognized with the use of mass spectrometers or some simpler devices derived from the same principle. In any case, the recognition of the labelled substances must be made by collecting the samples from the investigated substance and analysing them in the detecting device.

Labelling with radioisotopes enables one to observe the transfer without sampling or introducing any measuring device directly in the reaction medium. This is made possible, of course, by using the penetrating rays emitted by most of the radioisotopes. In addition, the speed and facility of such measurements makes labelling with radioisotopes very advantageous. There is not much the investigator must really know of the nuclear properties of the radioisotopes used. In most cases, he will only be interested in the exact knowledge of the decay scheme, which is necessary in planning the measuring method, and of the activity to be used in each experiment.

Sometimes a method of "post-radioactive labelling" can be used. It consists of labelling with a non-radioactive element, which is then detected and measured by subsequent neutron activation of collected samples. This method, rather simple in execution, has all the inconveniences mentioned above in connection with labelling with non-natural composition of stable isotopes. But it has also some benefits: low cost, the concentration of the labelling substance can be very low (a factor very important in the study of refining processes in the metallurgy of very pure metals and alloys), no health hazards, etc.

The labelling also gives some other possibilities: One of them is the investigation of the precursor-product relationship, and of reaction pathways. This can be also regarded as a special case of a transfer process. The suspected atoms, groups or molecules of a precursor are labelled with radioactive isotopes and then this radioisotope is sought in the supposed product. This application is of great importance in biochemistry, since the identification of complex metabolism pathways in the living organism is not easy.

The most interesting results can be obtained from the use of tracers in the study of process kinetics. Diffusion, exchange between two (or more) pools, and the turnover rate are some of the best known examples of such tracer applications.

The use of tracers enables also the measurement of some physico-chemical constants such as solubility of low-soluble substances, vapour pressure of low-volatile substances, partition coefficient between two phases, surface measurement of powders or porous matter, stability constants of complex compounds, etc. In all these cases, we make use of the fact that radioisotopic atoms can be detected and measured even in a very low concentration. Other tracers do not permit such dilution factors as with radioisotopic tracers. Some radioisotopes can be obtained almost carrier-free — e. g. the radioisotopes of elements represented in the fission products; in such cases, effectively weightless amounts of radiotracer can be detected easily. It is easy to calculate that a carrier-free radioisotope with a half-life of two weeks has an activity of about 3×10^5 Ci per gram, i. e. if we can measure an activity of 1 dps, which is quite easy, we can detect 10^{-16} g of the pure radiotracer.

There are also some analytical applications of radioisotopic tracers. Each analytical procedure requires two principal steps: separation and isolation of the analysed component from the sample and the measurement of the amount of the isolated component. In the past, the analytical chemists only used separation procedures of 100% efficiency, which means that the analysed component was isolated completely in a pure form for subsequent measurement of the mass.

But such methods are, in general, time-consuming and sometimes difficult to apply. Now, many analytical separation procedures have an efficiency lower than 100%. The determination of the actual efficiency can be carried out by adding a small quantity of labelled compound to the analysed substance. Then the labelled compound, which should be identical with the analysed component, is isolated. After measuring the ratio of activities before and after the separation or between two separated substances, it is possible to calculate the recovery of the analysed compound in the separation procedure and to take it into account for the end-result. This method also enables discovery of those steps in the separation procedure where losses occur.

A similar method using radioactive tracers is the method of isotope dilution. The aim of this method is the determination of masses or of volumes not accessible to direct measurement. The analytical use of this procedure is frequently demonstrated in the case of analysis of a mixture of amino acids. The quantitative isolation of a particular amino acid from such a mixture is very difficult, but it is possible to isolate only a part of the total content in a very pure form. If it is possible to know what part of the total content has been isolated and weighed, then the original amount of this amino acid will be known. The determination of the ratio of the weight of the isolated part to the total content can be performed by isotope dilution. It is only necessary to have this particular amino acid in labelled form. Then we add a known amount of tracer compound to the sample before starting the separation procedure. This radioactive reagent labels the total amount of the amino acid to be analysed. The labelled molecules are isolated with the same recovery as the non-labelled ones. We can easily measure the ratio of the specific activity of the added amino acid at the beginning to the specific activity of that isolated after the separation. This figure is exactly the ratio of the total weight of the amino acid to the weight of the added labelled reagent.

In geochemistry, the radioactive decay law is used for the determination of the age of rocks (geochronology). In this case, we make use of natural contamination of many minerals with some radioactive tracers: uranium, thorium, potassium, tritium and others. From the well-known law of radioactive decay, we can derive the formula

$$\lambda_I t = \ln (1 + N_{II} / N_I)$$

where N_{II}/N_I is the actual atomic ratio of the daughter and parent isotopes, e.g. ^{206}Pb and ^{238}U. This can be measured by mass spectrometry or, in some cases, by activation analysis. The successful application of this method requires the absence of the daughter isotope at the time of formation of the mineral and no subsequent chemical change in the composition of the mineral. With such pairs of isotopes as $^{207}Pb/^{235}U$; $^{206}Pb/^{238}U$; $^{208}Pb/^{232}Th$; $^{40}Ar/^{40}K$; $^{87}Sr/^{87}Rb$ it is possible to determine the age of rocks up to

several billions of years. For shorter periods ^{14}C is used (in the range of several thousand of years) and tritium (in the range of several tens of years). ^{14}C dating is frequently used in archeology and tritium dating is applicable in age determination of underground waters in hydrology. Precise knowledge of the half-life of the applied radioisotope is a fundamental requirement in the application of this method.

^{14}C and tritium tracers are examples of many other radioisotopes produced by the interaction of particles from cosmic rays with stable atoms. Some of them are short-lived (e. g. ^{37}Ar, 35 days), some are long-lived (e. g. ^{39}Ar: 270 years). The amount of these radioisotopes and the ratio of their respective activities can give information on the age of meteorites and the intensity of cosmic radiation in the interplanetary space.

The examples given above and some other facts demonstrate that there are many naturally occurring radioisotopes among the so-called "stable elements" (atomic number ≤ 82), e. g. rubidium, which is regarded as a stable element, consists to 28% of ^{87}Rb, which has a half-life of the order of 10^{10} years, about ten times longer than ^{238}U. ^{115}In is another noticeable example. Its abundancy in the natural element is 96%, and the half-life is of the order of 10^{14} years. About 30 natural isotopes with $Z \leq 82$ are suspected or have been proved to be radioactive, mostly with very long half-lives. Some other elements, as, e. g. krypton, are now "naturally" occurring radioactive isotopes as the result of continuous environmental pollution with fission products of uranium, one of which is ^{85}Kr.

Radioactive isotopes are also used for studying the structure of molecules or crystal lattices. One method consists of observing the rate of isotopic exchange between the radioactive and non-radioactive isotopes in the molecule. The kinetics of isotopic exchange depends on the strength of the chemical bond between this particular atom and the rest of the molecule. Also the position of the atom in the molecule has a certain influence. The central atom in complex compounds is well protected from isotopic exchange by the peripheral groups. When there is more than one atom of the same element in a molecule, there can be equivalence independent of the position of the atoms in the molecule, but sometimes such equivalence does not exist. In this last case, the rate of isotopic exchange will depend on the position of the radioactive tracer in the structure of the molecule. If the positions in the structure investigated are equivalent, then the rates of isotopic exchange will be equal and not dependent on the position of the radioisotopic tracer.

Another use of radioisotopes for structural studies is the Mössbauer effect. This effect is frequently applied for the investigation of bonds and fields in the crystal lattice.

From our short description of current applications of radioisotopes in chemistry we see that in most of the non-sophisticated applications only data on half-lives and disintegration schemes are needed, knowledge of which is necessary for successful use of radioisotopes in chemical research. Only for some analytical applications of radioactivity, especially activation analysis, which directly exploit some nuclear reactions, knowledge of cross-sections and exact information on the spectra of the emitted radiations are necessary.

DISCUSSION

J.A. CZUBEK: Although I am not involved personally in problems of chemistry, I would like to make two comments on nuclear data requirements in geochemistry which are of importance to those of us working in nuclear geophysics. We need a good knowledge of two constants which are also of interest for geochemistry. The first is the radioactive decay constant for ^{40}K (for gamma emission). The existing data range from 2.8 to 3.6 gamma/s per gram of natural potassium, which is of course quite unsatisfactory for us. The second is the fission decay constant for uranium, which is needed in geochemistry for age determination by trace detection in micas. The use for this purpose of the uranium glasses produced in Czechoslovakia during the 19th century is not quite satisfactory, owing to the short time elapsing from this period. The purpose of my comment is to encourage the measurement of these values, which are really needed by users.

L. HJÄRNE: When mentioning, for example, indium-115, Dr. Górski touched upon a matter which is of some importance to many of us. I am referring here to the natural abundances of isotopes. We often rely on one of the nuclide charts for information of this kind, but, when we need better accuracies, we have some difficulties finding good data.

I have been informed that in the next edition of the GE nuclide chart the revision of this kind of data will include a substantial reduction of the number of significant figures quoted. The reason is twofold:

(1) The natural variation of the abundances is greater than previously assumed; and
(2) The accuracies of measurements are not as good as previously believed.

Can anyone comment on whether this matter should be considered within the scope of nuclear data and on how unsatisfactory the situation really is?

M. LEDERER: The situation really is serious and the problem has been considered by the International Commission on Atomic Weights. It appears that most abundance measurements are accurate to no better than $\approx 1\%$ relative, with the exception of a few calibrated measurements, which may be accurate to $\approx 0.1\%$ relative. I believe the ICAW plans to review the abundances about every two years because of their importance to atomic weights. The most recent values are (apparently) those quoted on the latest GE chart. I have found no recent compilation on natural variations in the abundances. The ICAW notes certain elements for which natural variations limit the accuracy of atomic weight determinations.

D. BERÉNYI: The role of nuclear data on radioisotopes in X-ray fluorescence analysis was not mentioned in the review. This method is very important in widely different fields where the rapid analysis of samples is a requirement. What is your opinion on this subject?

L. GÓRSKI: The paper was devoted to applications in chemistry, to the exclusion of all analytical methods, which will be discussed in the various special sessions of this symposium. I agree that the knowledge of the cross-sections for production of X-rays in different isotopic sources of X-rays is very important for this application, but this is to some extent an extra-nuclear phenomenon.

NUCLEAR DATA REQUIRED FOR THE INTERPRETATION OF HOT-ATOM CHEMISTRY

A.H.W. ATEN
Euratom, Central Bureau for Nuclear Measurements,
Geel, Belgium

Abstract

NUCLEAR DATA REQUIRED FOR THE INTERPRETATION OF HOT-ATOM CHEMISTRY.

In hot-atom chemistry radioactive atoms are released by two processes from the bonds joining them to the molecule, in which they were originally contained. Either emission of a particle or a photon gives a recoil to the radioactive atom or a positive charge is given to the atom in question during the radioactive transformation and this charge, if sufficiently high, releases the atom. To understand what happens in hot-atom chemistry knowledge of these two phenomena is essential. In the case of neutron capture, the gamma processes determine the value of the recoil energy. The situation is even more difficult in those cases where bonds are broken by a positive charge. This may either be caused by the absence of electron pairs responsible for the chemical bond or by electrostatic repulsion between different parts of the charged molecule. In this case, the essential information is the value of the positive charge (or rather the fraction of cases in which each charge occurs). Positive charges normally arise from electron capture or from conversion of gamma rays. In the latter case, it is also essential to know the delay between the radioactivity process and the production of the converted gamma rays.

INTRODUCTION

The field of hot-atom chemistry covers the chemical reactions of those atoms in which the nucleus has just been formed by a nuclear reaction or by a radioactive process.

As such cases normally involve only a relatively small number of atoms, the usual technique is to study only those processes which produce radioactive nuclides and allow accurate measurements to be performed on very small amounts of material.

To understand the results of such reactions, information is required on the kinetic energy and the electrical charge of the atom and on the time scale of the separate processes involved.

For the various nuclear processes used in hot-atom studies the essential data are of a widely different nature, and we shall therefore consider separately the following possibilities:

1. Nuclear reactions induced by charged particles or by high-energy neutrons or photons. Nuclear fission also comes into this category, as does α-decay.
2. Neutron capture.
3. Electron capture.
4. Isomeric transitions.
5. β^--decay.
6. β^+-decay.

It will be seen that the situations are rather different depending on the way in which the nucleus has been formed.

1. NUCLEAR REACTIONS INDUCED BY CHARGED PARTICLES OR BY HIGH-ENERGY NEUTRONS OR PHOTONS. NUCLEAR FISSION, α-DECAY.

If a nucleus is produced by the action of a charged particle or a high-energy neutron or photon or by alpha-decay, it receives a recoil energy of the order of 10^4 to 10^5 eV. In the case of nuclear fission, the kinetic energy of the fission fragments is even higher, of the order of 10^8 eV.

Such energies greatly exceed normal ionization energies or chemical bond energies and therefore the radioactive nucleus will not be able to form a chemical compound until it has lost by far the larger part of its energy.

Under these circumstances, energy losses are caused mainly by ionization in the surrounding medium, and the radioactive particle itself will also lose a number of its electrons. Below about 10^3 eV various scattering processes are important in relieving the particle of its energy.

A large amount of radiation damage has now been done and the particle leaves behind it a track of radicals, and, if it is formed in a solid matrix, also of displacements. It will finally come to rest at a large distance, which even in condensed phase amounts to hundreds of angströms, away from the spot where it has been formed.

As the particle slows down its positive charge will diminish and it is usually assumed that by the time its energy has been reduced to about 10^2 eV it will have become electrically neutral. At this stage, it is able to react with molecules of the matrix or with radicals from its own track or from general radiation damage in the medium.

Under these circumstances, the final products formed will not be much influenced by the original condition or the original energy of the radioactive atom after its birth and no special information on the nuclear process is needed for the explanation of the products of these hot-atom reactions.

It may, however, happen that delayed γ-rays are emitted at a moment when the energy of the particle has already been reduced to a thermal value. If under these conditions, i.e. after a delay of, at least, the order of 10^{-13} to 10^{-12} seconds, a γ-ray is emitted, this will normally be a γ-ray of fairly low energy which will be converted to an appreciable degree. Under these circumstances, the atom will again be released from the molecule in which it is contained and will be capable of participating in one or more new chemical reactions. The results of such processes will be discussed in section 4.

At the moment when the particles come to rest – which occurs very roughly a few 10^{-13} s after the nuclear process – a fraction of them has already entered into the chemical combination in which they will finally be found. In most cases, however, another part is still present as single atoms, in free radicals, or in some other unstable form. As such they may persist for a much longer time before they reach a stable condition. In liquid and gaseous systems, this final stabilization process presumably involves diffusion over very appreciable distances.

2. NEUTRON CAPTURE

If a nucleus is activated by neutron capture, the energy gain of about 6 MeV (the binding energy of the neutron in the product nucleus) must be

dissipated by the emission of γ-rays. If the entire energy is emitted as a single γ-ray the recoil energy (E_R) of the nucleus is given by the equation

$$E_R = \frac{536}{M} E_\gamma^2$$

if E_γ is expressed in MeV and E_R in eV. It should, however, be realized that not all of this energy is available for breaking the chemical bond or bonds by which the radioactive is held in its mother molecule.

In simple molecules, the fraction of the recoil energy available for bond breaking is, at most, equal to (M-m)/M, where M designates the mass of the molecule and m that of the radioactive atom [1].

If more than one γ-ray is emitted, the situation is much more complicated as the total recoil energy imparted to the nucleus is determined by the angle under which the γ-rays are emitted, at least, if the two gamma-rays are produced not more than 10^{-15} to 10^{-14} seconds apart.

In the case of a thermal neutron capture reaction the recoil energy of the nucleus does not exceed normal chemical bond energies by a large factor. In a condensed phase, the particle will not move more than a few angströms from its original site and will not have to undergo more than a few collisions before it can form a stable chemical bond. In principle, it might even happen that, because of compensation of recoil processes, the particle gets such a small energy that it cannot leave the molecule or ion in which it was originally contained. This phenomenon, "primary retention", is, however, very rarely observed, if at all.

The situation is again complicated if delayed γ-rays are emitted by the product nucleus because in this case, as was already mentioned in section 1, after the radioactive particle has first formed a chemical combination, it will be released once more and will have to form a second molecule or ion in order to stabilize itself (see section 4).

3. ELECTRON CAPTURE

In the case of electron capture, the product nucleus, first of all, suffers a recoil due to the emission of a neutrino. In principle, one might expect that a neutral atom would be formed. If electron capture is followed by one or more γ-ray emissions, the latter processes give recoil energies to the nucleus comparable to that due to the neutrino emission, and the two (or more) recoil energies should be summed in the appropriate way.

However, the hole in the K-shell (or, in the case of L-capture, in the L-shell, etc.) will be filled up by an electron from one of the outer shells with emission of X-rays. Such a process is accompanied by the liberation of electrons (Auger effect) and this means that the product atom is left with a high positive charge (see Fig. 1). Moreover, this charge is by no means equal for all atoms produced but there is a certain probability distribution for atoms with various ionic charges [2]. If the atom in which electron capture takes place is part of a molecule, the electrical charge produced on the ion of the product nucleus will immediately spread over the entire molecule and the electrostatic repulsion created in this way is sufficiently strong to break it up. Also the deficiency in electrons of the molecule weakens the chemical bonds and may even in itself be sufficient to separate two atoms if both bonding electrons of a pair are absent at a certain moment.

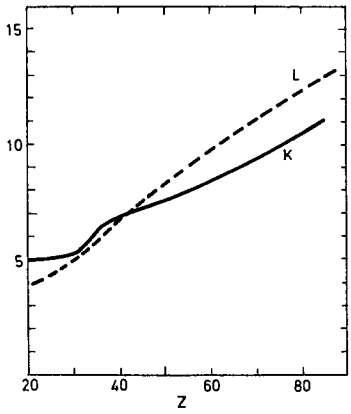

FIG. 1A. Average positive charge left on an atom in which a hole has been generated in the K- or L-shell.

The fact that the radioactive atom is left with a positive charge after the breaking-up of the molecule may also influence its ultimate chemical fate.

But here, too, we have the possibility that after electron capture and after the product nucleus has reached a stable chemical state, delayed γ-rays will be emitted, the conversion of which will again release the radioactive atom and force it to undergo a second hot-atom process, as will be explained in section 4.

4. ISOMERIC TRANSITIONS

In the case of a low-energy γ-ray emitted by a nucleus such a γ-ray is converted to an appreciable degree. This means that the energy is taken over by one of the electrons of the atom (normally a K-electron) and that the hole formed in the shell of this electron is filled up by an electron from a higher shell in the atom.

Owing to this process, a number of electrons finally leave the atom and, as in a case of K-capture, the final ion is left with a very appreciable charge (Fig. 2). (These charges will be roughly, but not exactly, equal to those produced by K-capture.) Thus, if the atom is part of a molecule it will be liberated by electrostatic repulsion or by the absence of the electrons constituting the chemical bond and, carrying – or having carried originally – a positive charge, it will react again with some constituent of the medium. In some cases, compounds of atoms with an excited nucleus can be used as such in hot-atom experiments, owing to the long half-life of some metastable nuclei, and then the results of delayed γ-emission can be studied by themselves. Important examples are the two products of neutron capture in the stable bromine isotopes. The radioactive isotopes produced – ^{80}Br and

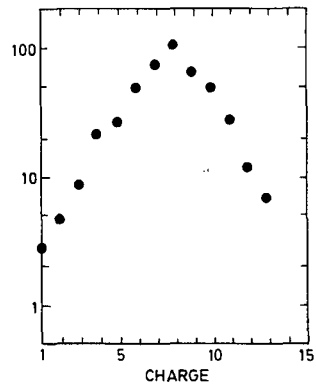

FIG. 1B. Relative frequency of formation of ions carrying different positive charges for the transition $^{131}Xe^{m} \rightarrow {}^{131}Xe$.

^{82}Br – both have an isomer, the first one with a half-life of 4 hours, the second of 6 minutes. Of the isomer $^{80}Br^{m}$ many compounds have been prepared and the hot-atom reactions following its highly converted gamma-emission have been studied.

Quite frequently, however, the delayed γ-emission follows other nuclear processes like beta-emission and the hot-atom reactions induced by the conversion process must be studied in the medium in which also the primary hot-atom reactions have taken place.

5. β^--DECAY

In the case of β^--decay, we have, first of all, to deal with the recoil process. In this case, it is more complicated than in that of electron capture because we now have two different recoils. One is due to the emission of the electron, and the other to that of the neutrino. As the two energies have quite comparable values, one has to know the angular distribution to compute the effective recoil energy available.

There is, however, a second effect which is not quite negligible. When a nucleus emits an electron, one would, in principle, expect to obtain a product ion which should be short of exactly one electron. However, in this case again secondary processes take place and in some product atoms electrical charges larger than one are observed (electron shake-off). Little is known about these phenomena but some estimates are given in Table I.

Evidently, any delayed converted γ-ray will cause a second hot-atom process and, in this way, will ultimately decide the fate of the radioactive product. But in the case of β-decay even γ-rays emitted within 10^{-13} s or less are important if they occur since the recoil energy due to them is not much lower than that due to the β-particle and the neutrino.

TABLE I. RELATIVE FREQUENCES OF IONIC CHARGES PRODUCED BY β-DECAY (GAS PHASE) [3]

$^{41}A \rightarrow {}^{41}K$		$^{133}Xe \rightarrow {}^{133}Cs$	
K^+	0.82	Cs^+	0.34
K^{2+}	0.12	Cs^{2+}	0.04
K^{3+}	0.03	Cs^{3+}	0.02
K^{4+}	0.01	Cs^{4+}	0.02
		Cs^{5+}	0.03
		Cs^{6+}	0.04
$^{85}Kr \rightarrow {}^{85}Rb$		Cs^{7+}	0.06
		Cs^{8+}	0.09
Rb^+	0.79	Cs^{9+}	0.12
Rb^{2+}	0.11	Cs^{10+}	0.09
Rb^{3+}	0.04	Cs^{11+}	0.06
Rb^{4+}	0.03	Cs^{12+}	0.03
Rb^{5+}	0.02	Cs^{13+}	0.02
Rb^{6+}	0.01	Cs^{14+}	0.01
		Cs^{15+}	0.01

6. β^+-DECAY

Very little is known about the chemical effects of positron decay. The primary product should be a negative ion, but it is most unlikely that such an ion is sufficiently stable to last until the final reaction of the radioactive atom takes place. However, positron emission is rarely used in hot-atom studies and this process will not be discussed in the present report.

CONCLUDING REMARKS

On the basis of the preceding discussion it is easy to recognize which items in the field of nuclear data are of interest to students of hot-atom chemistry. It will, of course, be realized that part of the data do not really refer to the nucleus in question, but rather to the atom as a whole.

In all cases it is of the highest importance to know whether there are any gamma-rays delayed by more than 10^{-13} s what their intensity per decay is, their conversion coefficient and the average ionic charge of the product atom, or – even better – the frequency distribution of the various ionic charges. (This problem is complicated by the fact that the charge

may not be independent of the composition of the matrix.) If the converted gamma ray is followed by one or more other gamma rays, details concerning the latter should also be known, as they determine the kinetic energy of the radio-atom at the stage where its final fate is decided.

For all reactions producing low-energy (< 50 eV) recoils (all categories except that under section 1), one should know the number of γ-photons emitted per decay (if any), their energies, and either their angular correlation or their delays, depending on whether the delay exceeds about 10^{-15} s or not.

In the case of electron capture, we also need more accurate information on the positive charges carried by the product atom, together with the mass difference between the parent and the daughter atom, whence we can derive the recoil energy given to the atom by the escape of the neutrino.

For β^--decay, one should have the same information as for electron-capture, but, in addition, the shape of the beta-spectrum should be known.

It will be evident that, at present, we are very far away from having the entire information asked for in the preceding paragraphs, and it is quite possible that we shall never be able to obtain all of it. Some of the more important aspects are, however, well within our reach. Concerning the de-excitation schemes of product nuclei of nuclear reactions and daughter nuclei of radioactive transitions, a good deal is already known and there do not seem to be any fundamental obstacles which could keep us from extending this knowledge to all nuclides which are of sufficient interest to hot-atom chemists to warrant the effort.

REFERENCES

[1] STÖCKLIN, G., Chemie heisser Atome, Verlag Chemie, Weinheim/Bergstr. (1969) 18.

[2] CARLSON, T.A., HUNT, W.E., KRAUSE, M.O., Phys. Rev. 151 (1966) 41; CARLSON, T.A., WHITE, R.M., Chemical Effects of Nuclear Transformations, (Proc. Symp. Vienna, 1964) 1, IAEA, Vienna (1965) 23.

[3] CARLSON, T.A., Phys. Rev. 131 (1963) 676; SNELL, A.H., PLEASANTON, F., Phys. Rev. 107 (1957) 740; 111 (1958) 1338.

DISCUSSION

K. H. LIESER (Chairman): I would like to stress the point that nuclear data give only an explanation of the very first step in hot-atom reactions. Hot-atom chemistry involves recoil effects, excitation of the hot atoms and secondary reactions as well as radiation effects. While the primary recoil effects depend on nuclear properties, the other effects, such as excitation, formation of radicals and secondary reactions, depend essentially on the properties of the atoms and of the surroundings. Thus, in hot-atom chemistry the situation is very complex.

A. H. W. ATEN: I would say that the second chapter is chemistry and the fact that the properties of the electrons already enter into what one calls the nuclear data is really a sign of the indiscrete behaviour on the part of the nuclear physicists, who have taken into the field of their activity part of the properties of the electrons of the atoms instead of restricting themselves to the nuclei.

Section VI

FISSION-PRODUCT NUCLEAR DATA

Chairman

G.B. YANKOV (USSR)

FISSION-PRODUCT CHAIN YIELDS FROM EXPERIMENTS IN THERMAL REACTORS*

E.A.C. CROUCH
Chemistry Division,
UKAEA Research Group,
AERE, Harwell, Berks,
United Kingdom

Abstract

FISSION-PRODUCT CHAIN YIELDS FROM EXPERIMENTS IN THERMAL REACTORS.

Published values of the yields of fission products from the thermal neutron induced fission of ^{227}Th, ^{229}Th, ^{233}U, ^{235}U, ^{239}Pu, ^{241}Pu, ^{242m}Am, ^{245}Cm, ^{249}Cf, and from the "pile"-neutron-induced fission of ^{227}Ac, ^{231}Pa, ^{232}Th, ^{232}U, ^{237}Np and ^{241}Am have been assessed and recommended values for the chain yields listed.

1. Introduction

Fission Product yields were last collected and assessed by a member of AERE in 1965 (Ref. 1). Since that time other collections, assessments, reviews and predictions have been made (Refs. 2, 3, 4, 5), but because of the continuous flow of new experimental results it becomes necessary to make the next assessment at approximately yearly intervals. Because the number of experimental results is getting too large to be conveniently handled in a card index file, and the simple arithmetic of adjustment and correction is increasing with each new assessment, a less onerous method of assessing the experimental results must be found. To this end there has been established at AERE a computer file library of fission product yields (Ref. 6), and an interrogation program (Ref. 7), to extract information from the library.

There are still lacunae in the experimental results even for ^{235}U thermal neutron fission (e.g. the yields at mass numbers 107, 108, 110, 113 and 116 among others, are undetermined experimentally), and there is a need both for academic and technological reasons, to have a sound means of estimating missing yields. It is intended that a mathmatical model of the fission process will be fitted to the available experimental results (e.g. Ref. 8 sets out some preliminary ideas), so that missing values in general shall be estimated with some confidence. Such a process is suited to fast and frequent computer processing and the methods of Refs. 6, 7 and 8 can be made automatic.

However, it seems prudent (and it may very well turn out to be necessary), to make preliminary assessment of the available results by the usual subjective methods so that starting estimates of the parameters of the fitted model shall be reasonable, and this paper is meant to provide part of such a necessary basis. Further papers dealing with fast fission and spontaneous fission will appear later as the work is completed. Independent yields will also be dealt with separately. In order that these assessments shall be the more easily applied to the objective methods

* The contents of this paper have been examined and recommended by the UK Chemical Nuclear Data Committee.

it was thought proper to make some estimates of the errors to be associated with each recommended chain yield. It is believed to be the first time that this has been done and the method used is described in detail. In such a compilation as this there are bound to be errors, and readers are asked to let the author know of any that they detect.

2. Basis of the Assessment

i) It would seem proper to define certain terms used by those engaged in the determination or use of Fission Product yields. There are three kinds of Fission Product yields as defined below and they are usually expressed as a number of fission product atoms formed per one hundred fissions i.e. in the form of a percentage.

a) Independent Yield

An independent yield is the probability of formation of a given nuclide in fission, after prompt neutron emission but before any radioactive decay of itself or it's precursors occurs. Sometimes independent yields are expressed as 'fractional independent yields' i.e. as a fraction of the chain yield.

b) Cumulative Yields

A cumulative yield is the probability of formation in fission of a nuclide after prompt and delayed neutron emission and before it decays, but including the independent yields of its precursors. A 'fractional' cumulative yield is a cumulative yield expressed as a fraction of the chain yield. Effectively a cumulative yield is the sum of all the independent yields in a decay chain up to and including the atomic number of the nuclide concerned.

c) Chain Yield

A Chain Yield is the probability of formation in fission of a given stable nuclide after prompt and delayed neutron emission and after the decay of all its precursors. It is effectively the sum of all the independent yields contributing to a given mass decay chain. Usually it is the cumulative yield of the last (stable) member of a decay chain of given mass number.

ii) Treatment of published results; yield adjustments

The published data for this assessment were stored in a computer file library (Ref. 6), and for each fissile isotope an interrogation program (Ref. 7), caused all cumulative and chain yields to be printed out. It was assumed that the printed list contained no duplicate values because during compilation of the library experimental results but not assessed values from compilations were included.

All entries were checked to ensure that values previously reported by the same author(s) were omitted if the new entry were a recalculation of the previous work and not a new determination. Corresponding to the print-out, punched cards were produced for the thermal fission products of the nuclides ^{233}U, ^{235}U, ^{239}Pu and ^{241}Pu, and the adjustments to be described below were applied to the reported results by means of computer routines which will be used in future computerised assessments using objective methods (see Ref. 8 for preliminary description). The results on the fission products of other fissile

isotopes, and those produced in fission induced by other neutron energies, were adjusted by hand calculations on the figures contained in the printed output of the interrogation routine.

As previously explained (Refs. 6, 7), there are three ways of classifying fission product yields depending on what corrections or adjustments have to be made to them before they can be combined with other similar results to give an average value. 'One-nuclide' yields are those yields relative to the yield of say ^{140}Ba or ^{99}Mo. Then if the reference yield is known the others can be adjusted relative to it.

'Other' yields (i.e. other than 'one-nuclide' or 'R-value'), are yields which have been determined absolutely or effectively absolutely, and which do not require or are not amenable to adjustment. This kind of yield is determined by simultaneously measuring the absolute number of fissions and the number of atoms of the resulting fission products. Sometimes the fissile isotope and the fission products are measured in the same piece of fissile material, sometimes the fissions are measured in a small quantity of the fissile material which is irradiated in close propinquity to the fissile material in which the fission products are measured.

In some cases yields are effectively absolute because after measuring the relative yields of a sufficient number of fission products, a smooth curve against mass-number is drawn and all the yields are multiples by a common factor which forces the area under the curve to sum to 200%. Usually no adjustment can be applied to the resultant yields.

'R-value' yields are calculated as follows:

$$y_1^X = y_2^X \left[\frac{A_1^X A_2^R}{A_2^X A_1^R}\right] \quad \frac{y_1^R}{y_2^R}$$

Where y is a yield and A an activity,

X is the nuclide of interest,
R is the reference nuclide, usually ^{99}Mo,
1 refers to the nuclear reaction of interest,
2 refers to the standard reaction, Thermal neutron fission usually of ^{235}U, less frequently, of ^{239}Pu.

The term in brackets in the above equation is called 'R-value' and is made up of measured radioactivities derived from the reaction of interest and from a simultaneous standard reaction irradiation. The other components of the right hand side must be absolutely determined or assumed.

The assessment process started with the thermal fission yields of ^{235}U. First all 'other' type yields were assembled i.e. those which required no adjustments. Mean values for such reference nuclides as ^{140}Ba, ^{99}Mo and ^{97}Zr were calculated and used to adjust the 'one-nuclide' type yields. If 'other' type yields were not available to establish a good absolute value for a reference nuclide of a 'one-nuclide' result then the adjustment was made by reference to the recommended value given in Ref. 2, which failing, Ref. 3. Finally all the results for a given mass number were used to find a mean and

its uncertainty; the chain yield recommended being composed of results determined as chain yields and cumulative yields eligible (see later), for inclusion as chain yields.

Attention was then turned to the ^{239}Pu fission yields. First all 'other' type results were assembled and absolute values for reference yields were obtained. The 'one-nuclide' yields were then adjusted in the same way as those of ^{235}U. 'R-value' yields were adjusted using the ^{235}U yields already established, along with the ^{239}Pu reference yield derived from 'other' and 'one-nuclide' yields. Finally the mean value and its uncertainty were found using all the results available. For a given mass-number the recommended chain yield contains those cumulative yields eligible for inclusion as chain yields.

The assessment process described above for ^{239}Pu, was applied to all the other fissile isotope fission yields. However, for some fissile nuclides not many experimental results are available so their values for reference nuclide yields cannot be established. In such cases authors commonly assume a reference nuclide yield and when this is so the assumed yield is indicated in the tables of results (below).

iii) Treatment of Published results: Error estimates

The uncertainties to be associated with a given measurement are reported by the authors in a variety of ways, and frequently not at all. Usually a mean value is given together with limits expressed as yield $X \pm x$, where x may be a standard deviation corresponding to the precision of the measurement only, not to the absolute accuracy of the measurement.

In this work two methods of expressing the experimental uncertainty or 'error' (the word being used in no pejorative sense), were used. In the first method the error (considered as a standard error), used in this paper (as opposed to the figure reported by the author), has been adjusted if necessary to what seemed to be a reasonable estimate of the absolute accuracy. Thus a yield given in an original paper as being subject to an error of $\pm$ 0.1% of the mean value, has been attributed a much larger error even if the yield were determined by mass-spectrometry. For this purpose no reported yield has been attributed a standard error of less than $\pm$ 3% of the mean value unless very good reason was shown in the paper. Likewise a yield reported without an estimate of its accuracy was attributed a standard error of $\pm$ 15% if the yield was determined radiochemically and $\pm$ 10% if by mass-spectrometry. There were occasions when better accuracy was attributed because there seemed good cause. Of course in those cases where reasonable errors were attributed to their results by the authors themselves, they were used unchanged.

The weighted mean of all the reported yields (after adjustment), for a given mass number in a given fission reaction was then calculated using the reciprocal of the square of the attributed standard error as weight for each result, together with the standard error of the weighted mean as follows:

$$\text{Weighted mean yield} = \sum_n \left(\frac{Y_n}{S_n^2}\right) \Bigg/ \sum_n \left(\frac{1}{S_n^2}\right)$$

where Y_n is the nth yield and S_n is its attributed standard error.

Standard error of the weighted mean yield = $\left[\sum_n \left(\frac{1}{S_n^2}\right)\right]^{-\frac{1}{2}}$.

The weighted sum of squares of the deviations of each included yield from the weighted mean (which should be distributed as χ^2) was then calculated,

$$\sum_n \left[\left(\frac{Y_n - \bar{Y}_w}{S_n}\right)\right]^2$$ where $\bar{Y}_w$ is the weighted mean yield.

If in fact it was significantly different from χ^2 then either the fission yields were inconsistent or the attributed errors were unrealistically small.

The second method of expressing the experimental uncertainty was simply to use the reported yields for a given mass number after adjustment, to calculate a simple mean and standard deviation directly. These two figures should agree with the weighted values found as described above. If they agreed then the attributed errors were realistic and the yields consistent, but if they differed then either the yields were inconsistent or the attributed errors were smaller than the errors indicated by the variations about the simple mean. It was also possible to find the attributed error larger than that calculated from the simple mean in cases whose only two or three reported results fortuitously agreed closely, although it was known that the experimental method was subject to larger error.

Finally the weighted mean yield was taken as the required assessed yield and the uncertainty (expressed as a standard error), was taken as the greater of the standard error of the weighted mean yield (see above), or the simple standard error calculated as

$$\left[\frac{\sum(Y_i - \bar{Y})^2}{(n-1)}\right]^{\frac{1}{2}} \Big/ n^{\frac{1}{2}}$$ where $\bar{Y}$ is the simple mean yield.

3. The assessed yields

The assessed fission yields are given[1] in Tables I-XV. The yields for ^{227}Ac, ^{231}Pa, ^{232}Th, ^{232}U, ^{237}Np and ^{241}Am are those obtained by "Pile" irradiations; they are not properly "thermal" yields and those who use them are urged to refer back to the orginal papers if considerations of the neutron energy distribution are at issue. Nevertheless they are listed here with the "thermal" yield as they will probably be used in conjunction. It must be noted in passing that the "thermal" yields here tabulated are not often obtained under conditions which eliminate the effects of fast neutrons present in the reactor. Reliance is placed upon the fact that thermal neutron fission reaction rates are in general far greater than the fission reaction rates due to fast neutrons.

[1] All tables are to be found at the end of this paper.

It should also be mentioned that the Tables show yields which were determined as chain-yields, and also cumulative yields which can be taken as chain-yields since the independent yields of nuclides of the same mass number, but greater atomic number, are negligible. An indication of the admissibility of cumulative yields for this purpose may be gleaned from Ref. 9 which tabultes independent yields. In general no cumulative yields have been used unless they account for 99.00% of the chain yield as calculated in Ref. 9.

4. References

[1] CROALL, I.F., "Yields from neutron induced fission", AERE-R 5086, (November 1965).

[2] MEEK, M.E., RIDER, B.F., "Summary of fission product yields for U^{235}, U^{238}, Pu^{239} and Pu^{241} at thermal, fission spectrum and 14 MeV neutron energies", APED-5398-A (Revised October 1968).

[3] FLYNN, K.F., GLENDENIN, L.E., "Yields of fission products for several fissionable nuclides at various incident neutron energies", ANL-7749, (December 1970).

[4] SIDEBOTHAM, E.W., "Fission product yield data extrapolated for some actinides", TRG Report 2134(R), (1972).

[5] VON GUNTEN, H.R., "Distribution of mass in spontaneous and neutron induced fission", Actinide Reviews, 1(1969), p 275.

[6] CROUCH, E.A.C., "A library of neutron induced fission product yields maintained and interrogated by computer methods. Part 1. Establishment of the library", AERE-R 6642 (December 1970).

[7] CROUCH, E.A.C., "A library of neutron induced fission product yields maintained and interrogated by computer methods. Part 2. Interrogation of the library", AERE-E 7207.

[8] CROUCH, E.A.C., "The Assessment of Fission Yields", Chemical Nuclear Data - measurements and applications. Proceeding of the International Conference, Canterbury (September 1971).

[9] CROUCH, E.A.C., "Calculated Independent yields in thermal neutrons fission of ^{233}U, ^{235}U, ^{239}Pu, ^{241}Pu and in fission of ^{232}Th, ^{238}U and ^{240}Pu, AERE-R 6056 (March 1969).

[10] HOLDEN, N.E., WALKER, F.W., "Chart of the nuclides", General Electric Company, Knolls Atomic Power Laboratory, Tenth Edition, (December 1968).

5. Explanation of the Tables

Mass Number (Col. 1)

This entry gives the mass-number of the fission product decay chain.

Element (Col. 2)

The symbol of the element used to estimate the chain yield. Several entries in this column does not imply that all were used in the calcula-

tion of the chain yield. Chain yields determined as "chain yields" are entered as such. A figure in brackets alongside an element symbol indicates that the nuclide is isomeric and the isomeric yield is given, the number is the order of the isomer in the 'Chart of the Nuclides'.

Literature Reference (Col. 3)

The number given in Column 3 gives the literature reference as set out in Table XVI.

Corrected value and error (Col. 4)

Column 4 gives the adjusted yield as a percentage followed by the error as a standard deviation expressed as a percentage of the yield. Thus the first entry for Br in Table I is to be read "7.00 $\pm$ 0.7%". The author's estimates of error are stated when they are given, otherwise an arbitrary default value is inserted (see para. 2 (iii) above).

Means: Weighted and simple (Col. 5)

The two figures entered on one line in column 5 are the mean as a percentage yield, the error as a percentage of the mean yield. The types of mean are differentiated by (w) for weighted and (s) for simple. Each mean is based on the values given in Column 4 as segregated by the horizontal lines. In some cases, usually when only two results are given in Column 4, the weighted mean only or the simple mean only appears in Column 5. This is because in the former case the weights are not equal and there would be no point in calculating a simple mean, or in the latter case there would be no point in calculating a weighted mean when the weights are equal or nearly so.

Note however, that the actual weights used in deriving the content of Column 5 from those of Column 4 are not necessarily those given in Column 4 which are the author's estimates or the default values (see paragraph 2 (iii) above).

Recommended Chain Yields (Col. 6)

Column 6 lists the recommended chain yield on the same line as the mass-number of the first column. The figures given in brackets are the indicators of yields still undetermined experimentally and they are interpolated values found by curve drawing through the neighbouring points. No attempt has been made to interpolate values when insufficient results are available to draw a smooth curve, or in regions where fine structure is likely to exist.

Table I

^{227}Ac Pile Neutron induced fission

1	2	3	4		5		6	
83	Br	229	7.00	10			7.00	10
89	Sr	229	7.89	10			7.89	10
91	Sr	229	5.82	10			5.82	10
97	Zr	229	0.31	10			0.31	10
99	Mo	229	0.11	10			0.11	10
105	Ru	229	0.88	10			0.88	10
109	Pd	229	0.24	10			0.24	10
111	Ag	229	0.16	10			0.16	10
112	Ag	229	0.14	10			0.14	10
121	Sn(2)	229	0.092	10			-	-
132	Te	229	4.59	10			4.59	10
140	Ba	229	8.23	10			8.23	10
143	Ce	229	6.17	10			6.17	10

Table II

^{227}Th Thermal Neutron induced fission

1	2	3	4		5		6	
77	As	211	1.4	15			1.4	15
83	Br	211	1.1	32			1.1	32
89	Sr	211	8.0	6			8.0	6
90	Sr	211	8.72	10			8.72	10
91	Sr	211	6.21	16			6.21	16
95	Zr	211	3.4	9			3.4	9
97	Zr	211	2.41	24			2.41	24
99	Mo	211	1.44	10			1.44	10
103	Ru	211	0.58	16			0.58	16
105	Ru	211	0.28	14			0.28	14
106	Ru	211	0.19	32			0.19	32
109	Pd	211	0.33	4			0.33	4
111	Ag	211	0.051	20			0.051	20
112	Pd	211	0.029	21			0.029	21
113	Ag	211	0.034	21			0.034	21
115	Chain	211	0.177	15			0.177	15
121	Sn(2)	211	0.11	36			-	-
125	Sn(2)	211	0.43	23			-	-
127	Sb	211	0.68	24	0.63	29	0.63	29
	Te(2)	211	0.53	47				
129	Te	211	1.36	21			1.36	21
131	I	211	2.61	18			2.61	18
132	Te	211	3.30	18			3.30	18
133	I	211	4.80	21			4.80	21
137	Cs	211	6.93	18			6.93	18
140	Ba	211	7.71	15			7.71	15
141	Ce	211	7.62	7			7.62	7
143	Ce	211	6.97	7			6.97	7
144	Ce	211	5.95	7			5.95	7
147	Nd	211	0.18	28			0.18	28

Table III

^{229}Th Thermal neutrons induced fission

1	2	3	4		5			6	
77	As	304	.106	15				.106	15
	Ge(1)	648	.011	15					
78	Ge	649	0.052	15				0.052	15
83	Br	304	8.11	15	(W)	6.48	7	6.48	9
		649	6.40	4	(S)	6.88	9		
		226	6.14	0.5					
84	Br	649	10.88	4	(S)	10.88	2	10.88	10
	Chain	226	10.88	4					
85	Chain	226	10.79	1				10.79	10
87	Chain	226	8.75	1				8.75	10
88	Rb	649	7.66	6	(S)	8.65	7.5	8.65	7.5
	Chain	226	9.64	.5					
89	Sr	304	7.3	15	(W)	8.46	9	8.46	12
		649	9.3	3	(S)	8.30	12		
90	Sr	226	2.7	20	(W)	7.72	9	7.72	9
		304	6.79	14					
		649	8.44	4					
91	Sr	304	5.78	17	(W)	6.81	9	6.81	9
	Y	649	7.40	5					
92	Y	649	6.40	9				6.40	10
93	Y	649	4.40	6				4.40	10
95	Zr	304	2.64	15	(W)	2.64	10	2.64	10
		649	2.60	15					
97	Zr	649	0.61	15				0.61	15
99	Mo	304	0.162	15	(W)	0.153	9	0.153	9
		649	0.15	4					
103	Ru	304	0.044	15	(S)	0.025	76	0.025	76
		649	0.006	10					
105	Ru	304	0.025	15	(S)	0.012	52	0.012	52
		649	0.008	3					
106	Ru	304	0.0203	15	(S)	0.016	27	0.016	27
		649	0.0117	8					
109	Pd	304	0.0132	15	(S)	0.0102	30	0.0102	30
		649	0.0071	10					

Table III (cont)

^{229}Th thermal neutrons induced fission

1	2	3	4			5		6	
111	Ag	304	0.0203	15	(S)	0.0207	7	0.0207	7
		649	0.021	4					
112	Pd	304	.0182	15	(S)	0.0196	7	0.0196	7
		649	.021	3					
113	Ag	304	.0167	15	(S)	0.0153	6	0.0153	11
		649	.0144	12					
115	Cd	304	.0213	15	(S)	0.0199	11	0.0199	11
		649	.0184	6					
117	Cd	649	.0163	12	(W)	0.0165	6	0.0165	6
	In	649	.0166	7					
118	Cd	649	.0174	5				0.0174	10
121	Sn(2)	649	.074	2					
125	Sn(2)	304	.040	15				0.042	11
	Sn(1)	649	.0022	14					
127	Sb	304	.04	15				0.042	11
		649	.0084	4					
	Te	304	.0405	15					
129	Te	304	.125	15	(W)	0.124	11	0.124	11
	Sb	649	.122	7					
131	Chain	227	.64	5	(W)	.595	5	.595	20
	I	304	.882	15	(S)	.651	20		
		649	.43	11					
132	Te	227	1.218	5	(W)	1.124	5	1.12	11
		304	1.125	15	(S)	1.113	11		
		649	0.87	6					
133	Chain	227	3.02	5	(W)	3.04	5	3.04	5
	I	649	4.00	24					
134	Chain	227	6.03	5	(W)	5.90	5	5.90	5
	I	649	5.30	13					
135	I	649	4.96	5	(W)	5.46	4	5.46	11
	Chain	227	6.10	5	(S)	5.53	11		
136	Chain	227	6.03	5				6.03	10

Table III (cont)

^{229}Th thermal neutrons induced fission

1	2	3	4		5			6	
137	Cs	304	5.98	15	(W)	6.94	5	6.94	9
		649	6.10	12	(S)	6.53	9		
	Chain	227	7.60	5					
138	Cs	649	8.00	3				8.00	5
139	Ba	649	8.96	1				8.96	5
140	Ba	304	7.30	15	(W)	9.74	5	9.74	17
		649	8.30	15	(S)	9.28	17		
	Chain	227	12.25	50					
141	La	649	8.35	0.5	(W)	8.03	6	8.03	6
	Ce	304	7.91	15					
		649	7.83	5					
142	La	649	8.50	9	(W)	5.66	5	5.66	23
	Chain	227	5.38	5	(S)	6.94	23		
143	Ce	649	8.87	3	(W)	5.48	5	5.48	27
	Chain	227	5.14	5	(S)	7.03	27		
144	Ce	304	8.72	15	(W)	6.15	5	6.15	16
		649	9.57	3	(S)	7.96	16		
	Chain	227	5.60	5					
145	Pr	649	5.40	15	(W)	3.30	5	3.30	27
	Chain	227	3.13	5	(S)	4.26	27		
146	Chain	227	2.14	5				2.17	10
147	Pr	649	1.83	15				1.83	15
148	Chain	227	1.07	5				1.07	10
149	Pm	649	0.71	15				0.71	15
150	Chain	227	0.18	5				0.18	10
151	Pm	649	0.046	15				0.046	15

Table IV

^{231}Pa Pile neutron induced fission

1	2	3	4			5		6	
83	Br	661	2.27	0.2				2.27	15
85	Kr(1)	587	4.46	3				-	-
89	Sr	230	6.62	10	(S)	6.99	4	6.99	11
		661	7.26	0.2					
91	Sr	661	7.34	15	(S)	6.85	4	6.85	9
		230	6.80	10					
	Y	587	6.40	0.5					
95	Nb	587	6.40	0.5				6.40	15
97	Zr	230	4.11	10	(S)	4.32	3	4.32	9
		661	4.50	15					
	Nb	587	4.36	2					
99	Mo	230	3.40	10	(S)	2.50	2.5	2.50	9
		661	2.59	15					
		587	2.51	1					
103	Ru	230	0.30	10	(S)	0.346	10	0.346	10
		661	0.33	15					
		587	0.41	1.3					
105	Ru	230	0.14	10	(S)	0.147	3	0.147	11
		661	0.154	15					
106	Ru	230	0.101	10	(S)	.105	3.5	0.105	11
		661	0.108	15					
109	Pd	230	0.076	10	(S)	0.080	4.5	0.080	11
		661	0.083	15	(W)	0.08	11		
111	Ag	230	0.081	10	(S)	0.90	10	0.90	10
		661	0.099	15					
112	Pd	230	0.047	10	(S)	0.054	13	0.054	13
		661	0.061	15					
113	Ag	230	0.060	10	(S)	0.067	12.5	0.069	13
		661	0.077	15					
115	Cd(2)	230	0.072	10				0.080	15
	Cd	661	0.080	15					
121	Sn(2)	230	0.068	10	(S)	0.074	6	0.072	11
		661	0.076	15					

Table IV (cont)

^{231}Pa Pile neutron induced fission

127	Sb	230	1.90	10				0.08	15
		661	0.080	15					
129	Te(2)	230	1.66	10	(S)	1.42	17	1.42	17
		661	1.18	15					
131	I	587	2.63	1.3				2.63	15
132	Te	230	2.83	10	(S)	3.24	9	3.24	9
		587	3.46	1					
		661	3.42	15					
133	Xe	587	5.21	1				5.21	15
135	Xe	587	6.69	34				6.69	34
140	Ba	230	6.25	10	(S)	6.80	5	6.80	8
		661	6.96	15					
	La	587	7.18	1					
141	Ce	587	6.88	1				6.88	15
143	Ce	230	5.58	10	(S)	5.61	6	5.61	8
		587	5.12	1					
		661	6.12	15					
144	Ce	587	4.79	3				4.79	15
147	Nd	587	1.89	2	(S)	2.17	13	2.17	13
		661	2.45	15					
149	Pm	587	0.95	3				0.95	15
153	Sm	661	0.079	15				0.079	15

Table V

^{232}Th Pile neutron induced fission

1	2	3	4		5			6	
72	Zn	348	.000136	15				.000136	15
73	Ga	326	.00035	50				.00035	50
77	Ge(2)	326	.009	22				.071	24
	As	228	.0106	0.5	(W)	.011	14		
		326	.0172	35	(S)	.014	24		
83	Br	228	1.98	7	(W)	1.98	7	1.98	9
		326	1.97	24	(S)	2.13	9		
		348	2.51	15					
89	Sr	15	7.20	6	(W)	6.96	5	6.96	5
		326	6.70	10	(S)	6.73	4		
		348	6.30	15					
90	Sr	15	7.55	6	(W)	7.24	3	7.24	4
		288	7.46	4	(S)	7.09	4		
		326	7.24	20					
		336	7.01	1					
		348	6.18	15					
91	Sr	228	6.81	8	(W)	5.18	5	5.18	11
		326	7.34	11	(S)	6.14	11		
		348	5.97	15					
	Y	15	4.44	6					
93	Y	367	7.86	15				7.86	15
95	Zr	228	5.30	6				5.30	6
97	Zr	228	4.15	14	(W)	4.65	9	4.65	9
		326	5.03	15	(S)	4.77	7		
		348	5.13	15					
99	Mo							2.78*	
103	Ru	228	0.149	5	(W)	0.149	4	0.15	6
		326	0.158	33	(S)	0.160	6		
		348	0.188	15					
		336	0.147	6					
105	Rh	228	0.031	5	(W)	0.072	14	0.072	14
		326	0.072	29					
		348	0.073	15					
106	Ru	228	.0405	5	(W)	.0425	5	.043	10
		326	.0435	10	(S)	.0498	10		
		336	.0612	15					
		348	.054	15					

* Taken as reference point in all papers.

Table V (cont)

^{232}Th Pile neutron induced fission

1	2	3	4		5			6	
109	Pd	228	0.05	8	(W)	0.050	7	0.050	7
		326	0.051	20	(S)	0.051	4		
		348	0.0492	15					
111	Ag	228	0.059	9	(W)	0.054	6	0.054	14
		326	0.047	20	(S)	0.058	14		
		336	0.081	15					
		348	0.046	15					
112	Pd	228	0.055	9	(W)	0.057	7	0.057	14
		326	0.049	15	(S)	0.063	14		
		348	0.061	15					
		336	0.089	15					
113	Ag	228	0.045	7				0.045	7
115	Cd(1)	228	.00052	15	(W)	0.05	13	0.050	13
	Cd(2)	228	.0465	15					
		348	0.055	15					
	(Cd chain)	326	0.0575	20					
117	In	228	0.048	11				0.048	11
121	Sn	228	0.046	5				0.046	15
123	Sn	228	0.0267	4				0.027	15
125	Sn	228	0.037	8				0.037	15
127	Sb	228	0.172	5				0.17	15
131	I	228	1.57	4	(W)	1.27	5	1.27	22
		326	1.18	50	(S)	1.39	22		
		336	2.14	15					
		348	0.68	15					
132	Te	326	2.24	29	(W)	1.76	14	1.76	15
		348	1.68	15					
137	Cs	228	4.5	1	(W)	4.76	5	4.76	9
		326	6.44	15	(S)	5.90	9		
		348	6.07	15					
		336	6.59	15					
139	Ba	228	7.60	0.5				7.60	10

Table V (cont)

^{232}Th Pile neutron induced fission

1	2	3	4		5			6	
140	Ba	228	8.38	3	(W)	7.59	4	7.59	7
		326	6.14	32	(S)	7.27	7		
		348	5.76	15					
		336	7.73	15					
		15	6.94	8					
	La	367	8.67	15					
141	Ce	15	6.59	5	(W)	7.60	3	7.60	6
		228	7.38	5	(S)	7.24	6		
		326	8.69	33					
		336	7.26	15					
		348	6.28	15					
143	Ce	367	7.12	15	(W)	6.81	4	6.81	4
	Pr	15	6.59	5	(S)	6.91	3		
		288	7.03	3					
144	Pr	228	6.98	0.5	(W)	7.10	4	7.10	4
	Ce	15	7.15	5	(S)	7.28	4		
		326	6.93	14					
		336	7.98	15					
		348	6.49	15					
		367	8.14	15					
147	Nd	15	2.71	8	(W)	2.96	5	2.96	6
		228	3.08	5	(S)	3.01	6		
		367	3.25	15					
149	Nd	367	1.57	15	(S)	1.22	30	1.22	30
	Pm	228	0.861	15					
151	Pm	367	0.46	15				0.46	15
153	Sm	367	0.22	15				0.22	15
156	Eu	228	0.0029	11				.0029	15

Table VI

^{232}U Pile Neutron induced fission

1	2	3	4		5			6	
85	Kr(1)	605	2.43	2				-	
91	Y	605	7.43	2				7.43	15
95	Zr	605	6.30	1	(W)	6.32	1	6.32	11
	Nb	605	6.36	2	(S)	6.33	1		
97	Zr	605	4.98	1	(W)	4.99	1	4.99	11
	Nb	605	5.07	2					
99	Mo	605	4.22	2	(W)	4.10	1	4.10	11
	Tc	605	4.08	1					
103	Ru	605	1.09	1				1.09	15
131	I	605	4.13	1				4.13	15
132	Te	605	4.77	1	(W)	4.80	1	4.80	11
	I	605	4.84	1					
133	I	605	5.76	4	(W)	5.64	1	5.64	11
	Xe	605	5.63	0.5					
135	Xe	605	6.40	11				6.40	15
137	Cs	605	8.14	1				8.14	15
140	Ba	605	7.26	1	(W)	7.17	1	7.17	11
	La	605	7.04	1					
141	Ce	605	6.61	1				6.61	15
143	Ce	605	4.68	1				4.68	15
144	Ce	605	4.32	4				4.32	15
147	Nd	605	1.15	2				1.15	15

Table VII

^{233}U Thermal neutron induced fission

77	Ge	347	0.00879	15				0.02	15
	As	347	0.0198	15					
78								(0.04)	
79								(0.08)	
80								(0.17)	
81	Se(1)	85	0.0141	14				0.33	12
	Se(2)	85	0.325	12					
82								(0.61)	
83	Se(2)	85	0.404	8				1.09	4
	Br	347	0.769	15	(W)	1.09	4		
	Kr	74	1.18	4	(S)	1.03	4		
		209	1.16	1					
	Chain	250	1.028	1					
84	Kr	74	1.97	4	(W)	1.81	3	1.81	4
		209	1.93	5	(S)	1.88	4		
	Chain	250	1.73	1					
85	Kr(2)	209	0.574	4				2.32	7
		590	0.512	2					
	Kr(1)	609	2.33	3					
	Rb	74	2,54	4	(W)	2 32	3		
	Chain	250	2.22	0.5	(S)	2.38	7		
86	Kr	74	3.30	4	(W)	3.06	3	3.06	4
		209	3.25	1	(S)	3.15	4		
	Chain	250	2.90	1					
87	Rb	74	4.61	4	(W)	4.18	3	4.18	7
	Chain	250	4.06	1	(S)	4.34	7		
88	Sr	17	5.30	6	(W)	5.47	2	5.47	2
		18	5.30	6	(S)	5.42	2		
		74	5.54	4					
		210	3.78	15					
		220	5.38	3					
	Chain	250	5.57	1					
89	Sr	32	6.91	2	(W)	6.12	3	6.12	5
		74	6.15	4	(S)	6.06	5		
		210	5.00	15					
		309	5.56	3					
		347	6.15	15					
	Y	220	6.61	4					

Table VII (cont)

^{233}U Thermal neutron induced fission

1	2	3	4		5			6	
90	Sr	17	5.80	7	(W)	6.33	3	6.33	4
		18	5.80	7	(S)	6.22	4		
		28	4.56	2					
		28	4.46	3					
		74	6.75	4					
		309	6.19	0.5					
	Zr	220	5.80	4					
	Chain	250	6.96	1					
91	Sr	32	6.59	2	(W)	6.56	2	6.56	2
		309	4.82	6	(S)	6.56	1.5		
		609	6.36	3					
	Y	76	6.90	10					
		309	3.55	2					
		347	4.50	15					
	Zr	74	6,45	4					
		210	6.31	15					
		220	6.74	3					
	Chain	250	6.60	1					
92	Zr	74	6.72	4	(W)	6.66	3	6.66	3
		210	6.37	15	(S)	6.58	2		
		220	6.53	4					
	Chain	250	6.69	1					
93	Zr	74	7.01	4	(W)	7.06	3	7.06	3
		210	6.88	15	(S)	6.99	1		
	Chain	250	7.09	1					
94	Zr	74	6.68	4	(W)	6.80	3	6.80	3
		210	6.92	15	(S)	6.80	1		
		220	6.69	4					
	Chain	250	6.91	1					
95	Zr	74	6.23	4	(W)	6.27	3	6.27	5
		309	5.01	12	(S)	6.02	5		
		347	6.26	15					
		609	6.17	2					
	Nb	309	5.16	12					
	Mo	210	6.92	15					
	Chain	250	6.40	1					
96	Zr	94	5.67	4	(W)	5.78	3	5.78	3
		210	6.78	15	(S)	6.00	2		
		220	5.69	5					
	Chain	250	5.84	1					

Table VII (cont)

^{233}U Thermal neutron induced fission

1	2	3	4		5			6	
97	Zr	609	5.73	2	(W)	5.57	3	5.57	5
	Nb	609	5.75	2	(S)	5.87	5		
	Mo	74	5.51	4					
		310	6.69	15					
	Chain	250	5.82	1					
98	Mo	74	5.22	4	(W)	5.24	3	5.24	7
		210	6.27	15	(S)	5.57	7		
	Chain	250	5.22	1					
99	Mo	76	4.80	10	(W)	5.08	3	5.08	3
		197	4.96	3	(S)	4.98	2		
		347	5.16	15					
		609	4.80	15					
	Chain	250	5.16	1					
100	Mo	74	4.49	4	(W)	4.50	3	4.50	16
		210	6.96	15	(S)	5.30	16		
	Chain	250	4.46	1					
101	Ru	74	2.87	4	(S)	3.10	3	3.10	3
	Chain	250	3.27	1					
102	Ru	74	2.10	4	(W)	2.31	3	2.31	3
	Chain	250	2.48	1					
103	Ru	43	1.71	6	(W)	1.61	4	1.61	15
		309	2.02	4	(S)	1.35	15		
		347	0.933	15					
		609	1.52	2					
104	Ru	74	0.94	4	(W)	1.00	3	1.00	3
	Chain	250	1.04	1					
105								(0.52)	
106	Ru	43	0.19	6	(W)	0.262	3	0.262	3
		309	0.26	12					
		347	0.263	15					
	Chain	250	0.262	1					
107								(0.105)	
108								(0.087)	
109	Pd	347	0.052	15				0.052	15
110								(0.032)	

Table VII (cont)

^{233}U Thermal neutron induced fission

1	2	3	4		5			6	
111	Pd	25	0.021	10	(W)	0.0203	7	0.02	7
	Ag	309	0.0187	1					
		347	0.0242	15					
112	Pd	309	0.0125	3	(W)	.013	9	0.013	9
		347	0.0154	15					
113								(0.014)	
114								(0.015)	
115	Cd(1)	347	0.0011	15				.019	15
	Cd(2)	347	0.0176	15					
(116)								(0.0154)	
117	Sn	246	0.0146	7				0.015	7
118	Sn	246	0.0151	7				0.015	7
119	Sn	246	0.0153	7				0.015	7
120	Sn	246	0.017	7				0.017	7
121	Sn(2)	347	0.0198	15				0.02	15
122	Sn	246	0.0189	6				0.019	6
123								(0.024)	
124	Sn	246	0.0313	5				0.031	5
125	Sn(2)	347	0.0593	15				0.116	11
	Chain	250	0.116	11					
126								(0.262)	
127	Sb	309	0.59	14				0.59	15
		347	0.101	15					
	Te	347	0.0736	15					
128								(1.04)	
129								(1.61)	
130								(2.40)	
131	I	309	2.84	7				3.51	2
		347	2.96	15					
	Xe	74	3.52	4	(W)	3.51	2		
		209	3.45	1	(S)	3.51	1		
	Chain	250	3.51	1					
		609	3.57	2					

Table VII (cont)

^{233}U Thermal neutron induced fission

1	2	3	4		5			6	
132	Te	309	4.32	6	(W)	4.41	6	4.81	6
		347	5.38	15					
	Xe	74	4.82	4	(W)	4.81	3		
	Chain	250	4.88	1	(S)	4.41	6		
		609	4.70	6					
133	I	309	3.37	9	(W)	5.85	2	5.88	2
	Xe	609	5.94	6	(S)	5.77	2		
	Cs	16	5.20	6					
		16	5.50	2					
		72	5.60	3					
		74	5.77	4					
		209	5.74	15					
	Chain	250	6.06	1					
		381	5.85	15					
		381	6.11	15					
		381	5.85	15					
		609	5.86	2					
134	Xe	74	6.18	4	(W)	6.14	3	6.14	3
		209	6.08	1	(S)	6.13	1		
	Chain	250	6.13	1					
135	I	273	4.59	1				5.81	3
	Xe	72	6.00	3	(W)	5.81	3		
		74	6.02	4					
		609	5.40	1					
136	I	347	1.87	15				6.89	5
	Xe	74	6.89	4					
137	Cs	16	5.80	5	(W)	6.12	2	6.12	3
		16	5.16	3	(S)	6.25	3		
		19	6.16	2					
		43	8.32	6					
		74	6.58	4					
		209	6.58	2					
		220	6.41	2					
		309	5.39	2					
		383	6.13	2					
	Chain	250	6.93	3					
		381	6.63	15					
		381	6.58	15					
		381	6.60	15					

Table VII (cont)

^{233}U Thermal neutron induced fission

1	2	3	4		5			6	
138	Chain	250	5.97	1	(W)	5.96	3	5.96	3
		381	5.74	15					
139	Ba	32	6.59	2	(S)	6.20	3	6.20	3
		609	6.13	2					
	La	19	5.91	4					
		220	6.15	4					
140	Ba	32	6.59	2	(W)	6.32	2	6.32	3
		276	6.59	1	(S)	6.16	3		
		309	5.21	5					
		609	6.07	2					
		347	6.59	15					
	La	609	6.02	1					
	Ce	16	5.45	9					
		16	6.16	4					
		74	6.72	4					
		220	6.41	4					
		290	5.60	3					
	Chain	250	6.53	1					
141	La	32	7.24	2	(W)	6.16	3	6.16	6
	Ce	76	7.11	10	(S)	6.28	6		
		309	5.30	2					
		609	6.69	2					
	Pr	19	5.57	3					
		220	5.79	3					
142	Ce	16	5.50	9	(W)	6.61	2	6.61	4
		16	6.06	4	(S)	6.29	4		
		74	7.00	4					
		220	6.30	4					
		290	5.60	3					
	Chain	250	6.71	1					
		381	6.83	15					
143	Ce	309	6.99	5	(W)	5.83	2	5.83	3
		609	5.67	2	(S)	5.81	3		
	Pr	76	5.71	10					
	Nd	16	5.00	6					
		16	5.19	3					
		72	6.45	3					
		74	6.22	4					
		220	5.40	3					
		259	5.86	15					
		290	5.15	6					
	Chain	250	5.85	1					
		381	5.98	15					
		381	5.90	15					
		381	5.90	15					

Table VII (cont)

^{233}U Thermal neutron induced fission

1	2	3	4		5			6	
144	Ce	76	4.48	10	(W)	4.52	2	4.52	4
		309	3.69	5	(S)	4.26	4		
		347	3.75	15					
		609	4.54	1					
	Nd	16	3.80	10					
		16	3.84	4					
		74	4.87	4					
		259	4.56	15					
		290	3.37	9					
	Chain	250	4.67	1					
		381	4.62	15					
		381	4.72	15					
		381	4.51	15					
145	Nd	16	2.82	9	(W)	3.29	2	3.39	3
		16	2.88	3	(S)	3.26	3		
		74	3.66	4					
		259	3.44	15					
		290	3.00	7					
	Chain	250	3.37	1					
		381	3.40	15					
		381	3.39	15					
		381	3.39	15					
146	Nd	16	2.20	7	(W)	2.46	2	2.46	3
		16	2.24	3	(S)	2.46	3		
		74	2.74	4					
		259	2.58	15					
		290	2.34	6					
	Chain	250	2.53	1					
		381	2.52	15					
		381	2.52	15					
		381	2.51	15					
147	Nd	76	1.73	10	(W)	1.82	3	1.82	6
		609	1.75	2	(S)	1.84	6		
	Pm	19	1.53	4					
		72	2.10	3					
	Sm	261	2.16	15					
	Chain	250	1.78	2					

Table VII (cont)

^{233}U Thermal neutron induced fission

1	2	3	4		5			6	
148	Nd	16	1.03	10	(W)	1.24	2	1.24	4
		16	1.07	4	(S)	1.23	4		
		74	1.40	4					
		259	1.31	15					
		290	1.15	4					
	Chain	250	1.30	1					
		381	1.30	15					
		381	1.27	15					
		381	1.27	15					
149	Pm	76	0.74	10	(W)	0.773	3	0.773	3
	Sm	16	0.66	20	(S)	0.748	3		
		16	0.70	4					
		72	0.30	3					
		74	0.79	4					
		261	0.77	15					
	Chain	250	0.773	1					
150	Nd	16	0.51	16	(W)	0.503	2	0.503	2
		16	0.49	4	(S)	0.507	2		
		74	0.57	4					
		259	0.521	15					
		290	0.51	8					
	Chain	250	0.50	1					
		381	.484	15					
		381	.491	15					
		381	.491	15					
151	Pm	76	0.36	10	(W)	0.338	3	0.338	3
	Sm	16	0.54	6	(S)	0.335	3		
		19	0.33	9					
		72	0.30	3					
		74	0.33	4					
		261	0.325	15					
	Chain	250	0.365	3					
152	Sm	19	0.21	10	(W)	0.198	3	0.198	4
		74	0.222	4	(S)	0.208	4		
		261	0.214	15					
	Chain	250	0.186	2					
153	Sm	76	0.099	10	(W)	0.0988	8	0.099	13
		347	0.0857	15	(S)	0.105	13		
	Eu	19	0.13	15					

Table VII (cont)

^{233}U Thermal neutron induced fission

1	2	3	4		5			6	
154	Sm	74	0.048	4	(W)	0.046	3	0.046	3
		261	0.047	15	(S)	0.0469	2		
	Chain	250	0.0458	1					
155								(0.0231)	
156	Eu	76	0.0114	10				0.0114	10
157	Eu	76	0.00674	10				0.0067	10
158								(.00235)	
159	Gd	76	.000908	10				.00091	10
160								.00031	
161	Tb	76	.000115	10				.00012	10

Table VIII

^{235}U Thermal neutron induced fission

1	2	3	4		5			6	
72	Zn	345	$.0_4$1539	15		-		$.0_4$15	15
73	Ga	345	$.0_3$1026	15		-		$.0_3$10	15
74	Ga	262	$.0_3$3408	15		-		$.0_3$34	15
77	Ge	307	$.0_2$2361	15		-		.0081	11
		345	$.0_2$3799	15		-			
	As	307	$.0_2$6882	15	(S)	.0081	11		
		345	$.0_2$9348	15					
78	Ge	307	.01847	15		-		.020	11
	Ge	345	.02053	15		-			
	As	307	.02053	15	(S)	.020	11		
	As	345	.02053	15					
79	As	158	.05506	10	(S)	.055	10	.055	10
80								(0.11)	
81	Se(1)	83	$.0_2$7586	12		-		0.21	10
	Se(2)	83	.2094	10					
	Se(1)	345	$.0_2$8218	15		-			
	Se(2)	345	.1364	15		-			
82								(0.333)	
83	Se	83	.2174	10	(W)	0.22	9	0.515	4
		345	.2165	15					
	Se(m)	83	.3392	6	0.34		6		
	Br	345	0.49	15	0.49		15		
	Kr	29	0.5529	2	(W)	0.515	1.2		
		344	0.5088	15	(S)	0.553	4		
	Chain	251	0.4967	1.5					
84	Br	83	0.9283	6	0.931		4	0.959	7
		308	0.9349	7					
	Br(m)	308	0.1929	16		-			
	Kr	29	1.011	2	(W)	0.9592	2		
		344	1.130	15	(S)	1.024	7		
	Chain	251	0.9297	2					
85	Kr	29	0.2977	2	(W)	0.286	1	1.30	3
		243	0.2727	3	(S)	0.296	5		
		344	0.3292	15					
		592	0.2843	1.2					
	Chain	251	1.297	1	1.297		1		

Table VIII (cont)

^{235}U Thermal neutron induced fission

1	2	3	4		5			6	
86	Kr	29	2.053	2	(W)	1.894	1	1.89	7
		344	2.17	15	(S)	2.01	7		
	Chain	251	1.807	2					
87	Sr	569	1.167	21				2.64	5
	Br	306	3.217	5					
	Chain	251	2.537	0.4	(S)	2.64	5		
	Chain	404	2.75	15					
88	Sr	210	3.617	15				3.69	5
	Chain	251	3.607	0.6	(W)	3.69	0.6		
	Chain	405	3.962	15	(S)	3.78	5		
89	Sr	34	4.752	5	(W)	4.774	1.4	4.77	1.4
		289	4.777	1.5					
		210	4.779	15					
		345	4.724	15					
90	Sr	4	5.607	4	(W)	5.888	1	5.89	11
		288	4.001	3	(S)	5.17	11		
	Chain	251	5.897	0.7					
91	Sr	34	5.726	5	5.68		4	5.90	2
		289	5.097	2					
		313	5.792	11					
		345	5.136	15					
	Y	75	6.208	10	(W)	5.887	0.5		
		288	5.325	4	(S)	5.904	2.2		
		345	6.060	15					
	Zr	210	6.032	15					
	Chain	251	5.897	0.5					
92	Sr	345	5.136	15	(W)	5.95	0.5	5.95	1
	Zr	210	6.093	15	(S)	6.02	1		
	Chain	251	5.947	0.5					
93	Y	240	6.107	10	(W)	6.34	0.6	6.34	3
		366	6.941	10	(S)	6.49	3		
	Zr	210	6.578	15					
	Chain	251	6.337	0.6					
94	Y	345	5.136	15				6.41	2
	Zr	210	6.618	15	(W)	6.41	0.6		
	Chain	251	6.407	0.6	(S)	6.51	1.6		

Table VIII (cont)

^{235}U Thermal neutron induced fission

1	2	3	4		5			6	
95	Zr	345	6.164	15	(W)	6.45	0.5	6.45	2
	Mo	210	6.618	15	(S)	6.41	2		
	Chain	251	6.447	0.5					
96	Zr	210	6.447	15	(W)	6.23	0.6	6.23	2
	Chain	251	6.227	0.6	(S)	6.35	2		
97	Zr	39	6.208	3.5	(W)	5.87	0.5	5.87	2.5
		40	6.084	2.7	(S)	6.07	2.5		
		289	5.50	3.5					
		313	4.775	1.1					
		345	6.368	15					
	Mo	210	6.396	15					
	Chain	251	5.857	0.5					
98	Nb(m)	393	0.064	19				5.77	2
	Mo	210	5.992	15	(W)	5.77	0.5		
	Chain	251	5.767	0.5	(S)	5.88	2		
99	Mo	198	6.25	3	(W)	6.14	0.85	6.14	0.85
		216	6.157	1.3	(S)	6.15	0.80		
		289	5.977	3.5					
		316	6.137	2.6					
		331	6.031	3.4					
		345	6.368	15					
	Chain	251	6.137	1.6					
100	Mo	210	6.648	15	(W)	6.24	0.5	6.24	3
	Chain	251	6.237	0.5	(S)	6.44	3.2		
101	Mo	331	5.519	4	(W)	5.05	0.8	5.05	5
	Chain	251	5.027	0.8	(S)	5.27	5		
102	Mo	331	4.19	1	(S)	4.19	1	4.19	1
	Chain	251	4.187	5					
103	Ru	41	2.963	6	(W)	3.03	3	3.03	6
		223	2.912	6	(S)	3.21	6		
		331	1.429	15					
		345	3.779	15					
		363	3.149	4					
104	Mo	315	2.032	15				1.82	3
	Chain	251	1.817	0.6					

Table VIII (cont)

^{235}U Thermal neutron induced fission

1	2	3	4		5			6	
105	Ru	331	0.8485	36	(W)	0.96	4	0.96	4
		345	0.9245	15					
		363	0.9654	4					
106	Ru	222	0.3828	8	(W)	0.39	1	0.39	12
		345	0.5341	15	(S)	0.44	12		
	Chain	251	0.3887	1					
107								(0.166)	
108								(0.070)	
109	Pd	39	.02938	2	(W)	0.03	1.3	0.03	3
		40	.02998	2	(S)	0.029	3		
		178	.02573	15					
		345	0.2875						
110								(0.0195)	
111	Pd	24	0.01822	10	(W)	0.017	1	0.017	1.6
	Ag	39	0.01689	1	(S)	0.0177	1.6		
		40	0.01746	2					
		178	0.01781	15					
		345	0.01847	15					
112	Pd	39	.008497	1	(W)	.008527	0.5	0.008537	1
		40	.008597	1	(S)	.008405	0.7		
		178	.008319	15					
		345	.008526	15					
		363	0.01217	5					
113								(.0086)	
114								(.0090)	
115	Cd	39	.008733	3	(W)	$.0_2877$	1.5	0.00952	14
		40	.008629	2	(S)	.01123	14		
		178	.01880	15					
		335	.009797	10					
		345	.01128	15					
		363	0.1015	6					
	Cd(m)	335	.0007097	10	(W)	$.0_3736$	9		
		345	.0008218	15					
116								(.0097)	

Table VIII (cont)

^{235}U Thermal neutron induced fission

1	2	3	4		5			6	
117	Cd	345	0.01026	15	(W)	0.01	2	0.01	2
	Chain	361	0.009997	2					
118	Chain	361	0.00999	2				0.01	2
119	Chain	361	0.011	2				0.011	2
120	Chain	361	0.011	2				0.011	2
121	Cd	337	.006397	8				.0111	4
	In(1)	337	.003197	15					
	Sn(2)	175	.01225	2	(W)	.0111	2		
		345	.01436	15	(S)	.01228	4		
		363	.01217	8					
		337	.01097	9					
	Chain	391	.01197	8					
		361	.01197	2					
122	Chain	361	.01297	2				.0130	2
123	Sn(1)	176	.01971	9				.0140	2
	Sn(2)	175	.001910	1.6					
		345	.001231	15					
	Chain	361	.01397	2					
124	Chain	361	.01697	2				.0170	2
125	Sn(1)	176	.0135	10				.0296	9
	Sn(2)	175	.01165	1	(W)	.01156	1		
		345	.01231	15	(S)	.01204	2		
		363	.01217	8					
	Sb	27	.02258	5	(W)	.02965	1		
		175	.02926	2	(S)	.02814	9		
		345	.02361	15					
	Chain	251	.02907	1					
		361	.03597	2					
126	Sb(2)	27	.000890	6				0.10	2
	Chain	361	.09997	2					
127	Sn(2)	175	.0674	1.5	(W)	.0675	1.5	0.25	2
		176	.0869	15	(S)	.0771	13		
	Sb	175	.1035	1	(W)	.104	1		
		178	.0921	15	(S)	.108	10		
		224	.1395	6					
		345	.0966	15					
		417	.394	10					
	Te(1)	345	.00339	15					
	Chain	361	.25	2					

Table VIII (cont)

^{235}U Thermal Neutron induced fission

1	2	3		4	5		6	
128	Sn(2)	175	.316	1.5	(S) 0.368	14	0.50	2
		176	.420	15				
	Chain	361	0.50	2				
129	Sn(2)	31	.173	6			1.0	2
	Sb	31	.396	8	(S) .767	21		
		175	.626	5	(W) .565	4		
		224	1.12	15				
		417	.926	7				
	Te(1)	345	.195	15				
	Chain	361	1.00	2				
130	Sb	283	2.58	2			2.00	2
	Chain	361	2.00	2				
131	Xe	29	2.91	2	(W) 2.85	1	2.85	1
		344	2.91	15	(S) 2.88	1.1		
		251	2.79	1.5				
		361	2.93	2.0				
132	Xe	29	4.35	2	(W) 4.26	1	4.26	1
		344	4.33	15	(S) 4.31	1		
		406	4.35	15				
	Chain	251	4.16	1.4				
		361	4.38	2.0				
133	Xe	233	6.62	33	(W) 6.72	0.5	6.72	0.5
		255	6.63	0.16	(S) 6.64	0.5		
		345	6.46	15				
	Cs	70	6.59	3				
	Chain	251	6.73	0.6				
		361	6.62	2				
		379	6.75	15				
		379	6.75	15				
134	Xe	29	8.00	2	(W) 7.76	1	7.76	1
		344	7.70	15	(S) 7.85	1.3		
		406	7.96	15				
	Chain	251	7.51	1.5				
		361	8.06	2				
135	Xe	70	6.41	3	(W) 6.39	3		
		345	6.06	16	(S) 6.23	3		
	Cs	279	6.51	10	(W) 6.45	2	6.45	2
	Chain	361	6.45	2	(S) 6.47	0.3		
	Chain	403	6.46	10				

Table VIII (cont)

^{235}U Thermal neutron induced fission

1	2	3	4		5		6	
136	Xe	29	6.41	2	(W) 6.54	1.4	6.54	2
		344	6.38	15	(S) 6.39	0.6		
		406	6.28	10				
	Chain	361	6.47	2				
137	Cs	47	6.24	3	(W) 6.27	0.5	6.27	1
		279	6.24	10	(S) 6.21	0.4		
	Chain	251	6.28	0.5				
	Chain	361	6.17	2				
		379	6.19	10				
		403	6.13	10				
138	Cs	45	7.24	4	(W) 6.80	0.4	6.80	2.5
	Chain	251	6.80	0.4	(S) 6.91	2.5		
		361	6.68	2				
139	Ba	34	6.59	5	(W) 6.44	1.6	6.44	2
		289	6.40	3.5	(S) 6.47	0.7		
		345	6.47	15				
	La	215	8.34	10				
	Chain	361	6.42	2				
140	Ba	154	6.36	4	(W) 6.32	0.4	6.32	0.5
		177	6.40	10	(S) 6.36	0.5		
		216	6.55	1.5				
		289	6.30	2				
		345	6.34	15				
		386	6.32	4				
	La	366	6.62	10				
	Ce	20	6.30	5				
		151	6.20	10				
		215	6.41	5				
	Chain	251	6.31	0.5				
		361	6.25	2				
141	La	34	6.32	5	(W) 5.70	0.5	5.70	3
	Ce	345	5.86	15	(S) 5.60	3		
	Pr	20	5.60	5				
		215	5.69	5				
	Chain	251	5.50	6				
		361	5.73	2				
142	Ce	20	5.80	4	(W) 5.87	0.5	5.87	1
		151	5.91	1	(S) 5.85	0.5		
	Chain	251	5.88	0.5				
		361	5.80	2				

Table VIII (cont)

^{235}U Thermal neutron induced fission

1	2	3	4		5		6	
143	Ce	313	5.89	4	(W) 5.89	1.5	5.89	2
		345	5.55	15	(S) 5.86	2		
		366	5.91	10				
	Pr	75	5.98	10				
	Nd	20	5.80	4				
		70	5.80	3				
		151	5.91	1				
		215	5.90	4				
		251	5.90	0.51				
		258	5.91	15				
		343	5.91	15				
	Chain	361	5.71	2				
		379	5.96	15				
		379	6.04	15				
		379	5.98	15				
144	Nd	20	5.60	5	(W) 5.42	0.5	5.42	2
		151	5.32	2	(S) 5.38	1.2		
		215	5.69	5				
		251	5.42	0.4				
		258	5.49	8				
		343	5.08	15				
	Chain	361	5.30	2				
		379	5.30	15				
		379	5.31	15				
		379	5.33	15				
145	Nd	20	4.00	3	(W) 3.87	0.5	3.87	1
		151	3.90	1	(S) 3.92	0.6		
		215	4.07	3				
		251	3.86	0.52				
		258	3.93	0.2				
		343	3.96	15				
	Chain	361	3.80	15				
		379	3.94	15				
		379	3.91	15				
		379	3.89	15				
146	Nd	20	3.20	15	(W) 2.95	0.5	2.95	2
		151	2.95	1	(S) 3.01	1.5		
		215	3.25	15				
		251	2.95	0.34				
		258	2.98	0.4				
		343	3.07	15				
	Chain	361	2.89	2				

Table VIII (cont)

^{235}U Thermal neutron induced fission

1	2	3	4		5		6	
147	Pm	20	2.90	14	(W) 2.17	1.2	2.17	4
		70	2.38	3	(S) 2.44	4		
	Nd	75	2.24	10				
		345	2.67	15				
		366	2.52	10				
	Sm	151	2.24	1				
		260	2.18	2				
	Chain	215	2.95	14				
		251	2.12	1.9				
		361	2.16	2				
148	Nd	20	1.70	6	(W) 1.688	0.6	1.69	1
		151	1.67	1	(S) 1.67	1		
		215	1.73	6				
		258	1.66	2				
		343	1.79	15				
	Sm	215	1.52	20				
	Chain	361	1.61	2				
		379	1.67	15				
		379	1.67	15				
		379	1.67	15				
		251	1.69	0.6				
149	Pm	75	1.06	10	(W) 1.01	1	1.01	6
		215	1.52	20	(S) 1.19	6		
		345	1.33	15				
	Sm	20	1.5	2				
		70	1.13	3				
		151	1.10	1				
		260	1.04	15				
	Chain	361	1.02	2				
		251	1.00	1				
150	Nd	20	0.70	14	(W) 0.66	5	0.637	1
		258	0.65	1	(S) 0.69	3		
		343	0.72	15				
	Sm	151	0.65	2	(W) 0.637	1		
	Chain	215	0.712	14	(S) 0.650	2		
		361	0.628	2				
		379	0.650	15				
		379	0.633	15				
		379	0.640	15				
		251	0.638	0.63				

Table VIII (cont)

^{235}U Thermal neutron induced fission

1	2	3	4		5		6	
151	Sm	20	0.45	3	(W) .410	2	0.410	2
		151	0.414	1	(S) .420	2		
		260	0.414	15				
		342	0.435	15				
	Chain	361	0.399	2				
		251	0.408	3				
152	Sm	151	0.266	1	(W) 0.234	2	0.234	5
		260	0.261	15	(S) 0.254	5		
		342	0.272	15				
	Chain	361	0.260	2				
		251	0.212					
153	Sm	75	0.161	10	(W) 0.149	4	0.150	3
		282	0.129	15	(S) 0.150	6		
		345	0.154	15				
		366	0.150	10				
	Eu	151	0.163	3	(W) 0.150	2		
		178	0.158	15				
	Chain	361	0.148	2				
154	Sm	151	0.0738	1	(W) 0.0652	2	0.0652	8
		260	0.0707	15	(S) 0.0736	8		
		342	0.0887	15				
	Chain	361	0.0724	2				
		251	0.0561	1.6				
155	Sm	345	.0318	15			.0294	5
	Eu	151	.0321	3	(W) 0.0294	2		
	Chain	361	.0291	2	(S) 0.0306	5		
156	Sm	345	0.0123	15			0.015	2
	Eu	75	0.0139	10	(W) .0129	5		
		170	0.0125	8	(S) .0131	3		
		178	0.0138	15				
		282	0.0119	15				
		345	0.0133	15				
	Chain	361	0.0150	2				
157	Eu	75	.00620	10	(W) .00677	2	.00677	6
		170	.00600	2	(S) .00670	6		
		345	.00760	15				
	Chain	361	.00700	2				

Table VIII (cont)

^{235}U Thermal neutron induced fission

1	2	3	4		5			6	
158	Eu	170	.00310	20	(W)	.00200	2	.00200	15
		345	.00205	15	(S)	.00238	15		
	Chain	361	.00200	2					
159	Eu	170	.00110	30				.00101	3
	Gd	75	.00104	10	(W)	.00101	2		
		183	.00113	11	(S)	.00105	3		
		282	.00104	15					
	Chain	361	.00100	2					
160								-	
161	Tb	75	$.0_4833$	10	(W)	$.0_4803$	7	$.0_4803$	7
		183	$.0_4824$	10	(S)	$.0_4793$	5		
		282	$.0_4720$	15					
162								-	
163								-	
164								-	
165								-	
166	Dy	265	$.0_7632$	50				$.0_7632$	50

Table IX

^{237}Np Pile neutrons induced fission

1	2	3	4		5		6	
83	Br	662	0.265	15	(S) .317	17	0.317	17
		231	0.368	15				
89	Sr	662	2.04	15	(S) 2.27	11	2.27	11
		231	2.49	15				
91	Sr	662	4.04	15	(W) 4.0	11	4.0	11
		231	3.95	15	(S) 4.0	2		
97	Zr	662	6.95	15			6.95	15
99	Mo	662	6.98	15	(W) 6.85	11	6.85	11
		231	6.71	15				
103	Ru	662	4.0	15	(W) 4.34	11	4.34	11
		231	4.68	15	(S) 4.34	8		
105	Ru	662	2.75	15	(W) 2.83	11	2.83	11
	Rh	231	2.90	15	(S) 2.83	3		
106	Ru	662	1.56	15	(W) 1.68	11	1.68	11
		231	1.79	15				
109	Pd(2)	662	0.30	15	(W) 0.34	11	0.34	11
		231	0.38	15	(S) 0.34	12		
111	Ag	662	0.085	15	(W) .092	11	0.092	11
		231	0.099	15	(S) .092	8		
112	Pd	662	0.072	15	(W) 0.059	11	0.059	22
		231	0.046	15	(S) 0.059	22		
113	Ag(2)	662	0.045	15	(W) 0.044	11	0.044	11
		231	0.042	15				
115	Cd	662	0.041	15	(W) 0.046	11	0.046	11
		231	0.051	15				
121	Su(2)	661	0.047	15	(W) 0.049	11	0.049	11
		231	0.051	15				
125	Su(2)	662	0.126	15	(W) 0.111	11	0.11	15
		231	0.094	15	(S) 0.11	15		
127	Sb	662	0.916	15	(S) 0.94	11	0.94	11
		231	0.97	15				

Table IX (cont)

^{237}Np Pile neutrons induced fission

1	2	3	4		5		6	
129	Te	662	2.60	15	(W) 2.66	11	2.66	11
		231	2.72	15				
132	Te	662	6.33	15	(S) 5.33	19	5.33	19
		231	4.33	15				
140	Ba	662	5.30	15	(S) 5.33	11	5.33	11
		231	5.35	15				
141	Ce	662	4.97	15	(S) 4.22	18	4.22	18
		231	3.46	15				
144	Ce	662	4.31	15	(S) 3.31	30	3.31	30
		231	2.31	15				
147	Nd	662	2.35	15			2.35	15
156	Eu	662	0.09	15			0.09	15

Table X

^{239}Pu Thermal neutron induced fission

1	2	3	4		5			6	
72	Zn	346	.000113	15				.00011	15
73								(.00026)	
74								(.00059)	
75								(.0013)	
76								(.003)	
77	As	159	.0071	5				.0071	10
78	As	159	.0256	5				.026	10
79								(.036)	
80								(.08)	
81	Se(1)	87	0.0045	32				0.182	10
		87	0.182	8					
82								(0.24)	
83	Se(1)	87	0.149	15				0.295	3
	Se(2)	87	0.169	15					
	Br	87	0.309	15	(W)	.295	3		
		159	0.291	8	(S)	.294	2		
	Kr	181	0.277	4					
		196	0.290	4					
	Chain	252	0.301	2					
84	Br(2)	87	0.415	10				0.478	4
	Kr	181	0.449	4	(W)	.478	2		
	Chain	252	0.487	2	(S)	.468	4		
85	Kr(1)	610	0.640	3				0.559	6
	Kr(2)	244	0.099	5	(W)	.120	2		
		592	0.128	2	(S)	.114	13		
	Rb	281	.512	4	(W)	.559	2		
	Chain	252	0.574	2	(S)	.543	6		
86	Chain	252	0.77	2				0.77	10
87	Rb	181	0.872	4	(W)	0.968	2	0.968	7
	Chain	252	1.00	2	(S)	0.936	7		
88	Sr	21	1.39	3	(W)	1.36	2	1.36	7
		181	1.37	4	(S)	1.28	7		
		237	1.02	15					
	Chain	252	1.35	2					
89	Sr	33	1.66	2	(W)	1.67	3	1.67	3
		181	1.63	4	(S)	1.72	3		
		263	1.74	3					
		346	1.85	15					

Table X (cont)

^{239}Pu Thermal neutron induced fission

1	2	3	4		5		6	
90	Sr	21	2.31	2	(W) 2.09	2	2.09	5
		181	2.07	4	(S) 2.05	5		
		237	1.72	15				
		263	2.05	2				
	Chain	252	2.09	2				
91	Sr	33	2.37	2	(W) 2.47	2	2.47	4
		346	2.36	15	(S) 2.43	4		
		610	2.03	3				
	Y	263	2.41	5				
		601	2.42	1				
		346	2.88	15				
	Zr	181	2.48	4				
	Chain	252	2.52	2				
92	Zr	181	2.98	4	(W) 3.01	2	3.01	2
	Chain	252	3.02	2				
93	Zr	181	3.77	4	(W) 3.91	2	3.91	2
	Chain	282	3.95	2	(S) 3.86	2		
94	Zr	181	4.26	4	(W) 4.45	2	4.45	2
	Chain	252	4.50	2				
95	Zr	263	5.06	7	(W) 4.90	3	4.90	5
		346	5.76	15	(S) 5.11	5		
		610	4.74	3				
	Chain	252	4.86	2				
96	Zr	181	4.91	4	(W) 5.08	2	5.08	2
	Chain	252	5.12	2	(S) 5.02	2		
97	Zr	346	5.45	15	(W) 5.54	3	5.54	3
	Mo	181	5.37	4	(S) 5.51	3		
	Chain	252	5.64	3				
98	Nb(2)	396	0.20	15			5.59	10
	Mo	181	5.59	4				
99	Mo	199	6.02	3	(W) 6.20	2	6.20	3
		263	5.61	6	(S) 6.30	3		
		346	6.27	15				
		688	6.17	3				
		682	6.79	2				
		682	6.66	1				
	Chain	252	6.59	3				

Table X (cont)

^{239}Pu Thermal neutron induced fission

1	2	3	4		5		6	
100	Mo	181	6.74	4			6.74	10
101	Ru	181	5.60	4	(W) 5.95	3	6.05	8
	Chain	252	6.50	4	(S) 6.05	8		
102	Ru	181	5.68	4	(W) 6.00	3	6.00	7
	Chain	252	6.65	4	(S) 6.09	7		
103	Ru	181	5.38	4	(W) 5.51	4	5.51	7
		346	5.63	15	(S) 5.89	7		
		610	6.65	7				
104	Ru	181	5.62	4	(W) 5.99	3	5.99	9
	Chain	252	6.61	4	(S) 6.12	9		
105	Rh(2)	263	5.47	1			5.47	10
		346	3.80	15				
106	Ru	181	4.33	4	(W) 4.34	3	4.34	4
		263	4.04	5	(S) 4.43	4		
		346	4.83	15				
	Chain	252	4.55	4				
107							(2.70)	
108							(1.70)	
109	Pd	204	1.94	2			1.08	5
		263	1.13	5	(S) 1.08	5		
		346	1.03	15				
110							(0.53)	
111	Ag	204	0.265	2	(W) .267	5	0.267	5
		263	0.280	14	(S) .274	2		
		346	0.277	15				
112	Pd	204	0.094	2	(W) 0.094	4	0.094	4
		263	0.093	3	(S) 0.097	4		
		346	0.103	15				
113	Ag	159	0.065	15			0.065	15
114							(0.052)	

Table X (cont)

^{239}Pu Thermal neutron induced fission

1	2	3	4		5			6	
115	Cd(1)	263	0.003	20	(W)	.0371	4	0.0371	11
		346	0.00308	15	(S)	.0408	11		
	Cd(2)	204	.034	2					
		263	0.033	6					
		346	0.0462	15					
116								(0.038)	
117								(0.039)	
118								(0.039)	
119								(0.040)	
120								(0.042)	
121	Sn(2)	346	0.0421	15				0.0421	15
122								(0.049)	
123								(0.058)	
124								(0.078)	
125	Sn(2)	346	0.0699	15				0.116	12
	Chain	252	0.116	12					
126								(0.24)	
127	Sb	263	0.55	6	(W)	.513	5	.513	20
		346	0.38	15	(S)	.415	20		
128								(0.83)	
129								(0.38)	
130								(2.30)	
131	I	263	3.80	4	(W)	3.69	2	3.69	2
		346	3.70	15	(S)	3.74	2		
		610	3.96	3					
	Xe	182	3.60	1					
		196	3.78	2					
	Chain	180	3.71	3					
		252	3.60	3					
132	Te	263	5.51	5	(W)	5.35	5	5.11	3
		346	5.04	15	(S)	5.17	4		
		610	4.97	2					
	Xe	182	5.02	1	(W)	5.11	3		
	Chain	180	5.26	3	(S)	5.12	2		
		252	5.09	1					

Table X (cont)

^{239}Pu Thermal neutron induced fission

1	2	3	4		5		6	
133	I	263	5.53	1	(W) 6.76	4	6.76	5
		346	5.14	15	(S) 6.37	5		
		610	6.70	2				
	Xe(2)	610	6.93	2				
	Cs	21	5.26	3				
		71	6.92	3				
	Chain	180	6.90	4				
		252	7.18	2				
		380	6.80	15				
134	Xe	182	7.13	1	(W) 7.24	3	7.24	3
	Chain	180	7.46	3	(S) 7.26	2		
		252	7.20	2				
135	I	274	6.89	2	(W) 6.71	5	7.08	4
		346	5.65	15	(S) 6.27	10		
	Xe	69	7.11	44	(W) 7.08	3		
		71	7.27	3	(S) 6.77	4		
		610	6.67	3				
	Cs	21	6.95	3				
		236	6.95	10				
		398	5.22	15				
	Chain	180	7.25	3				
136	I	346	1.95	15			6.33	10
	Xe	182	6.37	1	(W) 6.33	4		
		398	4.77	15	(S) 5.92	10		
	Chain	180	6.62	3				
137	Cs	21	6.50	3	(W) 6.48	3	6.48	6
		263	5.40	7	(S) 6.14	6		
		398	4.94	15				
	Chain	180	6.48	3				
		252	6.74	2				
		380	6.72	15				
138	Ba	21	6.26	3	(W) 5.71	3	5.71	5
	Chain	180	6.31	3	(S) 5.99	5		
		252	5.40	2				
139	Ba	33	5.89	2	(W) 5.77	5	5.77	5
		346	5.55	15	(S) 5.64	3		
		610	5.47	2				

Table X (cont)

		^{239}Pu Thermal neutron induced fission						
I	2	3	4		5		6	
140	Ba	13	5.31	3	(W) 5.57	2	5.57	5
		33	5.51	2	(S) 5.60	5		
		263	5 47	6				
		277	4.55	2				
		346	5.51	15				
		610	5.29	3				
	Ce	21	5.52	3				
		398	7.36	15				
	Chain	180	5.88	3				
		252	5.61	2				
141	La	33	5.56	2	(W) 5.78	3	5.78	4
		603	4.62	3	(S) 5.37	4		
	Ce	263	6.11	5				
		346	5.04	15				
		601	5.00	2				
		610	5.27	2				
	Pr	21	6.02	3				
142	La	610	5.24	4	(W) 5.05	3	5.05	6
	Ce	21	6.66	3	(S) 5.58	6		
		398	6.62	15				
	Chain	180	4.97	3				
		252	5.04	2				
		380	4.93	15				
143	Ce	263	4.28	5	(W) 4.42	2	4.42	5
		346	5.24	15	(S) 4.70	5		
		603	3.94	3				
		610	4.00	8				
	Pr	601	4.17	2				
	Nd	21	6.10	3				
		71	4.49	3				
		398	5.98	15				
	Chain	180	4.56	3				
		252	4.48	2				
		380	4.51	15				
144	Ce	263	4.09	5	(W) 3.85	3	3.85	6
		341	3.11	15	(S) 4.05	6		
		346	3.80	15				
		610	3.61	2				
	Nd	21	5.50	3				
		398	5.00	15				
	Chain	180	3.84	3				
		252	3.78	2				
		380	3.77	15				

Table X (cont)

^{239}Pu Thermal neutron induced fission

1	2	3	4		5		6	
145	Pr	603	3.48	2	(W) 3.14	3	3.14	6
	Nd	21	4.2	3	(S) 3.49	6		
		398	4.07	15				
	Chain	180	3.12	3				
		252	3.03	2				
		380	3.04	15				
146	Nd	21	3.53	3	(W) 2.52	3	2.52	8
		398	3.36	15	(S) 2.89	8		
	Chain	180	2.57	3				
		252	2.49	2				
		380	2.49	15				
147	Nd	263	1.46	6	(W) 2.07	2	2.07	6
		341	1.84	15	(S) 2.12	6		
		601	2.10	2				
		610	1.92	4				
	Sm	235	1.97	3				
		398	2.81	15				
	Pm	21	2.58	2				
		71	2.07	3				
		601	2.11	4				
	Chain	180	2.00	3				
		252	2.15	2				
148	Nd	21	2.30	2	(W) 1.71	3	1.71	5
		398	2.27	15	(S) 1.93	5		
	Chain	180	1.71	3				
		252	1.70	1				
		380	1.67	15				
149	Nd	603	1.13	4	(W) 1.24	2	1.24	7
	Pm	341	1.11	15	(S) 1.36	7		
		603	1.28	2				
	Sm	21	1.67	1				
		71	1.32	3				
		398	1.81	15				
	Chain	180	1.30	3				
		252	1.24	3				
150	Nd	21	1.35	2	(W) 0.97	3	0.97	3
		398	1.31	15	(S) 0.98	2		
	Chain	180	1.02	3				
		252	0.965	2				
		380	0.96	15				

Table X (cont)

^{239}Pu Thermal neutron induced fission

1	2	3	4		5			6	
151	Pm	603	0.724	3	(W)	.791	2	.791	6
	Sm	21	1.01	2	(S)	.867	6		
		71	0.79	3					
		235	0.821	2					
		398	1.10	15					
	Chain	180	0.802	3					
		252	0.821	6					
152	Sm	21	0.75	2	(W)	.575	3	.575	10
		235	0.538	3	(S)	.673	10		
		398	0.88	15					
	Chain	180	0.616	3					
		252	0.581	5					
153	Sm	341	0.368	15	(W)	0.385	10	0.385	10
		346	0.401	15					
		603	0.167	4					
154	Sm	21	0.36	3	(W)	0.255	3	0.26	12
		235	0.208	2	(S)	.306	1		
		398	0.40	15					
	Chain	180	0.293	3					
		252	0.27	2					
155	Sm	346	0.216	15				0.216	15
156	Sm	603	0.094	3	(W)	0.086	3	.086	12
	Eu	263	.062	7	(S)	.101	12		
		341	.102	15					
		346	.124	15					
		601	.122	2					
157	Eu	603	.075	3				.075	15
158								(0.04)	
159	Gd	341	.02	15	(W)	.021	10	.021	10
		603	.0213	1					
160								(0.01)	
161	Tb	341	.00406	15	(W)	.00466	9	.0047	12
		603	.00507	2	(S)	.00457	12		
162								(.0022)	
163								(.00106)	
164								(.00042)	
165								(.00017)	
166	Dy	341	.000068	15				.000068	15

Table XI

^{241}Pu Thermal neutron induced fission

1	2	3	4		5		6	
77	As	104	.000445	7			.00045	15
78	As	104	.00858	6			.0086	15
79							(.018)	
80							(.034)	
81							(.063)	
82							(.105)	
83	Br	104	0.204	5	(W) .201	3	.201	3
	Chain	253	0.20	3	(S) .202	1		
84	Br(2)	104	.343	4	(W) .353	3	.353	5
	Chain	253	.353	3	(S) .348	5		
85	Kr(2)	593	.086	4			.387	10
	Chain	253	.387	3				
86	Chain	253	.601	3			.601	10
87	Chain	253	0.741	3			.741	10
88	Chain	253	.954	3			.954	10
89							(1.19)	
90	Chain	253	1.53	3			1.53	10
91	Y	602	1.66	2	(W) 1.76	3	1.76	5
	Chain	253	1.82	3	(S) 1.74	5		
92	Chain	253	2.23	3			2.23	10
93	Chain	253	2.90	3			2.90	10
94	Chain	253	3.33	3			3.33	10
95	Zr	104	4.19	4	(W) 3.99	3	4.00	4
	Chain	253	3.92	3	(S) 4.06			
96	Chain	253	4.33	3			4.33	10
97	Zr	104	4.72	5	(W) 4.75	3	4.75	3
	Chain	253	4.76	3	(S) 4.74	1		
98							(5.5)	
99	Mo	104	6.04	4	(W) 6.14	3	6.14	3
		688	6.15	3	(S) 6.12	1		
	Chain	253	6.17	3				

Table XI (cont)

^{241}Pu Thermal neutron induced fission

1	2	3	4		5		6	
100							(6.0)	
101	Chain	253	5.94	5			5.94	10
102	Chain	253	6.32	5			6.32	10
103							(6.60)	
104	Chain	253	6.80	5			6.80	10
105							(6.60)	
106	Chain	253	6.08	4			6.08	10
107							(5.15)	
108							(4.15)	
109							(2.9)	
110							(1.4)	
111	Ag	104	0.485	8			0.49	15
112							(0.32)	
113	Ag	104	0.147	6			0.147	15
114							(0.065)	
115							(0.037)	
116							(0.033)	
117							(0.031)	
118							(0.030)	
119							(0.029)	
120							(0.029	
121							(0.030)	
122							(0.031)	
123							(0.032)	
124							(0.036)	
125	Chain	253	0.0416	12			0.042	15
126							(0.1)	
127							(0.21)	
128							(0.41)	
129							(0.82)	
130							(1.65)	
131	Chain	212	3.00	15	(W) 3.14	3	3.14	3
		253	3.15	3	(S) 3.08	3		
132	Chain	212	4.47	15	(W) 4.59	3	4.59	3
		253	4.64	3	(S) 4.55	2		
133	Chain	212	6.56	15	(W) 6.64	3	6.64	3
		253	6.71	3	(S) 6.59	1		
		382	6.52	15				
134	Chain	212	7.80	15	(W) 7.99	3	7.99	3
		253	8.06	3	(S) 7.93	2		

Table XI (cont)

^{241}Pu Thermal neutron induced fission

1	2	3	4	5	6
135	I	275	6.93	3	7.08 5
	Chain	212	7.08	15	
136	Chain	212	7.04	15	7.04 5
137	Cs	104	6.62	15 (W) 6.52 3	6.52 3
	Chain	212	6.62	15 (S) 6.49 2	
		253	6.60	3	
		382	6.14	15	
138	Cs	104	6.82	4 (W) 6.54 3	6.54 3
	Chain	212	6.82	15 (S) 6.67 3	
		253	6.37	3	
139					(6.30)
140	Ba	278	6.28	7 (W) 5.83 3	5.83 3
		688	5.64	2 (S) 5.89 3	
	Chain	212	5.78	15	
		253	5.86	3	
141	La	604	4.49	2 (W) 4.78 2	4.78 3
	Ce	104	5.14	4 (S) 4.81 3	
		602	4.74	2	
		688	4.81	3	
	Chain	212	4.84	15	
142	Chain	212	4.70	15 (W) 4.77 3	4.77 3
		253	4.80	3 (S) 4.75 2	
143	Ce	104	4.68	5 (W) 4.40 2	4.40 3
		604	3.89	2 (S) 4.36 3	
	Pr	602	4.29	1	
	Chain	212	4.43	15	
		253	4.48	3	
		382	4.38	15	
144	Ce	688	4.08	4 (W) 4.09 2	4.09 2
	Chain	212	4.07	15 (S) 4.09 1	
		253	4.13	3	
		382	4.08	15	

Table XI (cont)

^{241}Pu Thermal neutron induced fission

1	2	3	4		5			6	
145	Pr	604	3.01	3	(W)	3.14	2	3.14	2
	Chain	212	3.16	15	(S)	3.12	2		
		253	3.19	3					
		282	3.11	15					
146	Chain	212	2.71	15	(W)	2.65	2	2.65	2
		253	2.68	3	(S)	2.66	2		
		382	2.60	15					
147	Nd	602	2.34	2	(W)	2.26	3	2.26	3
	Pm	602	2.33	4	(S)	2.30	2		
	Chain	212	2.32	15					
		253	2.22	3					
148	Chain	212	1.91	15	(W)	1.87	2	1.87	2
		253	1.89	3	(S)	1.88	2		
		382	1.84	15					
149	Nd	604	1.47	3	(W)	1.47	3	1.47	3
	Pm	604	1.51	4	(S)	1.49	2		
	Chain	212	1.55	15					
		253	1.43	3					
150	Chain	212	1.23	15	(W)	1.14	2	1.16	4
		253	1.16	3	(S)	1.16	4		
		382	1.10	15					
151	Pm	604	0.846	5	(S)	0.903	6	0.903	6
	Chain	212	0.959	15					
152	Chain	212	0.757	15	(S)	0.741	4	0.741	4
		253	0.725	5					
153	Chain	212	0.559	15	(W)	0.54	4	0.54	4
		604	0.519	3					
154	Chain	212	0.408	15	(W)	0.379	3	0.379	5
		253	0.37	3	(S)	0.389	5		
155	Eu	602	0.231	9				0.231	9
156	Sm	604	0.158	3				0.17	5
	Eu	602	0.17	2					

Table XI (cont)

^{241}Pu Thermal neutron induced fission

157	Eu	604	0.13	3	0.13	5
158					(0.086)	
159	Bd	604	0.0462	2	0.0462	5
160					(0.024)	
161	Tb	604	0.00814	2	0.00814	5

Table XII

^{241}Am Pile neutron induced fission

1	2	3	4		5			6	
89	Sr	80	0.81	6	(W)	0.89	6	0.89	20
		301	1.20	8	(S)	1.00	20		
91	Y	80	1.16	3	(W)	1.47	5	1.47	14
	Sr	301	1.90	3	(S)	1.51	14		
	Sr	637	1.48	2					
92	Sr	301	2.30	5	(W)	2.20	4	2.20	5
		637	2.09	2	(S)	2.70	5		
93	Y	301	3.00	7				3.00	7
95	Zr	80	3.90	13	(W)	3.13	4	3.13	12
		301	2.70	4	(S)	3.55	12		
		637	4.04	5					
97	Zr	80	3.55	13	(W)	4.47	7	4.47	19
		637	5.16	8	(S)	4.36	19		
99	Mo	80	6.85	6	(W)	6.64	4	6.64	4
		301	6.30	3	(S)	6.68	3		
		637	6.90	4					
103	Ru	301	7.70	3	(W)	7.68	4	7.68	4
		637	7.65	3					
111	Ag	80	0.89	6	(W)	0.275	4	0.28	38
		301	0.22	15	(S)	0.76	38		
		637	1.19	3					
113	Ag	80	0.18	6	(S)	0.36	47	0.36	47
		638	0.49	2					
115	Cd(2)	80	0.046	7	(W)	0.050	6	0.05	24
		638	0.075	11	(S)	0.061	24		
121	Sn(2)	80	0.045	13					
127	Sb	638	0.66	5				0.66	10
129	Sb	638	1.32	4				1.32	10
131	I	80	3.71	5	(S)	2.89	17	2.89	17
		301	2.1	5					
		638	2.87	4					

Table XII (cont)

^{241}Am Pile neutron induced fission

1	2	3	4		5			6	
132	Te	80	4.48	7	(W)	3.70	4	3.70	10
		638	3.37	1	(S)	3.92	10		
	I	301	3.9	8					
133	I	301	4.00	5	(W)	4.67	4	4.67	15
		638	5.34	4	(S)	4.67	15		
135	I	301	4.50	6	(W)	4.63	4	4.63	4
	I	638	4.36	5	(S)	4.68	4		
	Xe	638	4.87	4					
137	Cs	80	9.20	20	(W)	6.22	13	6.22	25
		301	5.60	15	(S)	7.40	25		
138	Cs	301	6.40	6	(W)	7.25	5	7.25	14
		638	8.48	6	(S)	7.44	14		
139	Cs	80	6.22	5	(W)	7.45	4	7.45	17
		638	8.68	3	(S)	7.45	17		
140	Ba	80	6.0	6	(W)	5.53	4	5.53	5
		301	5.2	2	(S)	5.61	5		
		638	5.63	2					
141	Ce	80	5.04	13	(W)	4.63	4	4.67	4
		301	4.70	2	(S)	4.75	4		
		638	4.51	5					
143	Ce	301	3.40	3	(W)	2.83	4	2.83	10
		638	2.49	4	(S)	3.07	10		
	Pr	80	3.32	14					
144	Ce	80	3.15	13	(W)	3.19	6	3.19	6
		301	3.20	6					
147	Nd	80	2.06	16	(W)	1.42	10	1.42	23
		638	1.30	11	(S)	1.68	23		
153	Sm	80	0.76	16				0.76	16

Table XIII

^{242m}Am Fission induced by thermal neutrons

1	2	3	4		5	6	
83	Br	575	0.234	8		0.23	10
84	Br(2)	575	0.364	8		0.36	10
89	Sr	575	1.18	7		1.18	10
90	Sr	575	1.41	7		1.41	10
91	Y(2)	575	1.73	7		1.73	10
92	Sr	975	2.05	8		2.05	10
93	Y	575	2.56	8		2.56	10
95	Zr	575	3.23	6		3.23	10
97	Zr	575	4.21	7		4.21	10
99	Mo	575	5.36	7		5.36	10
103	Ru	575	6.95	7		6.95	10
109	Pd	575	3.29	9		3.29	15
111	Ag(2)	575	1.32	7		1.32	10
112	Ag	575	0.42	8		0.42	10
115	Cd(1)	575	0.0047	8		0.071	10
	Cd(2)	575	0.066	8			
	Chain	575	0.071	8			
121	Sn(2)	575	0.017	8		0.017	10
125	Sn(2)	575	0.0843	10		0.11	15
	Sb	575	0.111	12			
131	I	575	3.12	6		3.12	10
132	Te	575	4.78	6		4.78	10
133	I	575	5.82	7		5.82	10
134	I	575	5.95	7		5.95	10
135	I	575	6.49	8		6.49	10
137	Cs	575	5.84	12		5.84	15
139	Ba	575	5.55	7		5.55	10
140	Ba	575	5.40	7		5.40	10
141	Ce	575	4.94	8		4.94	10
143	Ce	575	4.23	7		4.23	10
144	Ce	575	3.55	8		3.55	10
147	Nd	575	2.32	8		2.32	10
149	Pm	575	1.61	8		1.61	10
151	Pm	575	1.13	8		1.13	10
153	Sm	575	0.73	8		0.73	10
156	Eu	575	0.313	7		0.31	10
157	Eu	575	0.164	9		0.16	10
161	Tb	575	0.0181	8		0.018	10

Table XIV

^{245}Cm Thermal neutron induced fission

1	2	3	4		5	6	
77	As	628	0.0048	24		.0048	24
83	Br	628	0.0229	22		.023	22
89	Sr	628	0.836	12		0.84	12
90	Sr	628	1.086	14		1.09	14
91	Y	628	1.21	24		1.21	24
95	Zr	628	2.47	13		2.47	13
97	Zr	628	3.05	11		3.05	11
99	Mo	628	4.18	10		4.18	10
103	Ru	628	6.25	14		6.25	14
105	Ru	628	6.10	21		6.10	21
106	Ru	628	5.83	24		5.83	24
109	Pd	628	5.16	12		5.16	12
111	Ag	628	3.21	19		3.21	19
112	Pd	628	1.35	25		1.35	25
113	Ag	628	1.72	25		1.72	25
115	Chain	628	0.40	17		0.40	17
121	Sn(2)	628	0.036	26		0.036	26
123	Sn	628	0.057	22		0.057	22
125	Sn(2)	628	0.053	25		0.091	21
	Sb	628	0.091	21			
127	Sb	628	1.083	16		1.08	16
129	Sb	628	1.76	21		1.76	21
	Te(1)	628	0.81	14			
131	I	628	2.89	13		2.89	13
132	Te	628	3.95	18		3.95	18
133	I	628	5.79	12		5.79	12
137	Cs	628	7.96	8		7.96	8
140	Ba	628	5.61	12		5.61	12
141	Ce	628	4.58	13		4.58	13
143	Ce	628	3.77	16		3.77	16
144	Ce	628	2.90	21		2.90	21
147	Nd	628	2.57	19		2.57	19
149	Pm	628	1.95	20		1.95	20
151	Pm	628	1.23	26		1.23	26
153	Sm	628	1.12	25		1.12	25
156	Eu	628	0.27	24		0.27	24

Table XV

^{249}Cf Thermal neutron induced fission

1	2	3	4		5	6	
89	Sr	208	1.17	25		1.17	25
95	Zr	208	1.72	15		1.72	15
97	Zr	208	2.35	20		2.35	20
99	Mo	208	3.42	7		3.42	10
103	Ru	208	5.27	12		5.27	12
106	Ru	208	5.09	21		5.09	21
109	Pd	208	4.92	25		4.92	25
111	Ag	208	5.16	11		5.16	11
112	Pd	208	3.48	16		3.48	16
113	Ag	208	2.92	11		2.92	11
115	Chain	208	2.46	20		2.46	20
121	Sn(2)	208	0.34	27		0.34	27
125	Sn(2)	208	0.24	25		0.24	25
127	Sb	208	1.23	24		1.23	24
129	Te	208	2.19	15		2.19	15
131	I	208	3.01	15		3.01	15
132	Te	208	3.95	7		3.95	10
133	Te	208	5.09	10		5.09	10
137	Cs	208	6.90	15		6.90	15
140	Ba	208	4.54	27		4.54	27
141	Ce	208	6.34	6		6.34	10
143	Ce	208	4.90	6		4.90	10
144	Ce	208	4.62	6		4.62	10
147	Nd	208	2.62	15		2.62	15

Table XVI

Reference List of Fission Yield Literature

[1 - 8] PETRZHAK, K.A., et al., AEC TR 4696.
[4 - 12] BAYHURST, B.P., TID 5787.
[13] CROUTHAMEL, C.E., KAFALAS, P., STUPEGIAS, D., ANL 5789.
[14] WEISS, H.V., REICHERT, W.L., Ad 627027; TR 943.
[15] CROOK, J.M., VOIGHT, A.F., IS 558.
[16] IVANOV, R.N., GORSCHKOV, V.K., ANIKINA, KUKAVADZE, G.M., ERSCHLER, B.V., J Nucl. Energy, 9 (1959) 46.
[17] ANIKINA, M.P., IVANOV, R.N., KUKAVADZE, G.M., ERSCHLER, B.V., J Nucl. Energy, 9 (1959) 167.
[18 - 21] ANIKINA, M.P., et al, P2040 Vol. 15 second Geneva Conf.
[22 - 26] AUMANN, D.C., FLYNN, K.F., GINDLER, J.E., GLENDENIN, L.E., Jinc., 31 (1969) 1935.
[27] ARAS, N.K., GORDON, G.E., Jinc., 28 (1966) 763.
[28] ANIKINA, M.P., ERSCHLER, B.V., J. Nucl. Energy, 6 (1957) 169.
[29] BLADES, A.T., FLEMING, W.H., THODE, H.G., Can. J. Chem., 34 (1956) 233.
[30] BUNNEY, L.R., SCADDEN, E.M., Jinc., 27 (1965) 1183.
[31] BIRGUL, O., LYLE, S.J., Radiochim. Acta., 8 (1967) 9.
[32 - 33] BARTHOLOMEW, R.M., MARTIN, J.S., BAERG, A.P., Can. J. Chem., 37 (1959) 660.
[34] BAERG, A.P., BARTHOLOMEW, R.M., Can. J. Chem 35 (1957) 980.
[35 - 38] BUNNEY, L.R., SCADDEN, E.M., ABRIAM, J.O., BALLOU, N.E., A/Conf15/P643, second Geneva Conference Vol. 15 449.
[39 - 40] BAYHURST, B.P., et al, Phys. Rev. 107 1957 325.
[41 - 44] BALCARCZYK, L., KERATSCHEV, P., LANZEL, E., Nucleonik, 7 1965 169.
[45] BARTHOLOMEW, R.M., BAERG, A.P., Can. J. Chem., 34 1956 201.
[46] BARTHOLOMEW, R.M., BROWN, F., HAWKINGS, R.C., MERRITT, W.F., YAFFE, L., Can. J. Chem., 31 (1953) 120.
[47] BROWN, F., Jinc., 1 (1955) 248.
[48] BROWN, F., YAFFE, L., Can. J. Chem., 31 (1953) 242.
[49] BROOM, K.M., Phys. Rev., 126 (1962), 627.
[50 - 51] BROOM, K., Phys. Rev., 133 (1964) 874.
[52 - 61] BURGUS, W.H., IDO-16797, TID-4500.
[62 - 65] BONYUSHKIN, E.K., et al., Sov. J. At. Energy, 10 (1961) 10.
[66 - 67] BAK, M.A., et al., Sov. J. Atom. Energy, 6 (1959) 429.
[68] BUNNEY, L.R., SCADDEN, E.M., Jinc., 27 (1965) 1183.
[69] BAYLY, J.G., DURET, M.F., POULSEN, N.B., TOMLINSON, R.H., Can. J. Phys., 39 (1961) 1391.
[70 - 72] BIDINOSTI, D.R., FICKEL, H.R., TOMLINSON, R.H., A/CONT.15/P201 Second Geneva Conf. Vol. 15 459.
[73] BORDEN, K.D., KURODA, P.K., Jinc., 31 (1969) 2623.
[74] BIDINOSTI, D.R., IRISH, D.E., TOMLINSON, R.H., Can. J. Chem., 39 (1961) 628.
[75 - 76] BUNNEY, L.R., SCADDEN, E.M., Jinc., 27 (1965) 273.
[77] BIRGUL, O., LYLE, S.J., Radiochim. Acta., 11 (1969) 108.
[78] GREENDALE, A.E., DELUCCHI, A.A., AD 686041.

Table XVI (cont)

Reference List of Fission Yield Literature

[79] CUNINGHAME, J.G., Jinc., 6 (1958) 181.
[80] CUNINGHAME, J.G., Jinc., 4 (1957) 1.
[81] CUNINGHAME, J.G., Jinc., 5 (1957) 1.
[82] CUNINGHAME, J.G., Jinc., 5 (1957) 1.
[83 - 86] CROALL, I.F., WILLIS, H.H., Jinc., 24 (1962) 221.
[87] CROALL, I.F., WILLIS, H.H., Jinc., 25 (1963) 1213.
[88 - 94] CUNINGHAME, J.G., KITT, G.P., RAE, E.R., Nucl. Phy., 27 (1961) 154.
[95 - 103] CUNINGHAME, J.G., FRITZE, K., LYNN, J.E., WEBSTER, C.B., Nucl. Phy., 84 (1966) 49.
[104] CROALL, I.F., WILLIS, H.H., AERE/R/6154.
[105 - 110] PRIVATE COMMUNICATION.
[111 - 146] COWAN, G.A., BAYHURST, B.P., PRESTWOOD, R.J., PNE-114F
[147 - 153] YUNG YEE CHU, UCRL-8926.
[154 - 157] CIUFFOLOTTI, L., Energia Nucleare, 15 (1968) 272.
[158 CUNINGHAME, J.G., Phil. Mag., 44 (1953) 900.
[159 - 161] CROALL, I.F., WILLIS, H.H., AERE-R4723.
[162] DELUCCHI, A.A., GREENDALE, A.E., STROM, P.O., Phys. Rev., 173 (1968) 1159.
[163] DENSCHLAG, H.O., Jinc., 31 (1969) 1873.
[164 - 167] BONYUSHKIN, E.K., AEC TR 4682.
[168 - 171] DANIELS, W.R., HOFFMAN, D.C., Phys. Rev., 145 (1966) 145.
[172] BIRGUL, O., LYLE, S.J., SELLARS, J., Radiochimica Acta, 12 (1969) 66.
[173 - 174] DAVIES, W., Radiochimica Acta, 12 (1969) 173
[175] ERDAL, B.R., WILLIAMS, J.C., WAHL, A.C., Jinc., 31 (1969) 2993.
[176] ERDAL, B.R., WAHL, A.C., DROPESKY, B.J., Jinc., 31 (1969) 3005.
[177 - 179] ENGELKEMEIR, D., FREEDMAN, M.S., STEINBERG, E.P., SEILER, J.A., WINSBERG, L., ANL-4927.
[180] FICKEL, H.R., TOMLINSON, R.H., Can. J. Phys., 37 (1959) 926.
[181] FICKEL, H.R., TOMLINSON, R.H., Can. J. Phys., 37 (1959) 916.
[182] FLEMING, W.H., THODE, H.G., Can J. Chem., 34 (1956) 193.
[183] FREILING, E.C., BUNNEY, L.R., BALLOU, N.E., Phy. Rev., 96 (1954) 102.
[184] FORD, G.P., AECD-3597, LADC-1200.
[185 - 195] FALER, K.T., TROMP, R.L., Phys. Rev., 131 (1963) 1746.
[196] FRITZE, K., MCMULLEN, C.C., THODE, H.G., A/CONF.15/P187, Second Geneva Conference.
[197] - 207] FORD, G.P., GILMORE, J.S., LA-1997.
[208] FLYNN, K.F., VON GUNTEN, H.R., Helv. Chim. Acta., 52 (1969) 2216.
[209] FLEMING, W., TOMLINSON, R.H., THODE, H.G., Can. J. Phys., 32 (1954) 522.
[210] FARRAR, H., FICKEL, H.R., TOMLINSON, R.H., Can. J. Phys., 40 (1962) 1017

Table XVI (cont)

Reference List of Fission Yield Literature

[211] FLYNN, K.F., VON GUNTEN, H.R., SM-122/1 Symposium on the Physics and Chemistry of fission.
[212] FARRAR, H., CLARKE, W.B., THODE, H.G., TOMLINSON, R.H., Can. J. Phys., 42 (1964) 2063.
[213 - 214] GRUMMITT, W.E., MILTON, G.W., Jinc., 5 (1957) 93.
[215] GORSHKOV, V.K., IVANOV, R.N., KORAVADZE, G.M., REFORMATSKY, I.A., Atomniya Energiya, 3 (1957) 11.
[216] VON GUNTEN, H.R., HERMANN, H., Radiochim. Acta, 8 (1967) 112.
[217 - 219] GRUMMITT, W.E., MILTON, G.M., Jinc., 20 (1961) 6.
[220] GORSHKOV, V.K., ANIKINA, M.P., Atomniya Energiya, 7 (1959) 144.
[221] GLENDENIN, L.E., STEINBERG, E.P., Jinc., 1 (1955) 45.
[222 - 223] HARDWICK, W.H., Phys. Rev., 92 (1953) 1072.
[224] HAGEBO, E., Jinc., 25 (1963) 615.
[225] HASTINGS, J.D., TROUTNER, D.E., Radiochim. Acta., 11 (1969) 51.
[226 - 227] HARVEY, J.W., CLARKE, W.B., THODE, H.G., TOMLINSON, R.H., Can. J. Phys., 44 (1966) 1011.
[228] IYER, R.H., MATTHEWS, C.K., RAVINDRAN, N., RENGAN, K., SINGH, D.V., RAMANIAH, M.V., etc., Jinc., 25 (1963) 465.
[229 - 231] IYER, R.S., JAIN, H.C., NAMBOUDIRI, M.N., RAJAGOPALAN, M., RAKISHORE, etc., Physics and Chem. of fission, Salzburg 1965.
[232] JADHAV, A.V., RAMANIAH, M.V., RAO, C.L., SHAHANI, C.J., Nukleonik, 9 (1967) 43.
[233] KATCOFF, S., RUBINSON, W., Phys. Rev., 91 (1953) 1458.
[234] KELLER, R.N., STEINBERG, E.P., GLENDENDIN, L.E., Phys. Rev., 94 (1954) 969.
[235 - 236] KRIZHANSKII, L.M., MALYI, Y., MURIN, A.N., PREOBRAZHENSKII, B.K., J. Nucl. Energy, 6 (1957) 260.
[237] KRIZHANSKII, L.M., MURIN, A.N., Sov. J. At. Energy 4 (1958) 95.
[238 - 239] KAFALAS, P., CROUTHAMEL, C.E., Jinc., 4 (1957) 239.
[240] KNIGHT, J.D., HOFFMAN, D.C., DROPESKY, B.J., FRASCO, D.L., Jinc., 10 (1959) 183.
[241] KENNETT, T.J., THODE, H.G., Can. J. Phys., 35 (1957) 969.
[242] KJELBERG, A., PAPPAS, A.C., Jinc., 11 (1959) 173.
[243 - 244] KATCOFF, S., RUBINSON, W., Jinc., 27 (1965) 1447
[245] LAIDLER, J.B., BROWN, F., AWRE-49/61.
[246 - 247] DE LAETER, J.R., THODE, H.G., Can. J. Phys., 47 (1969) 1409.
[248 - 253] LISMAN, F.L., MAECK, W.J., et al, IN-1277.
[254] DEL MARMOL, P., Jinc., 30 (1968) 02873.
[255] MACNAMARA, J., COLLINS, C.B., THODE, H.G., Phys. Rev., 78 (1950) 129.
[256 - 257] MENON, M.P., KURODA, P.K., Jinc., 26 (1964) 401.
[258 - 261] MELAIKA, E.A., PARKER, M.J., PETRUSKA, J.A., TOMLINSON, R.H., Can. J. Chem., 33 (1955) 830.
[262] MARINSKY, J.A., EICHLER, E., Jinc., 12 (1960) 223.
[263] MARSDEN, D.A., YAFFE, L., Can. J. Chem. 43 (1965) 249.
[264] TIN MO, RAO, M.N., Jinc., 30 (1968) 345.
[265] MUNTZE, R., GROSSE-RUYKEN, H., WAGNER, G., Kernenergie, 12 (1969) 380.

Table XVI (cont)

Reference List of Fission Yield Literature

[266] NERVIK, W.E., Phys. Rev., 119 (1960) 1685.
[267 - 268] NIECE, L.H., Diss. Abstr., 27 (1966) 1249.
[269 - 272] OKAZAKI, A., WALKER, W.H., BIGHAM, C.B., Can. J. Phys., 44 (1966) 237.
[273 - 278] OKAZAKI, A., WALKER, W.H., Can. J. Phys., 43 (1965) 1036.
[279] PETRUSKA, J.A., MELAIKA, E.A., TOMLINSON, R.H., Can. J. Phys., 33 (1955) 640.
[280 - 281] PETRUSKA, J.A., THODE, H.G., TOMLINSON, R.H., Can. J. Phys., 33 (1955) 693.
[282] PETROW, H.G., ROCCO, G., Phys. Rev., 96 (1954) 1614.
[283] PAPPAS, A.C., WILES, D.R., Jinc., 2 (1956) 69.
[284 - 286] PROTOPOPOV, A.N., TOLMACHEV, G.M., et al J. Nucl. Energy, A, 10 (1959) 80.
[287] PILLARY, K.K.S., MEYER, R.J., LARSEN, R.P., J. Radioanalyt. Chem., 3 (1969) 233.
[288] REED, G.W., Phys. Rev., 98 (1955) 1327.
[289] REED, G.W., TURKEVICH, A., Phys. Rev., 92 (1953) 1473.
[290] KUKAVADZE, G.M., ANIKINA, M.P., GOLDIN, L.L., ERSCHLER, B.V., AEC-TR-2435.
[291] RUNNALS, N.G., TROUTNER, FERGUSON, R.L., Phys. Rev., 179 (1969) 1288.
[292 - 294] REGIER, R.B., BURGUS, W.H., TROMP, R.L., Phys. Rev., 113, (1959) 1589.
[295 - 300] REGIER, R.B., BURGUS, W.H., TROMP, R.L., SORENSEN, B.H., Phys. Rev., 119 (1960) 2017.
[301] RICKARD, R.R., GOEKING, C.F., WYATT, E.I., Nucl. Sc. Eng., 23 (1965) 115.
[302] RAO, M.N., KURODA, P.K., Phys. Rev., 147 (1966) 884.
[303] RAO, M.N., Radiochim. Acta., 8 (1967) 12.
[304] RAVINDRAN, N., FLYNN, K.F., GLENDENIN, L.E., Jinc. 28 (1966) 921.
[305] SANTRY, D.C., YAFFE, L., Can. J. Chem., 38 (1960) 464.
[306] STEHNEY, A.F., SUGARMAN, N., Phys. Rev., 89 (1953) 194.
[307] SUGARMAN, N., Phys. Rev., 89 (1953) 570.
[308] SATTIZAHN, J.E., KNIGHT, J.D., KAHN, M., Jinc., 12 (1960 206.
[309] SANTRY, D.C., YAFFE, L., Can. J. Chem., 38 (1960) 421.
[310] SRINIVASAN, ALEXANDER, E.C., MANUEL, O.K., TROUTNER, D.E., Phys. Rev., 179 (1969) 1166.
[311] STROM, P.O., LOVE, D.L., GREENDALE, A.E., DELUCCHI, A.A., SAM, D. SAM, D., BALLOU, N.E., Phys. Rev., 144 (1966) 984.
[312] STROM, P.O., GRANT, G.R., PAPPAS, A.C., Can. J. Chem., 43 (1965) 2493.
[313] OHYOSHI, E., OHYOHSI, A., SHINAGANA, M., Radiochem. Radioanal. Ltrs., 3 (1970) 1
[314] STELLA, R., MORETTO, L.G., MAXIA, V., DI CASA, M., CRESPI, V., ROLLIER, M.A., Jinc., 31 (1969) 3779.
[315] TERCHO, G.P., MARINSKY, J.A., Jinc., (1964) 1129.
[316 - 325] TERRELL, J., SCOTT, W.E., GILMORE, S., MINKKINEN, C.O., Phys. Rev., 92 (1953) 1091.

Table XVI (cont)

Reference List of Fission Yie d Literature

[326] TURKEVITCH, A., NIDAY, J.B., Phys. Rev., 84 (1951) 52.
[327] TONG, S.L., FRITZE, K., Radiochim. Acta., 12 (1969) 179.
[328] TROUTNER, D.E., FERGUSON, R.L., OKELLEY, G.D., Phys. Rev., 130 (1963) 1466.
[329 - 330] WETHERILL, G.W., Phys. Rev., 92 (1953) 907.
[331 - 334] WILES, D.R., CORYELL, C.D., Phys. Rev., 96 (1954) 696.
[335] WAHL, A.C., BONNER, N.A., Phys. Rev., 85 (1952) 570.
[336 - 337] WEISS, H.V., BALLOU, N.E., Salzburg Symposium 1965.
[338] YOSHIDA, H., PAISS, Y., AMIEL, S., IA-1128.
[339 - 340] ROCHE, M.F., TID-24500.
[341] BUNNEY, L.R., SCADDEN, E.M., ABRIAM, J.O., BALLOU, N.E., Second Geneva Conf., Vol. 15 P444.
[342 - 350] CORYELL, C.D., SUGARMAN, N., Radiochemical Studies: The Fission Products, Vol. 2.
[351] VON GUNTEN, H.R., FLYNN, K.F., GLENDENIN, L.E., Jinc., 31 (1969) 3357.
[352 - 354] NETHAWAY, D.R., MENDOZA, B., VOSS, T.E., Phys. Rev., 182 (1969) 2151.
[355] THEIN, M., RAO, M.N., KURODA, P.K., Jinc., 30 (1968) 1145.
[356] JAMES, R.H., MARTIN, G.R., SILVESTER, D.J., Radiochim. Acta., 3 (1964) 76.
[357] LYLE, S.J., MARTIN, G.R., WHITELEY, J.E., Radiochim. Acta., 3 (1964) 80.
[358] VLASOV, V.A., ZYSIN, YU.A., KIRIN, I.S., LBOV, A.A., OSYAEVA, L.I., SELCHENKOV, L.I., AEC-TR- 4665.
[359] GANAPATHY, R., KURODA, P.K., Jinc., (1966) 2071.
[360] TIN MO, RAO, M.N., Jinc., 30 (1968) 345.
[361] FARRAR, H., TOMLINSON, R.H., Nucl. Phys., 34 (1962) 367.
[362 - 364] Cumulative yields in the 14MeV neutron fission of 232th and 238U in the etc., Can. J. Chem., 48 (1970), 641.
[365] RAO, M.N., Jinc., 29 (1967) 863.
[366 - 367] BRESESTI, M., BURIE, G., FERRARI, P., MORETTO, L., Jinc., 29 (1967) 1189.
[368] GORMAN, D.J., TOMLINSON, R.H., Can. J. Chem., 46 (1965) 1663.
[369] HARVEY, J.W., CLARKE, W.B., GORMAN, D.J., TOMLINSON, R.H., Can. J. Chem., 46 (1968) 2911.
[370 - 378] BORISOVA, N.I., DUBROVINA, S.M., et al., Sov. J. Nucl. Phys., 6 (1968) 331.
[379 - 382] RIDER, B.F., PETERSON, J.P., PRUIZ, C., SMITH, F.R., GEAP-5356.
[383] ONDREJCIN, R.S., Jinc., 28 (1966) 1763.
[384] YOUNG, B.G., THODE, H.G., Can. J. Phy., 38 (1960) 1.
[385] YAFFE, L., DAY, A.E., GREER, B.A., Can. J. Chem., 31 (1953) 48.
[386] YAFFE, L., THODE, H.G., MERRITT, W.F., HAWKINGS, R.C., BROWN, F., BARTHOLOMEW, R.M., Can. J. Chem., 32 (1954) 1017.
[387] WEISS, H.V., ELZIE, J.L., FRESCO, J.M., Phys. Rev., 172 (1968) 1269.
[388] WISH, L., Phys., Rev., 172 (1968) 1262.
[389] WYTTENBACH, A., VON GUNTEN, H.R., DULAKAS., Radiochim, Acta., 3 (1964) 118.

Table XVI (cont)

Reference List of Fission Yield Literature

[390] WEISS, H.V., BALLOU, N.E., Jinc., 27 (1965) 1917.
[391] WEISS, H.V., Phys. Rev., 139 (1965) 3304.
[392] WAHL, A.C., NETHAWAY, D.R., Phys. Rev., 131 (1963) 830.
[393] WAHL, A.C., FERGUSON, R.L., NETHAWAY, D.R., TROUTNER, D.E., WOLFSBURG, K., Phys. Rev., 126 (1962) 1112.
[397] WAHL, A.C., Jinc., 6 (1958) 263.
[398] WILES, D.M., PETRUSKA, J.A., TOMLINSON, R.H., Can. J. Chem., 34 (1956) 227.
[399] WOLFSBERG, K., NETHAWAY, D.R., MALAN, H.P., WAHL, A.C., Jinc., 12 (1960) 201.
[400 - 402] WAHL, A.C., Phys. Rev., 99 (1955) 730.
[403 - 405] WILES, D.R., SMITH, B.W., HORSLEY, R., THODE, H.G., Can.J. Phys., 31 (1953) 419.
[406 - 407] WANLESS, R.K., THODE, H.G., Can. J. Phys., 33 (1955) 541.
[408] VALLIS, D.G., THOMAS, A.O., AWRE Report O-58/61.
[409] LISMAN, F.L., et al., LA-4430-MS 16.
[410] WEISS, H.V., BALLOU, N.E., ELZIE, J.L., FRESCO, J.M., Phys. Rev., 188 (1969) 1893.
[411] LYLE, S.J., WELLUM, R., Radiochim. Acta., 13 (1970).
[412 - 413] NIECE, L.H., TROUTNER, D.E., FERGUSON, R.L., Phys. Rev. C, 1, (1970) 312.
[414] RUNNALLS, N.G., TROUTNER, D.E., Phys. Rev. C, (1970) 316.
[415] BOWLES, B.J., WILLIS, H.H., PRIVATE COMMUNICATION.
[416 - 418] BLACHOT, J., CARRAZ, L.C., CAVALLINI, P., GADELLE, A., MOUSSA, A., Vienna Symposium on Chem., Phys. of fission 1969.
[419] CHIEN-CHANG LIN, WAHL, A.C., Jinc., 32 (1970) 2501.
[420 - 421] CROUCH, .A.C., BROWNSWORD, M., MCKEAN, I.C., PRIVATE COMMUNICATION.
[422 - 427] TRACY, B.L., THODE, H.G., Can. J. Phys., 48 (1970) 1708.
[428 - 490] COWAN, G.A., BAYHURST, B.P., PRESTWOOD, R.J., GILMORE, J.S., KNOBELOCH, G.W., Phys. Rev., 144 (1966) 979.
[491] TROUTNER, D.E., EICHOR, M., PACE, C., Phys. Rev. C., (1970), 1044.
[492] WAHL, A.C., NORRIS, A.E., ROUSE, R.A., WILLIAMS, J.C., Second Symposium on the Chem. and Phys. of fission, Vienna 1969.
[493 - 560] COWAN, G.A., BAYHURST, B.P., PRESTWOOD, R.J., GILMORE, J.S., KNOBELOCH, G.W., Ans. Symp. on Engineering with Nucl. Explosives.
[561] BACHMANN, K., Radiochim, Acta. 9 (1968) 27.
[562 - 563] BAERG, A.P., BARTHOLOMEW, R.M., BETTS, R.H., Can. J. Chem., 38 (1960) 2147.
[564] TROUTNER, D.E., WAHL, A.C., FERGUSON, R.L., Phys. Rev., 134 (1964) 1027.
[565 - 566] MCHUGH, J.A., Jinc., 28 (1966) 1787.
[567] PARSA, B., GORDON, G.E., WENZEL, A., Jinc., 31 (1969) 585.
[568] TOMLINSON, L., HURDUS, M.H., Jinc., 30 (1968) 1995.
[569 - 571] CROALL, I.F., Jinc., 16(1961) 358.
[572 NETHAWAY, D.R., MENDOZA, B., Phys. Rev. C, 2 (1970) 2289.
[573 - 574] QAIM, S.M., DENSCHLAG, H.O., Jinc., 32 (1970) 1767.
[575 - 576] WOLFSBERG, K., FORD, G.P., LA-DC-12142.

Table XVI (cont)

Reference List of Fission Yield Literature

[577 - 580] WOLFSBERG, K., Phys. Rev., 137 (1965) 8929.
[581 - 584] HARBOUR, R.M., TROUTNER, D.E., Jinc., 33 (1971) 1.
[585 - 586] KRATZ, J.V., HERMANN, G., Jinc., 32 (1970) 3713.
[587 KEMMER, J., KIM, J.I., BORN, H.J., Radiochim. Acta., 13 (1970) 181.
[588] WOLFSBERG, K., Jinc., 33 (1971) 587.
[589] FORMAN, L., BALESTRINI, S.J., WOLFSBERG, K., JETER, .R., LA-DC 11500.
[590 - 593] LISMAN, F.L., ABERNATHEY, R.M., FOSTER, R.E., MAECK, W.J., Jinc. 33 (1971) 643.
[594 - 595] SWINDLE, D.L., WRIGHT, R.J., WARD, T.E., KURODA, P.K., Jinc. 33 (1971) 651.
[596] SWINDLE, D.L., WRIGHT, R.J., KURODA, P.K., Jinc. 33 1971) 876.
[597] KURODA, P.K., MENON, M.P., Nucl. Sc. Eng., 10 70.
[598] FARKER, P.L., KURODA, P.K., Jinc., 5 (1958) 153.
[599] ASHIZAWA, F.T., KURODA, P.K., Jinc., 5 (1957) 12.
[600] HEYDEGGER, H.R., KURODA, P.K., Jinc., 12 (1959) 12.
[601 - 602] SKOVORODKIN, N.V., et al., Sov. Radiochem., 12 (1970) 458.
[603 - 604] SKOVORODKIN, N.V., et al., Sov. Radiochem., 12 (1970) 453.
[605] KEMMER, J., KIM, J.I., BORN, H.J., Radiochim. Acta., 15 (1971) 113.
[606 - 607] HARBOUR, R.M., EICHOR, M., TROUTNER, D.E., Radiochim. Acta., 15 (1971) 146.
[608] DIERCKX, R., MARACCI, G., RUSTIGHELLI, F., J. Nucl. En., 25 (1971) 85.
[609] GORDON, G.E., HARVEY, J.W., NAKAHARA, H., Nucleonics, 24 (1966) 62.
[610] DANGE, S.P., JAIN, H.C., et al., IAEA Symp. Phys. and Chem. of fission, (1969) 741.
[611] FAHLAND, J., LANGE, G., HERMANN, G., Jinc., 32 (1970) 3149.
[612 - 615] HAWKINGS, EDWARDS, W.J., OLMSTEAD, W.J., Can. J. Phys., 49 (1971) 785.
[616] EICHOR, M., TROUTNER, D.E., Jinc., 33 (1971) 1543.
[617 - 618] GANAPATHY, R., ITOCHI, H., Jinc., 28 (1966) 3071.
[619] WUNDERLICH, F., Radiochim. Acta., 7 (1967) 105.
[620] MENKE, H., HERMANN, G., Radiochim. Acta., 6 (1966) 76.
[621] STEINBERG, E.P., GLENDENIN, L.E., Phys. Rev. 95 (1954) 431.
[622] TURKEVICH, A., NIDAY, J.B., TOMPKINS, A., Phys. Rev., 89 (1953) 552.
[623] COLEMAN, R.F., HAWKER, B.R., PERKIN, J.L., Jinc., 14 (1960) 8.
[624] ISHIMORI, T., UENO, K., KIMURA, K., et al., Radiochim. Acta., 7 (1967) 95.
[625 - 262] STEVENSON, P.C., HICKS, H.G., ARMSTRONG, J.C., GUNN, S.R., Phys. Rev., 117 (1960) 186.
[627] ARMANI, R.J., GOLD, R., LARSEN, R.P., ROBERTS, J.H., Trans. Amer. Nucl. Soc., 13 (1970) 90.

Table XVI (cont)

Reference List of Fission Yield Literature

[628] VONGUNTEN, H.R., FLYNN, K.F., GLENDENIN, L.E., Phys. Rev., 161 (1967) 1192.

[629 - 630] LYLE, S.J., MARTIN, G.R., RAHMAN, M.M., Radiochim. Acta., 9 (1968) 90.

[631 - 632] CUNINGHAME, J.G., GOODALL, J.A.B., WILLIS, H.H., PRIVATE COMMUNICATION.

[633 - 635] CUNINGHAME, J.G., GOODALL, J.A.B., WILLIS, H.H., AERE-R-6862.

[636] MCLAUGHLIN, T.P., Univ. Arizona Thesis, 1971 71-14509.

[637 - 639] NAKAHARA, H., FUJIWARA, I., OKAMOTOT, H., IMANISHI, N., ISHIBASHI, M., NISHI, T., Jinc., 33 (1971) 3239.

[640] TROUTNER, D.E., RUNNALLS, N.G., Jinc., 33 (1971) 2271.

[641] DEL MARMOL, P., PERRICOS, D.C., Jinc., 32 (1970) 705.

[642] SWINDLE, D.L., MOORE, D.T., BACK, J.N., KURODA, P.K., Jinc., 33 (1971) 3643.

[643] - 644] DENSCHLAG, H.O., QAIM, S.M., Jinc., 33 (1971) 3649.

[645] VLASOV, V.A., et al. AEC-TR-6665.

[646] FORD, G.P., STANELY, C.W., AECD-3551.

[647] NETHAWAY, D.R., LEVY, H.B., Phys. Rev., 139 (1965) 81505.

[648] PETRZHAK, K.A., TEPLYKH, V.F., PAN'YAN, M.G., Sov. J. Nucl. Phy. 11 (1970) 654.

[649] BORISOVA, N.I., et al., Sov. J. Nucl. Phy., 8 (1969) 404.

[650 - 651] SARANTITES, D.G., GORDON, G.E., CORYELL, C.D., Phy. Rev., 138 (1965) B353.

[652 - 653] BAECKMANN, A.V., FEUERSTEIN, H., Radiochim. Acta., 5 (1966) 234.

[654 - 655] BROWN, M.G., LYLE, S.J., MARTIN, G.R., Radiochim. Acta., (1966) 16.

[656 - 657] RAO, A.S., RAO, M.N., KURODA, P.K., Jinc., 31 (1969) 591.

[658 - 659] MO, T., KURODA, P.K., Jinc., 27 (1965) 503.

[660] ARINO, H., KURODA, P.K., Jinc., 30 (1968) 677,

[661 - 662] NAMBOODIRI, M.N., et al., Jinc., 30 (1968) 2305.

[663] TOMLINSON, L., HURDUS, M.H., Jinc., 33 (1971) 3609.

[664 - 670] ROBIN, M., BOUCHARD, J., DARROUZET, M., Int. Cong. Chem. Nucl. Data, Canterbury, 1971.

[671] HERRMANN, G., STRASSMANN, F., Zeit. Naturforsch., 11A (1956) 946.

[672] GANAPATHY, R., KURODA, P.K., Earth and Plan. Sc. Letters, 3, (1967) 89.

[673 - 675] KENNETT, T.J., THODE, H.G., Phys. Rev., 103 (1956) 323.

[676] MALY, J., KNOBLOCH, V., IMBRISOVA, D., PRASIL, Z., URBANEC, Z., Coll. Czech.

[677 - 680] KRAPPEL, W., SEUFERT, H., STEGEMANN, D., Nucl. Tech., 12 (1971) 226.

[681 - 682] RAMANIAH, M.V., JAIN, H.C., MATHEW, K.A., AVADHANY, G.V.N., Madras Conf., 1970.

[683 - 684] ROCHE, M.F., TROUTNER, D.E., Radiochim. Acta., 16 (1971) 66.

[685] BIRGUL, O., LYLE, S.J., WELLUM, R., Radiochim. Acta., 16 (1971) 104.

[686] TROUTNER, D.E., HARBOUR, R.M., Jinc., 34 (1972) 801.

[687 - 688] SOROKINA, A.V., et al., Atom. Energ., 31 (1971) 99.

DISCUSSION

M. LEDERER: Are these data available on magnetic tapes?

E.A.C. CROUCH: At present, only the input literature results are so available. We do hope to have them on magnetic tape but it may not be for some time yet. For this year, at least, we are publishing the final results in the form of reports.

F. FRÖHNER: In connection with Mr. Lederer's question, I might mention that Dr. Crouch was kind enough to turn over his library to the CCDN recently. We are now in the process of incorporating the data into our experimental data file and hope that we shall soon be able to answer requests from users in our service area or, for that matter, from other service areas via their respective neutron data compilation centres.

J. BLACHOT: Why do you sometimes have three significant figures and sometimes two?

E.A.C. CROUCH: Simply because I have not trimmed the figures to match the stated standard deviations; it is my omission entirely, and one must read the figures in conjunction with their stated standard deviations.

W.B. LEWIS: I saw no mention in your paper of neutron capture by fission products. Did you assume a value for this and then subtract or add it?

E.A.C. CROUCH: No corrections were made for neutron capture; it was assumed the author would have done this.

M. LAMMER: Do you estimate missing yield values from a mathematical model for the case of ^{235}U, ^{239}Pu etc. thermal fission as well, or only for types of fission where yields are not well known? What is the confidence level of such estimates?

E.A.C. CROUCH: We have not tested mathematical models to date, as the basic evaluations are more important to the UKAEA, although the references in the paper give some preliminary ideas. We have, however, done sufficient work to see that model fitting is possible; I would prefer not to say more at present.

M. LAMMER: Measured relative yields normalized in such a manner that the sum of yields totals 200% are based on interpolated values and radiochemical measurements from the earlier literature. At the time of evaluation these data were known far better. Such measurements must in any case be considered as relative yields. Why is an adjustment not possible, as indicated in section 2(ii) of your paper?

E.A.C. CROUCH: I would not say that adjustment is not possible. However, the very act of drawing a smooth curve through the exponential points implies the setting up of a model, the validity of which may be doubtful. So I prefer to leave such results as the author left them: he obviously hoped to make an estimate of absolute yields.

Miss K. WAY: Under what circumstances were data omitted? In other words, were data very different from the mean included in arriving at that average?

E.A.C. CROUCH: The χ^2 test was used with the weighted mean to establish if any results were obviously wrongly weighted. The weights were then adjusted so that no result was omitted although its weight might be so low as to render its effect negligible. The exception to this is the case where an error can definitely be detected in the paper; but as far as

my memory goes only one paper was ignored in the thermal yields. I ought to add that I do not include project progress reports in the evaluations; the results must have been made public somewhere!

C. DEVILLERS: Can you say whether the deviations which you observe in the yields as between your compilation and that of Meek and Rider are comparable with the uncertainties reported by the latter authors?

E. A. C. CROUCH: Most of the recommended yields agreed with Walker's and Meek and Rider's figures, within the figures taken as standard deviations for those works. I am not certain what exactly Meek and Rider meant by their error indicator letters.

W. H. WALKER: I should like to make a brief comment in this connection: the results of Meek and Rider in NEDO-12154('72) have been replaced by a new version currently available only as computer output. Some yields have been changed substantially, and most of the values quoted by Dr. Crouch have been changed.

CUMULATIVE YIELDS OF THERMAL NEUTRON FISSION PRODUCTS Some Results and Recommendations Based on a Recent Evaluation

W.H. WALKER
Chalk River Nuclear Laboratories,
Chalk River, Ontario, Canada

Abstract

CUMULATIVE YIELDS OF THERMAL NEUTRON FISSION PRODUCTS: SOME RESULTS AND RECOMMENDATIONS BASED ON A RECENT EVALUATION.

A careful analysis of cumulative yields in the thermal neutron fission of ^{233}U, ^{235}U, ^{239}Pu and ^{241}Pu has recently been completed. The methods used and some of the problems encountered are discussed. Errors are assigned to all yields and the effects of the corresponding uncertainties in neutron absorption and reactivity are estimated. A program of measurements which could reduce the major uncertainties requires mass-spectrometric measurements of radioactive and stable isobars for a given fissile species plus γ-ray measurements for all four fissile species of relative yields for a large number of radioactive nuclides that are isobaric with nuclides for which the yields have been measured mass-spectrometrically. These measurements are discussed and recommendations made for presentation of data in a way that will minimize uncertainties in future evaluations.

Though much effort has gone into the measurement and evaluation of fission product cross sections, there has been little support by reactor scientists of work on fission product yields. This is surprising since the rate at which neutrons are absorbed by a particular fission product is proportional to the product of its yield, y, and its cross section, σ, if σ is small, or to y only if σ is very large. In the most recent work on yields the interest has been primarily in their use as burnup monitors rather than in obtaining an improved knowledge of fission product absorption.

A recent evaluation of thermal fission yields at Chalk River [1] provides an excellent basis for determining uncertainties in fission product absorption since it includes an estimate of the error in the cumulative yields at each mass.

THE EVALUATION OF FISSION PRODUCT YIELDS

The new Chalk River evaluation of fission product yields is an improved version of the one for ^{235}U thermal fission presented at the Helsinki conference [2], extended to include data for ^{233}U, ^{239}Pu and ^{241}Pu. This evaluation is based mainly on mass spectrometric measurements which cover from 66% (^{241}Pu) to 92% (^{235}U) of the total yield. Radiometric data covering the same masses are used only to check final normalizations. They are also used to

obtain yields at masses where no mass spectrometric data are available, mainly the yields in the wings of the light and heavy mass peaks and in the valley between.

The evaluation method is, therefore, quite different from the usual one in which an error is assigned to every measured yield and the recommended yield at each mass is then obtained by a least squares analysis. This is the method used by Meek and Rider in a series of reports on fission product yields the last of which was published in 1972 [3]. The main disadvantage of this latter approach is that it is difficult to properly take account of the high accuracy with which the mass spectrometrist can measure both relative abundances of the isotopes of one element and the relative amounts of different elements. The second of these determinations is less accurate than the former, but even then is usually comparable in accuracy to the best radiometric measurements.

Although it is given in detail in [1] I will outline the evaluation method here for three reasons - first, to demonstrate the advantages referred to above more clearly, second, to provide background material for a discussion of possible future measurements, and third, because the version in [1] is quite detailed and is primarily of interest to a small group of specialists.

The method proceeds in three easily separated steps - the determination of isotopic abundances, the determination of relative element yields, and final normalization.

Isotopic Abundances

Table I is taken from [1] and shows the measured isotopic abundances of the Nd fission products, where isotopic abundance is defined as the number of atoms of one isotope divided by the number of atoms of the element, excluding relatively short-lived isotopes such as 11-day ^{147}Nd. The values of Lisman et al.[4] are averages of results from several samples of each fissile material and the assigned error is the standard deviation from the average. The errors assigned to the final averages are also standard deviations.

The first point to note about the data is the generally small scatter between measurements, with standard deviations often less than 1%. The greatest uncertainty, up to ~4% from the mean for ^{233}U fission, occurs for ^{150}Nd, which has a small isotopic abundance and is, therefore, more difficult to measure accurately. The fact that the standard deviation of the mean usually exceeds that of a single set of measurements (Lisman et al.[4]) indicates that there are probably small systematic errors in the different measurements.

Those results of Steinberg and Glendenin [5] that were not used require some comment. For ^{143}Nd the difference from the

TABLE I. RELATIVE YIELDS OF NEODYMIUM ISOTOPES

	^{143}Nd	^{144}Nd	^{145}Nd	^{146}Nd	^{147}Nd*	^{148}Nd	^{150}Nd
^{235}U							
Steinberg, Glendenin(1955)	.2820[x]	.2723[x]	.1849[x]	.1474[x]		.0814	.0325
Melaika et al. (1955)	.2861	.2672[1]	.1903	.1445		.0804	.0315
Farrar, Tomlinson (1958)	.2866	.2661	.1906	.1447	.1093	.0805	.0315
Chu (1959)	.2897	.2607	.1912	.1448		.0817	.0319
Rider et al. (1965)	.2927	.2593	.1911	.1441		.0816	.0313
Lisman et al. (1970)	.2884 ±0.4%	.2640 ±0.9%	.1893 ±0.6%	.1443 ±0.3%		.0827 ±0.5%	.0312 ±0.5%
Average	.2885 ±0.9%	.2635 ±0.9%	.1905 ±0.4%	.1445 ±0.2%	.1093	.0814 ±1.1%	.0316 ±0.8%
^{233}U							
Melaika et al. (1955)	.3201	.2506[1]	.1879	.1412		.0717	.0285
Ivanov et al. (1959)	.3224[2]	.2566[2]	.1821	.1412		.0663[x]	.0324[x]
Bidinosti et al. (1961)	.3197	.2503	.1881	.1408		.0720	.0291
Rider et al. (1966)	.3253	.2533	.1862	.1381		.0702	.0268
Lisman et al. (1970)	.3198 ±0.2%	.2574 ±0.4%	.1850 ±0.3%	.1389 ±0.3%		.0717 ±0.6%	.0272 ±2.4%
Average	.3215 ±0.7%	.2536 ±1.3%	.1859 ±1.4%	.1400 ±1.0%		.0714 ±1.2%	.0279 ±3.8%
^{239}Pu							
Wiles et al. (1956)	.2714	.2291[1]	.1849	.1523		.1029	.0594
Krizhanskii et al. (1957)	.2743	.2305	.1827	.1528		.0993	.0603
Fickel, Tomlinson (1959)	.2703	.2307[3]	.1852	.1522		.1014	.0603
Rider et al. (1966)	.2744	.2294	.1850	.1512		.1014	.0586
Lisman et al. (1970)	.2725 ±0.3%	.2286 ±0.9%	.1847 ±0.2%	.1518 ±0.2%		.1034 ±0.7%	.0590 ±0.4%
Average	.2726 ±0.7%	.2297 ±0.4%	.1845 ±0.5%	.1521 ±0.4%		.1017 ±1.6%	.0595 ±1.3%
^{241}Pu							
Farrar et al. (1964)	.2537	.2328	.1807	.1551		.1094	.0683[4]
Rider et al. (1967)	.2560	.2385	.1817	.1520		.1075	.0643
Lisman et al. (1970)	.2556 ±0.2%	.2356 ± 0.1%	.1819 ±0.1%	.1528 ±0.2%		.1077 ±0.2%	.0664 ±1.0%
Average	.2551 ± 0.5%	.2356 ±1.2%	.1814 ± 0.4%	.1532 ± 0.9%		.1082 ± 1.0%	.0663 ± 3.0%

* Yields for this isotope not included in normalization

[x] Not used in taking average. Remaining yields normalized assuming average value at this mass

[1] Corrected for change in $T_{\frac{1}{2}}(^{144}Ce)$ from 282 to 284.4 d – ^{235}U, +0.4% (see text); ^{233}U, +0.5%; ^{239}Pu, +1.0%.

[2] Corrected for change in $\hat{\sigma}(^{143}Nd)$ from 280 b to 325 b. See text.

[3] Corrected for change in $T_{\frac{1}{2}}(^{144}Ce)$ from 278 d to 284.4 d – ^{239}Pu, +1.5%.

[4] Results for two samples were quoted with relative ^{150}Nd yields differing by 4.4%. Only the value with the smaller standard deviation is used here.

average is only twice the standard deviation and would normally be included. While no details are available concerning the irradiation, I believe it was similar in integrated flux to those of Lisman et al. [4] where ^{143}Nd values were increased 2% or more to take account of loss by neutron capture. The ^{144}Nd isotopic abundance is decreased a corresponding amount. Since no mention of such a correction is made by Steinberg and Glendenin this is probably the source of the discrepancy and for this reason their mass 143 and 144 results are omitted. For masses 145 and 146 the differences are similar in magnitude, but cannot be explained by neutron capture since the ^{145}Nd cross section is only about 1/6 of the ^{143}Nd cross section. These results are omitted simply because they differ from the mean of the other values by more than ten times the standard deviations of the mean.

Proceeding in this manner with each element measured mass spectrometrically gives the shape of segments of the yield curve, each segment corresponding to an element, as shown in Figure 1(a) for the heavy masses in ^{235}U thermal fission.

Relative Element Yields

Isotope dilution is the most common method used to determine relative abundances of the different elements mass spectrometrically. A measured number of atoms of the same element are added to the fission product sample and the isotopic abundances of the mixed sample are determined. The added material is preferably a single isotope not produced in fission, but the naturally occurring element has also been used. The ratio of fission product atoms to added atoms is calculated from the isotopic abundances and from this data the number of fission product atoms for each element can be determined relative to a particular element.

The second method can readily be understood from Figure 1(a). It is not necessary to wait until all the radioactive isotopes have decayed before the mass analysis is made, and the open circles show where these have been measured. The final values for radioactive isotopes have, of course, been corrected for radioactive decay. To use the second method, isobaric linking, one simply equates the isotopic abundances of the two isobars to obtain the relative numbers of atoms of the two elements involved.

Table II, taken from [1], shows relative element yields for ^{235}U fission. The values listed are in atoms per atom of Zr for the light masses or Nd for the heavy masses. Those obtained by isobaric coupling are indicated by the superscript i. Note that the standard deviations are more variable than those in Table I, with a maximum of 6.3% for Sm.

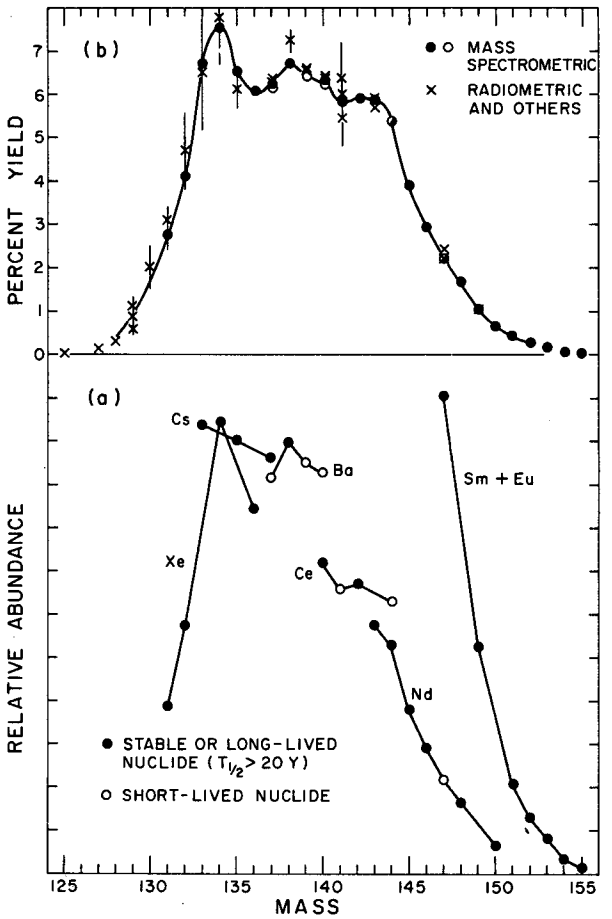

FIG.1. Heavy-mass data for the thermal neutron fission of ^{235}U:
a) Relative abundances of Xe, Cs, Ba, Ce, Nd, Sm and Eu isotopes; b) Percent yields.

Figure 1(b) shows how the individual element results of Figure 1(a) are fitted together in this way to give the shape of the bulk of the heavy mass peak in ^{235}U fission. Here the yields have been normalized so that the Nd element yield is 20.40% as determined by mass spectrometric measurements of the number of fissions. This value may be expected to have a 2-3% uncertainty. Note that the radioactive isobar yields agree with the stable isobar yields within their errors, even though they made only a minor contribution to determining relative yields.

TABLE II. RELATIVE ELEMENT YIELDS IN ^{235}U THERMAL NEUTRON FISSION

Element	Kr	Rb	Sr	Y	Zr	Mo	Ru
Isotopic masses included in element yield	83,84 86	85,87	88,90	89,91	91,92, 93,94, 96	97,98, 100	101,102 104,106
	Element Yields Relative to Zr						
Lisman et al. (1970)	.1124	.1252	.3084		1.000	.5796	.3707
Farrar et al. (1962)			.2992[i] ±0.7%	.3422[i]	1.000		
Steinberg, Glendenin (1955)			.3031		1.000	.5852	.3633[1]
Petruska et al. (1955)		.1238[2] (.3036)					
Average	.1124	.1245 ±0.6%	.3036 ±1.5%	.3422	1.000	.5824 ±0.5%	.3682 ±0.7%

Element	Xe	Cs	Ba	Ce	Nd	Sm
Isotopic masses included in element yield	131,132 134	133,137	138	140,142 144	143-146 148,150	147,149 151,152 154
	Element Yields Relative to Nd					
Lisman et al. (1970)	.7068	.6359	.3323	.860	1.000	.1838[3]
Rider et al. (1965,1967)		.6284	.3194		1.000	
Farrar, Tomlinson, (1962)	.7650[i,4]	.6346[i,6]	.3319	.8621[i]	1.000	.1979[i]
Chu (1959)				.8546	1.000	.2009
Petruska et al. (1955)					1.000	.2147
Steinberg, Glendenin (1955)		.5662[x]	.2627[x]	.8178[6,x]	1.000	
Average	.7068	.6330 ±0.6%	.3279 ±2.3%	.8592 ±0.5%	1.000	.1993 ±6.3%
From average relative yields (Tables 8,9)				.8642[i] ±1.6%		

[i] Using isobaric links
[x] Not used in taking average
[1] Based on absolute yield of ^{106}Ru determined by β-counting. Assigned half weight in taking average
[2] Based on an isotope dilution measurement giving Rb atoms/Sr atoms = 2.451 and assuming a Sr yield of 0.3036
[3] With ^{147}Sm reduced 2.5% (Table 10)
[4] Not used because it is based on an unpublished value of the ^{133}Xe yield for which no data on decay corrections is available
[5] From Cs yields of Petruska et al (1955b) using mass 137 isobars
[6] Based on mass 140 and 142 only, using average relative abundances of Table 8

Final Normalization

Finally, as shown in Figure 1(b), the radiometric yields are introduced. Their proper role can now be much more clearly understood - namely to define the yields in the valley between the light and heavy mass peaks, and in their wings, and to contribute to the final normalization of the mass spectrometric yields.

In the case of the ^{235}U heavy masses in Figure 1(b) the mass spectrometric yields as initially normalized sum to 95.6%, while the radiometric and interpolated yields add to 3.3%. The sum is thus short of the requisite 100% by 1.1% and this could be made up by increasing all radiometric yields by 1/3 of their value; however, even if one wished to argue that such a change is within their error range, this data is taken from so many different sources that one certainly could not claim that they would have a common systematic error of this magnitude. Since the required change to the set of mass spectrometric yields is less than the error assumed for the original normalization, it is much more reasonable to increase the mass spectrometric data only, and this is the course followed.

In the present case the more accurate radiometric measurements, those at masses 137, 139 and 140, support the ~1% increase in the mass spectrometric yields.

In [1] the yields are required to satisfy a second condition, in addition to $\Sigma\, y_i = 1.000$, in order to satisfy an additional requirement, namely that the mean number of nucleons of the final distribution should equal the number of fissioning nucleons less the average number of neutrons per fission,

$$\text{i.e. } \sum_i y_i A_i = A_f + 1 - \bar{\nu}$$

To satisfy this restriction a few adjustments were required, either in individual radiometric values, or by using different normalization factors for mass spectrometric yields above and below the peak, i.e. slightly skewing the original mass spectrometric shape of either the light or heavy mass peak. The changes were within the range allowed by the assigned errors.

ASSIGNMENT OF ERRORS AND THEIR EFFECT ON FISSION PRODUCT ABSORPTION

Because of the separation into three distinct steps used in this analysis the estimation of yield errors is relatively straightforward, consisting of that due to their isotopic abundance, the relative element yield, and final normalization. The errors for individual yields are correlated by both their dependence on relative elements yields and the normalization requirement that $\Sigma\, y_i = 1.000$. Thus a change within the range allowed by the errors for one yield, say an increase for one nuclide in

TABLE III. FISSION-PRODUCT ABSORPTION IN THERMAL REACTOR FUELS

Fission Product	$\hat{\sigma} \pm \Delta\hat{\sigma}$ - barns -	$y \pm \Delta y$ (%)				barns/fission (total no. of absorptions in nuclide ÷ (total fissions x irradiation)[a]								
		^{235}U	^{233}U	^{239}Pu	^{241}Pu	^{235}U[b]	^{236}U[b]	^{239}Pu[b]	Nat U[bc]	^{235}U[b]	^{239}Pu[b]	^{241}Pu[b]	Nat U+Pu[bc]	Th+^{233}[b]
^{135}Xe	$(345\pm14)10^4$	6.60±.16	6.21±.15	7.69±.24	7.06±.24	82.4±2.0	13.06	40.5	22.7±.4	7.71	17.72	16.32	16.66±.50	12.84±.32
^{143}Nd	329±10	5.95±.08	5.85±.10	4.53±.06	4.52±.06	7.72±.22	7.54	5.97	6.47±.19	6.89	5.47	5.45	5.98±.17	6.26±.19
^{149}Sm	$(69\pm2)10^3$	1.08±.07	.765±.021	1.29±.05	1.44±.04	17.2±1.1	3.52	9.00	5.49±.25	2.34	4.38	4.81	4.33±.18	2.54±.07
^{103}Rh	221±10	3.05±.20	1.8±.3	5.94±.29	6.65±.70	1.92±.14	2.69	4.92	3.74±.25	2.60	5.03	5.64	4.63±.34	1.63±.28
^{151}Sm	$(13\pm1)10^3$	.419±.027	.314±.008	.820±.029	.882±.024	6.92±.44	1.68	5.70	3.07±.14	1.27	3.01	3.26	2.75±.11	1.26±.03
^{147}Pm	311± 35	2.26±.04	1.70±.05	2.16±.07	2.20±.06	2.83±.28	2.30	2.47	2.17±.22	1.95	2.04	2.08	2.09±.21	1.63±.16
^{131}Xe	153±15	2.80±.07	3.53±.08	3.73±.09	3.12±.07	1.61±.15	1.86	2.42	2.13±.20	1.79	2.40	2.01	2.40±.28	2.53±.25
^{133}Cs	58.4±3.	6.78±.16	5.99±.21	6.92±.17	6.72±.18	1.82±.10	1.87	1.90	1.88±.11	1.85	1.89	1.83	2.16±.13	2.04±.13
^{152}Sm	399±15	.267±.017	.213±.006	.624±.022	.697±.019	1.12±.08	1.16	2.38	1.65±.08	1.11	2.22	2.43	2.01±.10	0.96±.04
^{105}Rh	$(18\pm2)10^3$	.95±.20	.53±.10	5.47±.16	6.75±.70	1.30±.28	0.20	3.16	1.16±.08	0.12	1.38	1.70	1.06±.09	0.12±.03
^{146}Nd	61±6	3.93±.06	3.38±.06	3.06±.04	3.22±.04	1.19±.12	1.15	0.91	1.05±.11	1.13	0.89	0.94	1.10±.12	1.10±.11
^{99}Tc	35±4	6.14±.09	5.01±.10	6.10±.36	6.20±.12	1.03±.12	1.04	1.03	1.05±.13	1.03	1.03	1.04	1.19±.12	1.01±.12
^{153}Eu	546±25	.167±.011	.105±.005	.38±.01	.522±.022	0.48±.04	0.67	1.30	1.00±.06	0.73	1.47	1.79	1.43±.08	0.62±.04
^{148m}Pm	$(24\pm)10^3$	(from capture in ^{147}Pm)				0.94±.10	0.85	0.88	0.79±.08	0.73	0.75	0.77	0.77±.08	0.60±.06
^{155}Eu	4200±200	.0321±.002	.023±.005	.17±.02	.231±.022	0.40±.03	0.35	1.28	0.78±.09	0.44	1.15	1.49	1.16±.13	0.41±.09
^{150}Sm	115±5	(from capture in ^{149}Sm)				0.58±.05	0.65	0.74	0.72±.05	0.66	0.75	0.83	0.83±.04	0.51±.02
^{154}Eu	1500±150	.074±.005	.046±.001	.286±.011	.378±.010	0.09±.01	0.37	0.55	0.57±.06	0.48	0.89	1.10	0.97±.09	0.42±.04
^{109}Ag	185±13	.030±.006	.047±.005	1.3±0.2	2.5±.5	0.03	0.03	1.16	0.47±.07	0.02	1.09	2.10	0.82±.13	0.04
^{95}Mo	20.9±1.5	6.53±.10	6.19±.10	4.98±.08	3.98±.09	0.15±.01	0.53	0.30	0.46±.03	0.58	0.40	0.32	0.53±.04	0.61±.04
^{83}Kr	210±10	.535±.013	1.00±.02	.295±.007	.202±.005	0.54±.03	0.48	0.28	0.38±.02	0.45	0.26	0.18	0.33±.01	0.82±.05
≥149						27.54±1.79	8.88	22.35	14.04±.65	7.54	14.88	16.90	14.39±.60	6.89±.19
Total Fission Product						134.4	44.8	92.0	61.8	26.7	58.6	61.2	57.3	41.6

a Integrated fissions and absorptions taken from LATREP (Nat U, Nat U+Pu, Th+^{233}U), pure fissile atom values are approximations (0.5 x barns per fission at mid-irradiation) using FISSPROD. All fluxes 3 x 10^{13}n/cm^{2}s

b Pure ^{235}U fuel irradiated to 0.6 n/kb; Nat U (with ^{235}U, ^{239}Pu components) to 2.6 n/kb; Nat U + Pu (with ^{235}U, ^{239}Pu, ^{241}Pu components) to 3.6 n/kb; Th+^{233}U to 4.0 n/kb. In the enriched fuels the Nat U contains 3.5 g fissile Pu/kg and the Th 14 g ^{233}U/kg.

c The fraction of fissions contributed are as follows - Nat U: ^{235}U,44.4%; ^{239}Pu,46.2%; ^{238}U,5.8%; ^{241}Pu,3.5% - Nat U + Pu: ^{235}U,28.1%; ^{239}Pu,54.2%; ^{241}Pu,11.8%; ^{238}U,5.9%

the heavy mass group, will require a comparable increase in the yields of other isotopes of the same element (assuming the isotopic abundance error is small) and a corresponding decrease in some or all of the other elements in the heavy mass range to keep $\Sigma\ y_i = 1.000$.

The use of yield errors to obtain uncertainties in fission product absorption is of considerable interest since it indicates where future efforts can most fruitfully be concentrated.

The basic data and estimated uncertainties (one standard deviation) are summarized in Table III. The first column lists the 20 most important fission products in their order of importance as determined by their average absorption in natural uranium irradiated in a CANDU reactor of the Pickering design. Other definitions of thermal fission product importance would require only minor changes in the order of the list and the nuclides included.

The second column lists effective cross sections in the same reactor using the notation of Westcott et al. [6]

$$\hat{\sigma} = \sigma_0(g+rs)$$

where σ_0 is the 2200 m/s cross section, $g\sigma_0$ is the effective cross section in a Maxwellian flux, r is the epithermal index (proportional to the fraction of neutron density in the epithermal range) and $s \propto I'/\sigma_0$, where I' is the resonance integral less the 1/v contribution from $g\sigma_0$. The values of $\hat{\sigma}$ and their assigned uncertainties are based on the evaluation of σ_0 and I' [7] associated with the yield evaluation discussed here, and $r = .057$.

The next four columns list the recommended yields of [1] with their overall error, taken as the square root of the sum of the squares of the 3 components already described.

The remaining columns list the contributions of these fission products in a variety of possible thermal reactor fuels - ^{235}U alone, natural U, natural U with Pu, and Th with ^{233}U - as well as in the main fissile components of the two natural U fuels. The mixed fuel calculations use a new version [8] of LATREP [9] and the quoted values are absorption in barns/fission using the total number of absorptions in the nuclide divided by the product of the irradiation and total fissions. The component contributions (columns 8, 9, 11, 12 and 13) are approximations based on FISSPROD [10] calculations using a value equal to half the calculated barns per fission at mid-irradiation.

The fission products may be separated for convenience into three categories depending on the magnitude of $(\lambda+\hat{\sigma}\phi)T$, where λ is the decay constant, ϕ is the flux and T is the irradiation

period. The three groups are rapidly saturating, partially saturating or non-saturating depending on whether $(\lambda+\hat{\sigma}\phi)T$ is much greater than, of the same order as, or much smaller than unity.

The dependence of the absorption of a particular fission product on its cross section, and consequently the degree to which it is sensitive to $\Delta\hat{\sigma}$ depends on the degree of saturation. The uncertainty in $\hat{\sigma}$ may be ignored for rapidly saturating fission products with $\sigma\hat{\phi}>>\lambda$, requires a partial weighting for partially saturating fission products or rapidly saturating fission products with $\hat{\sigma}\phi\approx\lambda$, and full weight for non-saturating fission products, or if $\hat{\sigma}\phi<<\lambda$.

Effect of Yield Correlations

Because of the correlations between yields it is impossible to calculate the uncertainty in the total fission product absorption. To illustrate the wide range of effects to be expected because of these correlations consider two cases associated with ^{135}Xe and ^{149}Sm.

In the ^{135}Xe case, the yields are based on single measurements of the relative abundance of the daughter, ^{135}Cs, for each of the fissile nuclides except ^{239}Pu, where three measurements are available. Because naturally occurring Cs is entirely ^{133}Cs, which is also a high yield fission product, isotope dilution measurements of the relative yield of Cs are difficult and these have an uncertainty exceeding 2% for both fissile Pu isotopes.

In the case of natural U it is a reasonably good approximation to assume that the uncertainty is 2½% and entirely due to the uncertainty in the relative Cs yield. It thus applies to all yields based on Cs (masses 133, 135 and 137) which total ~20% and have an absorption in natural U of 24.7 b/fission. Thus, if the Cs yields were increased the full 2½% the absorption would increase by 0.62 b/fission. On the other hand the remaining 80% of the high mass yield would have to be reduced by 0.6% to keep $\Sigma\, y_i = 100\%$. Since these contribute about 28 b/fission to the total absorption, the net increase in absorption is only 0.45 b/fission, or less than 3/4 what it would be without the requirement that $\Sigma\, y_i = 100\%$.

The second example concerns ^{149}Sm, or rather, absorption in all the masses from 149 up, since these are tightly linked together by capture transmutations. In the case of ^{235}U fission, the Sm and Eu isotopic abundances were measured relative to each other so in this case there is additional reason for treating this group as a single unit. Further, there appears to be a great deal of systematic uncertainty between the different isotope dilution measurements, so that the relative Sm-Eu yields are assigned an error of 6% in ^{235}U fuel. Since this group contributes 27.5 b/fission (2nd to last line in Table III) the increase

in absorption is 1.65 b/fission. On the other hand, the total yield for this group is only 2.7% so the compensating decrease in the remaining heavy masses will be small. Assuming the other yields are decreased uniformly the effect is approximately 0.06 x 0.027 x 100 or 0.15 b/fission, so that the net increase is 1.5 b/fission.

It is apparent that the correlations between yields will have different effects on different fuels, depending on the magnitudes of the yields and their corresponding absorption. In the case of isotopes of elements with large yields and low absorption, for example Zr or Ce, a yield increase may even result in a decrease in absorption.

Effect of Yield Uncertainties in Reactor Dynamic Calculations

Yield uncertainties also affect calculations of ^{135}Xe oscillations in large thermal reactors, and the ^{135}Xe, ^{106}Rh, ^{149}Sm and ^{151}Sm transient behaviour following reactor shutdown. In these cases the uncertainty in cross sections carry their full weight. The cost of these uncertainties will depend not only on the type of reactor but also on the method of control used (e.g. insertion of boosters, removal of absorbers).

It should be noted, however, that the cost of overriding the ^{135}Xe and ^{106}Rh transient after shutdown will probably be less in reactors fuelled with ^{233}U, not only because the cumulative yields of both nuclides are smaller, but because the direct yield of ^{135}Xe is much larger in this fuel than in natural U - 22% direct to Xe, only ~78% cumulative to I [11, 12].

To conclude this section on the effects of yield uncertainties, I would like to note that an estimate of uncertainties in fission product absorption was made previously [13] although the scope was restricted to ^{233}U, ^{235}U, ^{239}Pu and natural U. In comparison with that analysis, it would appear that we are a little less sure of the magnitude of fission product absorption, mainly because of the increase (by a factor of two) in the uncertainty in Sm yields in ^{235}U fission. This, in turn, can be attributed to the inclusion of the 1970 results of Lisman et al. [4].

FUTURE REQUIREMENTS

Table III is a useful indicator of where the major effort in improving fission product yields is required, although it does not cover all the shortcomings in yield measurements.

Table IV lists the six fission products having the greatest uncertainty in absorption in natural U fuel, with their uncertainties in natural U, natural U plus Pu and Th plus ^{233}U. For

TABLE IV. MAJOR SOURCES OF UNCERTAINTY IN ABSORPTION IN REACTOR FUELS

Nuclide	Absorption Uncertainty (barns/fission) in Natural U	Natural U + Pu	Th + 233U
>149	0.65	0.60	0.19
(149Sm)	(0.25)	(0.18)	(0.07)
135Xe	0.44	0.50	0.32
103Rh	0.25	0.34	0.28
147Pm*	0.22	0.21	0.16
131Xe*	0.20	0.28	0.25
143Nd*	0.19	0.17	0.19

*Most of the uncertainty is contributed by the cross section

several of these nuclides the major contributor to the uncertainty is the cross section and these are identified with an asterisk.

The uncertainties in the >149 mass group and ^{135}Xe are due primarily to uncertainty in the yields of Sm and Cs, respectively, relative to Nd. For ^{103}Rh the yield is based on limited radiometric data.

These are the three major sources of uncertainty. Of somewhat less importance are the uncertainties ($\sim$10%) in the ^{147}Pm and ^{131}Xe cross sections. In the case of ^{143}Nd, the last entry, the cross section is already known to $\pm$ 3%, so that a major effort would be required to reduce this uncertainty significantly.

In addition to the uncertainties in the Cs and Sm yields there are large differences in mass spectrometric measurements of the ^{138}Ba yields for both ^{239}Pu (15%) and ^{241}Pu (7.5%)[1]. Nor can the ^{241}Pu yields be considered satisfactory for many other masses. There is only one set of mass spectrometric measurements for the light masses [4]. These do not include Mo, which covers the light mass peak, and the Ru yields were determined radiometrically relative to ^{137}Cs. Also there are only three radiometric measurements covering the mass range from 107 to 130 so that there is considerable uncertainty in the final normalization of mass spectrometric data.

What is required to minimize the remaining uncertainties is a two-pronged assault using mass spectrometric methods to improve ^{235}U yields and radiometric measurements of yields of ^{233}U, ^{239}Pu and ^{241}Pu relative to those of ^{235}U.

Mass Spectrometer Measurements

Since the main source of uncertainty in mass spectrometric determinations of Cs, Ba and Sm yields appears to be systematic differences in the isotope dilution method, a more promising approach is to use isobaric coupling. Since this is a method used previously by Farrar and Tomlinson [14] for ^{235}U yields, I am, therefore, suggesting an independent check of their results. If good agreement is obtained I feel these results should be used in preference to those obtained by isotope dilution.

The links to be used are shown in Figure 1(a), namely ^{137}Cs-^{137}Ba, ^{140}Ba-^{140}Ce, and ^{147}Nd-^{147}Sm. Because of the long half-life of ^{137}Cs (30 y) an old sample of irradiated ^{235}U would be best for measuring the ^{137}Ba relative abundance.

The short-irradiation Ba measurement to obtain the ^{140}Ba relative abundance should also be used to check whether natural Ba is present since this is a possible explanation of some of the discrepancies observed.

The uncertainty in the mass 103 yield from ^{235}U fission is due to a lack of any mass spectrometric data, and it should be quite straightforward to determine the relative abundance of 40-d ^{103}Ru as has already been done for thermal fission of ^{239}Pu [15].

Since there has been only one isotope dilution measurement giving the yield of Ru relative to Zr in ^{235}U fission [4], it is unfortunate that there is no convenient isobaric link between Mo and Zr. This is because the two longest-lived fission product isotopes of Mo are 66-h ^{99}Mo and 14.6-m ^{101}Mo. The latter is too short-lived and the former decays to 10^5-y ^{99}Tc which intercepts the link to Ru.

Radiometric Measurements

Assuming that the above recommendations are acted on and are successful in reducing uncertainties in ^{235}U yields, the second prong of the attack is the radiometric measurement of yields of a wide range of radioactive nuclides for other fissile nuclides relative to those in ^{235}U thermal fission.

The measurement of relative yields radiometrically is by no means new. However, in comparing the results of relative radiometric yield measurement with mass spectrometric yields where that is possible, there are enough disagreements to convince me that a significant fraction is frequently lost, from one sample or the other, in extracting a particular element from different fissile samples.

A typical physicist's approach to this difficult problem is simply to leave the fissile sample sealed and use a Ge(Li)

detector to sort out the γ-rays. For those who believe that this approach is incapable of sufficient accuracy I note that it was used successfully as long ago as 1965 to determine the direct yields of ^{135}Xe in thermal fission of ^{233}U, ^{235}U, ^{239}Pu and ^{241}Pu [12].

Figure 2 is a composite of figures from that paper and shows the separation and accuracy achievable with a resolution of only 3.4 keV (FWHM) at 250 keV. With the resolutions now available, and improved electronics, ratios of 1-2 percent accuracy should be possible, especially using higher energy γ-rays and somewhat longer lifetimes.

The purpose of these measurements would be to check the mass spectrometrically determined relative element yields at many points in both light and heavy mass peaks with the main emphasis on resolving the discrepancies discussed.

Table V lists some of the nuclides with half-lives (generally >1 day) and γ-ray yields suitable for these measurements. In the light mass range the usual reference nuclide has been ^{99}Mo but ^{91}Sr is preferable for these measurements because it is an isobar of ^{91}Zr, and Zr has been measured mass spectrometrically for all four fissile nuclides and has been used as the normalizing element in [1].

In the heavy mass range ^{140}Ba is the usual reference standard and has considerable merit since it can be tied to the Ce yields through ^{140}Ce. However, the Ce yields are less accurate than the Nd yields, and ^{143}Ce would be a better choice.

Outside the mass spectrometer mass range (83 to 106 and 131 to 154) most of the yields are small and chemical separation will be necessary because in a sealed container their γ-rays would almost certainly be submerged in background radiation.

Reporting of Results

To conclude, I would like to make a plea for full documentation of irradiation conditions, elapsed times, correction factors and assumed constants in presenting yield data in order to make life easier for future evaluators, and, incidentally, to ensure that the results will not be discarded.

Many of the early measurements have not been used because of lack of information on corrections. A statement that the yield has been corrected "for decay of 282-day ^{144}Ce" is not much use many years later when the half-life has changed to 284.4 days.

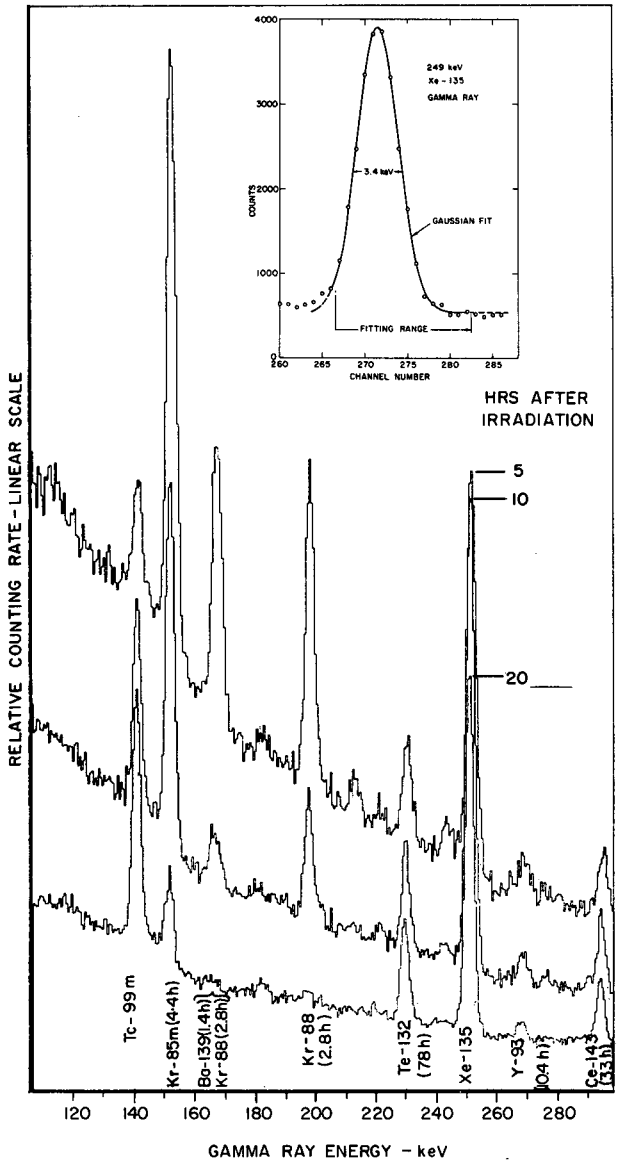

FIG. 2. Fission product γ-rays from irradiated ^{233}U at 5, 10 and 20 hours after the end of the irradiation. Inset: Gaussian fit to ^{135}Xe γ-ray.

TABLE V. NUCLIDES FOR RADIOMETRIC MEASUREMENT WITH Ge(Li) DETECTORS

Nuclide	Half-life	Main γ-rays with energies in keV and yields in γ's per 100 decays (in brackets) *
^{91}Sr	9.67 h	551(72), 645(14), 748(29), 1025(30), 1413(7)
^{93}Y	10.2 h	267(5)
^{95}Zr	65.5 d	724(44), 757(54)
^{95}Nb	35.1 d	765(100)
^{99}Mo	2.78 d	750(14); 149(90)
^{103}Ru	39.8 d	497(89), 610(5)
^{106}Ru	1.01 y	nil; 512(21), 622(10)
^{131}I	8.07 d	364(82)
^{132}Te	3.25 d	50(13.9), 228(85); 523(17), 630(14), 668(101), 773(78), 955(19)
^{133}I	21 h	530(89)
^{133m}Xe	2.26 d	233(14)
^{133}Xe	5.27 d	81(37)
^{137}Cs	30.2 y	662(85)
^{140}Ba	12.8 d	537(24); 328(24), 816(26), 1597(110), 2522(4)
^{141}Ce	32.5 d	145(49)
^{143}Ce	1.38 d	57(12), 293(40), 668(6), 725(7)
^{144}Ce	284.4d	134(11); 696(1.5), 2186(0.7)
^{147}Nd	11.06d	91(30), 531(13)
^{149}Pm	2.21 d	286(3)
^{151}Pm	1.18 d	340(23)
^{153}Sm	1.95 d	69(6), 103(32)

Semicolons separate the direct γ-rays from those of short-lived daughters that are in equilibrium with the parent.

* Values in original table were corrected after the meeting. The data shown is taken from M. J. Martin and P. B. Blichert-Toft (Radioactive atoms, Auger-electron, α-, β-, γ-, and x-ray data, Nuclear Data Tables 8 (1970)1) supplemented by C. M. Lederer, J. M. Hollander and I. Perlman ("Tables of Isotopes", 6th ed. (1967) Wylie and Sons).

On the other hand some early mass spectrometer measurements of Sm relative abundances ignored the hold-up in 11-d ^{147}Nd and used an out-of-date half-life for 2.62-y ^{147}Pm. However, because the irradiation and cooling periods were specified, corrections of 2.4% to 8% were made which brought the apparently discrepant results into excellent agreement.

REFERENCES*

[1] Walker, W. H., Fission product data for thermal reactors, AECL-3037, Part II - Yields, (1973).

[2] Walker, W. H., The evaluation of fission product yields, Proceedings of the second IAEA conference on Nuclear Data for Reactors, 1 (1970).

[3] Meek, M. E., and Rider, B. F., Compilation of fission product yields, Vallecitos Nuclear Center - 1972 NEDO-12154 (1972).

[4] Lisman, F. L., Abernathy, R. M., Maeck, W. J., Rein, J. E., Fission yields of over 40 stable and long-lived fission products for thermal neutron fissioned ^{233}U, ^{235}U, ^{239}Pu and ^{241}Pu, and fast reactor fissioned ^{235}U and ^{239}Pu, Nucl. Sci. Engng 42 (1970) 191.

[5] Steinberg, E. P., Glendenin, L. E., Survey of radiochemical studies of the fission products, Proceedings of the First Geneva Conference on Peaceful Uses of Atomic Energy 7 (1955) 3.

[6] Westcott, C. H., Walker, W. H., Alexander, T. K., Effective cross sections and cadmium ratios for the neutron spectra of thermal reactors, Proceedings of the Second Geneva Conference on Peaceful Uses of Atomic Energy 16, 70 (1958).

[7] Walker, W. H., Fission product data for thermal reactors, AECL-3037 Part I - Cross Sections (1972 revision).

[8] Milgram, M., The revision includes the production and removal of 45 fission products and additional heavy elements from Th to Cf.

[9] Phillips, G. J., Griffiths, J., LATREP users manual, AECL-3857, (1971).

[10] Lane, F., FISSPROD, a G-20 computer program, AECL-3038 (1969).

*AECL-XXXX: Report published by Atomic Energy of Canada Limited.

[11] Hawkings, R. C., Edwards, W. J., Olmstead, W. J., Independent yields of mass 135 xenons in the thermal neutron fission of ^{233}U, ^{235}U, ^{239}Pu and ^{241}Pu, Can. J. Phys. 49 (1971) 785.

[12] Okazaki, A., Walker, W. H., Bigham, C. B., The ratio of the direct to the cumulative yield of ^{135}Xe in the thermal neutron fission of ^{233}U, ^{235}U, ^{239}Pu and ^{241}Pu, Can. J. Phys. 44 (1966) 237.

[13] Walker, W. H., Fission product absorption in thermal reactors, Proceedings of the First IAEA Conference on Nuclear Data for Reactors 1 (1966) 521.

[14] Farrar, H., Tomlinson, R. H., Cumulative yields of heavy fragments in ^{235}U thermal neutron fission, Nucl. Phys. 34 (1962) 367.

[15] Fickel, H. R., Tomlinson, R. H., The cumulative fission yields of light mass fragments in the thermal neutron fission of ^{239}Pu, Can. J. Phys. 37 (1959) 916.

DISCUSSION

W. F. STUBBINS: Which fissioning isotopes have been adequately analysed, i. e. to the extent that the fragment spectra are known well enough to permit their use in calculations?

W. H. WALKER: Of the four fissile nuclides covered in my evaluation, the yields are generally well measured over the main part of the light and heavy mass peaks, i. e. by mass spectrometry. This is not the case for the light mass peak in ^{241}Pu fission and in the valley between the light and heavy peak there are only three radiometric yields. The result is that about 40% of the yield of the light mass peak is interpolated. The effect on calculations of fission product absorption is not very great (in thermal reactors) because most absorption is by the heavy meass fission products.

J. BLACHOT: I am in agreement with the view expressed in your paper that Ge/Li gamma spectrometry can in certain cases supplement mass spectrometric measurements. This method has two main advantages: (1) the possibility of normalization of results between heavy and light masses; (2) the sensitivity of the method, which requires a lower fission rate and therefore eliminates correction due to captures.

BIBLIOTHEQUE DE DONNEES RELATIVES AUX PRODUITS DE FISSION

C. DEVILLERS*, J. BLACHOT**, M. LOTT*,
B. NIMAL*, N'GUYEN VAN DAT*, J.P. NOEL*
Commissariat à l'énergie atomique

R. DE TOURREIL
Institut de physique théorique, Orsay,
France

Abstract-Résumé

FILE OF DATA RELATED TO FISSION PRODUCTS.

The authors describe the data necessary for calculating the concentrations and the β and γ activities of fission products. The file, which is based on the ENDF/B format, results from compilation and evaluation of the available data. It contains: the fission yields for the most common fissions; isobar chain schemes; the transition probability tables and the gamma spectra. The main work of compilation and evaluation relates to the decay schemes, for which the data, grouped for 622 isotopes (^{71}Zn to ^{170}Yb) are as follows: the period; Q_β (β transition energy) and the internal transition energy in the case of isomerism; the β transition probabilities and their energy; the relative or absolute gamma ray intensities and their energy; the references. The authors present residual power measurements which provide overall confirmation of the assembled body of data.

BIBLIOTHEQUE DE DONNEES RELATIVES AUX PRODUITS DE FISSION.

On décrit une compilation de l'ensemble des données nécessaires au calcul des concentrations et de l'activité β et γ des produits de fission. Cette bibliothèque, bâtie sur le format ENDF/B, résulte d'une compilation et d'une évaluation des données disponibles. Elle contient: les rendements de fission pour les fissions les plus courantes; les schémas des chaînes isobares; les tables de probabilités de transition et les spectres gamma. Le principal travail de compilation et d'évaluation porte sur les schémas de désintégration pour lesquels les données regroupées sur 622 isotopes (^{71}Zn à ^{170}Yb) sont les suivantes: la période; le Q_β (énergie de désintégration β), l'énergie de transition interne dans le cas d'isomérie; les probabilités de transition bêta et leur énergie; les intensités relatives ou absolues des raies gamma et leur énergie; les références. On présente des mesures de puissance résiduelle qui valident globalement l'ensemble des données retenues.

1 - INTRODUCTION -

Ce papier présente le format et le contenu de la bibliothèque de données sur les produits de fission qui a été développée pour permettre de calculer de façon théorique la concentration, l'activité et l'énergie dégagée par les produits de fission dans un combustible.

2 - APPLICATIONS DES CONSTANTES NUCLEAIRES SUR LES PRODUITS DE FISSION -

Des calculs de puissance résiduelle d'éléments combustibles de compositions diverses soumis à des régimes de fonctionnement variés

---

* Centre d'études nucléaires de Fontenay-aux-Roses.
** Centre d'études nucléaires de Grenoble.

sont en effet nécessaires pour déterminer le mode de refroidissement de ce combustible dans une gamme de temps de décroissance de l'ordre de la seconde à plusieurs années :

- problèmes de sûreté en cas de dépressurisation ou de défaut de refroidissement dans un coeur,

- problème du déchargement et du stockage du combustible,

- problème du transport et du retraitement.

Pour déterminer de façon précise la distribution des sources de chaleur dans le combustible et son environnement, il faut connaître également comment se répartit, en fonction du temps de décroissance, l'énergie émise, entre rayonnement bêta et rayonnement gamma, ainsi que le spectre des gamma émis.

Le spectre gamma permet en outre de calculer la protection des containers de transport.

Il est très important également, pour des problèmes de protection radiologique, de savoir calculer, dans un réacteur en fonctionnement, l'évolution de la concentration des produits de fission :

- pour prévoir les conséquences radiologiques d'un accident entraînant la libération des produits de fission,

- pour évaluer la contamination du circuit de refroidissement par les produits de fission qui traversent les gaines défectueuses.

Le développement de la production d'énergie nucléaire entraîne dans un autre domaine des études de prévision des quantités de produits de fission produites dans les différents types de réacteur en vue du conditionnement des déchets des usines de retraitement.

L'ensemble de ces questions joue un rôle important dans la sûreté, l'exploitation et l'économie des réacteurs.

Notons enfin le domaine d'application très vaste de l'analyse des produits de fission, en particulier par spectrométrie gamma (Ge/Li), pour l'étude des combustibles irradiés.

Pour répondre à cette gamme très large de problèmes, il était nécessaire d'une part de constituer une bibliothèque de données aussi complète que possible et d'autre part de développer des codes permettant de calculer la concentration et l'activité des produits de fission ainsi que l'énergie émise sous forme de bêta et de gamma par ces produits de fission (1, 2, 3).

Les premières éditions de la bibliothèque (4, 5, 6) ont été constituées en rassemblant les données mesurées ou évaluées, souvent éparses, publiées dans la littérature.

La quantité croissante de résultats nouveaux publiés, du fait de l'amélioration des techniques de mesure, nous a conduit à mettre au point une procédure de stockage et de mise à jour des données sur bande magnétique.

Le format choisi pour enregistrer ces données est celui de la bibliothèque ENDF (7), il est décrit dans le paragraphe 3.

3 - TYPES DE DONNEES -

La bibliothèque comprend essentiellement trois catégories de données :

- rendements indépendants de fission
- périodes, modes de filiation (désintégration, capture), énergies de désintégration, rapports de branchement
- données sur les spectres des rayonnements émis par désintégration.

Le contenu actuel de la bibliothèque comprend 622 produits de fission de masses comprises entre 71 et 170.

Les rendements de fission sont introduits pour trois noyaux fissiles :

U^{235} : fission thermique
fission rapide ($E \sim 1$ MeV)

U^{238} : fission rapide (E $\sim$ 1 MeV)

Pu^{239} : fission thermique
fission rapide (E $\sim$ 1 MeV)

3.1. Rendements indépendants de fission

Plusieurs compilations de rendements de fission ont déjà été publiées (10, 11) et nous avons choisi celle de MEEK et RIDER (8) qui nous a semblé la plus complète et la plus récente. Cette évaluation présente de plus la bibliographie de toutes les mesures effectuées depuis 1940, classées chronologiquement et indexées par noyau. Ces informations permettraient, si besoin était, de réévaluer certains rendements, par exemple en se basant sur l'étude de WALKER (9).

Dans la présente version de la bibliothèque, les rendements indépendants sont calculés par la formule :

$$Y(Z,A) = Y(A) \frac{1}{\sqrt{2\pi}\,\sigma(A)} \int_{Z-0,5}^{Z+0,5} \exp\left\{ - \frac{[Z'-Zp(A)]^2}{2\,\sigma^2(A)} \right\} dZ'$$

avec :

Y (A) : valeur recommandée du rendement de fission de la chaîne A

Zp (A) : valeur la plus probable de la charge des produits de fission de la chaîne A

σ(A) : paramètre de la distribution gaussienne.

Pour chaque chaîne de masse A, les rendements indépendants sont déterminés pour des charges variant de Z_{mini}(A) à Z_{max} (A), avec la condition de normalisation suivante :

$$Y(Z_{mini}, A) = Y(A) - \sum_{Z=Z_{mini}(A)+1}^{Z_{max}(A)} Y(Z, A)$$

En cas d'isomérie, les rendements indépendants calculés sont en général divisés également entre les isomères.

Le format ENDF permet d'introduire plusieurs jeux de rendements indépendants suivant l'énergie des neutrons produisant la fission.

Les rendements indépendants de fission ont été calculés ; pour la fission thermique ($E \sim 0$) et rapide ($E \sim 1$ MeV) pour U^{235} et Pu^{239}, pour la fission rapide ($E \sim 1$ MeV) dans le cas de U^{238}. Le mode d'interpolation proposé pour des fissions se produisant entre 0 et 1 MeV est le mode linéaire, en l'absence d'autre information.

3.2. Périodes et modes de filiation -

Contrairement aux rendements de fission, la littérature relative aux données radioactives est très abondante. La Table des Isotopes de LEDERER et al (12) est un document très complet mais il ne tient compte que des travaux publiés avant 1967 ; or le développement des détecteurs à germanium-lithium a permis depuis cette date des progrès très importants dans la connaissance des schémas de décroissance.

Les Nuclear Data Sheets (13) ont depuis 1966 publié huit volumes de données révisées. Ces publications comportent de plus des listes de références récentes indexées par masse qui permettent d'effectuer soi-même la révision des données (6). Les valeurs des énergies de désintégration qui n'ont pas été mesurées ont été tirées de l'évaluation de WAPSTRA et al.(15).

Le choix des données reportées dans la bibliothèque est coordonné par le laboratoire de Chimie Nucléaire du Centre de Grenoble sur la base de la nouveauté, de la qualité des techniques expérimentales et à l'aide de mesures expérimentales de contrôle (14).

La bibliothèque contient les références de toutes les valeurs numériques sélectionnées.

Un effort important reste à faire pour améliorer la connaissance des produits de fission de période inférieure à une heure et des intensités absolues des raies gamma.

Les modes de désintégration pris en compte dans la bibliothèque sont indiqués dans le tableau I.

TABLEAU I. FILIATIONS PAR DESINTEGRATION

Noyau père	Noyau fils	Energie de désintégration	Rayonnement émis
A, Z	A,Z + 1	QBF^-	β^-, γ
	A,Z - 1	QBF^+	β^+, γ
	A,Z + 1^m	QBM^-	β^-, γ
	A,Z - 1^m	QBM^+	β^+, γ
	A-1, Z + 1	QBF^-	β^-, γ, neutron
	A-4, Z - 2	EALPHA	α, γ
A, Z^m	A, Z	EIT	γ
	A,Z + 1	QBF^-	β^-, γ
	A,Z - 1	QBF^+	β^+, γ
	A,Z + 1^m	QBM^-	β^-, γ
	A,Z - 1^m	QBM^+	β^-, γ

Le format ENFB permet également d'introduire les filiations par capture neutronique comme l'indique le tableau II.

TABLEAU II. FILIATIONS PAR CAPTURE NEUTRONIQUE

Noyau père	Noyau fils	Energie de réaction
A, Z	A + 1, Z	Q F
	A + 1, Z^m	Q M
A, Z^m	A + 1, Z	Q F
	A + 1, Z^m	Q M

Les rapports de branchement pour les captures neutroniques conduisant à plusieurs isomères ont été tirés du BNL 325 (16).

Aucune évaluation relative aux sections efficaces différentielles de capture n'a été reportée dans la bibliothèque : leur place est prévue dans le format ENDF/B, à l'exclusion de toute donnée intégrale.

Les données intégrales, en l'absence de données différentielles suffisamment complètes ou détaillées sont introduites au niveau des programmes d'utilisation de la bibliothèque.

3.3. Spectres des rayonnements bêta et gamma émis par désintégration -

Au format ENDF/B nous avons ajouté la possibilité d'introduire, pour les produits de fission instables, d'une part des tables de probabilité de transition bêta et d'autre part des tables de spectre gamma (multiplicités).

Compte tenu du niveau inégal de connaissance de ces données suivant les nuclides considérés, on trouvera dans la bibliothèque quatre situations possibles schématisées comme suit :

Probabilités de transition bêta	Spectre gamma
non	non
non	oui
oui	non
oui	oui

L'énergie totale de désintégration est cependant supposée connue pour tous les nuclides instables.

Lorsque plusieurs modes de désintégration sont en compétition, par exemple, émission β^- et β^+, les tables introduites sont la résultante des probabilités ou spectres des divers modes.

Une table de probabilités de transitions bêta se présente sous la forme d'une suite de couples de valeurs : énergie de transition - probabilité, correspondant à chaque transition. Les probabilités sont normalisées à 100 en l'absence de transition interne, à 100-XEIT dans le cas d'une transition interne de probabilité XEIT. L'énergie d'une transition est aussi l'énergie maximale du spectre bêta émis lors de cette transition.

Une table de spectre gamma est constituée d'une suite de couples de valeurs : énergie de raie-intensité, correspondant à l'ensemble des raies dénombrées. Les intensités peuvent être données en valeurs relatives, avec la valeur 100 pour la raie la plus intense, ou bien en valeurs absolues, normalisées à 100 désintégrations.

4 - FORMAT DE LA BIBLIOTHEQUE -

Le format choisi est celui de la bibliothèque ENDF (7) auquel quelques additions ont été faites pour introduire les tables de probabilités de transition β et les spectres γ.

La structure générale d'une bande ENDF est schématisée à la figure 1. Dans la bibliothèque des produits de fission, chaque matériau ne comporte qu'une seule file (MF = 1).

Un matériau est identifié par son numéro MAT et parallèlement par l'indice ZAP = 1000 Z + A auquel il faut adjoindre un indice de niveau d'excitation. Des isomères sont considérés comme des noyaux indépendants.

Chaque matériau comporte une section d'information (MT = 451) comprenant :

- des indices annonçant les sections introduites dans la suite et permettant aussi de différencier les matériaux fissiles des produits de fission,

- des cartes commentaires comportant notamment les références des données,

- un dictionnaire indiquant le nombre de cartes contenues dans chaque section.

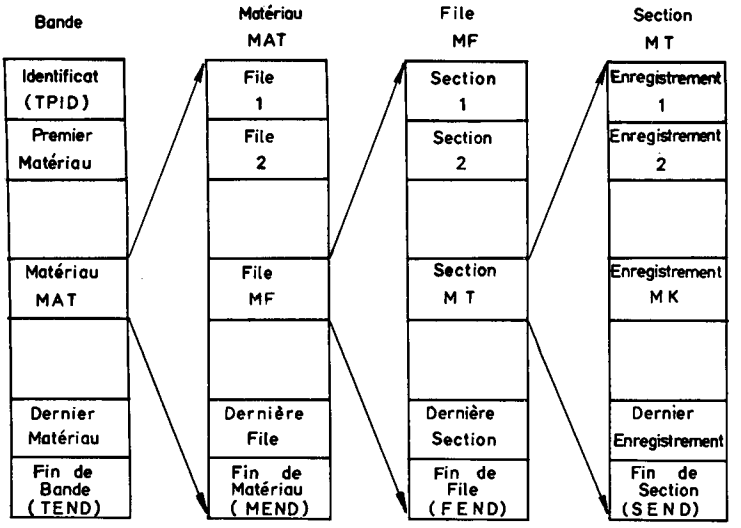

FIG.1. Structure générale d'une bande ENDF.

Les matériaux fissiles comportent, en plus de la section MT=451 :

- une section MT = 452 donnant le nombre de neutrons par fission $\bar{\nu}(E)$ (section obligatoire),

- une section MT = 454 donnant les rendements indépendants de fission (section facultative dans le format officiel ENDF).

La section MT = 454 peut contenir un ou plusieurs jeux de rendements, fonction ou non de l'énergie.

Chaque noyau produit par fission est caractérisé par :

- ZAFP : indice égal à 1000 Z + A

- un indice d'état :0 :fondamental ; 1 : 1er état excité....

- le rendement indépendant de fission à l'énergie considérée.

La somme des rendements est égale à 2.

Les produits de fission peuvent comporter les sections suivantes :

-Section MT = 453 : elle contient les données relatives aux divers modes de filiation par désintégration ou réaction neutronique (ou autre), en particulier, pour un noyau cible d'état donné (0 : fondamental ; 1 : 1er état excité ; etc....) :

-le nombre de noyaux fils produits (2 états d'excitation du même noyau sont considérés comme deux noyaux fils indépendants)

-pour chaque noyau fils produit :

- l'énergie de la réaction ou de la désintégration conduisant à ce noyau
- l'état du noyau produit (0,1....)
- le type de réaction :

  0.0. pour une désintégration spontanée quelle qu'elle soit

  MT pour une réaction neutronique
  (MT = 102 pour une capture radiative)

- le ZAP = 1000.Z + A du noyau produit
- la constante de désintégration, partielle pour le mode de désintégration considéré conduisant à l'état particulier du noyau fils considéré (0. dans le cas d'une réaction provoquée)
- les rapports de branchement pour la réaction considérée. Les rapports de branchement sont normés à 1 pour chaque type de réaction.

- Les deux sections suivantes (MT = 456, MT = 459) ne figurent pas dans le format officiel ENDF et ont été créées pour les besoins particuliers de notre bibliothèque de produits de fission.

- Section MT = 456 : elle contient la table des probabilités des transitions bêta résultant de l'ensemble des modes de désintégration du matériau.

- Section MT = 459 : elle contient le spectre des raies gamma résultant de l'ensemble des modes de désintégration du matériau.

Un indice permet de spécifier si le spectre est fourni en valeur relative ou absolue. Dans le premier cas, il est normalisé à la valeur 100 pour la raie la plus intense. Dans le second cas, les intensités correspondent à 100 désintégrations du matériau.

L'arrangement détaillé des données de chaque section est reporté dans l'annexe 1.

Les éléments nouveaux par rapport au format officiel ENDF sont repérés par un astérisque.

5 - APPLICATION DE LA BIBLIOTHEQUE AUX CALCULS DE PUISSANCE RESIDUELLE -

Le diagramme représenté à la figure 2 montre la procédure de gestion et d'exploitation de la bibliothèque des produits de fission pour les calculs d'évolution et d'activité des produits de fission et les calculs de puissance résiduelle.

5.1. Retraitement de la bibliothèque ENDF

La bibliothèque ENDF est retraitée par un programme qui aboutit à une bibliothèque élaborée après avoir effectué les opérations suivantes :

- établissement des chaînes de filiation à partir des données de la section 453 (types de réaction, constantes de désintégration, rapports de branchement) et de sections efficaces effectives de capture fournies par l'utilisateur

- calcul par le modèle de FERMI (17) des énergies moyennes des bêta et des neutrinos émis pour chaque transition bêta,lorsque la table des probabilités de transition est fournie. Calcul de l'énergie totale émise sous forme de bêta (EBM) et de neutrino (ENUM) pour une désintégration du noyau incluant tous les modes de désintégration possibles.

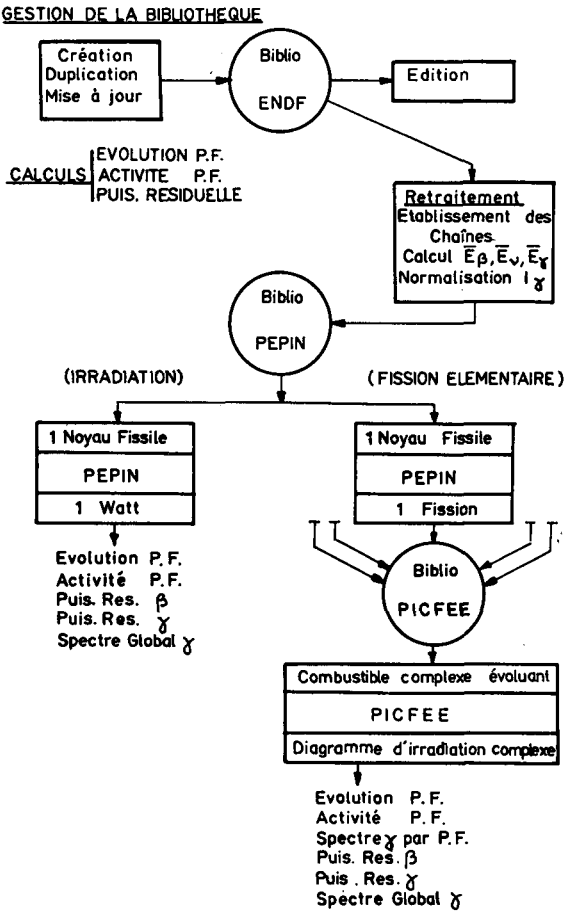

FIG.2. Gestion et application de la bibliothèque.

Calcul de l'énergie totale gamma émise (EGM) par l'expression :

$$EGM = \overline{EREL} - EBM - ENUM$$

où $\overline{EREL}$ est l'énergie totale libérée par une désintégration du noyau incluant tous les modes de désintégration possibles.

Lorsque la table des probabilités de transition n'est pas connue, les quantités EBM et ENUM sont introduites par l'utilisateur.

Dans le cas d'une transition interne, l'énergie apparaît uniquement sous forme de gamma.

Lorsque le spectre des gamma est connu, en valeur relative ou en valeur absolue, le programme renormalise les intensités des raies de manière que l'énergie totale gamma soit égale à EGM.

Les approximations faites portent sur les points suivants :

- le modèle de FERMI utilisé dans le calcul de l'énergie moyenne des bêta ne tient pas bien compte des transitions interdites. Un calcul pour l'ytrium-91 montre que le modèle de FERMI sousestime l'énergie moyenne des bêta de 4 %.

- dans son état actuel la bibliothèque ne distingue pas la désintégration β^+ et la capture électronique.

L'énergie totale correspondant à une désintégration où il y a compétition β^+, C.E. est égale à la différence des masses entre noyau père et noyau fils. Dans le cas d'une désintégration β^+ il y aurait lieu d'ajouter l'énergie apparaissant lors de l'annihilation du positon (1,02 MeV), le calcul de l'énergie totale émise est donc minorant.

Dans le cas d'une capture électronique au contraire, l'énergie est emportée presque totalement par le neutrino, le calcul de l'énergie totale bêta est donc majorant.

Cette approximation ne doit pas introduire d'erreur appréciable dans les calculs de puissance résiduelle étant donné les rendements faibles des produits de fission émetteurs β^+ ou C.E.

Au contraire, il est important d'améliorer le calcul de l'énergie moyenne bêta des émetteurs β^-.

L'amélioration des connaissances des énergies et probabilités de transition β^- et des énergies et intensités des spectres gamma, notamment pour les corps de période courte ($T < 1000$ sec.) est évidemment souhaitable.

TABLEAU III. ENERGIE LIBEREE APRES UNE FISSION THERMIQUE DE L'URANIUM-235

Temps de décroissance (sec)	Energie bêta (MeV/s)			Energie gamma (MeV/s)		
	1) Présent calcul	2) BATTAT et al.[20]	Rapport (1/2)	1) Présent calcul	2) BATTAT et al.[20]	Rapport (1/2)
10^1	$7,29 \cdot 10^{-2}$	$2,18 \cdot 10^{-2}$	3,34	$5,52 \cdot 10^{-2}$	$7,36 \cdot 10^{-3}$	7,5
10^2	$7,17 \cdot 10^{-3}$	$5,13 \cdot 10^{-3}$	1,40	$6,11 \cdot 10^{-3}$	$4,93 \cdot 10^{-3}$	1,24
10^3	$4,44 \cdot 10^{-4}$	$4,20 \cdot 10^{-4}$	1,06	$4,70 \cdot 10^{-4}$	$4,47 \cdot 10^{-4}$	1,05
10^4	$2,44 \cdot 10^{-5}$	$2,68 \cdot 10^{-5}$	0,91	$3,34 \cdot 10^{-5}$	$3,16 \cdot 10^{-5}$	1,06
10^5	$1,22 \cdot 10^{-6}$	$1,19 \cdot 10^{-6}$	1,03	$1,38 \cdot 10^{-6}$	$1,39 \cdot 10^{-6}$	0,99
10^6	$5,43 \cdot 10^{-8}$	$5,47 \cdot 10^{-8}$	0,99	$1,03 \cdot 10^{-7}$	$1,11 \cdot 10^{-7}$	0,93
10^7	$4,56 \cdot 10^{-9}$	$4,60 \cdot 10^{-9}$	0,99	$5,09 \cdot 10^{-9}$	$5,01 \cdot 10^{-9}$	1,02
10^8	$1,91 \cdot 10^{-10}$	$1,94 \cdot 10^{-10}$	0,98	$3,40 \cdot 10^{-11}$	$3,36 \cdot 10^{-11}$	1,01
10^9	$2,65 \cdot 10^{-11}$	$2,65 \cdot 10^{-11}$	1,00	$1,35 \cdot 10^{-11}$	$1,30 \cdot 10^{-11}$	1,04

5.2. Calcul de la puissance résiduelle pour une fission thermique de l'uranium-235

Le programme PEPIN (1) résout les équations différentielles gouvernant l'évolution des produits de fission soit avec une source continue correspondant à une irradiation constante de 1 watt de durée quelconque d'un échantillon constitué d'un seul nuclide fissile, soit dans le cas d'une source instantanée de produits de fission créée par une fission d'un nuclide fissile donné.

Il fournit dans les deux cas pour divers temps de décroissance l'évolution des produits de fission, de leur activité et de l'énergie libérée sous forme de bêta et de gamma par l'ensemble des produits de fission.

Les résultats d'un calcul de puissance résiduelle pour une fission thermique de l'uranium-235 sont présentés ici.

De nombreux calculs similaires ont été publiés dans la littérature (18-21) qui se distinguent par la rigueur du traitement numérique ou le caractère plus ou moins complet (nombre de produits de fission) ou plus ou moins récent des données.

Dans le tableau III nous présentons la comparaison entre notre calcul et le calcul de BATTAT et al. (20) pour des temps de décroissance variant de 10 à 10^9 secondes.

On notera pour les temps inférieurs à 1000 secondes l'augmentation résultant de l'introduction dans notre calcul de produits de fission de période courte alors que BATTAT et al. ne considèrent que des nuclides de période supérieure à 10 secondes. Au-delà de 1000 secondes, l'accord est satisfaisant, à mieux de 5 % près.

Les calculs PEPIN ont été comparés à une mesure calorimétrique effectuée à Fontenay-aux-Roses (22) sur un échantillon d'uranium-235 irradié en neutrons thermiques pendant 100, 1000, 5000, 10^5 et 6.10^5 secondes.

Une courbe de décroissance de la puissance résiduelle a été ajustée sur l'ensemble des mesures, corrigées des fuites d'énergie γ.

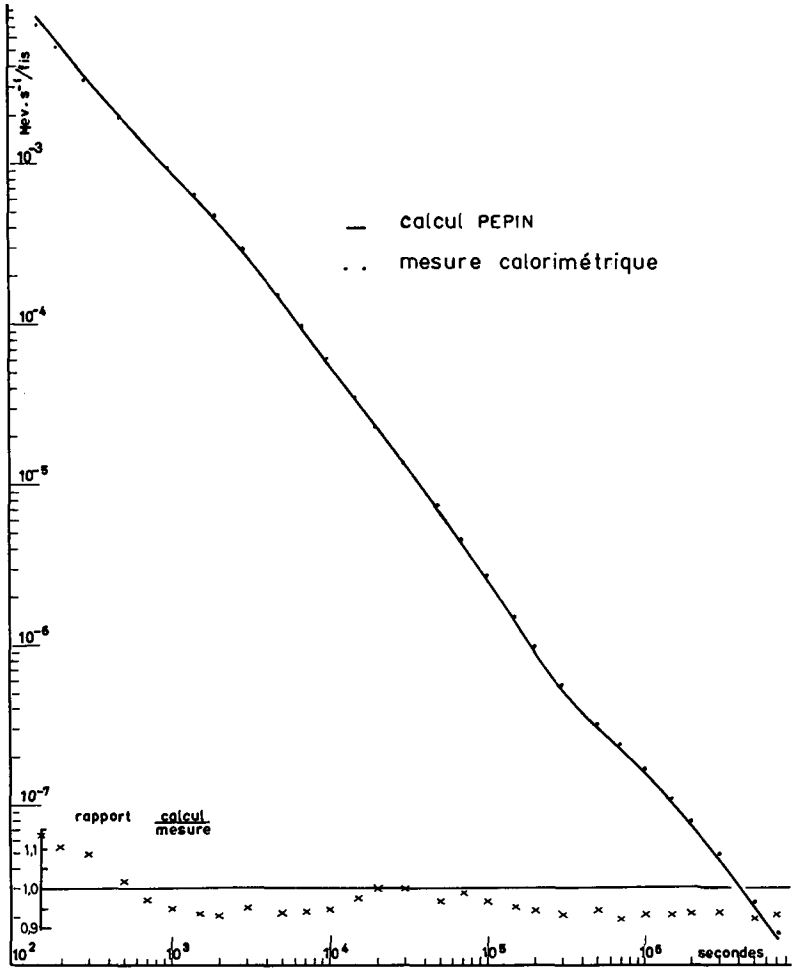

FIG.3. Décroissance de l'énergie libérée par les produits de fission thermique de l'uranium-235 (1 fission instantanée).

La comparaison entre le calcul et la mesure est reportée à la figure 3. De 100 à 600 secondes, le calcul est supérieur de 18 à 0 % à la mesure, de 600 à 7.10^6 secondes il est inférieur de 0 à 7 %. Le dépouillement d'autres mesures correspondant à des temps d'irradiation de 10 et 50 secondes respectivement permettront de recouper les points expérimentaux vers 100 secondes.

La précision annoncée de la mesure est ± 5 %. Le nombre de fissions intégrées par l'échantillon est mesuré par comptage de Ba-La 140 et recoupement par comptage de Cs 137.

L'écart entre le calcul et la mesure au-delà de 1000 secondes est donc significatif et quasi systèmatique. Il ne peut être imputé au traitement numérique des équations étant donné le bon accord de notre calcul avec celui de BATTAT et al. au-delà de 10^4 secondes ; il est à affecter soit aux données nucléaires et à leur traitement, soit à la mesure.

5.3. Calcul de la puissance résiduelle du combustible d'un réacteur à neutrons rapides

Dans le cas d'un combustible complexe constitué d'un mélange de nuclides fissiles en évolution et soumis à une irradiation irrégulière, le programme PICFEE (2-3) permet de calculer l'évolution des produits de fission, de leur activité, de leur spectre gamma et de la puissance résiduelle après l'arrêt du réacteur.

Le programme calcule l'évolution du combustible au cours de l'irradiation à partir de sections efficaces effectives, variables en fonction du temps, qui sont fournies par l'utilisateur. Il intègre ensuite les courbes correspondant à une fission élémentaire, fournies par le code PEPIN respectivement pour U235, U238 et Pu239, après avoir effectué les interpolations nécessaires pour tenir compte de l'énergie moyenne des neutrons provoquant les fissions.

Des comparaisons ont été faites entre des calculs de puissance résiduelle effectués par le code PICFEE et des mesures calorimétriques réalisées sur des aiguilles combustibles irradiées dans RAPSODIE à des taux moyens de combustion d'environ 9600, 37000, 47000 et 52000 MWJ par tonne de métal. Les nombres de fissions intégrées par les aiguilles ont été déterminés par mesure du néodyme formé, la précision est de ± 5 %.

Les mesures calorimétriques ont eu lieu après des temps de décroissance longs, de 1 à 4 ans.

Des comparaisons pour des temps de refroidissement plus courts (20 à 80 jours) ont été effectuées par COSTA et al. (23).

TABLEAU IV. PUISSANCE RESIDUELLE D'UN COMBUSTIBLE DE REACTEUR A NEUTRONS RAPIDES

Aiguille	1	2	3	4
Taux de combustion (%)	0,972	3,97	4,825	5,81
Temps d'irradiation *(jours)	257	537	670	553
Temps de décroissance*(jours)	1520	1250	1125	234
Puissance $\beta + \gamma$ calculée (watt)	0,04027	0,2044	0,2671	1,2111
Puissance α calculée (watt)	0,0564	0,0574	0,0574	0,0510
Activité des gaines mesurée (watt)	~0,0006	~0,0035	~0,0050	
Mesure globale (watt)	0,1066	0,2800	0,3356	1,314
Mesure**corrigée (watt)	0,05071	0,2235	0,2784	1,302
Calcul mesure	0,795	0,915	0,960	0,930

* Le temps d'irradiation comprend et le temps de décroissance ne comprend pas un temps de stockage d'environ 90 jours à 2,7 % de la puissance maximale.

** La mesure est corrigée de l'activité α, de l'activité des gaines et des fuites hors du calorimètre.

Les résultats de la présente comparaison sont reportés dans le tableau IV.

Compte tenu de la précision (± 2 %) de la mesure calorimétrique elle-même, de l'incertitude sur le taux de fission (± 5 %) et des corrections importantes effectuées sur les mesures pour soustraire l'énergie résultant de l'activité α, de l'activité résiduelle des gaines et pour tenir compte des fuites gamma, il est possible de conclure que la précision du calcul de puissance résiduelle des produits de fission, meilleure que 10 % sans doute, est suffisante, en particulier pour les problèmes d'ingénierie. Etant donné la complexité de l'analyse de ce type de mesure, il est au contraire improbable d'en tirer les conclusions quant à la nécessité d'améliorer encore la précision des données nucléaires utilisées.

6 - CONCLUSION

La bibliothèque de données nucléaires sur les produits de fission dans le format ENDF constitue un recueil de données cohérent et d'accès commode où l'ingénieur et le physicien peuvent prélever les informations qui leur sont nécessaires.

Le programme PICFEE calcule l'évolution des produits de fission, de leur activité et de l'énergie qu'ils émettent après des irradiations complexes d'échantillons comportant des mélanges de nuclides fissiles évoluant ; il a déjà fait l'objet d'applications très variées allant de la prévision de la composition chimique d'un combustible irradié au calcul des sources de rayonnement déterminant les conditions de manutention des combustibles irradiés.

L'ensemble des données et des programmes a été éprouvé sur certains problèmes dont quelques-uns ont été présentés ici. C'est la précision souhaitée par les utilisateurs dans les diverses applications et la comparaison avec l'expérience qui déterminera l'effort à poursuivre dans la mesure ou l'évaluation des données nucléaires. En ce qui concerne les questions de puissance résiduelle examinées ici, les prévisions théoriques sont correctes à mieux de 10 % près pour des temps de décroissance supérieurs à 200 secondes, et par conséquent on peut estimer que les données nucléaires qui interviennent : rendements, schéma de désintégration, spectres des rayonnements sont suffisamment bien connus. Le perfectionnement du calcul des énergies moyennes des bêta sera néanmoins poursuivi en tenant compte des spectres des transitions permises.

Pour des temps inférieurs, l'amélioration de la connaissance des rendements, schéma de désintégration et spectres de rayonnements des produits de fission de période inférieure à 1000 secondes est encore nécessaire.

Il faut noter que les sections efficaces d'interaction des neutrons (n, γ), (n, n'), (n, p) avec les produits de fission n'ont été considérées en détail ni dans la bibliothèque ni dans les applications mentionnées ici. Leur influence est en effet négligeable pour la majorité des problèmes de puissance résiduelle et d'activité. Le programme PEPIN utilise cependant des sections efficaces de capture effectives fournies par l'utilisateur.

L'introduction dans la bibliothèque des valeurs évaluées disponibles des sections efficaces différentielles de capture des produits de fission permettra de déterminer les sections efficaces effectives dans différents spectres de réacteurs et d'indiquer par des études de sensibilité pour quels isotopes des mesures ou des évaluations sont nécessaires.

ANNEXE 1

ANNEXE 1 (1).

File 1

MT = 451 (Indices et informations générales)

Zone 1	Zone 2	Zone 3	Zone 4	Zone 5	Zone 6	Type d'enregistrement
ZA	AWR	LRP	LFI	b	NXC	HEAD
b	b	LDD	LFP	NWD	NBG *	LIST
Cartes commentaire			n°1 n°2 n° NWD			
b	b	MF1	MT1	NC1	b	CØNT
b	b	MF2	MT2	NC2	b	CØNT
b	b	MF_{NXC}	MT_{NXC}	NC_{NXC}	b	CØNT
b	b	b	b	b	b	SEND

ZA : 1000.Z + A

AWR : masse atomique : rapport de la masse nucléaire du matériau à celle du neutron (masse du neutron : 1.008665 dans le système C12)

LRP : = 0 rien

= 1 des paramètres de résonance sont fournis dans la file 2

LFI : = 0 matériau non fissile

= 1 matériau fissile

NXC : nombre de cartes constituant le dictionnaire : une carte par section comportant :

MF : n° de file

MT : n° de section

NC : nombre de cartes de la section

LDD : = 0 rien

= 1 des données de filiation sont fournies dans la section MT = 453

LFP : = 0 rien

= 1 des rendements de produits de fission sont donnés dans la section MT = 454

NWD : nombre de cartes commentaire

NBG* : = 0 rien

= 1 tables de probabilité de transition bêta dans la section MT = 456

= 2 spectres gamma dans la section MT = 459

= 3 à la fois 1 et 2

ANNEXE 1 (2)

File 1

MT = 452 (nombre total de neutrons par fission)

LNU = 1 représentation polynominale : $\bar{\nu}(E) = \sum_{n=1}^{NC} C_n E^{(n-1)}$

Zone 1	Zone 2	Zone 3	Zone 4	Zone 5	Zone 6	Type d'enregistrement
ZA	AWR	b	LNU=1	b	b	HEAD
b	b	b	b	NC	b	LIST
C1	C2	------	-----	C_{NC}		
b	b	b	b	b	b	SEND

LNU : = 1 représentation polynominale

NC : nombre de termes du développement polynominal

C_n : coefficients du polynome

LNU = 2 valeurs tabulées de $\bar{\nu}$ (E)

ZA	AWR	b	LNU=2	b	b	HEAD
b	b	b	b	NR	NP	TAB 1
NBT (1)	INT (1)	NBT (2)	INT (2)	-----	-------	
------	------	-----	------	NBT (NR)	INT (NR)	
E1	$\bar{\nu}$ (E1)	E2	$\bar{\nu}$(E2)	------	-------	
------	------	-----	------	E_{NP}	$\bar{\nu}(E_{NP})$	
b	b	b	b	b	b	SEND

LNU : = 2 tabulation

NR : nombre de domaines d'interpolation

NP : nombre total de points d'énergie de la tabulation

NBT(I), INT (I) : mode d'interpolation pour $\bar{\nu}$ (E)

$\bar{\nu}(E_i)$: nombre total moyen de neutrons (prompts + retardés) par fission

Ei : énergie (eV)

ANNEXE 1 (3)

File 1

MT = 453 (données de filiation)

Zone 1	Zone 2	Zone 3	Zone 4	Zone 5	Zone 6	Type d'enregistrement
ZA	AWR	b	b	NS	b	HEAD
ZA ES (1)	AWR ES (2)	LIS -------	b ------	NE -------	NPR ES (NE)	LIST 1
$EREL_1$ $RTYP_1$	Q_1 ZAP_1	LFS_1 DC_1	b BR_1 (1)	NE + 3 --------	b BR_1 (NE)	LIST 2
-------	--------	-------				
$EREL_{NPR}$ $RTYP_{NPR}$	Q_{NPR} ZAP_{NPR}	LFS_{NPR} DC_{NPR}	b BR_{NPR} (1)	NE + 3 ------	b BR_{NPR} (NE)	LIST 2
b	b	b	b	b	b	SEND

NS : nombre d'états excités du noyau cible : (NS=1)* dans notre bibliothèque

LIS : état du noyau cible, 0 : fondamental ; 1 : 1er état excité ;
2 : 2ème état excité

NE : nombre d'énergies pour lesquelles sont introduits les rapports de branchement (NE = 2)*

NPR : nombre total de noyaux produits (des isomères sont comptés comme des noyaux indépendants)

ES (1), ES (2) : énergies pour lesquelles sont introduits les rapports de branchement ; pour les désintégrations : (ES (1) = 0 ; ES (2) = 2.10^7 eV)*

EREL : énergie totale libérée par le mode de désintégration considéré (gamma + particules) (eV)

Q : Q de la réaction considérée (eV)

LFS : état du noyau produit : 0, fondamental, 1 ....

RTYP : type de réaction : 0. : désintégration
MT : réaction (p.ex : MT = 102.pour capture radiative)

ZAP : 1000.Z+A du noyau produit

DC : constante de désintégration partielle (sec^{-1}) pour la filiation considérée

BR (1), BR (2) .... : rapports de branchement pour les désintégrations:(BR(1)=BR(2))*

ANNEXE 1 (4)

File 1

MT = 454 (rendements de fission indépendants)

Zone 1	Zone 2	Zone 3	Zone 4	Zone 5	Zone 6	Type d'enregistrement
ZA	AWR	LE + 1	b	b	b	HEAD
E1	b	LE	b	N1	NFP	LIST
$ZAFP_1$	FPS_1	YLD_1	------	------	------	
------	-----	-----	$ZAFP_{NFP}$	FPS_{NFP}	YLD_{NFP}	
EN	b	I_N	b	N1	NFP	LIST
$ZAFP_1$	FPS_1	YLD_1	-----	-----	-----	
------	-----	-----	$ZAFP_{NFP}$	FPS_{NFP}	YLD_{NFP}	
b	b	b	b	b	b	SEND

N1 : = 3 * NFP

NFP : nombre de produits de fission pour lesquels les rendements sont donnés

E_i : énergie des neutrons provoquant la fission (eV)

LE : = 0 : un seul jeu de rendements est donné

> 0 : (LE+1) jeux de rendements sont donnés pour LE + 1 valeurs d'énergie

I_1 : mode d'interpolation utilisé entre les énergies E_{i-1} et E_i (I_1 = 2 linéaire)*

ZAFP, YLD, FPS : pour chaque produit de fission

- 1000.Z+A
- rendement indépendant
- état du noyau produit : 0 fondamental
  1 1er état excité
  2 2ème état excité

ANNEXE 1 (5)

File 1

MT = 456 * (probabilités de transition bêta)

Zone 1	Zone 2	Zone 3	Zone 4	Zone 5	Zone 6	Type d'enregistrement
ZA	AWR	b	b	b	b	HEAD
b	b	b	b	NR = 1	NP	TAB 1
------	-------	b	b	b	b	
ET(1)	PB(1)	-----	-----	ET(NP)	PB (NP)	
b	b	b	b	b	b	SEND

NR : nombre de domaines d'interpolation

NP : nombre de transitions bêta (β^- et β^+ ou capture électronique)

NBT (1), INT (1) : mode d'interpolation (sans objet)

ET (i), PB (i) : énergie (eV) et probabilité de transition

MT = 459 * (spectres gamma)

ZA	AWR	LR	b	b	b	HEAD
b	b	b	b	NR = 1	NG	TAB 1
		b	b	b	b	
EG(1)	XG(1)	--------	------	EG (NG)	XG(NG)	
b	b	b	b	b	b	SEND

NG : nombre de raies γ

LR : = 0 spectre en valeurs relatives

= 1 spectre en valeurs absolues

EG(i), XG(i) : énergie (eV) et intensité du spectre γ total correspondant à l'ensemble des modes de désintégration du matériau.

REFERENCES

(1) R. de TOURREIL, Programme de calcul de l'activité des produits de fission, Note CEA.N.824 (Octobre 1967)

(2) B. BARRE, PICFEE : programme d'intégration de courbes de fissions élémentaires tenant compte de l'évolution des nuclides fissiles, Note CEA.N.1203 (Octobre 1969)

(3) C. DEVILLERS, N'GUYEN VAN DAT, PICFEE 2 : programme de calcul de la concentration et de l'activité des produits de fission et de la puissance résiduelle dans un combustible irradié, rapport SERMA N° 118/S (Janvier 1973)

(4) B. BARRE, R. de TOURREIL : Bibliothèque des activités β et γ des produits de fission, Note CEA.N.1269 (Avril 1970)

(5) B. BARRE, R. de TOURREIL : Bibliothèque de données nucléaires relatives aux produits de fission (2ème version), Note CEA.N.1423 (Mars 1971)

(6) J. BLACHOT, R. de TOURREIL : bibliothèque des données nucléaires relatives aux produits de fission (3ème édition), Note CEA.N.1526 (Mars 1972)

(7) M.K. DRAKE, Data Formats and Procedures for the ENDF Neutron Cross Section Library, BNL 50274, ENDF 102 vol 1 (1970)

(8) M.E. MEEK, B.F. RIDER, Compilation of Fission Product Yields NEDO-12154 (1972)

(9) W. H. WALKER, «The evaluation of fission product yields», Nuclear Data for Reactors (Compt. Rend. Conf., Helsinki, 1970) 1, AIEA, Vienne (1970) 685.

(10) C. MEIXNER, Jül-811, 812, 813 (1971)

(11) A. TOBIAS, RD/B/M 2356 (1972)

(12) C.M. LEDERER, J.M. HOLLANDER, I. PERLMAN, Table of Isotopes (6ème édition) John WILEY, sons (1967)

(13) Nuclear Data Sheets, Academic Press Inc.Volume B1-B8

(14) J. BLACHOT, L.C. CARRAZ, O. MARBACH, Raies gamma émises par quelques krypton et xenon de fission, rapport CEA-R. 4437 (1973)

(15) A.H. WAPSTRA, N.B. GOVE, Nuclear Data Tables, vol.A9, 267 (1971)

(16) BNL 325

(17) B. BARRE, R. de TOURREIL, Energie moyenne émise par les nuclides β^- instables - Note CEA.N.1285 (1970)

(18) J.F. PERKINS, R.W. KING, Nucl.Sci. Engng 3, 726 (1958)

(19) J.F. PERKINS, RR-TR-63-11 (1963)

(20) M.E. BATTAT, D.J. DUDZIAK, H.R. HICKS, LA-3954 (1968)

(21) J. SCOBIE, R.D. SCOTT, Jl of Nucl. Energy 25, 339 (1971)

(22) A paraître

(23) L. COSTA, J. RASTOIN, R. de TOURREIL, Jl of Nucl. Energy 26, 431 (1972)

DISCUSSION OF FISSION-PRODUCT YIELD EVALUATION METHODS AND A NEW EVALUATION

M. LAMMER*, O.J. EDER
Österreichische Studiengesellschaft für Atomenergie,
Seibersdorf, Austria

Abstract

DISCUSSION OF FISSION-PRODUCT YIELD EVALUATION METHODS AND A NEW EVALUATION.

Reliable data on fission product yields are necessary for interpretation of gammaspectrometric measurements on burnt fuel elements. Discrepancies among sets of fission yields recommended by different evaluators led to a detailed study of published experimental data. A new evaluation was performed. After a comprehensive description of the present state of experimental methods for obtaining fission product yields the previously adopted evaluation procedures are critically reviewed. An evaluation procedure is proposed which takes into account sources of experimental errors and accuracies of methods used. Examples of recently evaluated fission product yields for thermal fission of ^{233}U, ^{235}U and ^{239}Pu and for fast fission of ^{232}Th are presented. Data for ^{238}U fast fission and ^{241}Pu thermal fission are in preparation.

1. INTRODUCTION

For a number of years research work on fuel burn-up analysis has been done at the Research-Centre Seibersdorf [1-3]. With the use of high resolution semiconductor detectors the identification of many more fission products via gamma-spectrometry of irradiated fuel elements has been possible, than by application of NaI detectors. The aim of a fuel burn-up analysis is either to calculate fission product inventories and fuel burn-up (forward calculation) or to derive an appropriate fuel history from measured fission product gamma-spectra (backward calculation).

A survey of recent work in this direction will be presented in a separate paper at this conference [4]. Here it should only be noted that we are interested in fission products that can be identified by gamma spectrometry. Especially important for this work (see [4]) are fission yields for ^{95}Zr, ^{99}Mo, ^{134}Cs, ^{103}Ru, ^{106}Ru, ^{131}I, ^{133}Cs (capture product ^{134}Cs), ^{137}Cs, ^{140}Ba, ^{141}Ce, ^{144}Ce and ^{147}Nd. In addition several yields for fission products in the mass range from 149 to 153, which contribute to the activity of ^{154}Eu (activation product) through a series of neutron capture processes, are of importance in this context.

Checking the reliability of published fission product yields, that serve as input to our calculations, we found several discrepancies in recommended values of evaluations and recent experimental results[5,6]. In trying to find out the reasons for these discrepancies, we were naturally led to the consideration of:

- how are recommended values for fission product yields reached
- what are the experimental methods and the respective correction procedures.

---

* Present address: Nuclear Data Section, IAEA, Vienna, Austria.

2. SURVEY OF FISSION YIELD EVALUATIONS UP TO 1969

2.1. Information included in the evaluations

If the user of fission product yield evaluations does not want to just adopt one set of recommended yields at random, he wants to be given the following information:

- what is the general evaluation procedure
- which experiments (together with references) have been preferred for calculating recommended yields
- any information that allows a check on the reliability of yield values used, preferably a list of the individual experimental data together with references
- an indication of any changes of original experimental values and the nuclear data used by the evaluator to apply corrections
- uncertainties of recommended yields

Guided by these considerations evaluations available up to 1969 are surveyed. Fission product yield data for ^{233}U, ^{235}U and ^{239}Pu have been compiled in the works quoted, except where noted.

Steinberg and Glendenin [7] reviewed only very early measurements and will not be considered here in more detail.

Katcoff's [8] evaluation includes experimental data up to 1960, among these the first extensive series of mass spectrometric measurements, carried out at McMaster University, Canada [9 - 17]. A short introduction to the tables reviews the experimental methods. Mass-spectrometric data are preferred for recommended yields.

The tables contain recommended values. A list of references is given for each fissile nuclide. Adopted half-life values are also given. No information on original experimental data and methods or correction procedures is given. Uncertainties have not been assigned.

Ferguson and O'Kelly [18] evaluated ^{233}U yields only. Their report contains a detailed description of the data treatment and the evaluation procedure. They averaged readjusted mass spectrometric yields and finally normalized each mass peak to 100 % with the aid of radiometric and interpolated data.

This report contains separate tables for all original experimental data compared and adjusted values together with the recommended yields. The data sets are given with the respective references. Uncertainties are assigned as standard deviations only in those cases, where more than one experimental value was used for the final yield.

Croall [19] gives a more extensive discussion of experimental methods and correction procedures. He preferres mass-spectrometric data and experiments, where more than one yield has been measured. Corrections for new half-life values were applied, where possible.

The tables contain references together with each recommended yield and a list of adopted half-lives is also given. However, no information on preferred individual experimental data is included. Some highly discrepant values are given without comment for different isotopes belonging to the same mass chain in cases, where all of them represent essentially total chain yields. For each yield the 95% confidence limit is estimated.

Rider et al. [20] made a few renormalizations of relative yields, which they describe in detail. Their tables show original experimental data (and in some cases calculated yields) with references together with recommended values. For each yield the 95% confidence limit is estimated.

In their evaluation the authors included their own measurements [5] as well as those of Lisman et al. as published up to March 1967 (see [6]). These contain mass-spectrometric yields of the isotopes of Kr, Ru, Xe, Ce, Nd and Sm, the yield of ^{99}Tc determined spectrophotrometrically and of ^{137}Cs determined by gamma spectrometry, for ^{233}U and ^{235}U fission. However, the Kr yields of ^{235}U have been revised later by Lisman et al.[21].

The evaluation of Meek and Rider [22] was not available to us until recently. This work is based on [20], but contains yields of the isotopes of Rb, Sr, Zr and Cs and of ^{138}Ba for ^{235}U measured mass-spectrometrically by Lisman et al. [6]. It also includes the ^{239}Pu yields, as published in IN-1189, which were, however, completely revised in IN-1277 (see [6]). ^{233}U yields are not evaluated in this work. Meek and Rider have, with one exception, simply averaged published experimental yields from thermal fission. The tables include original experimental data with references, together with the recommended values, but also cumulative yields for the respective decay chains for a given mass number. No uncertainties are assigned.

Allen and Drake [23] give a more recent survey of ^{233}U fission yields, which was not published at the time of the preparation of the present paper.

2.2. Survey of discrepancies

Table I shows a survey of discrepancies among fission yield data from literature for the isotopes listed in the introduction. Some other important long lived fission products are also included. This table should reflect the situation at the time, when this evaluation was started. Therefore evaluations are also compared to the measurements of Lisman et al. [6,21]. Discrepancies are given in percent of the lowest value in column 3 and in percent of yields of Lisman et al. in column 4.

The evaluations compared are:
^{235}U: References [8, 19, 20, 22]
^{233}U: References [18, 19, 20, 23]
^{239}Pu: References [8, 19, 20, 22]

Other yields for Pu-241 thermal fission and ^{233}U, ^{235}U, ^{238}U, ^{232}Th and ^{239}Pu fast fission are not considered here, as published experimental results were rather scarce in the past and the most recent measurements [21, 24, 25, 26] are not included in the evaluations mentioned.

The overall agreement of compared yields is best for ^{235}U, which is, to a lesser extent also reflected in the values of table I.

3. EXPERIMENTAL METHODS FOR MEASURING FISSION YIELDS AND THEIR SOURCES OF ERROR:

In this chapter the mass spectrometric, the radiochemical and the ratio measurement technique are reviewed together with the sources of error and a discussion of the possibility for the evaluator to check and correct published experimental data. Based on these considerations, the previous evaluations will be discussed in 5. and new evaluation procedures are proposed in 6.

TABLE I. SURVEY OF DISCREPANCIES

Fissile isotope	Mass no. fission product	Discrepancies (percent of fission yield) between evaluations (maximum)	between evaluations and Lisman et al.[6]
^{235}U	^{90}Sr	< 4% [19] - [20]	2% [20] - 6% [19]
		>5% [19] - [22][a]	
	95	< 4% [8] - [19]	< 1% [19,20,22] -3% [8]
	99	about 1%	about 1%
	^{106}Ru	>2%[8,19]-[20,22][a)b]	0% [20,22]- 2%[8,19]
	^{125}Sb	≈ 0 (all)	≈40% (all)
	131	≈0 (all)	4% (all)
		6% I > Xe[19]	
	133	within 1.5% (all)	within 2% (all)
	^{137}Cs	<1% (all)	within 2% (all)
	140	within 2% (all)	within 2% (all)
	^{141}Ce	5% [20]-[22]	5.5% [20]- 10%[22]
	141	>10% difference La>Pr[19]	
	144	>5% [8,19]-[20][a)b]	0% [22]-4% [8,19]
	147	8% [8]-[22][a]	3.5[22] 8% [19],11%[8]
		~30% Nd - Pm [19]	
	149	11% [19] -[22][a)b]	4%[22],9%[20],15% [19]
	152	≈20% [8]-[22][a)b]	10% [22],15%[20],20%[19]
^{233}U	86	11% [19]-[20][b]	2% [20]- 13% [19]
	^{90}Sr	3% [18] - [23]	8% [23] - 11% [18]
	95	3% [18] - [23]	3% [18] - 6% [23]
	99	7% [20]-[23][b]	0% [20] - 7% [23]
	^{106}Ru	13% [20]-[18,23][b]	5%[20],10%[19],18%[18,23]
	^{125}Sb	100% [20] - [18,23]	16% [18,23];50%[19],80%[20]
	131	4% [23] - [19]	>1% [19] -<3% [23]
		22% I - Xe [19]	
	133	>2% [23] - [20]	<2% [20] - 4% [23]
	^{137}Cs	within 1% (all)[b]	>4% [19] ->5% [20]
	140	>3% [23] - [18]	≈0 [23] -<3% [18]
		>7% Ba - Ce [19]	

TABLE I (continued)

Fissile isotope	Mass no. fission product	Discrepancies (percent of fission yield) between evaluations (maximum)	between evaluations and Lisman et al. [6]
	141	<9% [23,18]-[20]	
	144	2.5% [18]-[20,23]	>1%[20,23]-3.5%[18]
	147	<4% [20]-[18][b]	>4%[20] - >8% [18]
	149	≈9%[23]-[19][b]	≈0 [20] - >5% [23]
	152	30% [23] - [18][b]	8%[20],<10%[23],18%[18]
^{239}Pu	^{90}Sr	≈7%[19]-[20,22]	2%[19]-5%[20,22]
	95	2.5% [19]-[20,22]	6% [20,22]
	99	<4% [19,20,22]-[8]	<8% [8] - 12% [19,20,22]
	^{106}Ru	13% [19] - [8]	
	^{125}Sb	8.5% [22]-[20]	35% [20]-40% [22]
	131	3% [22]-[19,20][a]	2.5% [22]-5.5% [19,20]
	133	>6%[20]-[8,19]	<4% [8,19]-9.5% [20]
	^{137}Cs	14% [19] - [8]	<2% [8], <3%[20,22],14% [19]
	140	<2% (all)	<2% (all)
	141	≈20% [8] - [19]	-
		6% [20,22] - [19]	
	144	<2% all except [8]	<2% all except [8]
		6.5% Ce Nd [19]	
	147	10%[20,22]-[19]	<4% [19]-13% [20,22]
		29% Nd - Sm [19]	
	149	<2% all	<5% [8]-6.5% [20,22]
	152	3.5% [20,22]-[19]	<2% all except [8]

a) Reference [22] includes values of [6] (see text)

b) Reference [20] includes values of [6] (see text)

3.1. Mass-spectrometric measurements

3.1.1. Description of techniques

Up to now mass spectrometric measurements of fission yields have been carried out for all stable and reasonably long lived fission products. Most commonly the isotopes of Kr, Sr, Zr, Mo, Ru, Xe, Cs, Ba, Ce, Nd and Sm have been studied, in some cases also isotopes of Y, Cd, Sn and Eu. The range of isotopes studied mass-spectrometrically can be extended by the use of on-line mass-spectrometers [27].

There are essentially two procedures used. Either the element to be investigated is chemically separated from the other fission products and the fissile element prior to mass-spectrometric analysis. Or, after separation from heavy elements like U or Pu, the sample containing all fission products is mounted on the filament of the mass spectrometer, making use of the different ionisation energies of the elements and thereby investigating the elements in succession. In the latter method complete separation of the elements is not always achieved (especially in the rare earth region) and careful corrections have to be applied for interference effects of either compound ions (e.g. LaO) and metal ions (e.g. ^{154}Sm), or isobaric isotopes (e.g. ^{144}Ce - ^{144}Nd).

The mass spectrometric measurements give precise relative yields for the isotopes of one element. As long as the half life of an isotope is at least of the order of the time needed for irradiation, handling and measuring, it can be investigated mass-spectrometrically in the conventional way. This makes possible the use of isobaric fission products to link different elements. Examples, where errors due to decay corrections can be kept small under suitable conditions, are ^{95}Zr - ^{95}Mo, ^{133}Xe - ^{133}Cs, ^{140}Ba - ^{140}Ce, ^{144}Ce - ^{144}Nd and ^{147}Nd - ^{147}Sm. For the above mentioned isobars this way of extending relative yields to neighbouring elements is generally superior to other techniques.

A suitable method to obtain the number of atoms of a particular fission product formed in an irradiated sample is the isotope dilution technique. In this technique, a known amount of a standardised solution is mixed thoroughly with a known amount of solution of either fission products or the chemically separated element under investigation. The standard solution contains a predetermined number of atoms of either a highly enriched "spike isotope" - preferably not formed in fission, or of the natural element. This mixture is measured again with the mass-spectrometer and the number of fission product atoms can be calculated by comparison with the pure fission product spectrograms.

Before leaving this technique one should mention the integral mass spectrographic method, as applied by Anikina et al. [28-30]. After determining the relative ionization coefficients of the elements under study for the spectrometer used, the ion currents are integrated for a given mass position of the investigated sample. Chemical separation of elements contained in the samples were not performed in these experiments. From the known ionization coefficients the relative concentrations can be determined. Absolute concentrations can be obtained by a determination of the number of atoms for one mass number, e.g. by isotope dilution.

3.1.2. Sources of error, corrections and accuracy

Rather high integrated neutron fluxes are required for accumulation of an amount of fission products sufficient to perform mass spectrometric measurements with reasonable accuracy. Therefore corrections have to be applied for neutron capture in fission products. If unstable isotopes are

also measured, then in-pile and out-of-pile decay corrections have to be applied, as the usual neutron fluxes require longer irradiation times and the radioactivity of the sample has to be sufficiently low for handling. Fission products like ^{135}Xe and some Sm isotopes have such high and rather uncertain capture cross-sections, which in addition depend strongly on the neutron spectrum that corrections can hardly be applied reliably under normal irradiation conditions. Therefore samples for measurements of the fission yields of these isotopes and their capture products have to be irradiated in very low fluxes.

In many cases cross-section and half-life data are known more accurately at the time of evaluation than when the experiment was performed. The correction of original yield data by the evaluator requires the knowledge of irradiation conditions and cooling time involved in the measurements, as well as either of the nuclear data used for corrections by the experimenter or of the uncorrected data.

Contamination of the fission product sample by naturally occuring isotopes in the same mass range can arise from the sample itself, the reagents, containers and apparatus used for post-irradiation treatment, or even from the filament of the mass-spectrometer, if surface ionization is used. Corrections can be applied to mass-spectrograms taking into account the abundance of an isotope not formed in fission. If this is not possible, unirradiated samples have to be carefully analysed. In many cases the amount of contamination cannot be determined exactly and can distort the abundances of fission product isotopes. For the Sm isotopes it is also essential to know, whether the contamination was present in the sample prior to irradiation, or not. In addition low yield ^{152}Sm and ^{154}Sm are very sensitive to corrections, as they have highest abundance in the natural element.

When the isotope dilution technique is applied, one has to consider mainly four sources of error:

- a fractionation of fission products (only partial recovery),
- an incomplete mixing of the fission product solution with the standardized solution,
- accuracy of the calibration of the standardized sample
- losses due to mass transport or reactions in the solution

Fractionation of fission products can be detected by measuring the activity of the residual solution. Also losses of fission products due to diffusion or migration can occur, but this can be avoided by properly encapsuled samples.

The accuracy of the determination of isotopic compositions depends on the amount of the investigated element, its ionization energy, the abundance of a particular isotope and the dynamical parameters of the mass-spectrometer used. Standard deviations quoted for fission products range typically between 0.1 and 2 percent.

Highly enriched spike solutions were used for isotope dilution by Lisman et al. [6,21]. The preparation of the spike is described in detail in [21] and a standard deviation of less than 0.5% is quoted for its standardization, leading to values around 0.5 percent for the determination of the number of fission product atoms.

The method of using the natural element for isotope dilution is less sensitive to changes in the isotopic composition of the sample. Therefore an overall accuracy of 0.3 to 3 percent can be assigned to the measurement of the number of fission product atoms present in a sample. However, in practice the deviations among measurements are sometimes larger, probably

due to systematic errors of the above mentioned kind. Therefore outstanding data can be rejected, if sufficient measurements are available to allow a check.

3.2. Radiochemical measurements

3.2.1. Description of techniques

The advantages of the radiochemical techniques are twofold:

- Sufficient radioactive nuclei are produced in rather short irradiation times. This makes fission yield determinations possible without the problem of interference caused by neutron capture processes.
- Natural element impurities do not contribute to the error of the measurements, as only radioactive fission products are measured and capture products arising from impurities can be neglected.

The fission products to be investigated are separated by suitable chemical procedures. This is done either directly after the dissolution of the irradiated sample, or the resulting solution is diluted to known volume and aliquots are drawn from this solution for further separation. So far the method is also applied for the mass-spectrometric isotope dilution technique. However, radiochemical measurements require rather very pure samples, which is achieved by a series of separation procedures, and the chemical yield is usually determined by weighing an inactive carrier. A known amount of solution is then investigated for fission products by counting techniques.

3.2.2. Sources of error, corrections and accuracy.

Errors arising from chemical separations can be due to:

- undetected losses of fission products
- the determination of the chemical yield
- incomplete separation from other fission products.

Other errors may arise from activity measurements, which require a number of corrections.

In earlier measurements mostly Geiger-Müller counters were used for the determination of the β-activity. Large corrections have to be applied for:

- efficiency, deadtime and geometry of the detector assembly
- absorption in the sample, air and detector window
- scattering of β-rays.

The 4π counter assemblies, more commonly used later, require less corrections than the Geiger-Müller counters. Corrections for self-absorption in the sample and absorption in the supporting film are still difficult to calculate directly. However, the high efficiency of 4π counters makes possible the use of very thin samples and films. Thus corrections can be kept reasonably small and be determined empirically.

Other counters require corrections similar to those mentioned. Uncertainties in the determination of the counter efficiency can be reduced by careful calibration against standardized detectors using standard sources, as has been done in most recent experiments (e.g. [31]).

Usually gross β-decay curves are measured at several time intervals. In the most straight-forward cases a suitable time interval can be chosen for the measurements, where the activity of the investigated fission product is clearly dominating and errors introduced by interfering activity can be kept negligible. Far more complicated are those cases where several fission products together with their daughter products

contribute to the total activity. Gross decay curves have to be resolved into components and final results depend strongly on the values used for the half lives. One erroneous value affects the other results as well. Decay data of precursors have to be taken into account, especially for calculations of the activity present at the end of the irradiation and after chemical separations.

From the evaluator's point of view it is almost impossible to correct old data for better known half life values or decay schemes. This would only be possible, if all the data points were available in addition to the experimental details, but even then attempts to do this for two experiments [32, 33] failed to improve the results. Corrections can be applied for a rather long lived fission product, where the original decay corrections introduce only small errors and the half life used is available. It is difficult to make a general statement about the accuracy of radiochemical measurements. This depends too strongly on any undetected failures during separation procedures and the detector equipment used for measurements. Considerable discrepances can also arise from various errors in the half-life values and decay schemes used, including precursors and daughters.

As such errors may be different for fission products investigated within the same experiment, it is then a question of how many yield data of one isotope are available for intercomparison to decide, which results are to be rejected.

In more recent experiments the efficiency calibration of the counters is accurate to about 2 percent [31]. Including corrections and chemical yield determination, excluding undetected losses, the overall accuracy should be within 3 - 5 %, in very early experiments up to around 10% and more.

In some experiments also gamma spectrometry is applied for the determination of disintegration rates. However, absolute intensities of gamma rays are accurately known only for a few fission products, and were even more uncertain in the past. Further, complex spectra cannot be resolved by NaI-detectors, which are most commonly used. Efficiency calibration introduces additional uncertainties.

The sources of error can be reduced by measuring the gamma spectra relative to a standard with known disintegration rate. Another suitable method is the determination of the detector efficiency for the investigated fission products by $4\pi-\beta-\gamma$-coincidence counting of pure samples of the isotopes.

Corrections can be applied by the evaluator without difficulty only for errors in gamma-ray intensities used.

3.3. Ratio measurements

3.3.1. Description of method

If a set of fission yields, e.g. those for ^{235}U, is assumed to be well known, an R-value can be measured, which is defined as

$$R = \frac{(Y_i/Y_{st})\ X}{(Y_i/Y_{st})\ ^{235}U}$$

Y_i . . . fission yield of isotope i

Y_{st} . . fission yield of a standard isotope (usually ^{99}Mo)

X . . . .the fissionable isotope under study

These ratios can be measured precisely, if irradiation times are either short compared to the half-lives of the investigated fission products or equal and measurement conditions are identical. In this case an absolute calibration of the equipment is not required and also the determination of absolute disintegration rates is not necessary, which avoids errors due to uncertainties in decay schemes.

3.3.2. Sources of error, corrections and accuracy

If the measurement conditions are identical and decay corrections of the same magnitude, errors depend only on the reproducibility of the chemical procedures, on the counting statistics and on the accuracy of the reference yields. Results from this type of measurement can easily be adjusted by the evaluator to a new set of reference yields, if the R-values obtained in the experiment are listed or if the reference yields used are quoted.

However, generally fractional independent yields of fission products, defined as the ratio of independent to cumulative or total chain yield, vary with fissionable isotope and neutron energy. If the independent yield of an investigated fission produot is significant in at least one type of fission, corrections have to be applied, if the half life of the precursor is comparable to the irradiation time or the cooling time until chemical separation.

The accuracy of this method can be better than 1%, but varies, depending on the fission product studied. In beta-ray measurements errors due to half-life values used cancel, if the gross decay curves have not too many components. In gamma ray measurements peak areas can be determined with rather high accuracy. But as fission products are not chemically separated, gamma spectra are complex and errors can be introduced by differences in background subtraction or interferences of other peaks. Due to these difficulties in the processing of the raw data, or any of the above mentioned errors, discrepancies are sometimes larger for single values.

3.4. Determination of the number of fissions

For the determination of absolute fission yields, the number of fissions, that have occurred in a sample, can be measured by essentially three methods.

3.4.1. Isotope dilution mass spectrometry

The technique itself has already been described and its application for the determination of the number of fissions shall be explained for the example of ^{235}U.

The isotopic composition and the number of atoms of Uranium are measured before and after irradiation. If the sample is highly enriched in ^{235}U, the total loss of U is almost entirely due to fissions of ^{235}U. Corrections for other losses of total U can be kept small enough to contribute a negligible error. This method has been applied by Lisman et al. [6,21], Rider et al. [5] and Meyer et al. [34] and requires a sufficiently large number of fissions.

3.4.2. Flux monitors

After measuring the neutron flux with a suitable monitor the number of fissions is calculated for a known amount of fissile material using published fission cross sections. The monitors mainly used in thermal fission yield measurements are ^{59}Co and sometimes Boron, where the change in the $^{10}B/^{11}B$ ratio is measured mass-spectrometrically.

The accuracy of this method depends on the self shielding corrections for monitor and sample, the values of the cross sections used and, in case a ^{59}Co monitor is used, on the half life value used for ^{60}Co. Reliable self shielding corrections cannot be applied, if the sample is very thick, i.e. these corrections should not exceed 10 - 15%.

2200 m/sc cross-section values have been used in many experiments. A recalculation of the number of fissions, based on recent adopted cross-section values, would require information about the neutron spectrum, which is, however, rarely available. The flux monitors usually have a 1/v cross section but the 2200 m/sc values can be used only if resonance absorption can be neglected, which is, however, not the case in a reactor neutron spectrum. E.g. for $r\sqrt{T/To} \approx 0.02$ about 1 barn would have to be added to the 2200 m/s cross section of ^{59}Co, which is about 3% of this value. U and Pu fission cross sections depend in addition strongly on the neutron temperature.

3.4.3. Fission Counters

In this method fission rates are determined directly by counting the emitted fission fragments, which, of course, requires very thin samples. These are irradiated together with "thick" samples, which serves for fission yield measurements, but has still to be thin enough to avoid large self-shielding corrections.

Errors in this method can further arise from corrections to the fission rate for sample thickness and in the determination of the counter efficiency, which varies with sample position in the counter.

3.5. Absolute fission yields

In many publications results are given as absolute fission yields in percent per fission. The evaluator has, however, to distinguish between those experiments, where absolute yields have actually been measured, and those, where relatively measured yields have been normalized by the authors in order to obtain absolute yields.

A measurement of absolute fission yields requires that the number of fissions, that occurred in the sample, have to be determined as well as the absolute number of atoms, or any equivalent quantity, of all investigated fission products from this sample. In this case the evaluator can only apply corrections for errors that have been introduced during the original processing of the raw data.

In many radiochemical measurements yields are determined relatively to a suitable standard, mostly ^{99}Mo or ^{140}Ba. The absolute fission yield of the standard is either measured separately or the value is taken from literature.

Sometimes absolute yields are obtained by normalizing relatively measured yields with the aid of interpolated and literature values in the mass ranges not covered by the experiment in such a way that the sum of yields is either 100 % for each mass peak or 200 % for both mass peaks. In experiments using radiochemical techniques this method has only been applied if no absolute yield of a suitable standard was available [26,35,36]. As many high yield masses have to be interpolated in such a work, the quoted absolute yields are not very accurate and cannot be compared to other results without readjustment. Mass spectrometric measurements cover in general most of the high yield range of at least one mass peak. In this case the reliability of absolute yields depends mainly on the number and accuracy of literature values in the range of yields not measured in the experiment.

All these results from relative measurements depend on earlier data and should therefore be renormalized by the evaluator, using his own adopted values.

4. MAIN PUBLICATIONS OF EXPERIMENTALLY DETERMINED FISSION YIELDS

When comparing published experimental fission yields one finds that discrepancies are often larger than one would expect from the accuracies quoted or from those we have assigned in the previous chapter. These discrepancies cannot always be explained, but are mostly due to systematic deviations, normalization procedures and, in the case of radiochemical measurements, resolution of gross decay curves. Knowledge of these discrepancies and of the experimentalist's measurement and data analysis techniques is essential for a discussion of existing evaluations and evaluation procedures. Therefore those publications of fission yield data, which receive heaviest weight in evaluations shall be briefly surveyed.

4.1. ^{235}U thermal fission yields

Thermal fission yields of ^{235}U have been determined mass spectrometrically by Farrar et al. [37,38], who used the isobaric technique, and by Rider et al [5], Lisman et al [6,21], Petruska et al [10,11], Steinberg and Glendenin [7] and Chu [39] who applied the isotope dilution technique. Gorshkov et al [29] applied the integral mass spectrographic method.

Rider et al [5] and Lisman et al [6,21] determined the number of fissions by isotope dilution mass spectrometry for one and four samples respectively. Additionally Lisman et al calculated all yields relative to ^{148}Nd, normalized the averaged values to 100% for the heavy mass peak and compared the resulting yields to absolute yields determined from the number of fissions in order to check the reliability of the normalization technique.

Petruska et al. [10,11] measured the neutron flux with a Boron monitor. In addition to their own measurements they used the relative Kr and Xe yields of Wanless and Thode [9] and normalized them to ^{85}Rb with the aid of a known branching ratio for ^{85}Kr and to ^{133}Cs with the aid of an unpublished ^{131}Xe: ^{133}Xe yield ratio respectively. Ce yields were linked to those of Nd through the common yield at mass 144, requiring, however, a rather large decay correction for ^{144}Ce.

Farrar et al [37,38] normalized relative yields in the heavy mass peak to 100% using the same Xe and Cs yields as Petruska et al [10,11] and interpolated values in the mass ranges not covered by their experiment. For the light mass peak they used relative yields of Kr and Rb and their normalization to Sr of Petruska et al [11] and obtained absolute yields relative to their predetermined yields in the heavy mass peak with the aid of an isotope dilution ratio also from [11]. Zr and Mo isotopes were linked to these yields by the isobaric technique. This technique depends on the accuracy of decay corrections.

Steinberg and Glendenin [7] used radiochemical, previous mass spectrometric and interpolated yields together with their own measurements and normalized the whole yield curve to 200%. Their relative Ru yields were normalized to a radiochemical value of the ^{106}Ru yield and the overall accuracy of absolute yields is rather low.

Chu [39] measured only relative fission yields in the rare earth region.

Gorshkov et al [29] (see also [28]) do not indicate, how they obtained absolute yields, which are given with low accuracy only.

The samples used for fission yield measurements at McMaster University [9-11, 37, 38] and by Chu [39] were irradiated in low integrated neutron fluxes and required only minor corrections for neutron capture. Yields obtained in these experiments agree well with those of Rider et al [5] and Lisman et al [6,21], who irradiated their samples in rather high integrated neutron fluxes, but used adequate nuclear data for corrections.
Heavy mass yields of Steinberg and Glendenin [7] obtained from high flux irradiations disagree severely with other mass spectrometric data, probably due to inadequate corrections and contamination. No details on irradiation and on cooling time are published. The same is true for the measurements of Gorshkov et al [29]. Although many of their absolute yields agree approximately with other published data, discrepancies become evident only when relative yields are compared. Sources of error due to the method itself are not indicated.

4.2. ^{233}U thermal fission yields

Lisman et al [6,21] and Rider et al [5]: same as for ^{235}U.

Bidinosti et al [40] made mass spectrometric measurements of stable and long lived fission products, but used different normalization techniques. Only final results are shown in the tables and no details on corrections and nuclear data used are included in their publication. The isotope dilution technique was applied for the isotopes of Sr, Cs, Nd and Sm and for ^{138}Ba. The isobaric technique has been used to link Ce to Nd through the common mass 144 and Zr to Mo through the common mass 95, but the half lives used for decay correction are not published. Making use of the Xe yields of Fleming et al [14] and Sm yields of Melaika et al [13] the heavy mass peak was normalized to 100%. However, for two samples the number of fissions were calculated from a neutron flux measurement and yields obtained in this way were said to be 2 and 4 percent lower than those obtained from the normalization technique and shown in the table. In the light mass peak Sr yields were calculated from the number of fissions. Kr yields were taken from [14] and normalized to the ^{133}Cs yield, and Rb yields were obtained with the aid of the ^{85}Kr branching ratio, which is not quoted.
Relative Ru yields were linked to the Zr-Mo yields by a radiochemically determined ratio and these relative yields together with interpolated and extrapolated values were normalized to total 100% minus the predetermined Sr, Rb and Kr yields and extrapolated values below mass 83. Absolute yields and even isotope dilution data disagree with other mass spectrometric measurements.

Steinberg et al. quoted in [7], have applied the method of isotope dilution mass spectrometry for the isotopes of Zr, Mo and Ru and normalized their relative yields to radiochemically determined values.

Anikina et al [30,41] (summarized in [28]) have applied the isotope dilution and mass spectrographic method. Details on the analysis of Sr isotopes by the former method are given in [41] and of Cs isotopes and the rare earth fission products by both methods in [30]. Information on the irradiation of the sample can be found in [42]. The original relative yields obtained by the method of isotope dilution agree after correction with those of [5] and [6], whereas the values obtained by the integral method disagree. The same sample was analysed later by Gorshkov and Anikina [43] for the isotopes of Zr and Sr as well as for ^{89}Y and ^{138}Ba by the integral mass spectrographic method. Relative and absolute yields calculated from the ^{233}U depletion [42] disagree completely with other mass spectrometric measurements. The good agreement achieved by the

isotope dilution method on the same sample indicates, that natural element contamination cannot account for the discrepancies. It seems that the integral mass spectrographic method is not suitable for accurate fission yield measurement.

4.3. ^{239}Pu thermal fission yields

Rider et al [5c] obtained absolute yields from the change in the isotopic composition of Pu in one sample, using a known capture to fission ratio. As for ^{233}U and ^{235}U relative yields obtained from the other two samples were normalized to agree in the sum of yields with one sample, for which the number of fissions have been determined.

Lisman et al [6j] used the method of isotope dilution mass spectrometry. However, they found their yields too low compared to the measurements of Fickel and Tomlinson [15] and therefore revised their yields later [6m, 21], using the normalization technique as described in 4.1.

Fickel and Tomlinson [15] used the method of isotope dilution mass spectrometry. Yields in the heavy mass peak were obtained from two samples, irradiated in the same position. For one sample they measured the neutron flux and the neutron temperature with the aid of Co and Sm monitors. The number of fissions were determined using g and s factors in the Westcott formalism. Yields obtained in this manner for both samples agree well for the isotopes of Nd and Ce. The yields of Sm and Cs isotopes, and hence also those of Xe, which were taken from Fleming et al [16] and normalized to ^{133}Cs, are about 5% lower for the Pu Al alloy sample. However, their final values were reached by a normalization of each set of yields to 100% and averaging them.

Yields in the light mass peak were obtained by isotope dilution relative to the predetermined ^{133}Cs yield, but generally from samples different to those used for measurements of the isotopic compositions of fission products. Only Zr yields were normalized to Mo yields at the common mass 95. The final set of yields contains also the Kr yields measured by Fritze et al. [17] and normalized to ^{85}Rb with the aid of the ^{85}Kr branching ratio.

Fritze et al [17] measured the absolute yield of ^{131}Xe by the isotope dilution technique together with a determination of neutron flux and temperature. Further, they measured relative Kr yields and the ratio of fission product Xe to Kr. Use was made of the relative yields of Fleming et al [16] to obtain absolute Xe and Kr yields.

Krizhansky et al [44,45] applied the method of isotope dilution mass spectrometry (results of isotope dilution measurements are given in [28]. Although there are several discrepancies among the other mass spectrometric measurements already mentioned, the results of Krizhansky et al disagree much more seriously. Even relative abundances of fission product elements cannot be compared to other measurements.

Finally the radiochemically determined yields of Marsden and Yaffe [46] should also be mentioned, as heavy weight was given to their data in the later evaluations [19,20,22]. Marsden and Yaffe measured the neutron flux with a Co monitor and calculated the number of fissions from the 2200 m/sec value of 742 barn for the fission cross-section of ^{239}Pu. This has been common practice in many experiments, but can introduce considerable error in the determination of ^{239}Pu fission yields due to its strong 0.3 eV resonance. The smallest possible value for a reactor neutron spectrum cross section (pure maxwellian at 20° C) is about 780 b and inclreases with increasing neutron temperature and contribution of epithermal neutrons [47].

An example of the influence of the ^{239}Pu cross section value is given in section 7.3. Surprisingly the absolute fission yields of Marsden and Yaffe agree fairly well with mass spectrometric measurements at several mass numbers. However, if absolute yields obtained from a flux measurement are included in an evaluation, the cross section data used have to be checked.

5. DISCUSSION OF EVALUATIONS AND EVALUATION METHODS.

In chapter 2 the information included in the previous evaluations have been summarized from a user's point of view. Now the evaluation procedures themselves and the treatment of experimental data shall be discussed in the light of the review of experimental methods and the individual experiments described in the previous chapter.

5.1. Treatment of data in previous evaluations

After a survey of existing fission yield measurements and knowledge of the methods used it is possible to better understand and analize previously used evaluation procedures.

Katcoff [8] evaluated yields for individual fission product isotopes within the same mass chain. He preferred mass spectrometric measurements where available and averaged results of equally reliable measurements or selected values he considered superior to others which avoids the averaging of discrepant data. Original data were renormalized by checking the sum of yields against 100% and corrected for neutron capture. When selecting ^{235}U fission yield measurements, the data of Anikina et al [28] were not used and the other mass spectrometric data [7, 10, 11, 39] averaged. For ^{233}U and ^{239}Pu the evaluation of recommended yields is not clear, as these do not correspond to individual experimental sets of yields, even after renormalization. Radiochemically determined yields were used for readioactive precursors of fission products measured mass spectrometrically. Therefore discrepant yields are given for isotopes belonging to the same mass chain, which are not consistent with charge distribution theory derived from measurements of independent yields [48,49].

Ferguson and O'Kelley [18] used mass spectrometric data only, for the mass ranges covered by these measurements. They have lowered all those yields reported by Bidinosti et al [40], that had been obtained by the isotope dilution technique, by 3%, according to the average difference between the normalization procedure and the flux measurement (see 4.2.). The yields of Zr, Mo and Ru isotopes remained unchanged. Relative yields reported by Gorshkov and Anikina [43] and Steinberg and Glendenin [7] for the light mass peak and by Anikina et al [28] for the heavy mass peak were readjusted to agree in the sum of yields with those of Bidinosti et al [40]. Only the data of [28,43] obtained by the integral mass spectrographic method were used and no corrections were applied to original data. Ferguson and O'Kelly used the normalization procedure, described in 3.5., to calculate absolute yields for each mass peak separately.

Although the yields reported in [28] and [43] were measured at different times, the same sample was used and hence the results are based on the same number of fissions. After the readjustment made by Ferguson and O'Kelley the ratio of yields in the light mass peak to those in the heavy mass peak is completely different from the ratio of originally determined yields. Large discrepancies between some reported experimental yield ratios of different elements were smoothed by the method of matching the sums of

yields. Although inconsistencies remained even after readjustment the yields were averaged by Ferguson and O'Kelley. However, at the time of their work no other mass spectrometric measurements were available to allow a check.

Croall [19] evaluated individual fission products belonging to some mass chain. Original data were corrected for decay and neutron capture. Relative measurements and R-values were readjusted to his adopted standard yields. The treatment of mass spectrometric data is not evident from the report. When comparing recommended yields with the original data of the references given, it appears that some readjustments were made, especially for discrepant absolute values. In some cases, where only one reference was used to obtain a recommended yield, this does not correspond to the original value. The measurements of Farrar and Tomlinson [38] and others published in laboratory reports [5,6,34] are not included in Croall's evaluation. The selection of preferred yields is also not evident, as sometimes obviously not all results from references have been used which are listed along with the recommended value. Radiochemical measurements were averaged together with mass spectrometrically determined yields. For ^{239}Pu the values reported by Marsden and Yaffe [46] were considered even superior over all other measurements and generally adopted as recommended yields. If sets of preferred experimental yields disagreed in a certain value, they were averaged. Yields adopted for different isobars within the same mass chain are sometimes highly discrepant and not consistent with charge distribution theory [48,49].

Rider et al [20] proceeded on a mass by mass basis comparing all isotope yields within a mass chain that essentially represent total chain yields. Generally no readjustments of originally reported absolute yields were made. Exceptions are pure relative yields that were normalized to adopted yields and the data of Anikina et al [28]. The data reported for ^{235}U were normalized to the adopted value of their relative standard and those reported for ^{239}Pu were renormalized to other measurements for mass 142 and above. This is, however, not valid and rather arbitrary, as the original normalization is established by a measurement of ^{142}Ce relative to ^{140}Ce [45] and therefore genuine, although in complete disagreement with other measurements.

^{233}U fission yields of [7,28,40,43] were used as adjusted by Ferguson and O'Kelley [18] and yields recommended by Katcoff [8] were also included in the averaging procedure. Thus, for example, the relative Xe yields of Wanless and Thode [9] are included 3 times: as adjusted by Katcoff [8], Petruska et al [10] and Farrar and Tomlinson [38]. Radiochemical measurements before 1960 were not used, later ones were averaged together with mass spectrometric data, but a few outstanding values were excluded from the mean.

Meek and Rider [22] evaluated not only chain yields but yields for all fission products by combining experimental results with charge distribution theory and decay schemes. They used essentially the same experimental data and renormalizations as Rider et al [20], except that they included some more recent measurements, and therefore the discussion shall not be repeated. But as they separated yields of isobars within the same mass chain sometimes lower yields of radioactive precursors of fission products were allowed for, which are not consistent with charge distribution theory. When differences were too large, yields of isobars were averaged. In no case was the cumulative yield of a daughter allowed to be smaller than the cumulative yield of its parent. As Rider et al [20] they used yields estimated by Weaver et al [95] for masses not covered by measurements. These estimates are, however, based on the earlier evaluation of Katcoff and do not agree with interpolations between more recent measurements.

In the discussion of their evaluation, Meek and Rider state that the unweighted averaging of data is not satisfactory and should only be considered as preliminary. They propose for a later evaluation estimates of uncertainties of individual experiments to obtain weighted averages. They also suggest the use of improved Gaussian charge distributions and calculations of unmeasured yields. We were only recently informed that in the meantime Meek and Rider have published a new evaluation [49]. Unfortunately this is not yet available to us and can therefore not be discussed for comparison.

5.2. Discussion of evaluation procedures

Discrepancies among evaluations do not only arise from the inclusion of different experimental data. They are also due to the procedure of evaluating absolute yields on a mass by mass basis. Differences in renormalizations of experimental data lead to different absolute yields that are compared. Depending further on the number of radiochemical measurements included, individual yields that show best agreement will also be different in the evaluations. It will be shown which consequences this procedure has and how the resulting drawbacks can be avoided.

Mass spectrometrically determined relative yields of the isotopes of one element agree, with some exceptions, also actually within 1%. Discrepancies due to decay or neutron capture can usually be corrected. Errors due to contamination of naturally occurring stable isotopes can often be detected by intercomparison of these relative yields.

For the linking of relative element yields by isotope dilution, isobaric technique or integral mass spectrographic method, the actual agreement among measurements is not as good. In the case of the isobaric technique ratios can be adjusted with the aid of better known half lives. Relative yields obtained by the first two methods agree generally still within a few percent. The consistency of data sets can again be checked by intercomparison and discrepant values can be excluded.

Poorest agreement show absolute yields. Exceptions are the data for ^{235}U [10,11,37,38,5,21], which is also reflected in the relatively good agreement among evaluations, and for ^{241}Pu [5d,62,21,118] . The values of absolute yields depend on the way, they were obtained. It has been shown in chapter 4 that these are widely different and not always straight forward. If the normalization technique is used, absolute yields depend also on errors introduced with the linking of relative element yields. Part of the mass yield curve will be lower, the other part higher than that determined in other experiments.

Discrepancies in absolute yields constitute a source of error in evaluations. Measurements, which show good agreement in relative yields, may disagree, if only absolute yields are compared. On the other hand measurements, which disagree in a comparison of relative yields may coincide with different sets of other data at different mass numbers, including radiochemical measurements. These coincidences may not only influence renormalizations, but can lead to preferred values, which are not consistent with relative mass spectrometric yields.

The accuracy of more recent radiochemically determined yields depends mainly on the accuracy of half life values used, the determination of the number of fissions and the decay curve resolution. If this is satisfactory, absolute yields can be of an accuracy comparable to some single absolute mass spectrometric yields. But as they are measured only for certain mass numbers and not for stable isotopes, their inclusion in averages may distort relative yields well established by mass spectrometric measurements.

In our work [4,51] the interpretation of gamma spectrometric measurements on burnt fuel elements is based on activity ratios of fission products listed in the introduction (1.). This method avoids large corrections that have to be applied in a determination of absolute activities. Therefore the accuracy of relative yields is most important for our work. For this reason and in order to avoid errors introduced if only absolute yields are compared, we concluded that the best suitable evaluation method would be to start with arbitrarily normalized relative mass spectrometric measurements and establish the shape of the yield curve in the peak regions in this way. These relative yields can then be normalized with the aid of absolute yields.Radiochemical yields should only be used for the final normalization and as a check of relative and absolute yields obtained in this manner. An evaluation based on these considerations was started in 1969 and the procedure used is outlined in the next chapter.

Independent from our work Walker made an evaluation based on similar conclusions. The first set of evaluated yields for ^{235}U was presented in 1970 [54]. This paper includes a detailed description of the treatment of experimental data and results of individual steps in his evaluation procedure. He normalized experimental mass spectrometric yields of different authors to agree in the sum of Zr yields for the light mass peak and in the sum of Nd yields for the heavy mass Peak. This selection is reasonable, as these elements cover the greatest parts of the respective mass peaks. By a selection of consistent relative yields he obtained the shape of the main portions of the mass peaks and normalized them as a group so that the sum over each mass peak is 100%.

Walkers evaluation would have been adequate for our work, had the results been available earlier. However, we learnt about the paper presented at the Helsinki Conference [54] only almost a year later. The evaluations of yields from other fissile isotopes were not published before last year [55b] and are still not yet available to us. These results could therefore not be compared to our evaluation, but will probably be presented at this conference [56]. Thus, our present calculation was carried out as a by-product of our investigations of irradiated fuel elements.

6. PROPOSAL OF EVALUATION PROCEDURES

6.1. The present evaluation procedure

The principle has already been outlined in the previous chapter. Some details shall be given as information to the recommended yields shown in tables IV to VII. The following evaluation procedure was adopted:

step 1: Mass spectrometric measurements were collected first and corrected, where possible, for differences in cross section and half life values between those used in the original work and those shown in table II. The cross section data shown in this table are based on Walker's comprehensive compilation [55a] and only updated for later measurements. For fission products,where no measurements are available, the capture cross sections calculated by Cook [58] are used. The half life values are based on the compilation of Martin and Blichert-Toft [52], but several more recent measurements were incorporated in a new evaluation carried out by one of us. The complete set of fission product half lives above 1 day will be published later as SGAE report. Table II includes values based on publications issued after the fission yield evaluation was started. Readjustments were made later, if necessary. The corrections to the published yield

data have been calculated with the aid of the computer programme CHAIN, briefly described in [4], by simulating the special irradiation conditions as given by the authors of the yield data.

Step 2: Corrected sets of relative mass spectrometric yields were compared and checked for consistencies. Data which suffered from incomplete or out of date corrections, and where no readjustment was possible, were rejected as well as those measurements that obviously disagreed severely with others.

Step 3: Relative yields of the isotopes of individual elements were averaged first. If sufficient measurements were available for comparison only consistent ratios were selected.

Step 4: Data for linking relative element yields were compared next.

As stated in 5.2 the agreement is not so good for these data. Therefore also ratio measurements (see section 3.3) were used for fissile isotopes other than ^{235}U, mainly to serve as a check. In some cases they were also included in the average, if their accuracy is comparable to that of isotope dilution data. Here the selection of preferred yields was not so easy, due to poorer overall agreement. Individual examples will be given in chapter 7.

Step 5: Relative element yields were linked according to the data obtained from step 4. This was adopted as especially in the experiments carried out at Mc Master University [9-17, 37,38,40] the samples used for isotope dilution measurements were not the same as those used for measurements of the isotopic distributions of fission products, or were even obtained in different experiments. Also the higher precision of relative measurements can be maintained.

During the actual evaluation this step had to be modified slightly. The procedure outlined above led to some disagreement between isotope dilution data and isobaric yields. Therefore neighbouring elements had to be adjusted together. But final yield ratios were always checked against those obtained in step 3.

Step 6: The original idea was to normalize the groups of relative yields to most accurate absolute yields and was applied to the first preliminary results used for the calculations. We learnt from Walker's evaluation [54] that sum of yields not measured mass spectrometrically was 11.015% (of which 6.16% is the well known ^{99}Mo yield,) for the light mass peak and only 3.635% for the heavy mass peak. Therefore this method of normalization seems to be well justified and was adopted in our first complete evaluation of ^{233}U and ^{235}U fission yields.

The final normalization was checked in several ways:

- The separate normalization of each mass peak was checked by comparing isotope dilution data of several isotopes from the light and heavy mass peak with the adopted values. This showed systematic deviations of the order of 1 - 2%.

- The adopted absolute yields were compared to most reliable absolute measurements based on determinations of the number of fissions. The agreement with radiochemical yields was within the limit of their errors. A comparison with mass spectrometric data showed good agreement for the heavy mass peak of ^{235}U, but again deviations of the order of 1-2% for the light mass peak and for both mass peaks of ^{233}U.

TABLE II. RECOMMENDED FISSION PRODUCT NUCLEAR DATA

fission product	half-life	Cross-sections (barn) type[b]	thermal[b]	Res. Int.[c]
^{83}Kr		maxw	200	150
^{85}Kr	10.73±0.06 a	pile	8	
^{89}Sr	50.52±0.05 d	pile	0.42	
^{90}Sr	28.6 ±0.4 a	pile	0.8	
^{91}Y	58.51±0.12 d	pile	1.4	
^{95}Zr	63.98±0.12 d	pile	1	
^{95}Nb	35.045±0.010 d	pile	4	
^{99}Mo	66.7 ±0.5 h	pile	2	
^{103}Ru	39.35±0.10 d	pile	10	
^{105}Rh	35.5 ±0.2 h	maxw	17000	17000
^{106}Ru	368.3 ±2.0 d	maxw	0.15	2
^{125}Sb	2.75±0.04 a	pile	1.6	
^{131m}Te	30 ±2 h	pile	0.1	
^{131}I	8.05±0.02 d [d]	maxw	0.94	8
^{131m}Xe	11.98±0.05 d	pile	50	
^{131}Xe		maxw	100	830
^{133}I	20.9 ±0.1 h [e]	pile	0.005	
^{133m}Xe	54 ±2 h	pile	50 [f]	
^{133}Xe	5.29±0.01 d	pile	190	
^{133}Cs		maxw	29.5	450
^{135}I	6.585±0.002 h	pile	0.05	

TABLE II (continued)

fission product	half-life	Cross sections (barn)		
		type [b]	thermal [b]	Res.Int. [c]
^{135}Xe	9.172± 0.005 h	2200	2.65x10^{6} [g]	
^{137}Cs	30.0 ± 0.2 a	pile	0.11	
^{141}Ce	32.55 ± 0.02 d	pile	29	
^{143}Pr	13.58 ± 0.03 d	maxw	100	150
^{143}Nd		maxw	325	60
^{144}Ce	284.5 ± 0.4 d	maxw	1	2.2
^{145}Nd		maxw	45	250
^{147}Nd	11.00 ± 0.03 d	pile	100	
^{147}Pm	2.623± 0.001 a	maxw	182 [h]	2400 [h]
^{147}Sm		maxw	61	646
^{148m}Pm	40.9 ± 0.2 d [i]	pile	25000	
^{148}Pm	5.37 ± 0.01 d	pile	3000	
^{149}Pm	53.08 ± 0.05 h	pile	1400 [g]	
^{149}Sm		2200	42100 [g]	
^{150}Sm		maxw	100	240
^{151}Sm		2200	15000 [g]	
^{152}Sm		maxw	206	3000
^{155}Eu	4.9 ± 0.1 a	pile	4040	

a Only fission products relevant for correction

b 2200 = 2000 m/s cross-sections
maxw = maxwellian average cross-sections at 20.4° C
pile = reactor spectrum cross-section

c Reduced infinite dilute resonance integral (above 1/v)

d Branching to ^{131m}Xe : 1.3 %

e Branching to ^{133m}Xe : 2.8 %

f Results of Reynolds and Emery [53] suggest that this cross section might be in the order of 10^{4} barn.

g Used with g and s factors in Westcott convention

h Production ratio: 47.24% to ^{148m}Pm, 52.76% to ^{148g}Pm

i 3% internal transition to ^{148g}Pm

Radiochemical yields in the range of masses 121 to 130 important for the final normalization show very large discrepancies, as can be seen for ^{235}U in the last column of table IV. Measurements in this mass range are very scarce for other fissile isotopes and the sum of yields in this mass range much higher. This introduces considerable uncertainties in the final normalizations. To avoid discrepancies as given above and reduce the overall uncertainty, the fission yields were reevaluated for both mass peaks together and finally normalized by a combination of the two procedures, which will be discussed individually in chapter 7.

As a further check the total number of neutrons (prompt + delayed), $\bar{\nu}_t$, can be calculated from the adopted set of yields according to:

$$\bar{\nu}_T = M_F - \bar{L} - \bar{H}$$

where M_F = mass number of fissile isotope + 1

$\bar{L}$ = average mass of light fragment

$\bar{H}$ = average mass of heavy fragment

$\bar{L} + \bar{H}$ can be calculated from:

$$\bar{L} = \left(\frac{\Sigma(\text{mass} \times \text{yield})}{\Sigma \text{ yield}} \right)_{\text{light}} \quad , \quad \bar{H} = \left(\frac{\Sigma(\text{mass} \times \text{yield})}{\Sigma \text{ yield}} \right)_{\text{heavy}}$$

The calculated value of $\bar{\nu}_T$ can be compared to recommended values [47]. This is, however, not a very meaningful check. On the one hand the value of $\bar{\nu}_T$ derived in this manner is rather sensitive to changes of individual yields. On the other hand errors may cancel. This can be seen from table III, where $\bar{\nu}_T$ calculated from fission yields is compared to [47]. For ^{235}U $\bar{\nu}_T$ was also calculated for the fission yields recommended by Meek and Rider [22] and by Walker [54]. Differences in $\bar{L}$ among the evaluations are compensated by differences in $\bar{H}$. The only conclusion that can be drawn from such a comparison is that at least part of the normalization is in error, if the calculated $\bar{\nu}_T$ disagrees severly with the recommended value.

TABLE III. COMPARISON OF ν_T VALUES

fissile isotope	Source	$\bar{L}$	$\bar{H}$	$\bar{\nu}_T$	recommended value[47a][a]
^{235}U	Walker [54]	94.855	138.650	2.495	
	Meek,Rider [22]	94.925	138.591	2.483	2.4229±.0066
	this work	94.849	138.660	2.492	
^{233}U	this work	93.377	138.159	2.464	2.4866±.0069
^{239}Pu	this work	98.814	138.116	3.070	2.8799±.0090

a In the 1973 evaluation the new ν_T values will be about 0.5% lower [47b]

Apart from the final normalization the present evaluation differs from that of Walker [54] only in two respects. Due to the separation of steps 3 and 4 relative yields of fission products, which were only measured in one experiment, are maintained as published. Examples for ^{235}U are the yields of ^{89}Y, ^{139}Ba and ^{141}Ce measured only by Farrar et al. [37,38] and of ^{135}Cs measured only by Petruska et al. [10], but the differences are only slight, if the two sets of yields are compared in table IV.

The second difference is that results of individual measurements have been used in our evaluation rather than yields averaged by the authors.

This has the advantage that more sets of data are available for comparison and the internal consistency of different experiments can be checked. Discrepant values, which may strongly influence the average yields of one experiment, can be excluded. Also a larger number of determinations within one experiment can be accounted for. This is important, as no weighted averages are taken in this evaluation.

This difference in procedures is reflected by a comparison of Xe yields for ^{235}U in table IV. These are based on the measurements of Lisman et al [6]. For the determination of the number of fission product atoms, and thus for relative yields, they quote about equal accuracies for all samples. The main difference in uncertainties among the samples arise from the determination of the number of fissions and is accounted for in the weighted average. The same trend can be observed if the Xe yields of Lisman et al. [6,21] determined from the number of fissions (column 6: "Fiss") are compared to those obtained by the normalization technique (column 7: "Norm") in table IV.

6.2. Proposal of an improved evaluation procedure

The drawback of a "hand" evaluation is that no weighted averages can be taken. During the evaluation of ^{239}Pu thermal fission yields we made the experience that discrepancies arise which can only be solved rather deliberately. Therefore we propose a computerized evaluation of fission yields that can simultaneously take account of all correlations. However, in advance to such a computer-fitting procedure the experimental data serving as input have to be analyzed carefully and errors have to be assigned individually. Also a pre-selection of experimental results has to be done. Such a computer programme could then include the following features:

- Relative abundancies of isotopes should be averaged first, according to step 3 in the previous section. Overall errors should be calculated.
- Then the yield curve could be adjusted simultaneously using isotope dilution data, isobaric yields and measured absolute yields. Changes of the relative yields, which were averaged first, should only be allowed for within the calculated errors.
- If there is disagreement among relative isotopic yields, these can be included in the simultaneous fitting procedure to determine, which value is in error. However, provision has to be made within the whole procedure that values, where the discrepancies exceed their errors, are not just averaged.
- Boundary conditions are: the total yield curve must sum up to exactly 200%. The split between the two mass peaks, $\bar{M}$, should be according to:

$$\bar{M} = \frac{M_F - \nu_s}{2} \pm \Delta\nu_s$$

M_F = mass of fissile isotope
ν_s = average number of neutrons emitted in symmetric fission near $\overline{M}$

$\Delta\nu_s$ = uncertainty in ν_s

These boundary conditions could serve to adjust interpolated and very uncertain yields. In addition, charge distributions could be incorporated into the fit to allow a check of experimental isobaric and independent yields.

7. RESULTS OF THE PRESENT EVALUATION

This paper is mainly devoted to a discussion of evaluation procedures and a justification of the present evaluation method. For the sake of completeness our results are also included, but space does not permit detailed descriptions of the treatment and selection of data. These will be published later as SGAE reports. Here only the general information shall be given together with some special features.

Our recommended yields for ^{235}U, ^{233}U and ^{239}Pu thermal fission and for ^{232}Th fast fission are compared to other evaluations in tables IV to VII respectively. The data of Lisman et al are included for the reasons given in chapter 2. Radiochemical measurements are also shown for illustration. In some cases they are in good agreement, also with our recommended yields, others are highly discrepant. Thermal fission yields for ^{241}Pu and fast yields for ^{238}U are still in preparation and only preliminary results available. Fast fission yields for ^{235}U and ^{239}Pu were not evaluated, as the complete set of yields measured by Lisman et al. [21] is presently adequate and further measurements in other laboratories are in progress.

For the calculation of yields other than total chain yields either measurements of independent yields were used as compiled for example by Wahl et al [48] or those calculated by Crouch [49]. The cumulative yield of ^{135}I was derived from the results of Hawkings et al [59].

7.1. Thermal fission yields of ^{235}U

Mass spectrometric measurements used are those of Lisman et al [21,57], Rider et al [5], Chu [39], the original experiments from McMaster University [9-13, 37, 38] and yields of the light mass peak reported by Steinberg and Glendenin [7]. Other measurements were not used for reasons already given in 4.1. The agreement between the selected experiments listed above is far better than that observed for mass spectrometric measurements of ^{233}U and ^{239}Pu yields.

Yields of the light and heavy mass peak were normalized arbitrarily to the sum of yields of ^{145}Nd and ^{146}Nd. This starting point was chosen because Nd isotopes were measured in most experiments and this sum is not affected by insufficient corrections for decay or neutron capture. Ce and Ba yields werelinked to Nd yields as a group, because the isotope dilution ratios for Ce and Ba were not consistent with the isobaric yield measurements of Farrar et al [38]. For the same reason Sr (Y), Zr and Mo yields were normalized together. Sm yields of Lisman et al [21] were not used, as they disagree with low flux measurements.

Relative yields of both the light and the heavy mass peak were normalized together in such a manner that the sum of yields in the light

mass peak only was 100%. The agreement with measured absolute yields was so good, and the sum of yields in the heavy mass peak was incidentally 100.0011, that no renormalization was considered necessary.

7.2. Thermal fission yields of ^{233}U

In this case the measurements used to establish the yield curve were:

Mass spectrometric: Lisman et al [21], Rider et al [5], Fleming et al [14], Bidinosti et al [40], Anikina et al [28,30,41] Steinberg and Glendenin [7] and Melaika et al [13].

Ratio measurements: Gordon et al [94] and Bunney and Scadden [92], after correction for ^{235}U reference yields.

First all mass spectrometric data were normalized to the sum of Nd isotopes, R-values at mass numbers 143 and 144, and the consistency checked. The yields of Anikina et al [28,30,41] could be corrected according to the ^{233}U depletion data given in [42] together with an approximate irradiation time and according to the decay corrections applied in the original work and the half lives used, as given in [30,41]. Only the isotope dilution values of Bidinosti et al [40] were used for this check.

The ratios of yields in the light mass peak and of Cs isotopes to those of Nd are in reasonable agreement for the data of Lisman [21], Rider [5], Gordon [94] and the isotope dilution values of Anikina [30,41]. The relative Sr and Cs yields of Bidinosti et al are about 10% lower than the averages of other data. As no details are given in their publication, their isotope dilution values were excluded and only relative element yields used in cases, where no remarkable corrections were required. Yields obtained by the integral spectrographic method [30,43] were not used, as even relative yields disagreed severely with other measurements, and sources of error of this method are not sufficiently known.

As the remaining sets of data are reasonably consistent, they were adjusted to agree in sums of yields of both mass peaks and the general procedure was followed as described in section 6.1.

Special attention had to be paid to Sm yields. No mass spectrometric measurements were made on samples irradiated in low integrated neutron flux. ^{147}Sm yields obtained in these experiments require large corrections for neutron capture and decay and were therefore considered no more reliable than the ^{147}Nd yields obtained from ratio measurements. The outstanding high value of Melaika et al [13] was not used. Calculated charge distributions [49] indicate that independent yields of ^{148}Pm and $^{150}Pm + ^{150}Sm$ could be 0.3% of ^{148}Nd and 9% of ^{150}Nd respectively. Corrections for natural Sm contamination based on this value for ^{148}Sm would lead to a "contamination correction" for ^{154}Sm of about 10 - 15% of its yield. Similarly, the amount of ^{150}Sm present in mass spectrometric measurements is generally added to the ^{149}Sm yield, but the calculated independent yields [49] of ^{150}Pm and ^{150}Sm together would be about 6% of the ^{149}Sm yield . As these independent yields have not yet been confirmed experimentally, no corrections were applied and the mass 149 yield shown in table V has to be considered as the sum of mass 149 cumulative yield and $^{150}Pm + ^{150}Sm$ independent yield.

Generally corrections for neutron capture in ^{151}Sm are not very reliable for high neutron flux irradiations, as its cross section depends strongly on the neutron spectrum. As the ^{235}U yields measured by Bunney

TABLE IV. ^{235}U FISSION YIELDS (THERMAL)

Mass No.	this work	Walker [44]	Meek Rider [22]	Croall [19]	Lisman et al [21,57] Fiss[a]	Lisman et al [21,57] Norm[b]	radiochemical measurements
72	16×10^{-5}		1.6×10^{-5}	1.6×10^{-5}			
73	0.0001		0.0001	0.00011			
74	0.00035	0.006[c]	0.00035	0.00035			
75	0.001[c]		0.0012[d]				
76	0.003[c]		0.0025[d]				
77	0.008	0.008	0.0083	0.0083			
78	0.02	0.02	0.02	0.020			
79	0.056	0.056	0.056	0.056			
80	0.11[c]	0.11[c]	0.094[d]				
81	0.22	0.22	0.18	0.22			.22±.02 [62]
82	0.35	0.35	0.24[d]				
83	0.532	0.53	0.52	0.55	0.526	0.529	.56±.04 [62]
84	1.000	1.00	0.97	1.00	1.00	1.01	.93±.05 [62]
^{85}Kr	0.288	0.273	0.271		0.2880		.273±.004 [63]
85	1.328	1.33	1.30	1.30	1.32	1.33	
86	1.97	1.96	1.89	2.03	1.94	1.95	
^{87}Br				3.2			
^{87}Rb	2.56	2.55	2.53	2.54	2.54	2.57	
88	3.62	3.62	3.58	3.55	3.61	3.61	
89	4.84	4.78	4.76	4.75			4.78±.07 [64]
90	5.91	5.88	5.83	5.55	5.90	5.93	4.02±.11 [65][e] 5.61±.22 [66][f]
91	5.93	5.91	5.90	5.8	5.90	5.92	5.62±.11[67],6.16[68]
92	5.98	6.02	5.98	6.03	5.95	5.98	
93	6.39	6.44	6.39	6.51	6.34	6.37	
94	6.45	6.47	6.44	6.50	6.41	6.45	
95	6.54	6.52	6.41	6.50	6.45	6.51	6.0±.3[69]
96	6.29	6.33	6.29	6.40	6.23	6.26	
97	6.00	6.05	6.21	5.9	5.86	5.92	5.42[64],6.2[69]
98	5.81	5.78	5.86	5.9	5.77	5.83	
99	6.11	6.16	6.16	6.14	6.14[gh]	6.24	6.16±.08 [70][h] 6.03±.08 [59][gh]

TABLE IV (continued)

Mass No.	this work	Walker [44]	Meek Rider [22]	Croall [19]	Lisman et al [21,57] Fiss[a]	Lisman et al [21,57] Norm[b]	radiochemical measurements
100	6.32	6.33	6.44	6.50	6.24	6.30	
101	5.05	5.07	5.02	5.2	5.03	5.08	
102	4.19	4.19	4.17	4.1	4.19	4.21	
103	2.95	2.85	3.0	2.85			2.92[71][h], 2.97[72][h] 1.4[73],3.7[74]
104	1.83	1.83	1.81		1.82	1.83	
105	0.90	0.83	0.90	0.83			.85±.20 [73]
106	0.387	0.39	0.39	0.38	0.389	0.389	.39±.03 [71]
107	0.17[c]	0.19	0.19	0.19			
108	0.057[c]	0.07[c]	0.07[d]				
109	0.024	0.03	0.03	0.03			.024±.003 [75]
110	0.017[c]	0.022[c]	0.018[d]				
111	0.014	0.018	0.019	0.018			.014±.002 [75]
112	0.010	0.016[c]	0.010				.012±.001 [75]
113	0.004	0.014[c]	0.016				
114	0.012	0.012[c]	0.014				
115	0.011	0.011	0.0104	0.0104			.0104[76], .0118[74]
116	0.011	0.011[c]	0.018				.010 [74]
117	0.011	0.011[c]	0.011				
118	0.011	0.011[c]	0.014				
119	0.012	0.011[c]	0.014				
120	0.013	0.012[c]	0.014				
121	0.014	0.014	0.014	0.015			.0145±.0010[31][i] .013±.002[77][i]
122	0.015	0.015[c]	0.015				
123	0.0164	0.018	0.016				.0164±.0012 [31]
124	0.024	0.022[c]	0.018				
125	0.028	0.029	0.021	0.021	0.0291		.0277[21][hj] .021[79] .0254[31][h] .036[78] .0297[31][h] .018[74]
126	0.063	0.06[c]	0.032				

TABLE IV (continued)

Mass No.	this work	Walker [44]	Meek Rider [22]	Croall [19]	Lisman et al [21,57] Fiss[a]	Norm[b]	radiochemical measurements
^{126}Sn	0.060						
127	0.11	0.13	0.137	0.10			Sn .143±.028[80] .128±.015[31] Sb .105±.004[31] .144±.020[81]
128	0.36	0.39	0.46				.36 [31][i]
^{129}Sb	0.63	0.90	1.0	1.12			.39±.03 [82] .63±.03 [31] 1.12±.28 [81]
^{129}I	0.64		1.0	0.9			.9 ± .2 [83]
130	2.00	2.0	2.1	2.0			2.0±.5 [84]
131	2.82	2.79	2.91	2.92	2.79	2.86	3.02[85],3.30[86]
132	4.20	4.16	4.26	4.37	4.16	4.27	4.49[85],4.21[86]
133	6.73	6.75	6.69	6.60	6.73	6.76	6.62[85], 7.48[86] 6.62[87], 6.75 [67]
134	7.67	7.57	7.80	8.03	7.51	7.73	8.00 [85]
135	6.55	6.51	6.43	6.41			6.37 [85]
136	6.18	6.10	6.46	6.44			
137	6.26	6.24	6.20	6.20	6.28	6.32	6.13[67],6.22[88] 6.23 ± .07 [6][j]
138	6.82	6.80	6.71	7.22	6.80	6.83	
^{139}Ba	6.55	6.56	6.48	6.55			Ba 6.55±.10 [70]
^{139}La	6.55		6.48	8.2			6.57±.02 [67]
140	6.37	6.34	6.34	6.40	6.31	6.35	6.36[88], 6.35[89] 6.36[90], 6.36[91]
^{141}Ce	5.85		6.10	6.0	5.50	5.53	
^{141}Pr	5.85	5.84	6.10	5.65			
142	5.91	5.92	5.90	5.9	5.88	5.90	
143	5.92	5.93	5.91	5.9	5.90	5.92	5.67[89], 5.93 [92]
144	5.44	5.41	5.40	5.62	5.42	5.45	
145	3.91	3.92	3.88	3.95	3.86	3.89	
146	2.96	2.97	2.95	3.05	2.95	2.97	

TABLE IV (continued)

Mass No.	this work	Walker [44]	Meek Rider [22]	Croall [19]	Lisman et al [21,57] Fiss[a]	Norm[b]	radiochemical measurements
^{147}Nd	2.22	2.23	2.19	2.24			2.23 [92]
^{147}Sm	2.22	2.23	2.19	2.30	2.12	2.14	
148	1.67	1.67	1.67	1.71	1.69	1.70	
149	1.05	1.06	1.04	1.1	1.00	1.01	1.05 [92]
150	0.644	0.65	0.65	0.67	0.638	0.640	
151	0.407	0.42	0.43	0.43	0.408	0.409	
152	0.262	0.26	0.24	0.265	0.212	0.213	
153	0.163	0.164	0.158	0.15			.160 [92]
154	0.072	0.073	0.064	0.077	0.0563	0.0564	
155	0.032	0.032	0.031	0.033			.031 [74]
156	0.014	0.013	0.0134	0.014			.0138 [92] .0125±.0010 [93]
157	0.0062	0.006	0.0066	0.0061			Eu .00618 [92] .0060 ± .0007 [83]
158	0.0031	0.0025	0.0037	0.002			.0031 ±.0006 [93]
159	0.00105	0.001	0.00105	0.001			Gd .00101 [92]
160	0.00035[c]	0.001[c]	0.00033				
161	9×10^{-5}		8.2×10^{-5}	8.7×10^{-5}			8.8×10^{-5} [92]

a Yields calculated from number of fissions

b Yields obtained by normalization technique (see text)

c Interpolated values

d Calculated yields

e Corrected for half life (28.5 a instead of 19.9 a) : 5.78
Adjusted for reference yields: 5.85 ± 0.16

f If a half life of 28.5 a instead of 28 a is used this yield becomes 5.72.

g ^{99}Tc yield determined spectrophotometrically

h Used for recommended yield

i Total chain yield

j Corrected for γ-ray intensity, as given in [52]

TABLE V. ^{233}U FISSION YIELDS (THERMAL)

Mass No.	This work	Rider et al [20]	Croall [19]	Ferguson, O'Kelly [18]	Lisman et al [6,21,57] Fiss[a]	Norm[b]	radiochemical measurements
72	0.0001[c]	9.9×10^{-5}					
73	0.00033[c]	0.00033[c]					
74	0.0009[c]	0.0009[c]		0.03[d]			
75	0.0023[c]	0.0023[c]					
76	0.0068[c]	0.0068[c]					
77	0.02	0.019	0.02	0.02			.019[96][g], .021[96][h]
78	0.04[e]	0.10[f]		0.1[e]			
79	0.09[e]	0.19[f]		0.19[e]			
80	0.18[e]	0.28[f]		0.28[e]			
81	0.33	0.46[f]	0.34	0.46[e]			.33±0.04 [62]
82	0.60[e]	0.69[f]		0.69[e]			
83	1.023	1.05	1.14	1.14	1.03	1.02	
84	1.69	1.76	1.91	1.91	1.73	1.71	.77±.08 [97] (Br)
^{85}Kr	0.507				0.512		
85	2.19	2.42	2.45	2.46	2.22	2.21	
86	2.86	2.96	3.32	3.20	2.90	2.88	
87	4.01	4.47	4.50	4.47	4.06	4.04	
88	5.54	5.37	5.36	5.36	5.57	5.56	
89	6.41	6.10	5.90	6.28			5.56[98],5.60[99] 6.66[100],6.5[96]
90	6.88	6.30	6.2	6.18	6.96	6.96	6.19[98], 6.53[99]
^{91}Sr	6.50		5.6				6.27[97],4.82[98]
^{91}Y	6.52		6.0				6.37[100] (Sr)
^{91}Zr	6.52	6.60	6.45	6.57	6.60	6.64	3.55[98] (Y)
92	6.65	6.63	6.60	6.63	6.69	6.69	6.76±.50[97](Sr)
93	7.04	7.02	6.90	7.02	7.09	7.08	6.35±.50[97](Y)
94	6.81	6.70	6.70	6.70	6.91	6.92	
^{95}Zr	6.21	6.13	6.10	6.22			5.01[98],6.15[99]
^{95}Mo	6.21	6.13	6.15	6.22	6.40	6.30	5.16[98] (Nb)
96	5.73	5.64	5.64	5.64	5.84	5.80	

TABLE V (continued)

Mass No.	This work	Rider et al [20]	Croall [19]	Ferguson O'Kelly [18]	Lisman et al [6,21,57] Fiss[a]	Norm[b]	radiochemical measurements
97	5.39	5.59	5.46	5.48	5.52	5.43	
98	5.14	5.25	5.20	5.25	5.22	5.16	
99	4.89	5.12	4.96	4.96	5.16	5.06	4.96[101],5.77[97]
100	4.38	4.49	4.45	4.49	4.46	4.41	
101	3.19	3.10	2.90	2.84	3.27	3.24	
102	2.42	2.38	2.22	2.16	2.48	2.44	
103	1.60	1.63	1.60	1.6			1.6[96][g],1.78[99] 2.02[98]
104	1.02	1.00	0.95	0.92	1.04	1.01	
105	0.54[e]	0.50[f]	0.15	0.5[e]			.146±.037 [98]
106	0.255	0.25	0.24	0.22	0.262	0.260	.259[98],.28[96][g] .23[99]
107	0.12[e]	0.12[f]		0.12[e]			
108	0.065[e]	0.07[f]		0.07[e]			
109	0.04	0.040	0.047	0.04			.04[96][g]
110	0.03[e]	0.03[f]		0.03[e]			
111	0.021	0.023	0.021	0.03			.025[96][g],.020[98] .0187±.0002 [97]
112	0.015	0.016	0.014	0.02			.0125[97],.016[96][g]
113	0.015[e]	0.02[f]		0.02[e]			
114	0.020[e]	0.02[f]		0.02[e]			
115	0.021	0.02	0.017	0.02			.020[96][g], .021[96][h]
116	0.021[e]	0.01[f]		0.01[e]			
117	0.022[k]	0.01[f]		0.01[e]			
118	0.022[k]	0.02[f]		0.02[e]			
119	0.023[k]	0.02[f]		0.02[e]			
120	0.025[k]	0.02[f]		0.02[e]			
121	0.027[e]	0.018		0.02[e]			^{121g}Sn .018[96][g]
122	0.030[k]	0.03[f]		0.03[e]			
123	0.038[e]	0.04[f]		0.04[e]			
124	0.050[k]	0.05[f]		0.05[e]			

TABLE V (continued)

Mass No.	This work	Rider et al. [20]	Croall [19]	Ferguson, O'Kelly [18]	Lisman et al [6,21,57] Fiss[a]	Norm[b]	radiochemical measurements
125	0.110[i]	0.05	0.060	0.1[e]	0.116		$^{125g}_{Sn}$ .050[96][g]
126	0.18[e]	0.26[f]		0.26[e]			
127	0.50[e]	0.61[f]	0.59	0.61[e]			.59 ±.08 [98]
128	1.00[e]	1.05[f]		1.05[e]			
129	1.56[e]	1.70[f]		1.7[e]			
130	2.40[e]	2.33[f]		2.33[e]			
131	3.54	3.46	3.55	3.41	3.51	3.50	2.84[98], 3.14[99]
^{132}Te	4.57[j]		4.32				4.32[98],4.18[99]
132	4.84	4.74	4.80	4.68	4.88	4.86	
^{133}I	6.00[j]		3.4				3.37[98],6.63[99]
^{133}Cs	6.03	5.96	5.90	5.88	6.06	6.05	
134	6.15	6.09	6.0	5.99	6.13	6.10	6.23[99] (I)
^{135}I	4.89[j]		4.78				4.84±.07[102]
135	6.27	5.2	6.0	5.84			I:4.64[99],5.21[103]
136	6.82	6.68	6.70	6.68			
137	6.85	6.58	6.65	6.64	6.93	6.94	5.39[98],6.13[104]
138	6.00	6.3	6.4	7.10	5.97	6.00	
139	6.34	6.64	5.9	6.61			6.34 [100]
^{140}Ba	6.35[j]	6.59	6.25				6.37[102],6.01 [99]
^{140}La	6.45		6.70				
^{140}Ce	6.45	6.59	6.71	6.71	6.53	6.48	
141	6.56	6.77	6.40	6.24			5.30[98],6.23[99] 7.00[100]
142	6.61	6.72	6.79	6.79	6.71	6.61	
143	5.88	5.86	5.9	5.91	5.85	5.82	6.99 [98]
^{144}Ce	4.60[j]	4.62	4.60	4.51	4.67	4.66	3.69[98],4.63[99]
^{144}Nd	4.64	4.62	4.60		4.67	4.66	
145	3.39	3.38	3.46	3.38	3.37	3.36	
146	2.53	2.54	2.60	2.58	2.53	2.52	
147	1.80	1.86	1.92	1.93	1.78	1.74	

TABLE V (continued)

Mass No.	This work	Rider et al [20]	Croall [19]	Ferguson O'Kelly [18]	Lisman et al [6,21,57] Fiss[a]	Norm[b]	radiochemical measurements
148	1.30	1.29	1.33	1.28	1.30	1.30	
149	0.76	0.77	0.80	0.77	0.773	0.744	
150	0.501	0.51	0.56	0.55	0.500	0.497	
151	0.32	0.36	0.33	0.35	0.365	0.364	
152	0.22	0.20	0.215	0.22	0.186	0.185	
153	0.107	0.12	0.13	0.15			
154	0.0449	0.03	0.048	0.047	0.0458	0.0445	
155	0.026	0.03		0.03			
156	0.012[j]	0.0116	0.0121	0.01			Eu .0117 [92]
157	0.0072	0.00635	0.00635				
158	0.0024[e]	0.0024					
^{159}Gd	0.00091	0.000905	0.00091	<0.01			
160	0.00035[e]	0.0003					
^{161}Tb	0.000118	0.00017	0.00017				

a Fission yield calculated from number of fissions

b Fission yield obtained by normalization technique (see text)

c Calculated yields of Weaver et al [95]

d Extrapolated yields

e Interpolated yields

f Assumed yields taken from reference [18]

g Data from [96], as revised by Steinberg [7]

h Data from [96], as revised by Katcoff [8]

i Reference [6], corrected for γ-ray intensity as given in [52]

j ^{132}Te, ^{133}I, ^{135}I, ^{140}Ba, ^{144}Ce and ^{156}Eu are assumed to be 94.5%, 99.5%, 78%, 98.5%, 99.2% and 96.5% of the total chain yield respectively

k Relative mass spectrometric yields of reference [61] normalized to yields of masses 115 and 125.

TABLE VI. ^{239}Pu THERMAL FISSION YIELDS

Mass No.	this work	Meek Rider [22]	Croall [19]	Katcoff [8]	Lisman et al[a] [21,57]	radiochemical measurements
72	0.00011	0.00011	0.00012	0.00012		1.1×10^{-4}[74]
73	0.00025[b]	0.00025[c]				
74	0.00062[b]	0.00062[c]				
75	0.0016[b]	0.0014[c]				
76	0.0035[b]	0.0031[c]				
77	0.0075	0.0072	0.0073			.0075[107]
78	0.028	0.026	0.025			.028[107]
79	0.06[b]	0.025[c]				
80	0.11[b]	0.048[c]				
81	0.186	0.178	0.182			.186±0.025[108]
82	0.24[b]	0.16[c]				
83	0.298	0.29	0.29	0.29	0.301	Br.312[107],.311[108]
84	0.482	0.47	0.47	0.47	0.487	Br .419[108]
^{85}Kr	0.129	0.12		0.127	0.130	.099±.004[63]
85	0.566	0.56	0.54	0.539	0.574	
86	0.764	0.75	0.75	0.76	0.770	
87	0.980	0.91	0.912	0.92	1.00	
88	1.385	1.41	1.42	1.42	1.35	
89	1.74	1.73	1.71	1.71		1.74±05[46],1.8[74],1.65[100]
90	2.13	2.2	2.05	2.25	2.09	2.05±.04[46]
^{91}Sr	2.53	2.42	2.6	2.43		2.3[74],2.37[100]
^{91}Y	2.53	2.60	2.41	2.9		2.41±.11[46],2.8[74]
^{91}Zr	2.53	2.60	2.6	2.61	2.52	Y 2.40[111]
92	3.05	3.06	3.12	3.14	3.02	
93	3.92	3.89	3.94	3.97	3.95	

TABLE VI (continued)

Mass No.	this work	Meek Rider [22]	Croall [19]	Katcoff [8]	Lisman et al.[a] [21,57]	radiochemical measurements
94	4.48	4.42	4.45	4.48	4.50	
^{95}Zr	5.07	5.2	5.06	5.8	4.86	5.06±.33[46],5.6[74]
^{95}Mo	5.07	5.2	5.0	5.03		
96	5.12	5.06	5.13	5.17	5.12	
^{97}Zr	5.61[j]	5.3	5.25	5.5	5.64	5.3[74]
^{97}Mo	5.70	5.61	5.61	5.65		
98	5.93	5.84	5.84	5.89		
99	6.33	5.9	5.86	6.10	6.59	5.61±.33[46],6.1[74] 6.66±.07[g],6.79±.15[h][109] 6.02±.18[101],6.1[110] 6.17±.19[112]
100	7.16	7.05	7.05	7.10		
101	6.01	5.86	5.86	5.91	6.50	
102	6.09	5.94	5.94	5.99	6.65	
103	5.86	5.6	5.79	5.67		5.79±.37[46],5.5[74]
104	6.03	5.88	5.88	5.93	6.61	
105	5.47	5.47	5.47	3.9		5.47±.06[46],3.7[74]
106	4.64	4.4	4.04	4.57	4.55	4.04±.22[46],4.7[74] 4.52±0.23[6m]k
107	3.3[b]	3.4[c]				
108	2.0[b]	2.6[c]				
109	1.13	1.2	1.13	1.40		1.13±.06[46],1.0[74] 1.6[110],2.0[101]
110	0.57[b]	0.75[c]				
111	0.27	0.25	0.28	0.23		.28±.04[46],.27[74] .26[101],.212[110]
112	0.11	0.10	0.093	0.12		.093±.003[46],.10[74] .15[101],.11[110]
113	0.065	0.072	0.065			.065[107]

TABLE VI (continued)

Mass No.	this work	Meek Rider [22]	Croall [19]	Katcoff [8]	Lisman et al.[a] [21,57]	radiochemical measurements
114	0.041[b]	0.055[c]				
115	0.036	0.039	0.036	0.041		.036±.002[46],.048[74] .035[101]
116	0.035[b]	0.037[c]				
117	0.035[n]	0.037[c]				
118	0.035[n]	0.035[c]				
119	0.036[n]	0.036[c]				
120	0.038[n]	0.037[c]				
121	0.041[b]	0.044		0.043		^{121}Sn .041[74]
122	0.045[n]	0.047[c]				
123	0.055[b]	0.056[c]				
124	0.075[n]	0.070[f]				
125	0.110[e]	0.069		0.071	0.116	
126	0.23[b]	0.16[c]				
127	0.55	0.46	0.55	0.39		.55±.03[46], .37[74]
128	1.0[b]	0.85[c]				
129	1.65[b]	1.7[c]				
130	2.6[b]	2.7[c]				
131	3.73	3.69	3.8	3.78	3.60	3.80±.14[46],3.6[74]
132	5.25	5.2	5.25	5.26	5.09	5.51±.27[46],4.9[74]
^{133}I	6.91[j]	5.3	5.53	5.2		5.53±.06[46],5.0[74]
133	6.94	6.6	6.90	6.91	7.18	I 6.97,Xe 7.23 [105]
134	7.43	7.31	7.47	7.47	7.20	

TABLE VI (continued)

Mass No.	this work	Meek Rider [22]	Croall [19]	Katcoff [8]	Lisman et al[a] [21,57]	radiochemical measurements
^{135}I	6.32[j]	5.7	5.97	5.7		6.04[i][102],6.36[i][103]
135	7.48	7.21	7.17	7.17	13.92	Xe 7.43 [105]
136	6.83	6.66	6.65	6.63		
137	6.62	6.56	5.8	6.63	6.74	5.40±.39[46],5.8[74]
138	5.46	5.91	6.28	6.31	5.40	
139	5.82	5.67	5.78	5.87		5.4[74],5.87[100]
^{140}Ba	5.49[j]	5.51	5.47	5.4		5.47±.32[46],5.36[74]
^{140}Ce	5.53	5.51	5.56	5.6	5.61	Ba 5.27[102]
^{141}La	5.24	5.75	5.47	5.7		5.56[100],4.58[111]
^{141}Ce	5.24	5.75	6.11	5.1		6.11±.31[46],4.99[111] 5.18±.13[112]
142	4.97	4.87	4.97	5.01	5.04	
^{143}Ce	4.48		4.28	5.3		4.28±.21[46],3.90[111]
^{143}Nd	4.48	4.52	4.57	4.57	4.48	Pr 4.16 [111]
^{144}Ce	3.75[j]		4.09	3.79		4.09±.20[46],4.9[74]
^{144}Nd	3.76	3.79	3.84	3.93	3.78	Ce 3.85±.09[112]
145	3.04	2.99	3.12	3.13	3.03	Pr 3.45[111]
146	2.49	2.45	2.57	2.60	2.49	
^{147}Nd	2.09		1.46	2.2		1.46±.08 [46]
^{147}Sm	2.09	1.87	2.07	2.07	2.15	
148	1.68	1.68	1.70	1.73	1.70	
149	1.24	1.30	1.31	1.32	1.24	Nd 1.11,Pm 1.27 [111]
150	0.97	0.96	1.01	1.01	0.965	
151	0.76	0.76	0.78	0.80	0.811	.72[111]
152	0.58	0.57	0.59	0.62	0.581	
153	0.44	0.36	0.37	0.37		.39[74],.36[111],.44[106]

TABLE VI (continued)

Mass No.	this work	Meek Rider [22]	Croall [19]	Katcoff [8]	Lisman et al[a] [6,21]	radiochemical measurements
154	0.273	0.25	0.29	0.29	0.27	
155	0.17	0.24[c]		0.23		.166[111]
156	0.12	0.09	0.07	0.11		.12[74],.062±.004[46] .121[111], .12[106]
157	0.080[j]	0.076[c]				Eu .074 [111]
158	0.045[b]	0.042[c]				
159	0.022	0.021	0.021	0.021		.021[111], .022[106]
160	0.011[b]	0.0098[c]				
161	0.0051	0.0039	0.0039	0.0039		Tb .0050[111],.0050[106]
162	0.0025[b]	0.0024[c]				
166	0.000076	0.000068	0.000068			

a Yields obtained by the normalization technique (see 4.1)
b Interpolated value
c Calculated yield, taken from Weaver et al [95]
d Original value corrected for half life (see 3.2.2, 28.5 years instead of 27.4. years.)
e Yield of Lisman et al [6 m] corrected for γ-ray intensity, as given by Martin and Blichert-Toft [52].
f Cumulative yield for stable ^{124}Sn. The independent yield for ^{124}Sb is given as 0.088 according to Marsden and Yaffe [46]
g Absolute measurement (for corrections see 7.3)
h Relative ^{99}Mo yield from ^{235}U fission. (for correction see 7.3)
i Relative ^{135}I yield normalized to 6.32 for ^{235}U thermal fission.
j Cumulative yields of ^{97}Zr, ^{133}I, ^{135}I, ^{140}Ba, ^{144}Ce and ^{151}Eu were taken to be 98.5, 99.6, 84.5, 99.2, 99,75 and 93 percent of total chain yield.
k Gamma spectrometric measurement by comparison with a ^{106}Ru standard source.
n relative mass spectrometric Sn yields (fuel rod) taken from reference [61], as relative yields do not change very much for different types of fission.

and Scadden [92] are in excellent agreement with our recommended values, the following procedure was adopted: the sum of ^{151}Sm and ^{152}Sm yields were averaged for mass spectrometric measurements. The ^{151}Pm yield of Bunney and Scadden [92], corrected for ^{151}Sm independent yield [49], was subtracted from this sum to calculate the yield of ^{152}Sm. Altogether the Sm yields shown in table V are not considered to be very reliable and have to be checked by measurements on samples irradiated in low neutron fluxes.

Relative yields of both mass peaks were normalized to the light mass peak only, as the sum of interpolated and radiochemical yields was only 3.766%. The corresponding sum in the heavy mass peak was 6.75% with the main contribution (5.55%) from interpolated yields at masses 128 to 130. Yields obtained by this normalization were 1 - 2% lower than absolute yields of [5] and [21]. The sum of absolute yields of Lisman et al [21] is 98.18% including the mass 89 value from our normalization. This could not possibly be brought in agreement with the sum of radiochemically determined yields, and therefore the normalization was left unchanged. Relative yields in the heavy mass peak were normalized to absolute Cs and Nd yields of [5] and [21] and the interpolated values for masses 128 to 130 were readjusted to make the sum of heavy mass yields 100 % . This can be justified, as the ratio of yields in the light mass peak to those of Nd and Cs obtained by Lisman et al [21] were 1-3% higher than those of other measurements [30, 41, 94].

7.3. Thermal fission yields of ^{239}Pu

Experimental data used for the evaluation of ^{239}Pu thermal fission yields are:

Mass spectrometric measurements: Lisman et al [21], Rider et al [5], Fickel and Tomlinson [15], Fritze et al [17], Fleming and Thode [16] and Krizhanski et al [45].

Ratio measurements: Dange et al. [105].

As the combined USSR measurements [28,44,45] disagreed with others, only some relative yields of [45] were used, as no corrections could be applied.

Evaluation of these yields was rather difficult because of several discrepancies that could not be resolved. Details cannot be given here and only the most important selections will be outlined.

Ru yields have only been measured for one sample by Fickel and Tomlinson [15], and disagree severely with those reported by Lisman et al [21] and Dange et al [105]. However, it was stated by Lisman et al [21] that Ru could not be completely recovered from sample dissolution. In addition their relative Ru yields (which were normalized by a ratio measurement of ^{106}Ru) are not consistent and yields in the light mass peak sum up to 103% when normalized to the heavy mass peak. Therefore only the Ru yields of Fickel and Tomlinson [15] were selected. The mass 99 yield is an average of the readjusted R-values of Dange [105] and Lisman [6m], which are in reasonable agreement. They were adopted rather than conflicting radiochemical measurements also for reasons given below.

Most difficult was the evaluation of Cs and Xe yields and needs some explanation. If the analyses of individual samples in [5,15,16,21,105] are compared, the values obtained for the ^{133}Cs yield are grouped around about 7.1% and 6.6% with no obvious systematic trends observed for measurements carried out at one laboratory. As a compromise all available ratios for this yield have been averaged. The ratio ^{133}Xe : ^{134}Xe

TABLE VII. ^{232}Th FAST FISSION YIELDS

Mass No.	This work	Harvey et al [25]	Croall [18]	Mass No.	This work	Harvey et al [25]	Croall [19]
77	0.010	0.014	0.015	104	0.08[a]		
78	0.035[a]			105	0.05		0.05
79	0.08[a]			106	0.041		0.058
80	0.2[a]	2.98[a]		107	0.04[a]		
81	0.4[a]			108	0.04[a]		
82	1.0[a]			109	0.041	0.56[a]	0.052
83	1.87	2.06	2.0	110	0.045[a]		
84	3.44	3.78	3.6	111	0.045		0.07
^{85}Kr	0.82						
85	4.0	4.01	3.9	112	0.062		0.07
86	5.66	6.21	6.0	113	0.06		0.045
87	5.99	6.57		114	0.06[a]		
88	6.32	6.92		115	0.057		0.065
89	6.72	7.14[a]	6.7	116	0.05[a]		
90	7.40	7.40	7.2	117	0.049		0.053
91	7.26	7.45	6.8	118	0.05[a]		
92	7.49		6.6	119	0.05[a]		
93	7.21	19.31[a]		120	0.05		
94	6.23[a]			121	0.055		
95	5.30	5.43	5.4	122	0.04[a]		
96	4.8[a]	4.97[a]		123	0.031	3.04[a]	0.029
97	3.96	4.52	5.2	124	0.03[a]		
98	3.4[a]	3.69[a]		125	0.033		0.025
99	2.76	2.86	2.80	126	0.05[a]		
100	1.9[a]			127	0.09		0.110
101	1.14[a]	3.97[a]		128	0.18[a]		
102	0.5[a]			129	0.36[a]		
103	0.146	0.146	0.16	130	0.8[a]		

TABLE VII (continued)

Mass No.	This work	Harvey et al [25]	Croall [18]	Mass No.	This work	Harvey et al [25]	Croall [19]
131	1.52	1.56	1.7	144	7.66	7.20	7.9
132	2.70	2.76	2.9	145	5.78	5.52	
133	3.74	3.75	3.3	146	4.95	4.73	
134	5.06	5.18	5.4	147	2.97	3.14	3.8
135	4.65	4.66	5.6	148	2.18	2.08	
136	5.30	5.44	5.7	149	1.44	0.88	0.9
137	4.61	4.60	6.5	150	1.09	1.04	
138	6.02[a]	5.79[a]		151	0.41		
139	7.38	6.99	6.8	152[a]	0.32	1.24[a]	
140	8.31	8.61	7.4	153	0.21		
141	7.28	7.74	7.3	154	0.06[a]		
142	7.22[a]	7.27[a]		155	0.01[a]		
143	7.12	6.79	7.3	156	0.0026	0.003	0.003

a Interpolated values

yields was measured by Fleming et al [16] for two samples with good agreement, however, in severe conflict with the Xe to Cs ratio of Lisman et al [21] which is based on separate determinations of these elements with rather large uncertainties for Xe. Therefore the ratio of Fleming was adopted for the normalization of Xe to ^{133}Cs and allowance was made for their margin of error towards the ratio of Lisman et al. This group of yields is, however, very unsatisfactory and should be reinvestigated.

The arguments and procedure for Sm yields are similar to that for ^{233}U, but the calculated independent yields of ^{148}Pm and ^{150}Pm are only 0.1% and 4% of the respective Nd yields.

As no direct and reliable absolute fission yield measurements are available, absolute yields were obtained by the normalization technique.

Finally, to support our argument not to rely on absolute fission yield measurements and to illustrate the uncertainty associated with such measurements, an example is given. Jain and Ramaniah [109] made two series of measurements of the ^{239}Pu fission yield of ^{99}Mo. One is based on the determination of the neutron flux, the other one relative to the ^{235}U fission yield of ^{99}Mo. They used the 2200 m/sec fission cross sections and obtained the results included in table VI, as well as 6.06% for the ^{235}U fission yield of ^{99}Mo. We recalculated their results using g and s factors from a recent survey [47b] according to

$$\hat{\sigma} = \sigma_0 (g + rs)$$

With r $\sqrt{T/To} \approx 0.0022$ calculated from the reported Cadmium ratio for Co of 200, we obtained the following results:

neutron temperature ⟶	20°C	40°C	60°C	80°C	100°C	120°C
U^{235}	6.13	6.17	6.20	6.22	6.24	6.25
Pu^{239} relative	6.32	6.22	6.09	5.98	5.84	5.71
Pu^{239} absolute	6.29	6.22	6.12	6.03	5.92	5.81

In spite of this example the data of Marsden and Yaffe were adopted for mass numbers not covered by the experiments listed above. They agree with our adopted yields at several mass numbers and therefore a renormalization was not considered necessary.

7.4. Fast fission yields of ^{232}Th

No complete set of mass spectrometric measurements is reported for fast fission yields of ^{232}Th. Therefore we had to rely mainly on ratio measurements. The references used are:

Mass spectrometric measurements: Kennett and Thode [113], Harvey et al [25];
Renormalized ratio measurements: Iyer et al [36], Harvey et al [25], Turkevich and Niday [35];
Radiochemical measurements: Bresesti et al [89], Crook and Voight [33], Broom [115], Wyttenbach and von Gunten [114].

We started with the most extensive set of yields of Iyer et al [36], normalized the mass spectrometrically determined Kr, Xe and Cs yields at mass numbers 132 and 137 and radiochemical yields at ^{140}Ba. Normalization points were selected for other data sets, which do not include those mentioned above. Mass spectrometric ratios were not changed and the gamma spectrometric measurements of Bresesti et al [89] were considered superior to others, especially for the yields of ^{141}Ce and ^{144}Ce, which depend on decay curve resolution in measurements of β-spectra. Fission yield ratios may change, when going from a fast reactor neutron spectrum to 3 MeV fission. But it is assumed, that a ratio of neighbouring mass yields will not change apreciably and therefore the ^{92}Sr yield reported by Broom was calculated relative to the adopted ^{91}Sr yield. Other yields reported for 3 MeV fission of ^{232}Th, including those of Lyle et al [116,117], were not used.

All relative yields were finally normalized to a total of 100% for the sum of yields in the heavy mass peak, as many mass numbers in the light mass peak are not covered by experiments. In the evaluation of Harvey et al [25], shown for comparison in table VII, each mass peak was normalized to 100%.

7.5. Uncertainties of recommended yields

It is difficult to assign uncertainties to values obtained by a normalization of relative yields. An attempt to derive accuracies of 235U fission yields from the data used will be discussed in detail

in a forthcoming publication. Judging from the overall agreement with experimentally determined absolute yields and the consistency of the data used to obtain relative yields, we assign the following uncertainties:

^{235}U: 0.7% - 1%, except Kr, Xe and Sm (about 2%)

^{233}U: 1.5% - 2%, except Sm (3%)

^{239}Pu: 2 - 3%, due to the unresolved inconsistencies

No comparison is possible for ^{232}Th and therefore the accuracy of these yields is believed to be not better than 5%.

REFERENCES

[1] BUBA, L., HICK, H., RUMPOLD, K., Atomkernenergie 11 (1966) 167.

[2] HIGATSBERGER, M.J., HICK, H., RUMPOLD, K., WEINZIERL, P., BURTSCHER, A., Int. Sympos. nuclear Materials Management (Proc. Sympos. Vienna,1965) IAEA, Vienna (1966) 817.

[3] PEPELNIK, R., HICK, H., Nucl. Instr. Meth. 68 (1969) 240.

[4] EDER, O.J., LAMMER, M., this symposium, paper SM-170/12.

[5] RIDER, B.F., RUIZ, C.P., PETERSON, J.P.,Jr., SMITH, F.R., Accurate Nuclear Fuel Burnup Analyses, quarterly prog. rep., USAEC documents

a) GEAP-5060 (1965) ^{235}U thermal fission yields
b) GEAP-5270 (1966) ^{233}U thermal fission yields
c) GEAP-5403 (1966) ^{239}Pu thermal fission yields
d) GEAP-5505 (1967) ^{241}Pu thermal and ^{238}U fast fission yields

[6] LISMAN, F.L., MAECK,W.J., REIN,J.E., FOSTER, R.E., Jr., ABERNATHEY,R.M., DELMORE,J.E., Jr., EMEL, W.A., KUSSY, M.E., MCATEE, R.E., WORKMAN, G.D., Burnup Determination of Nuclear Fuels, quarterly prog.rep., USAEC documents

a) IDO-14660 (1965), ^{235}U thermal fission yields, capsule 6-4-1
b) IDO-14663 (1965), ^{233}U thermal fission yields, capsule 6-4-2
c) IDO-14667 (1965), ^{233}U thermal fission yields, capsule 6-4-3, ^{235}U thermal fission yields, capsule 6-6-2
d) IDO-14676(1966), ^{235}U thermal fission yields, capsules 6-4-1 and 6-6-2.
e) IDO-14681 (1967), ^{233}U thermal fission yields, capsules 6-2-4 and 6-5-1.
f) IN-1064 (1967), ^{233}U and ^{235}U thermal fission yields, all capsules.
g) IN-1113 (1967), ^{233}U and ^{235}U thermal fission yields, all capsules.
h) IN-1157 (Rev.) (1967), ^{233}U and ^{235}U thermal fission yields, all capsules.
i) IN-1178 (1967), ^{235}U thermal fission yields, capsule 6-5-3
j) IN-1189 (1968), ^{239}Pu thermal fission yields
k) IN-1207 (1968), ^{235}U fast fission yields
l) IN-1215 (1968), ^{241}Pu thermal fission yields
Final Report
m) IN-1277 (1969), ^{239}Pu fast fission yields, revised ^{239}Pu thermal fission yields, ratio measurements, summary of all fission yields.

[7] STEINBERG, E.P., GLENDENIN, L.E., Int. Conf. peaceful Uses atom. Energy (Proc.Conf. Geneva, 1955) 7, UN, New York (1956)3.

[8] KATCOFF,S., Nucleonics 18 11 (1960) 201.

[9] WANLESS, R.K., THODE, H.G., CanJ.Phys. 33 (1955) 541.

[10] PETRUSKA, J.A., MELAIKA, E.A., TOMLINSON, R.H., Can.J.Phys. 33(1955)640.

[11] PETRUSKA, J.A., THODE, H.G., TOMLINSON, R.H., Can. J. Phys. 33 (1955) 693.

[12] BLADES, A.T., FLEMING, W.H., THODE, H.G., Can. J. Chem. 34 (1956)233.
[13] MELAIKA, E.A., PARKER, M.J., PETRUSKA, J.A., TOMLINSON, R.H., Can.J. Chem. 33 (1955) 830.
[14] FLEMING, W., TOMLINSON, R.H., THODE, H.G., Can.J. Phys. 32 (1954) 522.
[15] FICKEL, H.R., TOMLINSON, R.H., Can. J.Phys. 37 (1959) 916 and 926.
[16] FLEMING, W., THODE, H.G., Can.J. Chem. 34 (1956)193.
[17] FRITZE, K., McMULLEN, C.C., THODE, H.G., Int. Conf. peaceful Uses atom. Energy (Proc. Conf. Geneva, 1958) 15, UN, New York (1958) 436.
[18] FERGUSON, R.L., O'KELLY, G.D., USAEC Rep. ORNL-3305 (1962).
[19] CROALL, I.F., UKAEA Rep. AERE-R-5086 (1967).
[20] RIDER, B.F., RUIZ, C.P., PETERSON, J.P., Jr., SMITH, F.R., USAEC Rep. GEAP-5356 (1967).
[21] LISMAN, F.L., ABERNATHEY, R.M., MAECK, W.J., REIN, J.E., Nucl. Sci. Engng. 42 (1970) 191
[22] MEEK, M.E., RIDER, B.F., USAEC Rep. APED-5398-A (Rev.) (1968).
[23] ALLEN, M.S., DRAKE, M.K., quoted in USAEC Rep. GA-8854 (1969), 59.
[24] DAVIES, W., Radiochimica Acta 12 4 (1969) 173.
[25] HARVEY, J.W., CLARKE, W.B., GORMAN, D.J., TOMLINSON, R.H., Can. J.Phys. 46 (1968) 2911
[26] TOMLINSON, R.H., MATHEWS, C., (1965) unpublished.
[27] BORG, S., BERGSTRÖM, I., HOLM, G.B., RYDBERG, B., DE GEER, L.E., RUDSTAM, G., GRAPENGIESSER, B., LUND, E., WESTGAARD, L., Nucl. Instr. Meth. 91 (1971) 109.
[28] ANIKINA, M.P., ARON, P.M., GORSHKOV, V.K., IVANOV, R.N., KRIZHANSKY, L.M, KUKAVADSE, G.M., MURIN, A.N., REFORMATSKY, I.A., ERSHLER, B.V., Int. Conf. peaceful Uses atom. Energy (Proc. Conf. Geneva, 1958) 15, UN, New York (1958) 446.
[29] GORSHKOV, V.K., IVANOV, R.N., KUKAVADSE, G.M., REFORMATSKY, I.A., J. Nucl. Energy 8 (1958) 69.
[30] IVANOV, R.N., GORSHKOV, V.K., ANIKINA., M.P., KUKAVADSE, G.M., ERSHLER, B.W., J. Nucl. Energy 9 (1959) 56.
[31] ERDAL, B.R., WILLIAMS, J.C., WAHL, A.C., J. inorg. nucl. chem. 31 (1969) 2993.
[32] SANTRY, D.C., YAFFE, L., Can. J. Chem. 38 (1960) 421.
[33] CROOK, J.M., VOIGT, A.F., USAEC Rep. IS-558 (1963)
[34] LARSEN, R.P., MEYER, R.J., USAEC Rep. ANL-7225 (1966) 232, (details in ANL-6900 (1964) 339).
[35] TURKEVICH, A., NIDAY, J.B., Phys. Rev. 84 (1951) 52.
[36] IYER, R.H., MATHEWS, C.K., RAVINDRAN, N., RENGAN, K., SINGH, D.V., RAMANIAH, M.V., SHARMA, H.D., J. inorg. nucl. chem. 25 (1963) 465.
[37] FARRAR, H., FICKEL, H.R., TOMLINSON, R.H., Can. J. Phys. 40 (1962)72.
[38] FARRAR, H., TOMLINSON, R.H., Nucl. Phys. 34 (1962) 367.
[39] CHU, Y.Y., U. of Calif. Rep. UCRL-8926 (1959).
[40] BIDINOSTI, D.R., IRISH, D.E., TOMLINSON, R.H., Can. J. Chem. 39 (1961) 628.
[41] ANIKINA, M.P., IVANOV, R.N., KUKAVADZE, G.M., ERSHLER, B.W., J.Nucl. Energy 9 (1959) 167.
[42] KUKAVADZE, G.M., GOL'DIN, L.L., ANIKINA, M.P., ERSHLER, B.W., Int. Conf. peaceful Uses atom. Energy (Proc. Conf. Geneva, 1955) 4, UN, New York (1956)230.
[43] GORSHKOV, V.K., ANIKINA, M.P., Sovj. J. Atom. Energy 7 (1960) 649.
[44] KRIZHANSKY, L.M., MURIN, A.N., Soviet J. Atomic Energy 4 (1958) 95.
[45] KRIZHANSKY, L.M., MALY, YA., MURIN, A.N., PREOBRAZHENSKY, B.K., J.Nucl. Energy 6 (1957) 260.
[46] MARSDEN, D.E., YAFFE, L., Can.J. Chem. 43 (1965) 249.
[47] a) HANNA, G.C., WESTCOTT, C.H., LEMMEL, H.D., LEONARD, B.R., Jr., STORY, J.S., ATTREE, P.M., Atomic Energy Rev. 7 4 (1969) 3
b) LEMMEL, H.D., IAEA, private communication (December 1972), preliminary results of the 1973 revision of 2200 m/sec constants.

[48] WAHL, A.C., NORRIS, E.A., ROUSE, R.A., WILLIAMS, J.C., Int. Conf. Phys. Chem. of Fission (Proc. Sympos. Vienna, 1969), IAEA, Vienna (1969) 830.
[49] CROUCH, E.A.C., UKAEA Report AERE-R-6056 (1969)
[50] MEEK, M.E., RIDER, B.F., USAEC Report NEDO-12154 (1972)
[51] HICK, H., LAMMER, M., Int. Conf. Progress in Safeguards Techniques (Proc. Sympos. Karlsruhe, 1970) 1, IAEA, Vienna (1970) 533, and report SGAE-PH-98 (1970).
[52] MARTIN, M.J., BLICHERT-TOFT, P.H., Nuclear Data A 8 (1970) 1.
[53] REYNOLDS, S.A., EMERY, J.F., USAEC report ORNL-4466 (1970) 75.
[54] WALKER, W.H., Int. Conf. Nuclear Data for Reactors (Proc. Sympos. Helsinki, 1970) 1, IAEA, Vienna (1970) 685.
[55] WALKER, W.H., A.E. Canada reports
a AECL-3037, Part I (1969)
b AECL-3037, Part II (1973)
[56] WALKER, W.H., this symposium, paper SM-170/34.
[57] LISMAN, F.L., ABERNATHEY, R.H., FOSTER, R.E., Jr., MAECK, W.J., J. inorg. nucl. chem. 33 (1971) 643
[58] COOK, J.L., Australian A.E.C. Report AAEC/TM-549 (1970), UKAEA library of fission product cross sections.
[59] HAWKINGS, R.C., EDWARDS, W.J., OLMSTEAD, W.J., Can.J.Phys. 49 (1971) 785.
[60] LUM-HEE, G., TOMLINSON, R.H., A.E. of Canada report AECL-3776 (1970) 96.
[61] DE LAETER, J.R., THODE, M.G., Can.J. Phys. 47 (1969) 1409.
[62] CROALL, I.F., WILLIS, H.H., J. inorg. nucl. chem. 24 (1962) 221.
[63] KATCOFF, S., RUBINSON, W., J.inorg. nucl. chem. 27 (1965) 1447.
[64] REED, G.W., TURKEVICH, A., Phys. Rev. 92 (1953) 1473.
[65] REED, G.W., Phys. Rev. 98 (1955) 1327.
[66] BAYHURST, B.P., USAEC report TID-5787 (1957).
[67] BAERG, A.P., BARTHOLOMEW, R.M., Can.J. Chem. 35 (1957) 980.
[68] BUNNEY, L.R., SCADDEN, E.M., J. inorg. nucl. chem. 27 (1965) 273, ^{235}U yields renormalized to 6.11% for ^{99}Mo, ^{233}U yields readjusted to adopted ^{235}U yields and normalized at adopted ^{144}Ce yield for ^{233}U.
[69] CORYELL, C.D., SAKAKURA, A.Y., ROSS, A.M., Phys. Rev. 77 (1950) 755
[70] VON GUNTEN, H.R., HERMANN, H., Radiochim. Acta 8 (1967) 112
[71] HARDWICK, W.H., Phys. Rev. 92 (1953) 1072, readjusted to adopted ^{137}Cs and ^{140}Ba yields.
[72] BALCARCZYK, L., KERATSCHEV, P., LANZEL, E., Nukleonik 7 4 (1965) 169, readjusted to adopted ^{140}Ba reference yield.
[73] WILES, D.R., CORYELL, C.D., Phys. Rev. 96 (1954) 696.
[74] CORYELL,C.D., SUGARMAN,N., Eds., "Radiochemical Studies: the fission products", Appendix B, National Nuclear Energy Series, Div.IV, 9, McGraw-Hill, New York. (1951).
[75] FORD, G.P., LEACHMAN, R.B., (1965), quoted by Wahl et al [48].
[76] WAHL, A.C., BRONNER, N.A., Phys. Rev. 85 (1952) 570.
[77] WEISS, H.V., Phys. Rev. 139 (1965) B 304.
[78] GLENDENIN, L.E., FLYNN, K.F., (1966), quoted by Erdal et al [31].
[79] ARAS, N.K., GORDON,G.E., J. inorg. nucl. chem. 28 (1966) 763.
[80] PAPPAS, A.C., STROM, P.O., WESTGAARD, L., J. inorg. nucl. chem. 30 (1968) 890.
[81] HAGENBØ, E., J. inorg. nucl. chem. 28 (1966) 763.
[82] BIRGUEL, O., LYLE, S.J., Radiochim. Acta 8 (1967) 9
[83] PURKAYASTHA, B.C., MARTIN, G.R., Can. J. Chem. 34 (1956) 293.
[84] PAPPAS, A.C., WILES, D.R., J. inorg. nucl. chem. 2 (1956) 69.
[85] PAPPAS, A.C., Massachusetts Inst. of Technol., technical report no. 63 (1953), values as quoted by Steinberg and Glendenin [7].
[86] STROM, P.O., LOVE, D.L., GREENDALE,A.E., DELUCCHI, A.A., SAM , D., BALLOU, N.E., Phys. Rev. 144 (1966) 984.

[87] KATCOFF S., RUBINSON,W., Phys. Rev. 91 (1953) 1458.
[88] BROWN, F., J. inorg. nucl. chem. 1 (1955) 248
[89] BRESESTI, M., BUREI, G., FERRARI, P., MORETTO, L., J. inorg. nucl. chem. 29 (1967) 1189, readjusted to adopted value of ^{140}Ba reference yield.
[90] CIUFFOLOTTI, L., Energ. Nucleare 15 (1968) 272.
[91] SANTRY, D.C., YAFFE, L., Can.J. Chem. 38 (1960) 464.
[92] see reference [68].
[93] DANIELS, W.R., HOFFMAN, D.C., Phys. Rev. 145 (1966) 911.
[94] GORDON,G.E., HARVEY, J.W., NAKAHARA, H., Nucleonics 24 12 (1966) 62, readjusted to adopted ^{235}U reference yields and normalized to adopted ^{143}Ce and ^{144}Ce yields.
[95] WEAVER, L.E., STROM, P.O., KILLEEN, P.H., US Naval Radiol.Defense Lab report USNRDL-TR-633(1963).
[96] STEINBERG, E.P., SEILER, J.A., GOLDSTEIN, A., DUDLEY, A., USAEC report MDDC-1632 (1948), yields as revised by Steinberg (1954) and quoted in reference [7].
[97] CHUL LEE,AMIEL, S., YELLIN, E., ISRAEL AEC report IA-1168 (1967), readjusted to adopted value of ^{140}Ba reference yield.
[98] SANTRY,D.C., YAFFE,L., Can. J. Chem. 38 (1960) 421.
[99] GANAPATHY, R., TIN MO, MEASON, J.L., J. inorg. nucl.chem. 29 (1967) 257, readjusted to adopted value of ^{99}Mo reference yield.
[100] BARTHOLOMEW, R.M., MARTIN, J.S., BAERG, A.P., Can.J. Chem.37 (1959) 660, readjusted to adopted value of ^{140}Ba reference yield.
[101] FORD, G.P., GILMORE, J.S., USAEC report LA-1997 (1956).
[102] OKAZAKI, A., WALKER, W.H., Can. J. Phys. 43 (1965) 1036, values renormalized to adopted ^{235}U reference yields of ^{135}I and ^{140}Ba.
[103] NISLE, R.G. STEPAN, I.E., Nucl. Sci. Engng. 31 (1968) 241, values renormalized to adopted ^{235}U reference yield of ^{135}I.
[104] ONDREJCIN, R.S., J. inorg. nucl. chem. 28 (1966) 1763.
[105] DANGE, S.P., JAIN, M.C., MANOHAR, S.B., SATYAPRAKASH, K., RAMANIAH, M.V., RAMASWAMI, A., RENGAN, K., Int. Conf. Physics Chem. of Fission (Proc. Sympos. Vienna, 1969), IAEA, Vienna (1969) 741, readjusted to adopted ^{235}U reference yields and normalized to adopted ^{144}Ce yield.
[106] BUNNEY, L.R., SCADDEN, E.M., ABRIAM, J.O., BALLOU, N.E., Int. Conf. peaceful Uses atom. Energy (Proc. Conf. Geneva, 1958) 15, UN, New York (1958)444, readjusted to adopted ^{235}U reference yields and normalized to adopted ^{144}Ce yield.
[107] CROALL, I.F., WILLIS, H.H., Int. Conf. Phys. Chem. of Fission (Proc. Sympos. Salzburg, 1965) 1, IAEA, Vienna (1965) 355, readjusted to adopted ^{235}U reference yields and normalized to adopted ^{99}Mo yields.
[108] CROALL,I.F., WILLIS, H.H., J. inorg.nucl.chem. 25 (1965) 1213, readjusted to adopted yields of ^{99}Mo and ^{140}Ba.
[109] JAIN,H.C., RAMANIAH, M.V., Government of India AEC report BARC-584 (1971).
[110] KIRBY, L.J., USAEC report HW-77609 (1963) 3.1.
[111] SKOVORODKIN, N.V., SOROKINA, A.V., BUGORKOV, S.S., KRIVOKHATSKII, A.S., PETRZHAK, K.A., Radiokhimiya 12 (1970) 487, 492.
[112] SOROKINA, A.V., SKOVORODKIN, N.V., BUGORKOV, S.S., KRIVOKHATSKII, A.S., PETRZHAK, H.A., Atomnaya Energiya 31 (1971) 99.
[113] KENNETT, T.J., THODE, H.G., Can. J. Phys. 35(1957) 969.
[114] WYTTENBACH,A., VON GUNTEN, H.R., Int. Conf. Phys.Chem. of Fission (Proc. sympos. Salzburg, 1965) 1, IAEA, Vienna (1965) 414.
[115] BROOM, K.M., Phys. Rev. 133 (1964) B 874
[116] LYLE, S.J., MARTIN, G.R., RAHMAN, M., Radiochim. Acta 9 (1968) 90.
[117] LYLE, S.H., SELLARS, J., Radiochim. Acta 12 (1969) 43.
[118] FARRAR, H., CLARKE, W.B., THODE, H.G., TOMLINSON, R.H., Can.J. Phys. 42 (1964) 2063.

DISCUSSION

Miss K. WAY: Do you have any apprehensions about omitting values far from the average?

M. LAMMER: For the majority of omitted values, there were good reasons for leaving them out, for example, when the nuclear data were out of date and the measured values could not be corrected. In some cases we trusted the results of certain experiments more than others if we had the opportunity to check their reliability. On the other hand, let us take the case where three values agree and a fourth value does not: if this single value is in error it distorts the average but if it is the only correct one, the average will differ considerably from this value. Nevertheless, any rejected data should be referred to in an evaluation together with the reasons for not including them.

NEED OF NUCLEAR LEVEL SCHEMES FOR CALCULATED CROSS-SECTIONS OF FISSION-PRODUCT NUCLEI

H. GRUPPELAAR
Reactor Centrum Nederland,
Petten,
The Netherlands

Abstract

NEED OF NUCLEAR LEVEL SCHEMES FOR CALCULATED CROSS-SECTIONS OF FISSION-PRODUCT NUCLEI.

For many fission product nuclei, no measurements of fast neutron cross-sections are available; for other fission-product nuclei, only a few measured points are known. Therefore, calculated cross-sections are needed to provide a set of data with adjustable parameters. Adjustments to cross-section data can be applied by using experimental data of differential measurements from accelerators or by using results of integral experiments like the reactivity worths measured in the Dutch STEK reactor. In the energy range between 0.1 MeV and 3 MeV, which is important for fast-breeder reactors, a good knowledge of excitation energies, spins and parities of levels in the target nucleus is necessary for the calculation of both the neutron inelastic-scattering cross-section and the neutron absorption cross-section. In the present paper, the need of level-scheme information and the desirability of a compilation and/or evaluation of these data for practical calculations of fission product neutron cross-sections will be discussed.

1. INTRODUCTION

In fast breeder reactor calculations cross sections of about 150 fission product nuclei in the mass range $81 \leq A \leq 164$ are important. The required accuracy for the capture cross section at energies from about 100 eV to 10 MeV is generally stated to be ±10% [1,2]. Since for the majority of these nuclei no cross section measurements have been performed in the entire energy range of interest, one often has to rely on evaluations primarily based on calculations with phenomenological nuclear models. In some cases cross section measurements will hardly be possible, since for many isotopes not enough target material is available, or because targets are highly radioactive. To overcome these difficulties, effective cross section measurements in different well-defined fast reactor spectra might be of great help. Experiments of this kind are being performed at Petten in the STEK facility [8], where the reactivity of a large number of individual isotopes, listed in table I, is measured in five different neutron spectra. To evaluate the results of these integral measurements, the application of a statistical adjustment technique on calculated effective cross sections is foreseen [8]. The cross sections depend on a limited number of parameters which influence the cross section in a wide energy range and a large number of parameters which show a more local effect, such as resonance parameters, and excitation energies, spins and parities of the target nucleus. Uncertainties in these parameters need to be known before adjustment calculations can be applied. In the present note some remarks will be made about the influence of uncertainties in the level scheme of the target nucleus, particularly on the capture cross section of fission product isotopes as a result of competitive inelastic neutron scattering.

TABLE I. ISOTOPES MEASURED AT STEK[a)]

^{90}Zr	^{98}Mo	^{107}Pd	^{132}Xe	^{142}Nd	^{149}Sm
^{91}Zr	^{100}Mo	^{108}Pd	^{134}Xe	^{143}Nd	^{150}Sm
^{92}Zr	^{99}Tc	^{110}Pd	^{136}Xe	^{144}Nd	^{151}Sm
^{93}Zr	^{101}Ru	^{109}Ag	^{133}Cs	^{145}Nd	^{152}Sm
^{94}Zr	^{102}Ru	^{111}Cd	^{135}Cs	^{146}Nd	^{154}Sm
^{96}Zr	^{104}Ru	^{128}Te	^{137}Cs	^{148}Nd	^{151}Eu
^{92}Mo	^{103}Rh	^{130}Te	^{139}La	^{150}Nd	^{153}Eu
^{94}Mo	^{104}Pd	^{127}I	^{140}Ce	^{147}Pm	^{156}Gd
^{95}Mo	^{105}Pd	^{129}I	^{142}Ce	^{147}Sm	^{157}Gd
^{97}Mo	^{106}Pd	^{131}Xe	^{141}Pr	^{148}Sm	^{159}Tb

a) Underlined isotopes are fission products with a reactivity effect of more than 1% of the total fission product mixture in a typical fast reactor.

2. PRESENT SITUATION

Only for about one third of the isotopes listed in table I, one or more measured cross section points at energies above 0.1 MeV are available.

In the energy range from 1 keV up to 10 MeV evaluations of capture cross sections of many fission products, based on the statistical model, have been published by Benzi et al. [3,4] and Cook et al. [5], who used the same cross sections in the high-energy range. Calculations of fast neutron capture cross sections for inclusion in the ENDF/B-III nuclear data library have been reported by Schenter and Schmittroth [6]. All authors estimate a maximum error of about ±50% in the calculated cross sections.

Information on level schemes is currently being published in the Nuclear Data Sheets. Unfortunately, for about 50 of the 60 nuclei listed in table I the most recent evaluation is more than five years old. For nuclei in the mass range $91 \leq A \leq 139$ recent level schemes have been compiled without evaluation [7]. In general, the number of unambiguous spin-parity assignments is rather low and often uncertainties in the level scheme arise already at energies below 1 MeV.

3. EFFECTS OF UNKNOWN INELASTIC SCATTERING

To study the influence of unknown inelastic scattering on $\sigma_{n\gamma}$ and $\sigma_{nn'}$ Hauser-Feshbach calculations have been performed, using the codes FISPRO [9] and SASSI [10], which were kindly supplied to us by Prof. V. Benzi. The same parameters as used in [3,4] were utilized and only the level scheme of the target nucleus was varied.

For a number of nuclei (^{95}Mo, ^{103}Rh, ^{107}Pd, ^{109}Ag, ^{133}Cs), with recently evaluated level schemes, cross section calculations have been performed. The results of these calculations were compared with earlier evaluations of Benzi et al. [3,4]. In general deviations from 10% to 30% in the energy range from 0.1 to 3 MeV were found both in $\sigma_{n\gamma}$ and $\sigma_{nn'}$. Since for most of the nuclei investigated the present level schemes still do contain many ambiguities, uncertainties of the same order of magnitude might be expected even in the most up to date calculations.

As an example, consider the important unstable fission product nucleus ^{107}Pd for which a recent level scheme evaluation is available [11]. In table II is shown that for most excited states two J^π values are possible; the most probable one is given as the "first" possibility. The difference between the level scheme used in the 1970 cross section calculation [4] and the present one (both drawn in fig. 1) is the inclusion of five additional levels. As a result $\sigma_{n\gamma}$ decreases and $\sigma_{nn'}$ increases an amount of at most 30%, which can be seen from fig. 1. At neutron energies above 1.5 MeV the Weisskopf-Ewing model, which is also adopted in the FISPRO code, was used. In between 0.9 MeV and about 1.5 MeV a smooth curve is drawn in order to match the Hauser-Feshbach and continuum calculations.

In the above mentioned example the change in cross section was mainly caused by an increased number of levels and did not depend very much on the values of J^π, which was found from a calculation in which the second spin possibility, listed in table II, was prefered. Apparently this is due to the high value of the spin of the ground state ($J^\pi = 5/2^+$), which weakens the influence of the angular momentum and parity selection rules.

If the spin of the ground state is low and the level density not too high (e.g. for even-even nuclei), the spins and parities of individual excited states may be very important. This can be demonstrated clearly for ^{103}Rh, where the level scheme is well known [12] up to 0.65 MeV: J^π = $1/2^-$, $7/2^+$, $9/2^+$, $3/2^-$, $5/2^-$, $5/2^+$, $7/2^+$ for E_x = 0, 0.040, 0.093, 0.295, 0.358, 0.537, 0.650 MeV, respectively. If the spin of the excited state were 3/2 instead of 7/2, the capture cross section would decrease drastically with a maximum change of 40% in the region between 0.05 and 1 MeV, due to angular momentum selection rules. Less pronounced effects can be shown for a change in parity of some particular levels.

For a number of nuclei (e.g. ^{93}Zr, ^{129}I, ^{151}Sm) the level scheme is rather unknown, so that Hauser-Feshbach calculations cannot be performed in the energy region above 100 keV.

4. CONCLUSIONS AND FINAL REMARKS

Effects in $\sigma_{n\gamma}$ and $\sigma_{nn'}$ due to missing levels in the target nucleus or due to unknown J^π values can be large, with a maximum* of about 30-50% at energies between 0.1 and 3 MeV, which is larger than required in [1,2]. In general the spin and parity of the first excited state is well known, so that for many even-even nuclei uncertainties in the cross section do not occur below 0.5 MeV.

It can be concluded that level scheme information on fission product nuclei for excitation energies up to 3 MeV is important for accurate cross section evaluations. This might give additional stimulus to nuclear spectroscopists and level scheme evaluators. A convenient type of evaluation is that of Nuclear Data Sheets. It would be very useful if in case of ambiguities the most probable J^π value were clearly indicated (e.g. like in table II).

---

* Effects in the inelastic scattering to individual levels can be much larger.

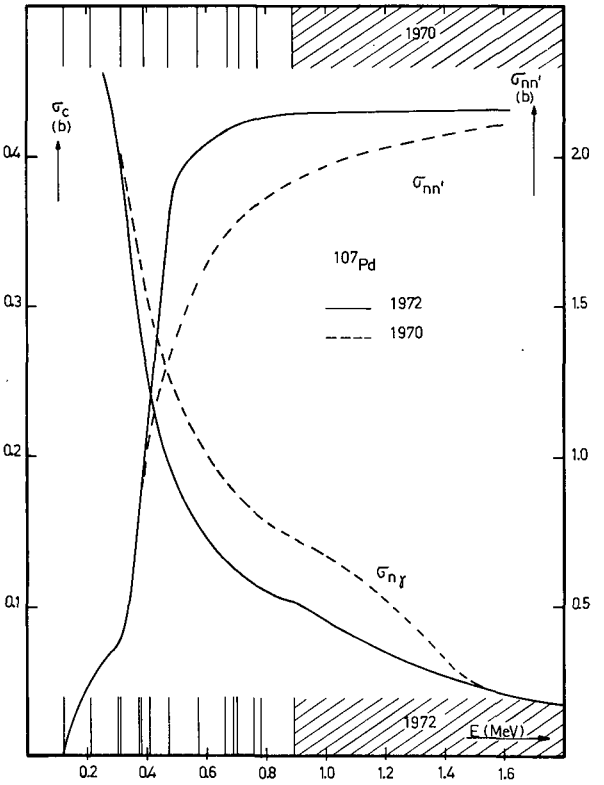

FIG. 1. Calculated capture and inelastic-scattering cross-section for ^{107}Pd for two different level schemes, labelled with "1970" and "1972" (see Table II). Continuum calculations have been performed for excitation energies above 0.9 MeV.

Some final comments will be made on the effects of level-scheme uncertainties on fast reactor parameters. For a fast breeder reactor the most important part of the neutron spectrum with respect to capture is below 0.2 MeV. In the worst case (50% change in $\sigma_{n\gamma}$ for $E_n = 0.2$ to 1.4 MeV), the change in the absorption reaction rate for an average fission product in a typical fast breeder reactor is not more than 4% (in the case of ^{107}Pd, Fig. 1, the level scheme uncertainty produces a 1% reactivity uncertainty). The influence of level-scheme uncertainties to the breeding ratio was not investigated. From a paper submitted to this symposium [13] it appears that the contribution of fission products to the breeding ratio cannot be neglected in this energy range. Errors of less than 15% [13] are required in $\sigma_{n\gamma}$ and $\sigma_{nn'}$ in the energy range where level-scheme uncertainties might influence the cross-sections. This has been calculated for a mixture of all fission-product nuclei. For individual fission-product nuclei it seems that the commonly assumed goal [1,2] of 10% inaccuracy in the capture cross-section is somewhat overestimated for present reactor calculations above 0.2 MeV.

TABLE II. LEVEL SCHEME OF ^{107}Pd

1970 [a]		1972 [b]	
E_x (MeV)	J^π	E_x (MeV)	J^π
0.0	$5/2^+$	0.0	$(5/2)^+$
0.115	$1/2^+$	0.1157	$1/2^+$
0.210	$11/2^-$	0.214	$(11/2)^-$
		0.3028	$(5/2,3/2)^+$
0.307	$7/2^+$	0.3122	$(7/2,9/2)^+$
		0.3482 [c]	
		0.366	$(7/2,9/2)^+$
0.390	$3/2^+$	0.3819	$(3/2,5/2)^+$
		0.3924 [c]	
		0.412	$1/2^+$
0.470	$3/2^+$	0.4712	$(3/2,5/2)^+$
0.570	$5/2^+$	0.5677	$(5/2,3/2)^+$
0.670	$7/2^+$	0.6701	$(5/2,3/2)^+$
		0.685	$(7/2^-)$ [d]
0.700	$1/2^+$	0.698	$1/2^+$
0.770	$3/2^+$	0.759	$(3/2,5/2)^+$
		0.781	$(1/2,3/2)^-$
		0.806 [c]	
0.890	$1/2^+$	0.889	$1/2^+$

a) Level scheme used in the 1970 cross section calculation [4].

b) Level scheme from [11]. If more than two J^π values are possible, the first possibility in general is more likely.

c) Not used in the cross section calculation shown in fig. 1.

d) Not adopted in [11].

In the last reactor core which is foreseen in the STEK project, the reactivity will be more sensitive to the MeV range. However, the change in reactivity for ^{107}Pd in the above mentioned example still is not more than 2.5%. In this reactor core, but also in some of the other STEK cores, inelastic scattering contributes significantly to the reactivity worth. Thus uncertainties in the level scheme will effect the calculated reactivity worth as a result of uncertainties both in $\sigma_{n\gamma}$ and $\sigma_{nn'}$. Therefore a good knowledge of the level scheme of a number of fission product isotopes is important for the evaluation of results from STEK.

REFERENCES

[1] GREEBLER, P., HUTCHINS, B.A., COWAN, C.L., Second Int. Conf. on Nuclear Data for Reactors (Proc. Conf. Helsinki, 1970), Vol. 2, IAEA, Vienna (1970) 17.
[2] Renda 72, IAEA, Vienna (1972), Rep. INDC(SEC)-27/L.
[3] BENZI, V., D'ORAZI, R., REFFO, G., VACCARI, M., Fast Neutron Radiative Capture Cross Sections of Stable Nuclei with 29 ≤ A ≤ 79, Rep. CNEN-RT/FI(72)6 (1972).
[4] BENZI, V., PANINI, G.C., REFFO, G., VACCARI, M., Discrete and Continuum Inelastic Scattering Cross Sections for Neutrons up to 10 MeV (1970), data available via CCDN Neutron Data Compilation Centre.
[5] COOK, J.L., Fission Product Cross Sections, Rep. AAEC/TM-549 (1970), and ROSE, E.K., The AAEC Fission Product Cross Section Libraries FISPROD.POINTXSL and FISPROD.GROUPXSL, Rep. AAEC/TM-587 (1971).
[6] SCHENTER, R.E., SCHMITTROTH, F.A., Cross Section Evaluations of 27 Fission Product Isotopes for ENDF/B-III, Rep. HEDL-TME-71-143 (1971).
[7] BASS, W.T., HOREN, D.J., EWBANK, W.B., Current Nuclear Level Schemes: A = 91 to 117, Rep. ORNL-4627 (1970), and HOREN, D.J., Current Nuclear Level Schemes: A = 118 to 139, Rep. ORNL-4730 (1971).
[8] BUSTRAAN, M. et al., STEK, The Fast-Thermal Coupled Facility of RCN at Petten, Rep. RCN-122 (1970).
[9] BENZI, V., PANINI, G.C., REFFO, G., FISPRO II: A Fortran IV Code for Fast Neutron Radiative Capture Calculations, Rep. CNEN-RT/FI(69) 44 (1969).
[10] BENZI, V., FABBRI, F., ZUFFI, L., SASSI - A Fortran Programme for the Calculation of Neutron Scattering from a Spherical Optical Potential, Rep. CNEN-RT/FI(71) 6 (1971).
[11] BERTRAND, F.E., HOREN, D.J., Nucl. Data B7 (1972) 1.
[12] AVIGNONE, F.T., FREY, G.D., Phys. Rev. C4 (1971) 912.
[13] USACHEV, L.N., MANOKHIN, V.N., these Proceedings.

DISCUSSION

M. LEDERER: You have raised an important point concerning measured versus "estimated best" data. For many levels, an excellent guess of the spin can be made, although there are no data (some such guesses would undoubtedly be better than "measured" values). This implies an entirely different type of compilation. However, one would not want to supply such guesses to a nuclear theorist, who might consider them as confirmation of his predictions.

H. GRUPPELAAR: In my paper I was not asking for such a compilation. However, it would be very useful if, in the case of two possible spin values, the most probable one were clearly indicated in the Nuclear Data Sheets. Your suggestion of a different type of compilation might be worthwhile for the purpose of cross-section calculations. However, it should not be included in the Nuclear Data Sheets, lest it give rise to confusion.

C. WEITKAMP: It is obvious that the ^{107}Pd inelastic scattering cross-section goes up as you switch from the 1970 to the 1972 level scheme. Is it also obvious that the capture cross-section goes down?

H. GRUPPELAAR: If the number of known levels increases, the capture cross-section will go down, since the total width of the compound state, which appears in the denominator of the expression for the capture cross-section increases. The total cross-section is not very sensitive to level scheme uncertainties.

EVALUATION OF THE RANGES OF FISSION PRODUCTS

F. RUSTICHELLI*
Physics Division, Joint Research Centre,
Euratom, Ispra, Italy
and
Dipartimento di Fisica, Facoltà di Ingegneria
dell'Università,
Ancona, Italy

Abstract

EVALUATION OF THE RANGES OF FISSION PRODUCTS.

In a very recent work, on the basis of the Lindhard, Scharff and Schiøtt theory and using available experimental data for average ranges in a few stopping elements, a complete set of ranges in all the natural elements for the median light, median-heavy, and overall median ^{235}U fission fragments was derived. A similar approach was used in the present paper to derive the corresponding quantities for the thermal-neutron-induced ^{239}Pu fission. By using the Lindhard, Scharff and Schiøtt theory and the few data existing for ^{239}Pu fission fragment ranges in air and Al, a complete set of average ranges of ^{239}Pu fission fragments in all the existing natural elements was obtained. This set includes, for each stopping element, ranges for the median-light, median-heavy, and overall median fission fragments. The method of fission product evaluation used is quite general and is being extended to the other fissile nuclei of interest.

INTRODUCTION

Most of the investigations on the energy loss of fission fragments in matter were concerned with individual fission fragments interacting with a few stopping elements. In this way, it was possible to obtain detailed information on the slowing-down mechanism of fission fragments in relation to the different physical parameters. However, very little information exists on general quantities as the average fission product ranges which, in addition to present physical interest, are of particular importance in nuclear technology.

To partially overcome this lack of information on general quantities related to the energy loss of fission fragments, we have derived in a very recent work [1] range values in all the natural elements for the median-light, median-heavy and overall median ^{235}U fission fragments. The derivation was based on the observation that the Lindhard, Scharff, Schiøtt (LSS) theory [2] is able to appropriately predict the relative stopping powers of different elements for the three types of ^{235}U median fission fragments. Furthermore, the few available experimental data on median fission-fragment energy loss was utilized in order to give an absolute character to the evaluated ranges. A similar approach was used here to evaluate the ranges of the median fragments produced in the thermal-neutron-induced fission of ^{239}Pu. The task was complicated in this case by the fact that, to our knowledge, no data exist on median fragments, but only on individual fragments originating in the ^{239}Pu fission.

* Present address: Institut Laue-Langevin, B.P. 156, 38042 Grenoble Cedex, France.

However, by using the existing experimental data together with LSS-theory, it was, also in the case of ^{239}Pu, possible to derive the ranges in all the natural elements for the median-light, median-heavy and overall median fission fragments, by means of a method to be described in the next section.

EVALUATION METHOD

The procedure used to evaluate ^{239}Pu median fission fragment ranges is very similar to that used in Ref. [1] to evaluate the ^{235}U median fission fragment ranges. This evaluation method is based on the fact that, in Ref. [3], it appeared evident that LSS-theory is able to predict in a satisfactory way the relative stopping powers of different elements for the ^{235}U overall median fission fragment. The validity of LSS-theory in correctly predicting relative stopping powers was confirmed by a close comparison [1] with experimental data on median-light and median-heavy ^{235}U fission fragments.

The unified expression obtained by LSS for the electronic atomic stopping power is [2]

$$-\frac{1}{N}\frac{dE}{dx} = \xi_e \, 8\pi^2 a_0 \frac{Z_1 Z_2}{(Z_1^{2/3}+Z_2^{2/3})^{3/2}} \frac{v}{v_0} \qquad (1)$$

where a_0 and v_0 are radius and velocity of the first Bohr orbit of hydrogen, respectively, v is the velocity of the projectile, N is the atomic density of the stopping material, e is the electron charge, Z_1 and Z_2 are the atomic numbers of the projectile and the stopping atom, respectively, and ξ is a constant "of the order of $Z_1^{1/6}$" [2]. The curves for the relative stopping powers referring to Al for the median-light and median-heavy ^{235}U fission fragments were obtained [1, 3] from the expression derived from Eq. (1):

$$S_{Al}(Z_2) = \frac{Z_2}{(Z_1^{2/3}+Z_2^{2/3})^{3/2}} \qquad \frac{Z_{Al}}{(Z_1^{2/3}+Z_{Al}^{2/3})^{3/2}} \qquad (2)$$

with Z_1 assuming the value of the ^{235}U light-fragment atomic number ($Z_\ell = 37.4$) and of the ^{235}U heavy-fragment atomic number ($Z_h = 54.6$), respectively. The curve for the relative stopping powers referring to Al for the overall median ^{235}U fission fragment was obtained by using the expression [1, 3]

$$\bar{S}_{Al}(Z_2) = \frac{Z_\ell^{1/6}[Z_\ell Z_2/(Z_\ell^{2/3}+Z_2^{2/3})^{3/2}]\left[\int_{E_\ell}^{0}(v_0/v)\,dE\right]^{-1} + Z_h^{1/6}[Z_h Z_2/(Z_h^{2/3}+Z_2^{2/3})^{3/2}]\left[\int_{E_h}^{0}(v_0/v)\,dE\right]^{-1}}{Z_\ell^{1/6}[Z_\ell Z_{Al}/(Z_\ell^{2/3}+Z_{Al}^{2/3})^{3/2}]\left[\int_{E_\ell}^{0}(v_0/v)\,dE\right]^{-1} + Z_h^{1/6}[Z_h Z_{Al}/(Z_h^{2/3}+Z_{Al}^{2/3})^{3/2}]\left[\int_{E_h}^{0}(v_0/v)\,dE\right]^{-1}} \qquad (3)$$

Figure 1 shows these curves in comparison with the available experimental range data for the overall median ^{235}U fission fragment. Of the experimental data reported in Fig. 1, only those of Segrè and Wiegand [4] and of Aiello, Maracci, Rustichelli [3] were directly recorded by means of an ionization chamber. In the Fulmer [5] and Alexander and Gazdik [6] experiments the energy-loss measurements were carried out separately on median-light

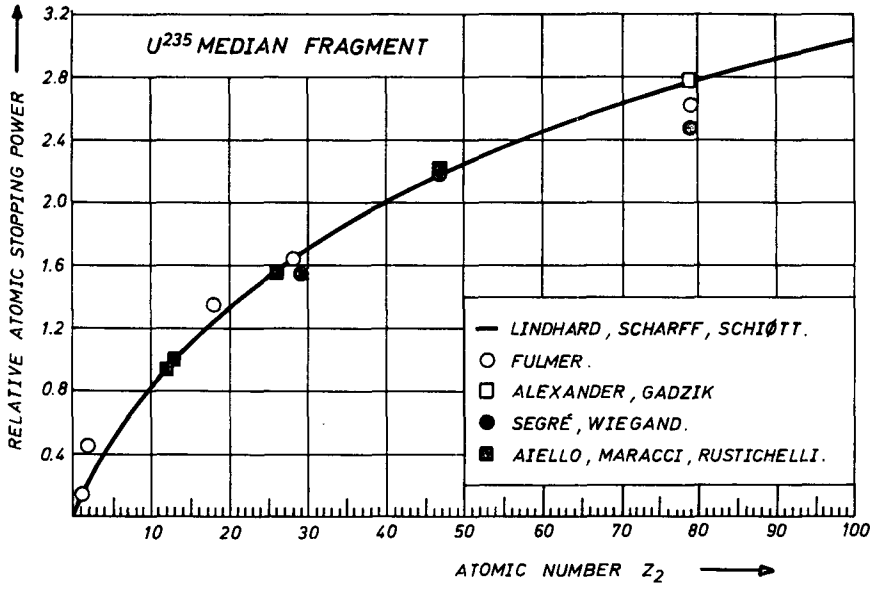

FIG. 1. Atomic stopping powers relative to Al for the overall median ^{235}U fission fragment as a function of the atomic number Z_2 of the stopping element [1].

and median-heavy ^{235}U fission fragments. The range $\langle R \rangle$ in a given stopping element for the overall median fission fragment was obtained by the equation reported in Appendix C of Ref. [3]:

$$\frac{1}{\langle R \rangle} = \frac{1}{2}\left(\frac{1}{R_\ell} + \frac{1}{R_h}\right) \tag{4}$$

where R_ℓ is the median-light fragment range and R_h is the median-heavy fragment range.

The comparison between experimental data and LSS-theoretical values of relative atomic stopping power for the median-light and median-heavy ^{235}U fission fragments was reported in Ref. [1] and was quite satisfactory, too. On this basis, the assumption was made [1] that LSS-theory is able to correctly predict the relative stopping powers of the different elements for the median-light, median-heavy and overall median ^{235}U fission fragments. On the other hand, no experimental data exist, to our knowledge, for the ^{239}Pu median fragments, which would have allowed us to check the validity of this assumption for the ^{239}Pu case, as it was made in Fig. 1 for the ^{235}U case. Despite this lack of direct verification, the present work is based on the assumption that LSS-theory is able to correctly predict the relative stopping powers of the different natural elements for the three types of ^{239}Pu median fission fragments. This assumption is justified if one considers that parameters like energies, atomic numbers, masses of fission fragments do not change very much between the thermal-neutron-induced fissions of ^{235}U and ^{239}Pu.

The energies of the two median fragments of the ^{239}Pu fission were taken from Ref. [7] where the data of Milton and Fraser [8] are reported: the energy of the median-light fragment is $E_\ell = (101.5 \pm 1.0)$ MeV and that of the median-heavy fragment is $E_h = (72.9 \pm 0.7)$ MeV. In Refs [7, 8] the masses of the two median fragments before neutron emission are reported, too: they are $A^*_\ell = 100.23 \pm 0.15$ for the light fragment and $A^*_h = 139.77 \pm 0.15$ for the heavy fragment. By assuming a value of 2.9 for the number ν of neutrons emitted per ^{239}Pu thermal fission [9] and by using the equation[1] [7]

$$\frac{A_\ell}{A_h} = \frac{E_h}{E_\ell} \tag{5}$$

where A_ℓ and A_h are the mass numbers after neutron emission of the light and the heavy-median fragments, respectively, the values $A_\ell = 99.1$ and $A_h = 138$ were obtained. The atomic number Z_h of the median-heavy fragment was obtained from the equation [12]

$$Z_h = {}^{UCD}Z_h = D(A_h) \tag{6}$$

where ${}^{UCD}Z_n$ is the atomic number obtained according to the unchanged charge density (UCD) distribution and $D(A_h)$ is the charge deviation that, according to Nörenberg [12], is roughly equal to 0.7 units for the ^{239}Pu fission fragment with $A = 140$.

The value for ${}^{UCD}Z_h$ was obtained from the equation

$${}^{UCD}Z_h = A^*_h \frac{Z_{Pu}}{A_{Pu}} \tag{7}$$

where Z_{Pu} and A_{Pu} are the atomic number ($Z_{Pu} = 94$) and the mass number ($A_{Pu} = 240$), respectively, of the compound Pu-nucleus. From Eqs (6) and (7), a value $Z_h = 54$ was obtained: the value of the atomic number for the median fragment was then $Z_\ell = 40$.

Figure 2 shows the relative atomic stopping powers for the median-light, median-heavy and overall median ^{239}Pu fission fragments, with Al being the reference element. The curves for the median-light and the median-heavy fragments were obtained from Eq. (2), with Z_1 assuming the value of the light fragment ($Z_\ell = 40$) and of the heavy fragment ($Z_h = 54$), respectively. The curve for the overall median fragment was obtained from Eq. (3). The numerical data corresponding to the three curves are reported in Table II.

Once the relative atomic stopping powers of the three median fragments are known it is sufficient to know only the absolute range value in one element for each kind of median fragment, in order to be able to derive the absolute ranges in all the other elements. In the evaluation of ^{235}U fission fragment ranges [1] several absolute range values for the different median fragments were available. By using all the existing experimental data, an effective range in Al was obtained for each ^{235}U median fragment:

---

[1] These two ratios are not precisely the same but, for the present purpose, can be considered identical. For detailed information see Refs [10, 11].

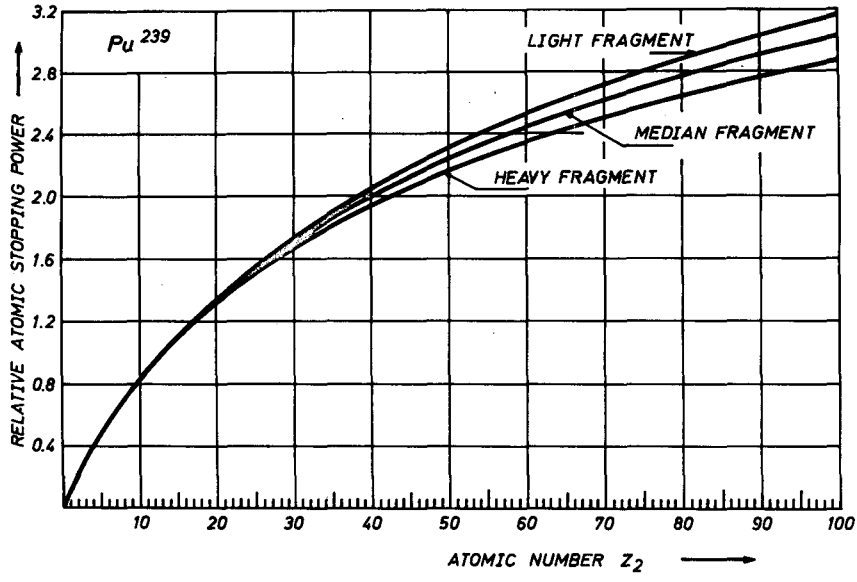

FIG. 2. Atomic stopping powers relative to Al for the median-light, median-heavy and overall median ^{239}Pu fission fragments as a function of the atomic number Z_2 of the stopping element.

$R_\ell = 3.676$ mg/cm^2 for the light fragment, $R_h = 3.021$ mg/cm^2 for the heavy fragment and $\langle R \rangle = 3.359$ mg/cm for the overall median fragment. These range values are slightly different from the measured ranges in Al, but they are more appropriate in view of the evaluation of the ranges in all natural elements, because they are the result of a sort of best fit, taking into account all the available experimental data.

Below, the problem of obtaining the corresponding ^{239}Pu values for the three median fragments' effective ranges in Al will be solved. Since no data exist, to our knowledge, on the ranges of ^{239}Pu median fragments, the procedure used for ^{235}U cannot be repeated exactly. However, experimental data exist for individual ^{239}Pu fission fragment ranges in air [13] and in Al [14]. The assumption will be made that the range of the light ^{239}Pu median fission fragment ($A_\ell = 100.23$) will be the same as that of the individual ^{239}Pu fragment having the mass number A = 100, and that the range of the heavy ^{239}Pu median heavy fragment ($A_h = 139.77$) will be the same as that of the individual ^{239}Pu fragment having the atomic number A = 140.

This assumption will now be justified. At first, it can be observed that the energies of the two ^{239}Pu individual fragments under consideration are equal, within a few percent, to the energies of the corresponding ^{239}Pu median fragment [7]. Furthermore, we shall check the validity of this assumption by comparing the measured ranges for individual ^{235}U fission fragments having the same mass numbers as the median ^{235}U fragments ($A_\ell = 95$), ($A_h = 140$) with the evaluated ranges [1] for the median-light and the median-heavy ^{235}U fission fragments, respectively.

TABLE I. ABSOLUTE RANGES FOR ^{239}Pu AND ^{235}U FISSION FRAGMENTS IN AIR AND Al.

Stopping element	Pu^{239} fission fragment A = 100			Pu^{239} fission fragment A = 140			Author
	Absolute range (cm)	Absolute range (mg/cm^2)	Average range value (mg/cm^2)	Absolute range (cm)	Absolute range (mg/cm^2)	Average range value (mg/cm^2)	
Air	2.783	3.354	3.354	2.206	2.658	2.658	Katcoff, Miskel, Stanley [13]
Al		4.046	4.046		3.210	3.210	Dange et al. [14]

Stopping element	U^{235} median light fragment		U^{235} median heavy fragment		Author
	Absolute range (mg/cm^2)	Average range value (mg/cm^2)	Absolute range (mg/cm^2)	Average range value (mg/cm^2)	
Air	3.55 3.02	3.285	2.59 2.29	2.440	Fulmer [5] Alexander, Gozdik [6]
Al	4.11 4.00	4.055	3.45 3.03	3.240	Fulmer [5] Alexander, Gozdik [6]

$$\left.\begin{aligned}\left[\frac{R_\ell(Pu^{239})}{R_\ell(U^{235})}\right]_{Air} &= 1.021\\ \left[\frac{R_\ell(Pu^{239})}{R_\ell(U^{235})}\right]_{Al} &= 0.998\end{aligned}\right\} \left\langle\frac{R_\ell(Pu^{239})}{R_\ell(U^{235})}\right\rangle = 1.010$$

$$\left.\begin{aligned}\left[\frac{R_h(Pu^{239})}{R_h(U^{235})}\right]_{Air} &= 1.089\\ \left[\frac{R_h(Pu^{239})}{R_h(U^{235})}\right]_{Al} &= 0.991\end{aligned}\right\} \left\langle\frac{R_h(Pu^{239})}{R_h(U^{235})}\right\rangle = 1.040$$

TABLE II. ABSOLUTE RANGES IN THE NATURAL ELEMENTS AND THE RELATIVE STOPPING POWERS FOR THE MEDIAN-LIGHT, MEDIAN-HEAVY AND OVERALL MEDIAN ^{239}Pu FISSION FRAGMENTS

Element	Symbol	Atomic Number (Z_2)	Median Light Fragment			Overall Median Fragment			Median Heavy Fragment		
			Relative Atomic Stopping Power	Relative Mass Stopping Power	Absolute Range (mg/cm^2)	Relative Atomic Stopping Power	Relative Mass Stopping Power	Absolute Range (mg/cm^2)	Relative Atomic Stopping Power	Relative Mass Stopping Power	Absolute Range (mg/cm^2)
Hydrogen	H	1	0.122	3.254	1.141	0.117	3.139	1.084	0.114	3.039	1.034
Helium	He	2	0.227	1.531	2.425	0.220	1.486	2.290	0.215	1.446	2.172
Lithium	Li	3	0.323	1.255	2.960	0.315	1.223	2.783	0.307	1.195	2.628
Beryllium	Be	4	0.410	1.229	3.022	0.402	1.202	2.830	0.394	1.179	2.664
Boron	B	5	0.492	1.228	3.025	0.483	1.205	2.823	0.475	1.186	2.650
Carbon	C	6	0.568	1.276	2.910	0.559	1.257	2.708	0.552	1.240	2.534
Nitrogen	N	7	0.640	1.232	3.013	0.632	1.217	2.796	0.625	1.203	2.611
Oxygen	O	8	0.707	1.193	3.112	0.700	1.181	2.881	0.694	1.171	2.684
Flourine	F	9	0.772	1.096	3.388	0.766	1.087	3.130	0.760	1.080	2.909
Neon	Ne	10	0.833	1.113	3.335	0.828	1.107	3.074	0.824	1.101	2.853
Sodium	Na	11	0.891	1.046	3.551	0.888	1.042	3.266	0.885	1.039	3.025
Magnesium	Mg	12	0.947	1.051	3.534	0.945	1.049	3.245	0.944	1.047	3.001
Aluminum	Al	13	1.000	1.000	3.713	1.000	1.000	3.403	1.000	1.000	3.142
Silicon	Si	14	1.051	1.010	3.677	1.053	1.012	3.364	1.054	1.013	3.102

TABLE II (continued)

Phosphorus	P	15	1.100	0.959	3.874	1.104	0.962	3.539	1.107	0.964	3.258
Sulfur	S	16	1.148	0.966	3.844	1.153	0.970	3.507	1.158	0.975	3.224
Chlorine	Cl	17	1.193	0.908	4.088	1.201	0.914	3.723	1.207	0.919	3.419
Argon	Ar	18	1.237	0.836	4.442	1.247	0.842	4.041	1.255	0.848	3.706
Potassium	K	19	1.280	0.883	4.204	1.292	0.891	3.818	1.302	0.898	3.498
Calcium	Ca	20	1.321	0.889	4.174	1.335	0.899	3.787	1.347	0.907	3.466
Scandium	Sc	21	1.361	0.817	4.545	1.377	0.826	4.118	1.390	0.835	3.765
Titanium	Ti	22	1.400	0.789	4.709	1.418	0.799	4.262	1.433	0.807	3.892
Vanadium	V	23	1.437	0.761	4.877	1.457	0.772	4.409	1.475	0.781	4.023
Chromium	Cr	24	1.474	0.765	4.855	1.496	0.776	4.384	1.515	0.786	3.997
Manganese	Mn	25	1.509	0.741	5.010	1.533	0.753	4.519	1.554	0.763	4.116
Iron	Fe	26	1.544	0.746	4.979	1.570	0.758	4.487	1.593	0.770	4.083
Cobalt	Co	27	1.577	0.722	5.143	1.605	0.735	4.630	1.630	0.746	4.210
Nickel	Ni	28	1.610	0.740	5.020	1.640	0.754	4.514	1.667	0.766	4.102
Copper	Cu	29	1.641	0.697	5.328	1.674	0.711	4.787	1.703	0.723	4.346
Zinc	Zn	30	1.672	0.690	5.380	1.707	0.705	4.829	1.738	0.717	4.381
Gallium	Ga	31	1.702	0.659	5.636	1.739	0.673	5.055	1.772	0.686	4.582
Germanium	Ge	32	1.732	0.644	5.768	1.771	0.658	5.169	1.805	0.671	4.683
Arsenic	As	33	1.760	0.634	5.856	1.802	0.649	5.244	1.838	0.662	4.747
Selenium	Se	34	1.789	0.611	6.075	1.832	0.626	5.436	1.870	0.639	4.917

TABLE II (continued)

Bromine	Br	35	1.816	0.613	6.056	1.862	0.629	5.414	1.901	0.642	4.894
Krypton	Kr	36	1.843	0.593	6.258	1.891	0.609	5.590	1.932	0.622	5.051
Rubidium	Rb	37	1.869	0.590	6.293	1.919	0.606	5.618	1.962	0.619	5.072
Strontium	Sr	38	1.895	0.583	6.364	1.947	0.599	5.677	1.992	0.613	5.123
Yttrium	Y	39	1.920	0.583	6.373	1.974	0.599	5.681	2.021	0.613	5.123
Zirconium	Zr	40	1.944	0.575	6.457	2.000	0.592	5.751	2.049	0.606	5.184
Niobium	Nb	41	1.968	0.572	6.496	2.027	0.589	5.782	2.077	0.603	5.209
Molybdenum	Mo	42	1.992	0.560	6.628	2.052	0.577	5.896	2.105	0.592	5.309
Technetium	Tc	43	2.015			2.077			2.131		
Ruthenium	Ru	44	2.038	0.544	6.826	2.102	0.561	6.065	2.158	0.576	5.454
Rhodium	Rh	45	2.060	0.540	6.875	2.126	0.557	6.104	2.184	0.573	5.487
Palladium	Pd	46	2.082	0.528	7.034	2.150	0.545	6.242	2.209	0.560	5.608
Silver	Ag	47	2.103	0.526	7.059	2.173	0.544	6.260	2.234	0.559	5.622
Cadmium	Cd	48	2.124	0.510	7.283	2.196	0.527	6.455	2.259	0.542	5.794
Indium	In	49	2.144	0.504	7.368	2.219	0.521	6.527	2.283	0.537	5.856
Tin	Sn	50	2.165	0.492	7.545	2.241	0.509	6.680	2.307	0.524	5.991
Antimony	Sb	51	2.185	0.484	7.669	2.263	0.501	6.786	2.331	0.517	6.083
Tellurium	Te	52	2.204	0.466	7.967	2.284	0.483	7.046	2.354	0.498	6.313
Iodine	I	53	2.223	0.473	7.855	2.305	0.490	6.943	2.377	0.505	6.218
Xenon	Xe	54	2.242	0.461	8.059	2.326	0.478	7.120	2.399	0.493	6.374

TABLE II (continued)

Cesium	Ce	55	2.261	0.459	8.090	2.346	0.476	7.144	2.421	0.491	6.393
Barium	Ba	56	2.279	0.448	8.293	2.366	0.465	7.320	2.443	0.480	6.547
Lanthanum	La	57	2.297	0.446	8.323	2.386	0.464	7.342	2.464	0.479	6.565
Cerium	Ce	58	2.314	0.446	8.331	2.406	0.463	7.346	2.485	0.479	6.566
Praseodymium	Pr	59	2.332	0.447	8.316	2.425	0.464	7.329	2.506	0.480	6.548
Neodynium	Nd	60	2.349	0.439	8.451	2.444	0.457	7.444	2.526	0.473	6.649
Promethium	Pm	61	2.366			2.462			2.547		
Samarium	Sm	62	2.382	0.428	8.685	2.481	0.445	7.644	2.566	0.461	6.822
Europium	Eu	63	2.399	0.426	8.719	2.499	0.444	7.670	2.586	0.459	6.843
Gadolinium	Gd	64	2.415	0.414	8.962	2.517	0.432	7.881	2.605	0.447	7.029
Terbium	Tb	65	2.430	0.413	8.999	2.534	0.430	7.909	2.624	0.446	7.052
Dysprosium	Dy	66	2.446	0.406	9.142	2.551	0.424	8.033	2.643	0.439	7.159
Holmium	Ho	67	2.461	0.403	9.221	2.569	0.420	8.099	2.662	0.435	7.216
Erbium	Er	68	2.476	0.399	9.294	2.585	0.417	8.159	2.680	0.432	7.267
Thulium	Tm	69	2.491	0.398	9.331	2.602	0.416	8.189	2.698	0.431	7.291
Ytterbium	Yb	70	2.506	0.391	9.502	2.618	0.408	8.335	2.716	0.423	7.419
Lutetium	Lu	71	2.521	0.389	9.553	2.635	0.406	8.376	2.734	0.422	7.454
Hafnium	Hf	72	2.535	0.383	9.690	2.650	0.401	8.493	2.751	0.416	7.555
Tantalium	Ta	73	2.549	0.380	9.769	2.666	0.398	8.560	2.768	0.413	7.512
Tungsten	W	74	2.563	0.376	9.872	2.682	0.394	8.646	2.785	0.409	7.687

TABLE II (continued)

Rhenium	Re	75	2.577	0.373	9.945	2.697	0.391	8.707	2.802	0.406	7.739
Osmium	Os	76	2.590	0.367	10.105	2.712	0.385	8.845	2.818	0.400	7.859
Iridium	Ir	77	2.604	0.365	10.159	2.727	0.383	8.889	2.835	0.398	7.895
Platinum	Pt	78	2.617	0.362	10.260	2.742	0.379	8.974	2.851	0.394	7.969
Gold	Au	79	2.630	0.360	10.307	2.757	0.378	9.012	2.867	0.393	8.001
Mercury	Hg	80	2.643	0.355	10.446	2.771	0.373	9.130	2.883	0.388	8.103
Thallium	Tl	81	2.655	0.351	10.592	2.785	0.368	9.255	2.898	0.383	8.212
Lead	Pb	82	2.668	0.347	10.688	2.799	0.365	9.335	2.914	0.379	8.281
Bismuth	Bi	83	2.680	0.346	10.730	2.813	0.363	9.369	2.929	0.378	8.309
Polonium	Po	84	2.692			2.827			2.944		
Astatine	At	85	2.704			2.840			2.959		
Radon	Rn	86	2.716			2.854			2.973		
Francium	Fr	87	2.728			2.867			2.988		
Radium	Ra	88	2.740			2.880			3.002		
Actinium	Ac	89	2.751			2.893			3.017		
Thorium	Th	90	2.763	0.321	11.558	2.906	0.338	10.071	3.031	0.352	8.916
Protactinium	Pa	91	2.774			2.919			3.045		
Uranium	U	92	2.785	0.316	11.762	2.931	0.332	10.242	3.058	0.347	9.063
Neptunium	Np	93	2.796			2.944			3.072		
Plutonium	Pu	94	2.807			2.956			3.085		

TABLE II (continued)

Americium	Am	95	2.818	2.968	3.099
Curium	Cm	96	2.828	2.980	3.112
Berkelium	Bk	97	2.839	2.992	3.125
Californium	Cf	98	2.849	3.004	3.138
Einsteinium	Es	99	2.859	3.015	3.151
Fermium	Fm	100	2.869	3.027	3.164

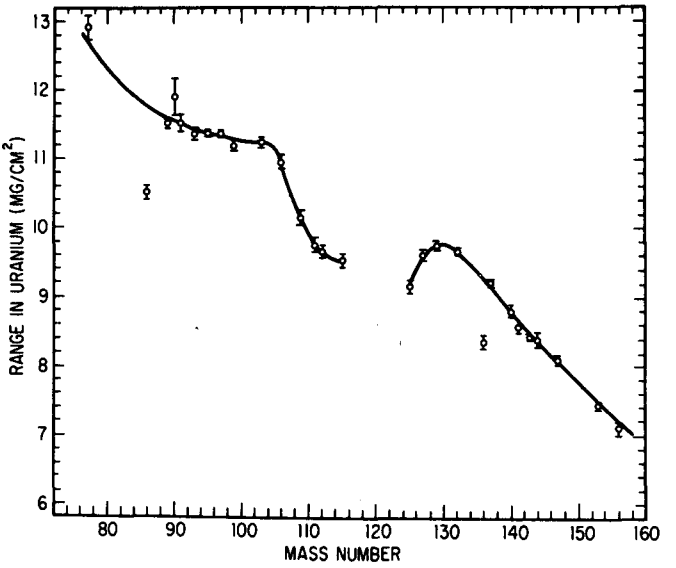

FIG. 3. Integral ranges of fission products of ^{235}U measured by Niday in uranium metal [7, 15].

The ranges of ^{235}U fission products in uranium were measured by Niday [15] and reported in Fig. 3. It can be seen that the dependence of the range on the mass number A_1, and, as a consequence, on the atomic number Z_1 of the projectile atom is quite regular and free from oscillations which were found in some other cases [16]. The range in uranium of the ^{235}U fragment with a mass number A = 95 appears to be, according to Fig. 3, equal to 11.4 mg/cm^2 and the range of the ^{235}U fragment with a mass number A = 140 appears to be equal to 8.8 mg/cm^2. These values are in good agreement with the values obtained in Ref. [1] for the range in uranium of the ^{235}U median-light fragment (R_ℓ = 11.893) and for the range of the ^{235}U median-heavy fragment (R_h = 8.686).

Table I reports the values of the ranges in air measured by Katcoff, Miskel and Stanley [13] for the ^{239}Pu fission fragments of mass number A = 100 and A = 140 and the ranges in Al of the same fragments measured by Dange et al. [14]. In addition, the range values in air and Al obtained experimentally for the median-light and the median-heavy ^{235}U fission fragments, discussed in Ref. [1] are reported. The data of Ref. [13] were obtained by using a radiochemical technique: the values reported in Fig. 3 are deduced from the figures and not from the tables in order to be coherent with the ^{235}U data referring to the maximum range. An air density value of ρ_{air} = 1.205 was used to convert the range data from cm to mg/cm^2. The range values of ^{239}Pu fission fragments in Al were obtained by using a high-resolution gamma-spectrometer.

The ratio in air and Al between Pu and U light-fragment ranges and between Pu and U heavy-fragment ranges are reported in Table I, too. The average values for the ratio range Pu/range U is 1.010 for the light fission fragment and 1.040 for the heavy fission fragment. The effective ranges in Al for the light and heavy ^{239}Pu median fragments were obtained by multiplying the effective ranges in Al of the light and heavy ^{235}U median fragments by these two experimental ratios. The effective range in Al of the ^{239}Pu median-light fragment was found to be $R_\ell = 3.713$ and of the ^{239}Pu median-heavy fragment $R_h = 3.142$. The ^{239}Pu overall median-heavy fragment was obtained from R_ℓ and R_h by using Eq. 4; the value obtained is $\langle R \rangle = 3.403$.

The absolute ranges for the three ^{239}Pu median fission fragments reported in Table II were obtained by dividing the effective range in Al of each of the median fragments by the theoretical relative mass-stopping powers referred to Al. The relative mass stopping powers were obtained by multiplying the relative atomic stopping powers by the atomic weight ratios [1].

RESULTS AND DISCUSSION

Table II reports the values of the relative atomic and mass-stopping powers, referred to Al, as calculated by LSS-theory for the median-light, median-heavy and overall median ^{239}Pu fission fragments. Finally, the evaluated absolute ranges for the three types of ^{239}Pu median fragments

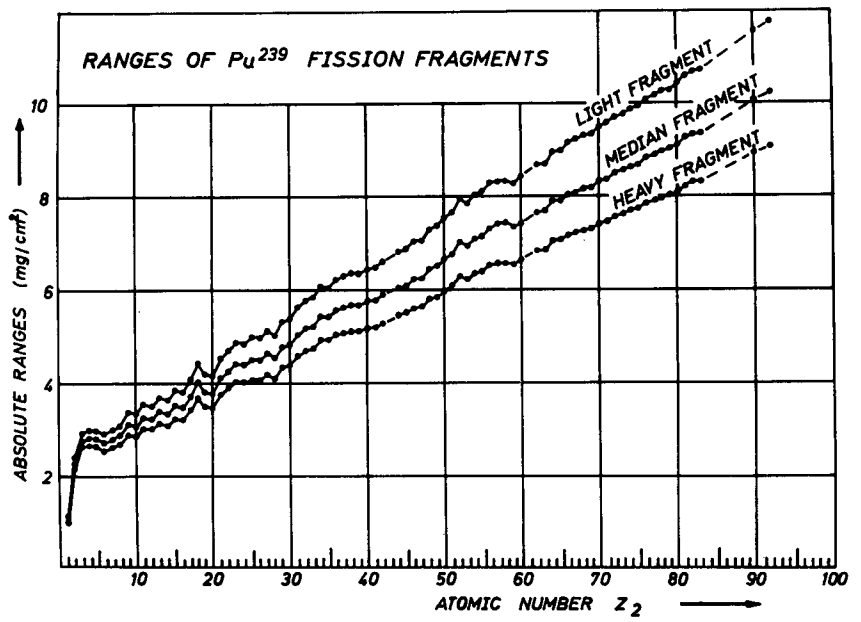

FIG. 4. Absolute ranges in the natural elements of the median-light, median-heavy and overall median ^{239}Pu fission fragments, as a function of the atomic number Z_2 of the stopping element.

are reported. A discussion of the physical meaning of the range of the overall median fission fragment was presented in Ref. [1]. In practical applications, it would be preferable to take the corresponding values for the median-light fission fragment instead of the overall median fission-fragment ranges. The absolute ranges for the three types of ^{239}Pu median fission fragments are reported in Fig. 4, as a function of the atomic number Z_2 of the stopping element. The results obtained are not too different from the corresponding ^{235}U values and, because of uncertainties in the approximations used, they should be considered in an absolute scale and not in reference to the ^{235}U data.

This work represents only a first attempt to produce general information on ^{239}Pu fission fragment ranges. The evaluation method is largely based on the ^{235}U experimental data: the precision would increase if new experimental data for ^{239}Pu were available. This procedure of estimating absolute ranges for median fission fragments is quite general and is now being applied to other fissile nuclei of interest.

REFERENCES

[1] RUSTICHELLI, F., Z. Phys., under press.
[2] LINDHARD, J., SCHARFF, M., SCHIØTT, H.E., Kgl. Dan. Vidensk. Selsk. Mat.-Fys. Medd. 33 14 (1963).
[3] AIELLO, V., MARACCI, G., RUSTICHELLI, F., Phys. Rev. 48 (1971) 3812.
[4] SEGRE, E., WIEGAND, C., Phys. Rev. 70 (1946) 808.
[5] FULMER, C.B., Phys. Rev. 108 (1957) 1113.
[6] ALEXANDER, J.M., GAZDIK, M.F., Phys. Rev. 120 (1960) 874.
[7] HYDE, E.K., "The Nuclear Properties of the Heavy Elements", 3, Chapter 6, Kinetic Energy of the Fission Fragments, Prentice-Hall, New Jersey (1964).
[8] MILTON, J.C.D., FRASER, J.S., Can. J. Phys. 40 (1962) 1626; 41 (1963) 817.
[9] Reactor Physics Constants, ANL-5800 (Second Edition) (1963).
[10] TERREL, J., Phys. Rev. 113 (1959) 527.
[11] BRUNTON, D.C., HANNA, G.C., Can. J. Res. 28A (1950) 190.
[12] NÖRENBERG, W., Phys. Rev. 5 (1972) C 2020.
[13] KATCOFF, J., MISKEL, J.A., STANLEY, C.W., Phys. Rev. 74 (1948) 631.
[14] DANGE, S.P., JAIN, H.C., MANOHAR, S.B., SATYAPRAKASH, K., RAMANIAH, M.V., RAMASWAMI, A., RENGAN, K., in Physics and Chemistry of Fission (Proc. Symp. Vienna), IAEA, Vienna (1969) 741.
[15] NIDAY, J., Phys. Rev. 121 (1961) 1471.
[16] EL-HOSHY, A.H., GIBBONS, J.F., Phys. Rev. 173 (1968) 454.

DISCUSSION

N. M. SPYROU: Do you intend extending your method to californium-252? If so you could then check your range calculations for selected elements against results obtained experimentally, e. g. by using surface barrier detectors, which are becoming increasingly available. This would be important from the medical point of view.

F. RUSTICHELLI: I am now applying the method to ^{233}U. But, I agree with you that it would be interesting to consider also ^{252}Cf. I shall certainly be doing that in the near future.

Section VII

ACCELERATOR AND SPACE SHIELDING

Chairman

W.W. HAVENS (USA)

USE OF NUCLEAR DATA IN DESIGNING SPACE-SCIENCE EXPERIMENTS

B.C. CLARK, P.G. KASE, J.P. MARTIN, J.G. MORSE
Martin Marietta Aerospace,
Denver, Colo.,
United States of America

Abstract

USE OF NUCLEAR DATA IN DESIGNING SPACE-SCIENCE EXPERIMENTS.

Scientific experiments for exploration of the planets and interplanetary space must be designed to operate in a number of severe environments, including the natural radiation in space (cosmic rays, solar flares, radiation belts, etc.). Man-made radiation environments may be also present, such as gamma and neutron emissions from radioisotope thermoelectric generators (RTG's) used as spacecraft power supplies, and/or emissions from radiation sources which are a part of the science instrumentation complement. Examples of the latter include alpha, beta, X-ray and radioisotope sources, miniature X-ray tubes, and neutron generators of the D-T accelerator type. Each experiment must survive the radiation damage as well as interferences during operation in such environments. The use of nuclear data in designing several instruments for exploration of Mars and Venus is discussed, with examples drawn from the X-ray fluorescence geochemical analyser scheduled for launch to Mars in 1975, plus an X-ray diffractometer, a gamma-ray spectrometer, and a neutron activation analyser under study for possible use on future missions. Constraints upon overall spacecraft design due to the nuclear environments are also discussed. The types of nuclear data employed include radioisotope emission characteristics, shielding of sources, shielding of cosmic rays and trapped particles, neutron scattering and activation cross-sections, and gamma-ray transport parameters. High costs in fully simulating such environments for spacecraft-sized equipment have dictated heavy reliance upon analysis rather than experimental test in verifying spacecraft compatibility. This greatly increases the economic value of the applicable nuclear data.

This paper describes science experiments which will be (or could be) carried on spacecraft designed to explore surfaces and/or atmospheres of planets, such as Mars, Venus and Jupiter. It is limited to those experiments in which beta, gamma and X-radiations are measured in order to ascertain requisite physical, chemical and biological properties, and it is concerned with the effect of radiation background on the measurements themselves.

RADIATION ENVIRONMENTS

The radiation environments of science experiments for the exploration of the planets and interplanetary space include both natural and man-made radiation sources.

The properties of radiation environments of the planets are influenced very strongly by the properties of their magnetic fields and their atmospheres. Planets having strong magnetic fields are likely to have belts of trapped proton and electron radiation, such as the well-known Van Allen belts of Earth. Since their discovery in 1958, the Van Allen belts have been extensively mapped and very detailed models of their properties are readily available [1, 2, 3, 4].

Planetary exploration so far has shown that the Moon, Venus and Mars have very weak magnetic fields and therefore no significant radiation belts. Except for atmospheric interactions, the radiation environments near these planets are essentially identical to the interplanetary environments.

Warwick [5] and Beck [6] have inferred from analysis of its synchrotron radio noise that Jupiter has a strong magnetic field, and probably has extensive radiation belts. Until the Pioneer spacecraft encounters Jupiter in December 1973, planners of missions to Jupiter are anticipating that its radiation belts contain the fluxes indicated by Figure 1, which shows the uncertainties of current forecasts of the trapped proton and electron fluxes [7]. The peak fluxes in this model occur in the plane of the Jupiter magnetic equator where it intersects the cloud layers visible in the atmosphere. Because the electron component of this belt is derived from measurements of Jupiter's synchrotron radiation noise, there is more confidence in this portion of the model. Nominally, the peak electron flux is 2.0×10^7 electrons/cm^2 sec; the upper limit of the electron flux is 6.0×10^7 electrons/cm^2 sec. These values are comparable to the fluxes at Earth, but are distributed through a considerably larger volume surrounding Jupiter. The proton component of Jupiter's radiation belt is inferred from the electron component, hence there is less confidence in this portion of the model. The peak proton fluxes are 3.3×10^8 protons/cm^{2}sec, nominal

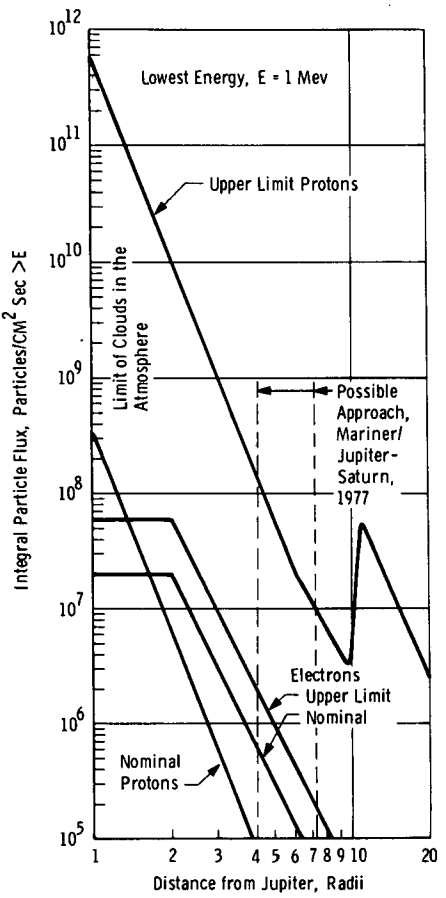

FIG. 1. Distribution of protons and electrons in the plane of the Jupiter magnetic equator.

and 6.0 x 10^{11} proton/cm^2 sec, upper limit. Again, the peak nominal proton flux is comparable to that at Earth, but the upper limit flux is nearly 2000 times greater. Spacecraft shielding is ineffective at the peak flux due to the extreme hardness of the energy spectrum [4]. However, the energy spectra are considerably softer at remote distances so that shielding may be used to reduce the flux when the closeness of approach is limited. The range of closest approach to Jupiter that may be expected during the Mariner/Jupiter-Saturn mission to be launched in 1977 is also shown on Figure 1. This range, from 4.3 to 7.3 Jupiter radii, is based on two considerations -- limitation of permanent damage to electronic devices within the spacecraft due to the considerable fluences accumulated during flight past Jupiter, and trajectory constraints imposed by the objective of flying past Saturn later in the mission. These trajectory constraints also force the spacecraft to remain close to Jupiter's equatorial plane. The fluences encountered during equatorial fly-by's of Jupiter are shown in Figure 2. When the radius of closest approach is 4.3 Jupiter radii, the nominal and upper limit electron fluences are respectively 1.0 x 10^{10} and 4.2 x 10^{10} electrons/cm^2; the proton fluences are respectively 1.3 x 10^9 and 3.4 x 10^{12} protons/cm^2.

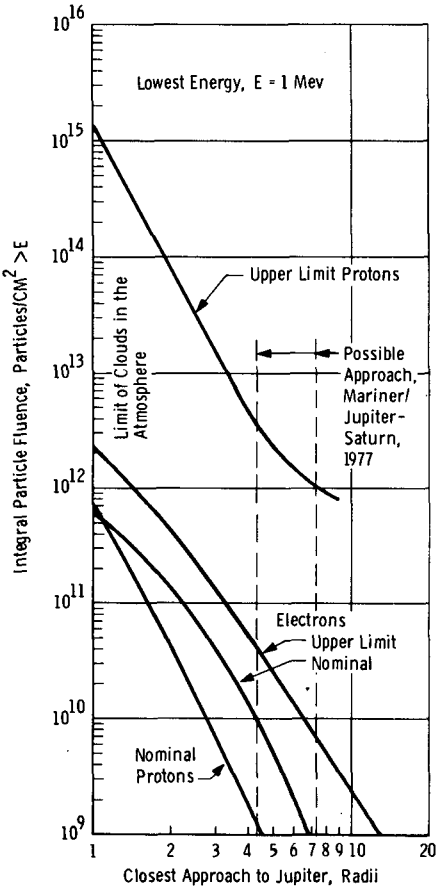

FIG. 2. Fluences of protons and electrons encountered during equatorial flights past Jupiter.

Kase [4] has shown that these values would be reduced as much as 50% if polar fly-by's were possible. There is little difference between these fluences and those accumulated during departure from Earth when the radius of closest approach to Jupiter is restricted. The radiation environments of probes that enter Jupiter's atmosphere would be approximately 100 times more severe.

Haffner [8] has indicated the possibility that Saturn has radiation belts. These belts are expected to have 1/100 the intensity of Jupiter's radiation belts. There is currently no evidence either for or against other planets or any moons of the planets having radiation belts.

The radiation environment in interplanetary space has three principal elements -- intergalactic cosmic radiation, the solar wind, and solar flares. The first two of these elements are essentially continuous, while solar flares are periodic, or wave-like. The properties of all of these sources are strongly influenced by the 11-year cycle of solar activity.

Galactic cosmic radiation consists of charged particles having the following abundances [7, 9]:

Charged Particle	Relative Abundance in the Universe
Hydrogen (Proton)	100,000
Helium (Alpha)	7,500
Lithium, Beryllium, Boron	3×10^{-3}
Carbon	10
Nitrogen	15
Oxygen	50
$10 \leq Z \leq 30$	30
$30 \leq Z$	8×10^{-4}
Electron	6,600

The cosmic radiation at solar minimum is approximately double that at solar maximum. The next solar maximum will occur early in the 1980's. Divine [7] indicates that the fluxes at solar minimum are 9.5 protons/cm^2 sec and 0.6 electrons/cm^2 sec, and their minimum energy is 100 MeV. Because these particles are extremely energetic, typical spacecraft shielding has very little effect. The fluences of protons and electrons encountered in the cosmic radiation environment are proportional to the mission duration. Missions to the inner planets, requiring on the order of a year, would encounter 3.0×10^8 protons/cm^2 and 2.0×10^7 electrons/cm^2. Missions to the outer planets entail 5 to 10 years; the preceding fluxes would be multiplied accordingly.

The solar wind is an electrically neutral plasma of protons, electrons, and other particles emitted by the Sun. It is believed that the solar wind emission is isotropic and, therefore, the particle flux is inversely proportional to the square of the distance from the Sun. Measurements at 1 a.u. have shown that the solar wind velocity is 300 to 800 km/sec; the flux is 1.5×10^7 to 2.4×10^8 protons and electrons/cm^2 sec; and the proton energy is 0.5 to 3 keV. Haffner [8] has shown that the velocity of the solar wind increases with distance from the Sun and that the effective temperature, or energy decreases. Because of the inverse square effect, the solar wind flux will vary considerably between inner and outer planets missions and the fluences will depend on the trajectory histories. At Venus, 0.72 a.u., the flux is approximately twice that at Earth. At Saturn, 5.2 a.u., the flux

is only 1/27 that at Earth. Diederich [10] has integrated the flux during year-long Viking flights to Mars to obtain solar wind fluence of 3.5×10^{15} protons/cm^2.

Solar flares consist of protons, alpha particles and electrons emitted by the Sun during solar storms. The energies of these particles may range from 1 MeV to several thousand MeV and the duration of the event as it passes a given location in space may be from hours to weeks. McDonald [11] discusses the morphology of solar flare events and indicates that a single event could result in a fluence at Earth of 4.0×10^9 protons/cm^2 having energies greater than 30 MeV, with a maximum flux during the event of 2.0×10^4 protons/cm^2 sec. The fluxes of electrons and alpha particles are in general equal to or considerably less than that of protons.

Various authors, including Modisette [12], have predicted the nature of the solar flare environment in future solar cycles. However, the model due to Diederich [10] has been adopted for this paper, which integrates the total fluence of all solar events during a year into one event measured at Earth. It is believed that the spatial distribution of solar flare particles relative to the Sun is inversely proportional to the square of distance, as in the case of the solar wind. This effect is shown in Figure 3, assuming that all of the year's events occur essentially instantaneously in

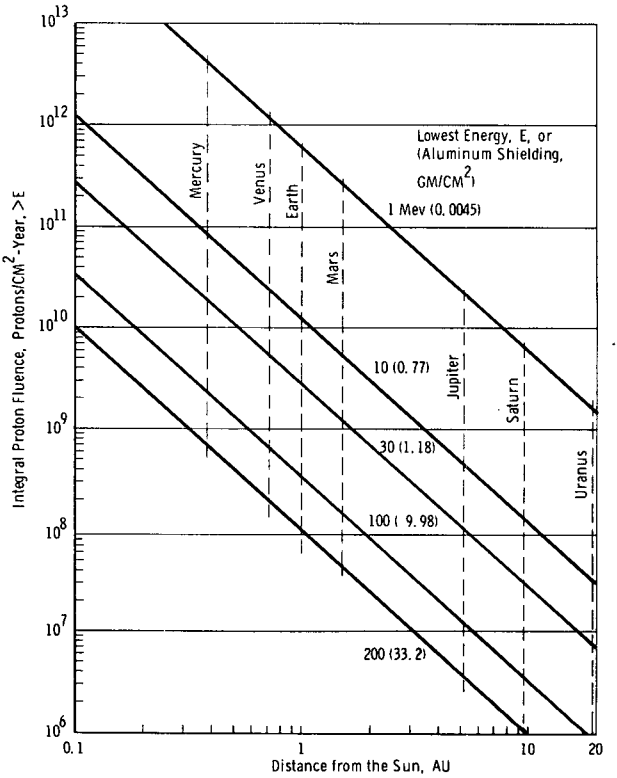

FIG. 3. Proton fluence from solar flares during interplanetary cruise.

the time frame of interplanetary flight. The fluence of solar protons with energies exceeding 1 MeV at Earth is 6×10^{11} protons/cm^2. Spacecraft shielding very effectively reduces this fluence, as shown by the figure. A 33 gm/cm^2 aluminum shield results in a fluence of only 10^8 protons/cm^2 penetrating to the interior of the spacecraft.

The atmosphere of a planet has profound effects on the radiation environment above and within the atmosphere and at its surface. When the planet has no atmosphere, as in the case of the Moon, the radiation levels at the surface are approximately ½ those in space because of the shielding effect of the planet's mass. The atmosphere of Venus is so dense that probably no radiation from space could reach its surface. However, at some altitude, the cascading effect of radiation from space interacting with the atmosphere results in a peak of secondary particles, as is observed in the Earth's upper atmosphere. On Mars, this increase in particle flux is estimated at 1.5 to 2.0 times the nominal value [31]. The effectiveness of the Martian atmosphere and bulk planet in totally absorbing lower energy particles is as follows [13]:

Radiation Source	Fraction of Space Value at Earth Penetrating to the Surface of Mars (6 millibar pressure)
Solar Flare	
Energy > 10 MeV	2.0×10^{-3}
Energy > 100 MeV	5.0×10^{-2}
Cosmic Radiation	> 0.4

The preceding data are consistent with the previous observation that solar flare spectra are softer then cosmic ray spectra and, therefore, are readily shielded by even a tenuous atmosphere.

Especially in the case of outer-planet missions, space science instruments may have to cope with man-made radiation sources on board the spacecraft. For instance, as the spacecraft moves away from the Sun, the amount of solar energy available to generate power in a solar cell system or to provide heat for thermal control diminishes. As in the case of the solar wind and solar flares, solar energy is inversely proportional to the square of the distance from the Sun. Solar cells are marginally effective at Mars, where the solar energy available is less than half that at Earth, excluding the effect of Martian dust; at Jupiter, the solar energy available is 1/27 that at Earth. Consequently, radioisotope thermoelectric generators (RTG) are to be used to power most outer-planet spacecraft, and radioisotope heating units (RHU) will provide heat in many instances. Pioneer, the Viking Lander and Mariner/Jupiter-Saturn all employ RTG's.

The radioisotope fuel to be used in the RTG's and RHU's of outer-planet vehicles is plutonium oxide, $^{238}Pu\ O_2$. This fuel is especially desirable because it has an 86.8 year half-life, provides 0.5 thermal watts of energy per gram, and produces low radiation emissions in comparison to other sources. The spontaneous emissions of this fuel are alpha particles, neutrons, and gamma rays. Though 99% of this radiation is alpha particles, these particles are of too low energy to penetrate the fuel container.

Though this fuel spontaneously emits about 2100 neutrons/gram second, several factors affect the total neutron emission rate. As discussed by Weddell [14] these factors include reaction with the oxygen component of the fuel, interactions with impurities in the fuel, such as boron, sodium,

magnesium, and aluminum, and multiplication due to the intrinsic size and power of the device. Weddell states that the neutron emission rate can vary from 20,000 to 314,000 neutrons/gram sec due to these factors, with the expected maximum about 40,000 in the case of the Mariner/Jupiter-Saturn spacecraft. The neutron spectrum includes energies up to 7 MeV.

Plutonium oxide fuel also emits gamma radiation. The natural decay of plutonium (^{238}Pu) is augmented by gamma radiation produced by impurities, such as ^{236}Pu, which are associated with the manufacture of the fuel. If 1 part per million of ^{236}Pu is present, Weddell indicates this impurity will multiply the total gamma production rate by a maximum factor of 7 at 18 years after initial purification; then the rate will decline. Noon [15] shows that aged fuel will produce about 2,000 photons/cm^2 sec in the energy range 100 to 200 keV at a location about 1 meter from the axis of the RTG canister. The entire gamma radiation spectrum includes energies up to 7 MeV. When the emission is lengthy, as in the case of Mariner/Jupiter-Saturn, it is desirable to assume that the fuel age is 18 years so that the gamma radiation environment is not underestimated.

The neutron fluences that should be anticipated at the science instruments of the Viking/Mars Lander and the Mariner/Jupiter-Saturn outer planets spacecraft are shown in Figure 4. This figure is based on fluxes calculated by Diederich [10] and Wertz [16] for the respective vehicles. In the case of the Viking Lander, the two 675 watt (thermal) RTG's used to power the vehicle are embedded in the spacecraft and all other systems, including the science experiments, are in close proximity. This is necessary because all vehicle systems must be within the heat shield during entry and descent through Mars' atmosphere. The fluxes at the science experiments calculated by Diederich do not include attenuation by the spacecraft structure or equipment. The neutron flux is 1.30×10^3 neutrons/cm^2 sec; the gamma flux is 1.65×10^4 photons/cm^2 sec. The mission of the Mariner/Jupiter-Saturn outer-planets spacecraft does not include entry of their atmospheres, so the configuration need not be compact. Therefore, the three 2,200 watt (thermal) RTG's that power this vehicle are mounted on a boom, deployed diametrically opposite to the science instrumentation. As a result, though considerably more radioisotope fuel is to be carried on the Mariner/Jupiter-Saturn spacecraft than on Viking, the fluxes at the science experiments are substantially less. Including attenuation by the spacecraft, Wertz calculates the fluxes to be 3.1 neutrons/cm^2 sec and 34 photons/cm^2 sec. The fluences shown in Figure 4 are plotted as functions of the time of flight so that the effects of several mission duration times could be indicated. However, the exposure of the science experiments and associated electronics to the RTG and RHU radiation sources actually commences earlier due to the necessity for integration and checkout of the spacecraft systems prior to launch. In the case of Viking, the prelaunch exposure is 120 days, whereas the Mariner/Jupiter-Saturn exposure will be only 30 days. These differences are due not only to differences in the vehicles but also to the need to limit the exposure of personnel at the launch complex to the larger RTG's of the latter spacecraft. Figure 4 indicates that the total neutron fluence during the Viking mission will be about 5×10^{10} neutrons/cm^2. The exposure of the science experiments of the Mariner/Jupiter-Saturn spacecraft will be 1.7×10^8 neutrons/cm^2 at Jupiter encounter and 3.5×10^8 neutrons/cm^2 at Saturn encounter. In all cases the fluences of gamma radiation are approximately 10 times the neutron fluences.

EXPERIMENTS IN DESIGN AND DEVELOPMENT

The Viking mission to be launched in 1975, is the United States' next mission to the planet Mars. Consisting of an integrated orbiter and lander,

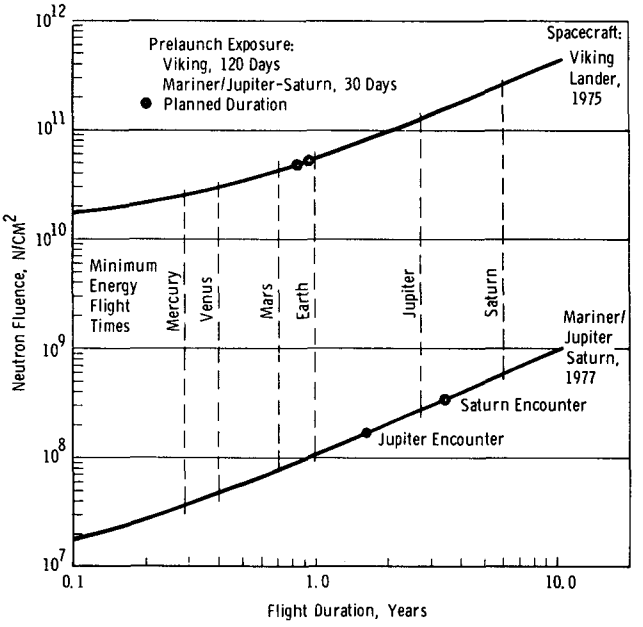

FIG. 4. Neutron fluence at science instrumentation of interplanetary spacecraft powered by radioisotope thermoelectric generators.

the Viking spacecraft will first go into Mars orbit and reconnoiter the potential landing sites before the lander is separated and allowed to enter the atmosphere and soft land on the Martian surface. Once landed, the radiation environment is a combination of the following: galactic and solar cosmic rays, cosmic ray interaction products (the relatively sparse Martian atmosphere produces a nearly maximum flux density of build-up secondaries), emission from the onboard RTG power supply, induced radioactivity in the lander body, and natural radioactivity in the Martian soil. In addition, planetary quarantine criteria for Mars have levied the requirement that the entire lander be heat sterilized just prior to launch, and this has in turn necessitated the use of quantities of thoriated magnesium alloy in the lander construction. It should be pointed out that although the RTG's and MgTh alloy can cause interference problems in several experiments, it is unrealistic to assume they can be replaced. The thoriated alloy is the most cost-effective means of achieving low-weight instrument housings.

For all present and proposed Viking lander experiments studied so far, the RTG emissions are more serious than any other ionizing radiation environment by at least an order of magnitude. Clearly, any experiment for the Viking spacecraft system must include the RTG radiation field as a required design criterion (along with, for example, weight and power constraints, thermal range, etc.).

Three experiments on the Viking-75 lander employ detectors of ionizing radiation. The first of these is an X-ray fluorescence spectrometer (XRFS)

to assay Martian soil for the concentrations of major, minor, and certain trace elements [17, 18]. In operation, this instrument provides two collimated X-ray beams to bombard the soil surface. The resulting fluorescent X-ray emissions are measured with energy-dispersive analysis by four "tuned-response" proportional counter detectors. The two beams are the 5.9 and 22.2 keV X-ray emissions of the radioisotopes ^{55}Fe and ^{109}Cd. Together, the four counters are sensitive over the energy range 1.0 to 25.0 keV. Since its inception, this spectrometer was designed with close regard for the interference problem. Although it is well-known that the major component of the counting-rate in proportional counters exposed to gamma fields is due to secondary electrons from the walls rather than direct gamma interactions in the gas, the theoretical response functions for this effect are apparently not yet developed. It is thus impractical to calculate proportional counter response to an RTG field to the accuracy desired. One consequence immediately applicable to design, however, is that the gamma ray counting rate should scale as the internal surface area of the detector. On the other hand, the counting rate of the fluorescent X-rays scales as the aperture of the thin entrance window. A large window with minimum wall area is therefore preferred, and a pancake detector indicated. Criteria of resolution, peak tailing, ruggedness and reliability rule out the pancake detector, and a conventional side-window cylindrical counter was selected instead. The counter design was then optimized for the minimum diameter and length (i.e., minimum internal wall area) consistent with requirements for adequate gas path for fluorescent X-ray absorption and uniform electric field geometry over the distance of the entrance window to give acceptable resolution. The signal-to-background ratio was then adjusted by sizing the radioisotope sources. In Figure 5 is presented a typical fluorescent spectrum overlaid by the spectrum measured in the field of a Pioneer RTG (S/N 42), as corrected for Viking RTG fuel-loading levels. This figure is for the counter which is most interfered with. Of the 12 elements analyzed for by the XRFS, only three (mg, Al, and Si) are measurably affected by the RTG interference at all. Statistical analysis of these data, based upon a nominal operating period on Mars, has shown sensitivity and accuracy to be limited chiefly by the finite resolution of the counters and strength of the sources, rather than the RTG interference background, even for these three elements.

Besides interference calculations, the XRFS experiment requires the best obtainable values of certain fundamental data: X-ray fluorescent yields, X-ray mass absorption coefficients, and X-ray mass scattering coefficients. These are used in a calculation from first principles of the element concentrations which would give rise to the observed spectra. In practice, we have found it necessary to employ empirical correction factors to the results. Better input data should allow reduction of these factors and a capability to accurately analyze a wider variety of sample compositions. Accordingly, we are presently updating our data base by replacing the fluorescent yield values of Fink [19] with the more recent compilations of Bambynek [20] and the X-ray mass interaction coefficients of Pletachy and Terrall [21] with those of Viegle [22]. These data are yet susceptible to improvement in accuracy, which would be quite welcomed for this application.

The second and third Viking-75 experiments which are susceptible to RTG interference are the carbon assimilation and labeled metabolite schemes for detecting Martian life forms. Each employs ^{14}C labeled compounds and assays for ^{14}C in the gas phase. By this tracer technique, reactions characteristic of metabolic processes can be detected. Sensitivity of these experiments in detecting life is directly related to the ability to reliably detect small levels of ^{14}C in the presence of the high RTG background.

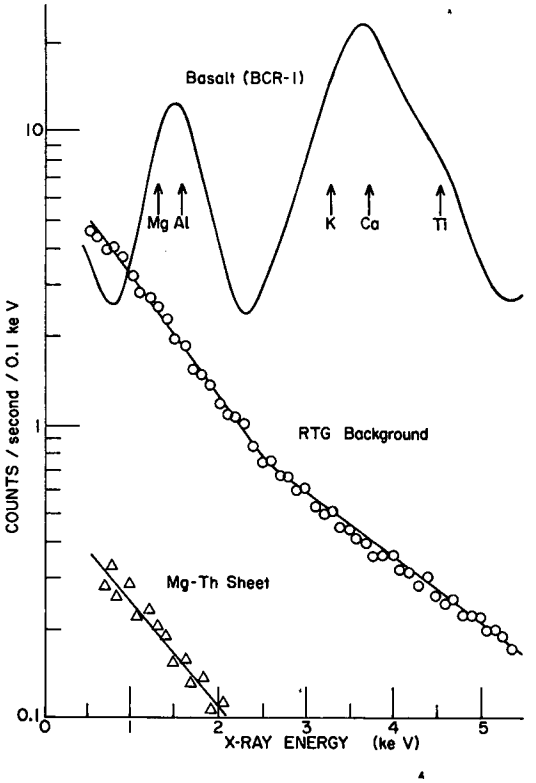

FIG. 5. X-ray fluorescence spectra due to RTG-emissions and signal from basalt sample (US Geological Survey Standard BCR-1).

Realizing this, the U.S. NASA initiated studies of this problem early in the development phase of the biology instrument. In one study, a number of different detector types were evaluated for inherent efficiency for ^{14}C and energetic gamma rays [23]. The second study resulted in the development and test of a detection system consisting of a spherical cavity proportional counter for internal counting of the ^{14}C labeled gas at very high efficiency. The walls of this counter were made of scintillator with a thin evaporated aluminum coating to provide a cathode ground return and good light collection. With optimum settings of the energy windows for the counter and scintillator outputs, the anti-coincidence output of the counter correctly registers most of the ^{14}C beta rays while rejecting most of the gamma interactions [24]. With this device, ^{14}C activities of 16 disintegrations per minute (dpm) could be detected in a one hour count with RTG background. This approach was not pursued, however, because of the significant weight penalty and a decision by the biology investigators that a minimum detection limit of 150 dpm would be satisfactory. On this basis, a theoretical, then experimental study was made which resulted in a detection system composed of two solid-state detectors, monitoring a pillbox-shaped gas cavity. Nuclear data used in the study included the ^{14}C beta ray energy spectrum, electron energy-loss rate and backscattering from the

dead layer and sensitive volume of the silicon detectors, and gamma ray absorption coefficients for silicon. The resulting system detects 150 dpm with 1300 counts/minute of background when a counting period of 24 hours is used. This long integration time has required the development of extremely stable and well temperature compensated amplifying and discrimination circuitry.

EXPERIMENTS FOR FUTURE MISSIONS

X-ray Diffractometry - Two instruments which have been proposed for future Viking missions to Mars are an X-ray diffractometer and a gamma ray spectrometer. The purpose of the diffractometer is to measure lattice spacings of crystallites in the surface material to identify the mineralogic species present. It consists of a miniature X-ray tube and goniometer/detector or position-sensitive detector. All detectors proposed to date are of the proportional counter type so that the considerations mentioned in connection with design of the XRFS apply here also. If the RTG's were absent, the X-ray tube would probably not be required and a radioisotope source such as ^{55}Fe could be used as a simpler, more stable, and more reliable substitute. Further work on X-ray diffraction is in progress. The nuclear data of concern are the X-ray coherent scattering cross-sections.

Gamma Ray Spectrometry - A gamma ray spectrometer is needed to measure the concentrations of the three naturally-occurring radioactive elements in the soil, viz., ^{40}K, ^{232}Th, and ^{238}U. If the Martian crust can be shown to contain high levels of these elements ($> 0.1\%$ for K and $>$ few ppm for Th and U), as is the case for both the Earth and the Moon, then one can immediately deduce that Mars has undergone a planetary-scale geochemical differentiation with significant depletion of the internal K, U, and Th content. Otherwise, the radioactive heating would render the planet entirely molten. Our problem here in implementing this experiment is once again the RTG interference, but much more severely so than in the preceding examples. In Figure 6 are plotted typical gamma spectra recorded in NaI scintillator for two slightly different SNAP units (the fuel-holding units used for the RTG's) along with a typical spectrum of natural emissions from Earth crustal rock [25, 26, 27]. The SNAP gamma intensity even at distances of 2 and 2.7

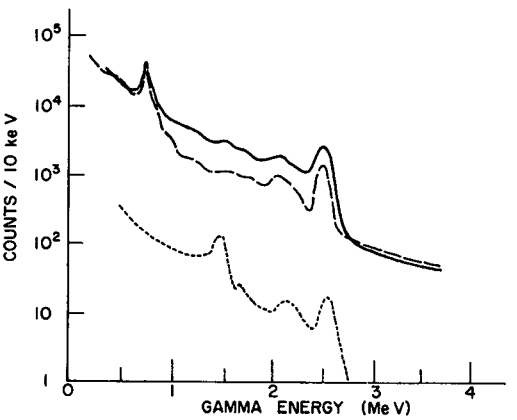

FIG. 6. Gamma spectra of RTG and Earth soil emissions as recorded by NaI(Tl) scintillator in 4 minutes count time. Solid curve: SNAP-27 at 2.7 metres [25]; dashed curve: SNAP-19 at 2.0 metres [26]; dotted curve: natural emission with detector 1.0 metre above the ground [27].

meters is two orders-of-magnitude or more greater than the terrestrial soil intensity. Since Martian soil could be only one-tenth as radioactive as terrestrial, it is desirable to reduce the RTG interference by at least a factor of 1000 from that shown in Figure 6. Shielding is out of the question from the weight standpoint - an adequate lead shield would weigh almost as much as the entire lander. Increasing the separation distance between spectrometer and RTG's appears to be the only practical way of reducing the interference to reasonable levels. To achieve the factor of 1000 would require removing the spectrometer to a distance of at least 60 to 80 meters from the lander.

One other way of possibly reducing the interference would be to employ a very high resolution gamma detector in lieu of the rather poor resolution scintillator and to use energy discrimination to distinguish between RTG gammas and soil gammas. Energy resolution provides only partial relief from interference, however, because although over half the RTG gammas are from ^{238}Pu, and therefore do not coincide with soil gammas, there is a very significant fraction due to the decay of ^{236}Pu (this isotope is present only at the one part per million level in the SNAP fuel - its removal would be extremely costly). The decay of ^{236}Pu is as follows:

$$^{236}Pu \xrightarrow{2.85\ yr.} {}^{232}U \xrightarrow{72\ yr.} {}^{228}Th \xrightarrow{(1.91\ yr.\ total)} \cdots \rightarrow {}^{208}Tl \xrightarrow{3\ min.} {}^{208}Pb\ (stable)$$

The most important gamma emissions are those of ^{208}Tl, viz. 2.615 MeV (100%), 0.80 MeV (12%), 0.58 MeV (86%), and 0.51 MeV (23%). Consider now the decay chain of the natural thorium isotope ^{232}Th:

$$^{232}Th \xrightarrow{1.4\times10^{10}\ yr.} {}^{228}Ra \xrightarrow{6.7\ yr.} {}^{228}Ac \xrightarrow{6.1\ hr.} {}^{228}Th \rightarrow \cdots \text{ etc.}$$

The key point here is that the thorium decay series intersects the ^{236}Pu decay series at ^{228}Th, with both proceeding identically thereafter. This is the reason we see the same peak of 2.615 MeV for all three spectra in Figure 6. Consequently, the RTG spectrum interferes not only from a flux standpoint, but also from the energy standpoint for the Th determination.

In summary, getting the spectrometer away from the lander seems to be the only reasonable solution. Because of the distances required, a boom is out of the question. A small mini-rover, of the tethered type, could adequately perform this task. In addition, such a rover could possibly travel over a hill or behind a boulder to attenuate the RTG signal even further (a single boulder 0.8 meters in diameter would attenuate by a factor of 1000).

X-RAY FLUORESCENCE OF VENUS CLOUDS

The basic scheme used for geochemical analysis of rocks collected by a Mars lander can be applied to the determination of atmospheric constituents by a descent probe through the dense Venus atmosphere. Thus, using unstable nuclei which decay by capture of K, L, and M shell electrons, X-rays can be generated to stimulate fluorescent X-radiation from atmospheric atoms. The experiment therefore would use two such X-ray sources (^{55}Fe and ^{109}Cd) and two proportional counters mounted external to the descent probe of the Pioneer Venus multiprobe mission (scheduled for launch in early 1977). The atmosphere is analyzed directly during the descent without the need of any sample collection devices. Fluorescent X-rays from all elements above

phosphorus in the periodic table fall within the energy range of the counters. The host atmosphere, mostly CO_2 causes very little attenuation of the X-rays, especially the 22.2 keV ^{109}CD X-rays. However, sensitivity of the experiment is greatest for heavy elements such as Hg, Br, I, Sb, and As which are thought to be cloud forming elements of the Venus atmosphere. The measurement is independent of the chemical and physical state of the fluorescing elements and thereby provides a complement to a mass spectrometer experiment which measures concentrations of gaseous components only.

NEUTRON DETECTION

The detection of fast neutrons in planetary atmospheres can be used as an effective tool in evaluating effects of cosmic radiation in the atmosphere and planetary surface. On Earth, such studies have been used to identify a mechanism for populating the inner part of the trapped radiation belt with protons and also to understand the production of ^{14}C in the atmosphere. Fast neutron detectors operating in the presence of other types of radiation must be designed to discriminate against these in favor of the more elusive neutrons. The method used historically in many studies involved surrounding a pair of gas filled proportional counters with a proton rich neutron moderator such as water or paraffin. The neutrons thus thermalized produced N-α reactions in a BF_3 gas, highly enriched in ^{10}B, in one of the proportional counters. The very high ^{10}B thermal neutron capture cross section thus enabled statistical discrimination of counts produced by other radiation by subtracting the counts from the other proportional counter filled with BF_3 gas depleted in ^{10}B.

A more recent scheme for discriminating directly rather than statistically against other radiation uses a proton-rich scintillation plastic or liquid. The neutrons are detected by observation of the ionization scintillation of recoil protons resulting from elastic n-p collisions in the detector. The detector is made totally unresponsive to protons and electrons entering the scintillator by surrounding it with a shell of an inorganic scintillator such as CsI or NaI. The ionization light pulse produced by the charged particle in this shell is much longer than that seen in the organic scintillator and can readily be separated electronically to reject such pulses as resulting from charged particles rather than neutrons entering the detector. An additional scheme is added to discriminate against X-rays which, like neutrons, can pass by the charged particle rejection shell and produce characteristic electron interactions in the organic scintillator. This involves using a special type of scintillator which results in a different ionization pulse shape by protons as opposed to electrons. Thus, recoil protons (produced by neutrons) can be separated electronically from Compton, photoelectric, or pair production electrons and positrons (produced by γ-rays). The electronically rejected pulses in this type of detector can also be used to detect the protons, electrons, and γ-rays which enter the counter.

NEUTRON ACTIVATION ANALYSIS

Elemental analysis using the technique of neutron activation is a very sensitive method for characterizing the chemical composition of planetary surfaces [28]. Although the technique was proposed by a number of investigators in the pre-Apollo or unmanned phase of the U.S.' lunar program, it is as yet untried in space for compositional analysis. Developments in the past few years, however, in the areas of detector technology, data reduction and analysis, and particularly the availability of Californium-252 which offers extremely high neutron yields through spontaneous fission, have rekindled interest in using neutron activation for planetary surface analysis.

This section of the paper will treat briefly the concern of background radiation interferences, and their minimization, in order to obtain statistically valid data.

Following absorption of neutrons, atomic nuclei generally emit gamma rays whose energy distribution provides "spectral signatures" which are characteristic of the elemental species and thus enable quantitative identification of the chemical elements. This radiation falls into two categories, namely: neutron capture gamma rays and delayed or activation gamma rays. In the former case, the gamma radiation is emitted in the range of 10^{-14} to 10^{-8} seconds. If the nucleus becomes radioactive, it will emit delayed gamma rays as it undergoes radioisotopic decay.

A promising approach to the minimization of interfering background radiation was developed to aid in minerals exploration of the ocean floor [29]. In this environment the natural background is severe owing to the decay chains of the uranium and thorium present, and potassium (^{40}K). Prompt capture gamma rays have energies up to 10 MeV, whereas delayed gammas are emitted up to about 1.5 MeV. Measurement of the former limits the extent of background interference, enables simultaneous irradiation of the surface and measurement of the gamma response, and because of the higher energies emitted, the technique allows placement of the detector within the protective enclosure of the spacecraft. The authors proposed a mathematical relationship to describe the usefulness of this approach, which is $S = I\theta/A$, where: S is defined as an index of elemental sensitivity, I is the number of gamma rays of a given energy emitted per 100 neutrons absorbed, θ is the microscopic cross section in barns. This concept required extension to and test of those elemental species anticipated in planetary surfaces.

A basic problem here is the resolution of the complicated spectra obtained in capture gamma ray measurements. A solution of this problem has been described using both ruggedized NaI (Tl) detectors and the development of sophisticated computer-based procedures for the analysis of the complex pulse-height spectrum [30].

The evidence indicates that background radiation, arising from the surface itself and the environment characteristic of the planet, can be minimized thus enabling the return of statistically valid data and provide elemental analysis of the planetary surface.

NUCLEAR DATA REQUIRED

It is evident from the foregoing that applications of nuclear techniques in space science are many. Likewise, the operating environments often give rise to significant radiation interferences. Successful design of a space experiment requires careful study, both from an experimental and theoretical standpoint, of the response of the experiment to its intended signal versus the background interference. The general body of nuclear data has been and will continue to be of considerable importance to experiment design. In Table I, we list some of the types of nuclear data that apply to the examples discussed. In many cases, improvement in the fundamental data and/or radiation transport calculations would allow more optimal experiment design.

TABLE I. TYPES OF NUCLEAR DATA USED IN ABOVE EXAMPLES*

Gamma (20 keV to 10 MeV)	Photoelectric and pair production absorption coefficients Coherent and incoherent scattering coefficients Scattering direction distributions
Beta Rays (0 to 150 keV)	Scattering and energy loss in thick absorbers
X-rays (1 to 20 keV)	Fluorescent yields Photoelectric absorption coefficients Coherent and incoherent scattering coefficients Fluorescent X-ray emission energies
Neutrons (thermal to 14 MeV)	Inelastic and elastic scattering cross-sections Activation cross-sections
Radioisotope Decay	Emissions of X-ray emitters and contaminants (^{109}Cd, ^{65}Zn, etc.) and gamma ray emitters (neutron activation products)
Protons, Charged Nuclei (1 MeV to 10 GeV)	Energy loss rates Spallation and activation cross-sections

*Because these examples cover only a limited number of cases in which nuclear instrumentation is used in space experiments, the breadth of types of nuclear data required is greater than shown here.

REFERENCES

[1] VETTE, J. I. et al, Models of the Trapped Radiation Environment, Vols. I through VII, NASA SP-3024, National Aeronautics and Space Administration, Washington, D. C. (1966 through 1971).

[2] SINGLEY, G. W., VETTE, J. I., The AE-4 Model of the Outer Radiation Zone Electron Environment, NSSDC 72-06, National Space Science Data Center, Greenbelt, Maryland (August 1972).

[3] TEAGUE, M. J., VETTE, J. I., The Inner Zone Electron Model AE-5, NSSDC 72-10, National Space Science Data Center, Greenbelt, Maryland, (November 1972).

[4] KASE, P. G., "The radiation environments of outer-planet missions," IEEE Transactions on Nuclear Science, Vol. NS-19, 6 (Dec. 1972) 141-146.

[5] WARWICK, J. W., Particles and Fields Near Jupiter, NASA CR-1685, Jet Propulsion Laboratory, Pasadena, California (October 1970).

[6] Proceedings of the Jupiter Radiation Belt Workshop, (BECK, A. J., Ed.) TM 33-543, Jet Propulsion Laboratory, Pasadena, California (1 July 1972).

[7] DIVINE, N., The Planet Jupiter (1970), NASA SP-8069, Jet Propulsion Laboratory, Pasadena, California (December 1971).

[8] HAFFNER, J. W., "Magnetospheres of Jupiter and Saturn," AIAA Journal, Vol. 9, No. 12 (December 1971) 2422-2427.

[9] Satellite Environment Handbook, (JOHNSON, F. S., Ed.) Stanford Univ. Press, Stanford, California (1961).

[10] DIEDERICH, D. R., Viking Radiation Environment, TN-3770040 (Rev. A), Martin Marietta Aerospace, Denver, Colorado (24 April 1972).

[11] Solar Proton Manual, (McDONALD, F. B., Ed.), NASA TRR-169, Goddard Space Flight Center, Greenbelt, Maryland (December 1963).

[12] MODISETTE, J. L., VINSON, T. M., HARDY, A. C., Model Solar Proton Environments for Manned Spacecraft Design, NASA TN D-2746, Manned Spacecraft Center, Houston, Texas (April 1965).

[13] Mars Engineering Model, M75-125-2, NASA Langley Research Center, Hampton, Virginia (14 April 1972).

[14] The Effects of Radiation on the Outer Planets Grand Tour, (WEDDELL, J. B., Ed.), SD71-770, North American Rockwell Corp., Downey, California (November 1971).

[15] NOON, E. L., ANNO, G. H., DORE, M. A., "Nuclear radiation sources on board outer-planet spacecraft," NS-18, IEEE Transactions on Nuclear Science (October 1971).

[16] Mariner/Jupiter-Saturn 1977 Spacecraft Description, (WERTZ, C., Ed.), Jet Propulsion Laboratory, Pasadena, California (12 July 1972).

[17] CLARK, B. C., X-ray Surface Sample Analyzer for Planetary Exploration," NASA High CR-127526 (1972), Accession No. N-72-27846.

[18] The design and execution of the Viking Inorganic Chemistry Experiment is the responsibility of a team of scientists consisting of Professor A. K. Baird of Pomona College, Dr. B. C. Clark of Martin Marietta Aerospace, Professor K. Keil of the University of New Mexico, Dr. H. J. Rose, Jr., of the United States Geological Survey, and Dr. P. Toulmin, III, of the United States Geological Survey (Team Leader).

[19] FINK, R. W., JOPSON, R. C., MARK, H., SWIFT, C. D., "Atomic fluorescence yields," Rev. Mod. Phys. 38 (1966) 513.

[20] BAMBYNEK, W., CRASEMANN, B., FINK, R. W., FREUND, H. U., MARK, H., SWIFT, C. D., PRICE, R. E., RAO, P. V., "X-ray fluorescence yields, Auger, and Coster-Kronig transition probabilities," Rev. Mod. Phys. 44 (1972) 716.

[21] PLECHATY, E. F., TERRELL, J. R., Integrated System for Production of Neutronics and Photonics Calculational Constants - Vol. 6 Photon Cross Sections 1 keV to 100 MeV, UCRL-50400 (1968).

[22] VEIGLE, W. J., BRIGGS, E., BATES, L., HENRY, E. M., BRACEWELL, B., X-ray Cross Section Compilation from 0.1 keV to 1 MeV, DNA 2433F (formerly DASA 2433) (1972) available from Director, Defense Nuclear Agency, Washington, D. C. 20305.

[23] WAINIO, K., ROGERS, W. L., An Analysis of Carbon-14 Radiation Detection Systems, Final Report to Contract NAS 2-5546, NASA/Ames Research Center (1969).

[24] CLARK, B. C., "Carbon-14 detection in a high background radiation," Nucl. Instr. Math. 89 (1970) 225.

[25] KAMINSKAS, R. A., RYAN, G. W., SMITH, C. A., RTG/Science Instrument Radiation Interactions for Deep Space Probes, TRW Rept. on Contract NAS 2-5222 with NASA/Ames Research Center (1969).

[26] BLOCK, S., SCHMIDT, C. T., KATHREN, R. L., Radiation Dosimetry and Spectral Distribution of the SNAP-19 Source, UCRL-50539 (1968).

[27] MINATO, S., KAWANO, M., "On the constitution of terrestrial gamma radiation," J. Geophys. Res. 75 (1970) 5825.

[28] KRUGER, P., Principles of Activation Analysis, Wiley - Interscience, New York, N. Y., (1971).

[29] SENTFLE, F. E., DUFFEY, D., WIGGINS, P. F., "Mineral exploration of the ocean floor by in-situ neutron absorption using a Californium-252 source," Marine Technology Society Journal 3, 5 (Sept.-Oct. 1969) 9.

[30] TROMBKA, J. I., SENTFLE, F. E., SCHMADEBECK, R., "Neutron radiative capture methods for surface elemental analysis," Nuclear Instruments and Methods 87 (1970) 37-43.

[31] Mars Scientific Model, Vol. 1, Jet Propulsion Laboratory Document No. 606-1 (1968).

DISCUSSION

F. RUSTICHELLI: I have heard recently that it would be useful from the point of view of space science, particularly in X-ray investigations, to have spherically curved monochromator crystals in order to get a focusing effect. Could you comment on this point? I might mention that we are developing this kind of crystal at the Institute Max von Laue-Paul Langevin in Grenoble in connection with neutron physics experiments. We get the curvature by chemical treatment of one of the faces of silicon crystals. After the treatment the crystals remain naturally curved, without any need for a mechanical or thermal device. This last-mentioned characteristic should be an advantage in space research.

B. C. CLARK: This development is of interest, especially if it results in a greater throughput efficiency for monochromatization of X-rays. I would be interested in learning more about this development.

R. NICKS: In your paper you mention the presence of neutrons in the atmosphere. Where do these neutrons come from, what is their intensity and what is their energy? Can you tell us something about the detection system?

B. C. CLARK: The origin of these neutrons is nuclear reactions between incoming charged particles (cosmic rays and solar flare particles) and the nuclei of the constituents of the earth's upper atmosphere. The energy spectrum of this so-called "neutron albedo" flux covers a broad range, extending up to the energy of the incoming particle. Several detection systems have been devised, including the BF_3-counter in a moderator described in the text. It is found that successful measurement of the neutron albedo requires the ability to identify and exclude the interference of primary cosmic ray counts. This is accomplished by surrounding the primary detector with a second detector (e. g. a scintillator shell) insensitive to neutrons and operated in anti-coincidence with the primary detector.

NUCLEAR DATA FOR SHIELDING AND ACTIVATION ESTIMATES FOR TRIUMF

I.M. THORSON, W.J. WIESEHAHN
TRIUMF Group, Simon Fraser University,
Burnaby, B.C., Canada

Abstract

NUCLEAR DATA FOR SHIELDING AND ACTIVATION ESTIMATES FOR TRIUMF.

The more important radiation transport and residual activity production estimates required for the high-intensity (100 μA) medium-energy (500 MeV), H^- isochronous cyclotron, external beam lines and targets of TRIUMF are enumerated and discussed. The gross features of the radiation field distribution during operation of the facility are primarily dependent on the hadronic cascade in the facility components and shields. Lacking adequate experimental data for the secondary particle spectra and angular distributions, almost exclusive reliance has been placed on the results from intra-nuclear cascade calculations. The residual activation and radiation field problems, which are more comparable, in intensity, to those found at fission reactors than previous generations of accelerator facilities, are complicated by the wide variety of product species from high-energy hadron reactions. The available experimental data are at best incomplete and often fragmentary. Extensive reliance for nuclear data requirements has been placed on compilations based on Rudstam's empirical formula; more recently activity production estimates based on Silberberg and Tsao's extended empirical formula have been used.

Nuclear Data for Shielding and Activation Estimates for TRIUMF

1. INTRODUCTION AND GENERAL DESCRIPTION OF TRIUMF

1.1 Description of the TRI-University Meson Facility

1.1.1 TRIUMF Accelerator:

TRIUMF [1] consists of a six-sector, isochronous cyclotron and, initially, two external beam lines as shown in Fig. 1. H^- ions are injected at 300 keV into the cyclotron and accelerated to any energy between 150 MeV and 500 MeV, where they are stripped to protons, for simple, clean, simultaneous extraction into either external beam line. The total, design specification beam intensity is 100 μA at 500 MeV limited by acceptable residual radiation fields produced by beam spill in the accelerator. If the final beam energy is reduced by ~10% the beam current capability of the accelerator should increase by a factor ~3, for the same spill.

1.1.2 Experimental Beam Lines:

The experimental areas of the facility are divided into a Meson Area and a Proton Area as shown in Fig. 1. In the first, the highest intensity proton beams produce mesons by nuclear reactions in targets in primary beam line BL1. For initial operations two secondary beam lines will collect pions produced in target T2; one, at 30° to the proton beam direction, and in the vertical plane, will transport π^- mesons into the Bio-Medical experimental area and the other at 135° to the

incident proton beam, and in the horizontal plane, will collect relatively low energy pions of either polarity and transport them through the shielding to the meson experimental area. Shortly after start-up of the facility, expected in early 1974, a second meson production target, T1, will be installed to provide energetic pions at near 0° to the incident proton direction into a secondary beam line to the meson experimental area. A third secondary beam from target T2 and a second from T1, not shown on Fig. 1, are also planned for the near future.

The Proton Area will be used for nucleon-nucleon and nucleon-nucleus experiments. Primary beam line BLIV is switched at the entrance to the area to either BLIV(a) or BLIV(b). Protons of variable energy in BLIV(a) will be used to produce polarized or unpolarized, mono-energetic neutrons in a liquid deuterium target and/or to bombard thin targets for reaction product studies in an evacuated scattering chamber. An experimental activity production facility with thin targets and gas transport of the species recoiling into the gas will be installed immediately ahead of the beam dump in BLIVa. The maximum proton beam current contemplated for BLIV(a) is 10 μA and the average is expected to be substantially lower.

BLIV(b) will have a proton beam current limit of 100 nA. It will feed protons to one, or possibly two general purpose target positions for (p, nucleus) reaction studies and to the target for a high resolution proton spectrometer designed to utilize the inherently narrow proton energy spread ultimately expected from the cyclotron.

1.1.3 Proton Beam Dumps:

The residual proton beams in the Proton Area will be dumped into low activation absorbers, such as graphite, surrounded by iron-concrete shields to achieve adequate dose-rates in inhabited areas at minumum cost. The beam intensity at BLI will, at full power, be high enough to make a useful neutron source for a thermal neutron facility. The residual protons will be stopped in a Pb or Pb/Bi target producing approximately 8 neutrons per incident 500 MeV proton. At 100 μA beam current the neutron source strength of 5×10^{15} s^{-1} will produce thermal neutron fluxes in the range $0.5\text{-}1.0 \times 10^{13}$ cm^{-2} s^{-1} in a small H_2O/D_2O moderator assembly.

Three tubes to neutron irradiation sites will be included in the vertical column used for access to the target-moderator assembly. Two horizontal tubes through the iron core shielding, off-set above the proton beam plane, will allow removal of neutron beams for experimental purposes. A separate proton irradiation facility for gross activity production will be installed immediately ahead of the thermal neutron facility target.

1.2 Radiation Sources, Shielding and Activity Production in TRIUMF

1.2.1 Accelerator:

Two beam loss mechanisms are expected to dominate in the accelerator: collisions with residual gas atoms in the cyclo-

tron vacuum chamber and dissociation of the H^- ions. Both will generally produce neutral H atoms which will then be lost tangentally into the side walls of the stainless-steel vacuum tank. Presuming no significant pressure gradients in the vacuum tank, the residual gas stripping will be uniform around the circumference and at the design, nitrogen-equivalent, residual pressure of 7×10^{-8} torr the fractional power loss from the accelerating beam is estimated to be 3.9%. The dissociation spill intensity follows the azimuthal variation of the magnetic field varying from 0 to 2.5 times the average at the vacuum tank wall. For normal operations with beam extraction at 500 MeV, the fractional power loss to vxB stripping is expected to be 7.6%, and essentially disappears for operations at 400 MeV or less.

Over most of the periphery of the cyclotron the void between the vacuum tank side wall and the main magnet return yoke will contain low activation shielding, thick enough to stop the spilled primary protons. At the gaps and thin sections in the main magnet return yokes, heavy-concrete block shielding around the periphery of the cyclotron will reduce the residual radiation levels in the cyclotron vault to allow general access within hours after shutdown of the facility. The 5 m thick concrete shielding walls between the cyclotron vault and the experimental areas are intended to reduce the operating dose rates in these areas below that for continuous occupation, i.e. 2.5 mrem h^{-1}.

As outlined above, the maximum beam intensity capability of TRIUMF is expected to be set by the residual radiation field constraints on maintenance and servicing operations in and around the cyclotron. The predicted residual radiation fields at the mid-plane of the service space when the vacuum tank lid and top halves of the cyclotron magnet sectors are raised 1.2 m, varies from $\lesssim 1$ rem h^{-1} at the center of the cyclotron to ~ 5 rem h^{-1} at a point opposite the tank periphery. This estimate assumes one day decay following a long operating period at 10 kW continuous spill. It is expected that at least semi-remote servicing operations will be required before residual fields reach these levels.

1.2.2 Proton Beam Lines and Targets:

All shielding in both the Proton and Meson experimental areas as shown in Fig. 1 will be in the form of demountable blocks. This approach was adopted primarily because of uncertainties in experimental space requirements over the lifetime of the facility. It has the additional advantage, however, of substantially reducing the precision requirements on operating dose-rate estimates at the design stage. The shielding shown for BLI is based on an assumed, uniform spill rate of 1 nA m^{-1}. This is not the level or distribution expected, but is the threshold level at which residual activation radiation fields begin to constrain access to the beam line after shutdown. This shielding also provides adequate protection against serious overexposure of personnel in the meson experimental area in the improbable circumstances that the entire 100 μA beam is lost at a point in the tunnel and goes undetected for an extended period of time.

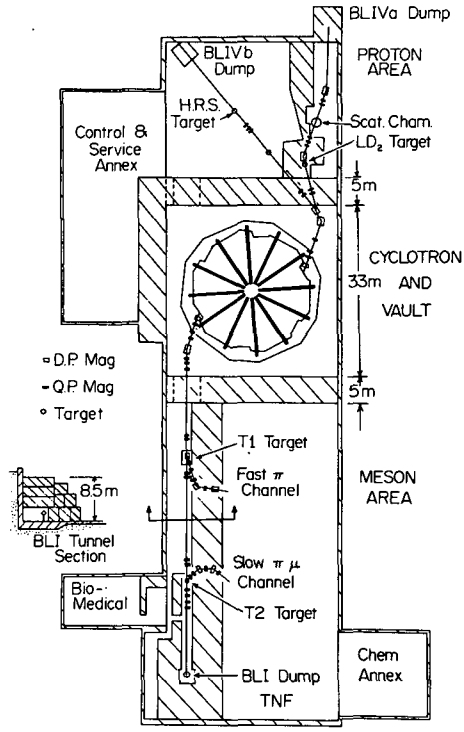

FIG. 1. Plan view of TRIUMF at primary beam line elevation.

Substantial proton beam spill is, of course, unavoidable at the meson and neutron production targets in the primary beam lines. Target T1 and BLI will be up to 4 g cm^{-2} thick of low Z material such as H_2O, C or Be; it will remove up to 7% of incident protons by elastic and non-elastic nuclear collisions. T2 targets will be limited to 20 g cm^{-2} of low or medium Z material (Be, Cu, etc.) and remove up to 25% of the incident protons by nuclear reactions. The Coulomb scattering will also be significant from medium Z targets at T2, and in the ultimate facility the residual proton beam will be collimated immediately after T2 for transmission to the proton beam dump - thermal neutron facility. Up to 25% of protons will be removed by the collimator.

Of the targets in the proton area only the liquid deuterium target, maximum thickness 1.7 g cm^{-2}, will remove substantial proton beam fractions, up to 3.3%. The other targets in BLIV(a) and BLIV(b) will remove less than 0.1% of the incident protons.

The general approach adopted at TRIUMF to accommodate residual activity problems resulting from high spill targets is to imbed the target assemblies in large monolithic shielding block, making all vacuum and cooling connections at the

outside of the block. The maximum block size that can be handled by the available lifting crane, 100 tons, affords a reduction of $\sim 10^{-3}$ in the high energy nucleon current, integrated over the outside surface, as compared to a simple target container. The residual radiation field at decay times short compared to the operating period are thus reduced from the order 10 R h^{-1} to the order 10 mR h^{-1} for distances of 10' from a thick target dissipating 5 kW of beam power. The actual target assemblies will be removable through a vertical access tube in the shield block to a shielding flask for transfer to hot-cell facilities.

1.2.3 Proton Beam Dumps:

The most intense sources of radiation both during operation and after shutdown are, of course, the beam dumps, and in particular the dump at the end of BLI, which will also have the function of a thermal neutron facility, as discussed above. For 50 kW of proton beam power on the stopping Pb-Bi target, approximately 10% emerges from the target as high-energy, "cascade" neutrons which, having the longest relaxation lengths, control the operating shield requirements. This 5 kW of cascade neutron power must be reduced by geometry and energy absorption to a radiation intensity of the order 10^{-11} W cm^{-2} for unrestricted personnel access. For distances of 10 m between the source and field points of interest, the geometry factor is 10^{-7} cm^{-2}; thus the attenuation factor for cascade neutron energy must be of the order 10^{-7} in directions of average intensity.

The residual activity accumulated in the Pb-Bi target after a long operating period at 50 kW beam power is ~40 kCi, of species with lifetimes longer than a few minutes. The residual radiation field at a distance of 10' from such a target a few hours after shut-down will be ~100 R h^{-1}.

2. OPERATING RADIATION INTENSITY ESTIMATES.

2.1 Hadronic Cascade Calculations

2.1.1 Collision Probability Calculations:

The essential problem in making reliable radiation transport estimates for high energy, "cascade" hadrons is an adequate treatment of the effects of the highly peaked angular distributions of secondary nucleons from non-elastic nuclear reactions. At the low-to-medium energies encountered at TRIUMF only neutrons need be considered in detail. The only significant energy loss mechanisms for neutrons in this energy region are non-elastic nuclear reactions: elastic nuclear reactions occur with approximately the same probability but the fractional momentum transfer is so small over most of the energy range of interest that they can, except for collisions with the lightest elements, be ignored. That the neutrons will dominate as the vehicles for transport of radiation energy through matter is obvious from a comparison of the collision mean free paths of various forms of radiation. At energies above about 100 MeV the mean free path between non-elastic neutron collisions varies smoothly from ~75 g cm^{-2} in

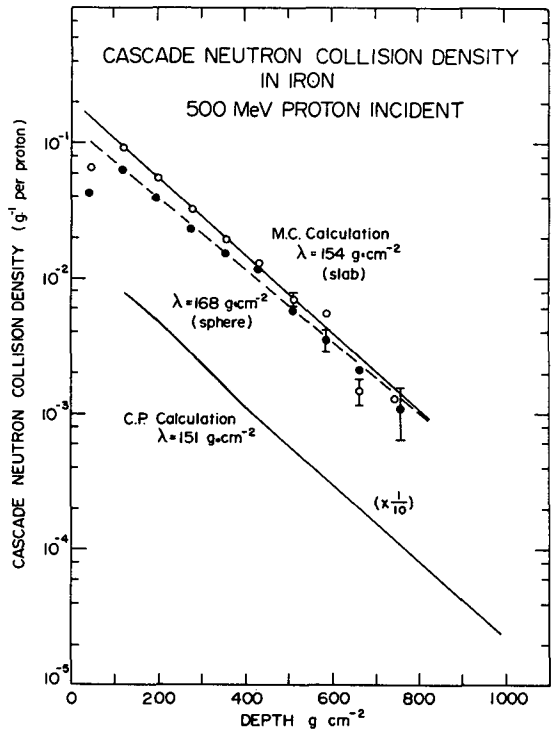

FIG. 2. Calculated collision density in iron of cascade neutrons with energy greater than 100 MeV. Monte-Carlo results are for slabs normal to, and 0 - 30° spherical cone sections centred on, the direction of protons incident at the centre of a 2 m cube. Collision probability results are for protons incident normally on a 1000 g·cm^{-2} plane slab.

carbon to ~200 g cm^{-2} in lead. By comparison, the mean free path for γ-radiation is in the range 10 - 25 g cm^{-2}. The cross-section for lower energy neutrons are generally higher, although there are a few isolated exceptions, one of which, the sharp dip in elastic scattering cross section in iron in the region of 26 keV, can be of practical significance.

To estimate the relaxation length for deep penetration of neutrons in various materials for the energy below 500 MeV, a series of numerical collision probability calculations were done [2]. The calculations were modelled on an infinite plane slab with nucleons incident on one face in discrete angular intervals and energy groups. The collision probabilities for successive generations of nucleons for each energy group, angular segment, and slab sub-interval, were computed by integrating over all relevant nucleon reactions in the previous generation. To obtain the results for the total internuclear cascade, a summation is carried out for all significantly contributing generations. The essential nuclear

reaction data requirements are the total non-elastic cross-section values, which were taken from experimental measurements [3], and the secondary particle distributions, which were derived from the parametric fits [4] to Bertini's intranuclear cascade results [5].

The bottom curve of Fig. 2 shows the results of one such calculation for 500 MeV protons incident on a 1000 g cm^{-2} slab of copper at near normal incidence. The non-elastic collision density for cascade neutrons with energies greater than 100 MeV, is plotted as a function of depth in the slab. The effective, broad beam, forward relaxation length at medium to large depths in the copper slab is 151 g cm^{-2} or 1.06 times the non-elastic mean free for high energy nucleons. For other materials this ratio was estimated to vary from 1.21 for carbon to 0.96 for Pb.

The model used for these calculations makes the estimates a useful guide for situations where broad beams are incident on plane or nearly plane shielding walls. Such a model does not have extensive application and its use can be justified only in the simplification it affords in solving the transport equation. For the more usual shielding situation near point radiation sources, the relaxation lengths deduced from this model can only be used with substantial contingency factors to allow for coupling effects between the geometrical divergence and secondary particle distributions from the nuclear reactions. More elaborate calculations have been undertaken recently to estimate the relaxation near point or line sources with more realistic models, as described in the next section.

2.1.2 Monte Carlo Calculations

In principle the Monte Carlo method is potentially exact in solving various problems in radiation transport, and the usual applications are in studying complicated systems that cannot be solved by less general methods. There are severe limitations on its application to problems involving low probability because of statistical accuracy problems. Deep shield penetration of radiation around high intensity facilities is a particular acute example. While special weighting techniques can be used they are tedious and require careful testing for most applications.

The Monte Carlo code NMT [6] which was developed at Oak Ridge for nucleon-meson transport studies, has been used to estimate the cascade particle fluxes around a few high intensity points in TRIUMF. The code uses Monte Carlo techniques for generating the intra- as well as the inter-nuclear cascade simulation, thus reducing the input data requirements to a minumum. The NMT code generates a series of particle histories and stores these, usually on magnetic tape, for subsequent analysis by separate codes. Several such analysis codes have been written at TRIUMF to compile collision densities and fluxes (COLLD), particle currents (ANNE), recoil energy distributions (RECOIL), residual product distributions (PROD) and detector spectral response (DECT).

The two upper curves of Fig. 2 show the cascade neutron collision densities in a 2 m cube of iron when 500 MeV protons are incident at the center. The top curve shows the col-

lision density sorted into slabs perpendicular to the incident direction, as a function of slab depth from the point of incidence. It is thus essentially equivalent to the collision probability calculation described above, and the slope of the curve gives a relaxation length of 154 g cm^{-2} in good agreement. The other curve is the collision density for cascade neutrons above ~100 MeV in the forward 0 - 30° cone, from the same NMT results. The slope of the curve gives a relaxation length of 168 g cm^{-2} for this "point" source geometry.

3. RESIDUAL ACTIVATION ESTIMATES

3.1 Experimental Data

The data requirements for making reliable residual activation estimates for medium and high energy proton accelerators are much greater than for either fission reactors or lower energy accelerators. In principle, the requirements for medium and high energy electron accelerators are as broad as those for proton machines, but for the same power dissipation neutron production and residual activation by electrons is a factor 10^{-2} to 10^{-3} less than for protons. For high energy hadron reactions a wide variety of products, as found in fission reactions, is combined with the universal target possibilities, as in neutron capture reactions. The situation is substantially relieved, however, by the much smoother variation in production cross-section as a function of residual species, target nucleus and hadron energy, as compared to the neutron capture case. This has led to the very valuable development of empirical formulae [7, 8] for reproducing experimentally known cross-sections and estimating unknown ones, as discussed in the following sections.

The experimental data available to 1964 has been compiled by Bruninx in CERN reports [9]. This compilation, and an internal Chalk River compilation [10] made in connection with the ING project, have been used extensively for estimating residual activity production at TRIUMF, especially for low-to-medium mass targets where the experimental data are relatively much more complete. For neutrons in the energy region below ~25 MeV the standard data compilation source for estimates at TRIUMF has, of course , been BNL-325 [11].

3.2 Empirical Activity Production Estimates

Empirical formulae defining the distribution of residual species following high energy nucleon-nuclear collisions have been used extensively in making residual activity estimates at TRIUMF. The original formulation, due to Rudstam [7], has also been used by Barbier and Cooper [12] in their very useful tabulation of source strengths and radiation fields for a wide variety of target elements, incident nucleon energies and decay periods. To provide estimates of residual activity for individual isotopes and the specific conditions at TRIUMF, a code, ACTA, and a decay data bank, similar to but more extensive than that used originally by Barbier and Cooper, were compiled. The code used a subroutine, RUDSTAM,

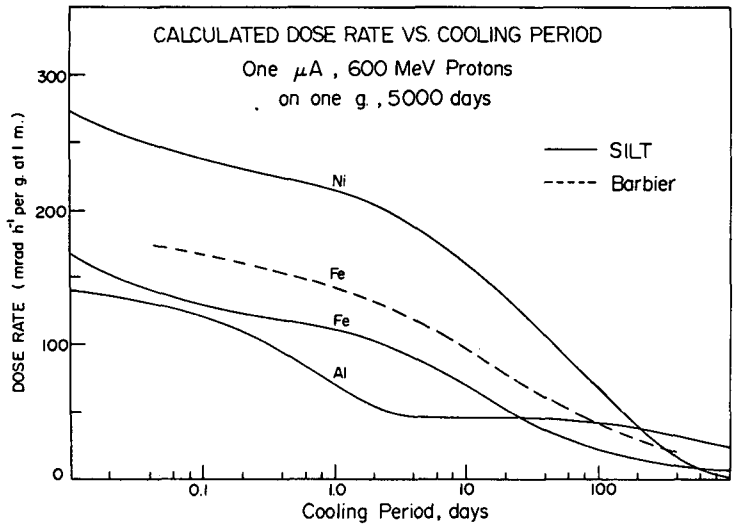

FIG. 3. Calculated residual radiation field decay curves for various elements using the empirical formulae of Silberberg and Tsao (SILT) and Rudstam (as estimated by Barbier).

for the activity production estimates which was based on a $^3/_2$ power exponential rather than Gaussian shape for the residual charge distribution.

A more recent empirical description of residual species distributions, similar to Rudstam, but extended in range of targets and residual species has been put forward by Silberberg and Tsao [8]. By the use of multiple sets of parameters for different ranges of nucleon energy, target and residual isotope, fairly good agreement with the available experimental data has been achieved for almost all target nuclei and reaction products. In particular they include "peripheral" reactions such as (p, 2p) and (p, pn), high excitation fission, which is important for high mass targets, and "break-up" of low mass targets as well as the usual spallation and evaporation processes.

A subroutine, SILT, has been written which uses Silberberg and Tsao's formula and parameters to estimate the production cross-sections in the residual activation code. Fig. 3 shows the results for 600 MeV protons on aluminum, iron and nickel from this code and subroutine. The dotted curve at Fig. 3 is Barbier's result for iron using Rudstam's formulae; Barbier's result for nickel is nearly identical to his iron curve. The newer results indicate that nickel is substantially worse than iron for residual activation, and that after long operating and decay periods aluminum is also worse than iron, in agreement with an observation by Wallace [13]. Fig. 4 shows the SILT results for stainless steel, concrete and limestone, all materials of practical importance at TRIUMF.

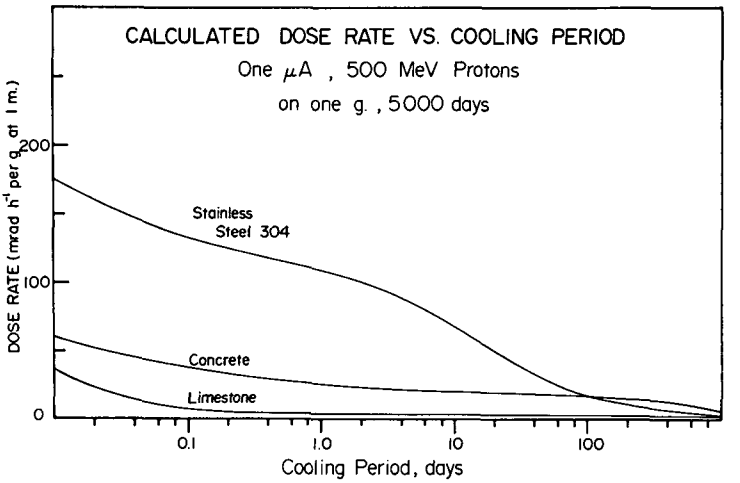

FIG. 4. Calculated residual radiation field decay curves for various construction materials as estimated by the empirical formulae of Silberberg and Tsao (SILT) and Rudstam (Barbier).

4. SUMMARY OF FUTURE DATA REQUIREMENTS

4.1 Radiation Transport Estimates

The most important uncertainties in radiation transport around medium-energy proton accelerator facilities like TRIUMF are in the angular dependencies, relative to the incident momentum, of the deep penetration relaxation lengths for the high energy neutrons, the dominant energy carrying component. The general solutions to these problems require both reliable nuclear reaction data and elaborate computational techniques and/or facilities. Any significant mismatching of these two components cannot, of course, be expected to yield optimum results. The Monte Carlo results for both intra- and inter-nuclear cascades, as employed, for example, in the NMT code, provide the most useful and reliable estimates for situations involving attenuation factors up to 10^{-3}.

When TRIUMF and other facilities in the same intensity range become operational the most reliable methods of making deep penetration radiation transport estimates will likely be by interpolation and extrapolation of the directly measured intensities. In the short term them, the incentive for the acquisition of the extensive secondary particle distribution data specifically for deep penetration shielding calculations is unlikely to increase. In the longer term the nuclear data requirements for shielding protection will be dependent on the introduction of machines of significantly higher intensity than those now coming into service. A substantial body of nuclear reaction data will be generated by facilities like TRIUMF from fundamental experimental programs. At the outset, at least, the effort is likely to be concentrated on simple

systems, i.e., light nuclei, and will probably not warrant, or require, much explicit effort for comprehensive compilation, at least for secondary particle distribution data.

An important operational problem found around medium and high energy accelerators is the variation in radiation leakage admixture and spectra. This problem is important because of inadequacies in the available personnel dosimetry techniques which are usually alleviated by making comprehensive dose and/or dose-equivalent measurements at "representative points" in the facility and relating these to particular components that are measured on personnel dosimeters. While the leakage spectra and admixture can, in principle, be determined entirely by experiment, recourse is usually indicated, at least as a supplement, to radiation transport calculations. Increasing attention will be required for such estimates at TRIUMF. The data requirements for these estimates, while the same in principle as those for the deep penetration calculations, are concentrated more at the lower, fission reactor energy range, where the data are fairly complete, than at the higher energies where recourse must be made to the intra-nuclear cascade results.

4.2 Residual Activity Estimates

As discussed above in section 3.3, the residual activity production by high energy reactions has been estimated at TRIUMF from experimental and empirical determined cross-section values. No strong incentive is forseen at this time to embark on cross-section measurements explicitly for residual activation estimates. Fairly extensive, fundamental physics programs at TRIUMF and other high intensity facilities are expected to yield substantially more data in this area over the next few years. These data should be assembled as soon as possible after publication into freely available compilations, preferable in conjunction with continuing refinements of the empirical production cross-section formulations.

REFERENCES

[1] TRIUMF Proposal and Cost Estimate, E. W. Vogt and J. J. Burgerjon, Editors, Nov. 1966.
TRIUMF Annual Reports, Edited by J. J. Burgerjon (1968), N. Brearley (1969, 1970, 1971), E. W. Vogt and A. Strathdee (1972).

[2] I. M. Thorson, Shielding and Activation in a 500 MeV Cyclotron Facility, TRIUMF Report TRI-68-4 (1968).

[3] R. G. P. Voss and R. Wilson, Proc. Roy. Soc. (London) A236 41 (1956).
M. H. MacGregor, et al., Phys. Rev. 111 1155 (1958).
T. Coor, et al., Phys. Rev. 98 1369 (1955).
F. Chen, et al., Phys. Rev. 99 857 (1955).
W. P. Ball, Nuclear Scattering of 300 MeV Neutrons, Report UCRL-1938 (1952).

[4] R. G. Alsmiller, M. Leimdorfer and J. Barish, Analytical Representation of Non-elastic Cross-Sections and Particle Emission Spectra from Nucleon-Nucleus Collisions in the Energy Range 25 to 400 MeV, Report ORNL-4046 (April 1967).

[5] H. W. Bertini, Phys. Rev. 131 1801 (1963) and Phys. Rev., AB2 (1965).

[6] W. A. Coleman and T. W. Armstrong, The Nucleon-Meson Transport Code NMTC, Report ORNL-4606 (1970).

[7] G. Rudstam, Phil. Mag. 46 344 (1955) and G. Rudstam, Z. Naturforsch 21a 7 (1966).

[8] R. Silberberg and C. H. Tsao, Partial Cross-Sections in High Energy Nuclear Reactions for Targets with $Z \leq 28$, (Pre-print, to be published, 1972) and Partial Cross-Sections in High Energy Nuclear Reactions for Targets Heavier than Nickel, (Pre-print, to be published, 1972).

[9] E. Bruninx, High Energy Nuclear Reaction Cross-Sections, Reports CERN61-1 (1961), CERN 62-9 (1962) and CERN 64-17 (1964).

[10] T. A. Eastwood and D. C. Santry, Private Communication (1963).

[11] Neutron Cross-Sections, 2nd Edition, BNL-325 (1956) and Supplements.

[12] M. Barbier and A. Cooper, Estimates of Induced Radioactivity in Accelerators, Report CERN-65-34 (1965).

[13] R. Wallace, Nucl. Inst. and Meth. 18, 19 405 (1962).

TRANSPORT OF NEUTRONS INDUCED BY 800-MeV PROTONS*

R.G. FLUHARTY, P.A. SEEGER, D.R. HARRIS,
J.J. KOELLING, O.L. DEUTSCH†
University of California,
Los Alamos Scientific Laboratory,
Los Alamos, N. Mex.,
United States of America

Abstract

TRANSPORT OF NEUTRONS INDUCED BY 800-MeV PROTONS.

Neutron transport calculations are presented for a pulsed neutron and proton research (Weapons Neutron Research, WNR) facility. Pulses of 800-MeV protons are obtained from the Los Alamos Meson Physics Facility (LAMPF) of 5 to 10 μs duration or 1 to 2% of the full LAMPF beam, yielding a maximum average neutron source strength of $1\text{-}2\times10^{15}$ neutrons/s. The calculated shield required to reduce this source to ~1 mrad/h consists of 2.6 m of steel plus 0.4 m of magnetite concrete and boron glass frit. The vertical proton beam and target require special consideration of the underground shielding to reduce floor dosage.

Neutron source, energy deposition, and activation calculations are based on two continuous-energy Monte-Carlo codes, NMTC and MCN, adapted to CDC 6600 and CDC 7600 computers. The NMTC code contains the detailed Monte-Carlo intranuclear-cascade calculations of Bertini. To maintain adequate statistical accuracy for deep penetration, a series of problems is run in which leakage neutrons from the previous problem are weighted and split as a source for the new problem containing added material. The low-energy MCN calculations, which use standard cross-section sets for energies below 20 MeV, are included in the last 1.2 m of thickness.

To provide more efficient calculational methods, a parallel effort has been undertaken to generate multigroup cross-section sets using the intranuclear-cascade model. An advantage of this method is that experimental values can also be incorporated. A library has been so constructed for iron and nine other elements, in a format for combination with ENDF libraries, for ten energy groups from 20 to 800 MeV. Comparison tests have been made on a spherical problem with a 1-m void followed by 2 m of iron. The multigroup Monte-Carlo program ANDY-MGCR, with source weighting and surface splitting, agrees with the SN transport code DTF-IV; however, the DTF results are only 60% of the results of the NMTC method described above. Since the difference is a relaxation-length effect, it probably reflects the inadequacy of the P_3 cross-section expansion tested to date. In addition to testing with higher-order cross-section sets, plans include experimental tests of thick iron shields.

1. INTRODUCTION

The Weapons Neutron Research (WNR) facility is being designed for neutron spectroscopy by means of neutron time of flight. The pulsed neutron source is to be produced by impinging pulses of 800-MeV protons from the Los Alamos Meson Physics Facility (LAMPF) on various thick targets. Pulses are to be obtained by separately switching the proton injector beam of LAMPF to produce pulses from 5-nsec to 5- or 10-μsec long while a pulsed switching magnet is activated. After the short pulse operation, the switching magnet is to be turned off and the normal 490-μsec pulse from the source is provided for the many other uses for the accelerator.[1] Thus, 1 to 2% of the LAMPF output (8 to 16 kW of target power) will be provided. A summary of the pulsed characteristics of LAMPF and WNR is given in Table I.

* Work performed under the auspices of the United States Atomic Energy Commission.

† Present address: Massachusetts Institute of Technology, Cambridge, Mass. 02139, United States of America.

TABLE I. LAMPF AND WNR CHARACTERISTICS

	LAMPF	WNR
Voltage (MeV)	800	800
Average Current (mA)	1	0.01-0.02
Macropulse Width (μsec)	500	0.008 to 5-10
Pulses per sec	120	120-240
Peak Macropulse Current (mA)	17	17
Micropulse Width (nsec)	0.08	0.3

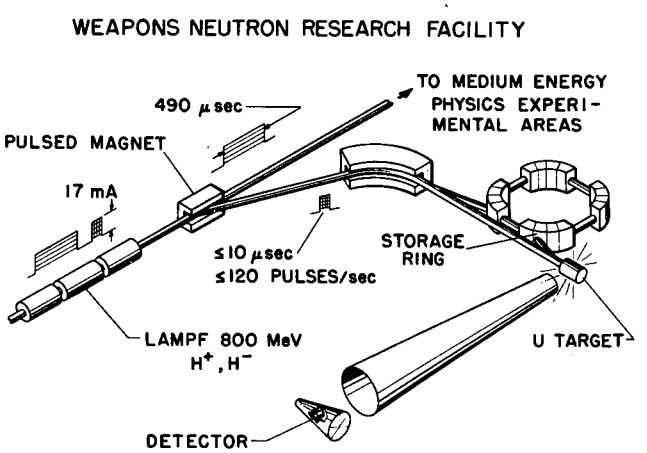

FIG. 1. Schematic showing how a short injector pulse of protons is deflected south by a pulsed switching magnet into the WNR transport system, through 90°, and onto the targets to produce neutrons. Neutron beams are represented using time of flight for the energy-dependent response of a detector. The major portion of the LAMPF beam is utilized elsewhere by turning the switching magnet off.

The LAMPF machine is a linear accelerator consisting of three types of accelerators. The 750-keV beam from a Cockcroft-Walton injector is accelerated to ~100 MeV in a 200-MHz Alvarez section, and then to 800 MeV in the 805 MHz side-coupled cavity system. At the end of the accelerator, the pulsed proton beam is transported to the WNR experimental area. First, the beam is deflected 90°, translated downward, and transported underground 150 to 200 m to the WNR experimental areas. This transport process is shown schematically in Fig. 1.

An isometric view of the WNR experimental area is given in Fig. 2, showing two principal target areas. In the first target, the beam is deflected 90° to point into the ground. Before it enters the ground, it impinges upon

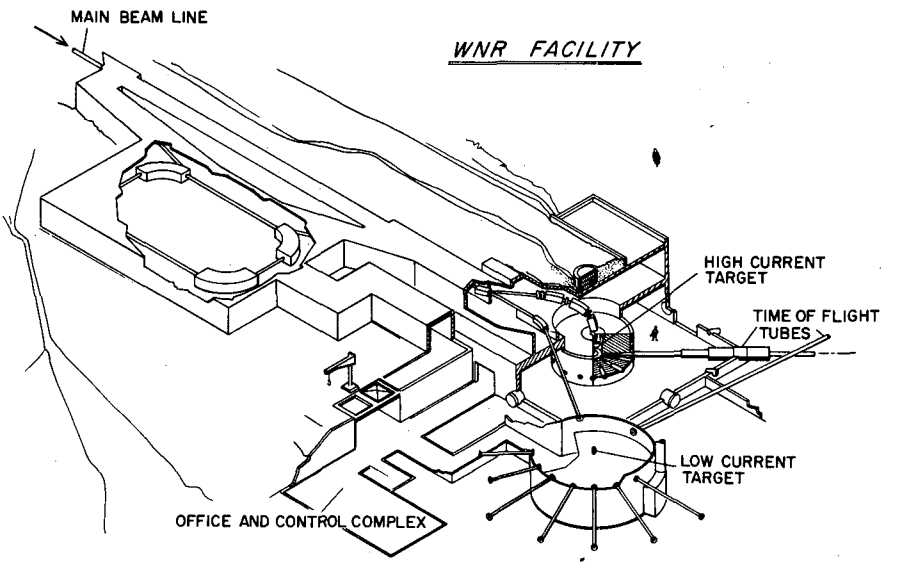

FIG. 2. A visual representation of the WNR target area. The high-power target is located in a vertical beam, allowing absorption of the forward high-energy neutrons in the earth. This high-power target has 11 neutron beam ports and requires a massive shield. The low-power target area provides for low neutron return from the walls.

a ^{238}U target of 4-cm diam. by 20-cm long to produce ~20 neutrons per proton. This target will absorb 8 to 16 kW from protons and 3 to 6 kW from fission (the rest of the proton energy is removed by fast neutrons). It is surrounded by a cylindrical void ~2-m diam. and 2-m high, and then by an iron-concrete shield ~3.7-m thick. There are to be 11 horizontal neutron beams penetrating to the experimental areas outside. One 200 m evacuated flight path (beam path) will have an illumination of 1.82-m diam. at the end. Other flight paths (5, 35, 50, 100 m) will have smaller apertures.

The second target area is shown in the foreground of Fig. 2; it is a large room where the central target position is at least 6 m from any wall, floor, or ceiling to reduce the back-scattered neutrons. This target area can be utilized for a horizontal target with ≤1% of the intensity of the first target or for a neutron scattering chamber utilizing a neutron beam from the first target. This second target area has great versatility for spectrum measurements, spectrum tailoring, and scattering measurements.

2. NEUTRON AND PROTON TRANSPORT

2.1 NMTC-MCN

A continuous energy Monte Carlo calculational system, NMTC-MCN,[2],[3] has been developed for use at the Los Alamos Scientific Laboratory for neutron, proton, and meson transport from 0 to 3.5 GeV, by P. A. Seeger. The system can be used on the CDC-6600 or CDC-7600 computers, and has options for MCN

geometry and time-dependence. Outputs are on tapes which contain complete individual particle records as requested for reaction events or surface crossings. Analysis programs for sorting and counting of the taped events provide tabular and graphic displays of the integrated information.

One code used, NMTC, is that developed at Oak Ridge National Laboratory for medium energy particle transport between about 15 MeV to 3.5 GeV. The nuclear portion by Bertini[4] assumes known input total reaction cross sections (elastic scattering is neglected) and calculates the reaction products by Monte Carlo assuming a cascade inside the nucleus pictured as a Fermi gas. This intranuclear cascade is terminated when the cascading particles have either escaped from the nucleus or have not enough energy to escape. Account is then taken of the residual nuclear energy by particle evaporation (mostly neutron). Escaping particles that have energies above an arbitrary cutoff are transported by Monte Carlo until another nuclear reaction occurs, a problem boundary is crossed, or (in the case of charged particles) they reach the cutoff energy. As NMTC was adapted to the CDC-6600 by H. I. Israel,[5] very detailed, individual particle-events (outside the nucleus) are recorded on a magnetic tape file. This very general tape also may include ionization losses, pion and muon production, etc.

Neutron transport for energies below the NMTC cutoff energy is continued with the continuous Los Alamos Monte Carlo code MCN, using the tape output of NMTC as the source. A cross-section library is maintained for this code, and the geometry routine is very general. The MCN geometry is now available as an option to the NMTC portion of the code, permitting a single geometrical description of the problem. A more concise optional tape format has been developed, suitable for both NMTC and MCN. Only the energy, position, velocity, time, statistical weight, and particle type for each particle are buffered and recorded, avoiding multiple tape reels. The high-energy output particles (p, n, π^+, and π^-) from NMTC and the low-energy neutrons from MCN may be written on a single tape.

2.2 Multigroup Cross Sections

In a parallel effort, the Bertini intranuclear cascade has been used to generate 41-energy group-average cross-section sets for ten elements (H, C, O, Si, Al, Fe, Ca, Mo, W, and Pb) in the ENDF/B format. This multigroup set provides access to faster running multigroup Monte Carlo and discrete ordinate transport programs. Currently, these cross sections are being used with the programs ANDY-MGCR[6] and DTF-IV.[7] The average cross-section approach allows ready adjustment to experimental cross-section evaluations. Currently, the cross sections are available with P_0, P_1, P_2, and P_3 Legendre coefficients for 20 to 800 MeV.

3. SOURCES

Neutron source optimization and source spectral adjustment are important objectives for the facility, so source studies are continuing. The NMTC-MCN system has been used to generate both primary and secondary sources, and output tapes can be used as sources for subsequent problems for both the NMTC-MCN and the multigroup systems. Examples where sources are used further involve shielding and moderator optimization for time-of-flight sources. In a previous study,[8] emphasis was placed on the generation of variable spectra sources and high neutron yield per proton.

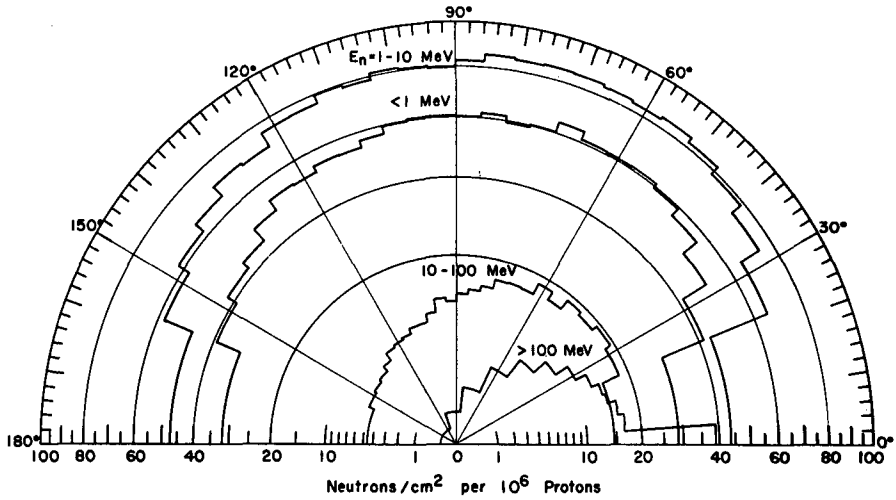

FIG. 3. The angular distribution at 1 m of neutrons emitted from a 4-cm-diam. by 15-cm-long target of ^{238}U is shown for 4 energy groups. Note the strong forward distribution for neutrons having energies above 100 MeV.

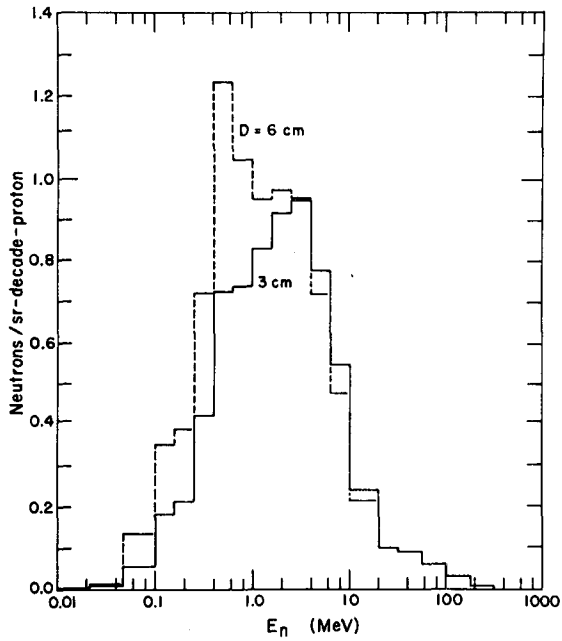

FIG. 4. The neutron spectra of 90° (averaged over ± 10°) for targets of ^{238}U with dimensions of 3-cm diam. by 15-cm long and 6-cm diam. by 15-cm long are shown. The added thickness converts the neutrons to a softer spectrum with more neutrons. Above 20 MeV, the two curves are not statistically different and have been averaged together.

A characteristic of the spallation source is the markedly forward component of the high-energy neutrons (>100 MeV). The anisotropy of this component is illustrated in Fig. 3, which shows the neutron current at 1 m produced by 800-MeV protons impinging along the axis of a 4-cm-diam. by 15-cm-long ^{238}U target. Below 20 MeV, the neutrons are emitted in a nearly isotropic pattern. Because the forward high-energy neutrons are poorly attenuated, the applied beams requiring lower neutron energies are taken off at angles of 90° or greater to the proton beam direction. For the first (high-power) target, the multiple beam ports are at 90° to the vertical proton beam.

Below 20 MeV, the calculated spectra can be characterized as evaporation spectra. Assuming a spectral shape used for fission spectra, the NMTC evaporation spectra from ^{238}U contain ~75% neutrons at 3-MeV temperature and 25% at 1-MeV temperature. Plots of the spectra at 90° from different ^{238}U targets are shown in Fig. 4. The targets are both 15-cm long and have diameters of 3 cm and 6 cm. It is seen that the additional radial thickness serves as a spectral converter wherein neutron inelastic scattering in the ^{238}U produces a new spectrum characteristic of a lower neutron temperature. Some portion of this conversion is also present in the smaller diameter target.

To a first rough approximation, the thick sources studied have one high-energy neutron per proton (between 20 and 800 MeV), and for neutron energies below 20 MeV, the number of neutrons is one-tenth the atomic number (A/10). Increased yields result from fission and (n,2n)(n,xn) processes as the neutrons are transported out of the target.[8] Experimental measurements, by Mady et al.[9] with 750-MeV protons yield ~30% more fast neutrons at 30 and 150° than predicted by NMTC. Because of their importance to accelerator shielding, these results need verification. Here the predictions of the code are utilized, but safety factors are included to allow for the experimental uncertainty.

4. SHIELDING

Monte Carlo calculations for deep penetration or large attenuations of radiation require weighting techniques--even with the fastest computers. Here, the principal method used is that of surface splitting, although exponential weighting should be better in theory. Secondarily, source weighting, Russian roulette, and variable energy cutoff as a function of position are resorted to. The success of this approach is based on the physical property that the penetration is propagated by the high-energy neutrons (above 100 MeV) where the lowest cross sections are encountered. The exception to this generalization involves the "windows"--particularly in Fe, where essentially zero cross sections are observed because of interference between s-wave resonances and potential scattering in spin-zero targets. To avoid this exception, a cardinal rule of neutron shielding is followed; namely, always construct shields of mixtures of elements. Thus, sufficient cross section is provided in the windows to avoid a "trapped" component, allowing neutrons to "stream" through the shield.

A major design study has been made on the shield for Target 1, which produces ~10^{15} neutrons/sec. A vertical cut of this shield is shown in Fig. 5; the target is located in a 6-ft by 6-ft cylindrical void surrounded by ~9 ft of steel plus 3 ft of heavy concrete. The external 1 ft of concrete will also contain boron glass to limit neutron-capture gamma rays to the relatively soft 476-keV boron component.

Calculations for the design of the Target 1 shield to reduce neutron dosages below 1 mrem/h were performed using the NMTC-MCN system. The procedure followed for these calculations was as follows:

(a) A cylindrical geometry was used.

(b) A series of problems were calculated in which successive layers were added to the previous calculations using NMTC only (E_n>20 MeV).

(c) The leakage neutrons from the previous problem were used as a source for the next problem with added thickness.

(d) The particles from each source tape, representing the output of the previous problem, were run three times to provide splitting given by the expected attenuation factor.

(e) Low-energy output tapes from NMTC for the last four thicknesses of shield were used as a source for MCN runs to calculate the leakage of low-energy neutrons.

(f) Neutron dosages are based on integrated or total neutrons or currents leaking from surfaces. This is considered to be a conservative estimate, compared with the more realistic fluxes (integral of particles/cosine of angle with respect to the surface normal).

Plots of the dosage as a function of vertical distance are presented in Fig. 6, for various radii corresponding to the tic marks on the neutron beam axis in Fig. 5. The significant feature to be noted in Fig. 6 is the large leakage near and under the floor or in the forward direction to the beam. Special care and tedious study were required to reduce the dosage at floor

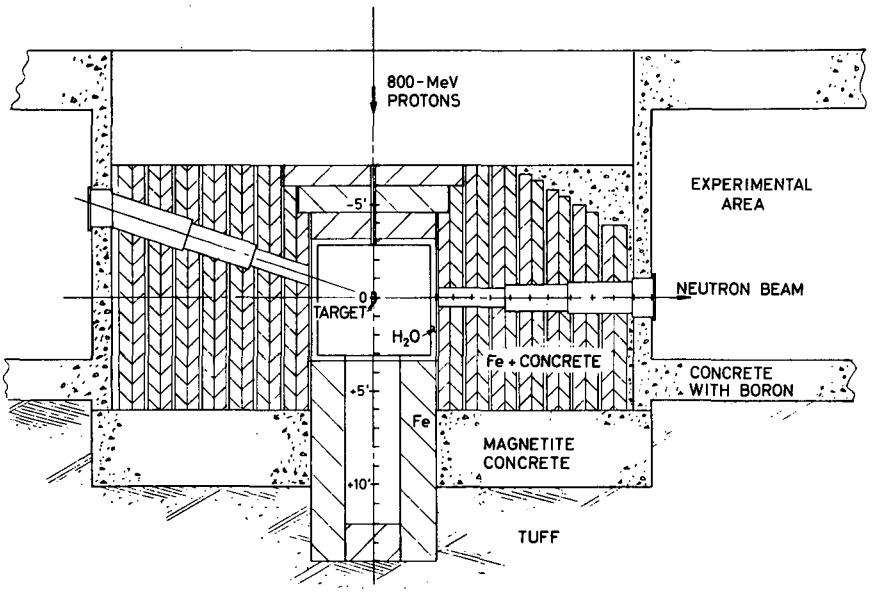

FIG. 5. A vertical cross-section of the high-power target shielding, as studied for shield design. It has been determined that a superior shield results from solid iron or lead shielding below the centre cavity instead of the hole into the ground. Tic marks on the neutron beam axis represent radial positions for which dosage is plotted in Fig. 6.

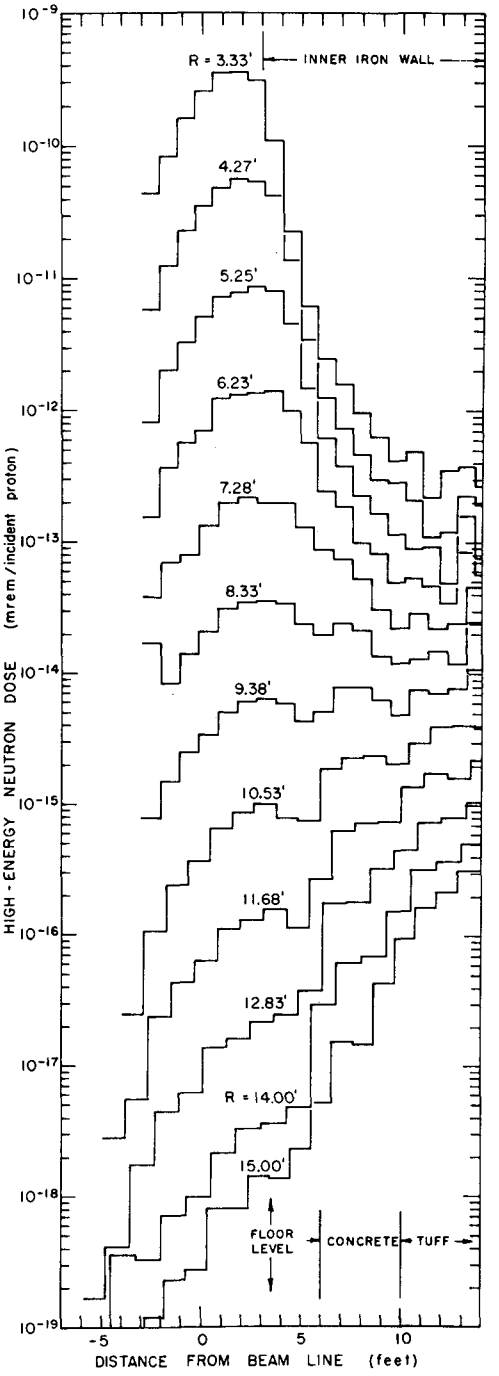

FIG. 6. Radiation dosage as a function of vertical distance from the neutron beam port level, at different radii from the centre of the proton beam. The positive vertical direction is in the proton beam direction (downward). Note the high dosage levels in the ground which cause high dosages at the floor level of the experimental room. This figure is scaled to Fig. 5.

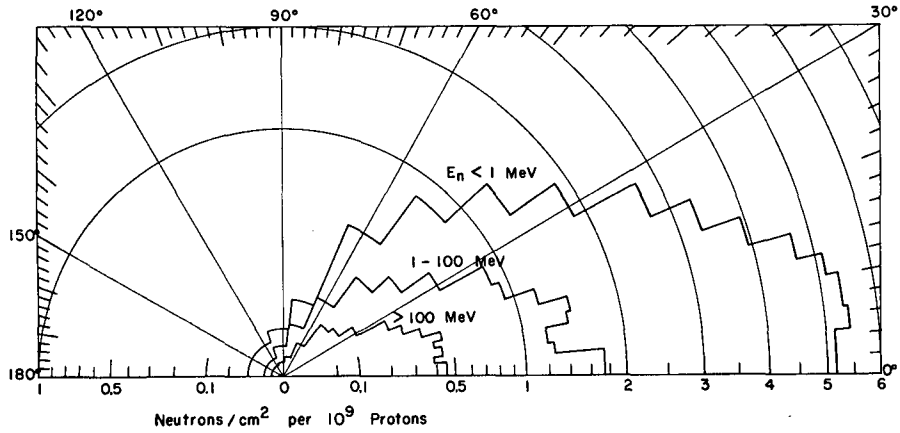

FIG. 7. The leakage neutrons/cm^2 (measured from the proton direction) on the outside of a 2-m-thick spherical iron shell, as a function of angular position. The inner radius of the shell is 1 m; the source neutrons entering the shell are shown in Fig. 3. Note that the dosage pattern for all neutron energies is equivalent to the angular distribution of the neutron spectrum component above 100 MeV.

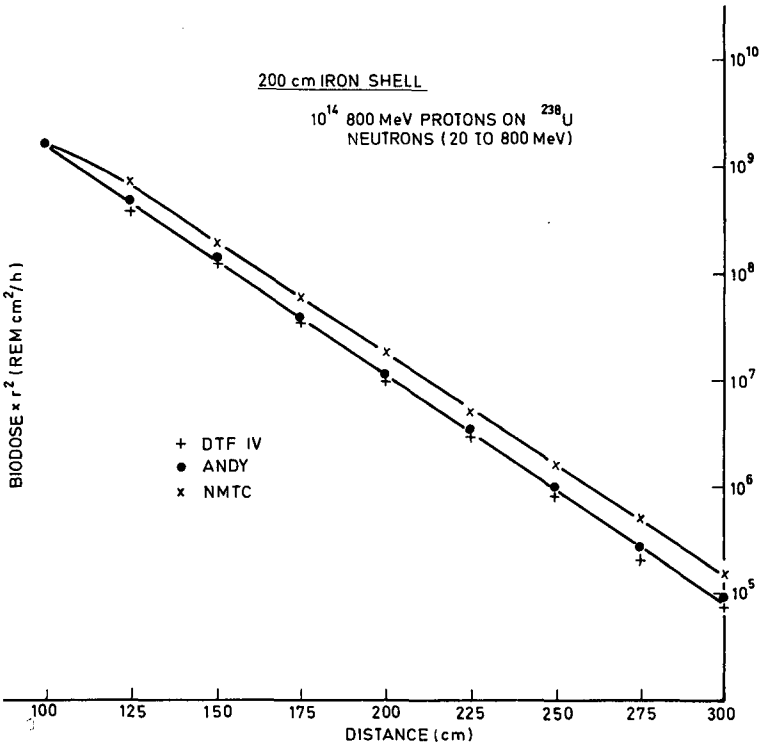

FIG. 8. A comparison of the average dosage over the surface of the spherical iron shell problem of Fig. 7, for three different calculational methods. NMTC-MCN is a continuous energy Monte-Carlo system, ANDY-MGCR is a multigroup Monte-Carlo system, and DTF-IV is a discrete ordinate method. The agreement is excellent, but Fig. 7 indicates that position information is also needed to compare the methods.

levels where neutrons leak through the ground and up through the floor; underground shielding was found necessary to reduce these levels. More recent studies reveal that a solid shield at the bottom of the void is preferable to the voided hole into the ground shown in Fig. 5.

To emphasis the importance of the angular distribution of the source, results from a calculation with a spherical iron shell are shown in Fig. 7. The same neutron source as shown in Fig. 3 was used, surrounded by a 1-m-radius void and then 2-m of iron. The results presented are the surface neutron leakage as a function of angular position, with respect to the proton beam direction. It is observed, from comparison with Fig. 3, that the surface dose in all energy bins essentially follows the angular distribution of the 100 to 800-MeV component of the source.

The same spherical iron problem has been also calculated by ANDY-MGCR and DTF-IV using average multigroup cross sections. A comparison of the dosage for high-energy neutrons averaged over the spherical surfaces as a function of radius is shown in Fig. 8. The agreement is considered satisfactory for such calculations, since the relaxation length by NMTC is only 1.3% higher than by using the average cross sections. Higher order polynomial expansion of the cross sections is being tested as a possible explanation. Some 15 to 20% of the difference may be explained by those protons which continue through the target into the iron shield. These are not considered in the multigroup treatments and are included in NMTC. Note that the same physical quantities for the dosage are present only at the outside surface for this problem. The NMTC approach truly calculates surface leakage as a function of sphere size, but the other calculation methods include multiply reflected neutrons across internal surfaces because only one calculation has been performed.

5. DISCUSSION

Despite early intentions to obtain general results which allow simplified methods to follow, the major effort has been on specific design problems. To accomplish this, considerable computer resources have been required which are not generally available. It is not our intention to imply that the techniques used here should necessarily be followed, because simpler techniques are clearly desirable.

The spherical iron problem can serve as a comparison standard; simple cylindrical problems, using earth and concrete, are being carried out. The discrete-ordinate methods (DTF-IV) and NMTC-MCN approach agree reasonably well, but the multigroup ANDY-MGCR-Monte Carlo approach is not completely understood. Although the spherical iron agreement is good, thick cylinders of earth currently present problems. Further testing of the multigroup cross-section sets are needed, and clean experimental comparisons are vitally needed. To carry out the spherical iron problem with NMTC-MCN, two to three hours of CDC-7600 time was required, and a factor of five more using the CDC-6600. In comparison, the multigroup ANDY-MGCR required ~5 min. (5 problems), and DTF ~30 sec (isotropic).

The results to date demonstrate the promise that point kernel and removal cross-section methods can be evolved. The major problem will be to account properly for source anisotropy in the high-energy region. The value of the computational system being developed for WNR has already been demonstrated in the understanding of the physics of the problems and in the design of the facility.

REFERENCES

[1] NAGLE, D. E., KNAPP, E. A., in Yale University Conference on Linear Accelerators, 1963 (Yale Univ. Press, New Haven, 1964), p. 171; in Proceedings of the Fifth International Conference on High Energy Accelerators, Frascati, Italy, 1965 (Comitato Nazionale Energia Nucleare, Rome, 1966), p. 403; IEEE Trans. Nucl. Sci. 12 623 (1965).

[2] COLEMAN, W. A., ARMSTRONG, T. W., "The Nucleon-Meson Transport Code, NMTC," ORNL-4606 (1970).

[3] CASHWELL, E. D., NEERGARD, J. R., TAYLOR, W. M., TURNER, G. D., "MCN: A Neutron Monte Carlo Code," Los Alamos Scientific Laboratory report LA-4751 (1972).

[4] BERTINI, H. W., Phys. Rev. 131 1801 (1963) and erratum Phys. Rev. 138 AB2 (1963).

[5] ISRAEL, H. I., COCHRAN, D. F., "DTF Shielding Calculations at 800-MeV LAMPF," Second International Conference on Accelerator Dosimetry and Experience, Stanford Linear Accelerator Center, Stanford, California (1969).

[6] HARRIS, D. R., "ANDYMG3, the Basic Program of a Series of Monte Carlo Programs for Time-Dependent Transport of Particles and Photons," Los Alamos Scientific Laboratory report LA-4539 (1970); HARRIS, D. R., FLUHARTY, R. G., KOELLING, J. J., WHITTEMORE, N. L., "Medium- and Low-Energy Cross Section Library," Trans. Am. Nucl. Soc. 15 962 (1972).

[7] LATHROP, K. D., "DTF-IV, A FORTRAN IV Program for Solving the Multi-Group Transport Equation with Anisotropic Scattering," Los Alamos Scientific Laboratory report LA-3373 (1965).

[8] FULLWOOD, R. R., CRAMER, J. D., HAARMAN, R. A., FORREST, R. P., Jr., SCHRANDT, R. G., "Neutron Production by Medium-Energy Protons on Heavy Metal Targets," Los Alamos Scientific Laboratory report LA-4789 (1972).

[9] MADEY, R., WATERMAN, F. M., submitted for publication, Kent State University, Kent, Ohio; see also Ref. [8], above.

DISCUSSION

I. M. THORSON: In Fig. 8 showing calculated relaxation of neutron flux in the spherical shields, what angle is the result for, or is it integrated over all outgoing directions?

R. G. FLUHARTY: It is integrated for all directions.

W. B. LEWIS: What is the difference between Russian Roulette and Monte Carlo?

R. G. FLUHARTY: I would prefer that an expert answer your questions about Russian Roulette, but my version is as follows: to avoid spending time on neutrons travelling back through the surface (inwards), the particles are randomly "killed" but they are accounted for by weighting methods.

W. B. LEWIS: In sections 4 and 5 of the paper there is reference to windows in iron shielding for certain neutron energies. What would you use instead of iron or in addition to it?

R. G. FLUHARTY: Because of cost considerations, iron is still the preferred shield material in spite of the windows. Hydrogen with 1.5 atom %, is considered adequate to eliminate window effects. More precisely, the optimum mixture is 1.5 atom % hydrogen.

R. NICKS: Your discussion is limited to neutron attenuation. What about photon production and propagation. Neutron capture and inelastic scattering will probably represent important gamma sources. Did you resolve the problem of photon propagation?

R. G. FLUHARTY: No, we did not calculate the gammas. However, this question has not been completely ignored because the gamma production will follow the penetrating high-energy neutrons and because the gamma attenuation is much more rapid than for these neutrons. Moreover, the outer 15-18 inches of the shield consists of magnetite aggregate concrete with a boron frit or glass. The hydrogen moderation and capture in boron largely eliminates the iron capture gammas. The 476-kW boron gammas can be easily shielded. Gamma production and transport options are available for the multigroup methods we are using.

R. NICKS: In calculating the neutron transport in the shield, you make use of DTF IV. I do not think that a code of this kind is adapted to handling the strong flux anisotropies. What was the order of the S_n-approximation?

R. G. FLUHARTY: I do not wish to state the order of the S_n approximation because I have forgotten the value.

H. RIEF: What is the cost estimate for the spallation target and the proton deflection facility? How long will it take to construct this facility?

R. G. FLUHARTY: The beam channel cost is estimated to be US $1 million and the budget for the whole WNR facility is $4.4 million. Completion is expected in two years.

G. A. KOLSTAD: All three speakers in this session have described very interesting applications – in space science, accelerator shielding, beam transport and beam tailoring. All have indicated that their calculations required nuclear data which are insufficient for their needs. Yet none of them listed the nuclear data needed, giving the bombarding energy, particle and resolution required.

Would it be possible for any of them to specify the required information in the form of request lists so that measurers of nuclear data can be stimulated to make the measurements which might meet their needs or future needs of a similar nature? Such tabulations could be included in the proceedings of this conference.

R. G. FLUHARTY: The Bertini approach is not expected to provide good answers for Be, C, N and O, so these have first priorities for angular dependent inelastic scattering cross-section measurements, i.e. (p; n'(E), θ), (n; n'(E), θ), (n; p(E), θ) [including xn', xp' products as well] for energies from 20 MeV up to 3 GeV. This should cover the applied accelerator field and space applications. Angular effects for isotopes spaced through the chart of A values are needed to confirm Bertini calculations. It would be useful to test the assumption that Al and Si have the same cross-sections.

Data are needed on high energy fission cross-sections (heat production as well as neutron), and the delayed neutron fractions are a vital question for possible booster expansion of the source capability. This latter question

is of sufficient interest to have made us decide to measure the delayed neutrons ourselves.

Deep penetration measurements are needed because the cross-section accuracy required can be obtained only in this manner.

W. W. HAVENS, Jr. (Chairman): I am afraid that we shall have to get these facilities operating and do some experiments with them before there will be adequate data in this energy range to get the information which is necessary for checking the calculations.

CHAIRMEN OF SESSIONS

Section I	G. A. KOLSTAD	USA
Section II	W. B. LEWIS	Canada
Section III	O. J. EDER	Austria
Section IV	A. H. W. ATEN	CCE
Section V	K. H. LIESER	Federal Republic of Germany
Section VI	G. B. YANKOV	USSR
Section VII	W. W. HAVENS	USA
Section VIII	Yu. F. CHERNILIN	IAEA
Section IX	R. L. JOLY	France
Section X	B. GRINBERG	France
Section XI	P. ALBERT	France
Section XII	G. A. BARTHOLOMEW	Canada
Section XIII	A. H. WAPSTRA	Netherlands
Section XIV	A. T. G. FERGUSON	UK
Section XV	H. P. MÜNZEL	Federal Republic of Germany
Section XVI	D. J. HOREN	USA

SECRETARIAT

Scientific Secretaries:	J. J. SCHMIDT L. HJÄRNE	Division of Research and Laboratories, IAEA
Administrative Secretary:	R. NAJAR	Division of Scientific and Technical Information, IAEA
Editor:	J. W. WEIL	Division of Publications, IAEA
Records Officer:	L. S. LIEBERMANN	Division of Languages, IAEA

HOW TO ORDER IAEA PUBLICATIONS

Exclusive sales agents for IAEA publications, to whom all orders and inquiries should be addressed, have been appointed in the following countries:

UNITED KINGDOM	Her Majesty's Stationery Office, P.O. Box 569, London SE1 9NH
UNITED STATES OF AMERICA	UNIPUB, Inc., P.O. Box 433, New York, N.Y. 10016

In the following countries IAEA publications may be purchased from the sales agents or booksellers listed or through your major local booksellers. Payment can be made in local currency or with UNESCO coupons.

ARGENTINA	Comisión Nacional de Energía Atómica, Avenida del Libertador 8250, Buenos Aires
AUSTRALIA	Hunter Publications, 58 A Gipps Street, Collingwood, Victoria 3066
BELGIUM	Office International de Librairie, 30, avenue Marnix, Brussels 5
CANADA	Information Canada, 171 Slater Street, Ottawa, Ont. K1 A OS 9
C.S.S.R.	S.N.T.L., Spálená 51, Prague 1 Alfa, Publishers, Hurbanovo námestie 6, Bratislava
FRANCE	Office International de Documentation et Librairie, 48, rue Gay-Lussac, F-75 Paris 5e
HUNGARY	Kultura, Hungarian Trading Company for Books and Newspapers, P.O. Box 149, Budapest 62
INDIA	Oxford Book and Stationery Comp., 17, Park Street, Calcutta 16
ISRAEL	Heiliger and Co., 3, Nathan Strauss Str., Jerusalem
ITALY	Libreria Scientifica, Dott. de Biasio Lucio "aeiou", Via Meravigli 16, I-20123 Milan
JAPAN	Maruzen Company, Ltd., P.O. Box 5050, 100-31 Tokyo International
NETHERLANDS	Marinus Nijhoff N.V., Lange Voorhout 9-11, P.O. Box 269, The Hague
PAKISTAN	Mirza Book Agency, 65, The Mall, P.O. Box 729, Lahore-3
POLAND	Ars Polona, Centrala Handlu Zagranicznego, Krakowskie Przedmiescie 7, Warsaw
ROMANIA	Cartimex, 3-5 13 Decembrie Street, P.O. Box 134-135, Bucarest
SOUTH AFRICA	Van Schaik's Bookstore, P.O. Box 724, Pretoria Universitas Books (Pty) Ltd., P.O. Box 1557, Pretoria
SPAIN	Nautrónica, S.A., Pérez Ayuso 16, Madrid-2
SWEDEN	C.E. Fritzes Kungl. Hovbokhandel, Fredsgatan 2, Stockholm 16
U.S.S.R.	Mezhdunarodnaya Kniga, Smolenskaya-Sennaya 32-34, Moscow G-200
YUGOSLAVIA	Jugoslovenska Knjiga, Terazije 27, Belgrade

Orders from countries where sales agents have not yet been appointed and requests for information should be addressed directly to:

Publishing Section,
International Atomic Energy Agency,
Kärntner Ring 11, P.O.Box 590, A-1011 Vienna, Austria

INTERNATIONAL
ATOMIC ENERGY AGENCY
VIENNA, 1973

PRICE: US $26.00
Austrian Schillings 486,-
(£10.00; F.Fr.110,-; DM 64,-)

SUBJECT GROUP: III
Physics/All